33rd International Conference on Solution Chemistry

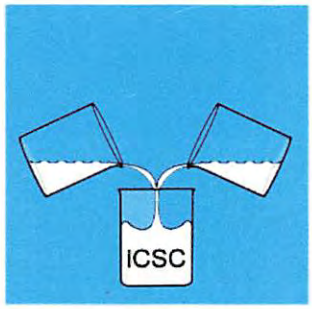

Book of Abstracts

Kyoto Terrsa, Kyoto, Japan
July 7th-12th 2013

JASC

Welcome to the 33rd International Conference on Solution Chemistry (33ICSC)

On behalf of the organizing committee, we are pleased to welcome you to the 33rd International Conference on Solution Chemistry held here in Kyoto from 7th July to 12th July 2013. During the two years since last we met in La Grande Motte, France, we organized the committee and prepared in all aspects to make this traditional conference very successful. We would like to express our sincere thanks to all staff members and students of universities and organizations and to foundations and private companies who have supported to hold this conference. We would like to thank all plenary and invited speakers and contributors of oral and poster presentations from overseas and domestic to bring together new results of their scientific works to present and discuss the new findings on various scientific and technological issues related to solution chemistry. Solution chemistry covers a broad and interdisciplinary area in chemistry, physics, and biology, pharmaceutical and medical sciences. With the advent of new theory, analytical methods, computers, and technology, the research area of solution chemistry has now been widely and deeply expanded, e.g. new solvents, such as room temperature ionic liquids and supercritical fluids, which are very promising in industrial applications, liquids and solutions in confinements and on interfaces, more complex systems like biomaterials and proteins, and nanotechnology. During the conference we arrange ample time for poster sessions so that presenters, in particular, young scientists like PhD students and postdocs, could discuss about their research results with eminent scientists from all over the world. Kyoto is an ancient capital of Japan, not bombarded in the World Wars, and thus there are many historical places to visit, some of them are registered as world heritage by UNESCO. The official travel agency TOPTOUR of the conference will help the accompanying persons enjoy sight-seeing and Japanese culture in Kyoto. We strongly wish that all attendees of the conference could bring home fruitful results and have memorable experiences and time in scientific and cultural events during this week.

Professor Toshio Yamaguchi
Chairman of the Organizing Committee of 33ICSC

Organization Committee

Conference Chair — Toshio Yamaguchi (Fukuoka University)

Secretary General — Masahide Terazima (Kyoto University)

Chairman of Program Committee — Toshihiro Tominaga (Okayama University of Science)

Chairman of Publication Committee — Yasuo Kameda (Yamagata University)

Chairman of Local Organizing Committee — Nobuyuki Matubayasi (Kyoto University)

Local Organizing Committee
- M. Kato (Ritsumeikan University)
- Y. Kimura (Doshisha University)
- H. Sato (Kyoto University)

Program Committee
- R. Akiyama (Kyushu University)
- M. Aratono (Kyushu University)
- F. Hirata (IMS, Ritsumeikan University)
- M. Iida (Nara Women's University)
- M. Irisa (Kyushu Institute of Technology)
- T. Kakiuchi (Kyoto University)
- M. Kanakubo (National Institute of Advanced Industrial Science and Technology)
- T. Kimura (Kinki University)
- K. Nishikawa (Chiba University)
- H. Ogawa (Tokyo Denki University)
- S. Okazaki (Nagoya University)
- M. Osawa (Hokkaido University)
- H. D. Takagi (Nagoya University)
- K. Tominaga (Kobe University)
- H. Torii (Shizuoka University)
- S. Tsukahara (Osaka University)
- Y. Umebayashi (Niigata University)
- H. Wakita (Fukuoka University)
- K. Yamanaka (Organo Corporation)
- Y. Yoshimura (National Defense Academy)

International Steering Committee
- I. Persson (Uppsala, Sweden)
  - Chairman

- G. Hefter (Murdoch, Australia)
- B. M. Rode (Innsbruck, Austria)
- P. Turq (Paris, France)
- T. Yamaguchi (Fukuoka, Japan)

- J. Barthel (Regensburg, Germany)
- B. Gill (Leeds, UK)
  - Honorary Members

Acknowledgements

The organizing committee of 33ICSC is grateful to the following organizations, companies and persons for financial support, contribution, insertion of the advertisement to the abstract book and participation to the exhibition of commercial products or catalogues.

Financial Support

Commemorative Organization for the Japan World Exposition '70

Morino Foundation for Molecular Science

Organization for the Prohibition of Chemical Weapons

Contribution

Chemicals Evaluation and Research Institute, Japan

BEL Japan inc.

TANAKA KIKINZOKU KOGYO K.K.

Yoshiyuki Asakura (HONDA ELECTRONICS CO., LTD.)

Masaharu Watanabe (TAIATSU TECHNO CORPORATION)

KOUATU SYSTEM CO., LTD.

Tokyo Riko Co., Ltd.

Professor Isao Okada

COMBEX CO., LTD.

Professor S. Y.

Contributions were given from other two companies.

Exhibition of Catalogue

BEL Japan inc.

Advertisement

Rigaku Corporation

BEL Japan inc.

TAIATSU TECHNO CORPORATION

KOEI CHEMICAL COMPANY LIMITED

Merck Ltd.

PerkinElmer Japan Co., Ltd.

SANSHODO CO., LTD.

SANKYO PUBLISHING Co., Ltd.

Exhibition Booth

KOEI CHEMICAL COMPANY LIMITED

HORIBA, Ltd.

ORGANO CORPORATION

Kyoto Electronics Manufacturing Co., Ltd.

Asahi Glassplant Inc.

This Conference is financially supported in part by

The Morino Foundation for Molecular Science

Koichi M. T. Yamada[‡]

Professor Yonezo Morino (1908* –1995+), an outstanding molecular scientist in Japan, founded the Morino Foundation for Molecular Science (or expressed simply as "the Morino Foundation") was in 1985 donating his personal property. The main intention of the foundation is to encourage young scientists of great promise, in the field of the molecular science, by supporting them financially. On his death in 1995, the fund received a rich legacy. Furthermore his wife, Mrs. Yoshi Morino, donated to the Morino Foundation all her inheritance on her death in 2005. The scientific work of Professor Morino is summarized in a special issue of the *Journal of Molecular Structure* in 1995, by Hirota, Kimura, Kuchitsu, and Tanimoto. The term "Molecular Science" was introduced in Japan by Professor Morino and others in early 1960's and the establishment of the Institute of Molecular Science in Okazaki, 1975, is a brilliant result of their endeavor.

Presently, the Morino Foundation supports four kinds of activities. The first one is the **Morino Lecture**. We invite excellent scientists from overseas and give young Japanese scientists chances to discuss directly with them. The first Morino Lecturer was Prof. Polanyi in 1986. We are very proud that we had invited him one year earlier than he got the Novel prize. Since then, we invite a few scientists each year as the Morino Lecturer.

The second activity is to offer **Research Funds** to promising young molecular scientists. Each year two or three awardees are selected.

The third activity is the support for **International Conferences** organized by molecular scientists in Japan.

The fourth activity is the support for **Traveling Expenses** to the molecular scientists in Japan who wish to report their results at the international meetings held abroad.

If you wish to have any support from the Morino Foundation, please contact the steering committee.

[‡]Chairman of the steering committee of the Morino Foundation; kmt.yamada@aist.go.jp

謝　辞

本国際会議開催に当たりに財政援助頂いた独立行政法人**日本万国博覧会記念機構**，公益法人**分子科学奨励森野基金**および**化学兵器禁止機関**（OPCW）に感謝致します。

助成 独立行政法人日本万国博覧会記念機構
Supported by the Commemorative Organization for the Japan World Exposition('70).
この助成金は，日本万国博覧会の収益を基にしています。

また，ご寄付，広告掲載および，機器・製品またはカタログ展示を頂いた下記，法人，企業，および個人様に心より御礼申し上げます。

寄付者（敬称略）

一般財団法人化学物質評価研究機構

日本ベル株式会社

田中貴金属工業株式会社

本多電子株式会社　研究部部長
朝倉 義幸

耐圧硝子工業株式会社　代表取締役
渡辺 正治

高圧システム株式会社

株式会社 東京理工

岡田 勲

コムベックス株式会社

匿名 S. Y.

他，2社様よりご寄付を頂きました。

カタログ展示企業

日本ベル株式会社

広告掲載企業

株式会社 リガク

日本ベル株式会社

耐圧硝子工業株式会社

広栄化学工業株式会社

メルク株式会社

株式会社 パーキンエルマージャパン

株式会社 三笑堂

三共出版株式会社

機器・製品展示企業

広栄化学工業株式会社

株式会社 堀場製作所

オルガノ株式会社

京都電子工業株式会社

株式会社 旭製作所

Access guide to the meeting place : Kyoto Terrsa

Address Kyoto TERRSA Shinmachi Kujo Minami-ku,Kyoto,Japan (Kyoto Citizen's Amenity Plaza)
TEL +81+75-692-3400 FAX +81+75-692-3402

Conference Banquet will be held at New Miyako Hotel located near J.R. Kyoto Station.
TEL : +81-75-661-7111 FAX : +81-75-661-7135

Kyoto Terrsa Access & Location

- 75minutes by train from Kansai international Airport to Kyoto Station
- 2hours and 30minutes by Shinkansen(bullet train) from JR Tokyo Station to Kyoto

Transportation

- 5minutes by subway (Karasuma Line) from Kyoto Station to Kujo Station.
  5minutes walk from Kujo Subway Station.
- 5minutes walk from To-ji Station on the Kintetsu Line
- 15minutes walk from Kyoto Station

Kyoto TERRSA

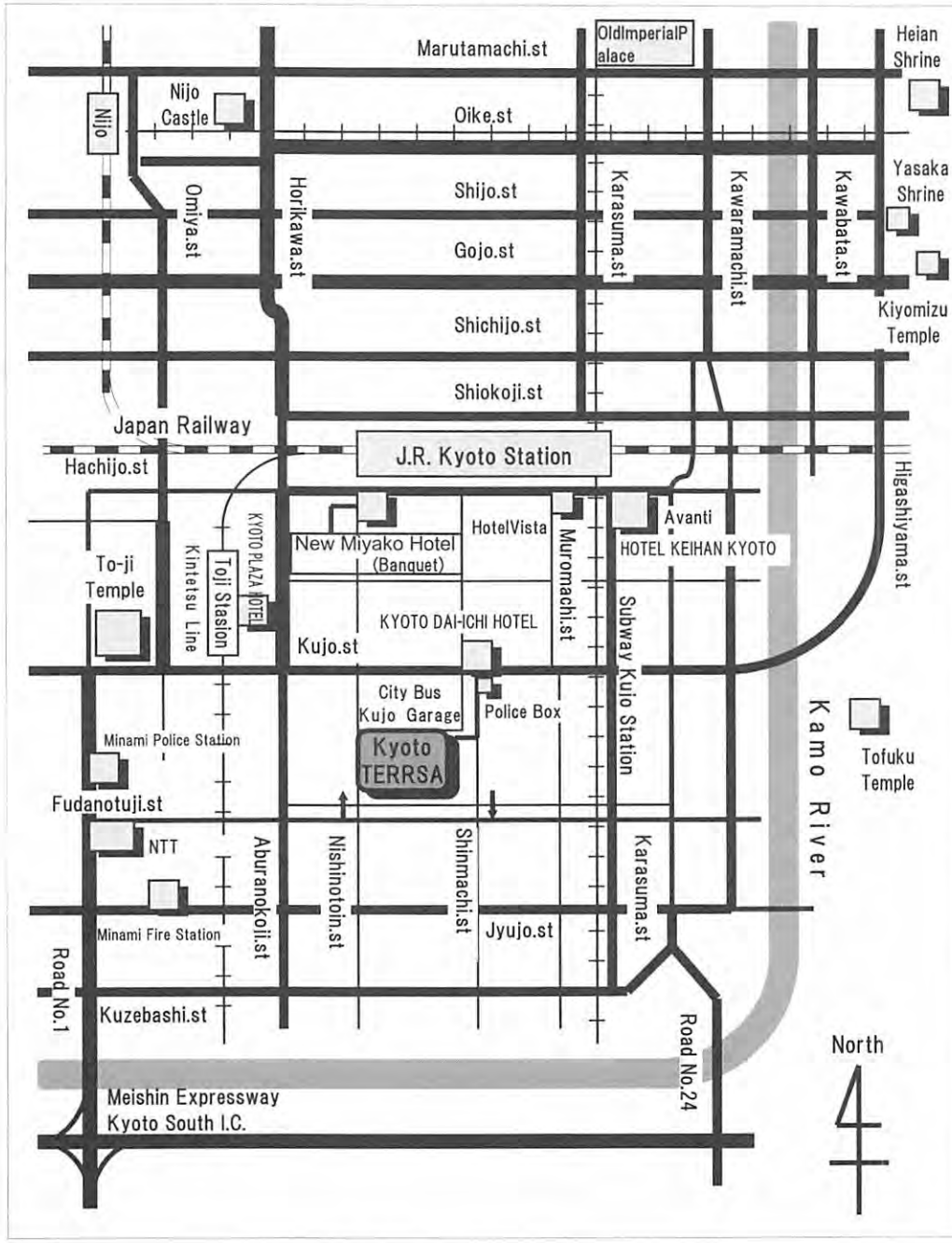

J.R. Kyoto Station Sketch

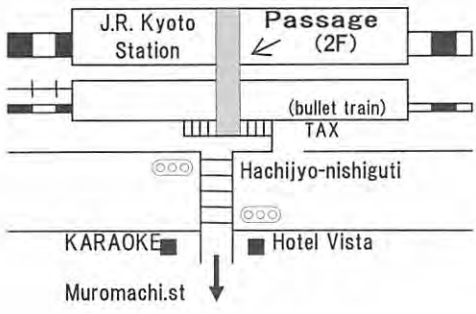

Sightseeing close by

- Toji Temple (10minutes walk)
- Tofukuji Temple (10minutes by Bus)
- Kiyomizu-dera Temple (20minutes by Bus)
- Yasaka Shrine (25minutes by Bus)
- Nijo Castle (30minutes by Subway)
- Heian Shrine (30minutes by Bus)

Kyoto TERRSA Floor Map

3F (East Building)

3-I.J.K.
Conference Room (Large)
- 3-I. Conference Room A
- 3-J. Conference Room B
- 3-K. Conference Room C

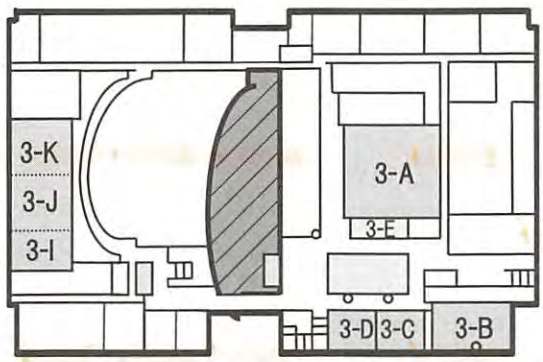

3F (West Building)

- 3-A.Conference Room No.1
- 3-B.Conference Room No.2
- 3-C.Conference Room No.3
- 3-D.Conference Room No.4
- 3-E.Conference Room No.5

2F (East Building)

2-A.B.C.Seminar Room
- 2-A.Seminar room No.1
- 2-B.Seminar room No.2
- 2-C.Seminar room No.3

2-D. Conference Room (Middle)
2-E.A V Study Room
2-F. Study Room
2-G.Cookery Room

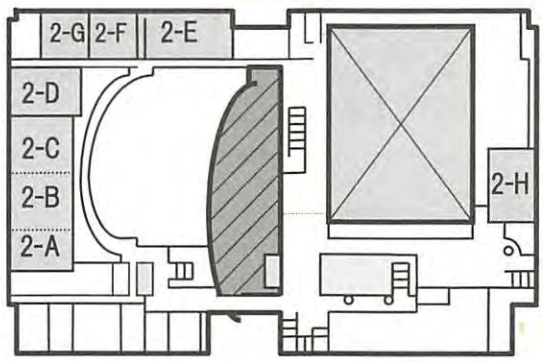

2F (West Building)

2-H.Rehearsal Room

1F (East Building)

Restaurant
"SUZAKU"

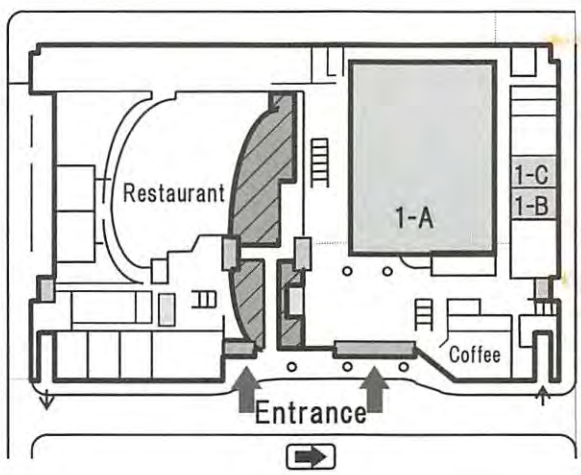

1F (West Building)

1-A.TERRSA Hall

1-B.Waiting Room No.1

1-C.Waiting Room No.2
(Japanese Type)

Coffee Shop
"heart garden"

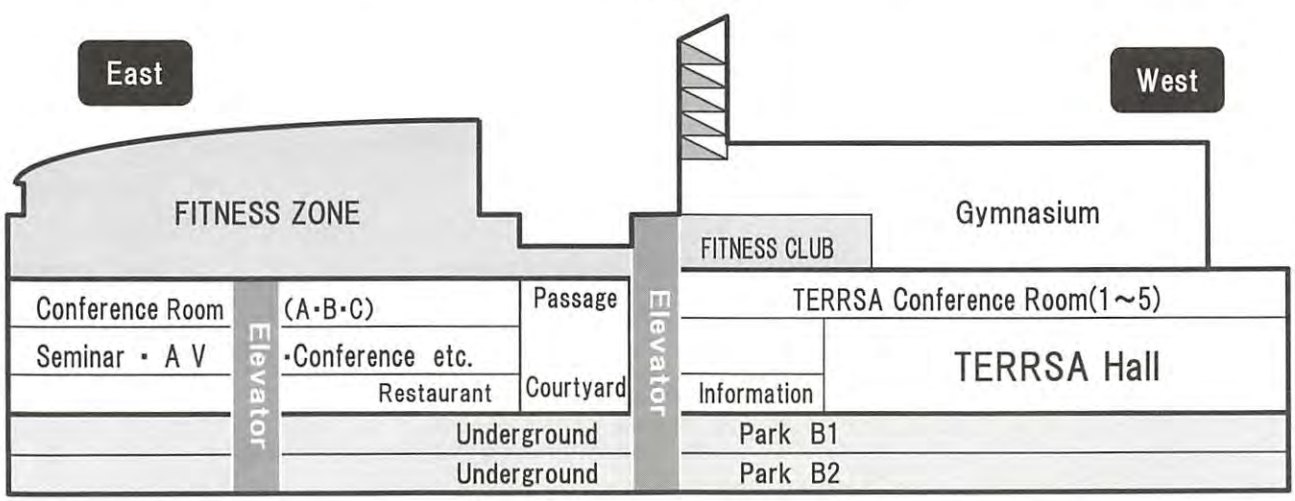

TIME TABLE

time/date	July											
	7 (Sun)	8 (Mon)			9 (Tue)			10 (Wed)		11 (Thu)		12 (Fri)	
Room		1-A	2-A	3-A	1-A	2-A	3-A	1-A	3-A	1-A	3-A	1-A	3-A
9 00		Opening Ceremony			PL02			PL03		PL05		Young Sceintist Session	
10													
20		PL01											
30													
40													
50													
10 00					2BK01	2M01	2CK01	3EI03	3DI01	4CI01	4DK01	5FO09	5JO12
10		Coffee Break										5FO10	5JO13
20					2BO01		2CO01	3EO03	3DO01	4CO07	4DO06	5FO11	5JO14
30		1AK01	1JI01	1FK01	2BO02	2M02	2CO02	3EO04	3DO02	4CO08	4DO07		
40												Coffee Break	
50		1AO01	1JO01	1FO01	Coffee Break			Coffee Break		Coffee Break		5FO12	5JO15
11 00		1AO02	1JO02	1FO02	2BI01	2M03	2EI01	3EK01	3DI02	4CI02	4DI03	5FO13	5JO16
10		1AI01	1JO03	1FI01	2BO03	2M04	2EI02	3EO05	3DO03	4CO09	4DO08	5FO14	5JO17
20			1JO04										
30		1AO03	1JO05	1FO03	2BO04	2M05	2EO01	3EO06	3DO04	4CO10	4DO09	Closing Ceremony	
40		1AO04		1FO04	2BO05	2M06	2EO02	3EO07	3DO05	4CO11	4DO10		
50						2M07							
13 00		Lunch			Lunch			Lunch					
10													
20													
30													
40													
50													
14 00													
10													
20													
30		1AI02	1II01	1GI01	Poster Session I			Poster Session II		Excursion / Lunch			
40													
50		1AO05	1IO01	1GO01									
15 00		1AO06	1IO02	1GI02									
10		1AO07	1IO03										
20	Registration			1GO02									
30		1AO08	1IO04										
40				1GO03									
50		Coffee Break											
16 00		1AO09	1II02	1GI03	2AO13	2JO06	2FO05	3JO08	3CO03				
10		1AO10			2AO14	2JO07	2FO06	3JO09	3CO04				
20			1IO05	1GI04									
30		1AO11			2AO15	2HO01	2FO07	3JO10	3CO05				
40			1IO06										
50		1AO12		1GO04	2AO16	2HO02	2FO08	3JO11	3CO06				
17 00													
10													
20													
30													
40													
50													
18 00													
10								PL04					
20													
30													
40													
50	Reception												
19 00							Public Lectures			Banquet			
10													
20													
30													
40													
50													

1-A Terrsa Hall (1F)
2-A Seminar Room (2-A, B, C) (2F)
3-A Conference Room (3F)
Registration Entrance Lobby (1F)
Reception Restaurant "SUZAKU" (1F)
Banquet New Miyako Hotel

A Ionic Liquids
B Spectroscopy
C High Pressures
D Coordination Chemistry
E Biophysics
F Colloids and Interfaces
G Analytical Chemistry on Liquids and Liquid Interfaces
H Structure and Dynamics of Electrochemical Interfaces
I Thermodynamics and Thermochemistry
J General
M Memorial Session for Professor Kazuyasu Ibuki

PL Plenary Lecture
K Keynote
I Invited Talk
O Oral Presentation

Program

Monday, July 8

9:00	**Opening Ceremony**		*1-A Terrsa Hall*

PLENARY SESSION			*1-A Terrsa Hall*
Chair	Y. Umebayashi		
9:30	PL01	Phase Behaviour of Ionic Liquid/Molecular Liquid Mixture H. Ohno and Y. Kohno	1

10:20 Coffee Break

PARALLEL SESSIONS

A: Ionic Liquids			*1-A Terrsa Hall*
Chair	M. Kanakubo		
10:40	1AK01	Chemistry in Ionic Liquids: Structure, Interactions, Solvation and Electron Transfer E. W. Castner, Jr.	6
11:10	1AO01	Do H-Bonds Explain Strong Ion Aggregation in Ethylammonium Nitrate + Acetonitrile Mixtures? T. Sonnleitner, V. Niktina, A. Nazet, and R. Buchner	31
11:30	1AO02	Dynamics, Solvation and Interionic Interactions in Mixtures of Room Temperature Ionic Liquid and Molecular Solvent: a Multitechnique Approach B. A. Marekha, A. Idrissi, O. N. Kalugin, and M. Bria	32
Chair	T. Takamuku		
11:50	1AI01	The Complex Structure of Ionic Liquids at an Atomistic Level: From "*Red-and-Greens*" to Charge Templates K. Shimizu, C. E. S. Bernardes, and J. N. C. Lopes	7
12:20	1AO03	Structure and Free Energy Analyses of CO_2 Solvation in Room-Temperature Ionic Liquids Y. Umebayashi, H. Doi, M. Kanakubo, T. Makino, K. Fujii, Y. Kameda, and N. Matubayasi	33
12:40	1AO04	Mixing State of Imidazolium-Based Ionic Liquid–Diglyme Solutions Studied by NMR and MD Simulations T. Shimomura, D. Kodama, M. Kanakubo, and S. Tsuzuki	34

J: Genaral			*2-A Seminar Room*
Chair	G. Hefter		
10:40	1JI01	Modeling Solvation of Some Cation-Crown Ether Complexes Using Density Functional Theory H. D. Pranowo, S. Hadisaputra, and R. Armunanto	30
Chair	H. Pranowo		
11:10	1JO01	Hydrophilic and Hydrophobic Hydration of Carboxylate Ions G. Hefter, H. Rahman, and R. Buchner	106
11:30	1JO02	Ethylene Glycol: Liquid Structure and H-bond Network Dynamics from MD Simulations A. Kaiser, O. Ismailova, A. Koskela, S. E. Huber, R. Nazmutdinov, and M. Probst	107
Chair	M. Probost		
11:50	1JO03	Observations of Weak Hydrogen Bonds C–H•••O as Intermolecular Vibration Modes in Solutions by Terahertz Time-Domain Spectroscopy K. Mizuno, T. Kikuchi, K. Murakami, Y. Aoike, K. Fukui, K. Yamamoto, and M. Tani	108
12:10	1JO04	Structure of Hydrogen-Bonded Associates in Primary Alcohols and Their Coordination to Aromatic Segments G. Matisz, A.-M. Kelterer, W. M. F. Fabian, and S. Kunsági-Máté	109
12:30	1JO05	Strength of Water-Water Interaction Depends on Local Environment T. Urbic	110

F: Colloids and Interfaces			*3-A Conference Room*
Chair	H. Matsubara		
10:40	1FK01	Turning Liquids Solid: Why Using Particles in Emulsions Makes All the Difference	22

		L. L. C. Wong, V. O. Ikem, R. Wu, A. Menner, and A. Bismarck	
11:10	1FO01	Interfacial Water over $CaCO_3$ Probed by FM-AFM H. Imada, K. Kimura, and H. Onishi	80
Chair	T. Takiue		
11:30	1FO02	Ultrasonic Relaxation Spectroscopy of SiO_2+Water Nanofluids S. Z. Mirzaev, S. K. Telyaev, and V. Avdievich	81
11:50	1FI01	Molecular Dynamics Study of Lipid Self-Assembly W. Shinoda	23
Chair	H.-J. Moegel		
12:20	1FO03	Surface Freezing of Binary Alcohol Mixtures T. Takiue, M. Tsuura, A. Shuto, H. Matsubara, and M. Aratono	82
12:40	1FO04	The Effect of pH and Counterion Property on the Surface Adsorption of Fe(III)-Edta Complex M. Villeneuve, M. Tanaka, and M. Abe	83

13:00 Lunch

PARALLEL SESSIONS

A: Ionic Liquids ***1-A Terrsa Hall***

Chair	Y. Ouchi		
14:30	1AI02	Solvation Dynamics in Ionic Liquids M. Liang, X.-X. Zhang, D. Roy, N. Ernsting, and M. Maroncelli	8
Chair	R. Kanzaki		
15:00	1AO05	High Pressure Transport Properties of Ionic Liquids K. R. Harris	35
15:20	1AO06	How Mesoscopic Bulk Structures Affect Interfaces of Ionic Liquids? T. Iwahashi, Y. Sakai, D. Kim, T. Ishiyama, A. Morita, and Y. Ouchi	36
15:40	1AO07	Solvation Structure of Poly(Ethylene Glycol) in 1-Ethyl-3-Methylimidazolium-Based Ionic Liquids K. Fujii, H. Asai, Y. Umebayashi, and M. Shibayama	37
16:00	1AO08	Phase Behavior and Dielectric Property of Ionic Liquid $(C_8mim)BF_4$ K. Watanabe, A. Nimonji, and K. Negita	38

I: Thermodynamics and Thermochemistry ***2-A Seminar Room***

Chair	T. Kimura		
14:30	1II01	Determination of Enthalpies of Solution, Limiting Solubilities and Partial Molar Heat Capacities of n-Alcohols in Water and Trehalose Crowded Media G. Bai, S. C. C. Nunes, M. A. A. Rocha, L. M. N. B. F. Santos, M. E. S. Eusébio, M. J. Moreno, and M. Bastos	28
Chair	J-Y. Coxam		
15:00	1IO01	Correlation between Thermodynamic Properties and Orientation Polarization for Binary Mixtures Containing Fluorinated Cyclopentane Y. Sato, H. Ogawa, and T. Minamihounoki	100
15:20	1IO02	Excess Molar Enthalpies of Binary Mixtures of {Water + Poly(Ethylene Glycol)} at T = 298.15 K H. E. Hoga, R. B. Tôrres, T. Kimura, and P. L. O. Volpe	101
Chair	M. Bastos		
15:40	1IO03	Combination of Molecular Simulation and Calorimetric Experiments to Describe Energies of Interaction in {Alkanolamine + Water} Systems M. R. Simond, K. Ballerat-Busserolles, J-Y. Coxam and A. A. H. Pádua	102
16:00	1IO04	Thermodynamics of Three-Phase Equilibrium in Argon Based on a Perfect Solid and a Perfect Liquid (v5) Y. Kataoka and Y. Yamada	103

G:Analytical Chemistry on Liquids and Liquid Interfaces ***3-A Conference Room***

Chair	A. Harata		
14:30	1GI01	Surface Propensity of Carboxylic Acids and Carboxylates and Surface Induced Reactions in the Water-Air Interface	24

		I. Persson, O. Björneholm and N. Ottosson	
Chair	T. Fujiwara		
15:00	1GO01	Ionic Liquid Salt Bridge Enables Accurate Determination of Single Ion Activities in Aqueous Electrolyte Solutions T. Kakiuchi and M. Yamamoto	94
Chair	M. Suwa		
15:20	1GI02	Interfacial Phenomena at Aqueous-Liquid Crystal Interfaces N. L. Abbott	25
Chair	S. Ishizaka		
15:50	1GO02	Anion Effects on Lateral Diffusion of Cationic Rhodamine B at Toluene/Water Interface Measured by Total Internal Reflection-Fluorescence Recovery after Photobleaching N. Shinomori and S. Tsukahara	95
16:10	1GO03	Surface Tension Determination through Measurements of Resonance Oscillation of a Small Surface Using Dielectric Force by a Localized Alternating Current Electric Field S. Tsukahara, T. Tsuruta, and T. Fujiwara	96

16:30 Coffee Break

PARALLEL SESSIONS

A: Ionic Liquids			***1-A Terrsa Hall***
Chair	M. Iida		
16:40	1AO09	Kinetics of Water-Mediated Fluctuations in Room Temperature Ionic Liquid: *N*, *N*-Diethyl-*N*-Methyl-*N*-(2-Methoxyethyl) Ammonium Tetrafluoroborate H. Abe, Y. Imai, M. Aono, H. Kishimura, T. Takekiyo, and Y. Yoshimura	39
17:00	1AO10	Structure and Physicochemical Properties for Solvate Ionic Liquids Composed of Glymes and Na[TFSA] or K[TFSA] T. Mandai, S. Terada, K. Yoshida, S. Tsuzuki, K. Ueno, K. Dokko, and M. Watanabe	40
17:20	1AO11	Solvation Structure of Ni(II) Ion in Imidazolium-Based Ionic Liquid-Molecular Liquid Mixtures H. Hoke, Y. Yamada, T. Shimomura, T. Umecky, and T. Takamuku	41
17:40	1AO12	Ionization Reaction Thermodynamics in Protic Ionic Liquid, Ethylammonium Nitrate R. Kanzaki, Y. Kusamura, X. Song, H. Doi, and Y. Umebayashi	42
I: Thermodynamics and Thermochemistry			***2-A Seminar Room***
Chair	H. Ogawa		
16:40	1II02	Dissolution of Carbon Dioxide in Aqueous Solutions of Amines: Experimental and Thermodynamic Modeling Studies J-Y. Coxam	29
Chair	Y. Kataoka		
17:10	1IO05	Molecular Simulation of Aqueous Electrolyte Solutions via the OEMC Algorithm and Applications W. Smith, F. Moučka, and I. Nezbeda	104
17:30	1IO06	Thermodynamics and Phase Diagrams of Systems with Ester Synthesis Reactions under the Isothermal Conditions M. Toikka, A. Toikka, M. Trofimova, and A. Golikova	105
G:Analytical Chemistry on Liquids and Liquid Interfaces			***3-A Conference Room***
Chair	S. Tsukahara		
16:40	1GI03	Polymer Structure at Water Interface K. Tanaka	26
17:10	1GI04	DNA-Carrying Colloidal Particles for Biosensing M. Maeda	27
Chair	T. Kakiuchi		
17:40	1GO04	*In Situ* Fluorescence Microscope Measurements of Digestion Reactions of Single DNA Molecules by DNase at the Interface of Aqueous Two-Phase System K. Katayama and S. Tsukahara	97

Tuesday, July 9

PLENARY SESSION			*1-A Terrsa Hall*
Chair	M. Aratono		
9:00	PL02	Solutions on Superamphiphobic Layers H.-J. Butt, X. Deng, L. Mammen, P. Papadopoulos, M. Paven, and D. Vollmer	2

PARALLEL SESSIONS			
B: Spectroscopy			*1-A Terrsa Hall*
Chair	K. Ohta		
10:00	2BK01	Time-Resolved IR Spectroscopic Studies of Highly Concentrated Ion Solutions H. Kim, S. Kim, and M. Cho	9
10:30	2BO01	Intermolecular Electron Density Modulations and the Terahertz Spectral Intensities of Liquid Water H. Torii	47
10:50	2BO02	Vibrational Spectral Diffusion and Hydrogen Bond Dynamics of Molecular Solute in Aqueous Solution: *Ab Initio* Molecular Dynamics Study of Formaldehyde and Uracil in Water V. K. Yadav and A. Chandra	48
M: Memorial Session for Professor Kazuyasu Ibuki			*2-A Seminar Room*
Chair	M. Ueno		
10:00	2M01	A Role Played by Kazuyasu Ibuki in Developing Electrolyte Solution Dynamics: Tribute to Him M. Nakahara	123
10:40	2M02	Diffusion and Diffusion Limited Reaction in Supercritical Fluids and Ionic Liquids Y. Kimura	124
C: High Pressures			*3-A Conference Room*
Chair	Y. Yoshimura		
10:00	2CK01	Amorphous Ices, the Glassy States of Water K. Amann-Winkel, P. H. Handle, M. Seidl, T. Loerting, C. Gainaru, H. Nelson, and R. Böhmer	11
10:30	2CO01	Phase Separation of Glassy Dilute LiCl Aqueous Solution and Water Polyamorphism Y. Suzuki and O. Mishima	52
10:50	2CO02	Pressure-Induced Liquid-Liquid Transitions: Search in a Polymer Melt A. Chiba, M. Takenaka, and N. Funamori	53

11:10 Coffee Break

PARALLEL SESSIONS			
B: Spectroscopy			*1-A Terrsa Hall*
Chair	H. Torii		
11:30	2BI01	Dynamics of Water: Fluctuations and Relaxations Revealed by Theoretical Third-order Nonlinear IR spectroscopy S. Saito, T. Yagasaki, and S. Imoto	10
12:00	2BO03	Some Weak Molecular Interactions Affected by the Structure and Composition of the Solvation Shell in Binary Solutions S. Kunsági-Máté	49
12:20	2BO04	Infrared Study of Water Complexes with Inorganic Compounds in KBr Matrix I. I. Grinvald, I. V. Vorotyntsev, I. Y. Kalagaev, E. A. Sutjagina, and A. N. Petukhov	50
12:40	2BO05	Vibrational Dynamics of $[RuCl_5(NO)]^{2-}$ in Aqueous Solution Studied by Nonlinear Infrared Spectroscopy K. Aikawa, K. Ohta, and K. Tominaga	51
M: Memorial Session for Professor Kazuyasu Ibuki			*2-A Seminar Room*
Chair	M. Nakahara		
11:30	2M03	Exploring the Arts and Aqueous Solutions with Kazuyasu Ibuki	125

		P. A. Bopp	
12:00	2M04	Terahertz Dynamics and Structure of Hydrated Protein Studied by X-ray Scattering K. Yoshida and T. Yamaguchi	126
12:20	2M05	Density Effects of the Translational Motion for Monovalent Ions in High-Temperature Liquid Alcohols T. Hoshina, N. Tsuchihashi, K. Ibuki, and M. Ueno	127
12:40	2M06	Temperature and Pressure Effects on the Reorientational Correlation Time of Water in FA- and DMF-Water Mixtures M. Okada, K. Ibuki, and M. Ueno	128
13:00	2M07	S. Ibuki	
E: Biophysics			***3-A Conference Room***
Chair	S. Miura		
11:30	2EI01	Transfer Models for Chemical Protein Denaturation B. Moeser and D. Horinek	19
12:00	2EI02	Shaping the Skin: How Geometry Determines Corneocyte Hydration M. E. Evans and R. Roth	20
12:30	2EO01	Hydration Water Distribution in *Eco*RV-DNA Complex Calculated by Using 3D-RISM R. Motomatsu, A. J. Yasuniwa, Y. Maruyama, N. Yoshida, A. Sarai, F. Hirata, and M. Irisa	73
12:50	2EO02	Molecular Dynamics Study of Lipid Bilayers Modeling the Plasma Membranes of Normal Murine Thymocytes and Leukemic GRSL Cells Y. Andoh, S. Shibayama, S. Okazaki, and R. Ueoka	74

13:10 Lunch

14:30 ***POSTER SESSION I***

PARALLEL SESSIONS			
A: Ionic Liquids			***1-A Terrsa Hall***
Chair	Y. Kimura		
16:40	2AO13	Possibility of Specific Proton Conduction in N-Methylimidazole-Acetic Acid Equimolar Mixture H. Doi, X. Song, K. Fujii, R. Kanzaki, T. Miyazaki, Y. Kameda, and Y. Umebayashi	43
17:00	2AO14	Excess Electron in an Ionic Liquid R. Musat, T. Kondoh, Y. Yoshida, and K. Takahashi	44
17:20	2AO15	Protonation and Copper(II)-Complexation in Protic Ionic Liquids Comprised of *N*-Hexylethylenediaminium Cation M. Iida, S. Takemura, M. Watanabe, and M. Harada	45
17:40	2AO16	Surface Analysis of Ionic Liquids with and without Lithium Salt Using XPS Spectroscopy T. Kurisaki, D. Tanaka, Y. Inoue, H. Wakita, B. Minofar, S. Fukuda, S. Ishiguro, and Y. Umebayashi	46
J: Genaral			***2-A Seminar Room***
Chair	G. Matisz		
16:40	2JO06	Glycerol-Based Solvents for Organic Synthesis A. Wolfson and D. Tavor	111
17:00	2JO07	Reaction Control in Double Electrospray Microreactor A. Wakisaka, M. Tsuchiya, Y. Hyodo, H. Kobara, and T. Ono	112
H: Structure and Dynamics of Electrochemical Interfaces			***2-A Seminar Room***
Chair	T. Yamaguchi		
17:20	2HO01	Microscopic View of Ion Pairing of Alkali Metal Halides in Aqueous Solutions: A Conductivity and Computer Simulation Study J. Gujt, B. H. Lee, and M. Bešter-Rogač	98
17:40	2HO02	Initial Molecular Photocurrent: Nanostructure and Motion of Weakly Bound Charge-Separated State in Organic Photovoltaic Interface Y. Kobori, R. Noji, and S. Tsuganezawa	99
F: Colloids and Interfaces			***3-A Conference Room***

Chair	M. Villeneuve		
16:40	2FO05	Molecular Junction Y.-H. Wang, Y.-L. Chen, M.-L. Guo, and S.-H. Hsu	84
17:00	2FO06	Phase Behaviour and Microstructural Transition of Sucrose Ester-Based Microemulsions S. Kim, W. K. Ng, and R. B. H. Tan	85
17:20	2FO07	Computer Simulation of Self-assembly of Rigid Linear and Facial Surfactant Molecules in Aqueous Solution H.-J. Mögel, M. Wahab, and P. Schiller	86
17:40	2FO08	Free Energy of Solubilization of Solute Molecules in SDS Micelle Solution Studied by Molecular Dynamics Calculations K. Fujimoto, N. Yoshii, and S. Okazaki	87

PUBLIC LECTURES **(市民講座)** ***3-A Conference Room***

These lectures are open for local citiznes and presented in Japanese.

Part 1	Scientific Research on Innovative Areas granted by the Ministry of Education, Culture, Sports, Science, and Technology "ATP Energetics with Emphasis on Water"
18:20～19:00	Nobuyuki Matubayasi (Institute for Chemical Research, Kyoto University) "Energetics of Water and Aqueous Systems"
Part2	Scientific Research on Innovative Areas granted by the Ministry of Education, Culture, Sports, Science, and Technology "Molecular Science of Fluctuations toward Biological Functions"
19:05～19:15	Masahide Terazima (Kyoto University) "Fluctuation Determines Biomolecular Chemical Reactions in Solution"
19:15～20:00	Ryuichi Ueoka (Sojo University) "Membrane-Targeted Nanotherapy with Hybrid Liposomes for Cancer Treatment without Side Effects"

第１部　新学術領域「水を主役としたATPエネルギー変換」	
18:20～19:00	京都大学化学研究所　松林伸幸 「水と水溶液のエネルギー論」
第２部　新学術領域「揺らぎが機能を決める生命分子の科学」	
19:05～19:15	京都大学大学院理学研究科　寺嶋正秀 「ゆらぎが溶液の化学反応を決める」
19:15～20:00	崇城大学大学院生命科学研究科　上岡龍一 「水溶人工細胞膜を用いた副作用の無いがん治療へ」

Wednesday, July 10

PLENARY SESSION ***1-A Terrsa Hall***

Chair	N. Matubayasi		
9:00	PL03	Structure, Fluctuation, and Function of Biomolecules in Solution Explored by Statistical Mechanics of Molecular Liquids F. Hirata	3

PARALLEL SESSIONS

E: Biophysics ***1-A Terrsa Hall***

Chair	M. Irisa		
10:00	3EI03	Hydration Study of Adenosine Phosphates (ATP) and ATP-Driven Proteins by Dielectric Relaxation Spectroscopy M. Suzuki, G. Mogami, A. Imao, T. Wazawa, and N. Morimoto	21
10:30	3EO03	Water Model Tuning To Better Reproduce Rotational Diffusion and NMR Spectral Density of Protein K. Takemura and A. Kitao	75
10:50	3EO04	Theoretical Extraction of Fusion Nanopores Topology and Energetics from Amperometric	76

		Measurements of Vesicular Exocytosis at Ultramicroelectrodes A. Oleinick, F. Lemaitre, M. G. Collignon, I. Svir, and C. Amatore	

D: Coordination Chemistry			*3-A Conference Room*
Chair	A. Odani		
10:00	3DI01	Speciation of Anticancer Ru(II,III) Compounds in Aqueous Solution T. Kiss, T. Jakusch, É. A. Enyedy, É. Sija, C. G. Hartinger and B. K. Keppler	15
10:30	3DO01	Solvation of Alkali Metal Ions by Sulfolane F. Pichierri	63
10:50	3DO02	Characterisation of Metal Complexes for Theragnostic Applications: Some Contribution of Coordination Chemists Z. Baranyai, I. Bányai, E. Brücher, F. Kálmán, G. Tircsó, and I. Tóth	64

11:10 Coffee Break

PARALLEL SESSIONS			
E: Biophysics			*1-A Terrsa Hall*
Chair	R. Akiyama		
11:30	3EK01	Reentrant Condensation, Liquid-Liquid Phase Separation and Crystallization in Protein Solutions Induced by Multivalent Metal Ions F. Zhang, F. Roosen-Runge, A. Sauter, M. Wolf, R. Roth, M. W. A. Skoda, R. M. J. Jacobs, and F. Schreiber	18
12:00	3EO05	Protein Salting out Observed at an Air-Water Interface Y. F. Yano, K. Nitta, and T. Uruga	77
12:20	3EO06	Thermodynamic Measurement of the Structural Fluctuation in the Signaling State of Phototropin Y. Nakasone, K. Zikihara, S. Tokutomi, and M. Terazima	78
12:40	3EO07	The Intermolecular Interaction and Dynamics of Bovine Serum Albumin Solutions. K. Yanase, R. Arai, R. Buchner, and T. Sato	79

D: Coordination Chemistry			*3-A Conference Room*
Chair	M. Hojo		
11:30	3DI02	Kinetic Study on Cyclopalladation in Palladium(II) Complexes Containing an Indole Moiety S. Iwatsuki, T. Suzuki, S. Tanooka, T. Yajima, and Y. Shimazaki	16
12:00	3DO03	Competitive Coordination of Dioxygen and Water to Porphyrin Oxygen Reduction Catalysts A. Trojánek, J. Langmaier, H. Kvapilová, S. Záliš, and Z. Samec	65
12:20	3DO04	Cyanide-Bridged Bimetallic Multidimensional Structures G. Pálinkás, A. Deák, T. Tunyogi, C. Jobbágy, Z. Károly, and P. Baranyai	66
12:40	3DO05	Synthesis, Characterization and Catalytic Activity of Silica Supported Coordination Complexes S. T. David, R. Antony, S. Asha, M. Seethalakshmi, R. B. Bennie, S. D. Abraham, and C. Joel	67

13:10 Lunch

14:30 ***POSTER SESSION II***

PARALLEL SESSIONS			
J: Genaral			*1-A Terrsa Hall*
Chair	T. Urbic		
16:40	3JO08	Tunnel Process Calculation for Molecular Systems Using Ab Initio Path-integral Instanton Method T. Kawatsu and S. Miura	113
17:00	3JO09	A Semigrand, Isothermal-Isochoric Ensemble View of the McMillan-Mayer Solution Theory J. L. Gómez-Estévez	114

Chair	M. Bešter-Rogač		
17:20	3JO10	Statistical Mechanics of Hydration and Ion-Binding in Biologically Relevant Amino Acid Solutions M. Fedotova	115
17:40	3JO11	Effects of Solvent Viscosity on Photoinduced Electron - Transfer Reactions T. Inada, H. Ikeda, and K. Kikuchi	116
C: High Pressures			***3-A Conference Room***
Chair	S. Sawamura		
16:40	3CO03	Molecular Dynamics Study of Aqueous NaCl Solution: Flush Crystallization Caused by Solution Phase Change K. Kobayashi, Y. Liang, and T. Matsuoka	54
17:00	3CO04	Vibrational Spectrum Line Shape for Supercritical Water: Effect of Rotational Couplings on Density, Temperature, and Hydrogen Isotopes Dependencies K. Yoshida, N. Matubayasi, Y. Uosaki, and M. Nakahara	55
17:20	3CO05	Local Structure in Sub and Supercritical Water: IR Spectroscopy and Molecular Dynamic Simulation Analysis F. Lafrad, T. Tassaing, and A. Idrissi	56
17:40	3CO06	Pressure and Temperature Effect on the β-Hairpin Model Peptides: Mutants of GB1 (41-56) K. Tsuchiya, K. Fujimura, and M. Kato	57

PLENARY SESSION			***1-A Terrsa Hall***
Chair	I. Persson		
18:10	PL04	Perspectives for Hybrid Ab Initio/Molecular Mechanical Simulations of Solutions – From Complex Chemistry to Proton Transfer Reactions T. S. Hofer	4

Thursday, July 11

PLENARY SESSION			***1-A Terrsa Hall***
Chair	S. Iwatsuki		
9:00	PL05	Polyacrylate Hydrogels: Construction, Characterization and Applications D.-T. Pham, X. Guo, R. K. Prud'homme, J. Wang, and S. F. Lincoln.	5

PARALLEL SESSIONS			
C: High Pressures			***1-A Terrsa Hall***
Chair	A. Chiba		
10:00	4CI01	Effect of Temperature on Pressure-Induced Freezing and Crystallization of Room Temperature Ionic Liquid: *N*, *N*-Diethyl-*N*-Methyl-N-(2-Methoxyethyl) Ammonium Tetrafluoroborate N. Hamaya and H. Abe	12
10:30	4CO07	Pressure-induced Conformational Change of 1-Butyl-3-Methylimidazolium Tetrafluoroborate M. Shigemi, T. Takekiyo, H. Abe, and Y. Yoshimura	58
10:50	4CO08	Molecular Rotational Relaxation in Room-Temperature Ionic Liquids at High Pressures N. Kometani and A. Tai	59
D: Coordination Chemistry			***3-A Conference Room***
Chair	Y. Shimazaki		
10:00	4DK01	A Size Comparison of the Lanthanoid(III) and Actinoid(III) Ionic Radii D. Lundberg and I. Persson	14
10:30	4DO06	Spectrophotometry Study of Th(IV) Hydroxo Complexes Destruction Kinetics in Aqueous Solution A.V. Radkevich, V. V. Torapava, and V. S. Labko	68
10:50	4DO07	Effect of pH on the Tautomerism of Various *Cyclo*-Imidophosphate Anions H. Maki, D. Kataoka, and M. Mizuhata	69

11:10 Coffee Break

PARALLEL SESSIONS

C: High Pressures *1-A Terrsa Hall*

Chair M. Kanakubo

11:30	4CI02	Solvent Characteristics of Supercritical Carbon Dioxide as a New Materials Design Media and Their Application to the Production of Organic Nanoparticles H. Uchida	13
12:00	4CO09	Complex Coacervation for Composites of ZnO Nanoparticles with a Fluoropolymer by Pressure-Induced Phase Separation of Supercritical Carbon Dioxide Solutions K. Mishima, R. Kawakami, H. Yokota, T. Harada, T. Kato, K. Irie, K. Mishima, and M. Fujiwara	60
12:20	4CO10	NMR Studies on Solution Structures of Methanol and Ethanol Saturated with CO_2 T. Umecky, T. Takamuku, T. Aida, T. Makino, T. Aizawa, and M. Kanakubo	61
12:40	4CO11	Near Infrared Spectroscopic Study of the Melting Point Depression under High-Pressure Carbon Dioxide Y. Takebayashi, K. Sue, Y. Hakuta, T. Furuya, and S. Yoda	62

D: Coordination Chemistry *3-A Conference Room*

Chair D. Lundberg

11:30	4DI03	One-Electron Oxidized Cu(II)-Salen Type Complexes; Relationship between Electronic Structure and Reactivity Y. Shimazaki	17
12:00	4DO08	Conductometric and UV-Visible Spectroscopic Studies on the Strong Association between Poly-Sulfonic or Carboxylic Acids and Their Conjugate Anions in Acetonitrile M. Hojo, K. Zei, and Z. Chen	70
12:20	4DO09	Uranyl-Halide Complexation in *N,N*-Dimethylformamide: Halide Coordination Trend Manifests Hardness of $[UO_2]^{2+}$ K. Takao, S. Takao, Y. Ikeda, G. Bernhard, and C. Hennig	71
12:40	4DO10	Complexation and Structural Studies on Trivalent Lanthanides with Dioxaoctanediamide (DOODA) S. Okumura, T. Tsukahara, and Y. Ikeda	72

13:10 Lunch/Excursion

18:00 Banquet *New Miyako Hotel*

Friday, July 12

9:00 *YOUNG SCIENTIST SESSION*

PARALLEL SESSIONS

F: Colloids and Interfaces *1-A Terrsa Hall*

Chair M. Takezaki

10:00	5FO09	Motions and Fluctuations of Phospholipid Molecules in Large and Cell Sized Vesicles by NMR E. Okamura, Y. Takechi, H. Saito, and N. Yoshii	88
10:20	5FO10	Re-entrant Lamellar/Onion Transition under Shear Flow in a Nonionic Surfactant/Water System D. Sato, Y. Kawabata, and T. Kato	89
10:40	5FO11	Gel-like Behaviors in a Mixture of Water / Organic Solvent / Antagonistic Salt Induced by Flow K. Sadakane, M. Shibayama, M. Takeda, R. Inoue, and H. Seto	90

J: Genaral *3-A Conference Room*

Chair K. Ishihara

10:00	5JO12	Accurate pH Determination of Acidic Solutions on the Basis of an Ionic Liquid Salt Bridge M. Shibata, M. Kato, Y. Iwamoto, S. Nomura, and T. Kakiuchi	117
10:20	5JO13	Quality Assurance Method for Simultaneous Determining of Polychlorinated Biphenyls (PCBs) and Organo-Chlorinated Pesticides (OCPs) Using Pressurized Liquid Extraction M. I. H. Helaleh and A. Al-Rashdan	118
10:40	5JO14	Gas Chromatography Ion Trap Mass Spectrometry for the Determination of Nitro Derivatives Compounds in Environmental Soil Samples A. Al-Rashdan and M. I. H. Helaleh	119

11:10 Coffee Break

PARALLEL SESSIONS			
F: Colloids and Interfaces			***1-A Terrsa Hall***
Chair	T. Kato		
11:20	5FO12	Fluorescence Quenching of Pyrenesulfonate by Anthoraquinonesulfonate on DDACl Aggregate Surfaces M. Takezaki, T. Izumi, S. Kitamura, and T. Tominaga	91
11:40	5FO13	Coating of Magnetite with Mercapto Modified Silica in a One-Pot Process Nuryono, N. M. Rosiati, A. H. Suhendi, S. C. W. Sakti, and S. Tanaka	92
12:00	5FO14	Relationship between Particle Charges and Coalescence Stability of Pickering Oil-in-Water Emulsions Prepared Using Microchannel Emulsification R. Murakami, T. Iwahashi, Y. Fujimoto, and M. Yamamoto	93
J: Genaral			***3-A Conference Room***
Chair	M. I. H. Helaleh		
11:20	5JO15	Adsorption of Silver(I) and Zinc(II) Ions from the Solution Using Blended Adsorbent of Dithizone-Natural Zeolite Mudasir, L. Rintinga, and B. Rusdiarso	120
11:40	5JO16	Red Ginger Rhizome Extract (*Zingiber Officinale Linn.Var Rubrum*) as an Deodorant Herbal Making Materials I. N. Fitriani, R. N. Amelia, and A. R. Puspitasari	121
12:00	5JO17	Reducing Resistance to Carbon Droplets Polarography M. Syauqillah and T. Herviyansyah	122

12:30 Closing Ceremony ***1-A Terrsa Hall***

A: Ionic Liquids

B:Spectroscopy

POSTER SESSION II ***1-A Terrsa Hall***

A: Ionic Liquids

Invitation to submit to the special issue in Journal of Solution Chemistry

All contributors, of both oral and poster presentations, to the 33ICSC are cordially invited to submit these for inclusion in the special conference issue of the Journal of Solution Chemistry Please, note that all submissions will be peer reviewed. The submission deadline is Sun. 24th November for publication in the special conference issue, which will be published in February or March in 2014.

Contributors who would like to submit their manuscript should consult the **Instructions for Authors** of the journal before submission (these are available at: (http://www.springer.com/chemistry/physical+chemistry/journal/10953).

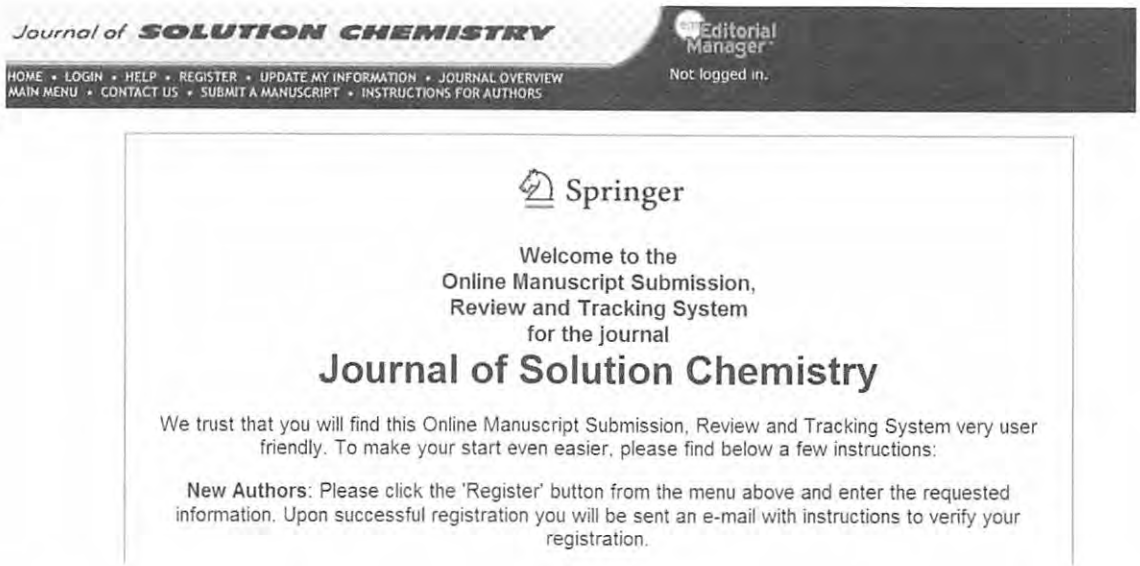

Online submission of manuscripts should be made through the journal's web-site (http://www.editorialmanager.com/josl/). Before submission, contributors who have not previously submitted to the journal should register to obtain their ID and set up their password. Please find the **REGISTER** link at an upper left side of the web page (see screen shot above).

It should be noted that, at the initial step of submission, the contributors must choose the special issue (S.I.:ICSC33) as Choose Article Type (see screen shot below) to ensure that their paper is included in the special conference issue.

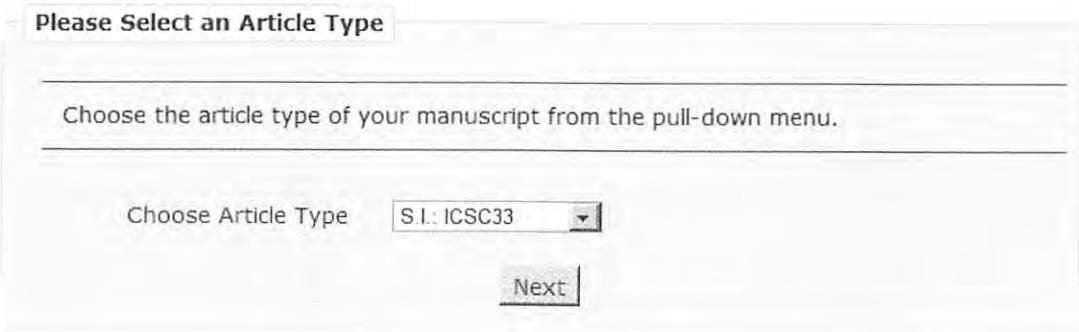

Plenary Lectures

PL01 Phase behaviour of ionic liquid/molecular liquid mixture

Hiroyuki Ohno[1,2] and Yuki Kohno[1,2]

[1]*Department of Biotechnology, Tokyo University of Agriculture and Technology, Koganei, Tokyo 184-8588 Japan*

[2]*Functional Ionic Liquid Laboratories (FILL), Graduate School of Engineering, Tokyo University of Agriculture and Technology, Koganei, Tokyo 184-8588 Japan*

e-mail : ohnoh@cc.tuat.ac.jp

There are many studies on the physico-chemical analyses of mixture of ionic liquids (ILs) and molecular liquids. Water is a typical molecular liquid and the number of studies on them is increasing. Since ILs are salts, they show high affinity with water. Apart from inorganic salts, it is easy to control hydrophilicity of ILs. Some ILs turned insoluble in water by increasing hydrophobicity of the component ions. There are many hydrophobic ILs known to show a clear phase separation with water. These clear phase separations are static and their separated phases are stable against outer stimuli. The phase separated IL/water mixture is interesting from the viewpoint of physical chemistry, and it also has industrial relevance. Unlike this static phase separation, dynamic phase change of IL/water mixtures between homogeneously mixed solution and separated phases has a wide variety of applications when the phase change was controlled by outer stimuli such as temperature. The miscibility of ILs with water generally increases upon heating, but a few ILs undergo a lower critical solution temperature (LCST)-type phase transition with water. As the phase transition can be controlled by changing the temperature for only a few degrees, the LCST-type phase response of IL/water mixture should be of great interest for solution chemists. Based on the physico-chemical analysis of many ILs having different hydrophobicity, we have found that there is a particular range of "hydrophobicity" of ILs to show the LCST-type phase transition. By increasing hydrophobicity of hydrophilic ILs, they turned immiscible with water. The point is that some ILs show the LCST-type phase transition with water only when these ILs have moderate hydrophobicity. The number of water molecules per ion pair of many ILs with different hydrophobicity was determined. When the hydrophobic IL has this value larger than seven, they show the LCST-type phase change with water. The number "**7**" seems to be a magic number of IL/water mixture because a few properties of hydrated ILs have been changed drastically around this water content.

Some applications of the LCST-type phase change of IL/water mixtures such as separation of water-soluble proteins as well as future aspect will also be mentioned at the lecture.

PL02 Solutions on Superamphiphobic Layers

H.-J. Butt, X. Deng, L. Mammen, P. Papadopoulos, M. Paven, D. Vollmer

Max Planck Institute for Polymer Research, Ackermannweg 10, 55128 Mainz, Germany

e-mail: butt@mpip-mainz.mpg.de

Superamphiphobic surfaces repel not only water but also nonpolar liquids and surfactant solutions. These liquids form contact angles greater than 150° and show low contact angle hysteresis. Tilting a superamphiphobic surface by a few degrees is already sufficient for a drop to overcome adhesion and to roll off. For applications, superamphiphobic layers need to be made in a self-assembled process. A simple method to fabricate transparent superamphiphobic layers will be described [1]. The optimal design of superamphiphobic layers will be discussed [2]. This leads to criteria of how to optimize such layers for a particular application. The considerations are based on stability criteria valid in the static case. For highly dynamic liquids additional effects are important. Therefore we carried out drop impact experiments. Possible applications of on superamphiphobic layers, such as solvent free chemistry and gas exchange membranes, will be discussed.

A drop deposited or impacting on a superamphiphobic surface rolls off easily, leaving the surface dry and clean. This remarkable property is due to a surface structure which favors the entrainment of air cushions beneath the drop, leading to the so called Cassie state. The Cassie state competes with the Wenzel (impaled) state, where the liquid fully wets the substrate. To utilize superamphiphobicity, impalement of the drop into the surface structure needs to be prevented. In order to understand the underlying processes we went one step back and studied the impalement dynamics of water into superhydrophobic surface in three dimensions by confocal microscopy [3]. While the drop evaporates from a pillar array, its rim recedes via step-wise depinning from the edge of the pillars [4]. Before depinning, finger-like necks form due to adhesion of the drop at the pillar's circumference. Once the pressure becomes too high, or the drop too small, the drop slowly impales the texture. The thickness of the air cushion decreases gradually. As soon as the water-air interface touches the substrate, complete wetting proceeds within milliseconds. This visualization of the impalement dynamics will facilitate the development and characterization of superhydrophobic surfaces.

References

[1] X. Deng, L. Mammen, H.-J. Butt & D. Vollmer, *Science* **335**, 67 (2012).

[2] H.-J. Butt et al., *Soft Matter* **9**, 418 (2013).

[3] P. Papadopoulos et al., *Langmuir* **28**, 8392 (2012).

[4] P. Papadopoulos et al., *Proc. Natl. Acad. Sci.* **110**, 3254 (2013).

PL03

Structure, Fluctuation, and Function of Biomolecules in Solution Explored by Statistical Mechanics of Molecular Liquids

F. Hirata

College of Life Science, Ritsumeikan University, Kusatsu, Shiga 525-8577, Japan

e-mail : hirataf@fc.ritsumei

There are two physicochemical processes which are essential for living bodies to maintain their life: "self-organization" and "molecular recognition." Protein folding and formation of cell-membrane are typical examples of the former process, in which biomolecules have to overcome the entropy barrier to organize themselves into some characteristic structure. It is well documented that a protein can perform its own function only when it takes such characteristic structure, or its native conformation. On the other hand, a molecular recognition process concerns whenever a biomolecule performs its function as a "molecular-machine." For examples, in order for the enzymatic reaction to occur, substrate molecules should be accommodated first by the protein in its reaction pocket to form so-called an enzyme–substrate (ES) complex. In order for hemoglobin to transport oxygen from lung to other organs, it has first to bind oxygen molecules in its heme-pocket.

The two processes may not proceed spontaneously if biomolecules and ligand molecules are exisiting by themselves in "vacuum," because those are not in favor with respect to entropy. For instance, the protein folding is a process in which a protein folds into a native conformation, the state of least entropy, from the random coil, the state of largest entropy. Then, why do those processes occur spontaneously in our body? It is because there is always "aqueous solution" in the real environment of a living body. It is water that help the biomolecules to do their own job.

We have been developing a statistical mechanics theory called "3D-RISM/RISM" for past few decades, which has proven itself to be capable of handling such processes stated above in biosystems. [1] The latest development of the theory has brought the structural fluctuation of biomlecules within scope of the science, which plays a crucial role in any biological activities. [2]

In the talk, I will provide a brief review of our study on biomolecular processes in solution based on the 3D-RISM/RISM theory, and address the new holizon in the statistical mechanics of solution.

References

[1] N. Yoshida, T. Imai, S. Phongphanphanee, A. Kovalenko, F. Hirata, *J. Phys. Chem.*B, 113, 873 (2009).

[2] B. Kim and F. Hirata, *J. Chem. Phys.*, **138**, 054108 (2013)

PL04 Perspectives for Hybrid Ab Initio/Molecular Mechanical Simulations of Solutions – From Complex Chemistry to Proton Transfer Reactions

T. S. Hofer

Theoretical Chemistry Division, Institute of General, Inorganic and Theoretical Chemsitry,University of Innsbruck, Innrain 80-82, A-6020 Innsbruck, Austria
e-mail : t.hofer@uibk.ac.at

As a consequence of the ongoing development of enhanced computational resources, theoretical chemistry has become an increasingly valuable field for investigations of a variety of chemical systems. This is particularly true for computational investigations of liquids, which are the most important but also the most challenging state of matter in chemistry.

Simulations employing a hybrid quantum mechanical/molecular mechanical (QM/MM) molecular dynamics (MD) technique have been shown to be a particular promising approach. In these methods the chemical most relevant part is treated with a suitable quantum mechanical technique, while empirical molecular mechanical potentials are considered to be sufficiently accurate to describe the remaining part of the system. Simulations of this type are particularly useful whenever ultrafast (i.e. picosecond) dynamical properties are to be studied, which are in many cases difficult to access via experimental techniques.

Details of the quantum mechanical charge field (QMCF) ansatz, an advanced QM/MM protocol, are discussed and simulation results for various systems ranging from solvated organic molecules and coordination complexes in solution will be presented.

A particularly challenging application is the description of proton transfer reactions in chemical simulations, which is a prerequisite to study acidified and basic systems. The combination of the QMCF methodology with a dissociative potential for the description of the solvent will presented. The results of a simulation study of a Lewis acid in solution will demonstrate the capabilities of this approach.

Acknowledgments: *This work was supported by the Austrian Ministry of Science BMWF Uni-Infrastrukturprogramm* as part of the Research Focal Point Scientific Computing at the University of Innsbruck. Financial support by the Austrian Science Fund (FWF) is gratefully acknowledged.

PL05 Polyacrylate Hydrogels: Construction, Characterization and Applications

D.-T. Pham[1], X. Guo[2], R. K. Prud'homme[3], J. Wang[2], and S. F. Lincoln.[1]
[1]*School of Chemistry and Physics, University of Adelaide, Adelaide SA 5005, Australia*
[2]*State Key Laboratory of Chemical Engineering, East China University of Science and Technology, Shanghai 200237, China*
[3]*Department of Chemical Engineering, Princeton University, Princeton, NJ 08544, USA*
e-mail: stephen.lincoln@adelaide.edu.au

Hydrogels are visco-elastic solids consisting dominantly of water compartmentalized by polymeric networks. Such hydrogels may be constructed from polyacrylates randomly substituted with hydrophobic substituents which aggregate in aqueous solution to form inter-strand cross-links in hydrogels with varying degrees of viscosity and elasticity depending on the nature of the hydrophobic substituents and the extent of their substitution on the polyacrylate backbone [1]. The range of hydrogels may be extended by introducing a second polyacrylate randomly substituted with α-, β- and γ-cyclodextrins (homochiral cyclic oligomers of 6-8 α-1,4- linked D-glucopyranose units, respectively) which complex the hydrophobic substituents of the first polyacrylate to form inter-strand cross-links in hydrogels [2]. A further variation arises when two or three cyclodextrins are linked together in small molecular entities which can act as di- and tritopic receptors for the hydrophobic substituents of a polyacrylate to form hydrogels [3]. Small molecular species such as dyes and drugs may be incorporated into such polyacrylate hydrogels and potentially have applications in controlled release of such species from the hydrogel.

To gain a good understanding of the interactions between the substituted polyacrylates and the substituted polyacrylates smaller molecular species with which they interact, studies are conducted over a range of concentrations ranging from very dilute where solutions a free flowing through to concentrations at which hydrogels form. This entails the use of a range of investigative techniques including ultraviolet-visible spectroscopy, fluorimetry, ^{1}H NMR spectroscopy, dynamic light-scattering, isothermal titration calorimetry and rheology.

References

[1] X. Guo, A. A. Abdala, B. L. May, S. F. Lincoln, S. A. Khan and R. K. Prud'homme, *Polymer* **47**, 2976 (2006).

[2] L. Li, X. Guo, J. Wang, P. Liu, R. K. Prud'homme, B. L. May, S. F. Lincoln, *Macromolecules* **41**, 8677 (2008).

[3] H.-T. Nguyen, D.-T. Pham, S. F. Lincoln, J. Wang, X. Guo, C. J. Easton, R. K. Prud'homme, *Polymer Chem.* **3**, 820 (2013)

Invited Presentations

1AK01 Chemistry in Ionic Liquids: Structure, Interactions, Solvation and Electron Transfer

Edward W. Castner, Jr.[1]

[1]*Department of Chemistry and Chemical Biology, Rutgers, The State University of New Jersey, Piscataway, NJ, 08854 U.S.A.*

e-mail : ed.castner@rutgers.edu

Ionic liquids (ILs) are finding a myriad of uses ranging from energy applications such as batteries and solar photoelectrochemical cells; drug delivery, and solubilization and conversion of biomass. Relative to water and organic solvents, ILs have many unique properties and thus affect chemical reactions in different ways. The higher viscosities of ILs are partly responsible for the observed heterogeneities in chemical reaction rates and solvation dynamics.[1-2] In common with molten salts, ILs have significant charge-ordering and adjacency correlations, but unlike molten salts, there is often a unique signature of intermediate range ordering observed in both molecular simulations and X-ray[3] and neutron scattering experiments.

I will present some of our most recent work on extending our growing understanding of ionic liquid structure, interactions and solvation dynamics. Our goal is to move beyond the properties of the bulk liquid to try to understand how the presence of a solute changes the local structure and interactions between ions. Our perspective is informed by careful analysis of X-ray and 2D-NMR nuclear Overhauser effect (NOE) experiments coupled with a theoretical analysis of molecular simulations done by our collaborators in the group of Prof. C. J. Margulis. Recently we have uncovered the reasons why the structures of ILs with ether-substituted cations are significantly different than the isoelectronic homologs with apolar alkyl-substituted cations.[4] How these properties affect reaction rates in ionic liquids will be discussed, focusing on intramolecular and bimolecular photo-induced electron-transfer reactions. Finally, a brief discussion of some novel reactive ionic liquids will be presented.

References

[1] E. W. Castner, Jr. and J. F. Wishart, *J. Chem. Phys.* **132**, 120901 (2010).

[2] E. W. Castner, Jr., C. J. Margulis, M. Maroncelli, and J. F. Wishart, *Annu. Rev. Phys. Chem.* **62**, 85 (2011).

[3] C. S. Santos, N. S. Murthy, G. A. Baker, E. W. Castner, Jr., *J. Chem. Phys.* **134**, 121101 (2011); H. K. Kashyap, C. S. Santos, H. V. R. Annapureddy, N. S. Murthy, C. J. Margulis and E. W. Castner, Jr., *Faraday Disc.* **154**, 133 (2012).

[4] H. K. Kashyap, C. S. Santos, R. P. Daly, J. J. Hettige, N. S. Murthy, H. Shirota, E. W. Castner, Jr. and C. J. Margulis, *J. Phys. Chem. B*, **117**, 1130 (2013); A. Triolo, O. Russina, R. Caminiti, H. Shirota, H. Y. Lee, C. S. Santos, N. S. Murthy, and E. W. Castner, Jr., *Chem. Commun.*, **48**, 4103 (2012).

[5] H. Y. Lee, J. B. Issa, S. S. Isied, E. W. Castner, Jr., Y. Pan, C. L. Hussey, K. S. Lee and J. F. Wishart, *J. Phys. Chem.* C, **116**, 5197 (2012).

1AI01 The Complex Structure of Ionic Liquids at an Atomistic Level: From "*Red-and-Greens*" to Charge Templates.

Karina Shimizu, Carlos E. S. Bernardes, José N. Canongia Lopes

Centro de Química Estrutural, Instituto Superior Técnico, 1049 001 Lisboa, Portugal
Instituto de Tecnologia Química e Biológica, Universidade Nova de Lisboa, 2780 901 Oeiras, Portugal
e-mail : jnlopes@ist.utl.pt

Any substance that is composed exclusively of anions and cations (a salt) must possess some kind of short-to-intermediate range organization in order to fulfill local electro-neutrality conditions. In the case of Ionic Liquids (ILs) such imposed short-range ordering does not lead, however, to long-range structures (crystalline forms) at room temperature. This unexpected fact is the defining characteristic of this amazing and complex class of compounds. The difficulty of forming stable crystalline structures in ionic liquids is associated in most cases with the size, asymmetry, charge dispersion, charge segregation and flexibility of the molecular ions that compose the ionic liquids. The presence of low charge density residues such as alkyl-side chains is often a controlling issue.

Taking all these facts into consideration it is not surprising that ionic liquids are presently regarded as meso-structured, nanosegregated fluids: if the ionic liquid has to order its polar parts into local structures that obey electro-neutrality conditions, then its non-polar parts must be segregated elsewhere. It is this interplay between the two types of regions/interactions (polar versus non-polar, long-range versus short-range) that eventually leads to the formation of nano-scale domains and the recognition of ionic liquids as polar networks permeated by non-polar regions.[1,2]

In this contribution we will show several examples of such interplay and illustrate the enormous variety of structural effects that can emerge when the nature of the ionic liquids or of their mixtures with molecular compounds is changed. We will explore the meso-structures that can be found in ionic liquids ranging from the original "red-and-green" representations, the interactions of ionic liquids with molecular species or solid substrates (ILs as charge templates), or the influence of the ubiquitous alkyl side chains (per-fluorinated, functionalized, symmetrical) in the morphology of the resulting structures.

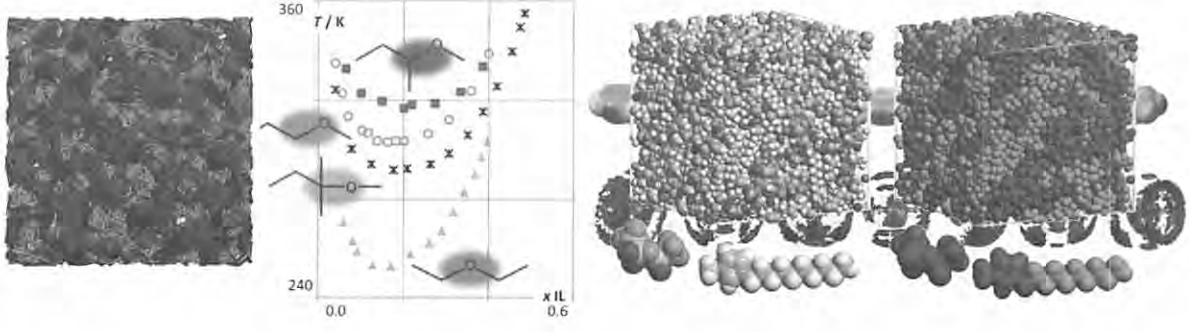

References

[1] J. Mol. Structure: TheoChem. **946**, 70(2010).

[2] Faraday Discus. **154**, 155(2012).

1AI02 Solvation Dynamics in Ionic Liquids

Min Liang[1], Xin-Xing Zhang[2,3], Durba Roy[1], Niko Ernsting[3], and Mark Maroncelli[1]

[1]*Department of Chemistry, Penn State, University Park, PA, U.S.A.*
[2]*Department of Chemistry, College of Physical Science, Nankai University, Tianjin, China* [3]
[3]*Department of Chemistry Humboldt Universität zu Berlin, Germany*

e-mail : maroncelli@psu.edu

Solvation dynamics, the response of a medium to electrical solute perturbations, is an important characteristic of polar liquids and directly tied how a solvent influences charge transfer processes. We have recently completed benchmark measurements of the complete (fs-ns) solvation response to the probe coumarin 153 in a representative collection of 21 ionic liquids.[1,2] These results confirm the presence of significant inertial dynamics taking place on the sub-picosecond time scale together with a broadly distributed structural component acting over the range 1 ps – 10 ns. Comparison to emerging dielectric measurements allow for definitive tests of dielectric continuum models of solvation. It is clear from these tests that solvation and dielectric relaxation involve closely related molecular dynamics, but the connection offered by simple continuum models underestimates solvation times by factors of at least 2-4. Simple continuum models also suggest that integral solvation times should be inversely proportional to the static conductivity of an ionic liquid.[3,4] Experimental data on 34 ionic liquids confirms the strong correlation between solvation times and inverse conductivity, albeit with a proportionality constant different by a factor of 2.4 from the continuum model prediction.[4] Computer simulations [1,5] provide insight into the relationship between solvation and dielectric response as well as mechanistic insights into the ion motions responsible for solvation. Whereas the sub-picosecond inertial dynamics entail easy-to-characterize translational motions of nearby ions, the structural relaxation responsible for the ps-ns dynamics is quite subtle, involving small amplitude motions of ions imperceptibly different from random molecular motion.

References

[1] M. Maroncelli, X.-X. Zhang, M. Liang, D. Roy, and N. P. Ernsting, *Faraday Discuss.* **154**, 409 (2012).

[2] X.-X. Zhang, M. Liang, N. P. Ernsting, and M. Maroncelli, *J. Phys. Chem. B*, DOI: 10.1021/jp305430a.

[3] X.-X. Zhang, C. Schröder, and N. P. Ernsting, *J. Chem. Phys.* **138**, 111102 (2013).

[4] X.-X. Zhang, M. Liang, N. P. Ernsting, and M. Maroncelli, *J. Phys. Chem. Lett.* **4**, 1205 (2013).

[5] D. Roy and M. Maroncelli, J. Phys. Chem. B 116, 5951 (2012).

2BK01 Time-Resolved IR Spectroscopic Studies of Highly Concentrated Ion Solutions

H. Kim[1], S. Kim[2], and M. Cho[1,2]

[1]*Department of Chemistry, Korea University, Seoul 136-713, Korea*

[2]*Multidimensional Spectroscopy Laboratory, Korea Basic Science Institute, Seoul 136-713, Korea*

e-mail : mcho@korea.ac.kr

Water structure ad dynamics are strongly affected by the presence of ions. One of the specific ion effects is known as the Hofmeister effect on protein stability. Depending on the chaotropic or kosmotropic nature of ions in aqueous protein solutions, the stability of tertiary structure of protein is affected by either making the hydrogen-bond network structure change or forming direct electrostatic interaction of ions with proteins [1]. One of the well-known and widely used denaturizing agents is thiocyanate. We first studied the ion pair formation dynamics of thiocyanate with lithium cation in aprotic solvents using two-dimensional IR spectroscopy of thiocyanate CN stretch mode [2,3]. The ion pair formation and dissociation time constants are on the order of a hundred picoseconds. To study thiocyanate vibrational dynamics in liquid water, we carried out a series of IR pump-probe studies of thiocyanate in highly concentrated aqueous solutions. To avoid self-attenuation problem in femtosecond IR pump-probe measurements, we focused on the vibrational dynamics of ^{13}C-labeled thiocyanate whose frequency is shifted towards low frequency region, while the total concentration of thiocyanate is controlled by adding unlabeled thiocyanate to the solution [4]. Analysing the population and rotational relaxations of thiocyanate ion in water, we found that the ions tend to form large ion aggregates at a high concentration. To elucidate possible ion-aggregation effects on water dynamics, the IR pump-probe studies of OD stretch mode of HOD in water were performed with varying potassium thiocyanate concentration. Using two-component analyses of the experimentally measured dispersed IR pump-probe spectra, we could separate the pump-probe spectrum of HOD molecules in bulk-like water and that of those interacting with thiocyanate ions. Since the two OD stretch modes have sufficiently different frequencies, it was possible to extract quantitative information on their rotational times and peak frequency shifts for varying ion concentration. The nonlinear dependence of the OD stretch frequency indicates that there is a critical concentration separating free ion phase and ion aggregate phase.

References

[1] H. Kim, H. Lee, G. Lee, H. Kim, and M. Cho, *J. Chem. Phys.* **136**, 124501 (2012).

[2] K.-H. Park, S. R. Choi, J.-H. Choi, S. Park, M. Cho, *ChemPhysChem.* **11**, 3632(2010).

[3] K.-K. Lee, K.-H. Park, D. Kwon, J.-H. Choi, H. Son, S. Park, and M. Cho, *J. Chem. Phys.* **134**, 064506(2011).

[4] H. Kim, S. Park, and M. Cho, *Phys. Chem. Chem. Phys.* **14**, 6233 (2012).

2BI01 Dynamics of Water: Fluctuations and Relaxations Revealed by Theoretical Third-order Nonlinear IR spectroscopy

S. Saito[1,2], T. Yagasaki[1,3], and S. Imoto[2]

[1]*Institute for Molecular Science, Okazaki, Aichi 444-8585, Japan*

[2]*The Graduate University of Advanced Studies, Okazaki 444-8585, Japan*

[3]*Present Address: Okayama University*

e-mail: shinji@ims.ac.jp

Water is the most abundant liquids on Earth, and also one of the most interesting liquids in physics and chemistry. Various experimental and theoretical studies have been conducted to elucidate the structure and dynamics of water. Now, it is known that the dynamics of water is characterized as HB network fluctuating with a wide range of time scales from tens fs to several ps. It is also known that the vibrational spectra are sensitive to HB environment. However, information obtained from linear spectroscopy is limited and, thus, we cannot examine the detailed dynamics. In contrast, third-order nonlinear IR experiments, for example two-dimensional IR spectra and pump-probe signals, are powerful tools to get information on fluctuations and relaxation dynamics that is not evident from the linear IR spectrum.

We examined the inter- and intra-molecular dynamics of liquid water in terms of third-order nonlinear IR spectroscopy by calculating third-order response function with non-equilibrium simulations.[1-3]. It has experimentally been known that the OH stretch shows the fast frequency fluctuation. We found, however, that the frequency fluctuation of the HOH bend is much faster than that of the OH stretch and that the libration motion also shows the fast frequency. We discuss the molecular origins of the fast frequency fluctuations of these motions. In addition to the frequency fluctuation, we analyzed the inter- and intra-molecular energy relaxation processes in liquid water by calculating the pump-probe signals and a newly developed method for the energy relaxation processes.[4,5] In particular, the newly developed method revealed the detailed energy relaxation processes and the involved structural changes. The detailed molecular mechanisms of the energy relaxation will also be discussed.

References

[1] T. Yagasaki and S. Saito, *J. Chem. Phys.* **128**, 154521 (2008), *Acc. Chem. Res.*, **42**, 1250 (2009), *Annu. Rev. Phys. Chem.*, DOI: 10.1146/annurev-physchem-040412-110150 (2013).

[2] T. Yagasaki, J. Ono, and S. Saito, *J. Chem. Phys.* **131**, 164511 (2009).

[3] S. Imoto, S. S. Xantheus, S. Saito, to be submitted.

[3] T. Yagasaki and S. Saito, *J. Chem. Phys.*, **134**, 184503 (2011).

[4] T. Yagasaki and S. Saito, *J. Chem. Phys.*, **135**, 244511 (2011).

2CK01 Amorphous ices, the glassy states of water

K. Amann-Winkel[1], P.H. Handle[1], M. Seidl[1], T. Loerting[1]
C. Gainaru[2], H. Nelson[2], R. Böhmer[2]

[1]*University of Innsbruck, Institute of Physical Chemistry, A-6020 Innsbruck, Austria*
[2]*Technische Universität Dortmund, Fakultät Physik, D-44227 Dortmund, Germany*

e-mail: katrin.winkel@uibk.ac.at

An understanding of the numerous anomalies of water is closely linked to an understanding of the phase diagram of the metastable non-crystalline states of ice. The discovery of high- (HDA) and low-density amorphous ice (LDA) [1] prompted the question whether this phenomenon of polyamorphism is connected to the occurrence of more than one supercooled liquid phase. Alternatively, amorphous ices have been suggested to be of nanocrystalline nature, unrelated to liquids.
In case of LDA the connection to the low-density liquid (LDL) was inferred from several experiments including the observation of a calorimetric glass-to-liquid transition [2,3] at ambient pressure. However, in case of HDA instead no calorimetric signature has been detected so far. Other experimental methods show a glass transition of HDA at elevated pressure [4,5,6]. We present here calorimetric and dielectric measurements on LDA and HDA, showing for the first time that HDA transforms into a liquid upon heating at ambient pressure.

Differential scanning calorimetry (DSC) is the most employed experimental method to investigate vitrification and devitrification transitions between glasses and liquids. The glass-to-liquid transition upon heating is evidenced by an endothermic step, which indicates that the liquid has a higher heat capacity than the glass due to an increase of molecular mobility, e.g., by unfreezing of translational motion. In the case of water, such a glass-softening endotherm has already been observed for hyperquenched glassy water (HGW) [3] as well as for LDA [2], showing a glass transition temperature Tg(LDA)=136 K (at a heating rate of 30 K/min).
Using a relaxed form of high-density amorphous ice [7,8] we demonstrate that the glass→liquid transition HDA→HDL , is astonishingly detectable at ambient pressure. In our measurements the corresponding calorimetric signature occurs at Tg(HDL)=116±2 K (at a heating rate of 10 K/min). Additionally we repeatedly cycle between the ultraviscous high-density liquid state HDL and the non-crystalline solid state HDA. The reproducibility of switching between solid-like and liquid-like dynamics confirms the existence of an ultraviscous high density bulk liquid at ambient pressure.

The glass-to-liquid transition can also be detected by dielectric spectroscopy via the appearance of an absorption peak centred at about 10^{-2} Hz. From the temperature dependent peak positions a relaxation map can be constructed. The good agreement between dielectric and calorimetric results convey for a clearer picture of water's vitrification phenomenon.

References

[1] O. Mishima, L. D. Calvert, E. Whalley, *Nature* **314**, 76(1985).
[2] Y. P. Handa and D. D. Klug, *J. Phys. Chem.* **92**, 3323(1988).
[3] I. Kohl, L. Bachmann, A. Hallbrucker, et al., *Phys.Chem.Chem.Phys.* **7**, 3210(2005).
[4] O. Mishima, *J. Chem. Phys.* **121**, 3161(2004)
[5] O. Andersson, *Proc. Natl. Acad. Sci. U.S.A* **108**, 11013(2011)
[6] M. Seidl et al., *Phys. Rev. B* **83**, 100201/1(2011)
[7] R. J. Nelmes, J. S. Loveday, T. Straessle, et al., *Nature Physics* **2**, 414(2006).
[8] K. Winkel, E. Mayer, T. Loerting, *J. Phys. Chem. B* **115**, 14141(2011)

4CI01 Effect of Temperature on Pressure-Induced Freezing and Crystallization of Room Temperature Ionic Liquid: *N*, *N*-Diethyl-*N*-methyl-*N*-(2-methoxyethyl) Ammonium Tetrafluoroborate

N. Hamaya[1] and H. Abe[2]

[1]*Graduate School of Humanities and Sciences, Ochanomizu University, Tokyo 112-8610, Japan*

[2]*Department of Applied Chemistry, National Defence Academy, Yokosuka 239-8686, Japan*

e-mail: hamaya.nozomu@ocha.ac.jp

Pressure gives large effects on intermolecular forces between anions and cations in ionic liquids by changing intermolecular distances. Recent study [1] of *N*, *N*-diethyl-*N*-methyl-*N*-(2-methoxyethyl) ammonium tetrafluoroborate, [DEME][BF_4], revealed its complicated phase behaviour involving liquid, glassy and crystalline states under high pressure. In this work, we studied the effect of temperature on pressure-induced freezing to glass, crystallization and melting in [DEME][BF_4].

The freezing pressure from the liquid state on compression increases with increasing temperature. Two successive crystallization that occurs on decompression from the glass phase is rather insensitive to temperature. The crystalline phase finally melts at a pressure much lower than the freezing pressure. This melting curve has a slope, dT/dP, steeper than the slope of the liquid−glass phase boundary.

[1] Y. Yoshimura, H. Abe, Y. Imai, T. Takekiyo, and N. Hamaya, J. Phys. Chem. B 117, 3264 (2013).

4CI02 Solvent Characteristics of Supercritical Carbon Dioxide as a New Materials Design Media and Their Application to the Production of Organic Nanoparticles

H. Uchida

Department of Chemistry and Material Engineering, Faculty of Engineering, Shinshu University, Nagano-city, 380-8553, Japan

e-mail : uchida@shinshu-u.ac.jp

Nanoparticles exhibit unique size-dependent properties compared to bulk counterparts and would enhance a variety of technologies including pharmaceutical, coating, environmental, chemical processing, electronic, and sensing applications. Therefore, it is desirable to develop the preparation methods of nanoparticles, which at least partially overcome the problems such as wide particle size distribution, high thermal and mechanical stress, impurity contamination from a comminution device and environmental pollution problems associated with the use of large amounts of organic solvents. As an alternative to the conventional techniques, various crystallization techniques using supercritical carbon dioxide have recently been proposed [1]. Supercritical carbon dioxide has been thought to be new-type attractive solvents and have been applied in various fields of industries such as separations, reactions and material processing because their solvent power is moderate, and their transport properties are favorable in mass transfer rates. In particular, recently new crystallization techniques using supercritical carbon dioxide such as rapid expansion of supercritical solutions (RESS), supercritical antisolvent recrystallization (SAS), and particles from gas saturated solutions (PGSS) processes have been proposed and the techniques have been paid much attention and have been expected as effective and environmentally friendly nanoparticle design methods [1].

The most well-known crystallization technique based on supercritical technique would be the RESS technique. The study on the production of nanoparticles of racemic ibuprofen and theophylline via RESS technique using supercritical carbon dioxide has been presented in this work. The supercritical carbon dioxide saturated with the solute was expanded rapidly through a drilled capillary nozzle (D = L = 50 μm) into a collection chamber of which temperature is controlled. The experimental temperatures and pressures are 308.2-338.2 K, and 13.5-22.0 MPa, respectively. We have successfully produced nano-sized particles of around 250-300 nm with the narrow particle size distribution, as shown in Figure 1. Moreover, the mean size of the micronized particles can be estimated by the supersaturation defined as the difference between the chemical potential of the solute at the section of preparing the supercritical solution saturated with the solute and that at the section of the collection of the produced particles.

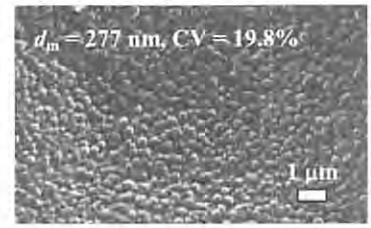

Figure 1. SEM photograph of particles of racemic ibuprofen produced by the RESS process.

References

[1] H. Uchida, *J. Soc. Powder Technol., Japan*, **48**, 641 (2011).

[2] J. Sakabe *et al.*, *Proc. 10th Int. Symp. Supercri. Fluids*, P-1505 (2012).

4DK01 A size comparison of the lanthanoid(III) and actinoid(III) ionic radii

D. Lundberg and I. Persson

Department of Chemistry, Uppsala BioCenter, Swedish University of Agricultural Sciences, P.O. Box 7015, SE-750 07 Uppsala, Sweden

e-mail : daniel.lundberg@slu.se

Using lanthanoid(III) ions as safe substitutes for the radioactive actinoid(III) ions in model compounds is commonplace in many nuclear reasearch areas. For instance, the highly radioactive actinoid ion americium(III) is often exchanged for the much safer europium(III) ion located in the same position in the lanthanoid series. There is, however, not much structural evidence that supports this view, and when placed in a greater perspective it becomes clear that the visual overlap in the periodic table does not correspond to the true ionic radii of these elements. Here, using structural data from both solution and solid state, we present a comparative view of the ionic radii of the two series.

3DI01 Speciation of anticancer Ru(II,III) compounds in aqueous solution

T. Kiss[1,2], T. Jakusch[1], É.A. Enyedy[1], É. Sija[2] C.G. Hartinger[3] and B.K. Keppler[3]

[1] *Department of Inorganic and Analytical Chemistry, University of Szeged, Hungary*
[2] *HAS-USZ Bioinorganic Chemistry Reserach Group, University of Szeged, Szeged, Hungary, e.mail: tkiss@chem.u-szeged.hu*
[3]. *Institute of Inorganic Chemistry, University of Vienna, Vienna, Austria*

Ruthenium compounds are highly potent antitumor agents. Many of them are currently undergoing preclinical and clinical studies. NAMI-A and KP1019 the two most promising Ru(III) compounds are in clinical Phase 2. The *in vivo* reduction of Ru(III) is assumed to be an important step in the activation mechanism and thus development of new organometallic Ru(II) compounds with potential antitumor activity also attracts attention [1,2] The solution properties of these compounds may provide key information for understanding their possible biotransfromation ways in biological millieu.

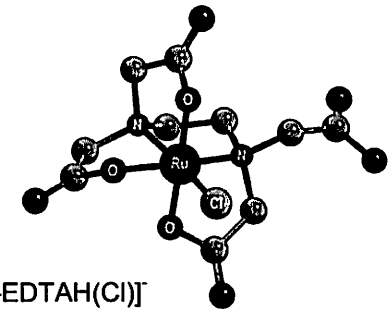

[Ru(III)–EDTAH(Cl)]$^-$

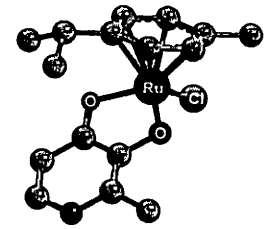

An example of the Ru(II) – cymene ternary complexes

In contrast with other Ru(III) compounds the EDTA complex of Ru(III) is kinetically labile in acidic pH [3] and the chloride ligand can be easily aquated. However, applying bidentate ligands (with (O,O), O,N) or (O,S) donor set) one of the carboxylates of the EDTA, besides the chloride, can also be replaced under fast kinetic conditions. Accordingly, this system gives us the chance to *compare* the binding ability of the different bidentate ligands to Ru(III) in the Ru(III)-EDTA-B ternary systems.

The pH dependent speciation of $[Ru(II)(\eta^6\text{-p-cymene})(H_2O)_3]^{2+}$ with some (O,O) type ligands had already been reported [4] As an extension of the work interactions with (O,N) and (O,S) type bidentate ligands have been studied in our laboratory by pH-potentiometry, UV-Vis spectrophotometry, and ^{1}H-NMR spectrometry.

The main finding is, that ruthenium in both oxidation states has much higher affinity to (O,S) type ligands than to (O,O) or (O,N), which may mean that the importance of the Ru-thiolate interaction during biotransformation reactions of the drug candidate compounds most probable are more important than believed earlier. This is in accordance with the higher cytotoxicity of the (O,S) type ternary complexes.

Acknowledgements.
The work was supported by the Hungarian Research Fund OTKA K77883 and the Hungarian Austrian Action Foundation. It was also financed by the EU in the frame of the TÁMOP-4.2.2.A project. ÉAE and TJ acknowledge the financial support of Bolyai J. Research Fund.

References:

[1] W. Kandioller, A. Kurzwenhart, M. Hanif, S.M. Meier, H. Henke, B.K. Keppler, C.G. Hartinger, *J. Organomet. Chem.*, **2011**, *696* 999.
[2] W. Kandioller, C.G. Hartinger, A.A. Nazarov, C. Bartel, M. Skocic, M.A. jakupec, V.B. Ariaon, B.K. Keppler, *Chem. Eur. J.*, **2009**, *15* 12283.
[3] T. Matsubara, C. Creutz, *Inorg. Chem.*, **1979**, *18* 1956.
[4] L. Biró, E. Farkas, P. Buglyó, *Dalton Trans.*, **2010**, *39* 10272.

3DI02 Kinetic study on Cyclopalladation in Palladium(II) Complexes Containing an Indole Moiety

S. Iwatsuki[1], T. Suzuki[2], S. Tanooka[1], T. Yajima[3], and Y. Shimazaki[2]

[1]*Department of Chemistry, Konan University, Kobe 658-8501, Japan,* [2]*College of Science, Ibaraki University, Mito 310-8512, Japan,* [3] *Department of Chemistry and Materials Engineering, Kansai University, Suita 564-8680, Japan*

e-mail : iwatsuki@center.konan-u.ac.jp

Various palladium complexes are known to be very useful catalysts in organic syntheses involving C–C bond formation and C–X bond activation. Most of these reactions have been considered to take place via Pd–C intermediates, and many Pd–C complexes have been developed to date, affording deep insights into the reaction mechanisms for useful catalytic reactions. On the other hand, the indole ring of the tryptophyl residue having the highest hydrophobicity among natural α-amino acids is known to provide a hydrophobic microenvironment for specific binding of molecules. In these points in mind, we have synthesized and characterized the Pd(II) complexes having an indole moiety and investigated their Pd–indole carbon bond formation.[1,2]

Pd(II) complexes of 2N1O-tridentate ligands having an indole moiety convert to the Pd–indole-C2 binding species through cyclopalladation (eq 1). In this Pd–C bond formation mechanism, the dissociated proton from the indole ring binds to the phenolate moiety. As a result, the reaction proceeds through intramolecular process. On the other hand, a Pd(II) complex of 2N-bidentate ligand having an indole moiety also converts to the indole binding complex (eq 2), and the Pd–C bond formation occurs simply by dilution of the solution. The kinetic analyses for these cyclopalladation reactions and their detailed mechanisms will be discussed.

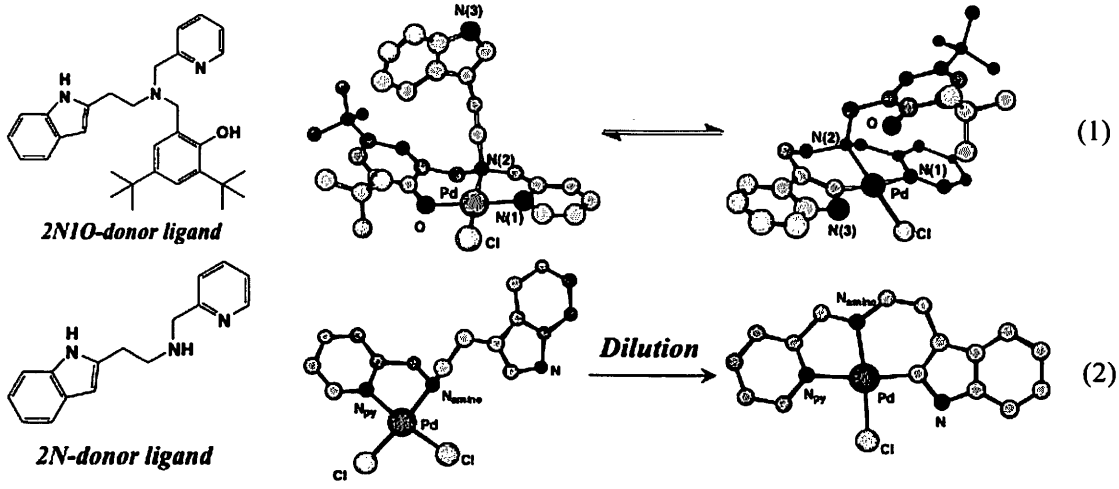

References

[1] Y. Shimazaki, M. Tashiro, T. Motoyama, S. Iwatsuki, T. Yajima, Y. Nakabayashi, Y. Naruta, O. Yamauchi, *Inorg. Chem.* **44**, 6044 (2005).

[2] S. Iwatsuki, T. Suzuki, T. Yajima, T. Shiraiwa, O. Yamauchi, Y. Shimazaki, *Inorg. Chim. Acta* **377**, 111 (2011).

4DI03 One-electron oxidized Cu(II)-salen type complexes; Relationship between electronic structure and reactivity

Yuichi Shimazaki

College of Sicence, Ibaraki University, Mito 310-8512, Japan

e-mail : yshima@mx.ibaraki.ac.jp

The Cu(II)–phenoxyl radical formed during the catalytic cycle of galactose oxidase (GO) attracted much attention, and the structures and properties of a number of metal–phenoxyl radical complexes have been studied. Some of functional model system of GO have been reported previously that the Cu complexes showed the oxidation of primary alcohols to aldehydes, and formation of the Cu(II)-phenoxyl radical species was revealed in the catalytic cycle. As an extension of the studies on Cu(II)–phenoxyl radical species, we synthesized one-electron oxidized square-planar Cu(II) complexes of 5- and 6-membered chelate salen-type ligands and characterized the valence state and reactivity of one-electron oxidized complexes.

The neutral and one-electron oxidized Cu(II) six-membered chelate **1,3-Salcn** complexes have been investigated and compared with the five-membered chelate **1,2-Salcn** complexes (Figure 1). Cyclic voltammetry of Cu(**1,3-Salcn**) showed two reversible redox waves at 0.45 and 0.63 V, which are only 0.03 V higher than those of Cu(**1,2-Salcn**). Reaction of the complexes with 1 equivalent of $AgSbF_6$ afforded the oxidized complexes. The electronic structures of the oxidized complexes were probed by X-ray crystal structures, UV-vis-NIR, resonance Raman, and EPR measurements, and theoretical calculations, indicating that [Cu(**1,2-Salcn**)]SbF_6 has a Cu(III)-phenolate ground state and valence tautomerisation between Cu(III)-phenolateand Cu(II)-phenoxyl radical in CH_2Cl_2 solution at room temperature, while [Cu(**1,3-Salcn**)]SbF_6 has the phenoxyl radical species whose electron is relatively localized on one phenolate moiety in the molecule. The reactivity of [Cu(**1,2-Salcn**)]$^+$ and [Cu(**1,3-Salcn**)]$^+$ with benzyl alcohol was also studied. Quantitative conversion of benzyl alcohol to benzaldehyde was observed, with a faster reaction rate of [Cu(**1,3-Salcn**)]$^+$ in comparison with [Cu(**1,2-Salcn**)]$^+$. These differences will be discussed based on the electronic structure difference.

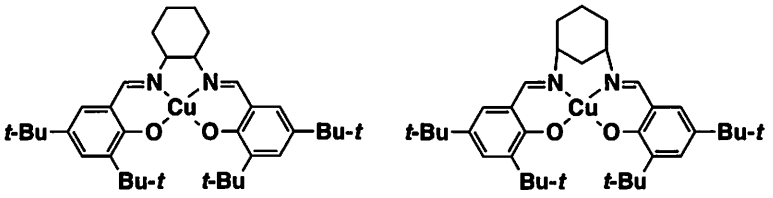

Figure 1. Structure of Cu(II) salen-type complexes

References

[1] T. Storr, *et al.*, *J. Am. Chem. Soc.* **130**, 14448 (2008).

[2] K. Asami, *et al.*, *Inorg. Chem.* **51**, 12450 (2012).

3EK01 Reentrant Condensation, Liquid-Liquid Phase Separation and Crystallization in Protein Solutions Induced by Multivalent Metal Ions

F. Zhang[1], F. Roosen-Runge[1], A. Sauter[1], M. Wolf[1], R. Roth[2], M.W.A. Skoda[3], R. M. J. Jacobs[4] and F. Schreiber[1]

[1]*Institut fuer Angewandte Physik, Universitaet Tuebingen, Auf der Morgenstelle 10, 72076, Tuebingen, Germany*

[2]*Institut für Theoretische Physik, Universität Tübingen, Germany*

[3]*STFC, ISIS, Rutherford Appleton Laboratory, Chilton, Didcot, OX11 0OX, UK*

[4]*Department of Chemistry, Chemistry Research Laboratory, University of Oxford, UK*

e-mail : fajun.zhang@uni-tuebingen.de

Reentrant condensation (RC) describes a type of phase behavior in colloid, protein, DNA and polyelectrolyte solutions in the presence of multivalent salt, in which a phase-separated regime occurs in between two critical salt concentrations. In particular, it has been shown that negatively charged globular proteins at neutral pH in the presence of multivalent counterions undergo a RC phase behavior [1,2], giving a metastable liquid-liquid phase separation (LLPS) [3]. This reentrant phase behavior corresponds to an effective charge inversion of proteins as confirmed by zeta-potential measurements and supported by Monte Carlo simulations [1,2]. Interestingly, protein crystallization follows both the classical and the "two-step" pathway under different conditions near the boundary of LLPS [3-5]. Further studies demonstrate that protein clusters formed *via* metal ion bridging can act as precursors for protein crystallization by reducing the energy barrier of nucleation [4,5]. Here, we briefly summarize the recent progress using multivalent metal ions to tune interactions as well as phase behavior in protein solutions. We will focus on the influence parameters and the mechanism of RC, as well as LLPS and protein crystallization in the condensed regime.

References

[1] F. Zhang *et al.*, Phys. Rev. Lett. **101**, 148101 (2008).

[2] F. Zhang *et al.*, Proteins: Structure, Function, and Bioinformatics **78**, 3450 (2010)

[3] F. Zhang *et al.*, J. Appl. Cryst. **44**, 755 (2011)

[4] F. Zhang *et al.*, Soft Matter **8**, 1313 (2012)

[5] F. Zhang *et al.*, Faraday Discuss. **159**, 313 (2012)

2EI01 Transfer Models for Chemical Protein Denaturation

B. Moeser, D. Horinek

Institut für Physikalische und Theoretische Chemie, Universität Regensburg, 93040 Regensburg, Germany

e-mail : dominik.horinek@ur.de

Protein denaturation by urea remained controversial after many decades of research: many results suggest that urea denatures by favorable solvation of both the side chains and the backbone, but the transfer model ascribes the denaturation power exclusively to urea's interactions with the backbone. On the path towards a complete understanding of the underlying physical-chemical principles, we present insight by molecular simulations in combination with liquid state theories. Peptide stability in concentrated solutions of urea is studied by a combination of interface thermodynamics, Kirkwood-Buff solvation theory, and molecular dynamics simulation results for pure urea/water mixtures and for peptide chains in these solvents. Different residue types and secondary structure motifs of the peptide are studied. The results are used for a rigorous evaluation of different implementations of the transfer model, which reveals that the established implementation gives an unsatisfactory prediction of the scaling of transfer free energies with the solvent accessible area. This scaling is well satisfied after an inconsistency in the treatment of the backbone contribution is corrected.

The new implementation works also best in the prediction of experimental m values of a set of 36 proteins. The separation into side chain and backbone contributions shows that they are in average of equal magnitude, which is in agreement with many other studies. Thus, our validations and proposed improvements further consolidate the transfer model as an outmost powerful tool for the prediction and interpretation of the solvation thermodynamics of proteins in mixed solvents.

2EI02 Shaping the skin: how geometry determines corneocyte hydration

M. E. Evans[1], and R. Roth[2]

[1]*Institute for Theoretical Physics, University of Erlangen-Nuremberg, Erlangen, Germany*
[2]*Institute for Theoretical Physics, University of Tübingen, Tübingen, Germany*
e-mail : myfanwy.e.evans@physik.uni-erlangen.de

The stratum corneum, the outer layer of mammalian skin, provides a remarkable barrier to the external environment, yet has highly variable permeability properties where it actively mediates between inside and out. On prolonged exposure to water, swelling of the corneocytes (skin cells) is the key process by which the stratum corneum controls permeability and mechanics. As for many biological systems with intricate function, the mesoscale geometry is optimised to provide functionality from basic physical principles: in this case, the woven geometry of the keratin intermediate filament (IF) organisation within corneocytes permits large swelling with full reversibility [1]. Here we show that macroscopic function of corneocytes can be identified from solvation and elasticity of helical tubes with woven geometry equivalent to the keratin IF arrangement. Our results show that the balance of solvation free energy [2], which drives water absorption, and elastic energy, which favours compactness, favours a set of geometric conformations corresponding to packing fractions for keratin IFs in native and fully hydrated corneocytes. The global free energy minimum is a swollen state of the corneocyte: given water, the corneocyte will expand and reach a natural barrier to further swelling, yet easily transform to the compact form once again with only a small force from evaporation once the water source is removed.

References

[1] M. E. Evans, S. T. Hyde, *J. R. Soc. Interface* **8**, 1274(2011).
[2] R. Roth, Y. Harano, M. Kinoshita, *Phys. Rev. Lett.* **97**, 078101(2006).

3EI03 Hydration study of adenosine phosphates (ATP) and ATP-driven proteins by dielectric relaxation spectroscopy

M. Suzuki[1], G. Mogami[1], A. Imao[1], T. Wazawa[1], and N. Morimoto[1]

[1]*Department of Materials Processing, Tohoku University, Sendai 980-8579, Japan*
e-mail : msuzuki@material.tohoku.ac.jp

Hydration properties of adenine nucleotides and orthophosphate (Pi) in aqueous solutions adjusted to pH=8 with NaOH were studied by high-resolution microwave dielectric relaxation (DR) spectroscopy at 20 °C. The dielectric spectra were analyzed using a mixture theory combined with a least-squares Debye decomposition method. Solutions of Pi and adenine nucleotides showed qualitatively similar dielectric properties described by two Debye components. One component was characterized by a relaxation frequency (fc=18.8–19.7 GHz) significantly higher than that of bulk water (17 GHz) and the other by a much lower fc (6.4–7.6 GHz), which are referred to here as hypermobile water (HMW) and constrained water (CW), respectively. By contrast, a hydration shell of only the latter type was found for adenosine (fc~6.7 GHz). The present results indicate that phosphoryl groups are mostly responsible for affecting the structure of the water surrounding the adenine nucleotides by forming one constrained water layer and an additional three or four layers of hyper-mobile water.[1] HMW was recently explained partly by statistical mechanical analysis using MD simulations.[2]

State changes of protein hydration were also studied with high-resolution DRS technique. For example, at low salt concentrations (e.g., less than several mM KCl), actin adopts a monomeric form, G-actin, whereas at higher salt concentrations (e.g., 50 mM KCl) and in the presence of adenosine triphosphate (ATP), actin polymerizes to a filamentous form, F-actin. This polymerization reaction is endothermic and occurs above a critical concentration. DRS measurements showed that F-actin exhibits dual hydration shells, CW and HMW [3], as a structure-maker and a structure-breaker, respectively. The present study revealed a significant increase of HMW around actin upon polymerization.[4]

References

[1] G. Mogami, T. Wazawa, N. Morimoto, T. Kodama, M. Suzuki, *Biophys. Chem.***154**, 1-7(2011).
[2] Y. Kubota, A. Yoshimori, N. Matubayasi, M. Suzuki, R. Akiyama, *J. Chem. Phys.* **137**, 224502(2012).
[3] S. R. Kabir, K. Yokoyama, K. Mihashi, T. Kodama, M. Suzuki, *Biophys. J.* **85**, 3154(2012).
[4] M. Suzuki, T. Wazawa, G. Mogami, T. Kodama, *J. Phys. Soc. Jpn.* **81**, SA003(2012).

1FK01 Turning Liquids Solid: Why using particles in emulsions makes all the difference

Ling L.C. Wong[1], Vivian O. Ikem[1], Ranting Wu[1], Angelika Menner[2]

and Alexander Bismarck[1,2]

[1] *Polymer & Composite Engineering (PaCE) Group, Department of Chemical Engineering, Imperial College London, South Kensington Campus, London, SW7 2AZ, UK.*
[2] *Polymer & Composite Engineering (PaCE) Group, Institute of Materials Chemistry & Research, Faculty of Chemistry, University of Vienna, Währingerstr. 42, 1090 Vienna, Austria*

e-mail : a.bismarck@imperial.ac.uk

High porosity, low density, interconnected porous polymers are attractive materials for numerous applications, ranging from supports for cell cultures, solid-state chemistry and setting retarded cements. Such polymers are also used in chromatography applications, ion-exchange modules and filters. Macroporous polymers can be prepared by various methods, such as chemical and physical blowing, salt leaching but also by emulsion templating; first reported by von Bonin and Bartl in 1962, emulsion templating has now emerged as effective method to synthesise macroporous polymers with tailored pore morphology and physical properties. High or Medium Internal Phase (ratio) Emulsions (HIPEs or MIPEs) with a continuous phase consisting of or containing monomers are used as templates for the preparation of interconnected macroporous polymers, called poly(merized)M/HIPEs, which are obtained after the removal of the internal template phase. PolyH/MIPEs are usually synthesized from emulsion templates stabilised by large volumes of surfactants (commonly between 10 - 20 wt.-%). The resulting polymers are interconnected and have porosities of up to 95%. However, applications of polyHIPEs remain limited mainly because of their poor mechanical properties but also because of their low permeability. In the last decade much research focused on improving the mechanical properties, which was achieved by incorporating particulate reinforcements, increasing the foam density by decreasing the internal phase volume of the emulsion templates or by using different monomers and polymerisation routes. Improving the permeability of macroporous polymers while maintaining sufficient mechanical properties was a more challenging task, increasing the porosity of interconnected porous polymers results in higher permeability but much reduced mechanical properties. Moreover, the maximum pore throat sizes of porous polymers produced from surfactant-stabilised emulsion templates are limited too by the droplet sizes in the emulsion, which also limits the permeability.

We introduced a new class of macroporous polymers called poly-Pickering-M/HIPEs, produced by polymerisation of particle stabilised (Pickering) M/HIPEs. Using particulate emulsifiers provides a number of processing advantages; it removes the need for structurally parasitic surfactant and allows to prepare macroporous polymers with much larger pores (up to 1500 μm) as commonly observed in polyHIPEs made from surfactant stabilized emulsions. However, poly-Pickering-M/HIPEs are typically closed-cell. Nevertheless, this new class of polyHIPEs with millimetre-sized pores should allow for very permeable polyHIPEs if the pores could be made interconnected. This was possible by introducing a surfactant to pre-made Pickering emulsion templates. The resulting open-porous poly-Pickering-HIPEs had a maximum gas permeability of 2.6 Darcy. Alternatively, if particles and surfactant were simultaneously used as emulsifiers, macroporous polymers with a hierarchical pore structure with enhanced mechanical properties while maintaining permeability were produced.

Now that we have a tool kit for new polyM/HIPE architectures, we believe that this can be combined with different polymer chemistries to produce a whole raft of novel interconnected macroporous polymers for new applications. By selecting appropriate particulate emulsifiers we could create functional macroporous polymers, which by virtue of the liquid template can be given any shape making this a versatile approach for the future.

1FI01 Molecular Dynamics Study of Lipid Self-Assembly

W. Shinoda

National Institute of Advanced Industrial Science and Technology (AIST), 1-8-31 Midorigaoka, Ikeda, Osaka 563-8577, Japan

e-mail : w.shinoda@aist.go.jp

We illustrate here our recent simulation work for investigating the morphology of lipid self-assembly using a coarse-grained (CG) force field model [1]. The CG model is designed to reproduce experimental surface/interfacial properties as well as distribution functions from all-atom (AA) molecular dynamics (MD) simulations. A series of MD simulations has elucidated that the CG model reproduces the phase diagram reasonably and produces the membranes with reasonable elastic moduli, surface and line tensions.

Using the free energy calculations, we have evaluated the stability of vesicle. [2] The calculated free energy barrier for the vesicle-to-disk transformation shows an overestimation of the energy barrier by a simple continuum theory. We discuss a possible extension of continuum theory to fill the gap.

The effects of lipid components and additives are also demonstrated. Especially the effect of fullerenes (carbon nanoparticles) on the membrane properties will be discussed in details.[3] The behavior of fullerenes in the bilayer membrane and the resultant membrane properties depend on the size of fullerene and bilayer thickness quite sensitively. To discuss these details, we need a chemically accurate CG model constructed based on extensive AA-MD results.

References

[1] W. Shinoda, R. DeVane, M. L. Klein, *Mol Simul* **33**, 27 (2007); *ibid*, *Soft Matter* **4**, 2454 (2008); *ibid*, *J. Phys. Chem. B* **114**, 6836 (2010); *ibid*, *Soft Matter*, **7**, 6178 (2011).

[2] W. Shinoda, T. Nakamura, S. O. Nielsen, *Soft Matter*, **7**, 9012(2011).; T. Nakamura, W. Shinoda, T. Ikeshoji, *J. Chem. Phys.* **135**, 094106 (2011). T. Nakamura, W. Shinoda, *J. Chem. Phys. in press.*

[3] R. DeVane *et al. J. Phys. Chem. B*, **114**, 6386 (2010); C. Chiu *et al. J. Phys. Chem. B* **114**, 6394 (2010). R. DeVane *et al. J. Phys. Chem. B*, **114**, 16364 (2010); A. Jusufi *et al. Soft Matter* **7**, 1139 (2011); C. Chiu *et al. Soft Matter*, **8** 9610(2012).

1GI01 Surface propensity of carboxylic acids and carboxylates and surface induced reactions in the water-air interface

Ingmar Persson,[a] Olle Björneholm[b] and Niklas Ottosson[b]

[a] Department of Chemistry, SLU, Box 7015, SE-750 07 Uppsala, Sweden,
[b] Department of Physics and Astronomy, Uppsala University, Box 516, SE-751 20 Uppsala, Sweden.

The relative surface propensity of the carboxylic acids and carboxylates has been obtained by monitoring their respective C1s signal intensities from a solution in which their bulk concentrations are equal.[1] All the acids are found to be enriched at the surface relative to the corresponding carboxylates. By monitoring the PE signals of acetic acid and acetate as a function of total concentration, the protonation of acetic acid is found to be nearly complete in the interface layer. This is in agreement with literature surface tension data, from which it is inferred that the acids are enriched at the surface while sodium, formate and acetate ions, but not the butyrate ion, are depleted. For butyric acid, the carboxylate form co-exists with the acid form in the interface layer. By comparing concentration dependent surface excess data with the evolution of the corresponding photoemission signals it is furthermore possible to draw conclusions about how the distribution of molecules that contribute to the excess is altered with bulk concentration. Chemical reactions thermodynamically not allowed to take place in aqueous bulk solution may instead take place in the interface aqueous solution-air due to a significant stabilization of one component in the interface, a surface promoted reaction. An example of such a reaction is the protonation of carboxylate ions, where the corresponding neutral carboxylic acid has a relatively long alkyl chain stabilized in the interface to such a degree that weak acids, as the ammonium ion, leave a proton. The results quantitative studies of such surface promoted reactions will be presented.

Reference

1. N. Ottosson, E. Wernersson, J. Söderström, W. Pokapanich, S. Kaufmann, S. Svensson, I. Persson, G. Öhrwall and O. Björneholm, *Phys. Chem. Chem. Phys.* **13** (2011) 12261-12267.

1GI02 Interfacial Phenomena at Aqueous-Liquid Crystal Interfaces

Nicholas L. Abbott

[1]*Department of Chemical and Biological Engineering, University of Wisconsin-Madison, Madison WI 53706, USA*

e-mail : abbott@engr.wisc.edu

Processes leading to the self-organization of molecules and colloids at the interfaces of isotropic liquids have been widely studied in the past. This talk will focus beyond those past studies by addressing interfacial and colloidal phenomena in systems in which the isotropic solvent is replaced by a nematic liquid crystal (LC). Observations related to two fundamental phenomena at aqueous-LC interfaces will be discussed. First, the influence of adsorbates on the ordering of LCs will be addressed, including the self-assembly of amphiphiles and recent observations connected to specific ion effects. Second, the influence of LCs on the interfacial ordering of amphiphiles and colloids will be discussed, with a particular focus directed to the influence of the elasticity of LCs on interfacial phase behaviour. Finally, the technological opportunities defined by these observations will be discussed, including designs for new analytical methods.

References

[1] Bai, Y.; Abbott, N.L.; "Recent Advances in Colloidal and Interfacial Phenomena Involving Liquid Crystals", *Langmuir*, 27(10), 5719-5738, **2011**

1GI03 Polymer Structure at Water Interface

K. Tanaka

Department of Applied Chemistry and International Institute for Carbon-Neutral Energy Research, Kyushu University, Fukuoka 819-0395, Japan

e-mail : k-tanaka@cstf.kyushu-u.ac.jp

Interfaces of polymers with "nonsolvents" play an important role in their functional properties such as wettability, friction with lubricants, cell adhesion, biocompability, etc. To design and construct highly functionalized polymers for applications that exploit these characteristics, aggregation states of the polymers at the liquid interfaces must be understood as the first benchmark. However, this is experimentally difficult because such interfaces are buried. In this study, we use specular neutron reflectivity (NR) and sum-frequency generation (SFG) spectroscopy to study, respectively, the density profile and local conformation of poly(methyl methacrylate) (PMMA) at the interface with air or gaseous nitrogen (N_2) and at water interfaces. The interface of PMMA with water was diffuse in comparison with the pristine interface with air. Interestingly, the PMMA film was composed of a swollen layer and the interior region, which also contained water, in addition to the diffused layer. To conserve mass, the swelling of the film by water is accompanied by an increase in the film thickness. The change in the film thickness estimated by NR was in excellent accord with the result of direct observation using atomic force microscopy (AFM). The modulus of PMMA in the vicinity of the water interface was also examined on the basis of force-distance curves measured by AFM. The modulus decreased closer to the outermost region of the film. The extent to which the modulus decreased in the interfacial region was consistent with the amount of water sorbed into the film. The local conformation of PMMA chains at the N_2 and water interfaces was studied by infrared (IR)-visible SFG spectroscopy. At the N_2 interface, hydrophobic functional groups such as α methyl, ester methyl and methylene groups were present. While the α methyl group was oriented along the direction normal to the interface, ester methyl and methylene groups were oriented parallel to the interface. Quantitative discussion concerning the orientation of the functional groups of PMMA at the N_2 interface was aided by a model calculation. Once the PMMA film was contacted with water, the carbonyl groups of the PMMA side chains were oriented to the water phase to form hydrogen bonds with water molecules, resulting in the migration of ester methyl into the internal region of the film. Concurrently, the methylene groups became randomly oriented at the water interface and/or in part migrated into the internal region. Interestingly, the α methyl groups still existed at the water interface oriented along the parallel direction. The outermost region of PMMA in water was consisted of hydrophilic and hydrophobic domains with sub-nanometer scale.

References

[1] Tanaka et al., *Langmuir* **24**, 296 (2008).

[2] Tanaka et al., *Macromolecules* **45**, 4638 (2012).

1GI04 DNA-Carrying Colloidal Particles for Biosensing

Mizuo Maeda[1]

[1]*Bioengineering Laboratory, RIKEN, Saitama 351-0198, Japan*
e-mail : mizup@riken.jp

DNA-Carrying nanoparticles disperse in an aqueous medium due to electrostatic repulsion between anionic phosphate groups in the DNA backbone. Interestingly, when complementary single-stranded DNA is added to the dispersion of DNA-carrying nanoparticles to form the fully matched double helix on the surface, the nanoparticles become unstable and spontaneously form aggregates in a non-crosslinking manner [1]. Furthermore, we have found that the double-stranded DNA-carrying nanoparticles acquire high colloidal stability to disperse in an aqueous medium when a terminal single-base mismatch exists at the interface between the DNA corona and the disperse medium. Exploiting the unique colloidal behavior of the DNA nanoparticles, we have devised a facile single-nucleotide polymorphism genotyping method [2-4]. We applied the SPR imaging technique on our original, power-free microfluidic devices to the detection of the gold nanoparticles aggregation [5, 6]. Through a combination of non-crosslinking aggregation of DNA-carrying nanoparticles and molecular recognition by aptamers or aptazymes, we have also developed bioanalytical systems for detecting cGMP, ATP, FMN, theophyllin [7, 8], and Hg(II) [9]. These analytical functions are designed based on unique properties of soft interface made from densely assembled double-stranded DNA on nanoparticle surface. We also studied intensively the thermo-responsive micellization and micellar stability of polyNIPAAm-g-DNA copolymers as well as of polyNIPAAm-b-DNA copolymers with the aid of synchrotron radiation solution small-angle X-ray scattering which allowed us to obtain detailed structural information [10].

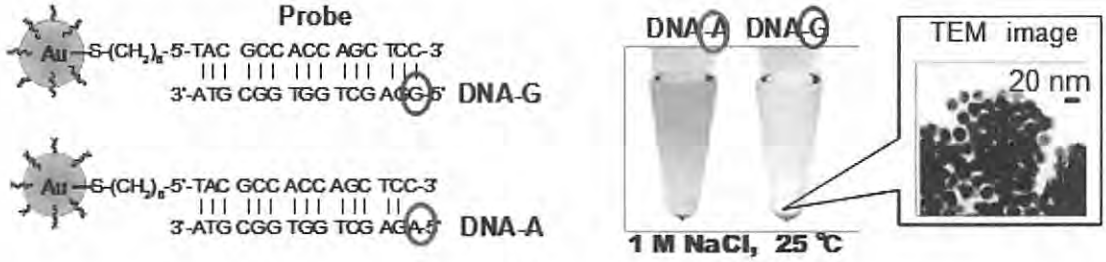

References

[1] K. Sato, K. Hosokawa, M. Maeda, *J. Am. Chem. Soc.*, **125**, 8102 (2003).
[2] K. Sato, K. Hosokawa, M. Maeda, *Nucleic Acids Research*, **33**, e4 (2005).
[3] K. Sato, M. Onoguchi, Y. Sato, K. Hosokawa, M. Maeda, *Anal. Biochem.*, **350**, 162 (2006).
[4] K. Hosokawa, K. Sato, N. Ichikawa, M. Maeda, *Lab Chip*, **4**, 181 (2004).
[5] Y. Sato, K. Sato, K. Hosokawa, M. Maeda; *Anal. Biochem.*, **355**, 125 (2006).
[6] Y. Sato, K. Hosokawa, M. Maeda, *Colloids Surf., B*, **62**, 71 (2008).
[7] A. Ogawa, M. Maeda, *Bioorg. Med. Chem. Lett.*, **18**, 6517 (2008).
[8] A. Ogawa, M. Maeda, *Chem. Commun.*, **45**, 4666 (2009).
[9] N. Kanayama, T. Takarada, M. Maeda, *Chem. Commun.*, **47**, 2077 (2011).
[10] P. Pan, M. Fujita, W.-Y. Ooi, K. Sudesh, M. Maeda, et al., *Langmuir*, **28**, 14347 (2012).

1II01 Determination of enthalpies of solution, limiting solubilities and partial molar heat capacities of n-alcohols in water and trehalose crowded media

Guangyue Bai[†], *Sandra C.C. Nunes*[‡], *Marisa A.A. Rocha*[†], *Luis M.N.B.F. Santos*[†], *M. Ermelinda S. Eusébio*[‡], *M. João Moreno*[‡], *Margarida Bastos*[†]

[†] CIQ (UP), Department of Chemistry and Biochemistry, Faculty of Sciences, University of Porto, R. Campo Alegre, 687, P-4169-007 Porto, Portugal

[‡] Department of Chemistry, University of Coimbra, 3044-535 Coimbra, Portugal

e-mail : mbastos@fc.up.pt

The cytoplasm is an aqueous solution with very high concentration of polar solutes, small molecules, macromolecules and supramolecular assemblies. Under these conditions of molecular crowding, the structure and dynamics of solutes is significantly different from the one adopted in dilute aqueous solution. Nevertheless, the majority of available biochemical and biophysical characterization of solute behaviour inside the cell is inferred from studies in dilute aqueous solutions.

In the present work we determine fundamental thermodynamic properties of solution of straight chain alcohols in HEPES buffer and in crowded media model, a 1 mol.dm^{-3} trehalose solution to ascertain the effect of molecular crowding on the thermodynamic properties of solution.

The measurement of ΔH_{sol} of n-propanol in both media, at $T = 298.15$ K, was performed in a Setaram C80 and the obtained values show already a significant effect of trehalose on this property. For the longer chain alcohols, n-butanol and for n-pentanol, an isothermal titration calorimeter (ITC) [1] was used and measurements were performed for both media at $T = 298.15$ K. This methodology allowed us to obtain the enthalpy of dissolution in the aqueous phase, the alcohol maximum solubility and the enthalpy of dissolution of the aqueous media in the alcohol phase. This is an innovative approach that allows a full characterization of the thermodynamics of the process, as we can also calculate ΔG_{sol} and ΔS_{sol} for the dissolution of the alcohols in the aqueous solutions. Finally the partial molar heat capacity of the solute, at infinite dilution was determined by use of a Drop heat capacity calorimeter (Drop-Cp), designed at Lund University, Sweden, and recently rebuilt at our Lab [2].The obtained results will be presented and discussed in light of the molecular crowding effect on the thermodynamic properties of the alcohols.

References

[1] M. Bastos, G. Bai, P. Gomes, D. Andreu, E. Goormaghtigh and M. Prieto *Biophys. J.*, **94**, 1-14 (2008)

[2] L. M. N. B. F. Santos, M. A. A. Rocha, A. S. M. C. Rodrigues, V. Štejfa, M. Fulem, M. Bastos *J. Chem Thermodynamics* **43**, 1818-1823 (2011)

Acknowledgements This work was mainly supported by FCT, Lisbon, Portugal, and European Social Fund through strategic projects Pest-C/QUI/UI0081/2011 awarded to CIQUP and Project PTDC/QUI/64565/2006.

1II02 Dissolution of carbon dioxide in aqueous solutions of amines: experimental and thermodynamic modeling studies

J-Y. Coxam[1,2]

[1]*Clermont Université, Université Blaise Pascal, Institut de Chimie de Clermont-Ferrand, BP 80026, F-63171 AUBIERE, FRANCE*

[2]*CNRS, UMR 6296, ICCF, BP 80026, F-63171 AUBIERE, FRANCE*

e-mail : jean-yves.coxam@univ-bpclermont.fr

Aqueous solutions of amines are known to be selective absorbents for separation of acid gases. The so-called "amine washing" capture processes initially developed for natural gas sweetening could be in next future applied to remove carbon dioxide from industrial post combustion effluents. However, the energy costs of processes working on absorption-desorption cycles have to be reduced. Research is currently carried out on the amine structure which will reduce the energy of solvent regeneration. This energy depends on the mechanism of CO_2 dissolution, which is mainly a combination of chemical reactions, leading to formation of bicarbonates, carbonates or carbamates. The products of chemical reactions and then the energy of absorption will depend on the amine type and its basicity. In order to establish relationships between the amine structure and its absorbent properties, it is necessary to study the mechanism of gas dissolution. This can be achieved with the development of thermodynamic models representative of equilibrium in {CO_2-amine-water} systems [1]. The models must consider non ideality and then all interactions in a system containing both molecules and ions. Due to a lack of experimental data for enthalpy of solution, most of thermodynamic models have been optimized to fit CO_2 solubility data.

The presentation will describe the thermodynamic models used to represent the absorption of carbon dioxide in aqueous solution of amines. Particular attention will be paid on their ability to predict enthalpy of solution [1-2]. The presentation will also focus on the experimental studies required to develop rigorous models taking into account non ideality of multiphase systems. Flow calorimetric techniques used in our laboratory to investigate the enthalpy of solution [3] or the enthalpy of amine protonation [4] will be described.

References

[1] Arcis, H.; Rodier, L.; Ballerat-Busserolles, K.; Coxam, J.-Y. *J. Chem. Thermodynamics* **2009**, *41*, 783–789.

[2] Kim, I.; Hoff, K. A.; Hessen, E.T.; Haug-Warberg, T.; Swendsen, H. F. *Chem. Eng. Sciences.* **2009**, 64, 2027–2038.

[3] Arcis, H.; Ballerat-Busserolles, K.; Rodier, L.; Coxam, J.-Y. *J. Chem. Eng. Data.* **2012**, 57(3), 840–855.

[4] Arcis, H.; Ballerat-Busserolles, K.; Rodier, L.; Coxam, J.-Y. *J. Sol. Chem..* **2012**, 41, 130–142.

1JI01 Modeling Solvation of Some Cation-Crown Ether Complexes Using Density Functional Theory

H. D. Pranowo, S. Hadisaputra, R. Armunanto

Austrian-Indonesian Center for Computational Chemistry (AIC),
Chemistry Department, Faculty of Mathematics and Natural Sciences,
Universitas Gadjah Mada, Yogyakarta, Indonesia
e-mail : harnodp@ugm.ac.id; harnopranowo@yahoo.com

The structures, energetic and thermodynamic parameters of some crown ethers with different cavity size, electron donating/withdrawing substituent groups and donor atoms have been determined with density functional method at B3LYP level of theory in gas and solvent phase. Small core quasi-relativistic effective core potentials was used together with the accompanying SDD basis set for cation and DZP basis set was used for crown ether atoms. Natural bond orbital (NBO) analysis was evaluated to characterize the distribution of electrons on the complexes. The interaction energy is well correlated with the values of Strontium charge after complexation, the second order interaction energies (E_2) and HOMO-LUMO energy gab (ΔE_{gab}). The interaction energy and thermodynamics parameters in gas phase are reduced in solvent phase as the solvent molecules weaken the metal-crown ether interaction. The thermodynamic parameters indicated that less feasibility to extract cations ion directly from pure water without presence of organic solvent. The theoretical values of extraction energy for salts from aqueous solution in different organic solvent is validated by the experimental trend. This study would have strong contribution in planning the experiments to the design of specific host ligand and screening of solvent for extraction of metal ion.

References

[1] P. R. Varadwaj, A.Varadwaj, H. M. Marques, *J. Phys. Chem. A,* **115**, 5592–5601 (2011).

[2] A. Boda, S. M. Ali, M. R. K. Shenoi, Rao, H., S. K. Ghosh, *J. Mol. Model.*, **18**, 3507-3522 (2012).

[3] G. A. Shamov, G. Schreckenbach, R. L. Martin, P. J. Hay, *Inorg. Chem.* 47, 1465 1475 (2008).

[4] M. Ansarifard, G. Rounaghi, J. Incl. Phen. Macro. Chem., **52**, 39–44 (2005).

[5] Yahmin, H. D. Pranowo, A. Ria, *Indo. J. Chem.,* 11, 1, 106-109 (2011).

[6] Diao, K. S., Wang, H. J., Qiu, J. M., *J. Mol. Struct. (THEOCHEM)*, 901,157–162 (2009).

Oral Presentations

1AO01 Do H-Bonds Explain Strong Ion Aggregation in Ethylammonium Nitrate + Acetonitrile Mixtures?

T. Sonnleitner[1], V. Nikitina[2], A. Nazet[1] and R. Buchner[1]

[1]*Universität Regensburg, Regensburg, Germany*

[2]*Moscow State University, Moscow, Russia*

e-mail : Richard.Buchner@chemie.uni-regensburg.de

Due to their ability to form a three dimensional hydrogen bond network accompanied by fast proton transport protic ionic liquids (ILs) offer a wide range of potential applications. Ethylammonium nitrate (EAN) is of particular interest as it is claimed that the ability of each ion to form multiple hydrogen bonds promotes a heterogeneous structure reminiscent to that of water.[1] Dominant feature of water structure is its percolating network of H-bonds, fluctuating on a picoseconds timescale. Disturbing the connectivity of this network by addition of other compounds leads to mesostructure with pronounced consequences for the dynamic and the thermodynamic properties of aqueous mixtures. Keeping in mind the similarities between EAN and water it is interesting to explore also EAN mixtures for such features as they will crucially affect possible applications.

In this contribution we expand previous investigations of the cooperative dynamics of neat EAN[2] and report a dielectric relaxation study of EAN+acetonitrile mixtures. We found that EAN rich mixtures ($x_{EAN} > 0.6$) behave similar to mixtures of aprotic imidazolium ILs with acetonitrile, i.e. they can be viewed as "lubricated molten salts" where dynamics are speeded up with respect to the pure IL but hardly changed in character.[3] However, more dilute mixtures behave rather differently from imidazolium IL + acetonitrile mixtures. They show a plateau for molar conductivity in the range $0.05 < x_{EAN} < 0.4$ and a pronounced peak for the static permittivity at $x_{EAN} \approx 0.1$, compatible with pronounced ion association at low EAN concentrations. Analysis of the ion-pair relaxation revealed that the association constant of EAN in acetonitrile exceeds that of imidazolium ILs (and other electrolytes, like tetraalkylammonium salts) by almost two orders of magnitude. Simultaneously, evalution of the solvent relaxation revealed that ion solvation by acetonitrile is very weak. The rather constant relaxation time of the mode associated with cation reorientation observed for $0.15 < x_{EAN} < 0.6$, combined with the rapidly decreasing ion-pair amplitude, suggests that in this range larger clusters are readily formed. Possible reasons for these peculiar features indicating microheterogeneity are discussed

References

[1] K. Fumino, A. Wulf and R. Ludwig, *Angew. Chem., Int. Ed.*, 2009, **48**, 3184.

[2] D. A. Turton, T. Sonnleitner, A. Ortner, M. Walther, G. Hefter, K. R. Seddon, S. Stana, N. V. Plechkova, R. Buchner and K. Wynne, *Faraday Discuss.*, 2012, **154**, 145.

[3] A. Stoppa, J. Hunger, G. Hefter and R. Buchner, *J. Phys. Chem. B*, 2012, **116**, 7509.

1AO02 Dynamics, Solvation and Interionic Interactions in Mixtures of Room Temperature Ionic Liquid and Molecular Solvent: a Multitechnique Approach

B.A. Marekha[1,2], A. Idrissi[1], O.N. Kalugin[2], M. Bria[3]

[1]*Université Nord de France, Lille 1, LASIR, CNRS-UMR A8516, 59655 Villeneuve d'Ascq Cedex, France*

[2]*V.N. Karazin Kharkiv National University, 4 Svobody sq, 61022, Kharkiv, Ukraine*

[3]*Université Nord de France, Lille 1, CCM-RMN, 59655 Villeneuve d'Ascq Cedex, France*

e-mail : marekha.bogdan@ed.univ-lille1.fr

Room temperature ionic liquids (RTILs) have already found an impressive number of applications due to the versatility of their properties which are determined by their composition. In case of electrochemical application of the RTILs the diversity of credible systems can also be expanded by combining RTILs with common electrochemical solvents like acetonitrile (ACN). Many practically important properties of these mixtures (such as conductivity, viscosity *etc.*) are modulated by phenomenon of ionic association to ion pairs or to ionic aggregates of higher order. From the microscopic point of view, these properties of the mixtures of RTILs with molecular solvents (which can be regarded as solutions of RTILs) are defined by strong interionic interactions, especially by the structure motif of ion pairs.

Here we report the results of combined investigations on solutions of imidazolium-RTIL 1-butyl-3-methylimidazolium trifluoromethanesulfonate (BmimTfO) in ACN, propylene carbonate (PC) and γ-butyrolactone (γ-BL) by using multitechnique approach. Full miscibility of the selected RTIL with mentioned polar molecular solvents allows one to study these systems in terms of structure, dynamics and underlying interactions over entire composition range.

Multinuclear NMR spectroscopy on ^{1}H, ^{13}C, ^{19}F and ^{17}O nuclei was used to establish the sites in the structure of cation, anion and solvent molecules which are the most sensitive to changes in concentration. Analysis of chemical shift variation upon mixing of RTIL and molecular solvent revealed that complete dissociation of ion pairs is observed only in very dilute solutions (RTIL molar fraction less than 1%).

^{1}H-^{1}H NOESY and ^{1}H-^{19}F HOESY studies on concentrated solutions showed formation of large ionic aggregates without specific arrangement of ions reflecting significant degree of ionic association.

Relative diffusion coefficients of cation and solvent molecules obtained from ^{1}H NMR-diffusometry show a clear change in dynamics of the studied systems when molar fraction of RTIL exceeds 20%.

Solvation of the RTIL by solvent molecules as well as interionic interactions were thoroughly investigated by means of Raman spectroscopy. Two-dimensional correlation spectroscopy was employed to deduce the relative preference of interactions upon changing the composition of mixtures and to analyze the fine structure of the representative bands.

1AO03 Structure and Free Energy Analyses of CO_2 Solvation in Room-temperature Ionic Liquids

Yasuhiro Umebayashi[1], Hiroyuki Doi[1], Mitsuhiro Kanakubo[2], Takashi Makino[2], Kenta Fujii[3], Yasuo Kameda[4], Nobuyuki Matubayasi[5]

[1]*Graduate School of Science and Technology, Niigata University, Niigata 950-2181, Japan*
[2]*National Institute of Advanced Industrial Science and Technology (AIST), Sendai, 983-8551, Japan*
[3]*Institute for Solid State Physics, The University of Tokyo, Chiba 277-8581, Japan*
[4]*Department of Material and Biological Chemistry, Yamagata University, Yamagata 990-8560, Japan.*
[5]*Institute for Chemical Research , Kyoto University, Kyoto 611-0011, Japan*
e-mail : yumescc@chem.sc.niigata-u.ac.jp

Since *Nature* publication by Blanchard et al., room-temperature ionic liquids have attracted much attention as a CO_2 absorber due to high CO_2 solubility. To achieve higher CO_2 solubility in ionic liquids, it is crucial to reveal CO_2 solvation in ionic liquids at a molecular level. Currently, it is believed that CO_2 is dissolved around anion species rather than cation in ionic liquids except acetate based ones. In fact, CO_2 solubility strongly depends on the anion species, while it is practically independent from the alkyl chain length in the cation composing ionic liquids.

We have so far investigated liquid structure of ionic liquids by means of large-angle X-ray scattering (LAXS) and also high-energy X-ray diffraction (HEXRD) techniques with the aid of molecular dynamics simulations.[1-9] This molecular simulation aided techniques can be applied to rather complicated systems of both molecular and ionic liquids. We extended our work to solvation structure in ionic liquids, for example polymer in ionic liquids. [10-11] In this contribution, we report CO_2 solvation structures in various ionic liquids. In addition, solvation free energy calculations of CO_2 in ionic liquids can be performed by using molecular simulations with recently developed the Energy Representation method. We discuss CO_2 solvation in ionic liquids from the viewpoint of structure and free energy.

References

[1] K. Fujii et al., *J. Phys. Chem.* B **112**, 9449 (2008).
[2] S. Fukuda et al., *J. Mol. Liq.* **143**, 2 (2008).
[3] K. Fujii et al., *J. Mol. Liq.* **143**, 64 (2008).
[4] Y. Umebayashi et al., *J. Comp. Chem., Jpn.* **7**, 125 ((2008)).
[5] K. Fujii et al., *Chem. Lett.* **38**, 340 (2009).
[6] R. Kanzaki et al., *J. Mol. Liq.* **147**, 77 (2009).
[7] Y. Umebayashi et al., *J. Phys. Chem. B* **114**, 11715 (2010).
[8] K. Fujii et al., *J. Chem. Phys.* **135**, 244502 (2011).
[9] X. Song et al., *J. Phys. Chem. B* **116**, 2801 (2012).
[10] M. Matsugami et al., *Anal. Sci.* **29**, 311 (2013).
[11] H. Asai et al., *Macromolecules in print* (2013).

1AO04 Mixing State of Imidazolium-Based Ionic Liquid–Diglyme Solutions Studied by NMR and MD Simulations

T. Shimomura[1], D. Kodama[1], M. Kanakubo[2], and S. Tsuzuki[3]

[1]*Department of Chemical Biology and Applied Chemistry, College of Engineering, Nihon University, Koriyama 963-8642, Japan*

[2]*Research Center for Compact Chemical System, National Institute of Advanced Industrial Science and Technology, Sendai 983-8551, Japan*

[3]*Nanosystem Research Institute, National Institute of Advanced Industrial Science and Technology, Tsukuba 305-8568, Japan*

e-mail : t-shimo@chem.ce.nihon-u.ac.jp

Ionic liquids (ILs) have unique properties, such as low vapor pressure, thermal stability, high polarity, and electroconductivity. Thus, ILs have been investigated in various fields as novel solvents. ILs are frequently used by being mixed with molecular liquids, such as water and alcohols, to change their physicochemical properties. Physicochemical properties of IL–molecular liquid solutions should derive from their mixing state at the molecular level; however, there are a few reports on the mixing state of IL–molecular liquid solutions.

In the present study, we have investigated the mixing state of imidazolium-based ionic liquid, 1-butyl-3-methylimidazolium bis(trifluoromethanesulfonyl)amide (C_4mimTFSA) and diglyme (diethylene glycol dimethyl ether) solutions by means of NMR and molecular dynamics (MD) simulations. ^{1}H and ^{13}C NMR chemical shifts of the solutions over the entire mole fraction range of diglyme, $0 \leq x_{\mathrm{diglyme}} \leq 1$, were observed to clarify intermolecular interactions between C_4mim^+ and diglyme from the changes in the electron densities of the hydrogen and carbon atoms. Furthermore, MD simulations were performed on C_4mimTFSA–diglyme solutions to elucidate the solvation structure of C_4mim^+ in the solutions.

The MD simulations revealed that the number of the $TFSA^-$ oxygen atoms that interact with the imidazolium hydrogen atoms of C_4mim^+ in pure IL is gradually decreased on addition of diglyme. This is probably because $TFSA^-$ at the imidazolium hydrogen atoms is replaced by diglyme due to the interaction between the imidazolium hydrogen atoms and diglyme. In fact, the MD and NMR results suggested that the oxygen atoms of diglyme interact with the imidazolium hydrogen atoms. However, the number of the $TFSA^-$ oxygen atoms that interact with the imidazolium hydrogen atoms in the C_4mimTFSA–diglyme solutions remained ~40% of that in pure IL ($x_{\mathrm{diglyme}} = 0$) even at $x_{\mathrm{diglyme}} = 0.9$. The electrostatic interaction between the imidazolium cation and $TFSA^-$ is sufficiently strong in the solutions even at the mole fraction. As a result, not only the $TFSA^-$ anion but also diglyme interact with the imidazolium cation in the C_4mimTFSA–diglyme solutions.

1AO05 High Pressure Transport Properties of Ionic Liquids

K. R. Harris

School of Physical, Environmental and Mathematical Sciences,
University College,
University of New South Wales,
Canberra, ACT2610, Australia
e-mail : k.harris@adfa.edu.au

High pressure measurements have been made of viscosities, ion self-diffusion coefficients and electrical conductivities of ionic liquids, including imidazolium, pyrrolidinium and phosphonium salts. Such measurements facilitate the separation of the competing effects of temperature and density. We review how these properties have been analysed in terms of the empirical Stokes-Einstein, Walden and Nernst-Einstein equations, and examine trends revealed by the phenomenological approach of velocity correlation coefficients and the more general theory of density scaling.

1AO06 How Mesoscopic Bulk Structures Affect Interfaces of Ionic Liquids?

T. Iwahashi[1], Y. Sakai[2], D. Kim[2], T. Ishiyama[3], A. Morita[3] and Y. Ouchi[1]

[1]*Department of Chemistry, Nagoya University, Nagoya 464-8602, Japan,*
[2]*Department of Physics, Sogang University, Seoul 121-742, Korea,*
[3]*Department of Chemistry, Tohoku University, Sendai 980-8578, Japan*
e-mail : ohuchi@chem.nagoya-u.ac.jp

Room temperature ionic liquids (RTILs) are ionic compounds that are composed solely of ionic species and are in a liquid phase under 100 °C. Though a number of reports have discussed the structural and physico-chemical properties of RTILs, not many papers have studied how RTIL-specific mesoscopic structures may affect those of surfaces and interfaces. In this study, we have carried out a series of experiments using interface selective IR-Vis sum-frequency generation (IV-SFG) vibrational spectroscopy[1-3] together with MD simulations to solve these unsolved problems.

Figure 1 shows SFG spectra of H_2O/[$C_n$mim][NTf_2] interfaces from n = 4 to 12. A broad peak at ~1170 cm^{-1} is assigned to the SO_2 symmetric stretch (SO_2-ss) mode inhomogeneously broadened by the presence of hydrogen bonding of H_2O molecules at the interface. It should be noted that the peak amplitude A_q of the SO_2-ss mode strongly depends on the alkyl chain length n of $[C_n\text{mim}]^+$ cation. The amplitude is much larger for n = 8 than that for n = 4, indicating that the $[NTf_2]^-$ anion configuration at the interface is strongly affected by the alkyl chains of cations. However, the peak amplitude is gradually decreased at n = 10 and 12, suggesting that another controlling parameter for molecular ordering at the interface should exist other than the length of the alkyl chain, n. Our MD simulations have successfully demonstrated that the interface structure for n = 12 is deteriorated by the presence of characteristic domain structure of bulk RTILs. Delicate balances of charge-ordering of RTILs and those with the water phase for the formation of liquid/liquid interfaces are important and will be discussed in detail.

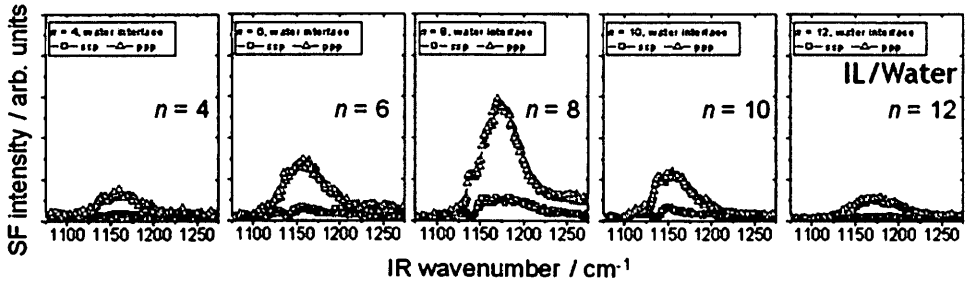

Figure 1 IV-SFG spectra(*ssp, ppp*) of water/[$C_n$mim][NTf_2] (n=4~12) interfaces.

References

[1] T. Iwahashi *et al.*, *ACS symposium series 1030*, (2009) 305- 316.

[2] T. Iwahashi *et al.*, *Phys. Chem. Chem. Phys.* **12**, 12943(2010).

[3] T. Iwahashi *et al. Faraday Discuss.* **154**, 289(2012).

1AO07 Solvation Structure of Poly(ethylene glycol) in 1-ethyl-3-methylimidazolium-based Ionic Liquids

Kenta Fujii,[1] Hanako Asai,[1] Yasuhiro Umebayashi,[2] and Mitsuhiro Shibayama[1]

[1] Institute for Solid State Physics, The University of Tokyo, 5-1-5 Kashiwanoha, Kashiwa, Chiba 277-8581, Japan.

[2] Graduate School of Science and Technology Niigata University, 8050, Ikarashi, 2-no-cho, Nishi-ku, Niigata City, 950-2181, Japan.

e-mail: k-fujii@issp.u-tokyo.ac.jp

Solvation structures of poly(ethylene glycol) (PEG) in 1-ethyl-3-methylimidazolium-based ionic liquids solution were studied by using high-energy X-ray diffraction (HEXRD) and molecular dynamics (MD) simulation in terms of dependences on the anion-type for ILs, molecular weight (M_w), concentration of PEG.[1] It was found from HEXRD experiment that there is no M_w dependence for PEG in 1-ethyl-3-methylimidazolium bis(trifluoromethansulfonyl)amide, [C_2mIm$^+$][TFSA$^-$] solution, implying that the local structure (r < 15 Å) is not influenced by the M_w. From the HEXRD results with the aid of MD simulations, it was found that C_2mIm cation preferentially solvates to PEG in all the ILs, and the anion (TFSA, FSA and BF_4 examined here) is distributed randomly with van der Waals and weak electrostatic interactions. The atom-atom pair correlation and space distribution functions evaluated from the MD simulations revealed that hydrogen bonding interactions are formed between C2 carbon within the imidazolium ring and O (PEG), which is essentially different from C4 carbon-O and C5 carbon-O interactions. Finally, we discussed the relationship between the obtained microscopic solvation structures and the macroscopic properties of PEG-based gel (swelling ratio and χ parameters).

[1] H. Asai, K. Fujii, K. Nishi, T. Sakai, K. Ohara, Y. Umebayashi, and M. Shibayama, *Macromolecules*, **46**, 3269 (2013).

1AO08 Phase behavior and dielectric property of ionic liquid $(C_8mim)BF_4$

K. Watanabe[1], A. Nimonji[1], and K. Negita[1]

[1]*Department of Chemistry, Faculty of Science, Fukuoka University, Fukuoka 814-0180, Japan*

e-mail : keisukew@fukuoka-u.ac.jp

Ionic liquids have been worth of remark among scientists and engineers. A large number of studies have been made on ionic liquids. However, it is not well known about the structure and the properties. One of the difficulties in the studies is that after temperature change ionic liquids need quite long time to reach thermal equilibrium, and hence true equilibrated values of physical quantities have been often hindered, which is pronounced especially at low temperature. Here our concern is to capture the phase behaviour and dynamics of ionic liquids steadily. To this end, we tried to obtain the temperature dependence of the dielectric constant of ionic liquid, 1-octyl-3-methylimidazolium tetrafluoroborate $(C_8mim)BF_4$, by taking sufficiently long equilibration time, more than 3000 s, at any temperature. The sample was outgassed under vacuum for 2 days to remove the water and other volatiles contained in the sample since impurity of ionic liquids tends to hamper such studies. The content of the water was confirmed by Karl-Fischer titration to be 164.7ppm.

– – The dielectric constant obtained was not particular on cooling from room temperature to the glass transition temperature, T_g. However, on heating from T_g an abrupt depression of the dielectric constant was observed around 223 K and then a steep, two-stage rise around 240 K. The former might correspond to crystallization and the latter melting point, T_m. It is noteworthy that, on the heating we observed quasi-periodic humps of the dielectric constant in the course of equilibration at 193 K, just above T_g, and 223 K, the crystallization temperature, respectively. Both periodicities were about 500 s, and intermittent crystal nucleation or growth is suggested, but it remains to be proved in future works.

Getting further into the crystallization, on a heating measurement we annealed the sample at 223 K in the course of the equilibration. The quasi-periodic humps of the dielectric constant became less and less intense as time passed, and the baseline was gradually lowered. After 5 days the baseline shift finished although the humps had still been observed. Assuming the shift stems mainly from the crystallization, it might have been almost completed. Further heating the crystal lead to a small peak of the dielectric constant just below T_m around 235 K, which indicated a solid-solid phase transition.

In a calorimetric study about 1-alkyl-3-methylimidazoim tetrafluoroborate $(C_nmim)BF_4$ (n = 0 – 18) by Holbrey et al.[1], they reported the melting and clouding points of ionic liquids with the alkyl chains longer than 10, indicating only a glass transition was found for $(C_8mim)BF_4$. The reason why the calorimetry detected neither crystallization nor melting may be the DSC scanning rate, 5 K min^{-1}, which was so fast that the crystallization couldn't occur due to its slowness.

References

[1] J. D. Holbrey, K. R. Seddon, *J. Chem. Soc., Dalton Trans.* **13**, 2133-2139 (1999).

1AO09 Kinetics of Water-Mediated Fluctuations in Room Temperature Ionic Liquid: *N*, *N*-Diethyl-*N*-methyl-*N*-(2-methoxyethyl) Ammonium Tetrafluoroborate

H. Abe[1], Y. Imai[1], M. Aono[1], H. Kishimura[1], T. Takekiyo[2], and Y. Yoshimura[2]

[1]*Department of Materials Science and Engineering, National Defense Academy, Yokosuka 239-8686, Japan*

[2]*Department of Applied Chemistry, National Defense Academy, Yokosuka 239-8686, Japan*

e-mail : ab@nda.ac.jp

Recently, room temperature ionic liquids (RTILs) are highlighted in terms of "green chemistry". The RTILs typically have vapour pressure near zero and are nano-heterogeneous. Water-mediated *N*, *N*-diethyl-*N*-methyl-*N*-(2-methoxyethyl) ammonium tetrafluoroborate, [DEME][BF_4], show anomalous mixing in phase diagram [1], liquid structure [2], hierarchy structure [3] and time evolution of *p*H [4]. Hydrogen bonding of water is a key to interpret the complicated behaviours.

By time-resolved small angle X-ray scattering (SAXS), it was found that fluctuations in [DEME][BF_4] – 70.8 mol% H_2O gradually developed at the fixed temperature (293 K) as shown in Fig. 1. Here, Q is provided to be $4\pi(\sin\theta)/\lambda$ (nm^{-1}). Time dependent SAXS depends extensively both on Q value and water concentrations. A significant finding is that SAXS intensities fluctuate at smaller Q-region. The Q dependent fluctuations might have a relation with the hierarchy structure in the liquid [3]. The kinetic the heterogeneity in the mixture has a relationship with *p*H rhythmic oscillations [4], where collective motion of proton is dominant in the mixtures.

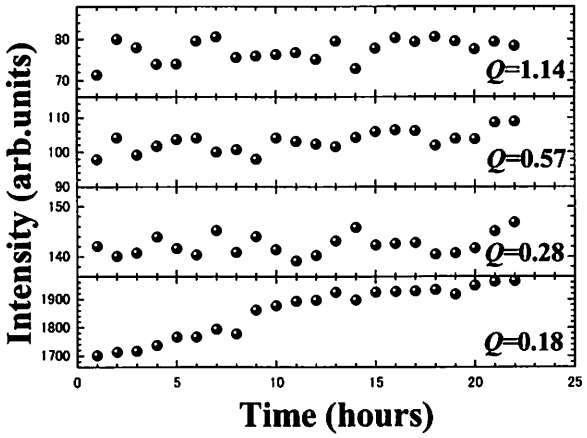

Fig. 1 Time dependence of SAXS in 70.8 mol% mixture.

References

[1] H. Abe, Y. Yoshimura, Y. Imai, T. Goto, H. Matsumoto, *J. Mol. Liq.* **150**, 16 (2009).

[2] H. Abe, Y. Imai, T. Takekiyo, Y. Yoshimura, *J. Phys. Chem. B* **114**, 2834 (2010).

[3] M. Aono, Y. Imai, Y. Ogata, H. Abe, T. Goto, Y. Yoshimura, T. Takekiyo, H. Matsumoto, T. Arai, *Metal. Mater. Trans.* **42**A, 37 (2011).

[4] M. Aono, Y. Tomita, H. Abe, Y. Yoshimura, *Chem. Lett.* **41**, 1532 (2012).

1AO10 Structure and Physicochemical Properties for Solvate Ionic Liquids Composed of Glymes and Na[TFSA] or K[TFSA]

T. Mandai,[1] S. Terada,[1] K. Yoshida,[1] S. Tsuzuki,[2] K. Ueno,[1] K. Dokko,[1] and M. Watanabe[1,*]

[1]*Department of Chemistry and Biotechnology, Yokohama National University, Yokohama, 240-8501, Japan*

[2]*National Institute of Advanced Industrial Science and Technology (AIST), Ibaraki 305-8568, Japan*

e-mail : mwatanab@ynu.ac.jp

Due to the characteristic physicochemical properties, equimolar binary mixtures of lithium salts and glymes have attracted much attention in recent years. Appropriate combination leads to molten mixtures at ambient temperature and they behave like typical ionic liquids.[1] The glymes and Li^+ ions form robust complex cations as component cations, and hence, they are categorized into "solvate ionic liquids". Although there are many reports on the solvate structures, physicochemical properties, and their applications as electrolytes for Li-secondary batteries,[2] studies on the mixtures involving other alkali metal salts are remarkably little. It can be anticipated that equimolar mixtures of Na- or K-salts and certain glymes are also regarded as solvate ionic liquids.

In this study, we focus on the binary mixtures composed of Na[TFSA] or K[TFSA] and a series of glymes, such as tetraglyme (G4), pentaglyme (G5) and hexaglyme (G6). Equimolar mixing of these salts and appropriate glymes results in the thermally, chemically, and electrochemically stable complexes. X-ray structure analyses revealed their solvate structures in the crystalline state. The characteristic solvate structures depending on the glyme length and the centre metal species were clarified (Figure). Melting point of $[K(G5)_1][TFSA]$ is 35.9 °C and this value is slightly higher than that of $[Na(G5)_1][TFSA]$ (31.7 °C) in spite of lower Lewis acidity of K^+ cation compared to Na^+ cation. Differences in the coordination and packing structures can cause this phenomenon. We will also discuss about the results of *ab initio* calculation and other physicochemical properties.

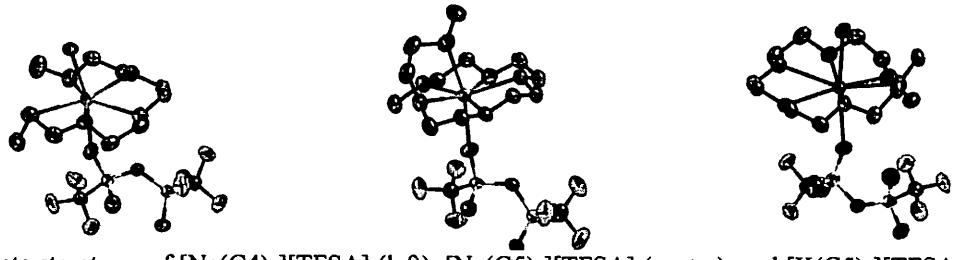

Figure. Solvate structures of $[Na(G4)_1][TFSA]$ (left), $[Na(G5)_1][TFSA]$ (center), and $[K(G5)_1][TFSA]$ (right) in the crystalline state.

References

[1] K. Ueno, K. Yoshida, M. Tsuchiya, N. Tachikawa, K. Dokko, M. Watanabe, *J. Phys. Chem. B*, **116**, 11323 (2012).

[2] (a) K. Yoshida, M. Nakamura, Y. Kazue, N. Tachikawa, S. Tsuzuki, S. Seki, K. Dokko, M. Watanabe, *J. Am. Chem. Soc.*, **133**, 13121 (2011). (b) N. Tachikawa, K. Yamauchi, E. Takashima, J. -W. Park, K. Dokko, M. Watanabe, *Chem. Commun.*, **47**, 8157 (2011).

1AO11 Solvation Structure of Ni(II) Ion in Imidazolium-based Ionic Liquid–Molecular Liquid Mixtures

H. Hoke[1], Y. Yamada[1], T. Shimomura[2], T. Umecky[1], T. Takamuku[1]

[1]*Department of Chemistry and Applied Chemistry, Saga University, Saga 840-8502, Japan*
[2]*Department of Chemical Biology and Applied Chemistry, College of Engineering, Nihon University, Fukushima 963-8642, Japan*
e-mail : takamut@cc.saga-u.ac.jp

Ionic liquids attract much attention from various research fields, such as electrochemistry and green chemistry. In analytical chemistry, many researchers have examined to use ionic liquids as extraction solvents for metal ions. Generally, ionic liquids have a high viscosity. This often prevents ionic liquids from being used in extraction. One of the possible solutions on this inconvenience is mixing of ionic liquids with molecular liquids, such as alcohols. To develop the application of ionic liquids to analytical chemistry as extraction solvents, information on solvation and complexation of metal ions in ionic liquids–molecular liquid mixtures is essential.

In this investigation, we have examined solvation structure of Ni(II) ion in imidazolium-based ionic liquid of 1-ethyl-3-methylimidazolium bis(trifluoromethanesulfonyl)amide (C_2mimTFSA) with methanol, acetonitrile, and dimethyl sulfoxide (DMSO). First, the mixing states of the mixtures were observed using ^{1}H, ^{13}C NMR and ATR-IR techniques. $Ni(TFSA)_2$ was then dissolved into the C_2mimTFSA–molecular liquid mixtures at various mole fractions of molecular liquid. The electronic spectra of the solutions were recorded on an UV/vis. spectrometer to clarify the solvation structure of Ni(II) ion. Furthermore, X-ray crystallographic analysis was conducted on crystals precipitated.

The electronic spectra of the $Ni(TFSA)_2$–C_2mimTFSA solutions showed that Ni(II) ion forms a complex with octahedral structure in the ionic liquid. In fact, the previous investigation revealed the formation of $[Ni(tfsa)_3]^-$ in TFSA-based ionic liquids, where $TFSA^-$ plays a role as a bidentate ligand [1]. With increasing molecular liquid content, $TFSA^-$ ions within the first coordination shell are replaced by molecular liquid molecules. The replacement significantly depends on the coordination properties of the molecular liquid molecules. DMSO molecules stoichiometrically replace $TFSA^-$ to form $[Ni(dmso)_6]^{2+}$. Actually, the X-ray analysis on a single crystal obtained from the DMSO solution revealed the formation of $[Ni(dmso)_6](TFSA)_2$. In acetonitrile solutions, the replacement of $TFSA^-$ by acetonitrile molecules is moderately taken place with increasing acetonitrile mole fraction. Methanol molecules showed the intermediate property between DMSO and acetonitrile. These findings are consistent with the Gutmann's donor number of D_N = 7 [2], 14.1, 19.0, and 29.8 for $TFSA^-$, acetonitrile, methanol, and DMSO, respectively.

References

[1] K. Fujii, T. Nonaka, Y. Akimoto, Y. Umebayashi, S. Ishiguro, *Anal. Sci.*, **24**, 1377 (2008).
[2] Y.-L. Zhu, Y. Katayama, T. Miura, *Electrochim. Acta*, **55**, 9019 (2010).

1AO12 Ionization Reaction Thermodynamics in Protic Ionic Liquid, Ethylammonium Nitrate

R. Kanzaki[1], Y. Kusamura[1], X. SONG[2], H. Doi[3], and Y. Umebayashi[3]

[1] *Graduate School of Science and Engineering, Kagoshima University, 1-21-35, Korimoto, Kagoshima 890-0065, Japan*

[2] *State Key Laboratory of Fine Chemicals, Dalian University of Technology, Linggong Road 2, Dalian 116024, P. R. China.*

[3] *Graduate School of Science and Technology, Niigata University, 8050, Ikarashi, 2-no-cho, Nishi-ku, Niigata 950-2181, Japan*

e-mail : kanzaki@sci.kagoshima-u.ac.jp

Ions are solvated by solvent-ions with opposite charge in ionic liquids. Solvent-effect on reactions involving ions in ionic liquids may be quite different from that in conventional molecular solvents. In this study, acid-base reactions were used for clarifying difference between molecular solvents and ionic liquids in their solvent-effect. The solute is ionized through acid-base reaction and the solvation state is changed while its chemical structure is mostly kept.

Ethylammonium nitrate (EAN), which is a typical protic ionic liquid (PIL), were used as a medium for acid-base reaction. Acid-dissociation constant pK_a, acid-base reaction enthalpy $\Delta H°$ and entropy $\Delta S°$ of 8 compounds of different-types (acetic acid, benzoic acid, phthalic acid, α- and β-alanine, trifluoroethylamine, adenine, phosphoric acid) have been determined by means of potentiometric and calorimetric titrations in neat EAN.

In most cases, pK_a values are larger in EAN than those in water. The difference in pK_a is around 1 without remarkable variation among compounds. That is, no practical deviation in the difference in pK_a is observed in any case including acetic acid that is ionized to an anion, trifluoroethylamine that is ionized to a cation, and zwitterionic alanines. This implies that solvation behaviour of EAN onto ions is similar to water. Dissociation enthalpies in EAN for most compounds are larger about 25 kJ/mol than that in water, and deviation among the compounds are not found. Therefore, the slightly larger pK_a than that in water is caused not by the difference in the solvation state of ions but mainly by the difference in the practical proton donor; HNO_3 in EAN and H_3O^+ in water. Dissociation entropies in EAN, shown in Fig. 1, are also larger in EAN than that in water. The difference shows slight deviation depending on the functional group implying a difference in the solvation manner while an exact interpretation is not established.

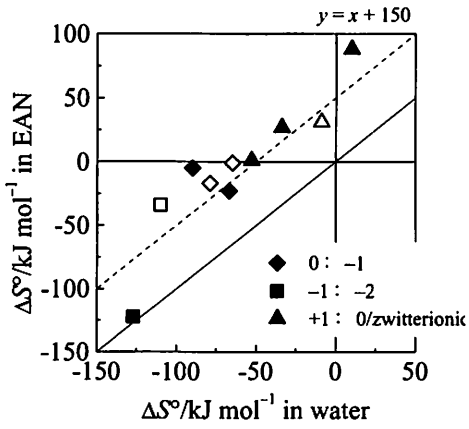

Fig. 1 Dissociation entropies in EAN vs. in water. Filled symbols are for hydrophilic compounds and opened symbols are for hydrophobic ones

2AO13 Possibility of specific proton conduction in *N*-methylimidazole-acetic acid equimolar mixture

Hiroyuki Doi[1], Xuedan Song[2], Kenta. Fujii[3], Ryo Kanzaki[4], Takuya Miyazaki[5], Yasuo Kameda[5], and Yasuhiro Umebayashi[1]

[1] *Graduate School of Science & Technology, Niigata University 950-2181, Japan*

[2] *State Key Laboratory of Fine Chemicals, Dalian University of Technology, Dalian 116024, P. R. China.*

[3] *Institute for Solid State Physics, The University of Tokyo, 277-8581, Japan*

[4] *Graduate School of Science and Engineering, Kagoshima University, 890-0065, Japan*

[5] *Department of Material and Biological Chemistry, Yamagata University, 990-8560, Japan*

e-mail : yumescc@chem.sc.niigata-u.ac.jp

Protic Ionic Liquids PILs with a dissociable hydrogen atom have attracted remarkable attention as electrolytes of fuel cells. Acid-base property of PILs as a solvent plays an important role in such an application. It is thus necessary to clarify the acid-base property of PILs quantitatively. Autoprotolysis constant K_s has been used as one of the measures of solvent acid-base property, so that it can be applied to PILs similarly. We reported thermodynamics of autoprotolysis reaction in ethylammonium nitrate based on direct pH measurements and precise calorimetry for the first time. [1-3] Recently, $pK_s = -\log K_s$ values were reported for *N*-methylimidazole C_1Im equimolar mixtures with various acids. [4] We found that pK_s for C_1Im and acetic acid AcOH equimolar mixture was practically negative, indicating that electrically neutral species of C_1Im and AcOH exist to some extent in the mixture, though it is believed that the mixture yields PIL of $[C_1hIm^+][AcO^-]$ by proton transfer from AcOH to C_1Im.

However, we focused on significant ionic conductivity of 4 mS cm^{-1} [5] for the mixture. For further insight into ion conduction in the mixture, ionic conductivity, viscosity and density were investigated at various temperatures. In addition, Raman spectroscopic study and quantum calculations were performed to reveal predominant species in the mixture; ions of C_1hIm^+ and AcO^- or electrically neutral molecules of C_1Im and AcOH. We found that ionic species are practically negligible in the mixture. Taking it into consideration, the Walden plots for the mixture located upper region of the ideal Walden line [6] proposed by Angell. This suggests specific proton conduction could occur in the mixture. Moreover, High Energy X-ray Diffraction experiments with the aid of MD simulations were carried out to elucidate hydrogen bonded network liquid structure of the mixture. Finally, we proposed a specific proton conduction mechanism operates in the mixture.

References

[1] R. Kanzaki et al., *Chem. Lett.*, **36**, 684(2007).
[2] R. Kanzaki et al., *Anal. Sci.*, **24**, 1347(2008).
[3] R. Kanzaki et al., *Chem. Lett.*, **39**, 578(2010).
[4] R. Kanzaki et al., *J. Phys. Chem. B*, **116**, 14146(2012).
[5] D. R. MacFarlane et al., *Chem. Commun.*, 1905(2006).
[6] W. Xu et al, *Science*, **302**, 422(2003)

2AO14 Excess Electron in an Ionic Liquid

R. Musat[1], T. Kondoh[2], Y. Yoshida[2] and K. Takahashi[1]

[1]*Institute of Science and Engineering, Kanazawa University, Kakuma-machi, Kanazawa, 920-1192, Japan*

[2]*The Institute of Scientific and Industrial Research (ISIR), Osaka University, 8-1 Mihogaoka, Ibaraki 567-0047, Japan*

e-mail : rmusat@se.kanazawa-u.ac.jp

Room Temperature Ionic Liquids (RTILs) have recently been exploited in numerous applications due to their properties. In particular their low volatility, recyclability, high conductibility and low flammability make them excellent candidates for "green" solvents in industrial applications and electrolytes in high performance Li-ion batteries. Their chemistry is currently being investigated, but despite intense efforts, debate still exists about the basic reactions governing it. Their degradation has turned the application of classical investigative methods to RTILs chemistry a challenge. We have used a single shot detection method coupled to pulse radiolysis studies to– study of excess charge dynamics in 1-butyl-1-methylpyrrolidinium bis(trifluoromethylsulfonyl)imide, $P_{14}NTf_2$. We were able to record the spectrum of the solvated electron in P14NTf2 and follow its reaction dynamics. Scavenging experiments allowed us to deconvolute the absorbance spectrum and assign each band. The solvated electron exhibits a two features absorbance spectrum with a peak at 1080 nm and one at 320 nm. The absorption spectrum measured in the UV region is more complex, as we observe a contribution from the hole in this region. Our experimental results confirm previous theoretical computation results.[1] The absence of spectral diffusion indicates that the solvation is complete within 2 ns (our time resolution limit). The decay kinetics at 900 nm and 320 nm show that the solvated electron has a relatively long lifetime, of a few hundred nanoseconds.

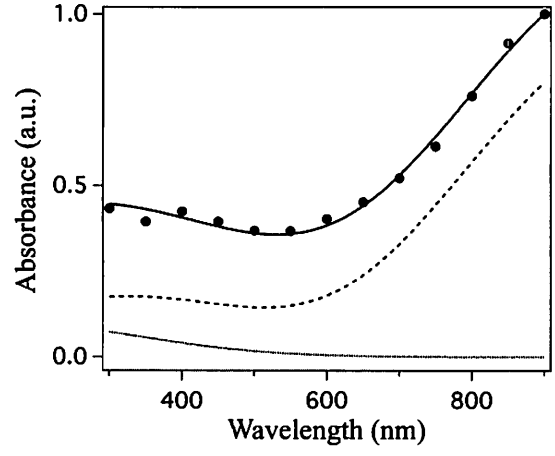

Figure 1. Experimental and fitted induced normalized absorbance spectra in $P_{14}NTf_2$ (black). Deconvoluted absorbance spectra of the electron (dashed line) and hole (dotted line) in $P_{14}NTf_2$ extracted from scavenging experiments. The individual spectra were offset for clarity.

References

[1] C.J. Margulis, H.V.R. Annapureddy, P.M. De Biase, D. Coker, J. Kohanoff, and M.G. Del Pópolo, *J.A.C.S.* **133**, 20186 (2011).

2AO15 Protonation and Copper(II)-complexation in Protic Ionic Liquids Comprised of *N*-Hexylethylenediaminium Cation

M. Iida[1], S. Takemura[1], M. Watanabe[1], and M. Harada[2]

[1] *Department of Chemistry, Nara Women's University, Nara 630-8506, Japan*

[2] *Department of Textile and Apparel Science, Nara Women's University, Japan*

e-mail : iida@cc.nara-wu.ac.jp

Protonation sites and complexations of copper(II) ions with a protic ionic liquid (PIL) comprised of *N*-hexyl-ethylenediaminium (= $HHexen^+$) bis(trifluoromethanesulfonyl)amide (= $TFSA^-$) (or trifluoroacetate (= TFA^-)) were studied by NMR, EXAFS, and VIS electronic spectroscopy. The protonation sites were dependent on the counter anion as described in Fig. 1. The present PILs are advantageous to accept metal ions owing to the chelating amine structure. The selective sites of the interactions for copper(II) ions in the PILs were clarified in comparing with such analogous liquids as hexylaminium (= HHexam)(TFSA)-PIL, neat *N*-hexylethylenediamine (= Hexen), and neat ethylenediamine (= En). The selective site-binding of copper(II) ion in the PIL system was monitored through paramagnetic broadenings of ^{13}C NMR spectra of the PILs by copper(II) ions. The ^{13}C NMR spectra showed that in the HHexen(TFSA)-PIL, copper(II) ion prefers the chelate amine of the HHexen cation rather than the TFSA anion while in the HHexam(TFSA)-PIL it prefers the TFSA anion over the amine.

Both the EXAFS and VIS electronic spectra showed that in the HHexen(TFSA)-PIL, copper(II) ion binds to the shorter four amines and to the longer two oxygen atoms of the TFSA anions. On the other hand, in the HHexen(TFA)-PIL, copper(II) ion tends to coordinate to the shorter four amines and to the longer two amines (Jahn-Teller effect), which is similar to that in the neat Hexen liquid.

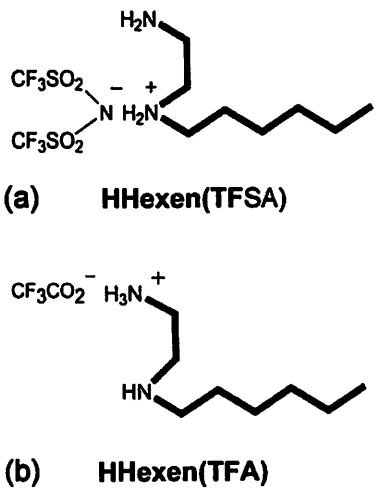

Fig. 1

2AO16 Surface Analysis of Ionic Liquids with and without Lithium Salt Using XPS Spectroscopy

T. Kurisaki[1], D. Tanaka[1], Y.Inoue[1], H.Wakita[1], B.Minofar[2], S.Fukuda[2], S.Ishiguro[2], and Y. Umebayashi[2]

[1]*Department of Chemistry, Fukuoka University, Fukuoka 814-0180, Japan*

[2]*Department of Chemistry, Kyushu University, Fukuoka 812-8581, Japan*

e-mail : wakita@fukuoka-u.ac.jp

XPS(X-ray photoelectron spectroscopy) was applied to a neat ionic liquid 1-ethyl-3-methylimidazolium bis(trifluoromethansulfonyl)imide [EMI^+][Tf_2N^-] and its lithium salt solution at room temperature to clarify the composition and structure of its near-surface region[1].

Core level peaks were recorded for Li 1s, N 1s, C 1s, F 1s, O 1s, S 2s, and S 2p. Valence band XPS spectra(0-40eV binding energy) were also studied. The XPS spectra were analysed using DV-Xα calculations[2]. Results show that the planar type isomer of the EMI^+ cation is dominant at the near-surface region of EMI- Tf_2N.

Results of XPS measurements show a spectrum of Li 1s in Li/ EMI- Tf_2N. The proposed models for the preferred orientation of the ions exhibit good agreement with results obtained from the DV-Xα calculations.

The details are as follows[1,2].

References

[1] T. Kurisaki, D. Tanaka, Y.Inoue, H.Wakita, B.Minofar, S.Fukuda, S.Ishiguro, and Y. Umebayashi, *J. Phys. Chem. B*, 116, 10870(2012).

[2] H. Adachi, M. Tsukada, C. Satoko, *J. Phys. Soc. Jpn.* 45, 875(1978): T.Kurisaki, S.Matsuo, R.C.C.Perera, J.H.Underwood, H.Wakita, *Adv. Quantum Chem.*, 54, 315(2008).: T.Kurisaki, S.Matsuo, I.Toth, H.Wakita, *Anal. Sci.*, 24, 1385(2008).

2BO01 Intermolecular Electron Density Modulations and the Terahertz Spectral Intensities of Liquid Water

Hajime Torii

Department of Chemistry, School of Education, Shizuoka University, 836 Ohya, Shizuoka 422-8529, Japan

e-mail : torii@ed.shizuoka.ac.jp

We can observe many kinds of dynamics in liquids with different choices of spectroscopic methods, and theoretical analysis is often helpful to know what the spectral profiles really mean. With regard to the IR and far-IR (THz) spectra, it is well known that the spectral profiles are determined by the correlation function of the system's dipole, and since the motions of any charged particles are involved, one sometimes faces the problem of the coupling between the motions of electrons and atomic nuclei. A simple idea would be that the electrons faithfully follow the atomic nuclei, and this is employed in the models with fixed atomic partial charges. The next step would be to take into account the intramolecular polarizations induced by intermolecular electrostatic interactions, for example, with the dipole-induced dipole model. However, there is no guarantee that this is (practically) sufficient for all cases.

Such a problem really exists for the THz spectrum of liquid water, especially the intensity of the band at ~6 THz (200 cm^{-1}). This band is known to arise from the H...O hydrogen-bond stretching motions (molecular translations with regard to the motions of individual molecules), but molecular translations of a neutral molecule do not give rise to IR intensity without intermolecular interactions. It has been pointed out that the IR intensity arising from intramolecular polarizations induced by intermolecular electrostatic (such as dipole-induced dipole) interactions is not sufficiently strong [1].

By analyzing the electron density modulations induced by molecular motions occurring in water clusters, it is shown that intermolecular transfer of electron density (called *intermolecular charge flux*) is induced by molecular translations of hydrogen-bonded water, and this is the main origin of the IR intensity of the band at ~6 THz [2]. There would be two ways for including this effect into the spectral simulations based on MD. One is to adopt the formula based on the time derivative of system's dipole for calculating the spectra, and combine the dipole derivatives with respect to molecular translations and rotations obtained by DFT calculations on water clusters and the molecular velocities and angular velocities in the liquid obtained from MD [2]. The other is to analyze the dependence of the extent of intermolecular transfer of electron density on molecular configurations, and include it in calculating the system's dipole in the course of the MD simulations. The results obtained with these two ways will be compared and discussed in the present study.

References

[1] M. Heyden, M. Havenith, *Methods* **52**, 74 (2010).

[2] H. Torii, *J. Phys. Chem. B* **115**, 6636 (2011).

2BO02 Vibrational spectral diffusion and hydrogen bond dynamics of molecular solute in aqueous solution: ab initio molecular dynamics study of Formaldehyde and Uracil in water

Vivek Kumar Yadav[1], and Amalendu Chandra[1]

[1]*Department of Chemistry, Indian Institute of Technology Kanpur,208016 India*
e-mail: viveky@iitk.ac.in

Various functional groups in chemical and biological systems are far from being simple and often complicated interplay of different order of interactions exists among them. Furthermore these systems being flexible are of dynamical nature. We present a first principle theoretical study of vibrational spectral diffusion and hydrogen bond dynamics in formaldehyde and uracil in aqueous solution without using any empirical potential at room temperature. The trajectories of the systems were generated by using *ab initio* molecular dynamics [1,2] and time series analysis was done by wavelet method [3] for frequency calculations. It is found that although a one to one relation does not exist between instantaneous frequency of an OD bond and the distance of its corresponding hydrogen bond, such a relation does hold on an average. We have employed the dispersion correction functional (BLYP-D) proposed by Grimme [4] in our simulations and compared it with our results having no dispersion corrections (BLYP). The dynamics of spectral-diffusion is investigated by means of frequency time correlation [5] and spectral hole dynamics calculations [6]. The results we obtained are compared with the existing theoretical and experimental findings.

References

[1] R. Car and M. Parrinello, *Phys. Rev. Lett.* **55,** 2471(1985).

[2] J. Hutter, A. Alavi, T. Deutsch, M. Bernasconi, S. Goedecker, D. Marx, M. Tuckerman, and M. Parrinello, CPMD Program, MPI für Festkörperforschung and IBM Zurich Research Laboratory.

[3] L. V. Vela-Arevalo, and S. Wiggins, *Int. J. Bifurcation Chaos Appl. Sci. Eng.* **11**,1359 (2001).

[4] S. Grimme, *J. Comput. Chem.* **25**, 1463(2004); *J. Comput. Chem.* **27**, 1787(2006); *Comp. Mol. Sci.*, **1**, 211(2011).

[5] B. S. Mallik, and A. Chandra, *J. Chem. Sci.* **124**, 215 (2012).

[6] B. S. Mallik, A. Semparithi, and A. Chandra, *J. Chem. Phys.* **129**, 194512(2008); *J. Phys. Chem. A* **112**, 5104 (2008).

2BO03 Some weak molecular interactions affected by the structure and composition of the solvation shell in binary solutions

S. Kunsági-Máté

[1]*Department of General and Physical Chemistry, University of Pécs, Ifjúság 6, H-7624 Pécs, Hungary*

[2]*János Szentágothai Research Center, Ifjúság 20, H-7624 Pécs, Hungary*

e-mail : kunsagi@gamma.ttk.pte.hu

Weak molecular interactions (ΔG~few tens kJ/mol) are an important group of chemical processes due to their reversible, temperature-dependent behavior. This weak property has significant consequences at wide scale of chemistry and biochemistry especially when the species interacted are surrounded in complex environment. Our previous works highlighted the unique structure of the solvation shell formed in binary solutions around molecules possessing aromatic moieties [1,2]. The stability of these solvation shells affects also the kinetics of complex formations [3]. To get deeper insights into this property, the dynamics of solvent molecules around a family of phenolic derivatives was examined first in ethanol – water mixtures [2]. Result shows significant change of the solvent relaxation times at a typical molar fraction of ethanol and highlights that the composition of the solvation shell in binary mixtures is far from the composition of the bulk solution [2]. To check some biological consequences, complexation ability of water-soluble tiacalix[4]arene-tetrasulfonate towards three aromatic amino acids (Phenylalanine, Tyrosine and Tryptophane) was studied in water-ethanol mixtures [4]. Interaction of Ochratoxin A towards Human Serum Albumin [5] and the effect of solvation shell structure on the structural transformations of weakly bounded antocyanine – polyphenol molecular complexes in water – ethanol mixtures was also studied [6].

Acknowledgement: Financial supports of the TÉT-10-1-2011-0043 and the SROP-4.2.2.A-11/1/KONV-2012-0065 project is gratefully projects are acknowledged.

References

[1] S. Kunsági-Máté, K. Iwata, *Chem. Phys. Lett.* **473**, 284 (2009).

[2] S. Kunsági-Máté, K. Iwata, *J. Solution. Chem.* **42**, 165 (2013).

[3] S. Kunsági-Máté, A. Kumar, P. Sharma, L. Kollár, M.P. Nikfardjam, *J. Phys. Chem. B* **113**, 7468 (2009).

[4] S. Kunsági-Máté, S. Lecomte, E. Ortmann, É. Kunsági-Máté, B. Desbat, *J. Incl. Phenom. Macrocycl. Chem.* **66**(1-2), 147 (2010).

[5] S. Kunsági-Máté, B. May, C. Tshiersch, D. Fetzer, I. Horváth, L. Kollár, M.P. Nikfardjam, *Food Res. International* **44**, 23 (2011).

[6] M. Poór, S. Kunsági-Máté, G. Matisz, Y. Li, Zs. Czibulya, B. Peles-Lemli, T. Kőszegi, *J. Lumin.* **135**, 276 (2013).

2BO04 Infrared study of water complexes with inorganic compounds in KBr matrix.

I.I.Grinvald, I.V. Vorotyntsev, I.Yu. Kalagaev, E.A. Sutjagina, A.N. Petukhov

Department of Chemistry, Nizhny Novgorod State Technical University, Nizhny Novgorod 603155, Russia

e-mail: *kalagaev@inbox.ru*

The investigations of samples containing water in infrared region are restricted owing to the sensitivity of optical materials to water action, whereas the stable components are transmitting in high frequency range only. We have proposed the variant of infrared measurements of such patterns in the KBr matrix. This approach based on the inputting of the investigated gas or liquid samples into KBr powder with the pressing of this one in pallet. Hereby we have presented the IR study results of the interaction of water with ammonia, carbon dioxide and ammonia-carbon dioxide mixture in KBr matrix.

Water-ammonia system in KBr matrix.

This system was investigated in two ways: **a**) gas passes through liquid water before KBr saturation, **b**) the water vapours and ammonia were inputted together into the KBr matrix. In first case a new bands at 3248 and 1405 cm^{-1} appear. They may be reasonably assigned to the proton vibrations in $[n(H_2O)\cdot(H_3O^+)\cdots m(NH_3)]$ complex. At the saturation of KBr powder with ammonia and water vapours (variant **b**) only band at 3237 cm^{-1} is observed. These results indicate that in both cases the water intermediates formate, but in variant (**b**) the proton transfer does not occur.

Water-carbon dioxide system in KBr matrix.

This samples were prepared in the same ways (**a** and **b**). In the first one we have observed the water bands at 3500 and 1640 cm^{-1}. The band, which can be assigned to the stretching of $[CO_3]^{-2}$ anion locates at 1405 cm^{-1} and is very weak. In the case (**b**) this band is observed at 1399 cm^{-1} and its intensity is close to the water bending band. At the same time the shoulder to the water stretching band (3580 cm^{-1}) arises at 3163 cm^{-1}. Both manifestations in the spectra indicate on the formation and transformation of water-carbon dioxide complex in KBr matrix. The quantum-chemical calculation in terms of DFT study predicts such opportunity.

Water - carbon dioxide- ammonium system in KBr matrix.

For this system the sample was prepared in the following way: carbon dioxide was passed through the water layer and was inputted together with the ammonia into the KBr matrix. The IR spectra show a few of new bands in comparison with the spectra of water, ammonia or carbon dioxide in KBr matrix. These bands resemble the spectral picture for ammonium and carbonic acid salts. That's why we can assume the formation of complexes with CO_2, NH_3 and water fragments.

Acknowledgment: This work has been financially supported by Russia Foundation of Basic Research, Grant No11-08-00707.

2BO05 Vibrational Dynamics of $[RuCl_5(NO)]^{2-}$ in Aqueous Solution Studied by Nonlinear Infrared Spectroscopy

Kyoko Aikawa[1], Kaoru Ohta[2], and Keisuke Tominaga[1,2]

[1] *Graduate School of Science, Kobe University, Japan*

[2] *Molecular Photoscience Research Center, Kobe University, Japan*

e-mail : tominaga@kobe-u.ac.jp

In aqueous solution, molecular dynamics is characterized by a wide time scale ranging from a few tens of femtoseconds to a few picoseconds. The characteristic behavior of water dynamics results from its three-dimensional network structures formed by intermolecular hydrogen bonds. The vibrational modes of solute molecule are a good probe to investigate local structure and microscopic dynamics around the oscillator. In this study, we examine vibrational dynamics of the NO stretching mode of $[RuCl_5(NO)]^{2-}$ (NR) in light and heavy water. We performed polarization resolved infrared (IR) pump-probe and two-dimensional (2D) IR spectroscopic methods to discuss the vibrational energy relaxation (VER), the rotational relaxation and the frequency fluctuation, $C(t)$.

The VER time constant of the NO stretching mode of NR at 293 K is 7.7 and 30.8 ps in H_2O and D_2O, respectively. These values decrease about 10% in both the solvents from 283 K to 313 K. The rotational relaxation time constant of NR at 293 K is 20 and 30 ps in H_2O and D_2O, respectively. These values decrease about 50% in both the solvents from 283 K to 313 K. The obtained 2D-IR spectrum is shown in Fig. 1(a). The center line slope (CLS) of the 2D IR signal is plotted against the population time T in Fig. 1(b). In order to simulate the CLS and the IR absorption spectra, we characterize the time correlation function (TCF) with a tri-exponential function. We have obtained the TCF of frequency fluctuation from three-pulse IR photon echo experiment using various anions in aqueous solutions [1]. From these studies, the TCF is modeled by two time constants. The slower component depends only on solvent, and it is 1–1.5 ps for aqueous solutions. It can be considered to originate from the structural fluctuation of the hydrogen-bond network of the water molecules surrounding the solute. In this study we detected a slower component with a time constant of several piscoseconds, which could be originated from dynamics of solvent molecules bound do the solute strongly.

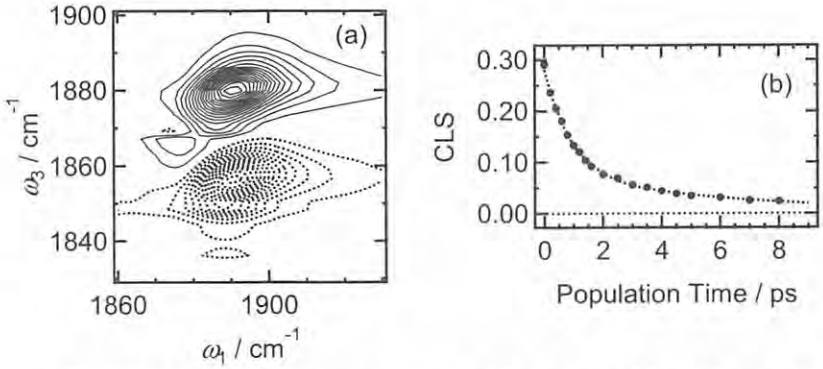

Figure 1. (a) The 2D-IR spectra of NR in H_2O at T = 200 fs. Solid and dotted line indicate positive and negative amplitude, respectively. **(b)** The CLS of NR in H_2O plotted against population time.

References

[1] K. Ohta *et al.*, *Acc. Chem. Res.*, **45,** 1982 (2012).

2CO01 Phase separation of glassy dilute LiCl aqueous solution and water polyamorphism

Yoshiharu Suzuki and Osamu Mishima

[1] *National Institute for Materials Science (NIMS), Ibaraki 305-0044, Japan*
e-mail : suzuki.yoshiharu@nims.go.jp

Introduction

Recent studies of the super-cooled liquid water (H_2O) suggest that two liquid waters, low-density liquid water (LDL) and high-density liquid water (HDL), exist at low temperatures and that a liquid-liquid-critical point (LLCP) relating to the two waters exists. Many experimental and theoretical results strongly suggest that this new concept for liquid water, so-called water polyamorphism, is plausible, although the existence of LLCP has not been shown experimentally. We think that the reconsideration of the water in aqueous solution from the viewpoint of water polyamorphism is important for the understanding not only of the anomalous properties of low-temperature liquid water but also of the dynamical properties of aqueous solutions. In this presentation we will talk about the relation between the state of solvent water in electrolyte aqueous solution and the two waters (LDL and HDL).

Experiment and Results

We vitrified lithium chloride aqueous solutions (LiClaq solutions) below ~10 mol% by cooling from room temperature to 77 K at 0.3 GPa. The solvent state of the glassy sample and its transformation by heating at 1 atm were examined using low-temperature differential scanning calorimetry and Raman spectroscopy.

As the LiCl concentration decreased, the Raman profile of glassy LiClaq solution gradually resembled that of high-density amorphous ice (HDA). [1, 2] This suggested that the solvent state of the glassy LiClaq solution was categorized in the HDL group. When the glassy LiClaq solution below ~10 mol% was heated at 1 atm, the separation into the low-density amorphous ice and the glassy highly-concentrated LiClaq solution occurred at ~130 K, not the glass-to-liquid transition which was commonly observed in the glassy LiClaq solution above ~10 mol%. The sudden switchover between the glass-to-liquid transition and the phase separation at ~10 mol% suggested that the phase separation related to the glass-to-liquid transition of the glassy dilute LiClaq solution. [2] Using these experimental results, we constructed a polyamorphic state diagram of LiClaq solution from a viewpoint of water polyamorphism. We will discuss that the phase separation in LiClaq solution is consistent with the water polyamorphism.

References

[1] Y. Suzuki, O. Mishima, *J. Chem. Phys.* **117**, 1673 (2002).

[2] Y. Suzuki, O. Mishima, *J. Chem. Phys.* **138**, 084507 (2013).

2CO02 Pressure-Induced Liquid-Liquid Transitions: Search in a Polymer Melt

Ayano Chiba[1], Mikihito Takenaka[2], and Nobumasa Funamori[3]

[1]*Department of Physics, Keio University, Yokohama 223-8522, Japan*
[2]*Department of Polymer Chemistry, Kyoto University, Kyoto 615-8510, Japan*
[3]*Department of Earth and Planetary Science, University of Tokyo, Tokyo 113-0033, Japan*
e-mail : ayano@phys.keio.ac.jp

Pressure-induced liquid-liquid phase transitions have been attracted a lot of attention. These are transitions between two liquids with different macroscopic properties such density, viscosity, entropy, and different microscopic structures. The existence of a first order transition of liquid phosphorous is now well known [1]. Also well-known is the amorphous-amorphous transition in ice which has been found in an experiment as early as 1985 [2], and liquid-liquid transition in water which has been theoretically proposed [3] and studied intensively so far.

If there are similar liquid-liquid transformations in polymer melts, it would be interesting to compare the phenomena between simpler small molecule based systems and polymer systems from the viewpoint of "polyamorphism". The aim of our study [4] is thus to do an in-situ search for a liquid-liquid transformation in a polymer melt by x-ray diffraction. A good candidate material is isotactic poly(4-methyl-1-pentene) (P4MP1), whose melting curve (temperature) shows a maximum as a function of pressure [5]. Our x-ray diffraction measurements at constant temperatures above the melting curve maximum shows a clear pressure-induced change at the peak around 0.6 $Å^{-1}$. This result suggests the structural change shown in the figure below. It was found that the change is clear but not first-order. The change is reversible with pressure increase and decrease. In the conference we briefly review some liquid-liquid transitions and show our results for P4MP1. We show the similarities of the structural changes of this polymer to that of simpler systems such as SiO_2 glass.

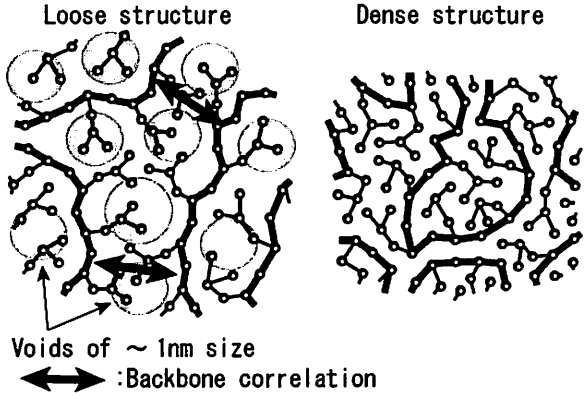

Figure: Two structures of P4MP1 melt; for the low-pressure range (left) and the high-pressure range (right).

References

[1] Y. Katayama, *et al.*, *Nature* **403**, 170 (2000).

[2] O. Mishima, L. D. Calvert, E. Whalley, *Nature* **314**, 76 (1985).

[3] P. H. Poole, F. Sciortino, U. Essmann, H. E. Stanley, *Nature* **360**, 324 (1992).

[4] A. Chiba, N. Funamori, K. Nakamura, Y. Ohishi, S. M. Bennington, S. Rastogi, A. Shukla, K. Tsuji, M. Takenaka, *Phys. Rev. E* **85**, 021807 (2012).

[5] S. Rastogi, M. Newman, A. Keller, *Nature* **353**, 55 (1991).

3CO03 Molecular Dynamics Study of Aqueous NaCl Solution: Flush Crystallization Caused by Solution Phase Change

K. Kobayashi[1], Y. Liang[1], and T. Matsuoka[1]

[1]*Environment and Resource System Engineering, Kyoto University, Kyoto 615-8540, Japan*
e-mail: kobayashi.kazuya.44n@st.kyoto-u.ac.jp

Aqueous solutions are essential to life, biology, chemistry, and geology because of their ubiquitousness in nature. In geological aspect, crystallization occurred under high pressure and high temperature condition (e.g. oceanic volcanoes in ocean ridges) receives much attention because it indicates how geological salt system formed [1]. In this condition, aqueous solutions can change its phase and the flush crystallization occurs due to the extremely low solubility of salt [2]. Here, molecular dynamics simulations of the salt-solution interfacial system were executed to observe the flush crystallizations at sub- and supercritical conditions (i.e. 150, 250, and 450 bar), respectively. At the phase boundary, we observed extreme reduction of solubility at all the pressures. Furthermore, differences in dynamics of flush crystallization were observed through the correlation coefficients of the density of fluids and the density of ions. At sub-critical conditions, the vapour phase of water (with extremely low concentration of salt) coexists with the salt crystal, while the liquid and vapour phases of solutions coexist with the crystals at supercritical conditions. The results provide us the classification of geological systems under high pressure and high temperature.

References

[1] M. Hovland, H.G. Rueslatten, H.K. Johnsen, B. Kvamme, and T. Kuznetsova, *Marine and Petroleum Geology*, **23**, 855-869(2006)

[2] F.J. Armellini and J.W. Tester, *J. Supercritical Fluids*, **4**, 254-264(1991)

3CO04 Vibrational Spectrum Line Shape for Supercritical Water: Effect of Rotational Couplings on Density, Temperature, and Hydrogen Isotopes Dependencies

K. Yoshida[1], N. Matubayasi[2,3,4], Y. Uosaki[1], M. Nakahara[2]

[1] *Department of Chemical Science and Technology, Faculty of Engineering, University of Tokushima, 2-1 Minamijosanjima-cho, Tokushima 770-8506, Japan*

[2] *Institute for Chemical Research, Kyoto University, Uji, Kyoto 611-0011, Japan*

[3] *Japan Science and Technology Agency (JST), CREST, Kawaguchi, Saitama 332-0012, Japan*

[4] *Elements Strategy Initiative for Catalysts and Batteries, Kyoto University, Katsura, Kyoto 615-8520, Japan*

e-mail : yoshida@chem.tokushima-u.ac.jp

The origin of the line shape of the O–H stretch vibrational spectrum for supercritical water was analyzed by using classical molecular dynamics simulation for the flexible point-charge model over a wide range of the temperature and the density (400–1200 °C, 0.01–1.0 g cm^{-3}). The SPC/Fw model was found to successfully reproduce the experimental IR spectrum at low densities of 0.01–0.04 g cm^{-3} and at 400 °C [1]. The spectrum line shape consists of broad rotational bands and a sharp component due to the O–H stretch oscillation. The rotational couplings get significant as the time-scale separation between the vibration and rotations becomes invalid for supercritical water at high temperatures. The molecular interpretations are presented in terms of the thermal acceleration of the rotations and the attractive (hydrogen-bonding) and repulsive (high-packing) potential effects dependent on density variation. The vibrational spectrum cannot be decomposed into definite chemical clusters for the thermodynamic and kinetic analysis because of the dynamic origin.

To observe the effect of the rotational velocities, we extensively investigated the line shapes as a function of the moment of inertia of the water through heavy hydrogen isotope substitutions [2]. The frequency differences between the sharp center peak and the rotational broad side-bands are found to be linearly correlated with the inverse of the moment of inertia, which is clear molecular-level evidence for the rotational couplings. We further elucidated that the sharp peak intensity is associated with the long-time component of the reorientational time correlation function for the stretching bond vector. The present analysis is not dependent on any intuitive assumptions specific to a particular thermodynamic state or a model, and thus provides a realistic molecular picture of the dynamics from the isolated molecule to the rather solvated ones in the low- to medium-density supercritical water.

References

[1] K. Yoshida, N. Matubayasi, Y. Uosaki, M. Nakahara, J. Chem. Phys., **137**, 194506 (2012).

[2] K. Yoshida, N. Matubayasi, Y. Uosaki, M. Nakahara, J. Chem. Phys., in press (2013).

3CO05 Local structure in sub and supercritical water: IR spectroscopy and molecular dynamic simulation analysis

F. Lafrad [1,2], T. Tassaing[2] and A. Idrissi[1]

[1]*Université Nord de France, Lille1 LASIR (UMR8516), Villeneuve d'Ascq, 59650, France*
[2]*Institute of Molecular Sciences (UMR 5255) University of Bordeaux I, Bordeaux 33405, France*
e-mail : nacer.idrissi@univ-lille1.fr

The purpose of this paper is to probe by infrared absorption spectroscopy and molecular dynamics simulations the evolution of the local order of sub- and supercritical water along the isobar 220 bar and in the temperature range between 298 and 612 K. Infrared absorption measurements were performed along this isobar using an isotopic water mixture of D_2O and H_2O with the molar ratio of 1:20 leading to a mixture of D_2O, HOD and H_2O with molar proportions of 1:40:400, respectively. The evolution of the shape of the infrared profiles associated with the O-D stretching mode of HOD and the combinations $\nu_3+\nu_2$ and $\nu_3+\nu_1$ of H_2O reveal a progressive weakening upon the temperature increase of the hydrogen bond network existing in liquid water at room temperature.

In order to get a molecular description of such experimental results, Molecular Dynamics simulations of water were performed using a cubic simulation box consisting of 864 water molecules modeled with the TIP4P potential in the (N,P,T) ensemble. We have characterized the local structure using the radial distribution function, the nearest neighbor approach, the Voronoi polyhedral (VP), the tetrahedral and the cluster distributions. Our results show that with increasing the temperature, the volume, the surface, the face area, and the vertex radius of the Voronoi Polyhedra distributions broaden and a second contribution at large values of these parameters appears at temperature higher than T_c at which the thermal expansion displays its maximum value. Furthermore, the rate of increase of the corresponding average values and the corresponding fluctuation increases drastically when approaching T_c. This behavior clearly indicates that the local structure as described by the VP becomes more and more heterogeneous when approaching this temperature. This heterogeneous distribution of water molecules is traced back to the increase of the large voids with increasing the temperature and is clearly seen in the behavior of the fluctuation of the local density as measured by the Voronoï polyhedral. More interestingly, the maximum in the heterogeneity coincide with the maximum of the fluctuation in the density of the VP.

3CO06 Pressure and Temperature effect on the β-hairpin model peptides: mutants of GB1 (41-56)

K. Tsuchiya[1], K. Fujimura[2], and M. Kato[1,2]

[1]*GraduateSchool of Life Science and* [2]*College of Pharmaceutical Sciences, Ritsumeikan University, Kusatsu 525-8577, Japan.*

e-mail to M. Kato: kato-m@ph.ritsumei.ac.jp

In general, protein folds into a unique structure and the structure unfolds by perturbing temperature and pressure. For understanding the mechanism of pressure unfolding of proteins, recently we have been performing systematic studies using model peptides. In the present study, we focus on the β-hairpin structure, which is the simplest β-structure. The current targeted peptides of research are some mutants for the GB1 segment peptide which are composed of residues 41-56 of the B1 domain of protein G (GB1). This β-hairpin peptide is well known to be stabilized by the hydrophobic interactions between W43 and V54, and between Y45 and F52. Previously, we have reported pressure effect on the secondary structure of Trpzip4, which is the triple mutant (W43Y45F52V54→W43W45W52W54) of GB1 segment peptide [1], showing the pressure-induced refolding. In the present work, we have expanded the research project to the other kinds of mutants, W43W45V52W54 (hereafter, WWVW) and W43W45F52W54 (hereafter, WWFW).

For analyses of the secondary structure, we used FTIR spectroscopy, which is available for measurements under high pressure. The infrared spectra of WWVW mutant showed the amide I' peaks around 1635 cm^{-1} and 1675 cm^{-1}, which are assigned to a typical antiparallel β-structure. These peak intensities decreased with increasing temperature (Figure 1) and pressure (Figure 2), indicating, respectively, the thermal- and pressure-induced unfolding the β-hairpin. We compare the results for WWVW and WWFW together with Trpzip4, and discuss the substitutional (hydrophobic) effects on the pressure-induced structural changes in the secondary structure of β-hairpins.

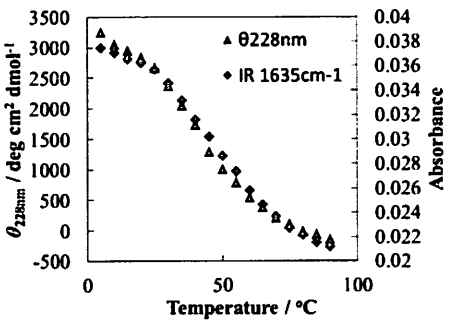

Fig. 1. Temperature dependence of CD results at 228 nm (left) and FT-IR spectra absorbance at 1635 cm^{-1} (right) of WWVW (7.2 - 86.0 °C).

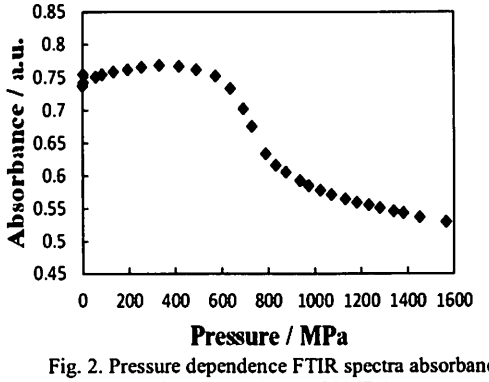

Fig. 2. Pressure dependence FTIR spectra absorbance at 1637 cm-1 of WWVW (0.1- 1566 MPa).

References

[1] Y. Yamaoki, K. Fujimura, H. Imamura, and M. Kato, 2010 International Chemical Congress of Pacific Basin Societies (December 15-20, 2010, Honolulu USA)

4CO07 Pressure-induced Conformational Change of 1-Butyl-3-methylimidazolium Tetrafluoroborate

M. Shigemi[1], T. Takekiyo[1], H. Abe[2], and Y. Yoshimura[1]

[1]*Department of Applied Chemistry, and* [2]*Department of Materials Science and Engineering, National Defense Academy, Kanagawa 239-8686, Japan*

e-mail : em51038@nda.ac.jp

Ionic liquids (ILs) comprising of an organic cation and an anion have received considerable attentions as environmentally benign solvents for their appealing properties such as negligible vapour pressure and thermal stability [1]. High pressure phase behavior of ILs have been studied to obtain the basic information of the recycling and purification of ILs. The study of conformational change of ILs under high pressure is necessary to clarify the moleculer orientation in conjunction with the complicated phase behavior. In our previous study, we reported that 1-butyl-3-methylimidazolium tetrafluoroborate ([bmim][BF_4], figure 1) didn't crystallize up to 1.4 GPa and the *gauche-trans* (*GT*) conformer of the N1-C7-C8-C9 and C7-C8-C9-C10 angles slightly increased with increasing pressure [2]. Su *et al.* [3] reported that the *GT* conformer of [bmim][BF_4] increased up to 2.25 GPa. On the other hand, some of other imidazolium-based ILs have been known to exhibit crystal polymorphism associated with the conformational changes of the alkyl chain of the cation at low temperature [4, 5] and high pressure [6]. Based on these results, we expected that the significant conformational change of [bmim][BF_4] may occur at higher pressure region.

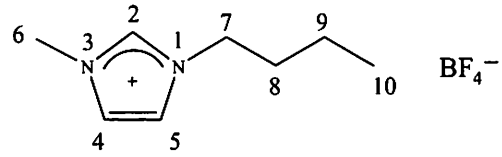

Fig. 1. The chemical structure of [bmim][BF_4] and the numbering of skeleton atoms of [bmim]$^+$.

In this study, we have investigated the pressure-induced conformational change and the phase behavior of [bmim][BF_4] by a JASCO NR-1800 Raman spectroscopy combined with the diamond anvil cell (DAC). Our results revealed that the *GT* conformer increases up to *ca.* 2.5 GPa but subsequently decreases above the pressure.

References

[1] T. Welton, *Chem. Rev.*, **99**, 2071 (1999).

[2] Y. Yoshimura, T. Takekiyo, Y. Imai, H. Abe, *Ionic Liquid - Classes and Properties*, Intech publishing Croatia Chap. 8, 150 (2011).

[3] L. Su, Z. Wang, X. Cheng, Y. Wang, C. Yuan, Z. Chen, C. Ma, F. Li, Q. Zhou, Q. Cui, *J. Phys. Chem. B*, **116**, 2216(2012).

[4] H. Hamaguchi, R. Ozawa, *Adv. Chem. Phys.*, **131**, 85 (2005).

[5] T. Endo, R. Kato, K. Tozaki, K. Nishikawa, *J. Phys. Chem. B*, **114**, 407 (2010).

[6] S. Saouane, S. E. Norman, C. Hardacre, F. P. A. Fabbiani, *Chem. Sci.*, **4**, 1270 (2013).

4CO08 Molecular Rotational Relaxation in Room-Temperature Ionic Liquids at High Pressures

N. Kometani, and A. Tai

Department of Applied Chemistry & Bioengineering, Graduate School of Engineering, Osaka City University, Osaka 558-8585, Japan

e-mail : kometani@a-chem.eng.osaka-cu.ac.jp

To probe the local chemical environments around solute molecules dissolved in room temperature ionic liquids (RTILs), the rotational relaxation dynamics of solutes has been investigated by several research groups. It has been revealed that the rotational relaxation time (τ_r) in RTILs can generally be accounted for within the framework of hydrodynamic theory, showing the proportional correlation between τ_r and η/T, where η and T represent the solvent viscosity and temperature, respectively. However, in most of previous studies, the solvent viscosity has been varied by altering the kind of solvent or changing temperature. This method is not suited for examining the pure viscosity dependence of τ_r, because the significant change of solvent structure or the simultaneous variation of η and T is inevitable. In this study, the viscosity has been changed by applying a high pressure to RTILs, which enables us to change the viscosity alone without the alternation of solvent structure and temperature. The rotational dynamics of perylene and its anionic derivative, MPTS, in three kinds of RTILs, 1-butyl-3-methylimisazolium tetrafluoroborate ([bmin]BF_4), 1-butyl-3-methylimisazolium hexafluorophosphate ([bmin]PF_6), and 1-hexyl-3-methylimisazolium hexafluorophosphate ([hmin]PF_6), were examined using time-resolved fluorescence depolarization spectroscopy from atmospheric pressure to 400 MPa at a fixed temperature of 318 K.

Fig. 1 shows a double logarithmic plot of τ_r vs η for perylene in RTILs. Here, viscosities at high pressures were taken from the literature data. As seen in Fig. 1, the rotational relaxation times are close to the prediction of hydrodynamic theory using slip boundary condition, indicating that perylene is located in a hydrophobic environment because it is known that perylene rotates with slip behaviour in organic oils like paraffin. More interestingly, the slop of these plots is shallower than predicted by hydrodynamic theory, which means that τ_r is less sensitive to the change of viscosity than that predicted by hydrodynamic theory. Such behaviour may be understood by "free space model" suggested by Dote, Kivelson, and Schwartz [1], implying the occurrence of robust network structure incorporating voids in RTILs.

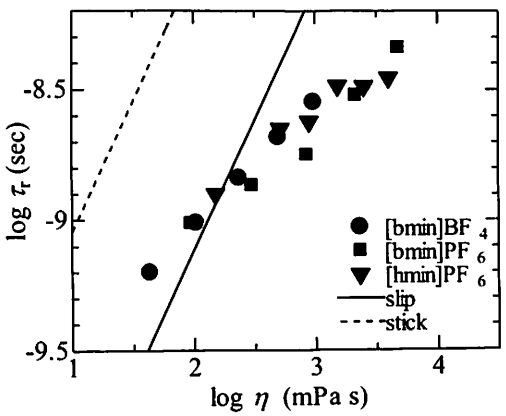

Fig. 1 The plot of τ_r vs η for perylene in [bmin]BF_4, [bmin]PF_6, and [hmin]PF_6 at high pressures.

References,

[1] J. L. Dote, D. Kivelson, R. N. Schwartz, *J. Phys. Chem.* **85**, 2169(1981).

4DO06 Spectrophotometry Study of Th(IV) Hydroxo Complexes Destruction Kinetics in Aqueous Solution

A.V. Radkevich, V.V. Torapava, and V.S. Labko

Joint Institute for Power and Nuclear Research - Sosny, Minsk 220109, Belarus

e-mail : artem-rav@yandex.ru

It is known that Th(IV) cations hydrolyze in aqueous solution with formation of different hydrolytic species: mononuclear – $Th(OH)_n^{(4-n)+}$, polynuclear – $Th_p(OH)_q^{(4p-q)+}$ hydroxo complexes, pseudocolloid and colloid particles. Therefore kinetics study of Th(IV) hydrolytic reactions is complicated by simultaneous presence of various metal ion forms possessing common chemical and physical properties. As a result there is a problem to obtain correlation between analytical signal and specific hydroxo complex concentration.

Our kinetics study of Th(IV) hydroxo complexes destruction was performed by spectrophotometry of Th(IV)–arsenazo-III complex. This complex, with absorption maximum at λ=665 nm, is formed with hydrated cation $Th(H_2O)_n^{4+}$ only, whereas complexes of hydrolyzed Th(IV) species with arsenazo-III don't have such optical characteristics. That's why we can determine selectively the concentration of Th^{4+}-cation in solution, containing various Th(IV) species.

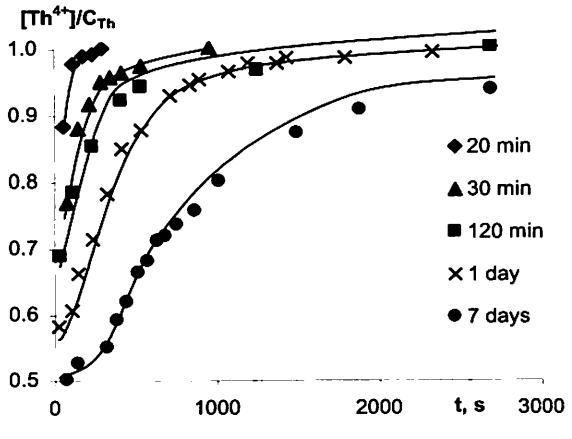

Influence of solution "aging" time on Th(IV) polynuclear hydroxo complexes destruction

Kinetics experiments were performed at $C_{Th}=1\cdot10^{-5}$ – $1\cdot10^{-3}$ M and pH 2.0 – 5.0. It was shown that the observed change in optical density correlate to Th(IV) polynuclear hydroxo complexes destruction.

Though the reaction kinetics is not elementary, in can by closely approximated by the following equation:

$$v = -\frac{d[Th_{poly}]}{dt} = k_{eff}[Th_{poly}][H^+]$$

The values of k_{eff} are shown in the table

"Aging" time	$k_{эфф}$, $M^{-1}c^{-1}$	"Aging" time	$k_{эфф}$, $M^{-1}c^{-1}$
20 min	6.01	1 day	0.79
30 min	1.45	7 days	0.26
120 min	1.04		

The obtained results significantly depend on "aging" time of solutions, that is the evidence of continuous hydrolysis process and transition to kinetically inert hydroxo complexes. This fact indicates, that metal-ion hydrolysis is a multi step reaction, and the reaction end cannot be always determined by such indirect features such as constant solution pH value.

4CO08 Molecular Rotational Relaxation in Room-Temperature Ionic Liquids at High Pressures

N. Kometani, and A. Tai

Department of Applied Chemistry & Bioengineering, Graduate School of Engineering, Osaka City University, Osaka 558-8585, Japan

e-mail : kometani@a-chem.eng.osaka-cu.ac.jp

To probe the local chemical environments around solute molecules dissolved in room temperature ionic liquids (RTILs), the rotational relaxation dynamics of solutes has been investigated by several research groups. It has been revealed that the rotational relaxation time (τ_r) in RTILs can generally be accounted for within the framework of hydrodynamic theory, showing the proportional correlation between τ_r and η/T, where η and T represent the solvent viscosity and temperature, respectively. However, in most of previous studies, the solvent viscosity has been varied by altering the kind of solvent or changing temperature. This method is not suited for examining the pure viscosity dependence of τ_r, because the significant change of solvent structure or the simultaneous variation of η and T is inevitable. In this study, the viscosity has been changed by applying a high pressure to RTILs, which enables us to change the viscosity alone without the alternation of solvent structure and temperature. The rotational dynamics of perylene and its anionic derivative, MPTS, in three kinds of RTILs, 1-butyl-3-methylimisazolium tetrafluoroborate ([bmin]BF_4), 1-butyl-3-methylimisazolium hexafluorophosphate ([bmin]PF_6), and 1-hexyl-3-methylimisazolium hexafluorophosphate ([hmin]PF_6), were examined using time-resolved fluorescence depolarization spectroscopy from atmospheric pressure to 400 MPa at a fixed temperature of 318 K.

Fig. 1 shows a double logarithmic plot of τ_r vs η for perylene in RTILs. Here, viscosities at high pressures were taken from the literature data. As seen in Fig. 1, the rotational relaxation times are close to the prediction of hydrodynamic theory using slip boundary condition, indicating that perylene is located in a hydrophobic environment because it is known that perylene rotates with slip behaviour in organic oils like paraffin. More interestingly, the slop of these plots is shallower than predicted by hydrodynamic theory, which means that τ_r is less sensitive to the change of viscosity than that predicted by hydrodynamic theory. Such behaviour may be understood by "free space model" suggested by Dote, Kivelson, and Schwartz [1], implying the occurrence of robust network structure incorporating voids in RTILs.

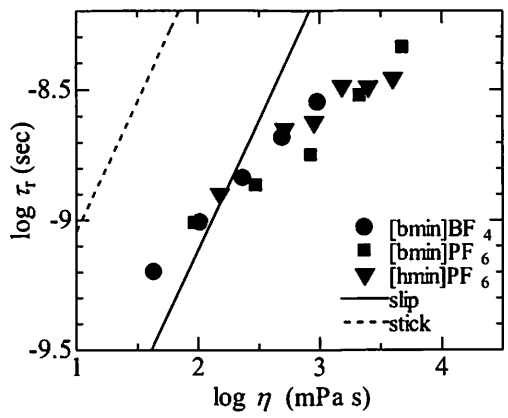

Fig. 1 The plot of τ_r vs η for perylene in [bmin]BF_4, [bmin]PF_6, and [hmin]PF_6 at high pressures.

References,

[1] J. L. Dote, D. Kivelson, R. N. Schwartz, *J. Phys. Chem.* **85**, 2169(1981).

4CO09 Complex Coacervation for Composites of ZnO Nanoparticles with a Fluoropolymer by Pressure-Induced Phase Separation of Supercritical Carbon Dioxide Solutions

K. Mishima[1], R. Kawakami[1], H.Yokota[1], T. Harada[1], T. Kato[1], K. Irie[2], K. Mishima[2], and M. Fujiwara[2]

[1]*Department of Chemical Engineering, Fukuoka University, Fukuoka 814-0180, Japan*
[2]*IDepartment of Neuropharmacology, Fukuoka University, Fukuoka 814-0180, Japan*
e-mail : mishima@fukuoka-u.ac.jp

We report a method for the complex coacervation for composites of ZnO nanoparticles with the fluoropolymer poly(heptadecafluorodecyl acrylate) (poly (HDFDA)) by pressure-induced phase separation of a supercritical CO_2 solution[1,2]. ZnO nanoparticles were synthesized with zinc acetate dihydrate and lithium hydroxide monohydrate[3]. ZnO nanoparticles were coated with 3-(trimethoxy-silyl)propylmethacrylate and poly(methyl methacrylate. A suspension of the ZnO nanoparticles in CO_2 and dissolved poly(HDFDA) were mixed in supercritical CO_2. After the system pressure was slowly decreased to atmospheric pressure, the microcapsules were obtained. Coacervation was achieved by the precipitation of poly(HDFDA) during the decrease in the pressure of CO_2; the solubility of poly(HDFDA) in CO_2 decreased with the pressure. The structure and morphology of the microparticles were investigated by using a scanning electron microscope (SEM) and an electron probe microanalyzer (EPMA) equipped with a wavelength dispersive X-ray spectroscope (WDX).

References

[1] K. Mishima, *Advanced Drug Delivery Reviews,*, **60**, 3,411-432 (2008).
[2] K. Matsuyama, K. Mishima, *Ind.Eng.Chem.Res.*, **46**(19), 6244-6250(2007)
[3] K. Matsuyama, K. Mishima, T. Kato, K. Irie, K. Mishima, *J. Colloid & Interface Sci.*, **367**, 171-177(2012).

4CO10 NMR Studies on Solution Structures of Methanol and Ethanol Saturated with CO_2

T. Umecky[1], T. Takamuku[1], T. Aida[2], T. Makino[2], T. Aizawa[2], and M. Kanakubo[2]

[1] *Graduate School of Science and Engineering, Saga University, Saga 840-8502, Japan*

[2] *National Institute of Advanced Industrial Science and Technology, Sendai 983-8551, Japan*

e-mail : umecky@cc.saga-u.ac.jp, m-kanakubo@aist.go.jp

Gas-expanded liquid systems are composed of condensed gases and organic solvents [1]. In recent years, they have been of growing importance in fractionation, particle formation, polymerization, and chemical reaction processes [2]. CO_2 is one of the promising condensed gases because it is nonflammable, nontoxic, and inexpensive. An understanding of the fundamental properties of CO_2-expanded liquids is definitely imperative to optimize operating conditions for some intended uses.

In the present work, ^2H and ^{17}O NMR relaxation times, $T_1(^2H)$ and $T_1(^{17}O)$, and ^2H NMR chemical shifts, $\delta(^2H)$, in CO_2-saturated CD_3OD and C_2D_5OD solutions were measured at 313.2 K over the pressure range up to ~6 MPa. The rotational correlation times, τ_r, of CD_3OD, C_2D_5OD, and CO_2 were determined from $T_1(^2H)$ and $T_1(^{17}O)$, and the susceptibility-corrected chemical shifts, δ_{corr}, were derived from $\delta(^2H)$. For C_2D_5OD system, δ_{corr} of the OD group gradually decreases with increasing the mole fraction of CO_2, x_{CO2}, whereas δ_{corr} of the CD_3 and CD_2 groups slightly increases. The negative change in δ_{corr} of the OD group is caused by the breakdown of hydrogen bondings. The positive changes in δ_{corr} of the alkyl groups are attributable to the enhancement of intermolecular interactions, presumably between the alkyl groups because CO_2 would not strongly interact with the alkyl groups. For CD_3OD system, δ_{corr} of the OD group remains virtually unchanged at lower x_{CO2} up to ~0.25 and then decreases at higher x_{CO2}, whereas δ_{corr} of the CD_3 group shows the monotonous increase. No change in δ_{corr} of the OD group indicates that the hydrogen bonding network persists at lower x_{CO2}. The discrepancy between CD_3OD and C_2D_5OD can be interpreted as the difference in the strength of the hydrogen bonds, $CD_3OD > C_2D_5OD$. In the presentation, we also report the results of τ_r and then discuss the structures of alcohol solutions in terms of the hydrogen bonding network and intermolecular interactions between alcohols and CO_2.

References

[1] G. R. Akien, M. Poliakoff, *Green Chem.* **11**, 1083 (2009).

[2] K. W. Hutchenson, A. M. Scurto, and B. Subramaniam (Eds), Gas-Expanded Liquids and Near-Critical Media, ACS Symposium Series 1006, American Chemical Society, Washington, DC, 2009.

4CO11 Near Infrared Spectroscopic Study of the Melting Point Depression under High-Pressure Carbon Dioxide

Y. Takebayashi, K. Sue, Y. Hakuta, T. Furuya, and S. Yoda

Nanosystem Research Institute, AIST, Tsukuba, Ibaraki 305-8565, Japan

e-mail : chikulin@ni.aist.go.jp

Introduction: Melting points of organic solids are often depressed by several 10°C under high-pressure CO_2, enabling various fluid processes, e.g., dispersion and micronization, of temperature-sensitive organic solids at relatively low temperatures. The melting point depression is due to the dissolution of CO_2 in the molten liquids. There have been few researches, however, of the solubility of CO_2 in molten liquids. Here we measured the solubilities of CO_2 in molten naphthalene and biphenyl at various temperatures and pressures by using near infrared spectroscopy.

Experimental: Solid naphthalene (1.2 g) was loaded in a high-pressure optical cell (2.5 cm^3) with sapphire windows, whose optical path length was 1.26 cm. The naphthalene was melted by heating it at 82.5°C. Near infrared spectrum of the molten naphthalene was measured with a fiber-optic spectrometer under various CO_2 pressures.

Results: The spectrum of molten naphthalene is shown in Fig. 1 as a function of the CO_2 pressure. Pure naphthalene had an absorption peak at 8780 cm^{-1} assigned to $3\nu_{C-H}$. The peak absorbance decreased with increasing CO_2 pressure, indicating a decrease in the molarity of naphthalene in the liquid phase due to the volume expansion of the molten liquid upon the dissolution of CO_2. The molarity of naphthalene at each pressure was determined from the variation in the peak absorbance.

Molarity of CO_2 dissolved in the molten naphthalene was determined from the $2\nu_1+\nu_3$ band at 5080 cm^{-1}, where the absorbance increased with increasing CO_2 pressure. Molar absorptivity of CO_2 was obtained from the density dependence of the peak absorbance of pure CO_2.

Figure 2 shows the mole fraction solubilities of CO_2 in molten naphthalene and biphenyl at various pressures and temperatures. The mole fraction of CO_2 monotonically increased with increasing CO_2 pressure up to ca. 0.6 at 20 MPa and slightly increased with decreasing temperature for both systems. At pressures above 10 MPa, however, the pressure and temperature effects on the solubility of CO_2 in molten biphenyl was smaller than those in molten naphthalene, respectively. In the conference, we will discuss the correlation between the solubility of CO_2 and the melting point depression for these systems.

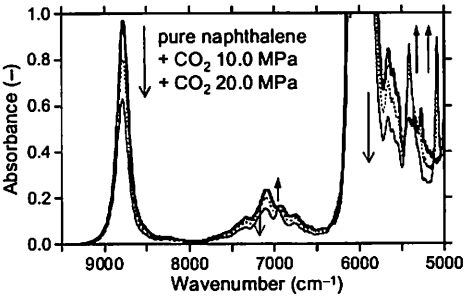

Fig. 1 Spectrum of molten naphthalene at 82.5°C and various CO_2 pressures.

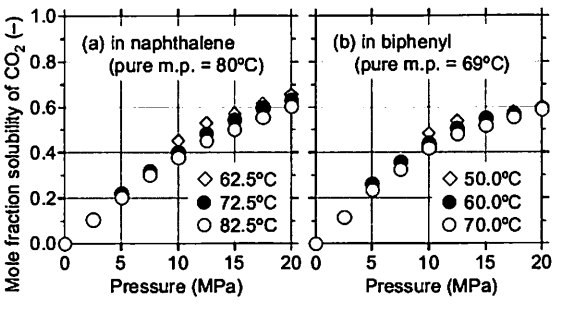

Fig. 2 Mole fraction solubility of CO_2 in molten naphthalene and biphenyl.

3DO01 Solvation of alkali metal ions by sulfolane

F. Pichierri[1]

[1]*Department of Applied Chemistry, Tohoku University, Sendai 980-8579, Japan*
e-mail : fabio@che.tohoku.ac.jp

Among dipolar aprotic solvents, sulfolane possesses a large dipole moment (μ=4.69 Debye), high relative permittivity, and a high Hildebrand solubility parameter [1]. Its high chemical stability towards both strong acid and bases makes it an ideal choice for carrying out industrial reactions at elevated temperatures. Furthermore, sulfolane has the ability to solvate cations by coordinating them via its sulfone group (SO_2).

So far, and to the best of our knowledge, no structural information about the coordination complexes of sulfolane with alkali metal ions is available. We have therefore investigated the geometries, electronic structure, and bonding characteristics of the complexes between sulfolane and alkali metal ions, Li^+ through Cs^+, with the aid of density functional theory (DFT) calculations. Figure 1 shows the DFT-optimized geometries of the binary sulfolane:Na^+ complex (left) and that of the corresponding ternary complex (right) with water. While in the binary complex both the sulfone oxygen atoms of sulfolane interact with the sodium ion, in the ternary complex only one sulfone oxygen interacts with Na^+ while the water molecule coordinates the ion and forms an H-bond with sulfolane. The interaction with Cs^+ is particularly interesting for the possibility of removing radioactive cesium (Cs-137) from sulfolane-treated materials. This approach therefore could be cost competitive with respect to the use of macrocycles with the ability to bind cesium ions [2].

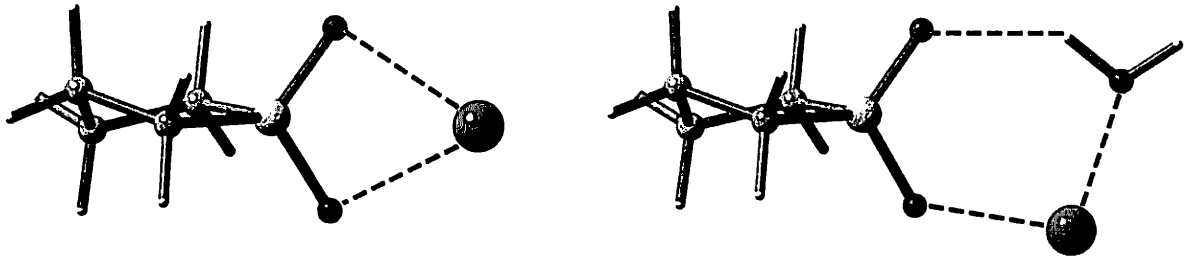

Sulfolane:Na^+ **Sulfolane:H_2O:Na^+**

Figure 1. DFT-optimized geometries of the binary and ternary complexes of sulfolane with Na^+.

References

[1] U. Tilstam, *Org. Process. Res. Dev.* **16**, 1273(2012).

[2] F. Pichierri, *Dalton Trans.* (2011) **DOI:** 10.1039/C2DT32180G.

3DO02 Characterisation of metal complexes for theragnostic applications: some contribution of coordination chemists

Z. Baranyai, I. Bányai, E. Brücher, F. Kálmán, G. Tircsó, I. Tóth

Department of Chemistry, University of Debrecen, Debrecen, Hungary

e-mail : imre.toth@science.unideb.hu

Metal complexes used in medical imaging and therapy have been intensively studied during the last few decades and are being used in screening, diagnosis, patient management, clinical research and in the development of new therapeutic drugs.[1] Although the modalities are based on very different physics for generating the image, there are many similarities in chemistry behind: metal ions are bound by organic ligands, the ligands are often bifunctional having a chelator and a biological vector for selective targeting anchored through a spacer, see the following scheme.

The coordination chemist seems to be focusing on the chelator and tries to develop ligands forming metal complexes with *high thermodynamic stability, high inertness (often called kinetic stability by medical researchers), high solubility, low osmolality, high effectivity* etc.. Our group has been involved in the chemical characterization of MRI contrast agents (CA) since the beginnings (i.e. from about 1980), studying equilibrium, formation and dissociation kinetics of lanthanide complexes formed with open chain and macrocyclic ligands (MC). Recently our research has been extended to some transition metals (especially manganese(II)) and main group metals (indium(III), gallium(III)) considered as MRI CA and radio diagnostics, respectively. The talk is going to summarize "state of the art" in chemistry of metal containing drugs. Comparison of open chain and MC ligands in terms of their stability and kinetics of the complex formation and dissociation will be done. New results in ligand design and in kinetics will be presented, especially the role of endogenous cations (Ca(II), Cu(II), Zn(II)) and anions (carbonate, citrate and phosphate) in transmetallation reactions will be discussed.

Acknowledgemenst: The research was supported by the EU and co-financed by the European Social Fund (ESF) under the project ENVIKUT (TÁMOP-4.2.2.A-11/1/KONV-2012-0043) and TÁMOP-4.2.2./B-10/1-2010-0024 project. Support from the Hungarian National Science Foundation (OTKA K-84291, PD-83253), COST CM1006 and TD1004 Actions are also acknowledged.

References

[1] E. Brücher, Z. Baranyai and G. Tircsó, The Future of Biomedical Imaging: Synthesis and Chemical Properties of the DTPA and DOTA Derivative Ligands and Their Complexes, *Chapter 5.2* in *"Biomedical Imaging. The Chemistry of Labels, Probes and Contrast Agents"*, ed. by M. Braddock, RSC Publishing, Cambridge, **2012.**

3DO03 Competitive Coordination of Dioxygen and Water to Porphyrin Oxygen Reduction Catalysts

A. Trojánek, J. Langmaier, H. Kvapilová, S. Záliš, Z. Samec

J. Heyrovsky Institute of Physical Chemistry of ASCR, Prague 8, Czech Republic

e-mail : zdenek.samec@jh-inst.cas.cz

The catalytic effect of 5,10,15,20-tetraphenylporphyrin (H_2TPP) and [5,10,15,20-tetraphenylporphyrin]cobalt (II) ($Co^{II}TPP$) in the reduction of dioxygen by ferrocene (Fc) and its methyl(Me)-substituted derivatives (Me_nFc) was studied by the stopped-flow kinetic measurements in 1,2-dichloroethane (DCE), and by cyclic voltammetry at the polarized water/DCE interface and DFT calculations [1-4]. Particular attention was paid to the effects of water and acid present in the DCE phase [1,2,4]. The reduction of O_2 with Fc or Me_nFc was shown to proceed remarkably faster in the presence of tetraphenylporphyrin diacid (H_4TPP^{2+}), which is formed in DCE from the H_2TPP free base either by addition of tetrakis(pentafluorophenyl)boric acid (HTB) [1,2,4], or by the interfacial transfer of proton from the acidified aqueous phase to DCE [3]. A mechanism was proposed, which includes the coordination of dioxygen to H_4TPP^{2+} in a competition with water and the acid anion, followed by the electron transfer from ferrocene (Fc) leading to the observed Fc^+ or Me_nFc^+, and to the regeneration of H_4TPP^{2+} [1,2].

On replacing H_2TPP with $Co^{II}TPP$, the reduction of O_2 with Fc proceeds with ca. two orders of magnitude higher rate, under the comparable experimental conditions (water content, acid concentration) [4]. The activation process is likely to involve the coordination of O_2 to the metal center, and the electron delocalization from the metal to O_2 followed by the protonation of the coordinated O_2, and the proton coupled electron transfer from Fc [4,5]. Strong inhibition of the catalyst by water was observed also in this case, while the effect of the acid anion was less pronounced [4]. The mechanism is supported by the DFT calculations.

This work was supported by grants no. P208/11/0697 from the Grant Agency of the Czech Republic.

References

[1] Z. Samec, A. Trojánek, J. Langmaier, S. Záliš, *Chem. Commun.* **48**, 4094 (2012).

[2] A. Trojánek, J. Langmaier, J. Šebera, S. Záliš, J.-M. Barbe, H. H. Girault, Z. Samec, *Chem. Commun.* **47**, 5446 (2011).

[3] A. Trojánek, J. Langmaier, Z. Samec, *Electrochim. Acta* **82**, 457 (2012).

[4] Z. Samec, A. Trojánek, J. Langmaier, H. Kvapilová, S. Záliš, in preparation.

[5] R. Partovi-Nia, B. Su, F. Li, C. P. Gros, J. M. Barbe, Z. Samec, H. H. Girault, *Chem.Eur. J.* **15**, 2335 (2009).

3DO04 Cyanide-bridged bimetallic multidimensional structures derived from organotin(IV) and dicyanoaurate building blocks: structure, ion exchange, luminescence, and gas sorption properties

Gábor Pálinkás, Andrea Deák , Tünde Tunyogi , Csaba Jobbágy,
Zoltán Károly, Péter Baranyai,
Research Centre for Natural Sciences, Hungarian Academy of Sciences,
Pusztaszeri út 59-67, 1025, Budapest, Hungary
palinkas.gaborg@ttk.mta.hu

The rational design and synthesis of cyanide-bridged bimetallic supramolecules containing cyanometallate building blocks are the focus of widespread research interest because of their interesting topological structures and diverse properties. Among many metal cyanide anions, the dicyanoaurate $[Au(CN)_2]^-$ building block, due to its affinity to bridge transition metal centers has been used in the construction of 2D and 3D cyano-bridged bimetallic Au–CN–M coordination polymers. The unique ability of linear $[Au(CN)_2]^-$ anion to form Au–Au aurophilic interaction plays a key role in controlling the dimensionality and topology of these dicyanoaurate-based heterometallic polymers. The cyanoaurate-based heterometallic polymers may exhibit unusual structural motifs and physical properties, such as luminescence, colossal thermal expansion, magnetism or ion exchange. This dicyanoaurate anion also has significant importance in industrial and medical applications.

We have previously reported the construction and structural characterization of multidimensional structures containing the Au–CN–Sn link generated by the reaction of the hard Lewis acidic organotin $R_nSn^{(4-n)+}$ cation and the soft Lewis basic dicyanoaurate $[Au(CN)_2]^-$ anion [1]. Single crystals of both compounds can be obtained by slow interdiffusion of aqueous solutions of Me_3SnCl or Me_2SnCl_2 and $K[Au(CN)_2]$.

We have also shown that the solvent-free mechanochemical method (grinding stoichiometric amounts of $K[Au(CN)_2]$ and metal chlorides in a mortar with a pestle) is a fast, simple, and efficient route to the synthesis of cyanoaurate-based heterometallic coordination polymers [2]. This mechanochemical method was successfully applied also to main group metals to obtain $Ph_3Sn[Au(CN)_2]$. In this presentation, we report the x-ray and infrared characterization, as well as the luminescence, gas sorption and ion exchange properties of these multidimensional structures.

References

[1] Deak A, Tunyogi T, Palinkas G, *J. Am. Chem. Soc* **131**(8):2815–2817 (2009).
[2] Jobbagy C, Tunyogi T, Palinkas G, Deak A, *Inorg. Chem.* **50** (15):7301–7308 (2011).

3DO05 Synthesis, Characterization and Catalytic Activity of Silica Supported Coordination Complexes

S.Theodore David, R.Antony, S.Asha, M.Seethalakshmi, R.Biju Bennie,
S.Daniel Abraham and C.Joel.

Post Graduate Department of Chemistry, St.John's College, Tirunelveli-627002, India.

e-mail : s.theodore.david@gmail.com

In the recent past, the organic-inorganic hybrid materials have been of much focussed materials, because of their diverse applications. Organic ligand based coordination complexes also belong to organic-inorganic hybrid materials. The organo modified silica supported coordination complexes play the key role in the catalytic reactions due to their stable catalytic efficiency for several cycles. In the present study, we have prepared the organo modified silica based Schiff base ligand from the condensation reaction of 3-aminopropyltriethoxysilane (APTES), silica gel and a ketone in toluene. From this Schiff base ligand, three different metal complexes with Co(II), Ni(II) and Cu(II) have been synthesized and characterized by FT-IR, UV-Vis., 1H NMR, and XRD spectroscopic techniques. The surface morphology and thermal properties of the complexes have been also studied by SEM TG-DTG methods, respectively. Further, the catalytic ability of the complexes has been investigated in the industrially important cyclohexane oxidation using hydrogen peroxide as oxidant.

Key words: Schiff base complex, Silica support, Spectral characterisation, Catalytic efficiency.

4DO06 Spectrophotometry Study of Th(IV) Hydroxo Complexes Destruction Kinetics in Aqueous Solution

A.V. Radkevich, V.V. Torapava, and V.S. Labko

Joint Institute for Power and Nuclear Research - Sosny, Minsk 220109, Belarus

e-mail : artem-rav@yandex.ru

It is known that Th(IV) cations hydrolyze in aqueous solution with formation of different hydrolytic species: mononuclear – $Th(OH)_n^{(4-n)+}$, polynuclear – $Th_p(OH)_q^{(4p-q)+}$ hydroxo complexes, pseudocolloid and colloid particles. Therefore kinetics study of Th(IV) hydrolytic reactions is complicated by simultaneous presence of various metal ion forms possessing common chemical and physical properties. As a result there is a problem to obtain correlation between analytical signal and specific hydroxo complex concentration.

Our kinetics study of Th(IV) hydroxo complexes destruction was performed by spectrophotometry of Th(IV)–arsenazo-III complex. This complex, with absorption maximum at λ=665 nm, is formed with hydrated cation $Th(H_2O)_n^{4+}$ only, whereas complexes of hydrolyzed Th(IV) species with arsenazo-III don't have such optical characteristics. That's why we can determine selectively the concentration of Th^{4+}-cation in solution, containing various Th(IV) species.

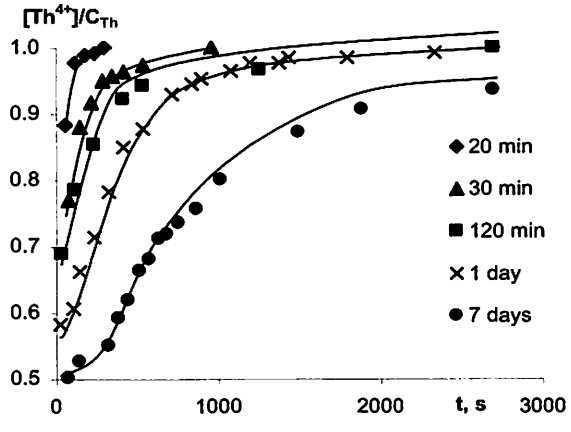

Influence of solution "aging" time on Th(IV) polynuclear hydroxo complexes destruction

Kinetics experiments were performed at $C_{Th}=1\cdot10^{-5}$ – $1\cdot10^{-3}$ M and pH 2.0 – 5.0. It was shown that the observed change in optical density correlate to Th(IV) polynuclear hydroxo complexes destruction.

Though the reaction kinetics is not elementary, in can by closely approximated by the following equation:

$$v = -\frac{d[Th_{poly}]}{dt} = k_{eff}[Th_{poly}][H^+]$$

The values of k_{eff} are shown in the table

"Aging" time	$k_{эфф}$, $M^{-1}c^{-1}$	"Aging" time	$k_{эфф}$, $M^{-1}c^{-1}$
20 min	6.01	1 day	0.79
30 min	1.45	7 days	0.26
120 min	1.04		

The obtained results significantly depend on "aging" time of solutions, that is the evidence of continuous hydrolysis process and transition to kinetically inert hydroxo complexes. This fact indicates, that metal-ion hydrolysis is a multi step reaction, and the reaction end cannot be always determined by such indirect features such as constant solution pH value.

4DO07 Effect of pH on the Tautomerism of Various *Cyclo*-imidophosphate Anions.

H. Maki, D. Kataoka, M. Mizuhata

Department of Chemical Science and Engineering, Graduate School of Engineering, Kobe University, 1-1 Rokkodai-cho, Nada, Kobe, 657-8501, Japan

e-mail : maki@kobe-u.ac.jp

Cyclic imidopolyphosphate anions, involving P-NH-P linkages, i.e., *cyclo*-μ-triimidotriphosphate anion, $P_3O_6(NH)_3^{3-}$, and *cyclo*-μ-tetraimidotetra-phosphate, $P_4O_8(NH)_4^{4-}$, contain non-bridging oxygen atoms as well as bridging nitrogen atoms as donor atoms for metal complexation. In addition to this interesting feature as ligand molecules, they have tautomerism equilibria as shown in Scheme 1. However, quite little has been known on the detail of the tautomerism equilibria in these ligands. A ^{15}N NMR technique is expected to provide deep insights into the microscopic hydrogen bond formation. ^{15}N enriched samples of these anions have been prepared and the hydrogen bond formation in the cyclic anions have been investigated precisely.

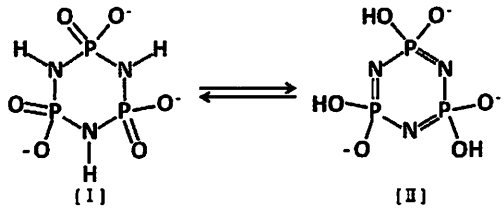

Scheme 1 Tautomerization of $P_3O_6(NH)_3^{3-}$. [I]cyclo-triphosphazane anion, [II]cyclo-triphosphazene anion

^1H decoupled ^{15}N NMR spectra of $[^{15}N]P_4O_8(NH)_4^{4-}$ anion consist of a triplet signal, indicating equivalent coupling due to two adjacent ^{31}P nucleus; $^1J(^{15}N\text{-}^{31}P)$ = 23 Hz, whereas the spectra of $[^{15}N]P_3O_6(NH)_3^{3-}$ anion are composed of a tripret of triplets signal, that is, the shorter distance coupling path gives an appreciably stronger coupling than the shorter distance path; $^1J(^{15}N\text{-}^{31}P)$ = 16 Hz and $^3J(^{15}N\text{-}^{31}P)$ = 6 Hz. The pH profile of the ^1H coupled ^{15}N NMR spectra of both anions(Fig. 1) gives most straight forward evidence for the tautomerism equilibria in these cyclic anions. At low and high pH regions, i.e., pH < 4 and pH > 10, ^1H coupling has not been observed for both anions, since the exchange of the acidic proton in the imino tautomer is much faster than the time scale of ^{15}N NMR FID. Whereas at medium pH region, i.e., pH = 5.5 – 9.0 for $[^{15}N]P_3O_6(NH)_3^{3-}$, and pH = 5.0 - 9.5 for $[^{15}N]P_4O_8(NH)_4^{4-}$, ^1H coupling with ^{15}N nucleus has become appreciable. It shows that the predominance of the imino tautomer which has N-H bonding, and the N-H bonding in these anions is relatively inert to the exchange of the imino proton in the medium pH region. The pH dependence of the localization of protons in the cyclic imidopolyphosphate molecules is very useful for the industrial application such as novel proton conductors.

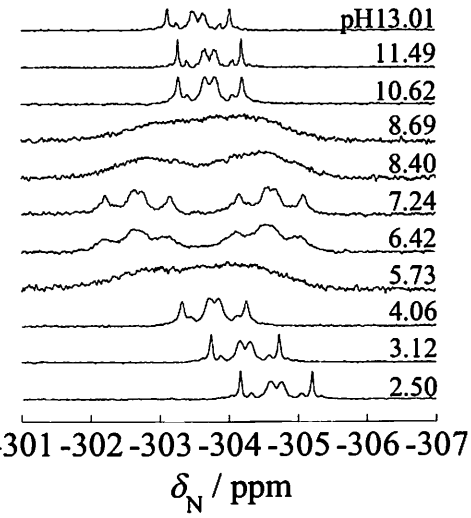

Fig. 1 Representative ^1H-coupled ^{15}N NMR spectra of $[^{15}N]P_3O_6(NH)_3^{3-}$ under various pH.

4DO08 Conductometric and UV-Visible Spectroscopic Studies on the Strong Association between Poly-Sulfonic or Carboxylic Acids and Their Conjugate Anions in Acetonitrile

M. Hojo[1], K. Zei[1], and Z. Chen[2]

[1]*Department of Chemistry, Kochi University, Kochi 780-8520, Japan*

[2]*Department of Applied Chemistry, Changzhou University, Changzhou, Jiangsu, 213164 China*

e-mail : mhojo@kochi-u.ac.jp

Conductometric titrations in non-aqueous solvents are often utilized because the properties of acids and bases in non-aqueous solvents differ much from those in aqueous solution. In an aprotic and protophobic solvent, such as acetonitrile (MeCN), the conjugate anion (A^-) generated from an acid (HA) may form the homoconjugate species (HA_2^-) through the hydrogen bonding force between A^- and mother acid (HA). In a previous paper [1], we reported the formation of the trimer [$A^-(HA)_2$] through the interaction between A^- and two HA molecules for sulfonic acids (e.g., methanesulfonic and benzenesulfonic acids) in benzonitrile (PhCN) by means of conductometirc titration. In MecN, however, such the homoconjugation reaction for the monosulfonic acids has been hardly observed.

In the present paper, we have studied homoconjugation reactions for di- and trisulfonic acids in MeCN. The multiple hydrogen bonding interaction between the conjugate anions and a mother polyprotonic acid may cause the favorite formation of associated species.

The conductometric titrations of 1,5-naphthalenedisulfonic acid (H_2A) with Et_3N in MeCN give conductivity maxima at the first equivalent point (cf. **Fig.1**). Other disulfonic acids, 2,6- and 2,7-derivatives, give results almost similar to 1,5-naphthalenedisulfonic acid. At the first equivalent point, all the H_2A should be converted to HA^- (Et_3NH^+), therefore, the conductivity maximum in a titration curve can be accounted for by the dimer formation [$(HA^-)_2$] between two HA^- species in MeCN (**Scheme 1**). The dimer formation constant has been estimated to be log K_d = 4.8 by means of the UV-Visible spectroscopic technique (**Fig. 2**). 1,3,6-Naphthalenetrisulfonic and dicarboxylic acids have been examined and effects of water and other solvents are fully discussed.

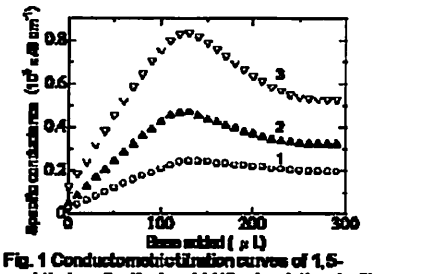

Fig. 1 Conductometric titration curves of 1,5-naphthalenedisulfonic acid (13 mL solutions) with triethylamine in MeCN at 25 °C. The concentrations of the acid and the added base are (1) 2.0×10^{-3} and 0.20, (2) 5.0×10^{-3} and 0.50, (3) 1.0×10^{-2} and 1.0 mol dm^{-3}.

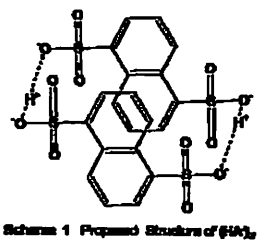

Scheme 1 Proposed Structure of $(HA)_2^-$

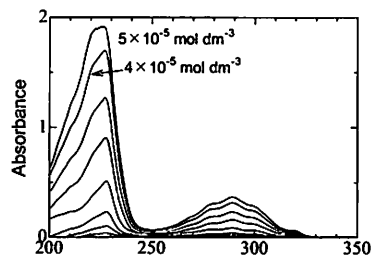

Fig. 2 UV spectra of tetraethylammonium hydrogen 1,5-naphalenedisulfonate ($NDSH^-$) over the concentration range of 1.0×10^{-6} – 5.0×10^{-5} mol dm^{-3} (0.1 cm path length).

Reference

[1] M. Hojo, Z. Chen, *Anal. Sci.*, **15**, 303-306 (1999).

4DO09 Uranyl-Halide Complexation in *N,N*-Dimethylformamide: Halide Coordination Trend Manifests Hardness of $[UO_2]^{2+}$

K. Takao[1,2], S. Takao[2,3], Y. Ikeda[1], G. Bernhard[2], and C. Hennig[2]

[1] *Research Laboratory for Nuclear Reactors, Tokyo Institute of Technology, Japan.*

[2] *Institute of Resource Ecology, Helmholtz Zentrum Dresden-Rossendorf, Germany.*

[3] *Innovation Research Center for Fuel Cells, University of Electro-Communications, Japan.*

e-mail : ktakao@nr.titech.ac.jp

Pearson's HSAB principle[1] is very simple, but quite helpful to explain interactions of metal ions with ligands. Stability of a halido complex is frequently used to demonstrate the hardness of a metal ion of interest. The halide (X^-) hardness increases like $I^- < Br^- < Cl^- < F^-$, while the formation constants of $[UO_2]^{2+}$-X^- complexes in aqueous system do not always follow this sequence. Although the coordination of the hardest F^- is actually strongest ($\log K_1 = 5.16$) and no evidences about the softest I^- coordination have been obtained, the difference between Cl^- ($\log K_1 = 0.17$) and Br^- ($\log K_1 = 0.22$) has not been clearly indicated[2]. Such a similarity could be related to the balance between the hydration strengths of $[UO_2]^{2+}$ and X^-. On this context, use of an organic solvent instead of water may help to more clearly differentiate the coordination strengths of $[UO_2]^{2+}$-X^- complexes. In this study, we selected *N,N*-dimethylformamide (DMF) as a solvent, because a fully DMF-solvated $[UO_2]^{2+}$ source is available. The complexation of $[UO_2]^{2+}$ with Cl^-, Br^-, and I^- in DMF was studied by UV-vis absorption spectroscopy and extended X-ray absorption fine structure (EXAFS).

In the Cl^- system, it was clarified that the Cl^- coordination to $[UO_2]^{2+}$ in DMF proceeds almost quantitatively. The coordination number of Cl^- increases up to 4 with increasing total $[Cl^-]$, *i.e.*, the limiting complex is $[UO_2Cl_4]^{2-}$. The logarithmic gross stability constants of $[UO_2Cl_x]^{2-x}$ (x = 1-4) were evaluated as $\log K_1 = 9.67$, $\log \beta_2 = 15.49$, $\log \beta_3 = 19.89$, and $\log \beta_4 = 24.63$ from UV-vis titration experiment. The EXAFS results well demonstrated not only the Cl^- coordination, but also the DMF solvation in the equatorial plane of $[UO_2]^{2+}$. The similar experiments were also performed for the Br^- and I^- systems. As a result, the Br^- coordination to $[UO_2]^{2+}$ stops at the 2nd step, *i.e.*, only $[UO_2Br]^+$ and UO_2Br_2 were observed. The molecular structure of each occurring species was confirmed by EXAFS. The evaluated $\log \beta_x$ of $[UO_2Br_x]^{2-x}$ (x = 1, 2) are 3.45 and 5.42, respectively. The much smaller $\log \beta_x$ than those of $[UO_2Cl_x]^{2-x}$ indicates that Br^- is much weaker ligand to $[UO_2]^{2+}$ than Cl^-. The EXAFS experiments revealed that the presence of I^- in the test solution does not modify any coordination structure around $[UO_2]^{2+}$. Thus, I^- does not form any stable $[UO_2]^{2+}$ complexes in DMF. Consequently, the stability of $[UO_2]^{2+}$-X^- complexes in DMF is exactly in line with the hardness order of X^- as expected. This trend clearly manifests hardness of $[UO_2]^{2+}$.

References

[1] R. G. Pearson, *J. Am. Chem. Soc.*, **85**, 3533(1963).

[2] R. Guillaumont, *et al. Update on the Chemical Thermodynamics of Uranium, Neptunium, Plutonium, Americium and Technetium*. Elsevier B.V.: Amsterdam, The Netherlands, 2003.

4DO10 Complexation and Structural Studies on Trivalent Lanthanides with Dioxaoctanediamide (DOODA)

S. Okumura[1], T. Tsukahara[1], and Y. Ikeda[1]

[1] *Research Laboratory for Nuclear Reactors, Tokyo Institute of Technology, Tokyo 152-8550, Japan*

e-mail : okumura.s.aa@m.titech.ac.jp

Neutral diamide compounds such as *N,N,N',N'*-tetraoctyl-glycoldiamide (TODGA) have been widely examined as extractants for separating trivalent actinide (An(III)) and lanthanide (Ln(III)) from high level liquid waste (HLLW) by solvent extraction. Recently, it was reported that *N,N,N',N'*-tetraoctyl-3,6-dioxaoctanediamide (DOODA-C8) extracts Ln(III) and An(III) effectively and showed different affinity to heavier Ln(III) compare with TODGA [1][2]. In order to explain the extraction mechanism and to find the factors for controlling selectivity, understanding of the structures of extracted species (complexes) must be crucial. However, the structures and properties of extracted complexes are still not elucidated. The number of extractant molecules and nitrate ions participating in solvent extraction, which are usually obtained from log*D*-log[L] plots ([L] : the concentrations of the extractant or nitric acid), are not always compatible with those in the crystal structures. DOODA extracts Ln(III)-nitrate as species with metal to extractant ratio of 1:2, whereas DOODA forms 1:1 complex with Ln(III) in crystal structures.

The complex formation of DOODA with Ln(III)-nitrate was studied by spectrophotometric (Ln: Nd and Ho) and NMR titration (Ln: except for Pm) methods. The changes in ^{1}H, ^{13}C chemical shift and relaxation time indicate that 1:1 and 1:2 complexes are formed in the acetonitrile solution.

The structures of Ln(III)-DOODA complexes were examined by ^{1}H-, ^{13}C- and ^{15}N- NMR spectra. The distances between observed nucleus and Ln(III) were determined through application of reduced Solomon-Bloembergen equation. As examples for 1:1 complexes, the Lanthanide Induced Shift (LIS) plot for methylene proton indicates that the structures of lighter and middle Ln(III) (Ln: La-Ho) are slightly different from those of heavier Ln(III) (Ln: Er-Lu). This difference was also detected by IR spectra of complexes in the solid state. The structural change in 1:1 complexes might be caused by the different coordination mode of the nitrate ions. The present study also demonstrates the existence of 1:2 complexes in the solution and is in agreement with the species expected from the log-log plot of the solvent extraction.

References

[1] Y. Sasaki, Y. Morita, Y. Kitatsuji and T Kimura, *Solv. Extr. and Ion Exch.*, **28**, 335.(2010)

[2] Y.Sasaki, Y. Kitatsuji, Y. Tsubata, Y. Sugo and Y. Morita, *Solv. Extr. Res. Dev. Jpn.*, **18**, 93.(2011)

2EO01 Hydration water distribution in *Eco*RV-DNA complex calculated by using 3D-RISM

Ryota Motomatsu[1], A. Junji Yasuniwa[1], Yutaka Maruyama[2] , Norio Yoshida[3],

Akinori Sarai[1], Fumio Hirata[4,5] and Masayuki Irisa[1]

[1] *Department of Bioscience and Bioinformatics, Kyushu Institute of Technology, Iizuka 820-8502, Japan*

[2] *Institute for Protein Research, Osaka University, Suita 565-0871, Japan*

[3] *Department of Chemistry, Kyushu University, Fukuoka 812-8581, Japan*

[4] *Institute for Molecular Science, Okazaki 444-8585, Japan*

[5] *TechnoComplex, Ritsumeikan University, Kusatsu 525-8577, Japan*

e-mail : irisa@bio.kyutech.ac.jp

Restriction enzymes recognize a specific sequence of DNA and selectively cut a double-stranded DNA. This hydrolysis reaction requires divalent cations. One of the type II restriction enzymes, *Eco*RV, is a homo dimer and requires Mg^{2+} ions in its function. In this study, hydration water and ion distributions in the *Eco*RV-DNA complex were calculated by using 3D-RISM [1], where the $MgCl_2$ aqueous solution was used as a solvent. The X-ray structure of *Eco*RV-DNA complex (PDB ID: 1rvb), which corresponds to the step prior to the hydrolysis reaction of a DNA fragment [2], was adopted as a solute structure. The calculated distribution of water molecules shows that in the minor groove of DNA strands two hydration water molecules bridge two DNA strands through hydrogen bonds at the both sides of the reactive site having the sequence, 5'-ATAT- 3', which should be cleaved at the centre of the sequence. This suggests the two hydration water molecules stabilize the both sides of the reactive site in order to support the cleavage reaction of the DNA fragment. The calculated water distribution around the active site in *Eco*RV is almost the same with/without the DNA fragment in the complex structure (1rvb). The calculated local densities of water at the locations of the three water molecules in the X-ray structure as the ligands, which are directly bonded to the Mg^{2+} ion at the active site, are twice higher in their values than the bulk one. In addition, Mg^{2+} ion has a sharp distribution at the same position in the active site with/without the DNA fragment. Probable process prior to the protein-DNA complex formation is that: some water molecules and ions cooperate with *Eco*RV to prepare for the docking with a DNA fragment. This work is the first step to pursue the hydrolysis reaction where both water molecules and the DNA fragment are substrates of the reaction. In such a situation, the 3D-RISM method must be suitable for the understanding of the reaction pathway in the framework of statistical mechanics.

References

[1] Norio Yoshida, Takashi Imai, Saree Phongphanphanee, Andriy Kovalenko and Fumio Hirata, *J. Phys. Chem. B*, **113**, 873-886(2009).

[2] Dirk Kostrewa and Fritz K. Winklera, *Biochemistry*, **34**, 683-696(1995).

2EO02 Molecular dynamics study of lipid bilayers modeling the plasma membranes of normal murine thymocytes and leukemic GRSL cells

Y. Andoh[1], S. Shibayama[1], S. Okazaki[1], and R. Ueoka[2]
[1]*Department of Applied Chemistry, Nagoya University, Nagoya 464-8603, Japan*
[2]*Graduate School of Life Science, Sojo University, Kumamoto 860-0082, Japan*
e-mail : okazaki@apchem.nagoya-u.ac.jp

A series of molecular dynamics (MD) calculations for the plasma membranes of normal murine thymocytes and thymus-derived leukemic GRSL cells in water have been performed under physiological isothermal–isobaric conditions (310.15 K and 1 atm) to investigate changes in membrane properties induced by canceration.

First, we performed MD calculations on the real membranes for normal and leukemic thymocytes composed of 23 and 25 kinds of lipids, respectively [1]. The membranes include phosphatidyl-choline (PC), phosphatidyl-ethanolamine (PE), phosphatidyl-serine (PS), phosphatidyl-inositol (PI), sphingomyelin (SM), lysophospholipids (lyso-PC, -PE), and cholesterol. The mole fractions of the lipids adopted were based on previously published experimental values [2]. Our calculations clearly showed that the calculated membranes of leukemic cells were considerably bulkier and softer in the lateral direction compared with those of normal cells. The tilt angle of the cholesterol and the conformation of the phospholipid fatty acid tails both showed a lower order in the leukemic cell membranes than in the normal cell membranes in accordance with fluorescence polarization measurements [3]. Further, the calculated lateral self-diffusion coefficient of the lipid molecules in leukemic cell membranes was almost double that in normal cell membranes. Furthermore, the calculated rotational and wobbling autocorrelation functions also indicated that the molecular motion of the lipids was enhanced in leukemic cell membranes. We demonstrated that the membranes of thymocyte leukemic cells are more disordered and more fluid than normal cell membranes.

Second, we performed additional MD calculations on the simplified model membranes for the normal and leukemic thymocytes composed of 3 and 2 kinds of lipids, respectively, with the hypothesis that the difference in membrane properties between the normal and leukemic membranes comes from the difference in (1) the molar ratio of cholesterol to phospholipids and (2) the mole fraction of unsaturated tails to saturated tails of phospholipids. The calculated static and dynamics properties of the simplified model membranes showed surprisingly good correspondence to those of the real membranes. Thus, we conclude that the changes in membrane properties by the canceration come mainly from the lipid composition changes in (1) and (2).

References

[1] Y. Andoh, S. Okazaki, R. Ueoka, *Biochim. Biophys. Acta*, **1828**, 1259 (2013).
[2] W.J. van Blitterswijk, G. de Veer, J.H. Krol, P. Emmelot, *Biochim. Biophys. Acta*, **688**, 495 (1982).
[3] W.J. van Blitterswijk, R.P. van Hoeven, B.W. van der Meer, *Biochim. Biophys. Acta*, **644**, 323 (1981).

3EO03 Water Model Tuning To Better Reproduce Rotational Diffusion and NMR Spectral Density of Protein

Kazuhiro Takemura[1], Akio Kitao[1,2]

[1] *Institute of Molecular and Cellular Biosciences, University of Tokyo, Tokyo 113-0032, Japan*

[2] *JST,CREST*

e-mail : ktakemur@iam.u-tokyo.ac.jp

A water model for molecular dynamics simulation was optimized to improve the reproduction of rotational diffusion and NMR spectral density of proteins [1]. The SPC/E_b model was developed from the original SPC/E model with a slight increase of the oxygen-hydrogen bond length by 1%. This tuning was based on an observation, that is, the translational diffusion constants significantly depend on the simulation box size [2]. The tuning has significantly improved the translational diffusion constant of water models when compared to the experimental values, whereas only small changes were observed in other thermodynamic properties. As shown in the figure, the overall tumbling correlation times (τ) from for proteins, ubiquitin, protein G, bovine pancreatic trypsin inhibitor and barstar C42/80A, were successfully reproduced using the SPC/E_b model. Site specific spectral densities of the main chain amide bond rotation in ubiquitin and protein G were calculated and in good agreement with those derived from NMR reduced spectral density mapping. Temperature dependent bond length tuning was also conducted to facilitate reproduction of the experimental τ around room temperature.

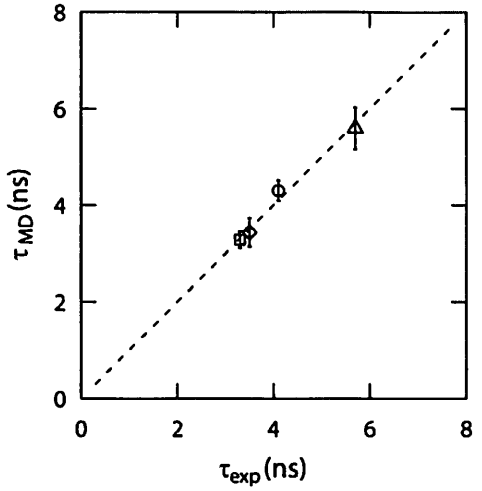

Figure: Correlation of the calculated and experimental τ. Symbols represent τ of ubiquitin (circle), BPTI (diamond), protein G (square), and barstar C40/82A (triangle) using SPC/E_b model.

References

[1] K. Takemura and A. Kitao, J.Phys. Chem.B., 116 (22), 6279-87 (2012).

[2] K. Takemura and A. Kitao, J. Phys. Chem. B, 111, 11870 (2007).

3EO04 Theoretical extraction of fusion nanopores topology and energetics from amperometric measurements of vesicular exocytosis at ultramicroelectrodes

A. Oleinick, F. Lemaitre, M. Guille Collignon, I. Svir, C. Amatore

[1]*CNRS-ENS-UPMC UMR 8640 PASTEUR, Département de Chimie, Ecole Normale Supérieure, 24 rue Lhomond, 75005 Paris, France*

e-mail : christian.amatore@ens.fr

Vesicular exocytosis is a natural nanoscale process. This involves a connection between nanometric vesicles contained inside a cell with the cell membrane occurring by creation of a fusion nanopore across the two membranes through which biologically active molecules contained inside the vesicle are released into the extracellular environment (synaptic cleft, circulating fluids). Despite the minute released amounts (attomoles), single exocytotic events can be studied by means of the 'artificial synapse' amperometric method [1], in which a cell is interrogated by a carbon fiber microelectrode collecting and oxidizing released molecules so that the finely-structured electrochemical current tracks quantitatively the exocytotic flux. In the ENS group we investigate essentially chromaffin cells which release adrenaline into the blood stream. Our purpose in this work was to derive topological, energetic and dynamic information about these vesicular exocytotic phenomena.

Such information is obtained by deconvoluting the experimental current by means of simulations involving self-adjustment of time-dependent radius of the fusion nanopore [2-3]. It should be noted, however, that due to the biological variability of the vesicles, the main parameters characterizing a spike (i.e., initial concentration of the neurotransmitter, its diffusion coefficient, vesicle radius, etc.) are not known *a priori*. Nevertheless, reconstruction is possible when at least one of the characteristic dimensions is known as an independent entry. To this end, we resorted to initial fusion nanopore radius values (1.2±0.35 nm), which are well established by patch-clamp measurements [4], for internal calibration of the reconstruction procedure. This resulted in the determination of the average neurotransmitter diffusion rate (D/R_{ves}^2) within the vesicle, which in turn allowed reconstructing the fusion nanopore dynamics from any given spike. Owing to the large number of spikes in amperometric experiments (several hundred spikes treated) this afforded statistically significant analysis of size distributions of initial fusion pore [3] as well as that in its final stage (full fusion). In turn this provided for the first time experimental access to the potential energy well governing the thermodynamics of such nanosystems suggesting their pure lipidic nature.

References

[1] C. Amatore, S. Arbault, M. Guille, F. Lemaître, *Chem. Rev.* **108**, 2585(2008).

[2] C. Amatore, A. I. Oleinick, I. Svir, *ChemPhysChem* **11**, 149(2010); **11**, 159(2010).

[3] A. Oleinick, F. Lemaître, M. Guille Collignon, I. Svir, C. Amatore, *Faraday Discuss.*, in press.

[4] A. Albillos et al., *Nature* **389**, 509(1997).

3EO05 Protein Salting out Observed at an Air-water Interface

Y. F. Yano[1], K. Nitta[2], and T. Uruga[2]

[1]*Department of Physics, Kinki University, Osaka 577-8502 Japan*
[2]*Japan Synchrotron Radiation Research Institute, Hyogo 679-5198, Japan*
e-mail : *yano@phys.kindai.ac.jp*

Protein crystallization is typically realized by the addition of a salt or an organic solvent to a supersaturated protein solution to decrease the protein solubility. "Salting out" is a method for separating proteins, in which the hydrated salt ions reduce the number of water molecules available for interaction with the proteins. Protein solubility is a macroscopic property resulting from various molecular interactions, including protein-protein, protein-ion, ion-water, and water-protein interactions, and depends on temperature, pH, ion species, and concentration.

The effect of ion species on the solubility of proteins is classified by the well-known Hofmeister series, defined by the concentration of a particular salt needed to precipitate proteins from whole egg white. The series are usually given in terms of the ability of the ions to stabilize the structure of proteins. Interestingly, the molar surface-tension increment of the salt also follows the rank order of the Hofmeister series.

Herein, we examine the protein adsorption process in salt solutions using time-resolved x-ray reflectometry [1] to investigate the salting-out phenomenon at the air-water interface. We found that the LSZ molecule initially adsorbed by adopting a flat, unfolded structure as a result of hydrophobic interactions with the gas phase [2, 3]. As the adsorption continues, protein refolding and a crystal nucleation with the refolded proteins are observed [4, 5]. We speculated that the observed phenomenon induced by screening of the positive charges in the LSZ by the salt anions. In the present study, therefore, to clarify the role of the salt ions in the protein crystal nucleation at an air-water interface, we investigate the effect of anion species on the structure of LSZ surface layer.

References

[1] Y.F. Yano, T. Uruga, H. Tanida, H. Toyokawa, Y. Terada, M. Takagaki, H *J. Synchrotron Rad.*, **17** 511-516 (2010).

[2] Y.F. Yano, T. Uruga, H. Tanida, H. Toyokawa, Y. Terada, M. Takagaki, H. Yamada, *Langmuir*, , **25,** 32-35 (2009).

[3] Y.F. Yano, *J. Phys.: Condens. Matter*, **24**, 50301 (2012)

[4] Y.F. Yano, T. Uruga, H. Tanida, H. Toyokawa, Y. Terada, H. Yamada, *J Phys. Chem. Lett.*, **2** 995-999 (2011).

[5] Y.F. Yano, T. Uruga, *Chem. Phys.*, in press (2013).

3EO06 Thermodynamic measurement of the structural fluctuation in the signaling state of phototropin

Y. Nakasone[1], K. Zikihara[2], S. Tokutomi[2] and M. Terazima[1]

[1]*Department of Chemistry, Kyoto University, Kyoto 606-8502, Japan*

[2]*Osaka Prefecture University, Osaka 599-8531, Japan*

e-mail : nakasone@kuchem.kyoto-u.ac.jp

In solution chemistry, the thermodynamic parameters are useful for characterizing the state of molecules. Here, we used the time-resolved thermodynamical measurements to study the nature of intermediate species of a protein, photoropin. Phototropin is a blue-light sensor protein in plants, which consists of two LOV domains, a kinase domain and a linker-helix, which connects the LOV2 and the kinase. As shown in Fig.1, dissociation and subsequent unfolding of the linker-helix are induced upon photo-excitation of the LOV2 domain [1]. A dynamic simulation study has shown that the fluctuation of the LOV2 domain was enhanced in the lit state, which might be responsible for the dissociation of the linker-helix [2].

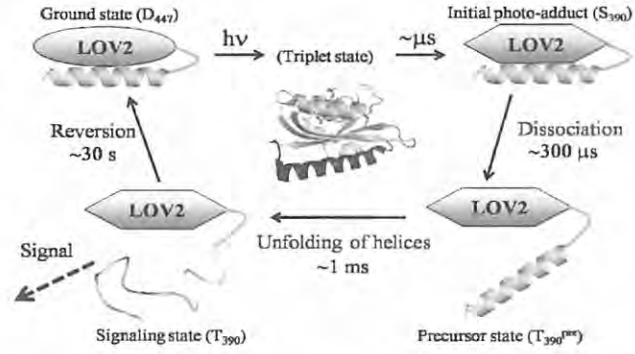

Fig.1 The reaction scheme of phototropin-LOV2 domain with linker

In order to experimentally observe the structural fluctuation, we used thermal expansion coefficient (α_{th}) and heat capacity (C_P) of protein, which represent the structural fluctuation and the entropic fluctuation, respectively. We measured the changes in α_{th} and C_P during photochemical reactions of phototropin1-LOV2 domain by the transient grating (TG) and transient lens (TrL) methods. These techniques can achieve a time-resolved quantitative measurement of the volume change (ΔV) and enthalpy change (ΔH). The α_{th} and C_P values were estimated by monitoring the temperature dependence of ΔV and ΔH, respectively. So far, we obtained clear temperature dependence of ΔV associated with the initial step of the photoreaction (adduct formation between chromophore and cysteine residue in the LOV2 domain), which can be interpreted as an enhancement of the structural fluctuation. We also found that C_P was increased both in the initial step and the unfolding process of the linker helix, which indicated that the entropic fluctuation was enhanced during these processes. Since the entropic fluctuation strongly depends on the solvent accessible surface area of protein molecule (*hydration effects*), the change of C_P was mainly attributed to the change of surface structure. The details of the structural fluctuation and the role of water molecules in the signaling process will be presented at the symposium.

References

[1] Y. Nakasone et al. *J. Mol. Biol.* **367**:432 (2007).

[2] P. L. Freddolino et al. *Biophys J.* **91**:3630 (2006).

3EO07 The intermolecular interaction and dynamics of bovine serum albumin solutions.

K. Yanase[1], R. Arai[2], R. Buchner[3], and T. Sato[1]

[1]*Department of Materials and Chemical Engineering, and* [2]*Division of Applied Biology, Shinshu University, Ueda 386-8567, Japan*

[3]*Institut für Physikalische und Theoretische Chemie, Univ. Regensburg, D-93040, Germany*

e-mail : takaakis@shinshu-u.ac.jp (T.S), 13fm527e@shinshu-u.ac.jp (K.Y)

By means of small and wide angle X-ray scattering (SWAXS) and dielectric relaxation spectroscopy (DRS), we investigated solution of bovine serum albumin (BSA), the most abundant plasma protein in bovine's bloodstream, to reveal its static structure and dynamics in solution. In this contribution, we report how intermolecular interactions of BSA differ depending on different ionic strength of solvent and a renovated assignment of dielectric relaxation processes in aqueous solution.

Using SWAXS, we investigated BSA solutions at protein concentrations of $5.0 \leq c$ / mgmL$^{-1} \leq 211$ in water to minimize ionic strength, and in 0.15 M phosphate buffer serine (PBS) to fulfil the physiological condition. We extracted the effective structure factor, $S(q)^{\mathrm{eff}}$, by dividing a normalized intensity, $I(q)/c$, by an experimental form factor, $P(q)^{\mathrm{exp}}$, determined at very low concentration. Further insights into the spatial correlations of BSA molecules were obtained by monitoring the effective (potential model-free) pair correlation function, $g(r)^{\mathrm{eff}}$, which was deduced by the inverse Fourier transformation of $S(q)^{\mathrm{eff}}$. In aqueous solutions, the mean nearest-neighbour distance between the proteins, d^*, was well described by that predicted from a charged colloidal model, i.e. $d^* \propto c^{-1/3}$, indicating that the system is governed by weakly screened electrostatic repulsion. On the other hand, d^* in PBS solutions decreased moderately with increasing BSA concentration. The d^* values for different solvent conditions coincided with each other at high c. The data demonstrate that electrostatic screening effect modifies the length scale of BSA-BSA interaction from long-ranged to short-ranged ones.

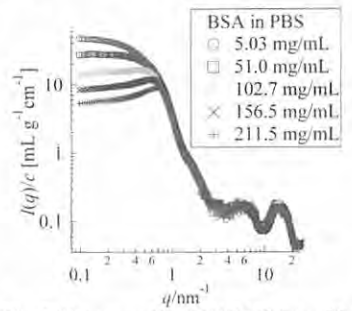

Fig. 1 The normalized SWAXS intensities, $I(q)/c$, of BSA in PBS at 25 °C.

The complex dielectric spectra of aqueous BSA required at least three relaxation processes. The relaxation time ca. 8 ps for the highest frequency process reflects the time scale of cooperative rearrangement of the hydrogen-bond network of bulk water. Beside, according to Stokes-Einstein-Debye equation, the relaxation time ca. 50 ns of the lowest frequency process yielded an effective molar volume of BSA identical to that predicted from its molecular weight. Thus, the process is assigned to the rotational diffusion of the BSA. Recent DRS studies on protein solutions have suggested that the intermediate frequency process centred at ca. 100 MHz is due to the orientational relaxation of water molecules in the hydration shell [2]. However, this assignment may be challenged if polarization fluctuation caused by counter ion crowd and charged groups on the protein surface is accounted for. We will discuss such an aspect in detail in the actual presentation.

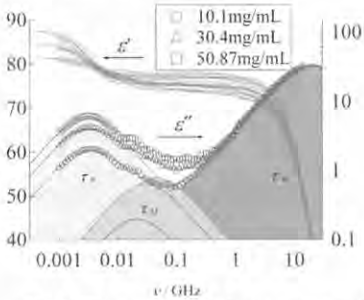

Fig. 2 The complex dielectric spectra of aqueous BSA solutions at 25 °C.

References

[1]T. Fukasawa, and T. Sato, *Phys. Chem. Chem. Phys.* **13**, 3187-3196 (2011).

[2] C. Cametti, S. Marchetti, C.M.C. Gambi, and G. Onori, *J. Phys. Chem. B,* **115**, 7144-7153 (2011).

1FO01 Interfacial Water over $CaCO_3$ probed by FM-AFM

H. Imada, K. Kimura, and H. Onishi

Department of Chemistry, Kobe University, Kobe 657-8501, Japan

e-mail : oni@kobe-u.ac.jp

Liquid-solid interfaces play an important role in chemistry and chemical engineering. Atomic force microscopy operated in frequency modulation mode (FM-AFM) provides a promising tool to observe the liquid structure as well as the solid topography at interfaces. The cantilever with a tip at the free end is resonantly oscillated and the shift of the resonance frequency (Δf), which represents liquid-induced force pushing or pulling the tip, was determined as a function of the vertical *and* lateral coordinates. The force distribution has been observed and related to the density distribution of interfacial liquids at a number of interfaces including water/mica [1, 2], water/Al_2O_3 [3], water/ *p*-nitroaniline [4], water [5] and alcohols [6] on OH- or COOH-terminated molecular monolayer, hydrocarbons/CH_3-terminated monolayer [7], and decanol/graphite [8]. In the present study, water on calcite was examined to show significant water structuring on this important polymorph of $CaCO_3$. Figure 1 shows the topography of a cleaved (104) surface of calcite and Δf distribution perpendicular to the surface and parallel to the [010] direction. Positive (or negative) Δf represents repulsive (or attractive) tip-surface force to be shown bright (or dark). Bright and dark patches were further recognized to suggest the solution structured over the surface. The patches were vertically and laterally ordered to present a checkerboard pattern commensurate to the topographic corrugations of calcite.

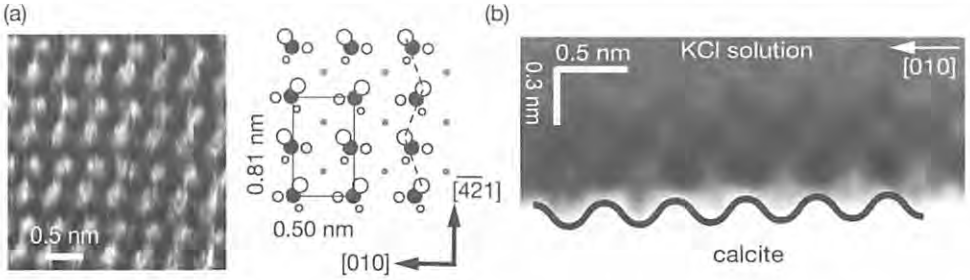

Fig. 1. Calcite (014) surface immersed in an aqueous KCl solution of 0.5 M. The surface topography and cross-sectional Δf distribution are shown in (a) and (b) together with an illustration of the atom arrangement of the surface. Dark, bright and gray spheres represent carbon, oxygen and calcium atoms, respectively. A rectangular unit cell is overlaid. The broken line traces the zigzag alignment of carbonate oxygen atoms protruding above the surface plane.

References [1] K. Kimura et al., *J. Chem. Phys.* **132**, 194705 (2010). [2] T. Fukuma et al., *Phys. Rev. Lett.* **104**, 016101 (2010). [3] T. Hiasa et al., *J. Phys. Chem.* **C114**, 21423 (2010). [4] R. Nishioka et al., *J. Phys. Chem.* **C117**, 2939 (2013). [5] T. Hiasa et al., *Phys. Chem. Chem. Phys.* **14**, 8419 (2012). [6] T. Hiasa et al., *J. Phys. Chem.* **C117**, 5730 (2013). [7] T. Hiasa et al., *Coll. Surf.* **A396**, 203 (2012). [8] T. Hiasa et al., *J. Phys. Chem.* **C116**, 26475 (2012).

1FO02 Ultrasonic relaxation spectroscopy of SiO_2+water nanofluids.

S.Z.Mirzaev, S.K. Telyaev, V. Avdievich
Institute of Ion-plasma and laser technologies, Uzbek Academy of Sciences,
Do'rmon yo'li str. 33, 100125 Tashkent, Uzbekistan
e-mail:sukhrobtillo@gmail.com

A fluid containing suspended nanometer-sized solid particles are called nanofluids. Since the concept of nanofluid has been introduced by Eastman and Choi [1], there have been many efforts to understand the mechanism of heat transfer enhancement by various experimental methods.

To understand the mechanism of heat transfer enhancement it is crucial to have the ideas on the aggregate formation within the fluid. Ultrasonic relaxation methods for aggregate characterization have many advantages. They are generally non-invasive, can be non-contact, are safe and often are economic [2].

It has been investigated the acoustic spectra of SiO_2+water nanofluids. Value of additional attenuation have been measured depending on sound frequency (in the frequency range from 300 kHz to 150 MHz), particle sizes (12 nm, 16 nm and 40 nm), and temperatures (278K, 283K, 293K, 303K, 313K). Two acoustical relaxation processes has been observed in this suspensions. Relaxation curve shift to the low frequencies area with decreasing nanoparticle size. The reverse tendency can be seen at temperature changes, i.e. shifting relaxation curve occurs to the high frequency area with decreasing of system temperature.

We suggested that the relaxation process arise due to aggregate formation of units in nanofluids. At low frequencies the mechanism causing losses of ultrasonic energy in investigated systems is the friction between aggregates and liquid. In the high frequencies area attenuation is caused by loss of the ultrasonic wave energy in the aggregates which arise owing to increasing viscosity of water in aggregate pores. Thus, the attenuation value and relaxation spectrum of studied systems is defined by aggregate properties. It explains behavior of relaxation spectrum with decreasing particle size and temperature, because physical parameters of the aggregate strongly depend both from the nanoparticle size and on temperature.

References

1. Eastman, J. and S. Choi, Anomalously Increased Effective Thermal Conductivities of Ethylene Glycol-Based Nanofluids, Applied Physics Letters 78, 718-720. 1995.
3. Povey, M. J. W.: Ultrasonic techniques for fluids characterisation. (Academic Press, San Diego) 1997.

1FO03 Surface Freezing of Binary Alcohol Mixtures

T. Takiue, M. Tsuura, A. Shuto, H. Matsubara, and M. Aratono

Department of Chemistry, Faculty of Sciences, Kyushu University, Fukuoka 812-8581, Japan

e-mail : t.takiue@chem.kyushu-univ.jp

Surface freezing (SF) is the phenomenon of the two-dimensional condensed film formation at liquid surface at temperature T_s which is a few degrees above the bulk freezing temperature T_b. Deutsch *et al.* have claimed that liquid alkanes with 16~50 carbon atoms and alkanols with 10~28 ones exhibit SF phenomena.[1] In this study, we aim at discussing the miscibility of molecules at the surface of the binary liquid mixture of alkanols from the viewpoint of the mutual interaction between the film forming molecules. We employed two kinds of mixtures; 1-undecanol (C11OH) – 1-dodecanol (C12OH) and 6-perfluorohexyl hexanol (F6H6OH) – C12OH mixtures.

The surface tensions (γ) of these mixtures were measured as a function of temperature (T) and composition of C12OH in the liquid mixture (x_2) under atmospheric pressure. X-ray reflectivity (XR) measurement was performed at BL37XU in SPring-8 as a function of scattering vector along the interface normal Q_z. Pure alkanols and their mixture were saturated with water at desired temperatures before measurements.

The γ vs. T curves of pure C11OH and C12OH systems show a sharp break point at T_s corresponding to the surface liquid (SL) – SF phase transition. The value of pure F6H6OH, on the other hand, decreases monotonically with increasing T. The entropy of surface formation Δs are large negative due to a well-ordered structure of SF layer. The value in the SF state is ca. -0.8 mJ K^{-1} m^{-2}, which is nearly twice of those in the condensed monolayer of the CnOH/water systems (ca. -0.4 mJ K^{-1} m^{-2}), suggesting that CnOH molecules form SF bilayer. The electron density profile obtained by XR indicated that the bilayer is stabilized by the hydrogen bonding between OH groups facing each other through water molecule intercalated in between them.

In the C11OH−C12OH system, the SL−SF transition was found at all x_2. The estimation of surface composition suggested that two components are miscible both in SL and SF states. The excess entropy of the surface $s^{\sigma,E}$ is almost zero in both states and thus it was concluded that the two components are mixed almost ideally at the surface. In case of F6H6OH−C12OH system at high x_2, on the other hand, SL layer is enriched in F6H6OH with lower surface tension than C12OH compared to bulk liquid. The negative $s^{\sigma,E}$ value in SL layer suggests that F6H6OH molecules form domain at the surface. The surface composition and electron density profile indicated that a small amount of F6H6OH mix with C12OH in the SF bilayer in which F6H6OH molecules preferentially exist in the upper layer of the bilayer.

References

[1] O. Gang, X.Z. Wu, B.M. Ocko, E.B. Sirota, M. Deutsch, *Phys.Rev. E,* **58**, 6086 (1998).

1FO04 The Effect of pH and Counterion Property on the Surface Adsorption of Fe(III)-edta Complex

M. Villeneuve, M. Tanaka, and M. Abe

Graduate School of Science and Engineering, Saitama University, Saitama 338-8570, Japan

e-mail : villeneuve@chem.saitama-u.ac.jp

The influences of pH of the aqueous solution and the hydration property of the counterion on the adsorption of iron(III)-ethylenediamine-N,N,N',N'-tetraacetic acid complex (Fe-edta) at the air/water interface were studied by surface tension measurement. Experimental data were analyzed with thermodynamic equations derived for mixed aqueous solutions of an alkali hydroxide (MOH) and Fe-edta, in which the following dissociation and association equilibria [1, 2] of Fe-edta complex were taken into account.

$[Fe(Hedta)(H_2O)] \rightleftharpoons [Fe(edta)(H2O)]^- + H^+$; $pKa_1 = 2.2$[1] (1)

$[Fe(edta)(H_2O)]^- \rightleftharpoons [Fe(edta)(OH)]^{2-} + H^+$; $pKa_2 = 7.6$[1] (2)

$2[Fe(edta)(OH)]^{2-} \rightleftharpoons [(edta)Fe\text{-}O\text{-}Fe(edta)]^{4-} + H_2O$; $pKd = -1.88$[2] (3)

At a given temperature and pressure, surface tension is expressed as a function of m and X_2.

$$-\mathrm{d}\gamma/(RT\Gamma_t^H) = (BX_1^H + CX_2^H)/m\ \mathrm{d}m + (DX_1^H + EX_2^H)\ \mathrm{d}X_2, \quad (4)$$

where B, C, D, E are determined by degrees of dissociation and association of Fe(III)-edta (eqs. (1) ~ (3)), m and X_2. Γ_t^H is the total surface density ($\Gamma_t^H = \Gamma_{c0}^H + \Gamma_{c1-}^H + \Gamma_{c2-}^H + \Gamma_d^H + \Gamma_{M+}^H$) and X_2^H is the interfacial composition of the Fe-edta ($X_2^H = (\Gamma_{c0}^H + \Gamma_{c1-}^H + \Gamma_{c2-}^H + \Gamma_d^H) / \Gamma_t^H$). Here, c_0, c_{1-}, c_{2-}, and d represent the nonionic specie $[Fe(Hedta)(H_2O)]$, the monovalent ionic specie $[Fe(edta)(H_2O)]^-$, the divalent ionic specie $[Fe(edta)(OH)]^{2-}$, and the dimer $[(edta)Fe\text{-}O\text{-}Fe(edta)]^{4-}$, respectively. Thus the surface tension and pH of aqueous solutions of MOH / Fe-edta mixture were measured at 298.15 K under atmospheric pressure as functions of m and X_2 ($m = m_1 + m_2$; $X_2 = m_2/(m_1 + m_2)$, m_1: molality of MOH, m_2: molality of Fe-edta).

The total surface density Γ_t^H vs. m curves at constant X_2 of the KOH / Fe-edta and the NaOH / Fe-edta systems were significantly different from each other as shown in the figure. The water-structure-breaking ion, K^+ brought Fe-edta to positive adsorption at most X_2, whereas the water-structure-making ion Na^+, negative adsorption at most X_2. The counter ion effect on pH dependence of the surface density will be discussed in detail at the conference.

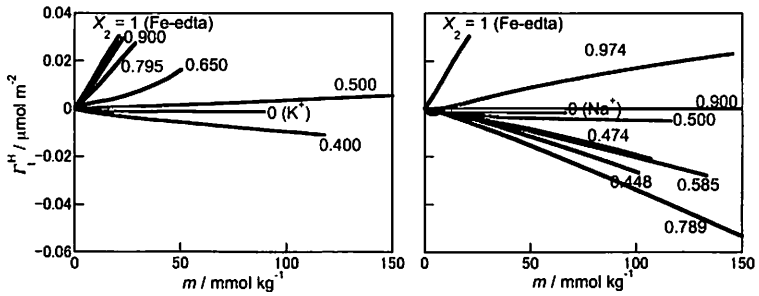

Fig. Γ_t^H vs. m curves at constant X_2: KOH / Fe-edta system (left); NaOH / Fe-edta system (right).

References

[1] J. L. Lambert, C. E. Godsey, L. M. Seitz, *Inorg. Chem.*, **1963**, 127-129.

[2] W. W. Frenier, *Canadian Journal of Chemistry*, **1980**, 1999-2005.

2FO05

Molecular Junction

Yi-Hong Wang[2], Yi-Ling Chen[1], Mei-Ling Guo[1], Shu-Han Hsu[1*]

[1] *Nano Device Laboratories, Hsinchu 300, Taiwan,*

[2]*Department of electrophysics, Nation Chiao-Tung University, Hsinchu 300, Taiwan,*

**E-mail : hsushuhan@ndl.org.tw*

Nowadays, devices scaling is the mainstream in semiconductor technology over the last few decade[1]. Along the gate scaling, the source/drain extension junction depths must scale down as well. However, conventional ion implantation poses random dopant fluctuations and caused the damage of transistor. Therefore, an emerging technique named monolayer doping (MLD) was utilized for possible device development.[2-3] They demonstrated the possibility of using self-assembled monolayer (SAM) as doping source to form shallow junction. However, the applied temperature above 1000°C is still too high for device integration. Here, a new strategy was presented to lower down the diffusion barrier of dopants with in-situ activation. Dopant diffused into the lattice position after in-situ thermal annealing, forming a ultra-shallow junction (~10 nm) with low sheet resistance (~307 Ω). By diode fabrication, the electrical performance clear observes its electrical characteristics from the monolayer doping. Different characterizations were utilized to confirm the junction formation, such as contact angle SIMS、XPS、TEM、and four-probe measurements.

By using this surface-rich chemistry of self-limiting monolayer formation on silicon, the dopant concentration could be well-controlled in sub-nano degree. Currently, this technology was under investigation for the non-plane structures such as nanowire and FinFET devices fabrications.

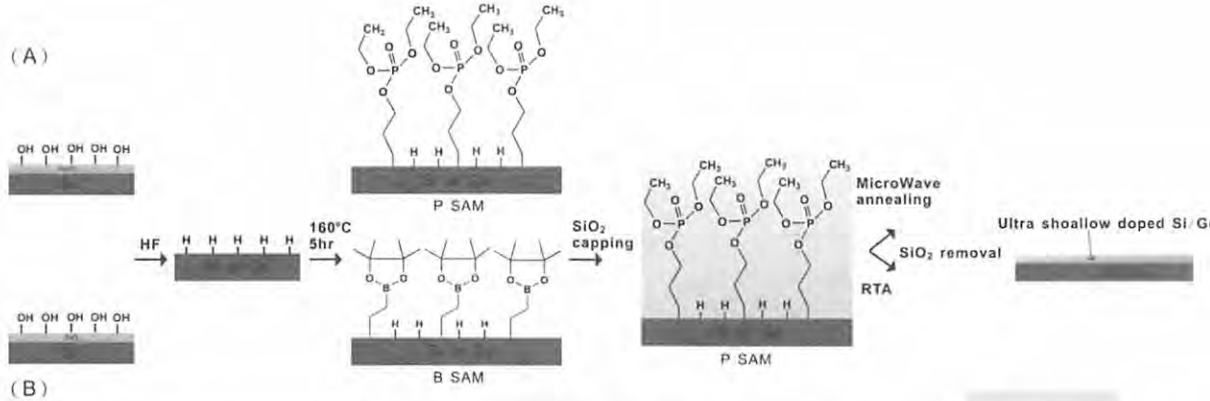

SAM	Blank θ(°)	P SAM θ(°)	Br SAM θ(°)
Si(100)	81±2	65±1	72±2
Ge(100)	70±2	63±1	78±3

Figure Scheme of the monolayer junction formation and its surface characterisation.

References

1. Claeys, C. VLSI Design 2004, 275–282 (2004).
2. Johnny C. Ho et al., Nat. Materials, vol.7, pp. 62-67, 2008.
3. Johnny C. Ho et al., Nano Letters. , vol. 9, pp. 725-730, 2009

2FO06 Phase Behaviour and Microstructural Transition of Sucrose Ester-Based Microemulsions

Sanggu Kim[1], Wai Kiong Ng[1], and Reginald B. H. Tan[1]

[1]*Formulation Science, Crystallization and Particle Science, Institute of Chemical and Engineering Sciences (ICES), Agency for Science, Technology and Research (A*STAR), 1 Pesek Road, Jurong Island, Singapore 627833*

e-mail : sanggu_kim@ices.a-star.edu.sg

In recent years, the growing interest in sugar-based surfactant microemulsions arises as potential candidates of food, cosmetic and drug delivery systems because of excellent thermodynamic stability, biocompatibility and biodegradability, less temperature sensitivity, and improved solubilization of poorly water-soluble compounds [1].

Sucrose ester microemulsions composed of sucrose laurate (SL), propylene glycol and water were prepared with the essential oil of *Melaleuca alternifolia* (TTO) as oil phase which show a broad spectrum of antimicrobial activity to investigate the phase behaviour and microstructure [2]. The identification of the constituents of crude TTO is strongly required because their structure and composition can influence on the formation of microemulsion. The major chemical components of TTO determined by gas chromatography–mass spectroscopy (GC/MS) analysis were terpinen-4-ol (42.65%), γ-terpinene (22.85%), and α-terpinene (10.36%). The pseudoternary phase diagrams were constructed by water titration with different surfactant and cosurfactant mixing ratios (K_m= surfactant/cosurfactant) between 1:1, 2:1 and 3:1 at room temperature. The extension of the microemulsion zone was found to be strongly dependent on the K_m ratios. The oil-in-water (o/w) microemulsion region increased when K_m ratio is increased from 1:1 to 3:1 and the solubility of TTO was increased with increasing the concentration of SL. Microstructural aspects were also studied by electrical conductivity and pulsed gradient spin echo (PGSE) NMR measurements along water titration line L28 (R_o = 2:8). The results showed that the microemulsion microstructure was changed as the water content increases. The microstructural inversion of w/o to bicontinuous microemulsions occurred at ~30 wt. % water while the transition from bicontinuous to o/w structure occurred at ~55 wt. % water. The results from these combined techniques were in good agreement in regard to the microstructure transition points.

References

[1] A.N. Garti, V. Clement, M. Fanun, M.E. Leser, *J. Agric. Food Chem.* **48**, 3945(2000).

[2] S. Kim, W.K. Ng, S. Shen, Y. Dong, R.B.H. Tan, *Colloids and Surfaces A:Physicochem. Eng. Aspect.* **348**, 289(2009).

2FO07 Computer simulation of self-assembly of rigid linear and facial surfactant molecules in aqueous solution

Hans-Jörg Mögel, Mirco Wahab, Peter Schiller

TU Bergakademie Freiberg, Institute of Physical Chemistry, Leipziger Strasse 29, 09599 Freiberg, Germany

e-mail: Hans-Joerg.Moegel@chemie.tu-freiberg.de

Linear and facial surfactant molecules with rigid hydrophobic cores and variously distributed hydrophilic groups of various sizes are investigated for their aggregation properties. Typical linear molecules used in this study are bolaform amphiphiles, which contain two hydrophilic groups terminating a rigid hydrophobic chain. As models for facial amphiphiles, the biologically important bile salts, consisting of a rigid hydrophobic steroid skeleton and attached hydro-philic groups, have been studied.

Using Molecular Dynamics and Monte-Carlo Simulation techniques for studying simple off-lattice coarse-grained models of surfactants, we found a large variety of structures ranging from micelles of varying shape and size to cubic structures and highly ordered linear aggregates. Depending on the temperature and concentration conditions of the surfactant solutions, we observed the occurrence of a diversity of phase structures and the growth of ordered nanostructures. The specific geometrical constraints introduced by the shape and the distribution of hydrophobic and hydrophilic groups within the architecture of the single molecules in combination with the rigidity of the backbone allows for the formation of diverse aggregates which even can be chiral. In this study, we have shown that very simple models built from hydrophobic and hydrophilic segments interacting with short range potentials including non-bonded mutually neighboured segments within 1.73 σ (σ is the diameter of spherical segments) are adequate to study the molecular aggregation of surfactants by self-assembly.

A particular interesting case of structure formation in solutions of rigid amphiphilic molecules is the self-limited self-assembly. We have found two types of molecules which form roughly monodisperse anisometric associates with a non-periodic internal order. The orientation of the the molecular axes changes regularly into radial direction up to a certain angle at the rim of the aggregate . For geometric and energetic reasons this change is not allowed to be continued and, in this way, the size of the anisometric aggregate is limited.

2FO08 Free energy of solubilization of solute molecules in SDS micelle solution studied by molecular dynamics calculations

K. Fujimoto[1], N. Yoshii[2], and S. Okazaki[3]

[1]*College of Pharmaceutical Sciences, Ritsumeikan University, 1-1-1 Noji-higashi, Kusatsu, Shiga 525-8577, Japan*

[2] *Center for Computational Science, Nagoya University, Furo-cho, Chikusa-ku, Nagoya 464-8603, Japan*

[3]*Department of Applied Chemistry, Nagoya University, Furo-cho, Chikusa-ku, Nagoya 464-8603, Japan*

e-mail : okazaki@apchem.nagoya-u.ac.jp

Above the critical micelle concentration (CMC), the surfactant molecules aggregate each other to form a micelle. A water-insoluble substance can be dissolved in this micelle solution such that the micelle accommodates the solute. This phenomenon is called "solubilization". The solubilization is utilized in various scientific and industrial processes. However, little is known at a molecular level still now. Thus, it is interesting to investigate interaction between the micelle and solubilized molecules in the solution.

In order to clarify the solubilization at a molecular level, free energy of transfer of a series of alkane, i.e. methane, ethane, butane, hexane, and octane as well as amphiphilic molecule such as methylamine, octylamine, methanol, and octanol from water phase to a sodium dodecyl sulphate (SDS) micelle has been calculated by thermodynamic integration method combined with molecular dynamics (MD) calculations. [1, 2] The free energy of transfer of all alkanes was negative, that is, the alkanes in the SDS micelle are more stable than in the water phase avoiding contact with water molecules. Further, the calculated free energy of transfer from water phase to the micelle core decreases almost linearly as a function of the number of carbon atoms of alkanes with a decrement of 3.3 kJ mol^{-1} per one methylene group. The free energy of transfer of methylamine, octylamine, methanol, and octanol from the water phase to the SDS micelle is all negative, i.e. they are stable in the SDS micelle. The longer the alkyl chains in the solubilized molecule are, the more stable the solubilized molecules in the SDS micelle. Further the methane and octane molecule are found in the SDS micelle core. The methylamine was adsorbed on the SDS micelle surface. The methanol is found everywhere in the system from the SDS micelle core to the water phase. The octylamine and octanol are solubilized in the SDS micelle with palisade layer structure.

References

[1] K. Fujimoto, N. Yoshii, and S. Okazaki, *J. Chem. Phys.* **133**, 074511 (2010).

[2] K. Fujimoto, N. Yoshii, and S. Okazaki, *J. Chem. Phys.* **137**, 094902 (2012).

5FO09 Motions and Fluctuations of Phospholipid Molecules in Large and Cell Sized Vesicles by NMR

E. Okamura[1], Y. Takechi[1,2], H. Saito[2], and N. Yoshii[1,3]

[1]*Faculty of Pharmaceutical Sciences, Himeji Dokkyo University, Himeji 670-8524, Japan*

[2]*Institute of Health Biosciences and Graduate School of Pharmaceutical Sciences, The University of Tokushima, Tokushima 770-8505, Japan*

[3]*Graduate School of Engineering, Nagoya University, Nagoya 464-8603, Japan*

e-mail : emiko@himeji-du.ac.jp

Lipid bilayer vesicle, the simplest model of cell membranes, is a confined space with fluid, soft interfaces. We have applied the pulsed-field-gradient (PFG) NMR measurement to large unilamellar vesicles (LUVs) in solution and reported the diffusion motions of lipids and trapped drugs in LUV [1,2]. The problem is that the observed diffusion is the sum of (i) the lateral diffusion of lipids and drugs on the vesicle surface, (ii) the rotational, and (iii) the translational diffusion of the vesicle as a whole, since they have not been separable in the experiment. We show that the lateral diffusion of lipids can be separated as a time-dependent part of the observed diffusion in LUV of 800-nm diameters, by systematically changing the diffusion time interval of the high-field-gradient NMR measurement [3]. This enables us to determine the precise value of lipid lateral diffusion coefficient in hydrated, freestanding bilayer membranes in a natural manner.

Although LUVs with hundred-nanometer diameters have been used as a suitable model for cell membranes, cell sized vesicles (CSVs), greater than ~10 μm in diameter, should be more suitable in view of the size that is comparable to the living cell. To shed light on how lipid motions and fluctuations are modified in cell sized biological membranes, we have also applied 2D NOESY and 1D transient NOE measurements to the CSV system, and systematically compared the results to LUVs from 100- to 800-nm diameters [4].

It is found that the lateral diffusion of lipids in the fluid phase is, at least, more than one order of magnitude faster than the rotational and the translational diffusion of the vesicle by the hydrodynamic continuum model [3]. Although the tumbling motion of the lipid is extremely slow in the giant CSV, the proximity between the lipid headgroup and hydrophobic chains is shown as a result of the large protrusion in the vertical direction to the CSV surface [4].

References

[1] E. Okamura, C. Wakai, N. Matubayasi, Y. Sugiura, M. Nakahara, *Phys. Rev. Lett.*, **93**, 248101 (2004).

[2] E. Okamura, N. Yoshii, *J. Chem. Phys.*, **129**, 215102 (2008).

[3] N. Yoshii, T. Emoto, E. Okamura, *Colloid Surf. B-Biointerfaces*, **106**, 22-27 (2013).

[4] Y. Takechi, H. Saito, E. Okamura, *Chem. Phys. Lett.*, 2013, http://dx.doi.org/10.1016/j.cplett. 2013.03.048.

5FO10 Re-entrant Lamellar/Onion Transition under Shear Flow in a Nonionic Surfactant/Water System

D. Sato, Y. Kawabata, and T. Kato

Department of Chemistry, Tokyo Metropolitan University, Tokyo 192-0397, Japan

e-mail : kato-tadashi@tmu.ac.jp

In the past 20 years, effects of shear flow on the structure of the lamellar phase have been studied extensively. Among them, the most striking result may be the transition from the lamellar phase to the "onion phase" where all the space is filled by multilamellar vesicles alone. Although this type of transition has been reported for many systems, neither the transition mechanism nor the conditions necessary for the onion formation has yet been established. Recently, We have found for the first time the reentrant lamellar/onion transition with varying temperature under constant shear rate by using simultaneous measurements of shear stress and small-angle X-ray scattering (Rheo-SAXS) for a nonionic surfactant ($C_{14}E_5$)/water system[1] (C_nE_m is an abbreviation of $C_nH_{2n+1}(OC_2H_4)_mOH$).

Figure 1 shows time evolutions of 2-dimensional SAXS pattern for the radial (a) and tangential (b) configurations and shear stress (c), and intensities of the Bragg peaks (d) at the shear rate of 3 s^{-1} in a $C_{14}E_5$/water system (50 wt%), which indicates re-entrant lamellar/onion (lamellar-onion-lamellar) transition with increasing temperature. The lamellar-to-onion transition with *decreasing* temperature has been reported for a $C_{10}E_3$/water system[2] whereas the transition with *increasing* temperature has been reported for a $C_{16}E_7$/water system[3]. The $C_{14}E_5$/water system exhibits both types of transition and therefore useful to investigate conditions of onion formation.

We have also derived a theoretical expression of the deformation energies stored in the edges and vertices of polyhedral onions in terms of bending modulus, saddle-splay modulus, and the lamellar spacing at rest, which is consistent with the re-entrant transition with varying temperature.

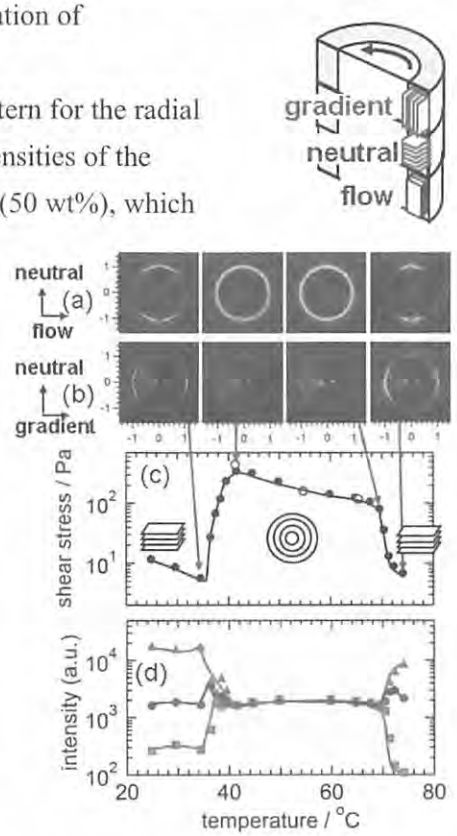

Fig. 1. Time evolutions of 2D SAXS pattern for the radial (a) and tangential (b) configurations, shear stress (c), and intensities of the Bragg peaks (d) at the shear rate of 3 s^{-1} in a $C_{14}E_5$/water system (50 wt%). The circles, squares, and triangles in the panel (d) indicate the intensities for the neutral, flow, and velocity gradient directions, respectively.

References

[1] D. Sato, K. Obara, M. Iwahashi, Y. Kawabata, and T. Kato, *Langmuir*, 29, 121 (2013).

[2] T. D. Le, U. Olsson, K. Mortensen, J. Zipfel, and W. Richtering, *Langmuir* ***17***, 999 (2001).

[3] Y. Kosaka, M. Ito, Y. Kawabata, and T. Kato, *Langmuir*, **26**, 3835 (2010), M. Ito, Y. Kosaka, Y. Kawabata, and T. Kato, *Langmuir*, **27**, 7400 (2011).

5FO11 Gel-like behaviors in a mixture of water / organic solvent / antagonistic salt induced by flow

K. Sadakane[1], M. Shibayama[2], M. Takeda[2], R Inoue[3], and H. Seto[4]

[1]*Department of Physics, Ritsumeikan University, Kusatsu 525-8577, Japan*
[2]*Institute for Solid State Physics, The Univ. of Tokyo, Tokai 319-1106, Japan*
[3]*Institute for Chemical Research, Kyoto University, Kyoto 611-0011, Japan*
[4]*Institute of Materials Structure Science, KEK,Tsukuba 305-0801, Japan*
e-mail : sadakane@fc.ritsumei.ac.jp

Mesoscopic structures, such as lamellar, are discovered in our recent studies in a mixture of water / organis solvent (3-methylpyridine) / salt ($NaBPh_4$) even though no surfactants or polymers are contained [1]. According to the theoretical investigations by Onuki [2], hydrophilic ion (Na^+ and hydrophobic ion (BPh_4^-) tend to adsorb near the interface between water and organic solvent. These ions reduce the interfacial tension between solvents, and mesoscopic structures may be induced as is the case with surfactant mixtures.

As a next step, we investigated the effect of shear-flow on lamellar-structures in a mixture of water / 3-methylpyridine / $NaBPh_4$. Figure 1(a) shows the results of polarization microscomic observation and visual observation. Lamellar structure changes to fiber-like stucture by shaking the mixture. At the same time, the fluidity of the mixture drastically decreased under this condition. Furthermore, shear thickening phenomena and onion-like structures are also observed by Rheo-SALS measurement in this mixture (see Fig. 1(b)) as is the case with polymer gels.

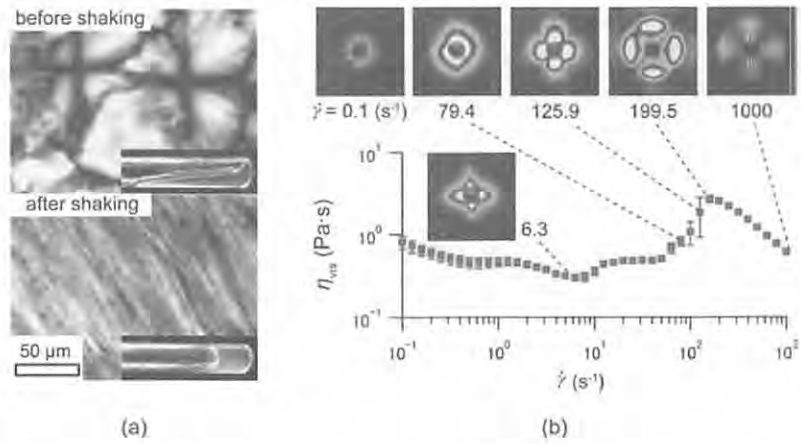

Figure1: (a) The results of visual and polarization microscopic observation on a mixture of D_2O / 3-methylpyridine / $NaBPh_4$. (b) The results of Rheo-SALS measurement.

References

[1] K. Sadakane, A. Onuki, K. Nishida, S. Koizumi, and H. Seto, *Phys. Rev. Lett.*, **103**, 167803 (2009).

[2] A. Onuki, *J. Chem. Phys.*, **128**, 224704 (2008).

5FO12 Fluorescence Quenching of Pyrenesulfonate by Anthoraquinonesulfonate on DDACl Aggregate Surfaces

M. Takezaki, T. Izumi, S. Kitamura, and T. Tominaga

Department of Applied Chemistry, Okayama University of Science, Okayama 700-0005, Japan

e-mail: mtake@dac.ous.ac.jp, ttominaga@dac.ous.ac.jp

Photoinduced electron-transfer reactions in microheterogeneous systems such as micelles and vesicles are important as models not only of two-dimensional bimolecular reactions but also of photosynthetic reactions. Pyrene (Py) and its derivatives have been widely used as fluorescent probes in micelles and vesicles to study microenvironments. Recently, we have reported the excimer formation and decay dynamics of pyrensulfonate (PyS^-) on micellar surfaces of a cationic monoalkyl surfactant, dodecyltrimethylammonium chloride[1]. In this study, we will report a photoinduced electron-transfer reaction from PyS^- to anthraquinone-1-sulfonate (AQS^-) adsorbed on aggregate surfaces of a cationic dialkyl surfactant, didodecydimethylammonium chloride (DDACl). Measurements were performed using a time-correlated single photon counting method at 25 °C.

Fluorescence decays for PyS^- adsorbed on the aggregate surfaces in the absence and presence of AQS^- also adsorbed on the aggregate surfaces are shown in Fig. 1. In the absence of AQS^-, the decay curve can be represented by a single exponential function. The decays in the presence of AQS^- cannot be fitted to the single exponential function but can be represented by the Tachiya-Infelta equation[2, 3].

$$I(t) = I_0 \exp(n\,(\exp(-k_q\,t)-1)-t/\tau) \quad (1)$$

where τ is the unquenched fluorescence lifetime, n is the number of quencher per aggregate and k_q is the quenching rate constant. The aggregation number of DDACl aggregates can be obtained to be 63 from the n values. Further study is being made to understand such small number.

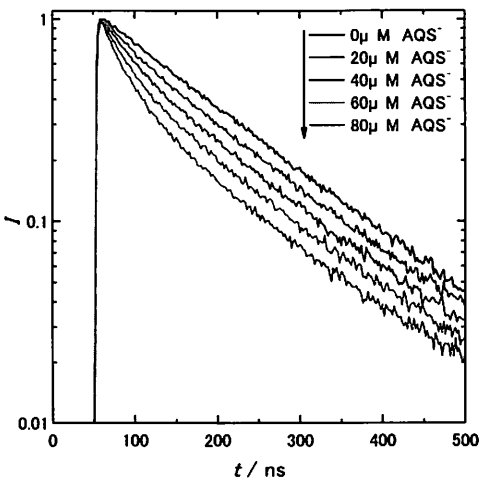

Fig. 1. Fluorescence decays for PyS^- quenched by AQS^- on the aggregate surfaces of 5 mM DDACl.

References

[1] M. Takezaki, T. Tominaga, *Chem. Lett.* **40**, 1300 (2011).

[2] M. Tachiya, *Chem. Phys. Lett.* **33**, 289 (1975).

[3] P. Infelta, *Chem. Phys. Lett.* **61**, 88 (1979).

5FO13 Coating of magnetite with mercapto modified silica in a one-pot process

Nuryono[1], N. M. Rosiati[2], A.H. Suhendi.[2], S.C.W. Sakti[3] and S. Tanaka[4]

[1]*Department of Chemistry, Universitas Gadjah Mada, Yogyakarta 55281, Indonesia*

[2]*Undergraduate Student at Department of Chemistry, Universitas Gadjah Mada, Yogyakarta 55281, Indonesia*

[3]*PhD Student at the Division of Environmental Material Science, Faculty of Environmental Earth Science, Hokkaido University, Japan*

[4]*Division of Environmental Material Science, Faculty of Environmental Earth Science, Hokkaido University, Japan*

e-mail: nuryono_mipa@ugm.ac.id

In this research, mercapto-silica coated magnetite (MSCM), Fe_3O_4-SiO_2-SH, has been prepared through sol-gel process in a one-pot. Preparation of magnetite using $FeCl_2$ and $FeCl_3$ mixtures was optimized by varying conditions including mixing techniques and ageing times. Before synthesis MSCM, coating magnetite with silica was carried out by mixing magnetite powder with sodium silicate solution extracted from rice hull ash at various volumes to to establish the maximum amount of silica that could be coated on the magnetite. The MSCM was prepared in nitrogen condition by mixing magnetite, 3-mercapto-propyltrimethoxysilane (MPTMS), and sodium silicate (Na_2SiO_3) solution extracted from rice hull ash, and the mixture pH was adjusted to reach 7.0 using hydrochloric acid and the kept the mixture overnight. The residue was washed with water, dried at 150 °C and MSCM was separated with an external magnetic field. In that work, the volume of MPTMS and Na_2SiO_3 was varied and the total amount of Si represented as silica was kept constant. Characters of the material including the functional group presence, the structure, the porosity, the morphology and acid stability were identified by Fourier-transform infrared (FT-IR) spectroscopy, X-ray diffraction, and acid treatment, respectively. Results indicated that mercapto modified silica has succeeded to be coated on magnetite with a simple one-pot process. XRD pattern showed that ultrasonic and nitrogen system for the mixing technique, 1 day ageing time and 150 °C drying were optimum conditions to prepare magnetite. The weight ratio of magnetite to silica to 5:9 is a composition of magnetite coated silica (Fe_3O_4- SiO_2), in which the maximum amount of silica could be coated on magnetite. Based on the IR spectra could be interpreted that there is no chemical interaction among magnetite, silica and mercapto groups; and the optimum composition of Fe_3O_4-SiO_2-SH was at the weight ratio of Fe_3O_4:SiO_2: MPTMS 11:10:14. Data of treatment with acid revealed that coating silica increased the chemical stability of magnetite. This high stability promizes prospective application in the future of the coated magnetite. However, it has to be noted that addition of MPTMS at a higher amount than the optimum composition leaded to the lower stability.

5FO14 Relationship between particle charges and coalescence stability of Pickering oil-in-water emulsions prepared using microchannel emulsification

R. Murakami, T. Iwahashi, Y. Fujimoto, M. Yamamoto

Department of Chemistry of Functional Molecules, Konan University, Kobe 658-8501, Japan

e-mail: murakami@konan-u.ac.jp

Emulsions stabilized by colloidal particles are called Pickering emulsions. One of the most important parameters in stabilizing the Pickering emulsions is wettability of particles against oils and water, quantified by a contact angle measured through a water phase (θ). The energy of adsorption of particles at oil/water interfaces is given by an equation: $\Delta G = \pi\gamma R^2(1-|\cos\theta|)^2$, where γ is an interfacial tension of oils and water and R is a particle radius. When $\theta < 90^\circ$, the ΔG value increases and the particles become strongly adsorbed at oil/water interfaces with increasing θ, implying emulsions stable against drop coalescence are formed with increasing θ.

Metal oxide particles, such as silica and alumina, are frequently used for particulate emulsifiers. The metal oxide particles are positively charged when pH is lower than isoelectric point (IEP), while they are negatively charged when pH is higher than IEP. For macroscopically flat surfaces of metal oxides, it has been shown that the surfaces of metal oxides are most hydrophobic when pH is around IEP[1].

In this study, we have used alumina-coated silica (ACS) particles and prepared particle-stabilized oil-in-water (o/w) emulsions using microchannel emulsification (Fig. 1). The emulsions were made as a function of pH and NaCl concentration (m_{NaCl}) of aqueous dispersions of ACS particles. The pH region where oil drops are stable against coalescence was determined, on the basis of monodispersity of oil drop size, at each m_{NaCl}. Combining experiments on emulsion stability against coalescence and zeta potential measurements (Fig. 2), it is found that monodispersed stable o/w emulsions are formed when pH of aqueous dispersions is around IEP, indicating that relatively less charged particles are relatively hydrophobic, so that they are more strongly adsorbed at oil/water interfaces than those when pH is apart from IEP.

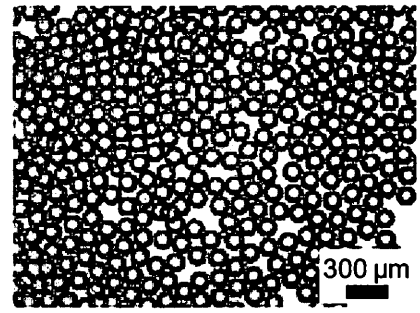

Fig. 1. Optical micrograph of o/w emulsion prepared at pH = 7.8 and m_{NaCl} = 0 mmol kg^{-1}.

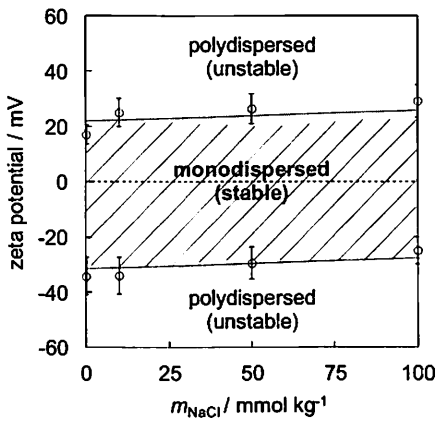

Fig. 2. Region of zeta potentials where stable o/w emulsions are formed.

References

[1] E. McCafferty, J. P. Wightman, *J. Adhesion Sci. Technol.* **13**, 1415 (1999).

1GO01 Ionic liquid salt bridge enables accurate determination of single ion activities in aqueous electrolyte solutions

T. Kakiuchi[1,3], M. Yamamoto[2]

[1]*Department of Energy and Hydrocarbon Chemistry, Graduate School of Engineering, Kyoto University, Kyoto 615-8510, Japan*

[2]*Department of Chemistry, Konan University, Kobe 658-8501, Japan*

[3]*pH Science and Technology Laboratory, Mizuo 3-16, Ibaraki, Osaka 567-0891, Japan*

e-mail : kakiuchi.takashi.55e@st.kyoto-u.ac.jp

Single ion activity is an elusive quantity, in that its definition and measurement are inevitably involved with a certain extrathermodynamic assumption, such as negligible liquid junction potential. This very nature of the single ion activities has raised an epistemological question whether it is a physical, that is, objectively measurable quantity. Whereas pH is one of the most frequently measured parameters in every facets of life, there is no way to escape from the elusiveness because pH is notionally defined in terms of single ion activity of hydrogen ions. The validity of the conventional definition of pH in terms of standardized pH solutions based on the Bates-Guggenheim convention and negligible liquid junction potential at the contact of a test solution and a salt bridge that consists of a concentrated KCl solution is only conditional.

An ionic liquid salt bridge (ILSB) comprised of a moderately hydrophobic ionic liquid in contact with an aqueous sample solution exhibits a stable liquid junction potential [1,2] and allows us to accurately determine pH of low ionic strength solutions, such as rain water and surface water [3,4].

A natural extension along this line is the determination of single ion activities of not only hydrogen but also other ions in wider concentration range, as the liquid junction potential developed at an ILSB is expected to be generally stable provided that the ions in the test solutions are hydrophilic enough. The single ion activities of H^+ and Cl^- in aqueous HCl solutions determined with an ILSB [5] are in good agreement with Fraenkel's recent predictions based on his smaller-ion shell (SiS) model [6] up to up to 0.2 mol dm^{-3}, but deviated significantly at higher ionic strengths [5]. The deviation is more significant in the case of aqueous HBr solutions [7]. Single ion activities in 1-2 and 2-1 electrolyte solutions will be reported.

References

[1] H. Sakaida, Y. Kitazumi, T. Kakiuchi, *Talanta*, **83**, 663 (2010).

[2] Y. Fujino, T, Kakiuchi, *J. Electroanal. Chem.*, **651**, 61 (2011).

[3] M. Shibata, H. Sakaida, T. Kakiuchi, *Anal. Chem.*, **83**, 164 (2011).

[4] M. Shibata, M. Kato, Y. Iwamoto, S. Nomura, T. Kakiuchi, to be published.

[5] H. Sakaida, T. Kakiuchi, *J. Phys. Chem. B*, **115**, 13222 (2011).

[6] D. Fraenkel, *Mol. Phys.*,**108**, 1435 (2010).

[7] K. Minami, T. Kakiuchi, to be published.

1GO02 Anion Effects on Lateral Diffusion of Cationic Rhodamine B at Toluene/Water Interface Measured by Total Internal Reflection–Fluorescence Recovery after Photobleaching

N. Shinomori[1] and S. Tsukahara[1]

[1]*Department of Chemistry, Graduate School of Science, Osaka University, Toyonaka 560-0043, Japan*

e-mail : shinomorin11@chem.sci.osaka-u.ac.jp

Introduction The lateral diffusion of molecules at liquid/liquid interfaces is one of the important factors to control their interfacial structure and interfacial reactivity. However, there are few studies on the interfacial diffusion. Therefore, we constructed an apparatus of fluorescence recovery after photobleaching (FRAP) measurements under the total internal reflection (TIR) conditions, and estimated the lateral diffusion coefficient (D) of a dye, rhodamine B, at liquid/liquid interfaces. We also investigated the effects of anions (HSO_4^-, NO_3^-, Cl^-) on the D of the cationic form of rhodamine B (HR^+).

Experimental Rhodamine B, which is adsorbed strongly at liquid/liquid interfaces [1], was used as a probe molecule. The aqueous and organic phases were aqueous acid solutions (H_2SO_4 / HNO_3 / HCl; 0.1 mol dm^{-3}) and a rhodamine B base (the lactone form of rhodamine B) toluene solution (1.0×10^{-8} – 1.0×10^{-6} mol dm^{-3}), respectively. The FRAP measurements were carried out with a thin-layer two-phase microcell. Two laser beams (532 nm), pulsed light of a higher power (150 mW) and cw-light of a lower power (< 2 mW), were used. The former enabled a brief laser irradiation causing the photobleaching of rhodamine B. The paths of the two laser beams were joined, and they were totally reflected at the toluene/water interface. Fluorescence of interfacial rhodamine B was collected with an inverted microscope and was detected with an avalanche photodiode [2].

Results and Discussion Figure 1 shows the dependence of the D values on the rhodamine B bulk concentrations with three different acid solutions. The D values become almost the same value (2.0×10^{-11} m^2 s^{-1}) in the higher concentration regions, which would be due to the molecular crowding effects at the interface. On the other hand, the D values are different in the lower concentration regions, which can result from the interaction between the anions and the cationic HR^+ at the interface.

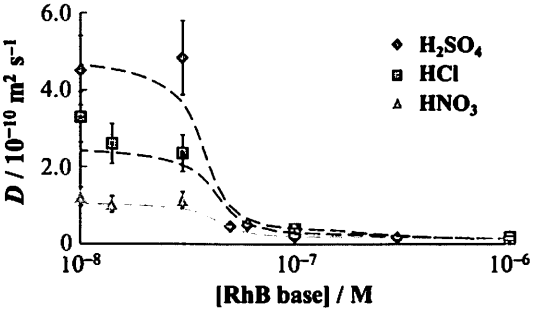

Figure 1. Dependence of D on the rhodamine B bulk concentration with three different acids.

References

[1] H. Watarai, F. Funaki, *Langmuir*, **12**, 6717 (1996).

[2] N. Shinomori, S. Tsukahara, *Chem. Lett.*, **42**, 444 (2013).

1GO03 Surface Tension Determination through Measurements of Resonance Oscillation of a Small Surface Using Dielectric Force by a Localized Alternating Current Electric Field

S. Tsukahara[1], T. Tsuruta[2], and T. Fujiwara[2]

[1]*Department of Chemistry, Graduate School of Science, Osaka University, Toyonaka 560-0043, Japan*

[2] *Department of Chemistry, Graduate School of Science, Hiroshima University, Higashi-Hiroshima 739-8526, Japan*

e-mail : sxt@chem.sci.osaka-u.ac.jp

Introduction Interfacial tension is a fundamental physical property, and interfacial concentration is frequently obtained from it. Various methods for the measurements of interfacial tension have been developed, and most of them are based on the Young–Laplace equation. These methods utilize the forces on curved interfaces. Few methods have been reported based on other principles. The present study employs an *in situ* optical microscope for the detection of the displacement of liquid surfaces. With this technique, we propose a new microscope method for the measurements of forced oscillation of the liquid surfaces induced by a localized alternating current (ac) electric field of variable frequencies as well as the quantitative analysis of the oscillation, leading to the determination of surface tension.

Experimental Eight liquids were employed. A liquid was added to a thin-layer microcell, and it was placed on a microscope stage. The bottom of a rod electrode (3.0 or 4.0 mmϕ) was placed 200 μm above the surface, and an ac was applied, whose voltage and frequency were 150 V (peak-to-peak) and 5–60 Hz, respectively. The present system consisting of an inverted microscope, a He–Ne laser, and an avalanche photodiode detector can be used for the measurements of the height change of liquid surfaces with about a 1 μm resolution.

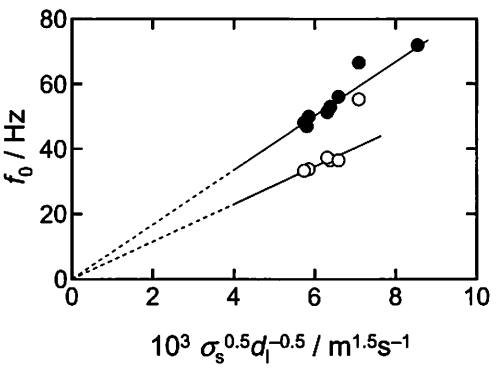

Figure 1 Proportional relationships between the resonance frequency (f_0) and $\sigma_s^{0.5} d_l^{-0.5}$ for the eight liquids. The radius of the microcell hole was (●) 3.5 and (○) 4.5 mm, whereas the depth was 2.0 mm.

Results and Discussion Liquids of a larger dielectric constant than air gathered under the electrode by a dielectric force, and thus the surface was oscillated. The oscillation was successfully analyzed with the forced oscillation model and the oscillation mode of two-dimensional circular membranes. A resonance oscillation (f_0) was observed, the frequency of which was well related to the ratio of surface tension (σ_s) to density (d_l) of the liquids, as shown in Figure 1. Therefore, the proposed novel method can be used for the determination of surface tensions of small surfaces with known densities [1].

References

[1] S. Tsukahara, T. Tsuruta, T. Fujiwara, *Analyst*, **138**, 2110 (2013).

1GO04 *In Situ* Fluorescence Microscope Measurements of Digestion Reactions of Single DNA Molecules by DNase at the Interface of Aqueous Two-Phase System

K. Katayama[1], and S. Tsukahara[1]

[1]*Department of Chemistry, Graduate School of Science, Osaka University, Toyonaka 560-0043, Japan*

e-mail : katayamak11@chem.sci.osaka-u.ac.jp

1. Introduction Single DNA molecules undergo a coil–globule transition corresponding to a conformational change from an elongated random-coil state to a collapsed globule state, depending on the concentrations of polyethylene glycol (PEG) and/or cations. On the other hand, an aqueous solution containing two kinds of polymer forms a two-phase system, called aqueous two-phase system. In the present study, an aqueous two-phase system with PEG and dextran was employed, and the rates of the conformational change and the digestion reaction of single DNA molecule at the liquid/liquid interface were measured by fluorescence microscopy.

2. Experiments An aqueous two-phase system contained 4.0% PEG (M.W. 7,400 – 10,200), 7.4% dextran (M.W. 500,000), and 12.5 mM $MgCl_2$. The top and bottom phases are a hydrophobic PEG-rich and a hydrophilic dextran-rich phases, respectively. λDNA (48,500 base pairs) which labeled with fluorescent 4',6-diammidino-2-phenylindole (DAPI) was used. As a DNase, Bsp1286 I was employed, which digests λDNA to 39 parts. λDNA was dissolved to the PEG-rich phase at 3.4×10^{-5} μg/μL, and Bsp1286 I was dissolved to both phases at the same concentration. Then, the dextran-rich phase was contacted with the PEG-rich phase in a thin-layer two-phase microcell again. The conformational change and the fluorescence intensity change of the single DNA molecules were measured with a fluorescence microscope (IX-51, Olympus).

3. Results and Discussions In the absence of Bsp1286 I, DNA molecules were in the globule state in the PEG-rich phase at 15°C, and the globular DNA molecules were adsorbed at the liquid/liquid interface. Then, when the temperature was raised to 30°C, the conformational change occurred from the globule state to the random-coil state. In presence of Bsp1286 I, the fluorescence intensity (I_F) of single DNA molecules did not change at 15°C, but I_F decreased at 30°C. Figure 1 shows the decreasing rate of I_F at [Bsp1286 I] = 0 – 1.0×10^{-2} U. When the Bsp1286 I concentration was lower than 2.5×10^{-3} U, the decreasing rate of I_F depended on the Bsp1286 I concentration. When the Bsp1286 I concentration was higher than 2.5×10^{-3} U, the decreasing rate of I_F was independent of the Bsp1286 I concentration. At such higher Bsp1286 I concentrations, the conformational change suppressed the digestion reaction because the cleavage sites were much fewer than Bsp1286 I molecules.

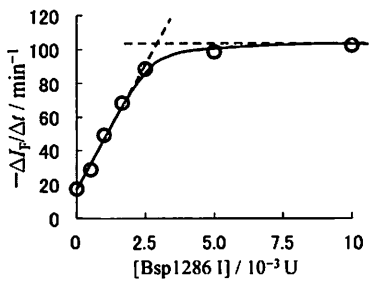

Fig 1 Dependence of the decreasing rate of the fluorescence intensity of single DNA molecules on the Bsp1286 I concentration.

2HO01 Microscopic View of Ion Pairing of Alkali Metal Halides in Aqueous Solutions: A Conductivity and Computer Simulation Study

J. Gujt, B. Hribar-Lee, and M. Bešter-Rogač

Faculty of Chemistry and Chemical Technology, University of Ljubljana, SI-1000 Ljubljana, Slovenia

e-mail : marija.bester@fkkt.uni-lj.si

Aqueous solutions of salts are ubiquitous and solvated ions greatly influence many naturally occurring processes. Charged species also affect the mechanism, and thus kinetics as well, of many chemical reactions. Consequently, solvated ions are still subject of many experimental and theoretical studies.

In this contribution a systematic investigation of the interactions between oppositely charged ions in simple alkali halide salts in water will be presented. At first glance, there is plenty of conductivity data of alkali metal halides in water, but they are in general limited to the temperature of 298.15 K and do not cover the diluted solutions sufficiently. Thus, appropriate data analysis on the literature data is not reliable, especially because the experimental quantification of weak association is not a trivial task. It has been reported recently that even conductivity-as one of the most established techniques for this purpose-yields only a rough estimation for the overall association constant $K_A<10$[1].

Therefore precise conductometric measurements on diluted aqueous solutions ($c<\sim0.005$ mol·L^{-1}) of all alkali metal chlorides and three iodides (NaI, KI, CsI) over broad temperature range were carried out. From the experimental data, association constants K_A, were determined by help of low concentration Chemical Model (lcCM)[2]. Small, but unambiguous differences in K_A among investigated salts were found. To explain these results on a microscopic K_A scale, a simple 2D water model[3] was used, that was parameterized to reproduce the association tendency qualitatively.

References

[1] Y. Marcus, G. Hefter, *Chemical Reviews* **106**, 4585(2006)

[2] J. M. G. Barthel. H. Krienke, W. Kunz, *Physical Chemistry of Electrolyte Solutions-Modern Aspects*, Steinkopff/Darmstadt, Springer/New York (1998)

[3] B. Hribar, N. Southall, V. Vlachy, K. Dill, *J. Am. Chem. Soc.* **124**,12302(2002)

2HO02 Initial Molecular Photocurrent: Nanostructure and Motion of Weakly Bound Charge-Separated State in Organic Photovoltaic Interface

Y. Kobori[1,2], R. Noji[3], and S. Tsuganezawa[3]

[1]*Department of Chemistry Graduate School of Science, Kobe University, Kobe 657-8501, Japan*

[2]*PRESTO, Japan Science and Technology Agency, Kawaguchi 332-0012, Japan*

[3] *Department of Chemistry, Faculty of Science, Shizuoka University, Shizuoka, 422-8529 Japan*

e-mail : ykobori@kitty.kobe-u.ac.jp

Organic bulkheterojunction (BHJ) blend films composed of the conjugated polymers as the electron donors and [6,6]-C_{61}-butyric acid methyl ester (PCBM) as the electron acceptor have been widely known to be useful for the highly efficient photovoltaic device as the organic thin film solar cells. Recent studies have demonstrated that the photoinduced, contact charge-transfer (CT) states are initially generated at the D/A domain-interfaces and play significant roles on the photocurrent generations. One of the most puzzling subjects has been that the photocarriers are escaped from the CT binding by the Coulomb attraction which energy is several hundreds of meV, leading to the photocurrent.

Despite the importance to understand how the interfaces play roles for the carrier dissociations, no study has experimentally characterized the conformational structure, the electronic interactions and the motions of the long-range charge-separated (CS) states that can conduct the photocurrents in the organic photovoltaic (OPV) systems. To elucidate the molecular mechanism of the efficient photocarrier generation, we have employed the time-resolved electron paramagnetic resonance method on the solid blends composed of PCBM and the P3HT polymers. The photoinduced CS states have been detected at the boundary regions between the P3HT polymer and the PCBM domains to characterize molecular geometries, electronic couplings, and molecular motions for the photo-carrier dissociations.[1] From the CS structure, it is indicated that the pentagonal or hexagonal aromatic rings of the buckyball in PCBM directly face the aromatic plane of the π -stacked P3HT surfaces. It has been concluded that the distant CS states are produced via fast hole delocalization process from the contact charge-transfer (CT) states. Such hole dynamics is explained by a coupling of the hole to librations of chains in the conjugated polymer. It has been concluded that both the enthalpy stabilization and the enhancement of the entropy occur through the orbital delocalization by the electron–phonon coupling, overcoming the initial CT binding to generate the molecular photocurrent.

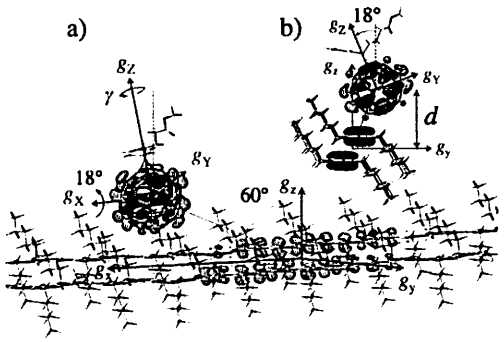

Figure 1. One of the geometries for the unpaired electron orbitals in the photoinduced CS state at the interface of the RR-P3HT:PCBM BHJ film.

References

[1] Y. Kobori, R. Noji, S. Tsuganezawa, *J. Phys. Chem. C* **117**, 1589-1599 (2013).

1IO01 Correlation between Thermodynamic properties and Orientation Polarization for Binary Mixtures Containing Fluorinated Cyclopentane

Y. Sato [1], Hideo Ogawa [1,2], T. Minamihounoki [2]

[1] *Graduate School of Tokyo Denki University, Hatoyama, Saitama, Japan*

[2] *Tokyo Denki University, Hatoyama, Saitama, Japan*

E-mail: hogawa@mail.dendai.ac.jp

Mixture containing fluorine organic compounds show complicated thermodynamic property compared to that of un-fluorinated them [1]. Such a characteristic might be brought by strong electronegativity of substituted fluorine atom. To understand the thermodynamic properties of solution containing fluorinated organic compound, refractive index and dielectric constant have been measured for binary mixtures containing 1,1,2,2,3,3,4- heptafluorocyclopentane (HFCP) or cyclopentane (CP) and orientation polarization, P_O was calculated from Onsager equation.

All results of excess enthalpy, H_m^E for the mixture with typical organic substances were disagreed between for mixture of HFCP and for of CP (Fig. 1). Large endothermic H_m^E observed for HFCP + hexane suggests weakening of dipole-dipole interaction between HFCPs (Fig. 1) and. Exothermic H_m^E (>0) of HFCP + ketone will be attributed hydrogen-bond formed between dissimilar molecules and which brings strong polarity and large dielectric loss. Negatively correlated relation was found for the mixture of HFCP (Fig 2) between H_m^E and the orientation polarization on mixing, ΔP_O, contrary to the constant value observed for mixture of non-polar CP.

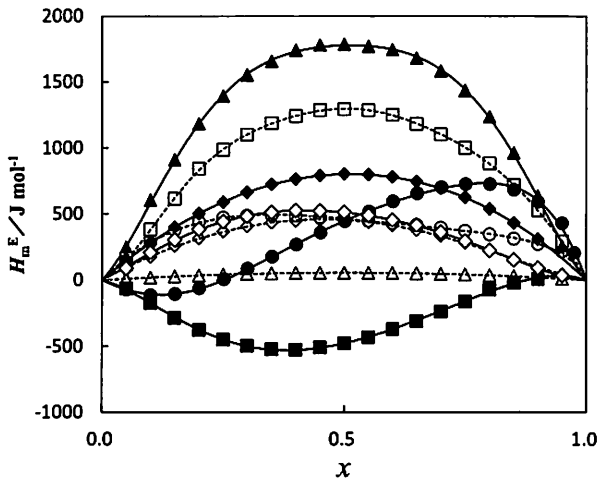

Fig.1. H_m^E at 298.15 K. Mixtures; HFCP + methanol(●) , + acetone(■) , + hexane(▲) or + benzene(◆) : CP + methanol(○), + acetone(□), + hexane(△) or + benzene(◇).

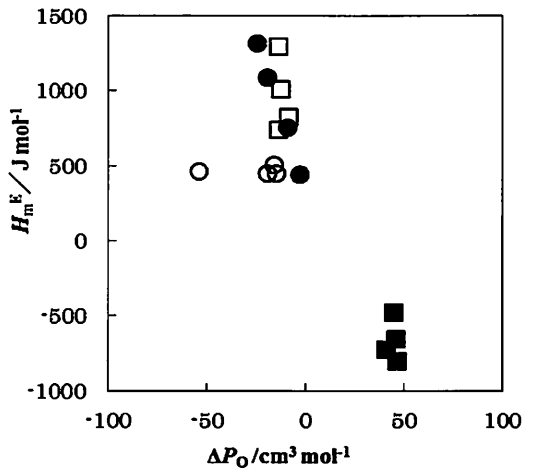

Fig.2. Correlation between ΔP_O and $H_m^E(x=0.5)$ at 298.15 K. Mixtures; HFCP + alcohols(●) or + ketones(■): CP + alcohols(○) or + ketones(□) .

Reference

[1]H.Ogawa, S.Karashima, T.Takigawa, S.Murakami, J.Chem.Thermodynamics, 35 (2003) 763-774.

1IO02 Excess molar enthalpies of binary mixtures of {water + poly(ethylene glycol)} at $T = 298.15$ K

Heloisa E. Hoga[1], Ricardo B. Tôrres[2], Takayoshi Kimura[3], Pedro L.O. Volpe[1]

[1]*Departamento de Físico-Química, Universidade Estadual de Campinas, Cidade Universitária Zeferino Vaz, 13083-970, Campinas, São Paulo, Brazil.*

[2]*Departamento de Engenharia Química, Centro Universitário da FEI, Av. Humberto de Alencar Castelo Branco, 3972, 09850-901, São Bernardo do Campo, São Paulo,Brazil.*

[3]*Department of Chemistry, Kinki University, Kowakae 3-4-1, Higashi-Osaka 577-8502, Japan*

E-mail:helhoga@iqm.unicamp.br

Aqueous solutions of Poly-ols show unique behavior. In order to clarify the behavior, viscosities of aqueous solution of monoethylene glycol, or + diethylene glycol, or + triethylene glycol, or + PEG200, or + PEG300, or + PEG400, or + PEG600 were determined at $T = 298.15$ K. In this work, enthalpies of mixtures of these binary systems were measured over the entire molar fraction composition range at $T = 298.15$ K using a microcalorimeter (Thermal Activity Monitor, Titration mode, LKB2277 Thermometric). Excess molar enthalpies were calculated from the experimental data and fitted to the Redlich-Kister polynomial. The results obtained from excess Gibbs energies of viscous flow and excess enthalpies of mixture were compared and discussed as viewpoint of size of poly-ols and also in terms of intermolecular interactions between unlike molecules.

Excess enthalpies of aqueous solutions of poly-ols were also estimated by a group contribution theory of UNIFAC and dielectric continuum solvation models (COSMO-RS), and compared with experimental results.

All interaction energy between water and poly-ols were performed with *Gaussian 09*. The interaction of water and poly-ols were optimized with MP2/6-311G(d,p) in solvent by self-consistent reaction field (SCRF) calculation. For the systems water + poly-ols will be discussed the role of interaction energies of electrostatic exchange, charge transfer and dispersion forces.

1IO03 Combination of molecular simulation and calorimetric experiments to describe energies of interaction in {alkanolamine + water} systems

M.R. Simond[12], K. Ballerat-Busserolles[12], J-Y. Coxam[12] and A.A.H. Pádua[12]

[1]*Clermont Université, Université Blaise Pascal, Institut de Chimie de Clermont-Ferrand, BP 80026, F-63171 AUBIERE, FRANCE*

[2]*CNRS, UMR 6296, ICCF, BP 80026, F-63171 AUBIERE, FRANCE*

e-mail : simondmickael@gmail.com

Carbon Capture and Storage (CCS) is one of the main options for carbon dioxide mitigation. Capture processes based on CO_2 dissolution in alkanolamine solutions are considered among the most adequate methods for decarbonation of post-combustion effluents [1]. An understanding of molecular interactions involved in {CO_2 + water + alkanolamine} systems is essential to optimize gas absorbents and reduce process costs. The aim of this work is to compare thermodynamic properties of {alkanolamine + water} mixtures obtained experimentally and from molecular simulations. Molecular simulation provides a detailed microscopic view into thermodynamics and transport properties and is complementary to experimental measurements. Simulation is also a promising tool for the prediction of properties required to design capture process. The insights into microscopic structure and energetics of {alkanolamine + water} mixtures obtained from simulation, such as differences in hydrogen-bond interactions between different alkanolamines, contribute to improve structure-property relationships.

A force field adapted to describe alkanolamines containing the N–C–C–O backbone was developed [2], taking into account the polar solvation environment. This new force field was validated through prediction of enthalpic and volumetric properties of seven alkanolamines, which are methyl- and ethyl-substituted monoethanolamine (MEA). The force field was then used to calculate the enthalpy of mixing of alkanolamines with water. The interaction between amine and water was modified adding a specific Lennard-Jones site in order to reproduce enthalpies of mixing of two {alkanolamine + water} systems. This model was then used to predict mixing properties for other systems. Simulation results are compared to experimental data obtained from mixing calorimetry using both flow mixing and titration techniques. The agreement observed was good and allowed the study of structural quantities, hydrogen bonding, cluster analysis, *etc.* The dependence of enthalpy of mixing with temperature was also investigated and comparison between experimental values and simulation is reported.

References

[1] Arcis, H.; Ballerat-Busserolles, K.; Rodier, L.; Coxam, J.-Y. *J. Chem. Eng. Data* **2011**, *56*, 3351–3362.

[2] Simond, M.; Ballerat-Busserolles, K.; Coxam, J.-Y.; Pádua, A. A. H. Chem. Phys. Chem. **2012**, 13, 3866–3874.

1IO04 Thermodynamics of Three-Phase Equilibrium in Argon Based on a Perfect Solid and a Perfect Liquid (v5)

Yosuke KATAOKA and Yuri YAMADA

Department of Chemical Science and Technology, Faculty of Bioscience and Applied Chemistry, Hosei University, 3-7-2 Kajino-cho, Koganei, Tokyo 184-8584, Japan

e-mail: yosuke.kataoka.7t@stu.hosei.ac.jp

Equations of state (EOS) are proposed for a system consisting of a perfect solid and a perfect liquid made up of single spherical molecules. The Lennard–Jones interaction is assumed for this system. Molecular dynamics simulations are performed to determine the temperature and density dependences of the internal energy and pressure. The super cooled liquid state is also examined. The internal energy term in the EOS is the sum of the average kinetic and potential energies at 0 K and the temperature-dependent potential energy. The temperature-dependent term of the average potential energy is assumed to be a linear function of the temperature and its coefficient is expressed as a polynomial of the number density. The pressure is expressed in a similar way, where the pressure satisfies the thermodynamic EOS [1-5]. The equilibrium condition is solved numerically for the phase equilibrium of argon. The Gibbs energy gives a reasonable transition pressure for three-phase equilibrium in argon (Fig.1 Fig.2). The thermodynamic properties at low pressures have significant temperature dependences.

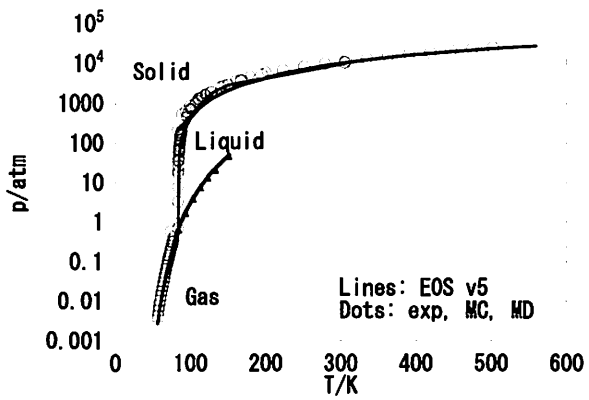

Fig. 1 Phase transition pressure vs. temperature for argon.

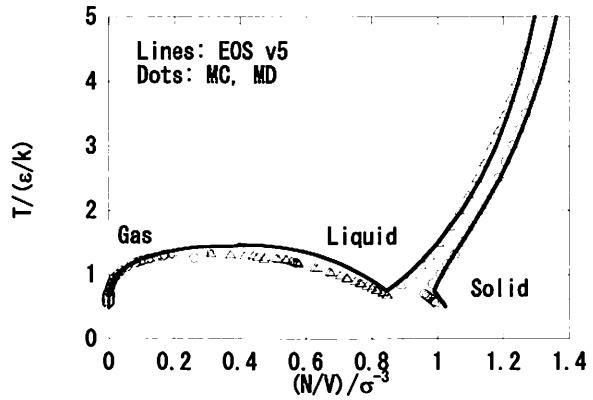

Fig. 2 Phase transition temperature vs. number density for argon. The constants ε and σ are Lennard-Jones parameters.

References

[1] Y. Kataoka and Y. Yamada, *J. Comput. Chem. Jpn.* **10**, 98-104 (2011)

[2] Y. Kataoka and Y. Yamada, *J. Comput. Chem. Jpn.* **11**, 81-88 (2012)

[3] Y. Kataoka and Y. Yamada, *J. Comput. Chem. Jpn.* **11**, 165-173 (2012)

[4] Y. Kataoka and Y. Yamada, *J. Comput. Chem. Jpn.* **11**, 174-183 (2012)

[5] Y. Kataoka and Y. Yamada, *J. Comput. Chem. Jpn.* in press.

1IO05 Molecular Simulation of Aqueous Electrolyte Solutions via the OEMC Algorithm and Applications

W.R. Smith[1,2], F. Moučka[3], and I. Nezbeda[3,4]

[1]*Faculty of Science, Un. of Ontario Institute of Technology, Oshawa ON L1H 7K4, Canada*
[2]*Department of Mathematics and Statistics, Un.of Guelph, Guelph ON N1G 2W1, Canada*
[3]*Faculty of Science, J.E. Purkinje University, Ústí nad Labem 400 96, Czech Republic*
[4]*E. Hála Laboratory of Thermodynamics, Institute of Chemical Process Fundamentals, Academy of Sciences, 165 02 Prague 6, Czech Republic*
e-mail : william.smith@uoit.ca

Aqueous electrolytes and their mixtures are important in many systems, and classical Molecular Dynamics and Monte Carlo simulation algorithms are important tools for understanding and predicting their chemical behaviour. Among the most important chemical properties of such systems are the chemical potentials of both the solute and the solvent, particularly at higher solute concentrations, in addition to the solubility of the salts. Other recent studies [1,2,3] have primarily employed computationally intensive thermodynamic integration procedures at specified concentrations, in conjunction with either Molecular Dynamics or Monte Carlo simulations. These calculations are primarily limited to moderate solute concentrations; in addition, the accurate direct calculation of the solvent chemical potential is extremely difficult.

The recently developed Osmotic Ensemble Monte Carlo (OEMC) algorithm [4] proceeds by a novel type of computationally efficient Semi-Grand Canonical Ensemble simulation of the solution phase, and calculates the solute concentration as a function of an externally imposed total electrolyte chemical potential. It can be viewed as an application of the Reaction Ensemble Monte Carlo algorithm [5] to the case of an inter-phase chemical reaction, by means of which the ions are formed from an external chemical potential reservoir. The method permits the efficient calculation of chemical potentials of both solutes and solvent, and can readily access the low concentration region. It can also directly calculate the solubility in a single simulation of the solution phase without the need for explicitly calculating chemical potentials. It also may provide a computational tool to investigate the onset of solid precipitation in supersaturated electrolyte solutions. We demonstrate the use of the OEMC algorithm for several model systems involving alkali halides, and also show its use as a tool to determine improved electrolyte force fields.

References

[1] S. Paluch, S. Jayaraman, J. K. Shah, E. J. Maginn, *J. Chem. Phys.* **133**, 124504 (2010).
[3] J.L. Aragones, E. Sanz, C. Vega, *J. Chem. Phys.* **136**, 244508 (2013).
[3] S. Joung, T. Luchko, D.A. Chase, *J. Chem. Phys.* **138**, 044103 (2013).
[4] F. Moučka, I. Nezbeda, W.R. Smith, *J. Phys. Chem.* **B116**, 5468 (2012).
[5] W.R. Smith, B. Tríska, *J. Chem. Phys.* 100, 3019 (1994).

1IO06 Thermodynamics and phase diagrams of systems with ester synthesis reactions under the isothermal conditions

Maria Toikka, Alexander Toikka, Maya Trofimova and Alexandra Golikova

Saint-Petersburg State University,
Faculty of Chemistry,
Department of Chemical Thermodynamics and Kinetics,
Universitetsky prospect 26, Petrodvoretz, 198504 Saint-Petersburg, Russia.
e-mail: masha-toikka@yandex.ru

This work deals with considering of thermodynamics and some peculiarities of multicomponent heterogeneous systems with mass-transfer. The main task is thermodynamic analysis of the features of liquid-liquid (LL) phase diagrams of the systems with equilibrium and non-equilibrium chemical reaction in solution. The thermodynamic conditions of mutual disposition of liquid-liquid tie-lines in ternary and quaternary systems, the interesting areas of the intersection of the binodal surfaces and chemical equilibrium (CE) surfaces including the complex of the transformed composition variables are presented.

The objects investigated are heterogeneous systems with ester synthesis reaction that were carried out both for basic and industrial purposes [1]: acetic acid – *n*-propanol – water – *n*-propyl acetate and acetic acid - ethanol - ethyl acetate - water systems. The simultaneous disposition of binodal and CE surfaces under the different isothermal conditions produces a variety of phase diagrams. Some results for these systems were presented in [2]. The existence of the area of the intersection of CE (Fig. 1) and LL equilibrium surface (Fig. 2) (at simultaneous consideration) in the system with *n*-propyl acetate synthesis reaction at 293.15, 303.15 and 313.15 K [3]. This area is also presented in transformed composition variables (2D composition complex).

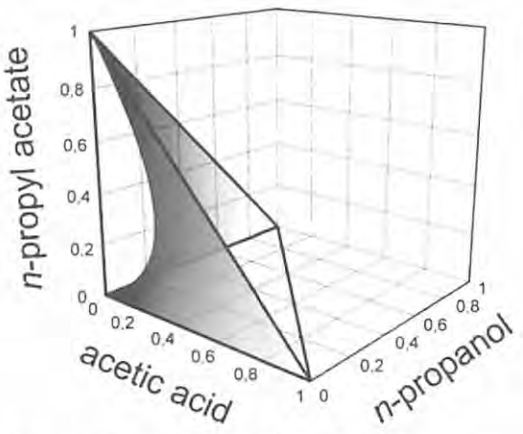

Fig. 1. The surface of CE of acetic acid – *n*-propanol – water – *n*-propyl acetate system at 293.15 K.

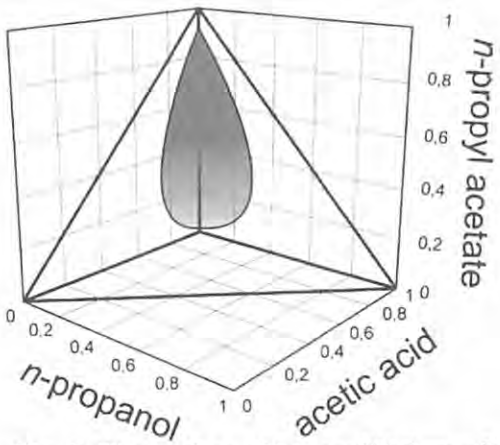

Fig. 2. The surface of LL equilibrium of acetic acid – *n*-propanol – water – *n*-propyl acetate system at 293.15 K.

The solubility phenomena in fluid reactive systems are the subject of interest from both basic and applied points of view. The data on LLE and CE should be taken into account for such processes as chemical synthesis in splitting solutions, extraction in reactive systems, etc. The database on thermodynamic properties of reactive LL systems is rather limited and needs to be developed.

This research was supported by Russian Foundation for Basic Research (grant 13-03-00985 A).

References.

[1] A. M. Toikka, M. A. Toikka, Yu. A. Pisarenko, L.A. Serafimov. *Theor.Found. Chem. Eng.* **43**, 129 (2009).
[2] M. Trofimova, M. Toikka, A. Toikka. *Fluid Phase Equilib.* **313**, 46 (2012)
[3] Maria Toikka, Alexander Toikka. *Pure Appl. Chem.* **85**, 280 (2013).

1JO01

Hydrophilic and Hydrophobic Hydration of Carboxylate Ions

Glenn Hefter[1], Hafiz Rahman[2], and Richard Buchner[2]

[1]*Chemistry Department, Murdoch University, Murdoch WA 6150, Australia*

[2]*Institut fur Physikalische & Theoretische Chemie, University of Regensburg, D-93040, Regensburg, Germany*

e-mail : g.hefter@murdoch.edu.au

Carboxylate groups are the most common anionic centres on biomolecules, for example in amino acids and peptides, and thus play a major role in the hydration of such molecules, which in turn influences their biological function. Despite numerous investigations over the years using diffraction methods, NMR spectroscopy, computer modelling, and so on, there is still much to learn about the hydration of carboxylate ions. In particular the interaction between the hydrophilic carboxylate moiety and neighbouring hydrophobic hydrocarbon entities, which are inevitably present in biomolecules, has been little studied. This paper will present recent measurements using broadband dielectric relaxation spectroscopy, a powerful but little used technique for the study of ion hydration, of a systematic series of low molecular weight sodium carboxylate salt solutions. Detailed analysis of the spectra as a function of solute concentration has shown that it is possible to separate and quantify both hydrophobic and hydrophilic hydration of substituted carboxylate ions. Estimates of the very weak association of carboxylate ions with sodium ions have also been made using the dielectric data.

1JO02 Ethylene Glycol: Liquid structure and H-bond network dynamics from MD simulations

Alexander Kaiser[1], Oksana Ismailova[1], Antti Koskela[2], Stefan E. Huber[1],

Renat Nazmutdinov[3], Michael Probst[1]

[1] *Institut of Ion Physics and Applied Physics, University of Innsbruck, 6020 Innsbruck, Austria*

[2] *Institut of Mathematics, University of Innsbruck, 6020 Innsbruck, Austria*

[3] *Kazan National Research Technological University, 420015 Kazan, Republic Tatarstan, Russian Federation*

e-mail : michael.probst@uibk.ac.at

The main aim of this investigation is the elucidation of the structure and dynamics of the hydrogen network in liquid ethylene glycole and how the rotational and translational mobility of the molecules can be potentially tuned by mixing with water.

Liquid ethylene glycol is modeled by means of classical molecular dynamics simulations. Four different OPLS-based force fields are compared. The radial distribution functions from all force fields are similar but the distributions of the intramolecular H-O-C-C and O-C-C-O angles show large discrepancies. The original OPLS-AA force field favors the trans conformer, the OPLS-AA-SEI and OPLS-AA-SEI-M force fields favor the gauche conformer in accordance with experiment and ab initio calculations. The mean number of intermolecular hydrogen bonds per EG molecule is ~3.7, varying only slightly with the force field. Intramolecular hydrogen bonds are strongly suppressed in the OPLS-AA-SEI-M case to 0.1% of the molecules compared to 15% in the original OPLS-AA field. Due to the number of possible hydrogen bonds per molecule EG builds up three-dimensional hydrogen-bonded structures with an estimated mean size of 15 molecules per cluster. The lifetimes are rather randomly distributed. Hydrogen bonds break regularly in timescales of a few picoseconds due to rovibrational motions and but be reformed later on. Clusters of 5-20 relatively long-lived hydrogen bonds (>100ps) can also be observed. The irreversible destruction of hydrogen-bonds due to diffusion happens on a time-scale of 80 ps. These results are relatively independent of the force field. This work is considered as a first step towards interpreting experimentally measured dielectric properties of EG and EG/water mixtures in terms of lifetimes of hydrogen-bonds, ro-vibrational motions and conformer changes. Finally, results from a new visualization tool "molvish" for the direct visualization of the hydrogen-bonds show that there is no obvious clustering of very long-lived (>500 ps) clusters.

Acknowledgements

This work was supported by the Austrian Science Fund (FWF) under projects I200-N29 and the DK+ project on Computational Interdisciplinary Modeling, by the RFBR Project 09-03-91001-a and by the Austrian Ministry of Science as part of the UniInfrastrukturprogramm 'Scientific Computing'.

1JO03 Observations of Weak Hydrogen Bonds C−H•••O as Intermolecular Vibration Modes in Solutions by Terahertz Time-Domain Spectroscopy

K. Mizuno[1], T. Kikuchi[1], K. Murakami[2], Y. Aoike[2], K. Fukui[2], K. Yamamoto[3], and M. Tani[3]

[1]*Depart. of Applied Chem. and Biotech., Graduate School of Engi., Univ. of Fukui*
[2]*Depart. of Electrical and Electronics Engi., Graduate School of Engi., Univ. of Fukui*
[3]*Research Center for Development of Far-Infrared Region, Univ. of Fukui*
e-mail : kmizuno@u-fukui.ac.jp

Abstract: We have carried out terahertz time-domain spectroscopic(TDS) measurements of propanoic acid, propionaldehyde, and dimethyl sulfoxide in solutions of cyclohexane with increasing each solute concentration. We observed absorption band at 30~180cm^{-1}, at 3~70cm^{-1}, and at 3~60cm^{-1}, respectively. We have also carried out measurements of IR spectra of the solutions, and observed the formation of intermolecular hydrogen bonds O−H···O=C, C−H···O=C, and C−H···O=S, respectively, from the C=O and S=O stretching vibration band for each solute in the concentration range smaller than ≈10^{-2}mol/l. We have also calculated the frequencies of intermolecular vibration modes in self-associated dimers of the three solutes using DFT calculation method. Then we could assign the spectra obtained from the terahertz TDS of propionaldehyde and dimethyl sulfoxide as the intermolecular vibration bands of the "weak hydrogen bonds" formed in their self-associated dimers.

A hydrogen(H−) bond has been generally expressed as X−H···Y, where X and Y had been noted to be electronegative atoms like O, N, or halogen until 1980 or 1990. In 1990's, however, two IR or Raman spectroscopic phenomena had been established on the formation of a weak H-bond such as C−H•••O, a blueshift of C−H stretching vibration band and a decrease of the absorption intensity of it in contrast to the conventional hydrogen bonds. New definition of hydrogen bond was recommended in 2011, in which C−H groups have been also assigned to H-bond donors [1]. We may notify at least that the electron negativity of carbon, 2.55, is much less than that of oxygen, 3.44, but larger than that of hydrogen, 2.20, as the reason why C−H can act as a H-bond donor.

When infrared spectrosopy is used to detect H-bond C−H···O=C, changes of the frequcncies for the intramolelcular vibration bands of C−H and O=C are detected. In the present work we have observed intermolecular vibration mode of C−H···O=C and C−H···O=S, in dimers of propionaldehyde, and dimethyl sulfoxide, respectively. Our results not only determined the structures of the dimers, but also detected weak hydrogen bonds in solutions experimentally.

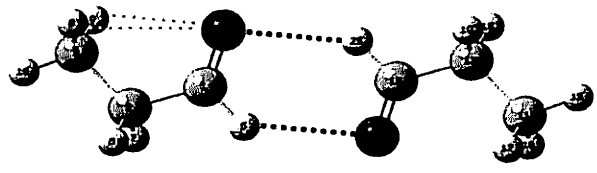

The optimized structure of self-associated dimer of propion aldehyde

References

[1] E. Arunan *et al., Pure Appl. Chem.* **83,** 1619, 1637(2011).

1JO04 Structure of Hydrogen-bonded Associates in Primary Alcohols and their Coordination to Aromatic Segments

G. Matisz[1,2], A-M. Kelterer[3], W.M.F. Fabian[4] and S. Kunsági-Máté[1,2]

[1]*Department of General and Physical Chemistry, University of Pécs, Ifjúság 6, H-7624 Pécs, Hungary*

[2]*János Szentágothai Research Center, Ifjúság 20, H-7624 Pécs, Hungary*

[3]*Institute of Physical and Theoretical Chemistry, Graz University of Technology, Stremayrgasse 9/I, A-8010 Graz, Austria*

[4]*Institute of Chemistry, Karl-Franzens University of Graz, Heinrichstr. 28, A-8010 Graz, Austria*

e-mail : gmatisz@gamma.ttk.pte.hu

Solvent relaxation time measurements showed [1,2] that in binary liquids the composition of the bulk phase differ from the composition and the structure of the solvation shell, while the solvation shell shows not easily interpretable dependence on the composition of the bulk phase.

With the aim to get deeper understand of the experimental results, theoretical studies have been done to describe the structural properties of the liquid phase [3,4] and the interaction of the solvent molecules with the solute [5]. The description of the bulk phase has been attempted by using the quantum cluster equilibrium (QCE) theory [6]. First extension of that model has been done recently [7] for binary solvents. Results obtained using the QCE theory will be discussed. Furthermore, with the aim to study the aforementioned solute – solvent interactions, quantum chemical calculations have been performed [5] to augment some experimental findings [8], i.e. how the clusters of molecules of the solvent interact with the aromatic segment.

Acknowledgement: The quantum chemical calculations were run on the Hungarian HPC infrastructure (NIIF Institute, Hungary). Financial support of the SROP-4.2.2.A-11/1/KONV-2012-0065 project is gratefully acknowledged.

References

[1] S. Kunsági-Máté, K. Iwata, *Chem. Phys. Letters* **473**, 284 (2009).

[2] S. Kunsági-Máté, K. Iwata, *J. Solution. Chem.* **42**, 165 (2013).

[3] G. Matisz, W.M.F. Fabian, A-M. Kelterer, S. Kunsági-Máté, *Theochem* **956**, 103 (2010).

[4] G. Matisz, A-M. Kelterer, W.M.F. Fabian, S. Kunsági-Máté, *J. Phys. Chem.* **B115**, 3936 (2011).

[5] G. Matisz, A-M. Kelterer, W.M.F. Fabian, S. Kunsági-Máté, *J. Phys. Chem.* **A115**, 10556 (2011).

[6] F. Weinhold, *J. Chem. Phys.* **109**, 367 (1998).

[7] B. Kirchner et al., *Comp. Phys. Comm.* **182**, 1428 (2011).

[8] R.N. Pribble, F.C. Hagemeister, T.S. Zwier, *J. Chem. Phys.* **106**, 2145 (1997).

1JO05 Strength of water-water interaction depends on local environment

T. Urbic[1]

[1]*Faculty of Chemistry and Chemical Technology, University of Ljubljana, Askerceva c. 5, 1000, Ljubljana, Slovenia*

e-mail : tomaz.urbic@fkkt.uni-lj.si

Accurate knowledge of water-water interaction potential is important for devising and evaluating simple water models, if they are to accurately describe water properties and reflect various solvation phenomena.

Interaction potential between two water molecules depends on their inter-molecular distance, relative orientation and local environment as well [1,2]. When finding themselves at a favorable distance and orientation, two water molecules experience a particularly strong attractive interaction called hydrogen bonding. Although hydrogen bond is very important for its effects on the elements of life, industrial applications, and bulk water properties, there is no scientific consensus on its true nature and origin. In this study we use quantum mechanical methods to calculate the strength of the hydrogen bond in different local environments, such as, next to other water molecules, next to an ion, a nonpolar solute, and non-polar plane. The local environment effects are considerable even for the second coordination shell. The results will be compared with the conventional models of water. These calculations provide novel insights into the nature of hydrogen bonding and its influence on the intermolecular potential in water.

References

[1] M. Hus and T. Urbic, *J. Chem. Phys.* **136**, 144305 (2012).

[2] V.S. Znamenskiy and M.E. Green, *J. Chem. Theory Comput.* **3**, 103(2007).

2JO06 Glycerol-based solvents for organic synthesis

Adi Wolfson* and Dorith Tavor

Green Processes Center, Chemical Engineering Department, Sami Shamoon College of Engineering, Bialik/Basel Sts. Beer-Sheva, 84100 Israel. *adiw@sce.ac.il.

The sustainability of a chemical process is derived from its materials and energy consumption, reaction performance, and separation procedures. As organic chemistry is traditionally carried out in solution, and as solvents are responsible for a large part of the waste and pollution generated by chemical processes, a key factor to enabling a sustainable chemical process is solvent selection. In the past two decades a variety of environmentally benign solvent alternatives have been proposed, including water, ionic liquids, fluorous solvents, and supercritical fluids. Yet, despite their green character, their implementation in industrial processes is still very limited due to a lack of experimental date and familiarity, as well as operational restrictions and high costs.

Several years ago we introduced glycerol, for the first time, as an alternative sustainable solvent for catalytic and non-catalytic organic transformations. Since then, we have explored the scope and limitation of organic synthesis in glycerol while many other research groups employed glycerol as solvent for organic synthesis. A non-toxic, non-hazardous, non-volatile, biodegradable, and recyclable liquid produced as a by-product in the transesterification of oil from renewable sources, glycerol has been successfully employed as a sustainable solvent in a wide variety of organic reactions and synthesis methodologies, showing its versatility as a solvent for organic synthesis. In many reactions, the presence of glycerol as a solvent has improved product yield and selectivity and enabled easy product separation and catalyst recycling. Glycerol can dissolve many organic and inorganic compounds and transition metal complexes, and also enables easy product separation and simple recycling of transition metal complexes by extraction with glycerol immiscible solvents such as ethers and esters and with supercritical carbon dioxide. Furthermore, its high boiling point and polarity make glycerol the perfect candidate for non-conventional heating and mixing reactions such as ultrasound- and microwave-assisted reactions. In addition, glycerol has also been used simultaneously as both solvent and reactant in the catalytic transfer-hydrogenation of various unsaturated organic compounds and as acyl acceptor in the transesterification of ester and in the kinetic resolution of esters racemates.

Yet, despite the promise of glycerol as a sustainable solvent for liquid phase catalytic and non-catalytic organic syntheses, several drawbacks are connected with its utilization, such as the high viscosity and low solubility of highly hydrophobic compounds and gases. Hence, the use of glycerol derivatives whose properties can be tailored, tuned and adjusted according to the requirement of each reaction and separation was also explored. It was found that glycerol-based solvents and their mixtures can be also successfully employed as green reaction mediums for various representative organic transformations. Both, reaction performance and product separation as well as catalyst recycling were found to be affected by the type and the polarity of the solvent in all reactions. It appeared that substrate solubility was the main determinant of reaction activity while the product solubility in the solvent determined the effectiveness of its extraction.

2JO07 Reaction Controll in Double Electrospray Microreactor

A. Wakisaka[1], M. Tsuchiya[2], Y. Hyodo[1], H. Kobara[1], T. Ono[3]

[1]*National Institute of Advanced Industrial Science and Technology, Tsukuba 305-8569, Japan*

[2]*Department of Applied Chemistry, Cluster of Applied Sciences, National Defense Academy, 239-8686, Japan*

[3]*National Institute of Advanced Industrial Science and Technology, Nagoya 463-8560, Japan*

e-mail : akihiro-wakisaka@aist.go.jp

For a chemical reaction started by the mixing of two kinds of solutions, it will be hard to stop the reaction at a certain stage, if the reaction rate is fast and some sequential reactions take place therein. In order to control such a chemical reaction in the liquid state, the rapid mixing of two solutions and the sudden stop of the reaction by the rapid extracting of the products will be necessary. For this purpose, here we designed a reaction field with double electrosprays.

When the positively and the negatively charged liquid droplets with diameters around 1 μm (femtoliter-scale volume) were simultaneously generated by the double electrosprays in an electric field, they collided to be merged through their electrostatic attractive force. This made it possible to mix two kinds of solutions within a femtoliter-scale liquid droplet. This femtoliter-scale reaction field was applied to the synthesis of gold nanoparticles to avoid the self-aggregation. The gold nanoparticles around 5nm were synthesized easily when a $HAuCl_4$ solution and an ascorbic acid solution were sprayed from the anode and the cathode electrospray nozzles, respectively. The Au^{3+} was reduced to Au by the ascorbic acid in the merged liquid droplets, and the self-aggregation of Au was stopped by collecting the resulting Au from the merged liquid droplet into a colloidal polymer solution. This indicates that the smallest reaction field given by the double electrosprays functions as a key factor to control miscellaneous reactions in the liquid state.

3JO08 Tunnel Process Calculation for Molecular Systems using ab initio Path-integral Instanton Method

T. Kawatsu[1,2], and S. Miura[2]

[1] *Institute for Molecular Science, Okazaki 222-8585, Japan*

[2] *Graduate School of Natural Science and Technology, Kanazawa University, Kanazawa 920-1192, Japan*

e-mail : kawatsu@fukui.kyoto-u.ac.jp

When a molecular system has degenerated states in the nuclear states, the quantum theory predicts that the energy of a vibration state splits to the parallel and anti-parallel states by the tunnel coupling. The path-integral theory presents strong methods to calculate the tunnel splitting as path-integral Monte Carlo or molecular dynamics methods. However, nuclear coordinate sampling of these methods sometimes tasks heavy computational cost when the potential calculation for the system is expensive. The instanton method is an approximated statistical technique to reduce such computational cost [1,2]. We have intended to spend the computational resource to calculate accurate interatomic potential using quantum chemical method with relatively large basis functions and electronic correlation instead of spending the sampling. We then have developed an ab initio path-integral instanton method and applied to the tunnel splitting problem [3].

The ammonia flipping is a popular problem of the tunnel splitting. Ammonia is a polar molecule and polarization functions and electronic correlation are required to reproduce the molecular coordinates of its grand and transition states. We have applied the ab initio path-integral instanton method to the ammonia flipping with quantum chemical methods that can reproduce the molecular coordinates in preliminary calculations. The computed tunnel splitting agreed the experimental results in condition of at least MP2 level and more than one polarization functions as shown in Table. It is advantage of this method that we can select even high level QM method which can reproduce the molecular coordinates in limited computational resource.

Table: Tunnel splitting of ammonia flipping using ab initio path-integral instanton method (kcal/mol)

(QM method)	NH_3	ND_3
MP2/ktvzpp	0.72	0.045
MP2/6-31++G(3d,3p)	0.81	0.053
MP2/6-31++G(2d,2p)	0.83	0.053
Exp.	0.79	0.05

References

[1] G. V. Mil'nikov, H. Nakamura, *J. Chem. Phys.* **115** 6881(2001).

[2] J. O. Richardson, S. C. Althorpe, *J. Chem. Phys.* **134** 054109(2011).

[3] T. Kawatsu, S. Miura, *J. Phys. Conf. Ser.* in press.

3JO09 A Semigrand, Isothermal-Isochoric Ensemble View of the McMillan-Mayer Solution Theory

J. L. Gómez-Estévez

Department de Física Fonamental, Facultat de Física,
Universitat de Barcelona,
Diagonal 645, E-08028, Barcelona, Spain
e-mail : jlgomez@ffn.ub.es

The McMillan-Mayer (MM) theory of Solutions was formulated originally in the context of the grand canonical ensemble (GCE) [1-3]. If we consider a solution formed only by a solute σ and a solvent s, the "natural variables" are $(\mu_\sigma, \mu_s, T, V)$ where μ_i is the chemical potential of each component. Because the GCE approach is not so much familiar as the canonical ensemble[3], a more suitable approach is needed. In this work a new version of the MM theory which employs a semigrand isothermal-isochoric ensemble is presented. By using the maximum term method[3], a semigrand partition function is obtained from the grand canonical partition function of the original MM theory. Now, the natural variables are (N_σ, μ_s, T, V) where N_σ is the number of solute particles. The pair correlation function for the solute and the thermodynamic properties of the solution are derived in a very general form. Also, the possibility for obtaining the thermodynamics of the solution by means of a charging process is discussed. Finally, after the explicit calculation of the thermodynamic properties of an "ideal solution", the definition of excess thermodynamic functions is given and their relationship with an "effective canonical-like" partition function found.

If time permits, a historical overview of previous works (Guggenheim, ..., Saito, Hill, Kodýtek) that used a semigrand ensemble treatment and that are scattered in the bibliography will be given.

References

[1] W.G. McMillan, J.E. Mayer, *J. Chem. Phys.* **13**, 276(1945).
[2] J. L. Gómez-Estévez, *Pure Appl. Chem.* **85**, 105(2013).
[3] T. L. Hill, *Introduction to Statistical Thermodynamics*, Addison Wesley, Reading, MA (1960).

3JO10 Statistical Mechanics of Hydration and Ion-Binding in Biologically Relevant Amino Acid Solutions

M. Fedotova[1,2]

[1]*G.A. Krestov Institute of Solution Chemistry of the Russian Academy of Sciences, Academicheskya st., 1, Ivanovo, 153045, Russia*

[2]*Ivanovo State University, Physical Department, Ermak st., 39, Ivanovo, 153025, Russia*

e-mail : mvf@isuct.ru

Amino acids as free molecules as well as constituents of proteins are invariably in an aqueous medium and play an important role in different biochemical processes in living organisms. Depending on their nature, the addition of salts to the solution can cause significant changes in many biomolecular properties, such as protein solubility, hydration, denaturation, aggregation, etc.[1, 2]. As salts and other electrolytes are ubiquitous in biological systems, understanding their effects on protein behavior at molecular level is important to quantify their interactions in biological and biochemical processes. Some progress has been made in understanding the effects of simple ions[3, 4] but so far a clear understanding of their molecular origins in complex biological systems has been elusive.

In this report we present results of a statistical mechanics study of the hydration structure and possible ion-binding of three amino acids with significantly differing residues, R, in biologically relevant electrolyte solutions (NaCl(aq), KCl(aq)). As the examples, we have chosen glycine (no R) in the zwitter-ion form, Gly-ZW, para-aminobenzoic acid (aromatic R) as a neutral molecule and its anion, PABA and $PABA^-$ correspondingly, and L-proline (heterocyclic R) in the zwitter-ion form, L-Pro-ZW. The presented structural information has been obtained by the integral equation method in the framework of the 1D-RISM and 3D-RISM (Reference Interaction Site Model) approaches. The structural features of amino acid-water and amino acid-water-salt systems will be discussed in terms of radial and spatial distribution functions and spatial functions of the potential of mean force. For PABA, $PABA^-$, and L-Pro-ZW cylindrical distribution functions will be also used to characterize ring hydration. The probability for ion-molecular complex formation between inorganic ions and the charged functional groups of the amino acids will be discussed and a structural mechanism for this process given.

This work was supported by funding from the European Union' Seventh Framework Program (FP7-PEOPLE-2009-IRSES, Marie Curie Project) under grant agreement No. 247500 and by the Russian Foundation for Basic Research (grant No. 12-03-97508–r_centre_a).

References

[1] P.H. von Hippel, T. Schleich, *in: S.N. Timasheff, G.D. Fasman (Eds.), Structure and Stability of Biological Macromolecules.* Vol. 2, Marcel Dekker, New York, 417(1969).

[2] M. Cacace, E. Landau, J. Ramsden, *Q. Rev. Biophys.* **30**, 241(1997).

[3] W. Kunz, J. Henle, B. W. Ninham, *Curr. Opin. Colloid Interface Sci.* **9**, 19(2004).

[4] K. Collins, M. Washabaugh, *Q. Rev. Biophys.* **18**, 323(1985).

3JO11 Effects of Solvent Viscosity on Photoinduced Electron - Transfer Reactions

T. Inada[1], H. Ikeda[2], and K. Kikuchi[3]

[1]*School of Science, Kitasato University, Sagamihara, 252-0373, Japan*
[2] *School of Engineering, Osaka Prefecture University, Sakai, 599-8531, Japan*
[3]*Kansei Fukushi Research Center, Tohoku Fukushi University, Sendai, 981-0943, Japan*
e-mail: tinada-@kitasato-u.ac.jp

Electron Transfer (ET) reaction is one of the most important phenomenon in chemistry and biology. The rate constant of ET is well known to depend on various factors such as the free energy change (ΔG) of full ET, the solvent polarity, the reaction distance, the molecular properties of the electron donor and acceptor and so on.

In this work, the fluorescence quenching ET and the following ET reactions such as back ET within geminate radical pairs, and the free radical recombination in a viscous polar solvent, ethylene glycol were studied using aromatic molecules as fluorescers and (i) aromatic hydrocarbons as neutral quenchers, and (ii) viologen derivatives as dicationic quenchers. The present results were compared with the results obtained for same fluorescer /quencher pairs in a non-viscous polar solvents (acetonitrile, methanol) to make clear the effects of solvent viscosity on the intermolecular photoinduced ET.

On analysis of the ΔG dependence of the rate constant of fluorescence quenching, the effective quenching distance, the yields of free radical and fluorescer triplet in fluorescence quenching, and the rate constant of free radical recombination, it is found that the switchover of fluorescence quenching mechanism occurs at ΔG = -0.25 eV, and the molecular charge of quenchers is not effected on the fluorescence quenching mechanism. The fluorescence quenching is induced by a exciplex formation when ΔG > -0.25 eV, and the fluorescence quenching is induced by a long-distance ET when ΔG < -0.25 eV. The shift of switchover ΔG from -0.5 eV in non-viscous polar solvents to -0.25 eV in ethylene glycol may be explained by the difference in the diffusion coefficients of electron donor and acceptor. Moreover it was found that the back ET occurs at longer reaction distance (r =12 Å on average) in ethylene glycol than non-viscous polar solvents (r =8 Å on average), and the ΔG dependence of the rate constant of back ET and the rate constant of free radical recombination are satisfactorily interpreted within the limits of the Marcus theory.

5JO12 Accurate pH Determination of Acidic Solutions on the Basis of an Ionic Liquid Salt Bridge

M. Shibata[1], M. Kato[1], Y. Iwamoto[1], S. Nomura[1], and T. Kakiuchi[2]

[1]*Research & Development Division, HORIBA, Ltd., Kyoto 601-8510, Japan*

[2]*Department of Energy and Hydrocarbon Chemistry, Graduate School of Engineering, Kyoto University, Kyoto 615-8510, Japan*

e-mail : manabu.shibata@horiba.com

Accurate determination of pH is of fundamental importance in not only science and technology but also many facets of our life and environments. Potentiometry by use of a pH glass combination electrode equipped with a concentrated KCl salt bridge (KClSB) has been used as a reliable and convenient method of pH measurements. However, the potentiometry with KClSB is not accurate enough for solutions of very low, as well as high ionic strengths. In this work, we show that pH values of 20-200 μmol dm^{-3} H_2SO_4 solutions and are estimated more reliably by use of the electrochemical cell with an ionic liquid salt bridge (ILSB) that consists of tributyl(2-methoxyethyl)phosphonium bis(pentafluoroethanesulfonyl)amide ($TBMOEPC_2C_2N$) than those bu use of KClSB-type. Table 1 lists the difference between the experimental and theoretical pH values in 20-200 μmol dm^{-3} H_2SO_4 solution obtained by use of ILSB type pH glass combination electrode. Metcalf reported that the error in the case of potentiometric pH measurements of 50 μmol dm^{-3} sulfuric acid was 0.055 ± 0.05 pH (positive bias ± two standard deviations) due to the residual liquid junction potential (RLJP) at the contact of KClSB with the sample solution[1]. The ILSB-type thus determines more accurately pH of the dilute sulfuric acid than KClSB-type. However the experimental pH values, pH_{ex}, at five different concentrations are still higher than the corresponding calculated pH values, pH_{cal}, by 0.005 to 0.032 pH unit. Taking account of the effects of finite solubility of IL in water and the diffusion potential of IL in the H_2SO_4, the difference between pH_{ex} and pH_{cal} values is smaller by 0.002-0.008 than those in Table 1.

The liquid junction potential between $TBMOEPC_2C_2N$ and 1 mol dm^{-3} HCl was estimated to be 0.6 mV, where the potential is referred to the inner potential of the $TBMOEPC_2C_2N$ phase, which fact opens the way for accurate pH determination of highly acidic solutions potentiometrically.

Table 1: The experimental and calculated pH value of 20 – 200μmol dm^{-3} H_2SO_4 solutions

$C_{H_2SO_4}$ / μmol dm^{-3}	$m_{H_2SO_4}$ / mol kg^{-1}	pH_{cal}	Mean pH_{ex}±95% confidence interval	pH_{ex}-pH_{cal}
20	20.06	4.401	4.433 ± 0.011	0.032
50	50.15	4.007	4.030 ± 0.003	0.023
100	100.30	3.710	3.710 ± 0.003	0.008
150	150.45	3.538	3.544 ± 0.004	0.006
200	200.59	3.416	3.421 ± 0.002	0.005

References [1] R. C. Metcalf, *Analyst* **112**, 1573-1577 (1987).

5JO13 Quality assurance method for simultaneous determining of Polychlorinated biphenyls (PCBs) and Organo-chlorinated pesticides (OCPs) using pressurized liquid extraction

Murad I. H. Helaleh[1], Amel Al-Rashdan[1]

[1]*Kuwait Institute for Scientific Research (KISR), Deputy General Director Office for Research, P.O. Box 24885, Safat 13109, Kuwait.*

e-mail: mrhelala@yahoo.com OR murad.helaleh@mailcity.com

Polychlorinated biphenyls (PCBs) and organo-chlorinated pesticides (OCPs) were belongs to persistence organic pollutant (POPs), and in accordance to Stockholm Convention of 2001, POPs must be controlled in water, soil, air and foodstuffs. POPs can be biologically accumulated in the fat tissues of humans and animals [1], which has resulted in concern about human exposures and adverse human health effect [2]. Simultaneous extraction with an integrated clean-up and removal of fat from fish tissue using pressurized liquid extraction (PLE) has been recently developed for fast and cost-effective analysis of polychlorinated biphenyls (PCBs) and organo-chlorinated pesticides (OCPs) in fish samples. Several experimental parameters such as: temperature, solvent composition, pressure, time and amount of adsorbent (i.e. florisil) have been tested to obtain an optimize conditions. The removal of fat content in fish tissue samples was effectively removed using 20 g of florisil (fat retainer) and solvent mixture composition of 10% DCM:H. Higher composition of dichloromethane resulted in a co-elution of interference and fat with the extracted sample. One-step method (extraction, clean-up, removal of fat and extract concentration) was successfully performed for the target analytes. Spiked sample recovery was applied in order to test the accuracy and precision of the developed method. Recovery of the method was satisfactory and minimum presence of matrix-interfering compounds was obtained. Quality parameters of the GC-MS (NCI) method was established, achieving good quality, low limits of detection, good precision and accuracy.

References

[1] E.N. Barkatina, I.A. Zastenskaya, O.V. Shulyakovskaya, A.L. Pertsovskii, N.V. Bunevich, T.A. Fedorova, *J. Anal. Chem.***62(9),** 868-871(2007).

[2] L.W. Robertson, L.G. Hansen, PCBs recent advances in environmental toxicology and human effect, University press of Kentucky, Lexington, KY, 2001.

5JO14

Gas Chromatography ion trap mass spectrometry for the determination of Nitro derivatives compounds in environmental soil samples

Amel Al-Rashdan[1],Murad I. H. Helaleh[1]

[1]*Kuwait Institute for Scientific Research (KISR), Deputy General Director Office for Research, P.O. Box 24885, Safat 13109, Kuwait.*

e-mail: dramel_alrashdan@yahoo.com

A rapid, accurate and reproducible method was developed for quantitative determination of thirteen nitro derivative compounds in soil at trace levels (μg/kg) by gas chromatography-ion trap mass spectrometry. The nitro derivative compounds were extracted from soil by sonication with acetonitrile, followed by clean up with silica cartridge and florisil. Two Calibration curves were drawn and the correlation coefficient (r^2) for each nitro derivative compounds were ranged from 0.995-0.999 units are missing and 0.984-1.000 units are missing for calibration curve 1 and 2, respectively. The method provides detection limits ranging from 0.98 μg/kg for NB full name of NB to 0.01 μg/kg for 3,5-DNA full name of NB. The method was validated by different analysis. The method gave good recovery (60.49-97.65 %), good precision (0.99-25.38 %), excellent reproducibility, and proved to be suitable for real routine work sample analysis. The method appeared to be effective by the analysis of soil samples in several soil samples from test fields in Kuwait.

5JO15 Adsorption of Silver(I) and Zinc(II) Ions from the Solution Using Blended Adsorbent of Dithizone-Natural Zeolite

Mudasir, L. Rintinga, and B. Rusdiarso

Chemistry Department, Faculty of Mathematics and Natural Sciences, Universitas Gadjah Mada, Sekip Utara, Yogyakarta 55281, Indonesia.

e-mail: mudasir@ugm.ac.id

The research about the ability of blended dithizone-natural zeolite (DNZ) for the adsorption of Ag(I) and Zn(II) ions from the solution has been done and the results were compared to those adsorbed by non-modified activated natural zeolite (NZ). Preparation of DNZ was done by stirring the mixture of NZ and dithizone in toluene for 24 h at room temperature and the obtained adsorbent was filtered and characterized using FT-IR spectrophotometer and X-Ray Diffraction analysis[1]. The adsorption study included pH optimization, adsorption kinetics, isotherm adsorption and sequential desorption of metal ions. The amount of Ag(I) and Zn(II) ions adsorbed from the solution were calculated by the concentration differences before and after adsorption processes which is determined using flame-AAS.

Table Langmuir-Hinshelwood isotherm adsorption parameters for Ag(I) and Zn(II)

Metal ions	Blended Adsorbents	Parameters of Langmuir-Hinshelwood isotherm adsorption			
		capacity/*b* (mol g^{-1})	Equilibrium constants/*K* (mol^{-1} L)	Energy/*E* (kJ mol^{-1})	Graph linearity (R^2)
Ag(I)	NZ	1.03×10^{-4}	6417.44	21.72	0.990
	DNZ	1.26×10^{-4}	8770.51	22.49	0.996
Zn(II)	NZ	5.19×10^{-5}	9813.14	22.77	0.992
	DNZ	6.11×10^{-5}	18230.5	24.31	0.996

Characterization results of the obtained adsorbent suggest that dithizone has been successfully blended on the surface of NZ and the process does not significantly alter the crystalline of NZ. Adsorption study reveals that the optimum pH for the adsorption of both Ag(I) and Zn(II) ions is reached at pH 6. Calculation of kinetic parameters for the adsorption of Ag(I) ion using Langmuir-Hinshelwood equation gives adsorption rate constants (*k*) of 1.0×10^{-3} and 3.0×10^{-3} $mins^{-1}$ for NZ and DNZ, respectively. The equilibrium constants (*K*) for NZ and DNZ are respectively 8104 and 9630 mol^{-1} L. For Zn^{2+} ion, the adsorption *k* is respectively 3.43×10^{-4} and 3.87×10^{-4} $mins^{-1}$ for NZ and DNZ, while the *K* for NZ and DNZ is found to be 4118 and 4338 mol^{-1} L, respectively. Evaluation of isotherm adsorption parameters using Langmuir-Hinshelwood equation gives the larger adsorption capacity (*b*), equilibrium constants (*K*) and adsorption energy (*E*) for DNZ compared to those of NZ (see Table). Sequential desorption study suggests that many interactions contribute to the adsorption processes of Ag(I) and Zn(II), i.e. complex formation, hydrogen bonding, ion exchange, and entrapment. In conclusion, it has been demonstrated that the blending of dithizone to natural zeolite has enhanced the adsorption ability of zeolite towards metal ions in the solutions.

References

[1] Mudasir, D. Maryanti, G. Pramiyanti, Roto, *J. Ion Exchange* **18**, 370 (2009).

5JO16 Red Ginger Rhizome Extract (*Zingiber officinale Linn.Var rubrum*) as an Deodorant Herbal Making Materials

Ika Nur Fitriani[1], Rizki Nor Amelia[1], and Anggi Ristiyana Puspitasari[1]

Department of Chemistry, Yogyakarta State University, Indonesia

e-mail : ika7x.gates93@yahoo.com

This research aimed to determine the optimal conditions for deodorant made from red ginger rhizome extract and knowing the effectiveness of product seen from the organoleptic test and bacteria test. The method consists of four stages, consist of making the red ginger extract, making of deodoran stick, tested the bacteria in the laboratory, and organoleptic tests. The results of this research is red ginger extract have 2.85345% oleoresin. It could potentially used as an anti-bacterial of *Staphylococcus aureus*. The process of making deodorant stick of red ginger rhizome extract had two ways. First, manufacture of red ginger rhizome extract by soxhletasi method. Second, mixing red ginger rhizome extract with sodium stearate and propylene glycol to form a solid. Test the inhibition of the growth of *Sthapylococcus aureus* bacteria do with Mueller-Hinton medium. Analysis of variance ANOVA of antibacterial activity in bacteria S. Aureus showed that the concentration did not show a significant effect. This suggests that deodorants ginger has antibacterial activity similar to the growth of *S. Aureus* test results for each concentration of 10%, 20%, and 30% of the inhibition obtained respectively 11.33 mm, 11.33 mm, and 11 mm. It can concluded that deodorant effective on concentration of 10%.

Keywords– Deodorant stick, red ginger rhizome extract, *Staphylococcus aureus*

5JO17 Reducing Resistance to Carbon droplets Polarography

M.Syauqillah[1],T.Herviyansyah[2]

[1]*Departement Chemistry, University of Indonesia, Depok West Java 16424, Indonesia*

[2]*Departement Chemical Engineering, University of Indonesia, Depok West Java 16424, Indonesia*

email: msyauqillah@gmail.com

In Asia, Liquid electrodes for polarography start to studied. Fluid carbon electrodes for polarography is a mixture of dioctyl phthalate and diiodomethane was found to be suitable to prepare a dropping carbon electrode[1]. We are now constructing a new electrode holder using a Teflon opening. In addition, the potential distribution on the surface of the electrode may affect the shape of the polarogram, if the resistance of the carbon paste is significantly high. In this study the parameters are explained in the reduction of carbon paste, thus obtained carbon electrodes have wide potential windows to more positive potentials, which cannot be reached by mercury electrodes[2].

References

[1] Hirosuke Tatsumi, Minami Shiba, Journal of Electrochemistry Communications **20** (2012)160–162

[2] P.A. Giguère, D. Lamontagne, Science **120** (1954) 390.

2M01 A Role Played by Kazuyasu Ibuki in Developing Electrolyte Solution Dynamics: Tribute to Him

Masaru Nakahara

Institute for Chemical Research, Kyoto University, Uji, Kyoto 611-0011, Japan

e-mail: nakahara@scl.kyoto-u.ac.jp

Dr. Kazuyasu Ibuki died on the 21st of May, 2012, at the age of 50, from a sudden heart attack during sleeping. Ibuki-san was the Professor of the Physical Chemistry Laboratory, the Department of Molecular Chemistry and Biochemistry, the Faculty of Science and Engineering, Doshisha University, after Professors K. Shimizu and M. Ueno. Just three days before his sad news I had an opportunity to meet him together with Profs. M. Ueno and Y. Yasaka and enjoyed exchanging our ideas and dreams on research and education and spent fantastic, never-forgetting time in discussing about our new research plan in Doshisha University. I promised to be back soon to continue our discussion in more detail but in vain. At this time of our last meeting nothing was wrong in his health conditions despite his heavy obligation as the department chairman. He continuously made contributions to the Japan Society of Solution Chemistry as a member of the steering committee. He was born on the 25th of February, 1962 as a son of a famous Kyoto Nishijin textile maker. Thus he loved the history and culture of Kyoto. He played a large brass tube instrument, euphonium and did a conductor for a group composed of young amateurs. He was good at music, mathematics, and chemistry. Under my supervision he received the Ph. D. degree from Kyoto University in 1989.

He was an outstanding scientist in the field of solution chemistry, contributing a wealth of valuable research findings in the field of electrolyte solution dynamics from the theoretical and experimental viewpoints. The main topics challenged theoretically and experimentally by him are: (1) ionic conductivity in solution, (2) solution viscosity studied by viscometer and NMR, and (3) diffusion-controlled rapid reactions. When he was in the Graduate Course of the Faculty of Science of Kyoto University the study on electrolyte conductivity met a new era as suggested by Evans, Tominaga, Hubbard, and Wolynes; JPC, **83**, 2669 (1979). He elucidated the reliability and limitations of the Hubbard-Onsager dielectric friction theory for the translational and rotational modes of ion movement beyond the simple Stokes-Einstein-Debye law originally for Brownian motion of molecules. He extended the dielectric friction theory to the viscosity B coefficient in electrolyte solution. In a series of papers he intensively analysed the effects of temperature, pressure, and solvent (including mixed solvent) on the ion dynamics and elucidated the contribution of the dielectric friction besides the viscous friction by systematically varying the solvent viscosity and dielectric properties (pioneering work by Josef Barthel) and the ionic valence and size. I am going to make every effort to tell you my happy research time spent together with Ibuki-san. Let you know what a scientist he was, how he worked on ionic solution dynamics, and how he was motivated to solve the solution problems. He published a number of epoch-making papers in The Journal of Chemical Physics and The Journal of Physical Chemistry in the 1980s. He kept enthusiastic interest in solution dynamics, in particular, various levels of diffusion processes.

2M02 Diffusion and diffusion limited reaction in supercritical fluids and ionic liquids

Y. Kimura

Department of Molecular Chemistry and Biochemistry, Faculty of Science and Engineering
Doshisha University, Kyotanabe, Kyoto 610-0321, Japan
e-mail : yokimura@mail.doshisha.ac.jp

Diffusion coefficients of molecules dissolved in solution reflects various solute-solvent interactions. We have investigated the diffusion coefficients dissolved in various unique fluids such as supercritical fluids and ionic liquids both by experimentally and theoretically[1-8]. In supercritical fluids, it has been discussed how the local density enhancement affect the diffusion coefficient dissolved in fluids. We have demonstrated that the local density enhancement makes the solute diffusion slower[1,2]. On the other hand, in the case of hydrophobic solute in supercritical water, the solute diffusion is much faster than that of attractive solute[4]. These predictions were partially demonstrated experimentally by applying the transient grating spectroscopy[3].

Molecular diffusion in ionic liquids attracts much attention of a lot of chemists because of its importance in electrochemistry and reaction chemistry. We have studied solute diffusion coefficients in ionic liquids under various conditions by applying the transient grating spectroscopy[5-8]. For example, we have investigated the diffusion coefficient of diiodide in ionic liquids. By comparing the disproportionate reaction rate of diiodide ions, we have revealed that the charge of the diiodide ion is shielded by surrounding ions and that the reaction rate is not affected by the repulsive charge between the reactant molecules (diiodide), in contrast to the case of the reaction in conventional liquid solvent such as ethanol[8]. The details will be presented at the conference.

Acknowledgement

I am very grateful to the late lamented Prof. K. Ibuki for useful discussion on the theoretical aspects of the diffusion and diffusion limited reaction in fluids.

References

[1] T. Yamaguchi, Y. Kimura, and N. Hirota, *Mol. Phys.* **94**, 527 (1998).
[2] T. Yamaguchi and Y. Kimura, *Mol. Phys.* **98**, 1553 (2000).
[3] T. Ohmori, Y. Kimura, N. Hirota, and M. Terazima, *J. Phys. Chem. B*, **107**, 5958 (2003).
[4] T. Ohmori and Y. Kimura, *J. Chem. Phys.* **119**, 7328 (2003).
[5] Y. Nishiyama, M. Fukuda, M. Terazima, and Y. Kimura, *J. Chem. Phys.* **128**, 164514 (2008).
[6] M. Demizu, M. Terazima, and Y. Kimura, *Analytical Sciences*, **24**, 1329 (2008).
[7] Y. Nishiyama, M. Terazima and Y. Kimura, *J. Phys. Chem B*, **113**, 5188 (2009).
[8] M. Demizu, M. Terazima, M. Harada, K. Saijo, and Y. Kimura, *Bull. Chem. Soc. Jpn.* **84**,70 (2011).

2M03 Exploring the Arts and Aqueous Solutions with Kazuyasu Ibuki

Philippe A. Bopp

Department of Chemistry, Université de Bordeaux
351 Cours de la Libération, FR-33405 Talence CEDEX
e-mail : philippebopp@yahoo.com

I have known Kazuyasu Ibuki since 1988 when he was a graduate student in Kyoto with M. Nakahara. It soon turned out that both of us were greatly interested in two things: the arts, and our science. His (together with Y. Kimura) 'guided tour' of Kyoto temples and shrines on a marvellous winter day is at the source of my later deep love and interest in Japanese art and classical literature. These exchanges deepened during his sabbatical year in Bordeaux, where his family and he integrated very well into French life. They bought a car, and travelled; he indulged in his love of opera, mainly Italian, and I tried to introduced him to the subtleties of 17th and 18th century French music (and Bordeaux wine).

Scientifically, our interest has been focused on the liquid state, in particular on the physical chemistry of solutions. A very large body of work was accumulated during his sabbatical year, which could up to now only be partly published [1][2]. We decided to revisit very carefully, in new MD simulations, the solutions of LiCl in water, since this salt is soluble at room temperature up to very high concentrations. These systems thus allow a realistic, yet systematic, variation of the interaction energies between the various constituents. We were still working on this (through the internet) when his wife's shocking message telling me about his so unexpected demise arrived one morning on my computer and left me stunned.

I shall mainly report on some of the results that were elaborated at this time and show how small variations (of the order of a few percent) in the assumed cation-water interactions (which have to be combinable with all other ones (water-water, anion-water, cation-anion, etc.)), lead, depending on the salt concentration, to quite drastic changes in the overall structure of the liquid.

References

[1] K. Ibuki and Ph. A. Bopp, **J. Mol. Liq.** *147*, 56-63 (2009).

[2] Ph. A. Bopp and K. Ibuki, **Condensed Matter Physics**, *15,2,* 23001, 1 (2012).

2M04 Terahertz dynamics and structure of hydrated protein studied by X-ray scattering

K. Yoshida[1], T. Yamaguchi[1]

[1] *Department of Chemistry, Fukuoka University, 8-19-1 Nanakuma, Jonan-ku, 814-0180 Fukuoka, Japan*

e-mail : kyoshida@fukuoka-u.ac.jp

Terahertz spectroscopy of biological samples has recently attracted much attention for chemical biologists since the dynamics of proteins in terahertz domain is concerned with their functions. Neutron scattering and terahertz absorption spectroscopy reflect single particle dynamics of protons in hydrated protein and dynamics of total dipole moment of water and proteins, respectively. An anharmonic oscillation mode was observed in a hydrated protein, while the mode was not seen in a dry sample [1, 2]. Since X-ray scattering is coherent and the wavelength is comparable with an atomic distances, inelastic X-ray scattering (IXS) of hydrated proteins would reveal the collective dynamics of the protein and hydration water as a function of wavevector Q. Therefore, the IXS would complement to the neutron scattering and the terahertz absorption spectroscopy. In the present study, IXS of hydrated proteins (β-lactoglobulin (β-Lg) [3], antifreeze protein, and filamentous actin) was measured at 180 – 298 K. The IXS experiments were performed using a high-resolution spectrometer installed at the beamline BL35XU of the SPring-8. Moreover, the static structure of the hydrated protein was measured by X-ray diffraction.

The dynamical structure factor of the hydrated proteins was fitted by a damped harmonic oscillator (DHO) model which consists of a Lorentzian for the central peak and a damped oscillator for both side peaks. The dispersion relation between the DHO excitation energy and Q for the hydrated proteins closely resembles that observed in pure liquid water. On the other hand, for the dry sample, such an excitation mode was not found. This indicates that the collective dynamics in the hydrated protein is very different from that in the dry protein, which is consistent with the results of the single particle dynamics. High frequency sound velocity is defined as the ratio of the DHO excitation energy to a Q value. The values for the hydrated proteins were almost constant against temperature, contrary to the results of the neutron scattering and the terahertz absorption spectroscopy. This could be explained in terms the fact that IXS spectrum is reflected from not the single particle dynamics but the collective dynamics, while the terahertz absorption spectrum includes both dynamics.

References

[1] M. Ferrand, et al., *Proc. Natl. Acad. Sci.* **90**, 9668 (1993).

[2] S. Kawaguchi, et al., *Phys. Chem. Chem. Phys.* **12**, 10255 (2010).

[3] K. Yoshida, et al., *J. Chem. Phys.* **133**, 134501 (2010).

2M05 Density Effects of the Translational Motion for Monovalent Ions in High-Temperature Liquid Alcohols

T. Hoshina[1], N. Tsuchihashi[2], K.Ibuki[2], and M. Ueno[2]

[1]*College of Industrial Technology, Nihon University, Chiba 275-8575, Japan*
[2]*Faculty of Science and Engineering, Doshisha University, Kyoto 610-0321, Japan*
e-mail : hoshina.takaaki@nihon-u.ac.jp

For a better understanding of transport process in solutions, it is necessary to investigate the density effect over a wide range of thermodynamic conditions. In ionic solutions, the electric conductivity measurement is one of the most reliable methods to disclose general trends of the density dependence of ionic mobility. We have reported the electric conductivities of 1:1 electrolytes (alkali metal halides and tetraalkylammonium bromides) in liquid alcohols (methanol and ethanol) along the liquid-vapor coexistence curve [1–5], and examined the validity of the Hubbard-Onsager (HO) dielectric friction theory [6, 7] based on the sphere-in-continuum model.

The molar electrolyte conductivities of dilute solutions of 1:1 electrolytes were measured in alcohol at high temperature. The limiting molar electrolyte conductivities and the molar association constants were obtained from the analysis of the concentration dependence of the conductivity. The translational friction coefficients for the monovalent ions were estimated from the limiting electric conductivities. The density effects of the friction coefficient of experimental data together with literature values were examined.

For monatomic ions [1, 2, 4], the translational friction coefficient decreased with decreasing density. The density dependences of the translational friction were well explained by the HO theory at medium and high densities. The application limit of the HO theory lay at about 2.0 times of the critical density in methanol and about 2.2 times in ethanol. For tetraalkyaammonium ions [3, 5], the density dependence of the translational friction coefficients was similar to that for monatomic ions. For the tetramethylammonium ion, the solvent structure loosening effect was important in methanol, whereas the dielectric effect was important in ethanol. For the tetraethylammonium ion, the structure loosening effect was showed in methanol, but a transition of the important factors from the structure loosening to the dielectric friction ones were observed with decreasing density in ethanol. For the tetra-*n*-butylammonium ion, the friction coefficients were determined mainly by the dielectric friction effect in methanol and the bulky size effect in ethanol.

References

[1] T. Hoshina, N. Tsuchihashi, K. Ibuki, and M. Ueno, *J. Chem. Phys.* **120**, 4355(2004).
[2] T. Hoshina, K. Tanaka, N. Tsuchihashi, K. Ibuki, and M. Ueno, *J. Chem. Phys.* **121**, 9517(2004).
[3] T. Hoshina, K. Tanaka, N. Tsuchihashi, K. Ibuki, and M. Ueno, *J. Chem. Phys.* **122**, 104512(2005).
[4] K. Takahata, T.Hoshina, N. Tsuchihashi, K. Ibuki, and M. Ueno, *J. Chem Phys.* **132**, 114501(2010).
[5] T. Matsui, T. Hoshina, N. Tsuchihashi, K. Ibuki, and M. Ueno, *J. Chem Phys.* **134**, 124509(2011).
[6] J. B. Hubbard and L. Onsager, *J. Chem. Phys.* **67**, 4850(1997).
[7] J. Hubbard, *J. Phys. Chem.* **68**, 1649(1978).

2M06 Temperature and Pressure Effects on the Reorientational Correlation Time of Water in FA- and DMF-Water Mixtures

M. Okada[1,2], K. Ibuki[2], and M. Ueno[2]

[1]*Depertment of Applied Chemistry, Nagoya University, Aichi 464-8603, Japan*
[2]*Depertment of Molecular Chemistry and Biochmistry, Doshisha University, Kyoto 610-0321, Japan*
e-mail : sk112652@mail.doshisha.ac.jp

In the study on the hydrophilic and hydrophobic interactions, amide-water mixtures have an advantage that we can systematically change the hydrogen-bonding ability and the hydrophobicity by substituting the functional groups. A formamide (FA) molecule consists of two hydrophilic groups and can be both a proton donor and an accepter in hydrogen-bonds. A *N*,*N*-dimethylformamide (DMF) molecule can only be a proton accepter, on the other hand, because the two hydrogen atoms in the amino group of an FA molecule are substituted by methyl groups in a DMF molecule. Both molecules have relatively large dipole moments, 3.73 D (FA) and 3.82 D (DMF), respectively, in gas phase and are miscible with water in arbitrary portions.

In this work[1-3], we determined the reorientational correlation times (τ_c) of heavy water (D_2O) in FA- and DMF-D_2O mixtures from the measurements of NMR relaxation times at 5, 25 and 45 °C under atmospheric pressure and at 25 °C under high pressure up to 196.1 MPa, and discussed the hydrophilic and hydrophobic interactions between amides and water. In order to support our discussion, we also performed the molecular dynamics (MD) simulations.

In the FA-D_2O mixture, τ_c increased with increasing FA content except for the water-rich region at 5 °C, where a shallow minimum appeared in the composition dependence of τ_c. On the other hand, τ_c in the DMF-D_2O mixture showed a remarkable maximum around 40 mol% of DMF at each temperature and pressure. The results on NMR measurements and MD simulations suggested the following as for the pressure dependence of τ_c in the mixtures. In the FA-D_2O mixture, the dipole interactions and the hydrogen bonds between FA-D_2O play an important role in the retardation of the rotational motion of D_2O molecules at high pressure. On the other hand, in the DMF-D_2O mixture, the methyl groups of DMF immobilize not only the water molecules directly contacting them but also those around the aldehyde group. Under high pressure, a condensed hydration structure is built up around the methyl groups of DMF by compression. The water molecules hydrated to methyl groups of DMF thus play an important role in determining the pressure dependence of τ_c in the mixture.

References

[1] M. Okada, K. Ibuki, M. Ueno, *Bull. Chem. Soc. Jpn.* **85**, 189(2012).
[2] M. Okada, K. Ibuki, M. Ueno, *Bull. Chem. Soc. Jpn.* **85**, 1192(2012).
[3] M. Okada, K. Ibuki, M. Ueno, *Bull. Chem. Soc. Jpn.* **86**, to be published.

Poster Session I

2PA01 A study on the phase behaviors and their dynamics of alicyclic-based ionic liquids by multi-faceted approach

Y. Shimizu[1], T. Yamamoto[1], K. Fujii[1], M. Imanari[2], and K. Nishikawa[1]

[1]*Graduate School of Advanced Integration Science, Chiba University, Chiba 263-8522, Japan*

[2]*Center for Analytical Instrumentation, Chiba University, Chiba 263-8522, Japan*

e-mail : k.nishikawa@faculty.chiba-u.jp

Ionic Liquids (ILs) are the materials composed of solely ions and characterized by low melting temperature. It has been elucidated that the physical properties of IL are greatly influenced by flexibilities of constituent ions[1, 2]. As for ILs with imidazolium-based cations ($[C_nmim]^+$), which are typical aromatic ones, we should consider only dynamics of alkyl chains of the cation. In the case of alicyclic-based ILs, it is also necessary to note the conformational analysis of the ring itself in addition to that of alkyl chains. We have investigated the phase behaviors and their dynamics of alicyclic-based ILs by multi-faceted approach.

As investing sample of alicyclic-based ILs, we adopted 1-butyl-1-methylpyrrolidinium hexafluorophosphate ($[C_4mpyr]PF_6$). We simultaneously performed calorimetry and Raman spectroscopy using own developed apparatus[3]. We also measured longitudinal and transverse relaxation times (T_1 and T_2) for ^1H, and ^{13}C spectra as a function of temperature.

The plural endothermic peaks corresponding to solid-solid phase transitions were observed in the heating process. The supercooled region of ILs is usually wide. However, that of $[C_4mpyr]PF_6$ is very small in comparison with $[C_nmim]X$. We confirmed the regions of the same solid phase on the calorimetric curve by Raman spectroscopy. In the range between 200 and 1200 cm^{-1}, no Raman band shift of $[C_4mpyr]PF_6$ is observed though some of $[C_4mim]PF_6$ are. However, there is the band which becomes broad with the temperature increasing. In the proton-relaxation measurement, the T_1 curve almost continuously changed in the both cooling and heating process. However, several discontinuous changes were observed in the T_2 curve. It may be suggested that there are plural phase transitions in the cooling process. The FID (Free Induction Decay) signals of ^1H, which observed in the temperature range with discontinuous change of the T_2 values, composed of long and short components. The ratio of the long and short components changed with depending on temperature. Therefore, there are two components of hard and soft in the solid state of these samples[4].

In addition to the above-mentioned results, we will discuss ^{13}C-T_1, ^{13}C spectra, DFT calculation for $[C_4mpyr]PF_6$ and those of 1-butyl-1-methylpiperidinium hexafluorophosphate ($[C_4mpip]PF_6$).

References

[1] Endo et al., *J. Phys. Chem. B*, **114**, 407 (2010).

[2] Umebayashi et al., *J. Phys. Chem. B*, **113**, 4338 (2009).

[3] Endo et al., *Jpn. J. Appl. Phys.*, **47**, 1175 (2008).

[4] Imanari et al., *J. Phys. Chem. B*, **116**, 3991 (2012).

2PA02 Alkyl-chain Length Dependence on Structural Fluctuations of $[C_nmim]NTf_2$ (n=2,4,6,8) + CO_2 Mixtures

T. Morita, S. Okumura, M. Ushio, and K. Nishikawa

Graduate School of Advanced Integration Science, Chiba University, Chiba 263-8522, Japan
e-mail : moritat@faculty.chiba-u.jp

Ionic liquids dissolve a large amount of carbon dioxide, as provided by Brennecke *et al.*[1] Despite such a large dissolution of carbon dioxide into ionic liquids, only small volume expansion is observed in ionic liquid phase. We have investigated relationship between this anomalous behavior and dissolution process from the viewpoint of structural fluctuations of ionic liquids. We obtained preliminary result of dependence of alkyl-chain length of the imidazolium-based ionic liquids on the structural fluctuations of ionic liquids saturated with pressurized carbon dioxide.

Small-angle X-ray scattering (SAXS) measurements were performed for the imidazolium-based ionic liquids using synchrotron facility, BL-15A and 6A stations at Photon Factory, up to 20 MPa. We constructed SAXS sample holder entirely made of titanium and titanium alloy[2]. Titanium spacer was set between two free pistons with X-ray windows made of single crystal diamond, so that path length was certainly kept to be constant under high-pressure conditions. We constructed and used in-situ beam monitoring detector [2,3] for determination of absorption coefficients of the mixtures, which affect absorption correction of the obtained SAXS signals exponentially. For evaluation of volume expansion of ionic liquids caused by the dissolution, measurements of the density were carried out in the same pressure range by means of X-ray absorption method using home-made measurement system. Incident and transmitted X-rays were measured with specially designed PIN Si photodiode with thin layer, 50 μm in thickness, and PIN Si photodiode, respectively. Uncertainty of the apparatus was estimated to be ±3% in density up to 20 MPa.

SAXS profiles even up to 20 MPa were analogous to those of the neat ionic liquids. The results indicate that the structural fluctuations of ionic liquids caused by the dissolution are very small. However, $I(0)$ values, SAXS intensities at zero-angle, had slight pressure dependences, especially for n=2 in high-pressure region and n=8 in the whole pressure region. The density slightly decreased with pressure from 0.1 to 10 MPa, whereas carbon dioxide qualitatively dissolves into space and void in ionic liquids in the pressure region. The density increased with pressure from 10 MPa. The pressure corresponds to that saturated region of carbon dioxide solubility. Dependence of alky-chain length of the cations on absorption process is discussed in the basis of structural fluctuations evaluated from $I(0)$ and density.

References [1] L. A. Blanchard, D. Hancu, E. J. Beckman, and J. F. Brennecke, *Nature* **399**, 28 (1999). [2] T. Morita, M. Ushio, K. Kanoh, E. Tanaka, and K. Nishikawa, *Jpn. J. Appl. Phys.* **51**, 076703 (2012). [3] T. Morita, Y. Tanaka, K. Ito, Y, Takahashi, and K. Nishikawa, *J. Appl. Crystallogr.* **40**, 791 (2007).

2PA03 Phase Behaviors of Amide-based Ionic Liquids accompanied by conformational change

K. Fujii[1], M. Imanari[1, 2], T. Endo[3] and K. Nishikawa[1]

[1]*Graduate School of Advanced Integration Science, Chiba University, Chiba 263-8522, Japan*
[2]*Center for Analytical Instrumentation, Chiba University, Chiba 263-8522, Japan*
[3]*University of California Davis, California, U.S.A.*
e-mail : fujii.kozo@chiba-u.jp

Ionic liquids have unique properties, such as low melting point, premelting over a wide temperature range, excessive supercooling, tendency toward glass formation from liquid state upon cooling, and extreme thermal history.

We have investigated phase behaviors of 1,3-dimethylimidazolium bis(fluorosulfonyl)amide ($[C_1mim]FSA$), 1,3-dimethylimidazolium bis(trifluoromethanesulfonyl)amide($[C_1mim]NTf_2$), and 1,3-dimethylimidazolium bis(pentafluoroethanesulfonyl)amide($[C_1mim]BETA$) by measuring of calorimetry, Raman spectroscopy and NMR, focusing on the crystallizing and melting processes. Since $[C_1mim]^+$ ion has no conformational freedom, it is noted on conformational analysis of the anion only. Every ions of FSA^-, NTf_2^- and $BETA^-$ were known to have two respective stable rotamers. To determine their structures in the liquid and the solid states, we made simultaneous measurements of Raman spectroscopy and calorimetry focusing on the crystallizing and melting process by using own developed apparatus[3]. At the heating process before melting, an endothermic peak corresponding to a crystal-crystal transition was detected on every samples. Concomitantly Raman spectra were measured at the temperature before and after the peak. Raman spectra revealed the peak shift in several wavenumbers which would be related to the conformational change of the anion.[4,5] According to DFT calculations, those peak shifts correspond to the conformational change of anion. Therefore, it is expected that the phase transition occurs accompanied by conformational change of the anion. These transitions of crystallization and melting were corresponded to T_1 and T_2 for ^1H and ^{19}F in NMR. After crystallization, the trace of T_1 and T_2 against temperature for ^1H and ^{19}F revealed the difference of dynamics for the cation and the anion.

We revealed that in a crystal system of $[C_1mim]FSA$, the conformation of FSA^- is Cisoid. We will discuss the relation between potential energy and conformations for FSA^-.[6]

References

[1] T. Endo, et al.: *J. Phys. Chem.* **B114**, 407(2010).
[2] M. Imanari,et al.: *J. Phys. Chem.* **B 116**, 3991(2012).
[3] T. Endo, et al.: *Jpn. J. Appl. Phys.*, **47**, 1775(2008).
[4] K. Fujii, et al.: *J. Phys. Chem. B Lett.*, **110**, 8179(2006).
[5] J.C. Lassegues, et al.: *J. Raman Spectrosc.*, **38**, 551(2007).
[6] J.N.Canongia Lopes, et al.: *J. Phys. Chem.* **B112**, 9449(2008).

2PA04 Physicochemical Properties of Water in Ionic Liquids Studied by the Chemical Shift and H/D Exchange Reaction

K. Saihara[1], H. Abe[2], Y. Yoshimura[3], and A. Shimizu[1]

[1]*Dept. Environmental Engineering for Symbiosis, Soka Univ., Tokyo 192-8577, Japan*
[2]*Dept. Applied Chemistry, National Defence Acad., Kanagawa 239-8686, Japan*
[3]*Dept. Materials Science and Engineering, National Defence Acad., Kanagawa 239-8686, Japan*

e-mail : ksaihara@kph.biglobe.ne.jp

Ionic liquids are known as room temperature molten salts, because they exist as liquid state at room temperature even they are composed solely of ions. Ionic liquid/water mixtures have attracted much attention in recent years due to their unique properties; *e.g.*, *cytochrome c* can keep the activity high in ionic liquid/water mixtures. Recently, we found that the NMR peak of water splits into two in certain ionic liquid/water mixtures [1]. In this study, to obtain more detailed information about this, we have investigated the chemical shift of water and the H/D exchange reaction between cation and D_2O in ionic liquid/water mixtures by NMR.

Following seven typical ionic liquids/water mixtures were used; 1-butyl-3-methyl imidazolium tetrafluoroborate ([bmim][BF_4]), [bmim][Cl], [bmim][Br], [bmim][I], [bmim][SCN], 1-ethyl-3-methylimidazolium tetrafluoroborate ([emim][BF_4]), *N*,*N*-diethyl-*N*-methyl-*N*-(2-methoxyethyl) ammonium tetrafluoroborate ([DEME][BF_4]). Chemical shift of water was gradually shifted to high magnetic field with increasing water concentration. An extrapolation of the chemical shift to 0 mol% water concentration was in agreement with the Jones-Dole *B* coefficient of anion determined by viscosity measurements. Generally viscosity *B* coefficient represents the strength of ion-water interactions in a dilute aqueous solution [2]. The present results, however, indicate that the trend of ion-water interaction in water-rich region was maintained even in water-poor region. This result is also consistent with the report by Zong *et al.* [3]; anion-water interactions are more prominent than cation-water interactions in [bmim][BF_4]/water mixtures.

Next, the H/D exchange reaction between the exchangeable C2-H proton of imidazolium cation and heavy water in 50 mol% ionic liquids/water mixtures were investigated. We found that the peak at lower magnetic field can be assigned to the proton located close to C2-H of cation. Additionally, there occurred no H/D exchange reaction between the split (two) NMR signals for water observed in 50 mol% ionic liquids/water mixtures suggesting that the waters exist as isolated each other.

References

[1] S. Ohta, *Master Thesis. Soka University*, 2012
[2] H. Donald, B. Jenkins, Y. Marcus, *Chem. Rev*, 95, 2695-2724, 2012
[3] X. Zhong, Z. Fan, Z. Liu, D. Cao, *J. Phys. Chem*, 116, 3249-3263, 2012

2PA05 Correlation between the H/D Exchange Reaction and the Conformational Change of Imidazolium Cation in Imidazolium-based Ionic Liquid-D_2O Mixtures

Y. Yoshimura[1], N. Hatano[1], T. Takekiyo[1], H. Abe[2]

[1]*Dept. Applied Chemistry, National Defence Acad., Kanagawa 239-8686, Japan*
[2]*Dept. Materials Science and Engineering, National Defence Acad., Kanagawa 239-8686, Japan*

e-mail: muki@nda.ac.jp

Recently, studies of room temperature ionic liquid (RTIL)-water mixtures have gained much attention and the unique properties have been reported [1-3]. The presence of water might affect the dynamics of constitute ions in RTILs [4-6]. Therefore, a detailed understanding of the behavior of RTIL-water mixtures is of importance to extend the range of applications for these materials.

In this study, we have studied the effect of deuterated water on the conformational equilibrium of the imidazolium cation in mixtures of water and imidazolium type ionic liquids. Raman spectroscopy is a powerful tool to investigate the inter- and intra-molecular interactions.

Raman spectra were measured at room temperature (298 K) using a JASCO NR-1800 Raman spectrophotometer equipped with a single monochromator and a CCD detector. The 514.5-nm line from a Lexel Ar+ ion laser was used as an excitation source with a power of 250 mW. As sample RTILs, we used 1-butyl-3-methylimidazolium tetrafluoroborate (denoted as [bmim][BF_4]), [bmim][Cl], [bmim]SCN], [bmim][CH_3COO], [bmim][PF_6], and [bmim][NO_3].

Here, we provide Raman spectroscopic evidence of that the conformational dynamics of the [bmim] cation in D_2O is directly related to the H/D exchange reaction of the C-H group at position 2 of the imidazolium ring. The H/D isotopic exchange induced the increase in a *gauche* conformer of the [bmim] cation in the mixtures, though the results show versatility depending on the anion.

References

[1] L. Cammarata, S. G. Kazarian, P. A. Salter, T. Welton, *Phys. Chem. Chem. Phys.*, **3**, 5192 (2001).

[2] S. Saha, H. Hamaguchi, *J. Phys. Chem. B*, **110**, 2777 (2006).

[3] Y. Jeon, J. Sung, D. Kim, C. Seo, H. Cheong, Y. Ouchi, R. Ozawa, H. Hamaguchi, *J. Phys. Chem. B*, **112**, 923 (2008).

[4] A. Adhikari, K. Sahu, S. Dey, S. Ghosh, U. Mandal. K. Bhattacharyya, *J. Phys. Chem. B*, **111**, 12809 (2007).

[5] W. Jiang, Y. Wang, G. A. Voth, *J. Phys. Chem. B*, **111**, 4812 (2007).

[6] M. Moreno, F. Castiglione, A. Mele, C. Pasqui, G. Raos, *J. Phys. Chem. B*, **112**, 7826 (2008).

2PA06 Water Concentration Dependences of NMR Longitudinal Relaxation Times and Self-diffusion Coefficients of Lithium Ion in Hydrophobic Ionic Liquid

T. Umecky[1], T. Takamuku[1], M. Takagi[2], E. Kawai[2], T. Matsumoto[2], and T. Funazukuri[2]

[1] *Graduate School of Science and Engineering, Saga University, Saga 840-8502, Japan*

[2] *Faculty of Science and Engineering, Chuo University, Tokyo 112-8551, Japan*

e-mail : umecky@cc.saga-u.ac.jp

Ionic liquids (ILs) have several excellent advantages, e.g., low-volatility and low- flammability, over conventional organic liquid solvents. Due to this, a variety of attempts to use ILs as reaction, extraction, and electrochemical media have been made. Water is one of contaminants in ILs. Because water molecules strongly interact with monoatomic ions such as lithium ion in a general way, understandings how water molecules exist in ILs with lithium electrolyte and play roles in microscopic properties, i.e., solution structures and dynamic characteristics, in the IL solutions are quite important to elucidate mechanism of metal ion extraction from water phase into (hydrophobic) IL one. As far as we know, the microscopic properties of the IL solutions including lithium electrolyte and water have not been sufficiently investigated.

In the present work, we focused on the effects of water dissolution on rotational and translational motions of lithium ion in hydrophobic IL. ^{7}Li NMR longitudinal relaxation times and self-diffusion coefficients of 1-ethyl-3-methylimidazolium bis(trifluoromethanesulfonyl)amide ([C_2mim]TFSA) solutions including lithium bis(trifluoromethanesulfonyl)amide at 0.020 mol dm^{-3} were measured as a function of water content. As the water concentration rises, a steep decrease in rotational correlation times, which were determined from the longitudinal relaxation times obtained with two field-different NMR spectrometers, of lithium ion in the [C_2mim]TFSA solution is followed by a gradual reduction at the water concentration of ~0.3 mol dm^{-3}. In contrast to the result of the rotational correlation times, the self-diffusion coefficients of lithium ion obtained by pulsed field gradient NMR technique markedly increase with rising water content up to ~0.3 mol dm^{-3} and then moderately elevate. In view of a decrease in the viscosity of [C_2mim]TFSA (without lithium electrolyte) with an increase in water content [1], the enhancements of the rotational and translational motions of lithium ion caused by water dissolution are due probably to the drop in the viscosity of the [C_2mim]TFSA solution with lithium electrolyte. In the presentation, we will report the correlation between the rotational correlation times and the self-diffusion coefficients, and then discuss the solvation structure of lithium ion in the [C_2mim]TFSA solution including water.

Reference

[1] J. A. Widegren, A. Laesecke, J. W. Magee, *Chem. Commun.* 1610 (2005).

2PA07

The analysis of diffusion coefficient in silicone ionic liquid studied by transient grating method

Shinya Nemugaki, Yukie Ohta, Yusuke Hiejima, Kenji Takahashi.
Kanazawa university, Kakuma-machi, Kanazawa 920-1192, Japan
e-mail : nemu@stu.kanazawa-u.ac.jp

Ionic liquids (ILs) have various interesting properties, for example, low vapor pressure, fire retardancy, high electrical conductivity, chemical stability. Due to these unique properties, ILs can overcome the drawback of organic solvents such as high vapor pressure and flammability. Therefore it is attracted much attention as an electrolysis solution in Li ion battery. However it is known that molecular diffusion in IL is generally slow, because viscosities of ILs are higher than that of organic solvent. On the other hand, it has been reported that molecular diffusion in silicone oil is higher than that in organic solvents with the same viscosity. Therefore we expected that siloxane fanctional group may improve the rate of molecular diffusion. Our present purpose is analysis of transport property in silicone ionic liquids (SiILs) which is applicable to electrochemical devices.

SiILs were synthesized by anion exchange method. As shown in Fig. 1, *N*-Methylpyrrolidine and siloxane with chloride group were reacted. Then lithium-bis(trifluoromethanesulfonyl)amide is made to react and SiILs were created. We synthesized four different SiILs.

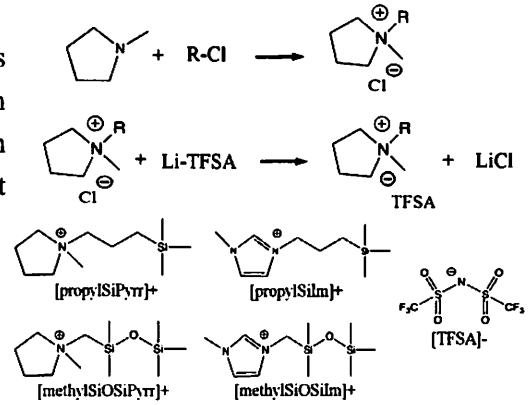

Fig. 1. Synthetic scheme and structure of silicone ionic liquids.

We applied the transient grating (TG) method in order to determine diffusion coefficients in SiILs. We used the photo-dissociation reaction of diphenylcyclopropenone (DPCP) for the TG method. After the photo-excitation, DPCP dissociates into diphenylacetylene (DPA) and carbon oxide (CO). The 355 nm of Nd:YAG laser was used as an excitation pulse. By this reaction, we determined the diffusion coefficient of CO, DPA, and DPCP in SiILs.

Compared with calculated values by Stokes-Einstein equation, diffusion coefficient of CO measured by TG method are found to be much larger. Fig. 2 shows a plot of diffusion coefficients of CO in SiILs against viscosity η. Compared with literature values, CO in SiILs are slightly larger than that in other ILs. In addition, diffusion coefficients of CO in ILs have weak dependence on the viscosity.

We think that these results caused by complex structure of ILs. A small molecule such as CO can diffuse fast through big voids in ILs. We are now investigating the correlation between the void size and diffusion coefficients.

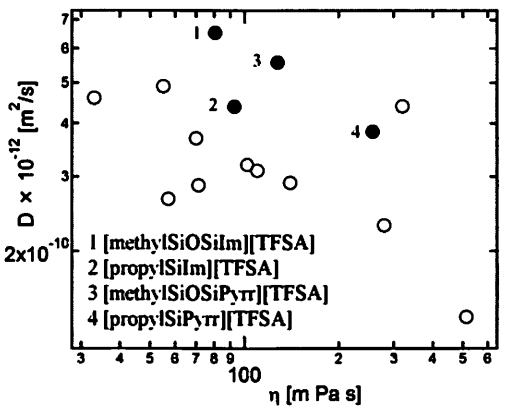

Fig. 2. A plot of diffusion coefficients of CO in ionic liquids against viscosity η.

2PA08 Dynamics of the Polymer-RTILs Solutions which Show LCST Behaviour

A. Iwata[1], K. Fujii[2], T. Ueki,[3] M. Shibayama[2], M. Watanabe[4], M. Terazima[1], and Y. Kimura[5]

[1]*Department of Chemistry, Graduate School of Science, Kyoto University, Kyoto 606-8502, Japan*

[2]*Institute for Solid State Physics, The University of Tokyo, Chiba, 277-8581, Japan.*

[3]*Department of Materials Engineering, Graduate School of Engineering, The University of Tokyo, Tokyo, 113-8656, Japan*

[4]*Department of Chemistry and Biotechnology, Yokohama National University, Yokohama, 240-8501, Japan*

[5]*Department of Chemical Science and Technology, Faculty of Bioscience and Applied Chemistry, Hosei University, Tokyo, 185-8584, Japan*

e-mail : ykimura@hosei.ac.jp

It has been reported that the solution of poly(benzylmethacrylate) (PBnMA) in ionic liquids (ILs) shows the LCST behaviour [1]. For example, the solution of PBnMA in ethylmethylimidazolium bis(trifluoromethanesulfonyl)amide ([EMIm][NTf_2]) shows the phase separation at around 100 °C. Fujii et al. studied the structure change of the solution by using dynamic light scattering and small angle neutron scattering, and found the existence of clusters of the polymer (ca. 3000Å) near below the phase separation temperature. In this paper we will report the dynamics of this polymer solution by using the transient grating (TG) spectroscopy. In the TG method (Fig.1), the sample solution is irradiated by two laser pulses simultaneously, and the transient optical fringe is produced by the interference of the pulses. Then successive photo-reaction in the solution produces the modulation of the refractive index of the solution, which is monitored by the diffraction intensity of the probe beam.

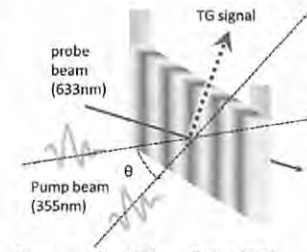

Fig.1 Principle of the TG method

Figure 2 shows a typical TG signal of the PBnMA in [EMIm][NTf_2]. This signal was ascribed to the diffusion dynamics of the fragmented PBnMA by the laser light. It was found that the diffusional dynamics of the fragment did not obey the Stokes-Einstein relation. Further near the critical temperature of the solution, we have detected the TG signal due to the phase separation. The details will be discussed in the presentation.

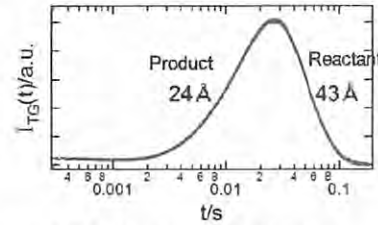

Fig.2 TG signal of PBnMA in [EMIm][NTf_2]

Acknowledgement

This work is supported by the grants from JSPS (No. 23350006).

References

[1] K. Fujii, T. Ueki, K. Niitsuma, T. Matsunaga, M. Watanabe, M. Shibayama, *Polymer*, **52** 1589 (2011).

2PA09 Photoisomerization quantum yields of novel ionic liquids with phenylazo group

T. Yoshida, T. Monji, D. Kawamori A. Kawai, and K. Shibuya

Department of Chemistry, Tokyo Institute of Technology,
2-12-1 H-89 Ohokayama Meguroku Tokyo 152-8551, Japan
e-mail : yosida.t.aa@m.titech.ac.jp

Ionic liquids (ILs) are salts which exist as liquid around room temperature and have many characteristic features such as non-volatility, non-flammability and electro-conductivity. One of the most interesting aspects of ILs is that it is possible to control physical properties by a choice of cation and anion components. Recently, we have synthesized novel ILs which have phenylazo group attached to imidazolium cation [1]. Phenylazo group is known to show photochromism through isomerization of N=N bond. The structures of these ILs are shown in Figure 1. It has been reported that 2PA-RmimX undergoes photoisomerization from E-form by UV or Vis light in diluted solution [1] and neat liquid [2]. In this study, we report quantum yields for photoisomerization of 2PA-RmimX diluted in various ILs and organic solvents to understand their photochromic property.

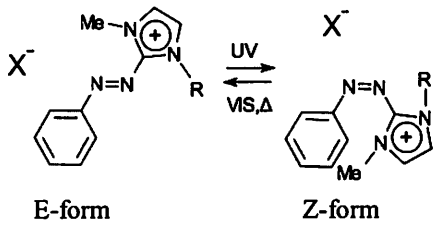

Figure 1 Structure of novel ionic liquids, 2PA-Rmim X and the isomerization reaction scheme. R= B (Butyl), MOE ($CH_3OC_2H_4$) and X= Tf_2N { $(CF_3SO_2)_2N$ }, Pf_2N

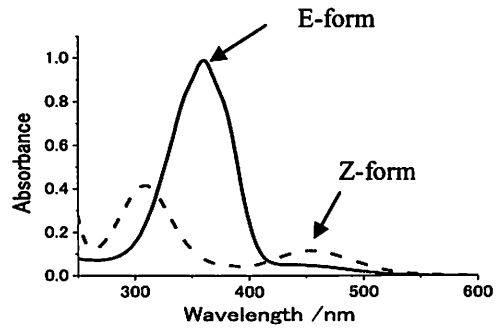

Figure 2 Absorption spectra of 2PA-MOEmim$^+$ in N,N-dimethyl-N-(2-methyl) ammonium Tf_2N.

Photoisomerization of 2PA-MOEmimTf_2N diluted in various solvents is monitored by UV-Vis absorption spectroscopy. Figure 2 shows absorption spectra of E- and Z-forms of 2PA-MOEmim$^+$. Time evolution of photoisomerization was monitored by absorbance at 360 nm which is responsible only to E-form. We measured time dependences of absorbance for 2PA-RmimX solutions and the standard sample, azobenzene in isooctane. From the analysis, quantum yields of photoisomerization were determined. The yields were low in ILs having imidazolium cation. We discuss the solvation effect of ILs on 2PA-Rmim$^+$ isomerization on the basis of the quantum yields.

References

[1] T. Asaka, N. Akai, A. Kawai, K. Shibuya *J. Photochem. Photobiol. A.* **209**, 12-18(2010).

[2] A. Kawai D. Kawamori, T. Monji, T. Asaka, N. Akai, K. Shibuya *Chem.Lett.* **39**, 230-231(2010).

2PA10 Anion effects on fluorescence lifetimes of methylene blue in ionic liquids

T. Hirano, K. Nakada, T. Hidemori, A. Kawai and K. Shibuya

Department of Chemistry, Graduate School of Science and Engineering, Tokyo Institute of Technology, Tokyo, Japan

Ionic liquids are organic salts whose melting points are near room temperature. They have unique physical properties such as nonvolatility and nonflammability, and have been proposed as "green" alternative to conventional environmentally detrimental volatile solvents. For a choice of appropriate solvent for one's purpose, it is definitely important to know their physical properties. Effect of ionic liquids on the photo-excited state lifetime is one important feature of solvent in photochemical point of view. Our group has been investigating triplet deactivation processes of methylene blue dissolved in degassed ionic liquids by means of a nanosecond transient absorption spectroscopy. It was found that the triplet lifetime of methylene blue depends on anion components of ionic liquids. In particular, there found strong correlation between anion donor number and the triplet lifetime. This result suggested that charge transfer type triplet quenching may occur in ionic liquids with anion of high donor number. In the present study, we focus on anion induced charge transfer quenching of singlet excited state in ionic liquids.

Fluorescence lifetime of methylene blue in ionic liquids was measured by means of a time correlated single photon counting (TCSPC) method. In TCSPC method, a picoseconds diode laser (pulse width 30 ps) was used as light source and fluorescence was detected by a combination of Nikon G500 monochromator (wavelength resolution 2 nm), avalanche photodiode (time resolution 50 ps) and photocounting board. IRF of the apparatus was 0.7 ns. Ionic liquids used as solvent are 1-R-3-methylimidazolium (R = Butyl, or Hexyl) salts with various anions such as BF_4^-, PF_6^-, SCN^-, $CF_3SO_3^-$, $(CF_3SO_2)_2N^-$, and halide ions with different donor numbers.

Fig.1 shows fluorescence time profiles of methylene blue in ionic liquid [Hmim][Tf_2N] in the presence of [Hmim][Br]. Decay parts of the profiles were well fitted by single exponential function. The decay rate linearly depends on the concentration of [Hmim][Br] and the Stern-Volmer analysis for various samples provided fluorescence quenching rate constant, k_q. ΔG^0 values of charge transfer reaction for various anions were calculated and the quenching mechanism was discussed on the basis of the correlation between k_q and ΔG^0 values.

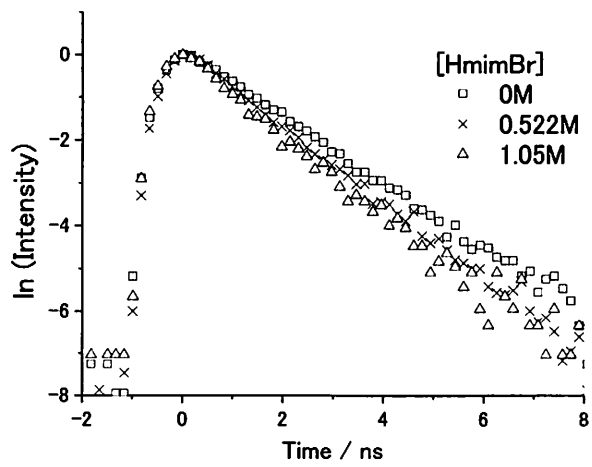

Fig. 1 Fluorescence time profiles of methylene blue in [Hmim][Tf_2N] in the presence of quencher, [Hmim][Br].

2PA11 Study on the Excitation Wavelength Dependence of the Photo-induced Proton Transfer Reaction

K. Suda[1], S. Hayaki[2], H. Sato,[2] M. Terazima[1], and Y. Kimura[3]

[1]*Department of Chemistry, Graduate School of Science, Kyoto University, Kyoto 606-8502, Japan*

[2] *Department of Molecular Engineering, Graduate School of Engineering, Kyoto University, Kyoto 615-8510, Japan*

[3]*Department of Chemical Science and Technology, Faculty of Bioscience and Applied Chemistry, Hosei University, Tokyo, 185-8584, Japan*

e-mail : skayo@kuchem.kyoto-u.ac.jp

It has been suggested that the combination of the charge parts and the nonpolar part of typical ionic liquids (ILs) makes a local structure in ILs, which results in a unique solvent properties. In this study, we focused on the intramolecular proton transfer (PT) reaction of 4'-*N,N*-diethylamino-3-hydroxyflavone (DEAHF). DEAHF exists in a normal form in the ground state, and after the photo-excitation the molecular undergoes PT in the excited state producing the tautomer form (see Figure. 1). The reaction dynamics can be monitored by the fluorescence from the normal (N*) and the tautomer (T*) forms at different wavelength. Interestingly, it has been found that the yield of PT is dependent on the excitation wavelength[1,2]. By moving to the red-wavelength for the excitation, the yield of the tautomer decreased. In this paper, we will present the detailed study on the dynamics of PT in various ILs at various excitation wavelengths.

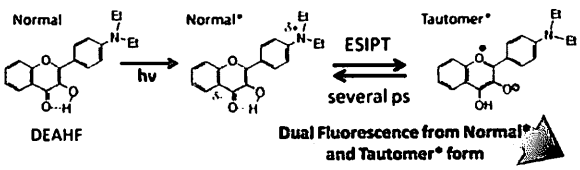

Figure 1. Reaction scheme of DEAHF.

Figure 2 shows the fluorescence dynamics of DEAHF in $[P_{2,2,2,8}][NTf_2]$ for different excitation wavelengths (400 nm and 450 nm). It has been found that the initial dynamics of the reaction is strongly modified by the excitation wavelength. Clearly the rise of the tautomer fluorescence when excited at 450 nm is slower and the fluorescence intensity from the tautomer at 200 ps is rather small. Similar trend was observed for other ILs. The detail will be discussed in the presentation.

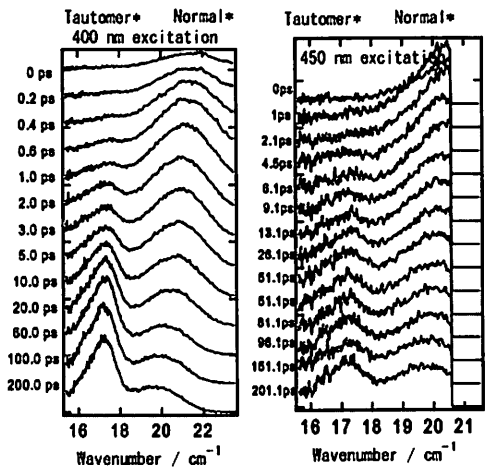

Fig. 2. Time resolved fluorescence spectra of DEAHF in $[P_{2,2,2,8}][NTf_2]$ obtained by the different excitation wavelengths.

Acknowledgement

This work is supported by the grants from JSPS (No. 23350006).

References

[1] Y. Kimura, M. Fukuda, K. Suda, M. Terazima. *J. Phys. Chem. B* **114**, 11847 (2010).

[2] K. Suda, M. Terazima, Y. Kimura, *Chem. Phys. Lett.* **531**, 70 (2012).

2PA12 Structure of ionic liquids at the mercury interface studied using electrocapillary measurements

N. Nishi, A. Hashimoto, E. Minami and T. Sakka

Department of Energy and Hydrocarbon Chemistry, Graduate School of Engineering, Kyoto University, Kyoto 615-8510, Japan

e-mail : nishi.naoya.7e@kyoto-u.ac.jp

Ionic liquids (ILs), which are liquid salts at ambient temperature and are composed of entirely ions, have potential applications in electrochemical devices, because of their unique properties such as negligible volatility and peculiar solvation toward solutes. The differential capacitance (C_d) at the electrochemical interface of ILs has been intensively measured and reported by using electrochemical impedance spectroscopy (EIS) with a fast frequency, e.g. 1 kHz, of a.c. perturbation voltage. However, we recently demonstrated that the interfacial structure of ILs shows ultraslow relaxation, on the order of seconds or minutes, in response to the electric potential change [1-4]. The ultraslow relaxation leads to deviation of the C_d values obtained by EIS from the static C_d (C_d at zero frequency). The measurements of the static C_d would be desirable, because the static C_d reflects the interfacial structure of ILs at equilibrium and it can be compared with theoretical results such as molecular dynamics simulations. Moreover, the static C_d would be more valuable than high-frequency C_d for the study of ILs for the possible application to energy storage devices.

Here, we will present the static C_d at the IL|Hg interface, by using electrocapillary (interfacial tension, γ, *vs.* potential) measurements. Long-time measurements of γ enabled us to track the ultraslow relaxation of the structure at the IL|Hg interface to the potential change and to evaluate γ at equilibrium, which was used in thermodynamic analysis to obtain the static C_d. In this paper, we will discuss IL-specific shape of the static C_d *vs.* potential curve and the dependence of the curve on IL-constituting ions.

References

[1] Y. Yasui, Y. Kitazumi, R. Ishimatsu, N. Nishi, T. Kakiuchi, *J. Phys. Chem. B*, 113(2009)3273.

[2] Y. Yasui, Y. Kitazumi, N. Nishi, T. Kakiuchi, *J. Phys. Chem. B*, 114(2010)11141.

[3] Y. Yasui, Y. Kitazumi, N. Nishi, T. Kakiuchi, *Electrochem. Commun.*, 12 (2010) 1479.

[4] S. Makino, Y. Kitazumi, N. Nishi, T. Kakiuchi, *Electrochem. Commun.*, 13 (2011) 1365.

2PB01 3D-RISM-SCF Study of Solvent Effects on Excitation Spectra of Merocyanines

Y. Tanaka, N. Yoshida, and H. Nakano

Department of Chemistry, Graduate School of Sciences, Kyushu University, Fukuoka 812-8581, Japan

E-mail: ta-chan@ccl.scc.kyushu-u.ac.jp

Merocyanines exhibit solvatochromism, the color change of solution dependent on the varieties of solvents. The origin of it is known mainly to be the polarity of the solvents. However, to understand and control the chromism from microscopic point of view, studies of the solvent effects based on molecular theory is crucial. In the present study, the excitation spectra of streptopolymethinemerocyanine (SPMC; $H_2N(C_2H_2)_nCHO$ (n = 1-8); Figure 1) and solvent effects on them are investigated using the three-dimensional reference interaction site model self-consistent field (3D-RISM-SCF) method. A focus is placed on the dependencies on the chain length and the varieties of solvents since it is widely known that the excitation energy is correlated with the chain length.

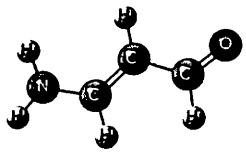

Fig. 1 SPMC (n = 1)

Figure 2 shows the π-π^* and n-π^* excitation energies against n. In the calculations, LC-BOP/cc-pVDZ were used as the exchange and correlation functionals and the basis set, and the solvents examined were water, methanol, and acetonitrile. With the extension of chain length, both the π-π^* and n-π^* excitation energies decreased monotonically. The solvent effect was different depending on the protic/aprotic solvents and the chain length. In the case of protic solvents, water and methanol, the π-π^* excitation energy decreased by solvation for all the chain lengths, whereas the n-π^* excitation energy increased on the contrary. In the case of aprotic solvent, acetonitrile, both the excitation energies behaved in the same way as in water and methanol for the shorter chain length (π-π^*: less than n = 4; n-π^*: less than n = 5), while the π-π^* excitation energy increased and the n-π^* excitation energy decreased by solvation for the longer chain lengths (π-π^*: n = 4 and more; n-π^*: n = 5 and more). The change in excitation energy can be well explained by the change in orbital energy due to the solvation (and associated hydrogen bonds).

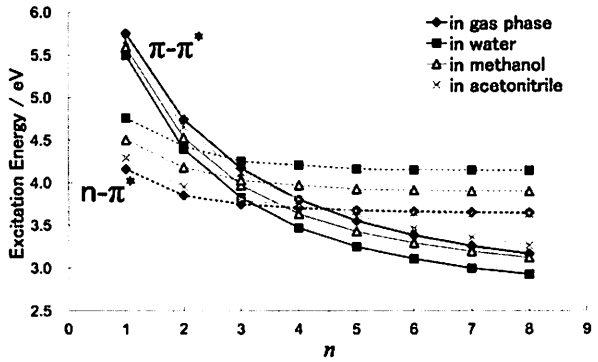

Fig. 2 π-π^* and n-π^* excitation energies of SPMC

2PB02 Salt Effect on Hydration Water in Protein Aqueous Solutions Studied by Terahertz Time-Domain Spectroscopy

K. Aoki[1], K. Shiraki[2], and T. Hattori[1]

[1] *Institute of Applied Physics, University of Tsukuba, Tsukuba 305-8573, Japan*

[2] *Faculty of Applied Sciences, University of Tsukuba, Tsukuba 305-8573, Japan*

e-mail : hattori@bk.tsukuba.ac.jp

Solubility of protein in aqueous solutions changes by addition of salts. Understanding of the molecular mechanism of the solubility change is an important issue in biology and pharmaceutics. Terahertz spectroscopy is unique in its ability of observing the picosecond to subpicosecond dynamics of water molecules in the hydration layer. In protein aqueous solution, motion of hydration water molecules on the protein surface slows down and the absorption coefficient in terahertz region decreases compared with that of bulk water. Here, we investigated the states of hydration water on the protein surface using terahertz time-domain spectroscopy (THz-TDS). We used hen egg white lysozyme (HEWL) as a model protein, and studied the effect of salt on the THz absorption by adding ammonium sulfate (AS) and ammonium thiocyanate (AT) to the solution.

Sample solutions were prepared by mixing 267-mg/mL HEWL stock solutions and AT or AS aqueous solutions; the final concentration of the HEWL was 200 mg/mL. Salt concentration was changed in the range where no precipitation took place.

Figure 1 shows absorption coefficient of HEWL and HEWL-salt-mixture solutions subtracted by that of water and the salt solution contained in these solutions. Black line shows the spectrum of HEWL aqueous solution, which confirms that motion of the hydration water of HEWL is slower than that of bulk water. AS increases the absorption coefficient, which indicates that the motion of the hydration water becomes faster and/or that the hydration number of HEWL (the number of hydration water molecules for a HEWL molecule) is reduced. AT decreases the absorption coefficient, which indicates that the motion of the hydration water slows down and/or that the hydration number of HEWL increases. These results are consistent with a hydration model [1], and suggest that hydration water at a protein surface is of great importance for protein solubility.

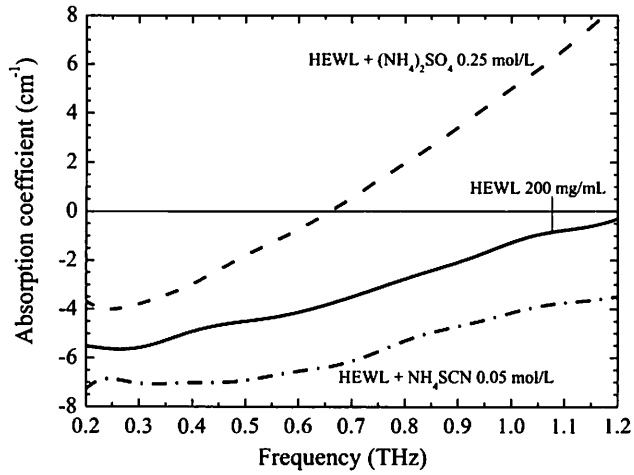

FIG. 1. Difference of absorption coefficient of HEWL-salt mixture solutions from solution baseline; with no salt (solid line), AS (dashed line), AT (dashed-dotted line).

References

[1] K. D. Collins, Methods **34**, 300 (2004).

2PB03 The effect of the solvent pre-orientation in the ground state for the photoinduced electron transfer in ionic liquids.

M. Muramatsu[1], S. Morishima[1], T. Katayama[1,2], S. Ito[1], Y. Nagasawa[1,2], H. Miyasaka[1]

[1]*Department of Chemistry, Osaka University, Osaka 560-8531, Japan*

[2]*JST-PRESTO*

e-mail : muramatsu@laser.chem.es.osaka-u.ac.jp

Room temperature ionic liquid (IL) is a molten organic salt at room temperature. Its peculiar properties, such as high ionic conductivity, nearly zero vapor pressure, and high viscosity, have been attracting much attention. We have been studying photoinduced intramolecular charge transfer (CT) reaction of 9,9'-bianthryl (BA) in imidazolium ILs and proposed that the CT reaction of BA can be explained by a multi-dimensional reaction coordinate model; the fast CT reaction is induced by the ultrafast local dynamics of IL, while the produced CT state is stabilized slowly by the reorganization of larger scale structure of IL[1, 2]. In the present work, we have investigated the photoinduced CT and solvation processes of asymmetric solutes, 4-(9-anthryl)-*N,N*-dimethylaniline (ADMA) and Coumarin 153 (C153), in ILs (fig. 1) by means of time resolved fluorescence measurements, so as to elucidate the role of pre-oriented solvent molecules on solvation dynamics.

Fig. 2 shows time profiles of the fluorescence maximum of ADMA and BA (dynamic Stokes shift: DSS). In $DemeBF_4$ (Fig. 2 (a)), DSS time profiles for ADMA and BA show similar dynamics in 0.03-100 ns region, while remarkable difference was observed in subpicosecond time region. Similar dynamic behaviors as Fig. 2 (a) were confirmed in most of ILs except for PhosTFSI, where the solvation dynamics of BA is slightly slower even in the >0.03 ns regions and no ultrafast solvation process was observed as shown in Fig. 2 (b). From these dynamic behaviors, we will discuss the hierarchical solvation process in IL and the role of the rapid motion of IL for the CT reaction.

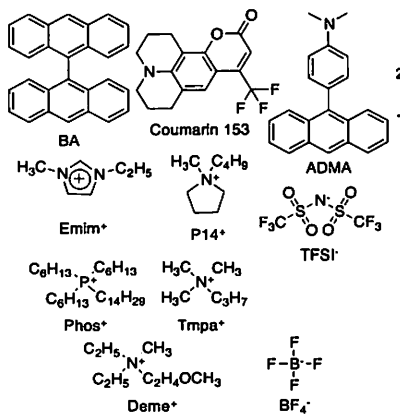

Fig. 1 Molecular structures of solutes and ionic liquids

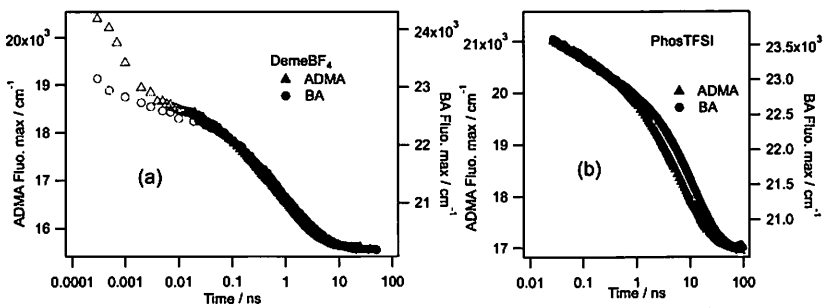

Fig. 2 Time dependence of the fluorescence peak wavenumber for ADMA (triangle) and BA (circle) in $DemeBF_4$(a) and PhosTFSI(b). Solid marks are the data points by the time correlated single photon counting method and open points are obtained by the femtosecond transient absorption measurement.

References

[1] Y. Nagasawa et al., *J. Phys. Chem. B.* **112**, 15758(2008).

[2] Y. Nagasawa, and M. Muramatsu et al., *J. Phys. Chem. C.* **113**, 11868(2009).

2PB04 Spectroscopic and computational investigation of a structure of a new isomer of salinomycin

Radosław Pankiewicz

Faculty of Chemistry, Adam Mickiewicz University in Poznań, Umultowska 89b, PL-61-614 Poznań, Poland

e-mail: radek@px.pl

Polyether ionophores make a wide class of natural and synthetic compounds. They are used to control ketosis and bloat in cattle and are applied as growth promoting feed additives. The main feature of this group is the ability to complex ions and transport them through the natural and synthetic membranes. Ionophores are host molecules that bind ionic guests and transport them across a membrane such as a bulk organic phase or a phospholipid bilayer. They can transport and hence regulate the concentrations of the main biological cations such as Li^+, Na^+, K^+, Ca^{2+} [1,2], heavy metal cations Pb^{2+}, Cd^{2+} and some anions (Cl^-) or neutral molecules (NH_3).

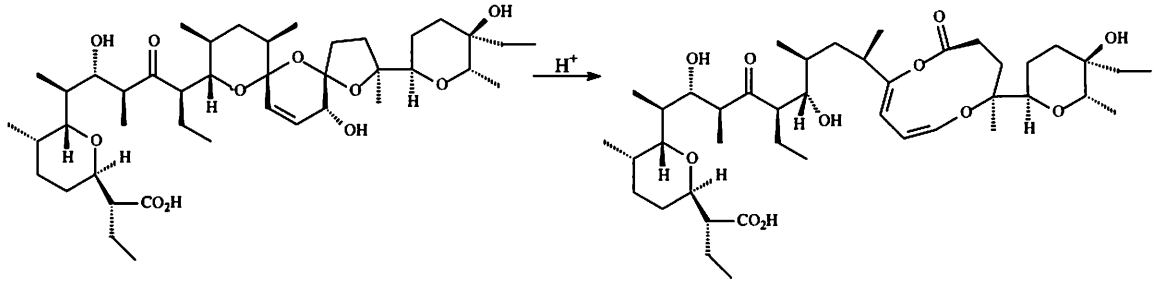

A new derivative of polyether ionophore salinomycin was obtained as a result of a rearrangement catalysed by sulphuric acid in two-phase medium of water/methylene chloride solution. The new isomer was fully characterized by multinuclear 2D NMR, NOESY and MALDI-TOF. To obtain full assignments of ^1H and ^{13}C, the 2D NMR techniques, ^1H–^1H COSY, ^1H–^{13}C HSQC and ^1H–^{13}C HMBC were used. The properties of the new compound were additionally study by semiempirical (PM5) and *ab-initio* DFT (B3LYP) methods. A potential mechanism of the rearrangement was also proposed [3].

The author thanks the Polish Ministry of Science and Higher Education for financial support under Grants No. NN 204 338237 in the years 2009–2013.

References

[1] P. Malfreyt, Y. Pascal, J. Juillard, *J. Chem. Soc. Perkin Trans.*, **2** 2031(1994).

[2] R. Pankiewicz, G. Schroeder, B. Gierczyk, G. Wojciechowski, B. Brzezinski, F. Bartl, G. Zundel, *Biopolymers:Biospectroscopy*, **62**, 173(2001).

[3] R. Pankiewicz, *unpublished results* (2013).

2PB05 Solvent Re-orientation Dynamics of Benzophenone-Water Clusters on Triplet State Potential Energy Surface

H. Tachikawa

Division of Materials Chemistry, Graduate School of Engineering, Hokkaido University, Sapporo 060-8628, Japan

e-mail : hiroto@eng.hokudai.ac.jp

Solvation is the most important initial process in chemical reaction and it sometimes affects strongly the reaction path and mechanism. Therefore, a lot of investigations of the effects of solvent and solvation on the reactions have been carried out from experimental and theoretical points of view. The solvation process is strongly dependent on the electronic state of solute. However, its nature is still unclear. It is known that an absorption spectrum of molecules with a C=O carbonyl is affected by solvent effect. For example, benzophenone (Bp) has two typical excited states (two typical absorption peaks) corresponding to $n\pi^*$ (S_1) and $\pi\pi^*$ (S_2) transitions from the ground state (S_0). It is known that the $n\pi^*$ and $\pi\pi^*$ excitation bands are shifted to be blue and red regions by the polar solvent, respectively. Also, benzophenone has another important point in which quantum yield to form triplet state (i.e. efficiency of $S_1 \rightarrow T_1$ intersystem crossing) is close to 1.0. The T_1 state is consisted of $^3(n\pi^*)$ in Bp. The structure of fluorenone (Fl) is very similar to that of Bp, but the T_1 state of Fl is consisted of $^3(\pi\pi^*)$ state. Therefore, one can obtain the solvation dynamics dependent on the electronic states by comparing the solvation process of Bp with that of Fl.

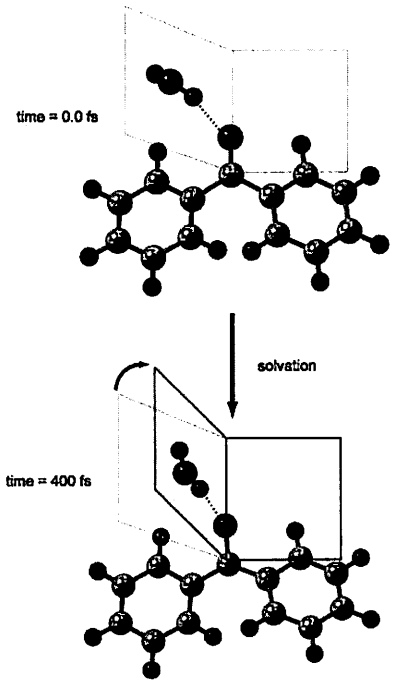

Figure 1. Snapshots of $Bp(H_2O)$ on the T_1 state calculated by means of direct ab-initio MD method.

In the present study, solvation dynamics of triplet state of $Bp\text{-}H_2O$ clusters following the electronic excitation of neutral to the triplet state by means of direct ab-initio MD method [1,2] to elucidate a possibility of real time solvation dynamics. The direct AIMD calculation showed that the structure of $Bp\text{-}H_2O$ is drastically varies as a function of time following the electronic excitation from S_0 to T_1 state. Snapshots of $Bp\text{-}H_2O$ are illustrated in Figure 1. The position of H_2O relative to the C=O carbonyl was drastically changed as a function of time. At time zero, the H_2O molecule orients to the n-orbital of C=O, whereas the structure is changed to π^*-orientation form at 400 fs.

References

[1] H. Tachikawa, T. Iyama, Phys. Chem. Chem. Phys., 4, 5806-5812 (2002).

[2] H. Tachikawa, T. Iyama , K. Kato, Phys. Chem. Chem. Phys., 11, 6008-6014 (2009).

2PB06 Study of Electron Transition for the liquid benzene and mono-substituted benzenes by using far-ultraviolet spectroscopy and quantum chemical calculations

Y. Uematsu[1], M. Yasunaga[1], Y. Morisawa[2] and Y. Ozaki[1]

[1]*Department of Chemistry, Kwansei Gakuin University, Gakuen, Sanda, Hyogo, Japan*

[2]*Department of Chemistry, Kinki University, Kowakae, Higashiosaka, Osaka, Japan*

e-mail : yuuki3105@kwansei.ac.jp

【Introduction】 Absorbance coefficients of benzene and its derivatives are so strong that only far-ultraviolet spectra in the gas phase had been measured. These spectra in the liquid phase can be measured easily by using attenuated total reflection for the far-ultraviolet region (ATR-FUV) spectrometer that was developed by our group. One can get information about molecular interaction of liquids by comparing FUV spectra between gases and liquids. In this study, we measured FUV spectra of pure liquids and cyclohexane solutions of benzene and mono-substituted benzenes. In addition, we tried to assign peaks of a FUV spectrum of liquid benzene by using quantum chemical calculations taking into account molecular interaction.

【Experiment】 We prepared pure liquids and some cyclohexane solutions of benzene and eight types of mono-substituted benzenes, and we measured their FUV spectra by using the ATR-FUV spectrometer. Moreover, we applied Kramers-Kroning transformation to observed spectra, and calculated absorption indexes (κ). In quantum chemical calculations, we optimized molecular configuration in B3LYP/cc-pVTZ level, and calculated electron transition by TD-CAM-B3LYP method. All calculations were carried out by Gaussian 09.

【Result】 We observed four peaks (160, 180, 200, 260 nm) in a FUV spectrum of a pure liquid of benzene. Three peaks of them (180, 200, 260 nm) are due to $\pi \rightarrow \pi^*$ (HOMO→LUMO) transitions, and they were also observed in a gas spectrum. A peak which was observed at about 160 nm is not observed in the gas spectrum. According to chemical calculations, we suggest this peak is due to HOMO-1→LUMO transition.

Next, we compared FUV spectra of liquids of mono-substituted benzenes. In this study, we focused on the intensity ratio of peaks at about 180nm and 200nm (180nm/200nm). In the result, we could divide nine samples into two groups (Fig.1). One group, the intensity ratio decreases as sample's concentration increases. However, the other group, the intensity ratio doesn't decrease as sample's concentration increases. We discussed the reason that why the intensity ratio changes as sample's concentration changes.

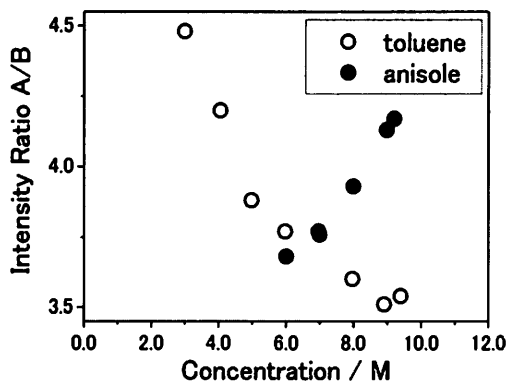

Figure1. Intensity ratio of toluene solutions and anisole solutions

2PB07 Structures and Electronic States of Benzophenone-Water Clusters

T. Iyama and H. Tachikawa

Division of Materials Chemistry, Graduate School of Engineering, Hokkaido University, Sapporo 060-8628, Japan

e-mail : ulmus.davidiana@gmail.com

The C=O carbonyl compounds are widely used for organic-semiconductor, molecular devices, electroluminescence (EL) and photoconductivity, photoredist materiasl. For example, polymethyl-metacrilate (PMMA) and poly-vinyl (benzophenone) are utilized for photo- resist and photo-sensitive polymers. In these compounds, the photo-absorption efficiency is strongly affected by impurity doped to the carbonyl compounds. This is due to the fact that the impurity changes strongly the excitation energy of the carbonyl compounds. The most typical impurity in the organic semi-conductor is a residual water in the system. Therefore, studying the effects of the residual water on the excitation energy of the carbonyl compounds is an important theme in the technology of organic semi-conductor.

In the present study, the structure and electronic states of benzophenone (Bp) and benzophenone-water clusters $Bp(H_2O)_n$ (n=1-8) are investigated by means of hybrid-density functional theory (DFT) methods in order to shed light on the effect of water molecules on the structures and electronic states of carbonyl compounds. We focus our attention mainly on the effect of water molecules on the excitation energies of Bp.

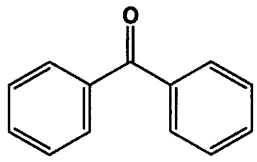

Benzophenone

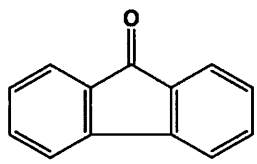

Fluorenone

The structures of Bp and $Bp(H_2O)_n$ (n=1-8) were fully optimized at the B3LYP/6-311G(d,p) level of theory. The excitation energies are calculated by means of time-dependent DFT (TD-DFT) calculation using the optimized structures obtained by several levels. For comparison, the fluorenone and water clusters $Fl(H_2O)_n$ (n=1-8) were investigated with the same manner. The structure of Fl is very similar to that of Bp, but the T_1 state of Fl is consisted of $^3(\pi\pi^*)$ state.

Structures and excitation energies of benzophenone-water complexes $Bp(H_2O)_n$ (n=1-8) have been investigated by means of density functional theory (DFT) calculations at the B3LYP/6-311++G(d,p) level. Solvation energy of H_2O to Bp (per one water molecule) is 6.1 kcal/mol in BpH_2O 1:1 complex. The solvation energy of $n\pi^*$ transition of Bp was blue-shifted by the solvation, whereas the excitation energy of the $\pi\pi^*$ transition was red-shifted. The excitation energy of $n\pi^*$ transition was saturated in n=4-5. The electronic states of $Bp(H_2O)n$ were discussed on the basis of theoretical results.

References

[1] H. Tachikawa, T. Iyama, *Phys. Chem. Chem. Phys.*, **4**, 5806-5812 (2002).

[2] H. Tachikawa, T. Iyama ,K. Kato, *Phys. Chem. Chem. Phys.*, **11**, 6008-6014 (2009).

2PB08 Effect of the Coexisting Anions on the Decomposition Rate of Silver(II) Macrocyclic Complexes

S. Ichimura[1], M. Matsushita[1], R. Yamamoto[1], E. Kikuta[1], K. Tomono[2], and K. Miyamura[1]

[1]*Department of Chemistry, Tokyo University of Science, Tokyo 162-8601, Japan*
[2]*Department of Chemical and Biological Engineering Ube National College of Technology, Yamaguchi 755-0097, Japan*
e-mail : jb112702@ed.tus.ac.jp

The macrocyclic ligands such as *cyclam* (1,4,8,11-tetraazacyclotetradecane) provide ideal coordination site and form stable complexes with various metal ions. Ag(I) ion induces disproportionation reaction in the presence of macrocyclic ligand, resulting in isolation of silver mirror and Ag(II) complex[1]. We succeeded in isolating Ag(II)LX (**L** : *C*-meso-1,5,8,12-tetramethyl-1,4,8,11-tetraazacyclotetradecane) complex salts **1-4** (**1** X=ClO_4^-, **2** X = NO_3^-, **3** X=Cl^- , **4** X=Br^-). Although these Ag(II)**L** complexes are known to be decomposed in aqueous solution by irradiation of visible light, but the detailed behaviour of the complex is not clarified yet. The purpose of this study, therefore, is to investigate the characterization of these complexs and the effect of the counter anions on the decomposition rate.

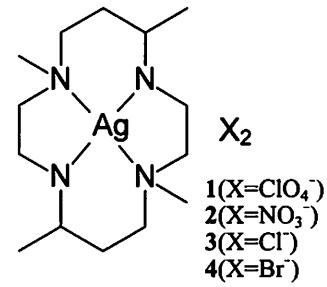

Fig.1 Ag(II)LX complex salts

When the Ag(II)**L** macrocyclic complexes is irradiated by UV-vis, decreasing of the peak at ca. 350nm due to the decomposition of the complex took place in aqueous solution of **1-4**. The rate of decomposition was in the order of **1** < **2** < **3** < **4**, especially in the case of **4**, the decomposition proceeded rapidly after a certain period of time(Fig. 2). These results could be explained as follows. First, Ag(II)**L** is decomposed into Ag(I) ion and **L** in aqueous solution by visible light. The ligand **L** may be subject to oxidation. Then, the oxidised macrocyclic ligand reacts with Ag(I) to reform Ag(II) complex together with Ag^0 by disproportionation. In the case of **4**, AgBr easily precipitated and removed from the solution. Thus, the regeneration of Ag(II) complex is depressed in **4**.

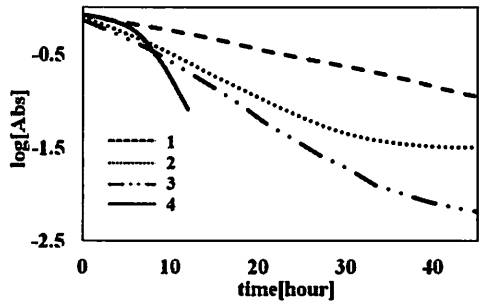

Fig.2 Time course of absorbance

References

[1] I. J. Clark and Mac B. Harrowfield, *Inorg. Chem. 23*, 3740(1984).

2PB09 Effect of Specific Interaction on Carbonyl Vibrational Dynamics of the Excited State 4-Aminopthalimide

M. Kondo, K. Ohta and K. Tominaga

Molecular Photoscience Research Centre, Kobe University, Kobe 657-8501, Japan

e-mail : mkondo@sapphire.kobe-u.ac.jp

4-Aminopthalimide (4-AP, Fig.1) is one of well-known fluorescence probe molecules because it shows the large fluorescence quantum yield and the electronic spectra sensitively depend on solvent polarity. Therefore, 4-AP has been used to study the solvation and rotational dynamics in complex media such as ionic liquids and confined liquids as well as pure solvents [1]. 4-AP contains both electron donor and accepter moiety in the structure, forming the hydrogen bonds with various solvent molecules in polar solvents. The photophysical properties of 4-AP studied previously and concluded that the formation of hydrogen bonding complex between 4-AP and solvents stabilized the excited state 4-AP leading the significantly large electronic spectral shift deviating from Lipperd-Mataga polarity $f(\varepsilon, n^2)$ and the quenching of fluorescence lifetimes [1-3]. In our current study, the steady state symmetric and anti-symmetric C=O stretching modes, appearing at about 1750 and 1700-1730 cm^{-1}, respectively, were measured in both aprotic and protic solvents. Both modes showed large solvent dependent spectral shift. The C=O vibrational dynamics of the excited state 4-AP were studied using sub-picosecond visible-pump IR-probe spectroscopy. In addition, the steady state and excited state C=O vibrational dynamics of 4-amino-N-methylpthalimide (4-AMP) was studied and compared to those of 4-AP. In 4-AMP the hydrogen of imide group was replaced by methyl group and the formation of hydrogen bonding between imide group and solvent molecules was inhibited. DFT and TDDFT calculations performed for electronic structure and infrared modes in the ground state and the excited state 4-AP molecule, respectively.

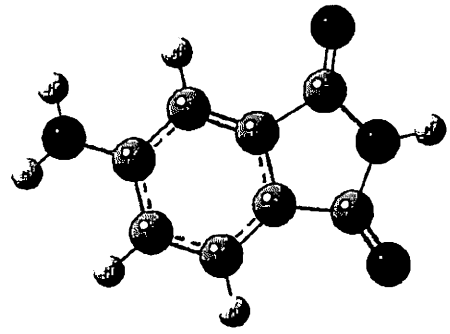

Fig. 1 4-Aminopthalimide

References

[1] C. F. Chapman, and M. Maroncelli, J Chem. Phys. B. **95** (1991) 9095.

[2] E. Krystkowiak, K. Dobek, and A. Maciejewski, J Photochem Photobiol A **184** (2006) 250.

[3] M. Sajadi, T. Obernnhuber, S. A. Kovalenko, M. Mosquera, B. Dick, and N. P. Ernsting J Chem. Phys. A. 113 (2009) 44.

2PB10 Weak, weaker, weakest ammonia: journey from ambient to supercritical region

Vivek Kumar Yadav[1], and Amalendu Chandra[1]

[1]*Department of Chemistry, Indian Institute of Technology Kanpur,208016 India*
e-mail: viveky@iitk.ac.in

We present a first principles molecular dynamics study of vibrational spectral diffusion and hydrogen bond dynamics in deuterated ammonia without using any empirical potential at ambient and supercritical region. The calculations are based on ab initio molecular dynamics simulations [1,2] for the generation of trajectories and for frequency calculations, time series analysis [3] is employed by using wavelet method. In ammonia although one-to-one relation does not exist between the instantaneous frequency of an ND bond and the distance of its associated hydrogen bond but this relation hold on average. By frequency-time correlation and spectral hole dynamics calculations, the dynamics of the spectral diffusion has been investigated at molecular level. We have also used the dispersion correction functional (BLYP-D) proposed by Grimme [4] in our simulations and compared it with our results having no dispersion corrections (BLYP) for both ambient as well as for supercritical ammonia. The details of the time constants of frequency correlations [5] and spectral shifts are found to be depend on the frequencies of chosen ND bonds and are analyzed in terms of the dynamics of hydrogen bonds of varying strengths and also for free non-hydrogen bonded ND groups. In supercritical ammonia, there exists interplay between the dynamics of hydrogen bonds, dangling ND groups, and the inertial rotation of the ND bonds that determines the time scales of spectral diffusion in a subtle manner.

References

[1] R. Car and M. Parrinello, *Phys. Rev. Lett.* **55,** 2471(1985).

[2] J. Hutter, A. Alavi, T. Deutsch, M. Bernasconi, S. Goedecker, D. Marx, M. Tuckerman, and M. Parrinello, CPMD Program, MPI für Festkörperforschung and IBM Zurich Research Laboratory.

[3] L. V. Vela-Arevalo, and S. Wiggins, *Int. J. Bifurcation Chaos Appl. Sci. Eng.* **11**,1359 (2001).

[4] S. Grimme, *J. Comput. Chem.* **25**, 1463(2004); *J. Comput. Chem.* **27**, 1787(2006); *Comp. Mol. Sci.*, **1**, 211(2011).

[5] B. S. Mallik, A. Semparithi, and A. Chandra, *J. Chem. Phys.* **129**, 194512(2008); *J. Phys. Chem. A* **112**, 5104 (2008).

2PD01 A quantum chemical study on hydration structure of Ra(II)

Aya Matsuda, Hirotoshi Mori

Department of Chemistry and Biochemistry, Ochanomizu University, Tokyo 112-8610, Japan.

E-mail: matsuda.aya@ocha.ac.jp

[Introduction] Radium (Ra) is the heaviest alkaline earth metal in the periodic table. Even Ra was found over 100 years ago [1], the hydration chemistry of Ra has not been still well known due to the danger associated with the experimental handling as well as the chemical instabilities of Ra isotopes. In this work, we have studied the hydration structure of Ra^{2+} using quantum chemical calculations and compared it with those of the other hydrated divalent alkaline earth (AE) metal ions.

[Methods] To investigate hydration structure of Ra^{2+}, we constructed both static and dynamic hydration models. For comparison, we also studied hydration structures of other AE divalent ions using the static solvation model.

In the static solvation model, we mainly focused on structures of the first solvation shell using $[AE(H_2O)_n]^{2+}$ (AE = Mg, Ca, Sr, Ba, and Ra; n = 1-9) aqua complex models. The effects from second or further solvation shells were taken into account through the conductor-like polarizable continuum (C-PCM) method. Geometry optimizations of the aqua complexes at the *ab initio* HF, MP2 and B3LYP levels of theory were performed. The solvation free energies, *i.e.* thermodynamic stabilities, were compared among AE^{2+} hydrates.

In the dynamic model, we focused on fluctuation of the aqua ligands using recently developed FMO-MD simulation [3], where FMO is abbreviation of fragment molecular orbital method for large-scale ab initio molecular orbital calculation. To simulate thermal fluctuation of the hydrated Ra^{2+}, we applied water droplet model confined within a sphere (radius = 9.0 Å). The coordinates of the central Ra^{2+} ion was kept fixed during the molecular dynamics simulation. The time step for FMO-MD was 1.0 fs, and the simulation temperature was kept to be 300 K using the Nosé–Hoover chains method. A 1 ps equilibration and a subsequent 2 ps production MD run were performed, and radial distribution function (RDF) of water molecules was statistically analyzed.

In both models mentioned above, we applied MCPdzp basis sets for AE [2]. For O and H, 6-31G** and 6-31G were used in the static and dynamic solvation models, respectively.

[Results] **1. Static Model** Increasing the number of water molecules (n), we could observe monotonic elongation of the AE-O bond length and a corresponding monotonic decrement of the AE-H_2O binding energy (per an AE-O bond) . As the he solvation free energies for n=6-9 gave similar values (-267.6, -267.5, -266.8, -265.1 kcal mol^{-1}), we concluded that that the hydration number of Ra^{2+} is in the range of 6-9. Thus, different from the lighter alkaline earth metal ions, Ra^{2+} does not have clear coordination number.

2.Dinamic Model Radial distribution functions (RDFs) of solvent water molecules around Ra^{2+} are shown in Fig. 1. The RDF peaks of Ra-H_{water} and Ra-O_{water} positions predicted by our FMO-MD simulations are 2.85 Å, 3.45 Å, respectively. The coordination number of water to Ra was computed to be *ca.* 8. The first peak of the RDF showed very broad feature (the width of the peak is 1.0 Å). This means that the structure of hydrated Ra^{2+} is very flexible.

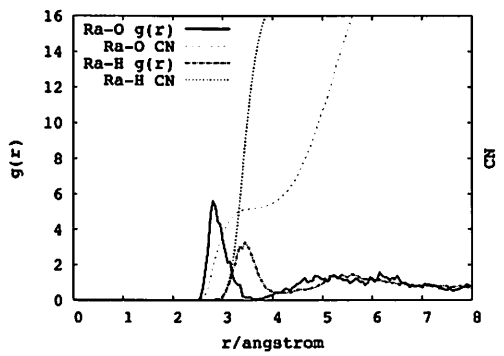

Fig. 1 Ra–O (Solid line) and Ra–H (Dashed line) RDF and their running integration numbers.

References [1] M. P. Curie *et al.*, *Comptes Rendus 127*, 175(1898) [2] Anjima, H. *et al.*, J. Comput. Chem. **28**, 2424. (2007) [3] Y. Komeiji *et al.*, *Chem. Phys. Lett.*, *372*, 342(2003)

Acknowledgment AM would acknowledge a fund for young scientist by Japan society for promotion of sciences (JSPS).

2PD02 Reusable Palladium Catalysts Derived from Ionic Liquids of Xanthines and Their Applications in Organic Synthesis

Fen-Tair Luo and Hung-Kun Lo

Institute of Chemistry, Academia Sinica
128, Sec. 2, Academia Rd., Nankang, Taipei 11529, Taiwan
e-mail: luoft@gate.sinica.edu.tw

Recently, we have reported the synthesis of a new and soluble polystyrene-supported palladium complex as an excellent and recyclable palladacycle catalyst for the carbon-carbon bond formation in Heck-Mizoroki, Suzuki-Miyaura, and Sonogashira reactions. In view of the NHC-metal complexes have been proved to be more effective in many catalytic reactions than phosphine-metal complexes, we developed a simple and highly efficient synthesis of bis-NHC-palladium catalyst derived from the ionic liquid of caffeine, one of the natural methylated xanthine, and its applications in Suzuki-Miyaura, Heck-Mizoroki, and Sonogashira cross-coupling reactions in aqueous solution with or without adding additives[1]. In order to support the development of sustainable chemistry and to apply the high recyclability and the development of polystyrene in organic synthesis, herein, we report another simple synthesis of polystyrene-supported bis-NHC-palladium catalyst derived from ionic liquid of theobromine, one appropriate natural methylated xanthine, in four steps and its applications in Suzuki-Miyaura reactions in water without adding other additives. Initially, the attempts to do the copolymerization of bis(1-allyl-3,7,9-trimethylxanthine-8-ylidene)palladium diiodide, obtained from the allylation of theobromine followed by the methylation and palladation with palladium acetate and sodium *t*-butoxide, with six equivalents of styrene with or without a catalytic amount of free radical initiator such as azobisisobutyronitrile (AIBN) or benzoyl peroxide in benzene, toluene, THF or DMF at 70 °C to 150 °C were all failed. We then turned our attention to the use of *p*-styrylmethylene group at the N1-position in theobromine. The copolymerization of six equivalents of styrene with bis(1-*p*-vinylbenzyl-3,7,9-trimethylxanthine-8-ylidene)palladium diiodide in the presence of a catalytic amount of AIBN at 150°C in DMF for 48 h could give the air-stable polystyrene-supported bis-NHC-palladium complex after repeatedly washed by the solvent of THF/*n*-hexane in a Soxhlet extraction apparatus. To test the applicabilities of palladium complexes in the carbon-carbon bond formation reactions, we examined the Suzuki-Miyaura cross-coupling reaction of phenylboronic acid with *p*- or *m*-bromotoluene and sodium *t*-butoxide or potassium carbonate as the base in the absence or presence of a catalytic amount of complex in water.

Reference

[1] F.-T. Luo, H.-K. Lo, *J. Organomet. Chem.* **696**, 1262(2011).

2PD03 Reduction Reaction of Copper(II) complex bearing 1,3-Di(pyridine-2-carboxaldimino)propane (pitn) by Decamethylferrocene in Acetonitrile

A. Yamada[1], Y. Watanabe[1], K. Noda[1], S. Itoh[1], N. Kishikawa[1], K. Ishihara[2], M. Inamo[3], R. M. Hassan[4] and H. D. Takagi[1]

[1] *Research Center for Materials Science, Nagoya University, Nagoya 464-8602 Japan;* [2] *Department of Chemistry, School of Science and Engineering, Waseda University, Tokyo 169-8555, Japan;* [5] *Department of Chemistry, Aichi University of Education, Kariya 448-8542, Japan;* [6] *Department of Chemistry, Faculty of Science, Assiut University, Assiut 71516, Egypt.*

email: h.d.takagi@nagoya-u.jp

Outer-sphere Gated electron transfer process is important in biological reactions involving some metalloenzymes. In Gated reaction systems, either the reaction of thermodynamically unfavoured direction is accelerated or the reaction of thermodynamically favoured direction is slowed down so as to control the concentration of metabolically important species in solution, by means of the conformational changes around the metal centers.

In this study, we report reduction reaction of Cu(II)-pitn by $Fe(Cp^*)_2$ in acetonitrile. Cu(II)-pitn has a distorted square planar structure with a small dihedral angle of 17.14° between the two planes having one Schiff-Base nitrogen and one pyridine ring.

The observed pseudo-first order rate constant exhibited saturation kinetics with increasing the excess concentration of $Fe(Cp^*)_2$. Detailed analyses revealed that the reaction was controlled by a structural change prior to the electron transfer step, rather than a Marcusian bimolecular electron transfer process preceded by the ion-pair (encounter complex) formation.

(1) Ion-pair formation followed by the electron transfer step.

$$Cu^{II}(pitn)^{2+} + Fe^{II}(cp^*)_2 \overset{K_{OS}}{\rightleftharpoons} \{Cu^{II}(pitn)^{2+}, Fe^{II}(cp^*)_2\}$$

$$\{Cu^{II}(pitn)^{2+}, Fe^{II}(cp^*)_2\} \xrightarrow{k_{ET}} \{Cu^{I}(pitn)^{+}, Fe^{III}(cp^*)_2^{+}\}$$

$$k_{obs} = \frac{k_{ET} K_{OS}[Fe^{II}(cp^*)_2]}{1 + K_{OS}[Fe^{II}(cp^*)_2]}$$

(2) Electron transfer reaction regulated by slow structural change

$$Cu^{II}(pitn)^{2+} \underset{k_{QO}}{\overset{k_{OQ}}{\rightleftharpoons}} Cu^{II}(pitn)^{2+*}$$

$$Cu^{II}(pitn)^{2+*} + Fe^{II}(Cp^*)_2 \xrightarrow{k_{B2}} Cu^{I}(pitn)^{+} + Fe^{III}(Cp^*)_2$$

$$k_{obs} = \frac{k_{B2} k_{OQ}[Fe(cp^*)_2]}{k_{QO} + k_{B2}[Fe(cp^*)_2]}$$

The rate constant for the structural change, k_{OQ}, was estimated as 275 ± 13 s^{-1} at 298K ($\Delta H^{\ddagger}$ = 33.3 ± 1.0 kJ mol^{-1}, $\Delta S^{\ddagger}$ = -86 ± 5 J mol^{-1} K^{-1}). The observed structural change is the fastest among the Gated reactions for CuN_4 complexes examined to date. The large k_{OQ} value was attributed to the relatively small energy requited for the twist(B_2 normal mode vibration) to the D_{2d} structure from the slightly distorted square planar structure in the ground state.

References

[1] Kaim, W.; Schwederski, B. In *Bioinorganic chemistry.*; *Inorganic Elements in the Chemistry of Life.*; Wiley: Chichester, 1994.

[2] Itoh, S.; Noda, K.; Yamane, R.; Kishikawa, N.; Takagi, H. D., *Inorg. Chem.*, **2007** *46*, 1419.

2PD04 Reaction mechanism of head-to-head pivalamidato-bridged Pt(III) binuclear complex having equatorial bromide ligand with acetone

Masatoshi Kishi,[1] Yu Kuraishi, [1] Koji Ishihara, [1] and Kazuko Matsumoto [2]

[1]*Department of Chemistry and Biochemistry, Advanced School of Science and Engineering, Waseda University,* [2]*NanoCarbon Research Institute, Ltd., Asama Research Extension Center (AREC), Faculty of Textile Science & Technology Shinshu University, 3-15-1 Tokida, Ueda, Nagano 386-8567 Japan* e-mail: ishi3719@waseda.jp

Head-to-head (HH) Pt^{III} binuclear complexes $[(L)Pt(NH_3)_2(\mu\text{-amidato})_2Pt(NH_3)_2(L)]^{n+}$ (amidato = α-pyridonato, α-pyrrolidonato, and pivalamidato, L = NO_3^-, NO_2^-, H_2O, Cl^-, Br^-) have two non-equivalent Pt atoms. One is coordinated by two ammine nitrogen and two amidate oxygen atoms ($Pt(N_2O_2)$), and the other is coordinated by two ammine and two amidate nitrogen atoms ($Pt(N_4)$), which are connected by a Pt-Pt bond. These complexes act as catalysts in the oxidation reactions of olefins to aldehydes, ketones, epoxides, and α,β-diols.[1] In a series of study on the reaction mechanism of amidato-bridged Pt^{III} binuclear complexes with organic compounds, we have reported mechanisms of the reactions with olefins,[2] phenol,[3] isoprene,[4] and acetone[5] in acidic aqueous solution.

In this study, we report reaction mechanisms of HH pivalamidato-bridged Pt(III) binuclear complexes having equatorial bromide ligand (**1** and **2**) with acetone in acidic aqueous solution.

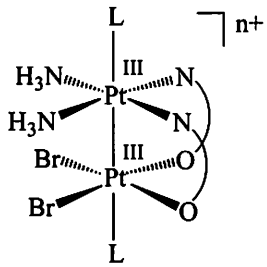

Head-to-Head

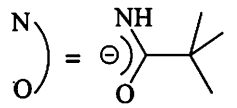

pivalamidate

L = H_2O (**1**) or Br^- (**2**)

In the consecutive reaction of complex (**1**), enol-acetone coordinates to the $Pt(Br_2O_2)$ to form π-complex, then the π-complex transforms to σ-complex (acetonyl Pt^{III} binuclear complex), whereas in the consecutive reaction of complex (**2**), fast enol-acetone coordination to the $Pt(N_4)$ is followed by the rate-determining enol-acetone coordination to the $Pt(Br_2O_2)$, then π–σ bond conversion on $Pt(Br_2O_2)$ and release of π-coordinated acetone from the $Pt(N_4)$ occur.

References

[1] K. Matsumoto, K. Sakai, *Adv. Inorg. Chem.*, **49**, 375–427 (1999).

[2] N. Saeki, N. Nakamura, T. Ishibashi, M. Arime, H. Sekiya, K. Ishihara, K. Matsumoto, *J. Am. Chem. Soc.*, **125**, 3605–3616 (2003); M. Arime, K. Ishihara, K. Matsumoto, *Inorg. Chem.*, **43**, 309–316 (2004).

[3] S. Hyodo, M. Kishi, H. Fukushima, S. Iwatsuki, K. Ishihara, K. Matsumoto, *Eur. J. Inorg. Chem.*, 5571–5577 (2012).

[4] J. Nagashima, K. Shimazaki, H. Sekiya, S. Iwatsuki, K. Ishihara, K. Matsumoto, *Dalton Trans.*, **40**, 6998–7007 (2011).

[5] H. Fukushima, H. Mori, M. Arime, S. Iwatsuki, K. Ishihara, K. Matsumoto, *Eur. J. Inorg. Chem.*, 1930–1936 (2011).

2PD05 Study of Multi-Equilibria in Protein by pH Titration - Drug and Metal Binding in Human Serum Albumin -

M. Kamei, T. Katsuno, R. Takeuchi, Y. Miyai, T. Kiwada, K. Ogawa, and A. Odani

[1] *Division of Pharmaceutical Sciences, Graduate School of Medical Sciences, Kanazawa University, Kakuma, Kanazawa, 920-1192, Japan*

e-mail : odani@p.kanazawa-u.ac.jp

Multi-equilibra in protein such as metal/drug binding to protein could be written as pM + q(protein) + r(drug) + sH <=> (M)p(protein)q(drug)rHs $\beta_{pqrs} = [(M)_p(protein)_q(drug)_rH_s] / [M]^p[protein]^q[drug]^r[H]^s$, though H^+ term has been ignored and the constant is conditional. The H^+ number s in human serum albumin (HSA)-Hs system were determined from pH titration data (25°C, I=0.1(KCl)) since HSA-drug interaction is important for evaluation of drug efficiency. Resultant s were not 1 by 1 and separated by 2 - 5. In a big molecule HSA there may be multi-equilibria. Finally we obtained only one set of s and overall stability constants involving with H^+ β_{010s} values.

The advantages of using β_{pqrs} are 1) physical equilibrium constant, 2) simple expression in multi-equilibra including metal coordination and non-covalent interaction with drug. pH titration analysis for HSA-salicylate-H system revealed non-covalent adducts (up to 3 salicylate) of HSA-salicyalte-Hs where salicylate is $C_6H_4(OH)(COO^-)$. The species distributions evaluated from β_{pqrs} values showed pH and concentration dependences. In the human serum condition of HSA : 0.6 mM and pH : 7.4, the [salicylate] dependence showed 1 and 2 salicylate adducts from the low [salicylate]. Two salicylate binding sites in HSA were estimated because two salicylate adduct formation were observed in the crystal structure of HSA-2salicyalte adduct [1]. The salicylate adduct populations also suggested the assignment of 1st and 2nd binding salicyaltes from pH dependences.

The concomitant formation of 1 and 2 adducts was observed in antimicrobial newquinolone drug Ciprofloxacine, which contains COO^- and C=O while COO^- and OH (phenol) in salicylate. This indicated HSA served same binding sites for salicylate and Ciprofloxacine.

pH titration method extended to ternary systems. The Cu(II)-HSA-salicylate-H system revealed (1) Cu coordination to HSA with deprotonation of $2H^+$, (2) non-covalent adducts of HSA-salicyalte and (Cu-albumin)-salicylate, where anti-inflammatory drug Cu-salicylate complex became broken and ternary Cu-albumin-salicylate-Hs complexes were major species, as estimated from spectral study [2], because the Cu(II) at N-terminal site of HSA assisted the salicylate binding. This is a first finding in metal-drug interaction on albumin and such interactions are not studied quantitatively by authentic methods such as dialysis, fluorescence probe, etc. Other examples will be discussed. Thus, β_{pqrs} evaluated by pH titration could serve valuable information and pH method would play an important role in the multi-equilibrium study of protein-drug interactions.

References

[1] L. Zhu, F. Yang, L. Chen, E. J. Meehan, M. Huang, J. Struct. Biol., **162**, 40-49 (2008).

[2] F. T. Greenaway, J. J. hahn, N. Xi, J. R. Sorenson, Biometals, **11**, 21-26(1998).

2PD06 Syntheses, Crystal Structures and Ligand Field Properties of Iron(II) Complexes with PNP Ligands: Origin of Large Ligand Field by Phosphorous Donor Atom

T. Mabe[1], H. Yamaguchi[1], M. Fujiki[1], K. Noda[1], K. Ishihara[2], M. Inamo[3], R. M. Hassan[4], S. Iwatsuki[5], T. Suzuki[6*], and H. D. Takagi[1*]

[1]*Research Center for Materials Science, Nagoya University, Nagoya 464-8602;* [2]*School of Science and Engineering, Waseda University, Tokyo 169-8555 Japan;* [3]*Department of Chemistry, Aichi University of Education, Kariya, 448-8542 Japan;* [4]*Department of Chemistry, Assiut University, Assiut, 71516 Egypt;* [5]*Department of Chemistry, Konan University, Kobe, 658-8501 Japan; and* [6]*Department of Chemistry, Okayama University, Okayama, 700-8530 Japan* E-mail: h.d.takagi@nagoya-u.jp

New iron(II) complexes with two tridentate hybrid ligands having phosphorous and nitrogen donor atoms were synthesized, to quantitatively estimate the difference of the ligand-field strengths of phosphorous and nitrogen donor sites in cationic metal complexes. Iron(II) complexes with bis(dimethylphosphinoethyl)amine (PNP) and 2,6-bis(diphenylphosphinomethyl)pyridine (PpyP) ligands crystallized as *ufac*-$[Fe(PNP)_2](PF_6)_2 \cdot CH_3NO_2$ and *mer*-$[Fe(PpyP)_2](CF_3SO_3)_2$, respectively, as expected from the steric congestion and from the tendency to avoid mutual *trans* influence between two phosphorous donor sites. Both complexes were in the low-spin electronic state up to 400K. The pseudo-D_{4h} coordination geometry of the PpyP complex made it possible to separate axial (2 x N) and equatorial (4 x P) contributions to the overall ligand-field by means of the spectrophotometric method in acetonitrile: the difference in the ligand-field strengths by the equatorial Ph_2P- donor sites and by the axial 2,6-disubstituted pyridine donor sites was ca. 13200 cm^{-1}. A significantly reduced inter-electronic repulsion parameter (425 cm^{-1} for both PNP and PpyP complexes) from the value of the free ion (1060 cm^{-1}) indicated covalent interaction between Fe(II) and P atoms.

Table– 10*Dq* and Racah *B* parameter for some Fe(II) complexes

Complex	$^1A_{1g} \rightarrow {}^1T_{1g}$ / cm^{-1}	$^1A_{1g} \rightarrow {}^1T_{2g}$ / cm^{-1}	10*Dq* / cm^{-1}	*B* / cm^{-1}
$[Fe(mmtp)_2]^{2+}$ a)	2.33 x 10^4	2.82 x 10^4	2.45 x 10^4	306
$[Fe(PNP)_2]^{2+}$ a)	2.15 x 10^4	2.83 x 10^4	2.32 x 10^4	425
$[Fe(tacn)_2]^{2+}$ b)	1.66 x 10^4	2.59 x 10^4	1.89 x 10^4	581
$[Fe(PpyP)_2]^{2+}$ b, c)	1.80x 10^4($^1A_1 \rightarrow {}^1E$)	2.70 x 10^4($^1A_1 \rightarrow {}^1B_2 + {}^1E$)	2.19 x 10^4	425

a) Measured in acetonitrile. b) Measured in H_2O. c) Three absorption bands corresponding to the $^1A_1 \rightarrow {}^1E$, $^1A_1 \rightarrow {}^1A_2$, and $^1A_1 \rightarrow {}^1T_2(O_h)$ [= $^1B_2 + {}^1E$ in D_{2d}] transitions were observed: another band corresponding to the $^1A_1 \rightarrow {}^1A_2$ transition was observed at 24600 cm^{-1}. mmtp stands for 1,1,1-(tris-dimethylphosphinomethyl)ethane, and tacn for 1,4,7-triazacyclononane.

References

[1] K. Kashiwabara, Y. Ozeki, M. Kita, J. Fujita, K. Nakajima, *Bull. Chem. Soc. Jpn.* **1995**, *68*, 3453–3457.

[2] S. Iwatsuki, S. Kashiwamura, K. Kashiwabara, T. Suzuki, H. D. Takagi, *J. Chem. Soc., Dalton Trans.* **2003**, 2280–2292.

2PD07 Relative kinetic reactivity of boronic acid and boronate ion towards 1,2-diols

A. Tanaka,[1] T. Okamoto,[1] T. Miyazaki,[1] S. Iwatsuki,[2] M. Inamo,[3] H. D. Takagi,[4] and K. Ishihara[1]

[1]*Department of Chemistry and Biochemistry, Advanced School of Science and Engineering, Waseda University, Tokyo 169-8555, Japan;* [2]*Department of Chemistry, Konan University, Kobe, 658-8501 Japan;* [3]*Department of Chemistry, Aichi University of Education, Kariya 448-8542, Japan;* [4]*Research Center for Materials Science, Nagoya University, Nagoya 464-8602 Japan* e-mail: ishi3719@waseda.jp

Boric acid ($B(OH)_3$) and boronic acid ($RB(OH)_2$, R = Ph, Me, etc.) react reversibly with bidentate ligands such as dicarboxylic acids, α-hydroxy carboxylic acids, 1,2-diols including sugars, etc. to form chelate complexes in aqueous solution. For this reason, a lot of boronic acid-based receptors and sensors for saccharides[1] have been reported in literature, however, a fundamental understanding of the complexation reaction of boronic acid, which provides a basis for the reception and sensing reactions, is lacking. For example, it has long been accepted that borate ($B(OH)_4^-$) and boronate ($RB(OH)_3^-$) ions are much more reactive towards bidentate ligands than their conjugate acids of borate and boronate ions.[2] However, the reactive species were not specifically identified; i.e. the rate constants of the borate and boronate ions were not directly measured, until recently in our previous studies,[3–6] in which we measured directly the reaction rate constants of boronate ions with several diprotonated bidentate ligands (H_2L), and concluded that the reactivity order was: $RB(OH)_2 > RB(OH)_3^-$.

In this study, we set up several reaction systems of boronic acids with monoprotonated bidentate ligands (HL^-) without proton ambiguity, on the basis of the results of our previous studies, and performed kinetic measurements for these systems in aqueous solution, in order to validate our recent conclusion mentioned above,[3–6] that is, to correct the widely accepted misunderstanding in kinetic reactivity of boronic acid.

References

[1] D. G. Hall, in Boronic Acids, 2nd ed., ed. D. G. Hall, Wiley-VCH, Weinheim, 2011, p. 23-25 and references cited therein.

[2] R. D. Pizer, C. A. Tihal, *Polyhedron*, **15**, 3411–3416 (1996) and references cited therein.

[3] S. Iwatsuki, S. Nakajima, M. Inamo, H. D. Takagi, K. Ishihara, *Inorg. Chem.*, **46**, 354–356 (2007).

[4] C. Miyamoto, K. Suzuki, S. Iwatsuki, M. Inamo, H. D. Takagi, K. Ishihara, *Inorg. Chem.*, **47**, 1417–1419 (2008).

[5] E. Watanabe, J. Fujii, K. Kojima, S. Iwatsuki, M. Inamo, H. D. Takagi, K. Ishihara, *Inorg. Chem. Commun.*, **13**, 1406–1409 (2010).

[6] E. Watanabe, C. Miyamoto, A. Tanaka, K. Iizuka, S. Iwatsuki, M. Inamo, H. D. Takagi, K. Ishihara, *Dalton Trans.*, in press.

2PD08 Synthesis and Characterization of Ionic Iridium Complexes for the Fabrication of Light-emitting Devices

C. D. Sunesh, M. Chandran, and Y. Choe*

Department of Polymer Science and Chemical Engineering, Pusan National University, Busan 609-735, South Korea

e-mail : suneshdamodar4@gmail.com

Recently, light-emitting electrochemical cells (LECs) containing ionic iridium complexes have been attracting a significant attention as electroluminescent devices which produce visible light at low operating voltages and have potential applications for display and lighting devices [1-3].For the purpose, two new cationic iridium complexes were synthesised using benzimidazole based ancillary ligand and were characterized by spectroscopical, electro-chemical and photophysical methods. LECs were fabricated based on the resulting complexes and their electrical properties were studied and compared. Furthermore, the electrical properties of the devices were studied by doping ionic liquid (IL), 1-butyl-3-methylimidazolium hexafluorophosphate ($BMIMPF_6$) into the light emitting layer.

References

[1] Q. Pei, G. Yu, C. Zhang, Y. Yang, A.J. Heeger, *Science* **269,** 1086(1995).

[2] J.K. Lee, D.S. Yoo, E.S. Handy, M.F. Rubner, *Appl. Phys. Lett.* **69,** 1686(1996).

[3] J.D. Slinker, A.A. Gorodetsky, M.S. Lowry, J.J. Wang, S. Parker, R. Rohl, S. Bernhard, G.G. Malliaras, *J. Am. Chem. Soc.* **126,** 2763(2004).

2PD09 Electroluminescent properties of LECs based on ionic transition metal complex using tetrazole-based ancillary ligand

Y. Kwon, J.Heo, and Y. Choe*

Department of Chemical Engineering, Pusan National University, Busan 609-735, South Korea

e-mail : dltmf3575@naver.com

Light-emitting electrochemical cells(LECs) are a promising type of electroluminescent device[1-2]. In this study, LECs based on ionic transition metal complex (iTMC) containing tetrazole based-ancillary were prepared and their electrical properties were investigated. Two new iridium(Ⅲ) complexes with tetrazole based ancillary ligands, namely, [Ir(ppy)2(tetrazole)]PF6 and [Ir(dfppy)2(tetrazole)]PF6 (ppy is 2-phenylpyridine, dfppy is 2-(2,4-difluorophenyl)pyridine, tetrazole is 5-bromo-2-(2-methyl-2H-tetrazol-5-yl)-pyridine and PF6 is hexafluorophosphate) have been synthesized and characterized. These synthesized complexes were used for the fabrication of LEC devices. Our work suggests that the light emission of cationic iridium complexes can easily tuned by substitutents on cyclometalated ligands. Moreover, through the addition of ionic liquids (ILs), we can get enhanced luminance of the devices.

References

[1] Q. Pei, G. Yu, C. Zhang, Y. Yang, A.J. Heeger, *Science* **269,** 1086(1995).

[2] J.D. Slinker, A.A. Gorodetsky, M.S. Lowry, J.J. Wang, S. Parker, R. Rohl, S. Bernhard, G.G. Malliaras, *J. Am. Chem. Soc.* **126,** 2763(2004).

2PD10 Selective complex formation of a deepened cavitand derivative towards copper and iron ions in acetonitrile – water binary solutions

Y. Li [1,2], Zs. Csók[2,3], G. Matisz[1,2], L. Kiss[1,2], L. Kollár[2,3], S. Kunsági-Máté [1,2]

[1] *Department of General and Physical Chemistry, University of Pécs,7624, Hungary;*
[2] *János Szentágothai Research Center, Ifjúság 20., 7624 Pécs, Hungary*
[3] *Department of Inorganic Chemistry, University of Pécs,7624, Hungary*
e-mail : kunsagi@gamma.ttk.pte.hu

Chemical sensor molecules, which possess both molecular recognition and fluorescent moieties, have received much attention due to their great significance in various fields such as analytical chemistry, biological research and environmental chemistry. The detection of transition metal ions is of particular importance. For instance, copper ions (Cu^{2+}) is one kind of major pollutants in water. Exposure to such kind of water will cause great health risks. It was reported that exposure to a high amount of copper ions (Cu^{2+}) can lead to gastrointestinal disturbance and damage of liver or kidney. As an essential element in biological system, iron is very famous for its responsibility of oxygen transportation and enzyme activity. Therefore, the detection of Cu^{2+} and Fe^{3+} is very meaningful in the field of biology and medicine.

Resorcin[4]arene and its derivatives are important host compounds in the field of molecular recognition. It is well known that these molecules are able to capture cations, anions and neutral species in their cavities. They have received remarkable attention due to their selectivity character. In our previous studies, it was found that their binding properties depend on several factors such as cavity shape [1,2], solvent effect [3] and flexibility of their skeleton [4].

In this work, in order to develop selective chemosensor for Cu^{2+} and Fe^{3+}, a novel resorcin[4]arene-based deepened cavitand was synthesized and characterized by NMR. Fluorescence emission spectra of this cavitand in the presence of Ni^{2+}, Hg^{2+}, Mn^{2+}, Cd^{2+}, La^{3+}, Cu^{2+}, Fe^{3+}, Cr^{3+}, Ag^{+}, Zn^{2+} and Co^{2+} in tetrahydrofuran / water binary solvent were recorded. Thermodynamic parameters were obtained by using van't Hoff theory. The results suggest that Cu^{2+} and Fe^{3+} can significantly quench the fluorescence emission intensity of the cavitand. Thermodynamic study shows that the interactions of Cu^{2+} and Fe^{3+} with the cavitand are both entropy-driven processes.

Acknowledgement: Financial support of the SROP-4.2.2.A-11/1/KONV-2012-0065 project is gratefully acknowledged.

References

[1] S. Kunsági-Máté, I. Bitter, A. Grün, G. Nagy, L. Kollár, *Anal. Chim. Acta.* **443**, 227 (2001).
[2] S. Kunsági-Máté, G. Nagy, P. Jurecka, L. Kollár, *Tetrahedron* **58**, 5119 (2002).
[3] S. Kunsági-Máté, I. Bitter, A. Grün, G. Nagy, L. Kollár, *Anal. Chim. Acta.* **461**, 273 (2002).
[4] S. Kunsági-Máté, Z. Csók, K. Iwata, E. Szász, L. Kollár, *J. Phys. Chem.* **B115**, 3339 (2011).

2PD11 Complex formation of hydrotropic *p*-toluene sulfonate with hydroxyacetophenone isomers

K. Szabó[1], P. Wang[2], B. Peles-Lemli[1], Y. Fang[2], L. Kollár[2,3], S. Kunsági-Máté[1,3]

[1] *Department of General and Physical Chemistry, University of Pécs, Ifjúság 6, Pécs, H-7624, Hungary*

[2] *Key Laboratory for Nano-Photonics and Nano-Structure, Capital Normal University,Xi San Huan Bei Lu 83, Beijing 100089, China*

[3] *Department of Inorganic Chemistry, University of Pécs, Ifjúság 6, Pécs, H-7624, Hungary*

[4] *János Szentágothai Research Center, Ifjúság u. 34., 7624 Pécs, Hungary*

e-mail : kunsagi@gamma.ttk.pte.hu

Compounds that cause increase of aqueous solubility are called hydrotropes, or chaotropes. The improvement of water-solubility by hydrotrope molecules is based on the molecular self-association of these materials and on the association of hydrotrope molecules with the solute.

According to our previous studies [1-3] on the interaction of aromatic species, in the present work we examine the effect of the electron density distribution of the aromatic rings on the molecular association between *para*-toluene sulfonate and different hydroxy-acetophenone derivatives [4]. The interaction between sodium *para*-toluene sulfonate (NaPTS) and hydroxyacetophenones (*o*- and *p*-HAPs) was investigated by photoluminescence (PL) methods. To clarify the role of molecular vibrations in the molecular association, Raman analyses were performed and the experimental results were compared to model calculations. The results show that there are characteristic peaks for the monomers and aggregates in the PL spectra during the aggregation process in case of sodium *para*-toluene sulfonate. The Gaussian deconvolution of the spectra showed that the aggregates have two different conformations which have different thermodynamic properties. The molecular interactions between the *para*-toluene sulfonate and hydroxyacetophenone molecules are preferably based on the interaction of aromatic moieties of the species. The strength of interaction is moderated by the site of hydroxy substitutent (*ortho*- or *para*-) of HAP molecules.

Acknowledgement: Financial supports of the TÉT-10-1-2011-0126 and the SROP-4.2.2.A-11/1/KONV-2012-0065 projects are acknowledged.

References

[1] S. Kunsági-Máté, K. Iwata, *Chem. Phys. Lett.*, **473**, 284 (2009)

[2] S. Kunsági-Máté, K. Szabó, B. Desbat, J.L. Bruneel, I. Bitter, L. Kollár, *J. Phys. Chem. B*, **111**, 7218 (2007)

[3] S. Kunsági-Máté, Z. Csók, K. Iwata, E. Szász, L. Kollár, *J. Phys. Chem. B*, **115**, 3339 (2011).

[4] K. Szabó, P. Wang, B. Peles-Lemli, Y. Fang, L. Kollár, S. Kunsági-Máté, *Colloid. Surface. A*, **422**, 143 (2013).

2PD12 Isomerization Reaction of Dinitrosyl-Molybdenum Complexes with 4,6-Dimethyl-2-mercaptopyrimidine

Y. Mashimo & T. Yonemura

Department of Applied Chemistry, Kochi University, Kochi 780-8520, Japan

e-mail: yonemura@cc.kochi-u.ac.jp

Nitric oxide (NO) has been identified as an important biological molecule, which has roles in neurotransmission, and in the immune responses to tumor cells and intracellular parasites. The regulation of NO in the creature has led to the NO-synthase or the controlled release of NO.

We report the characterization and the reaction of some dinitrosyl-molybdenum complexes with thiolate ligands. Now we investigate the syntheses and some properties of dinitrosyl-molybdenum $[Mo(L\text{-}N,S)_2(NO)_2]$-type complexes {L: 2-pyrimidinethiolate (pymt), 4-methyl-2-pyrimidinethiolate (mpymt), 4,6-dimethyl-2-pyrimidinethiolate (dmpymt)}. The pymt and mpymt complexes have trans(S,S) configuration, on the contrary, the dmpymt complexes has trans(N,S) one [1,2]. It is revealed that the structures are on the basis of their X-ray diffraction and IR absorption and ^{13}C NMR spectral data.

These complexes exhibited a remarkable time-course change under the room light, which decrease of the absorbance of the MLCT band in the UV-Vis absorption spectra. In the IR absorption spectra, it is thought that disappearance of one of two NO stretching bands seen in a starting materials indicate the elimination of the coordinated one nitrosyl ligand.

The clear reaction of pymt or mpymt complex with metal salt is not observed. While, only dmpymt complex exhibited a drastically change with copper(II) nitrate, which is blue-shift of the MLCT band in the UV-Vis absorption spectra. It is confirmed by the ^{13}C NMR, IR, and UV-Vis absorption spectral data that the reaction is isomerization to trans(S,S) from trans(N,S).

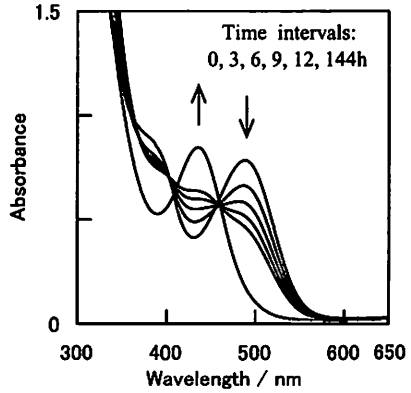

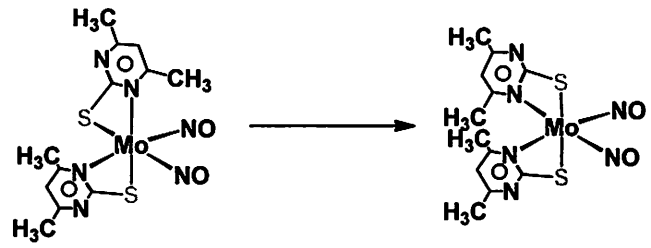

References

[1] T. Yonemura, J. Nakata, M. Kadota, M. Hasegawa, K. Okamoto, T. Ama, H. Kawaguchi, and T. Yasui, *Inorg. Chem. Commun.*, **4**, 661(2001).

[2] T. Yonemura, T. Hashimoto, M. Hasegawa, T. Ikenoue, T. Ama, and H. Kawaguchi, *Inorg. Chem. Commun.*, **9**, 183(2006).

2PE01 Transient compressibility during protein reaction; phototropin LOV2 domain with the linker helix

K. Kuroi[1], F. Sato[2], Y. Nakasone[1], K. Zikihara[3], S. Tokutomi[3], and M. Terazima[1]

[1]*Department of Chemistry, Kyoto University, Kyoto 606-8502, Japan*

[2]*Maringa University, Brazil,* [3]*Osaka Prefecture University, Japan*

e-mail : kyk@kuchem.kyoto-u.ac.jp

Compressibility is a property representing conformational fluctuation. We use this property to reveal the importance of structural fluctuation for functioning of proteins. For that purpose we are trying to measure the compressibility of reaction intermediates by the transient gating (TG) and transient lens (TrL) techniques under high-pressure conditions. By using these techniques, we evaluated the change in the isothermal compressibility with a high time resolution, which directly reflects the change of volume fluctuation during the photoreaction.

In this study, we applied this method to the LOV2 domain of a blue light sensor protein, phototropin from *Arabidopsis*. Although the LOV domain is one of the most versatile blue-light sensor domains, its molecular signal transduction mechanism remains still unclear. Only minor structural change around its chromophore has been observed upon light-excitation. In this regard, we have expected that the transient fluctuation of the intermediate might play an important role in this step. For proving this speculation, we studied the fluctuations of the LOV2 domain with Jα helix construct. The photoreaction of this sample has been intensively studied so far. After the photo-excitation of its chromophore FMN, it is converted into the triplet state (named as L660) at 30 ns and the L660 state forms the covalent bond between FMN and LOV core at 2μs (this state is called as S390), and finally Jα helix of S390 unfolds with the time constant of 1ms to generate the final product (T390).[1]

The volume fluctuation in each intermediate was estimated from the signal intensities at various pressures and was summarized in Figure. It shows the first intermediate L660 had the largest volume fluctuation. This enhanced fluctuation was reduced with the proceeding of the photoreaction. Our results support a possibility that the photoreaction of LOV domain need to generate the structural flexibility in the excited state to carry out its signal transduction.

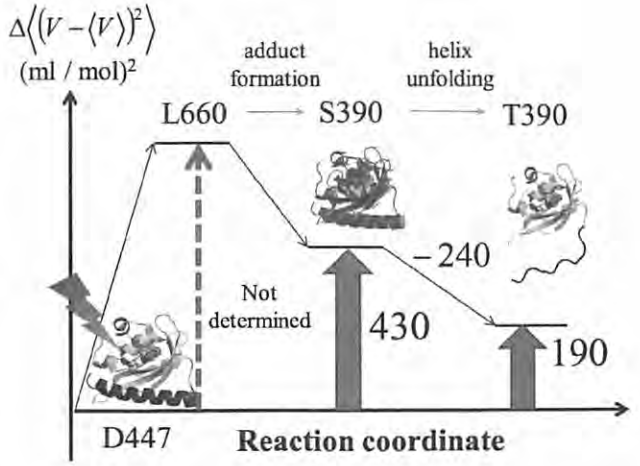

References

[1]Nakasone, et. al. (2007). J Mol Biol 367, 432-42.

2PE02 Role of multivalnet cations in association between macroanions based on simple model

S. Fujihara[1] and R. Akiyama[1]

[1]*Department of Chemistry, Kyushu University, Fukuoka 812-8581, Japan*

e-mail : sfujihara@chem.kyushu-univ.jp

Although G-actin is negatively charged, the monomers form fibrils (F-actin). HNC-OZ theory with a simple model was examined to explain those phenomena. The calculated results indicated that strong attraction between macroanions was mediated by counter charged ions[1]. In the previous study, we did not examine the dependence of effective interaction on the ionic valence. However, Murakami *et al.* suggested that Mg^{2+} is the mediator in case of fibril formation of actin[2]. Therefore, the effect of divalent cations was examined in this study.

In the present study, the electrolyte solution consisted of four components: solvelnt molecules, monovalent cations, monovalent anions, and divalent cations. Charged hard spheres were adopted for the electrolyte solution. We set the concentrations of ions to mimic biofluid. The correlation functions were also calculated on the basis of HNC-OZ theory. Fig. 1 shows the dependence of binding free energy ε on the concentration of divalent cations in a solution containing 150mM monovalent cations. When the concentraion of divalent cations is lower than 0.1mM, |ε| is smaller than the thermal energy, k_BT. The stability of dimer increases as the concentration of divalent cations becomes larger. The minmum ε approaches about -7.5 k_BT around 20 mM, and it is much larger than thermal energy. Our analyses suggest that the monovalent cations at the location A(see Fig. 1) are exchanged for the divalent cations around the minimum, and the attraction between macroanions is correlated with this exchange. These results correspond to the structural experiments[2]. We will discuss the relation between these results and the fibril formation of actin in the poster presentation.

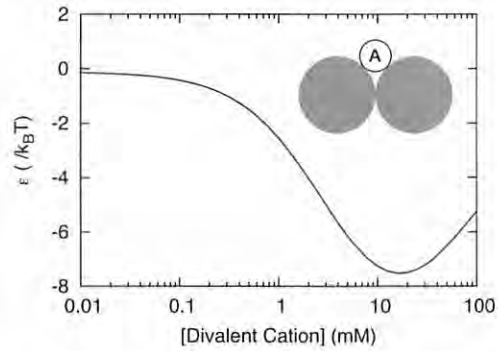

Fig. 1. Dependence of binding free energy of the macroanions(gray spheres) charged -11e on the concentration of divalent cations. Effective interaction is mediated cations located at A.

References

[1] R. Akiyama, R. Sakata: *J. Phys. Soc. Jpn.* **80** 123602 (2011).

[2] K. Murakami, T. Yasunaga, T. Noguchi, Y. Gomibuchi, K, X. Ngo, T, Uyeda, T, Wakabayashi: *Cell* **143** 275-287 (2010).

2PE03 Accelerated Dielectric Relaxation of Water around an Ion

Y. Kubota[1], A. Yoshimori[2], N. Matubayasi[3], M. Suzuki[4], and R. Akiyama[1]

[1]*Department of Chemistry, Kyushu University, Fukuoka 812-8581, Japan*

[2]*Department of Physics, Kyushu University, Fukuoka 812-8581, Japan*

[3]*Institute for Chemical Research, Kyoto University, Uji 444-8585, Japan*

[4]*Department of Materials Processing, Tohoku University, Sendai 980-8579, Japan*

e-mail : ykubota@chem.kyushu-univ.jp

Suzuki and co-worker observed dielectric spectra for aqueous solutions of alkali halide and of various proteins, such as actin filaments, in the frequency range 0.2 - 26 GHz. The spectra involved a component higher than the peak of bulk water [1, 2]. The observation suggests that the dielectric relaxation of water in the hydration shell is faster than that of bulk water and named hyper-mobile water (HMW). HMW was assigned to the structure-breaking region, i.e., in the second and/or third hydration layers. On the other hand, it has been difficult to show the faster relaxation by molecular dynamics simulations with usual force fields for water and ion.

We derived a time-correlation function $c_z^{[i]}(t)$ for dielectric relaxation of water in the i-th hydration shell on the basis of linear response theory. We calculated dielectric relaxation of water around the ion using molecular dynamics simulations. Figure 1 shows that the dielectric relaxation $c_z^{[i]}(t)$ near the ion is faster than that of bulk, although the orientational relaxation $s_z^{[i]}(t)$ near the ion is slower. With the distance from the ion, the relaxation curves $c_z^{[i]}(t)$ and $s_z^{[i]}(t)$ get close to the bulk results. The ratio of the relaxation time between the fast component in the nearest hydration shell and that of bulk is about 60 - 80 %. This calculated ratio is consistent with that between the hyper-mobile water and bulk water in the experiments for alkali halide aqueous solutions [3]. Our results show that HMW is located near the ion, in other words, in the structure-making region. Therefore, we improved the picture of the dielectric relaxation of hydrated water around ions.

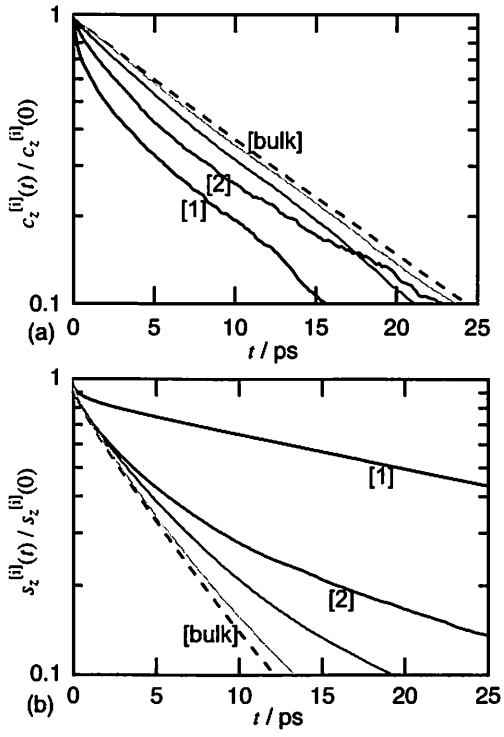

Fig. 1. (a) Dielectric relaxation function $c_z^{[i]}(t)$ and (b) orientational relaxation function $s_z^{[i]}(t)$ around an ion. The labels [1] and [2] indicate the results for the first and second hydration shells in our definition, respectively.

References

[1] S. Kabir, *et al.*, Biophsy. J. **85** (2003) 3154.

[2] T. Miyazaki, *et al.*, J. Phys. Chem. A **112** (2008) 10801.

[3] Y. Kubota, *et al.*, J. Chem. Phys. **137** (2012) 224502.

2PE04 Cation distribution in EcoRV-DNA complex calculated by using 3D-RISM

Shunya Sunaba[1], Ryota Motomatsu[1], Norio Yoshida[2],

Akinori Sarai[1], Fumio Hirata[3,4] and Masayuki Irisa[1]

[1] *Department of Bioscience and Bioinformatics, Kyushu Institute of Technology, Iizuka 820-8502, Japan*

[2]*Department of Chemistry, Kyushu University, Fukuoka 812-8581, Japan*

[3]*Institute for Molecular Science, Okazaki 444-8585, Japan*

[4]*TechnoComplex, Ritsumeikan University, Kusatsu 525-8577, Japan*

e-mail : sunaba@irisa-lab.bio.kyutech.ac.jp

Restriction enzymes recognize a specific sequence of DNA and selectively cut a double-stranded DNA. This hydrolysis reaction requires divalent cations. One of the type II restriction enzymes, *Eco*RV, is a homo dimer and requires Mg^{2+} ions in its function. In this study, cation distributions in the *Eco*RV-DNA complex were calculated by using 3D-RISM [1], where NaCl or $MgCl_2$ aqueous solution was used as a solvent. The X-ray structure of *Eco*RV-DNA complex (PDB ID: 1rvb), which corresponds to the step prior to the hydrolysis reaction of a DNA fragment [2], was adopted as a solute structure. The calculated distributions of both Na^+ and Mg^{2+} cations in the corresponding aqueous solutions show higher local densities in the minor groove of the DNA fragment than the bulk at the both sides of the reactive site having the sequence, 5'-ATAT-3', which should be cleaved at the centre of the sequence. The calculated local densities of divalent cation, Mg^{2+}, at the active site in *Eco*RV with a $MgCl_2$ aqueous solution are about twice as high as those of monovalent cation, Na^+, with a NaCl aqueous solution. Both the distributions of Na^+ and Mg^{2+} cations around the active site are similar, but slightly different from each other. The distribution of Na^+ ions has a sharp peak at the same position in the active site, where a Mg^{2+} ion is found in the X-ray structure. The distribution extends to the polypeptide side chains which are directly bonded to the Mg^{2+} ion in the X-ray structure. On the other hand, the distribution of Mg^{2+} ions also has a sharp peak at almost the same position as the previous Na^+ case, but extends to the interface region between the DNA fragment and the polypeptide side chains, both of which have negative charges. This difference in the distributions is probably caused by the difference in the valency numbers between the two cations. This work is the first step to pursue the reaction of restriction enzyme, where divalent cations are required in its function.

References

[1] Norio Yoshida, Takashi Imai, Saree Phongphanphanee, Andriy Kovalenko and Fumio Hirata, *J. Phys. Chem. B*, **113**, 873-886(2009).

[2] Dirk Kostrewa and Fritz K. Winklera, *Biochemistry*, **34**, 683-696(1995).

2PE05 Free-Energy Analysis of Cosolvent Effects on Functional Molecules in Solution

Nobuyuki Matubayasi

Institute for Chemical Research, Kyoto University, Kyoto 611-0011, Japan

e-mail : nobuyuki@scl.kyoto-u.ac.jp

The structure of a functional molecule such as protein can be strongly modified by adding a cosolvent. In aqueous system, water and cosolvent form a mixed solvent, and the effect of cosolvent is typically observed as a difference in solvation behavior between the mixed solvent and pure water. To control and utilize the cosolvent effect, it is desirable to analyze the cooperation and/or competition of intra- and intermolecular interactions among the solute, water, and cosolvent at atomic resolution. In the present work, we address the cosolvent or mixed-solvent effect by focusing on protein solvation and on molecular binding in lipid membrane.

A commonly utilized effect of cosolvent on protein is the denaturation, and a widely used denaturant is urea. When urea is added into an aqueous system with protein, the intermolecular interaction of protein is operative against both urea and water, leading to two views on urea-induced denaturation. One view emphasizes the direct interaction between protein and urea, and is called direct mechanism. The other focuses on the effect of water modified by the presence of urea, and is called indirect mechanism. We analyze the solvation free energies of amino-acid analogs and cytochrome *c* in pure water and in urea-water mixed solvent to discuss the urea effect from the viewpoint of energetics. The free-energy computation is carried with all-atom force field using molecular dynamics simulation combined with the method of energy representation. The transfer free energy from pure water to urea-water mixture is then decomposed into the contributions from urea and water. Urea is found to act as the stabilizer of transfer, and water is so only for the hydrophobic ones. When the focus is on the interaction component such as van der Waals or electrostatic, the transfer free energy is strongly correlated to the van der Waals component between the solute and solvent. There is no correlation against the electrostatic component due to the compensation between the loss of interaction with water and the gain with urea. The direct mechanism through the van der Waals interaction is thus the dominant factor of urea effect.

We also discuss the molecular binding into lipid membrane as a solvation in a mixed solvent. To do so, the lipid and water are viewed as mixed solvent and the molecule to be bound is seen as solute. The membrane binding is then treated as a solvation in an inhomogeneous mixed solvent, and the corresponding free energy of solvation is computed with the energy-representation method to determine the strength and location of binding. To highlight the effect of each of lipid and water, the binding free energy is decomposed into the contributions from lipid and water. The water contribution is found to delocalize the spatial distribution of hydrophobic solute within the membrane, and it is pointed out that the role of water is common among membrane/water interface, air/water interface, and supercritical water.

2PE06 Theoretical Analysis of Co-Solvent Effects on Intramolecular Proton Transfer Reaction of Glycine in Water-Acetonitrile Mixture

Yukako Kasai, Norio Yoshida, and Haruyuki Nakano
Department of Chemistry, Graduate School of Sciences, Kyushu University, Fukuoka 812-8581, Japan
E-mail:yukako@ccl.scc.kyushu-u.ac.jp

The proton transfer reaction is known to be a basic chemical reaction, and therefore a number of studies have been conducted so far on this reaction. However, many proton transfer reactions occur in solution phase, and for deep understanding of the reaction the consideration of the solvents that affect the reaction mechanism is essential. In the presentation, we report the free energy profile of intramolecular proton transfer reaction of glycine in solution. First we consider the free energy profile in the gas and pure solvents. In highly polar solvents, glycine is present as an ionic molecule, since the zwitterion form (ZW) is more stable than the neutral form (NF). Then, we examine the profile in water-acetonitrile mixture and discuss the solvent effect on it.

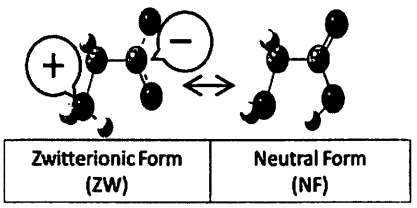

We used the reference interaction site model self consistent field (RISM-SCF) method to take account of the interaction between the solute and solvent, such as hydrogen bonding. The RISM-SCF method is a hybrid method of *ab initio* electronic structure theory and statistical mechanics for molecular liquid.

We first confirmed from the calculations for the gas and pure solvents that NF was more stable than ZW in gas phase and acetonitrile solution and that, in contrast, ZW was more stable than NF by 10.62 kcal/mol in aqueous solution. Figure 1 shows the free energy profile for the water-acetonitrile mixture, where M stands for molar fraction of acetonitrile. The reaction coordinate was defined as $R = r(\text{N-H}) - r(\text{O-H})$ and the energy of NF was taken to be the energy origin. According to the figure, we can see that as the molar fraction M increases, the relative free energy of ZW increases and the reaction barrier height from ZW to NF decrease. From the energy decomposition analysis of the free energy of solvation (ΔA), we found that the contribution of the excess chemical potential ($\Delta\mu$) on ΔA was larger than that of the electronic reorganization energy. We also found from the radial distribution function and coordination number analysis that the major factor which stabilizes ZW as M decreases was the hydrogen bond between a hydrogen atom in solvent water and the oxygen atom in solute glycine.

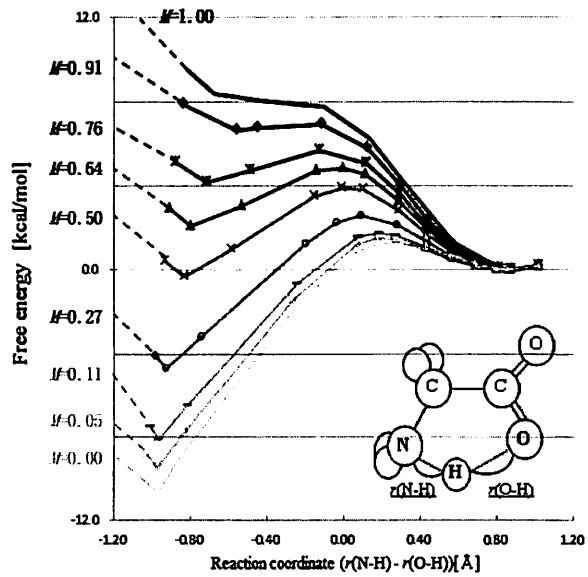

Figure 1.Free energy profile for the water acetonitrile mixture
(The energy of NF is taken to be zero.)

2PE07 Thermal and Quantum Structural Fluctuation of Small Protonated Water Clusters: A Path Integral Molecular Dynamics Study

Y. Sumita[1] and S. Miura[1]

[1]*Graduate School of Natural Science and Technology, Kanazawa University, Kakuma, Kanazawa 920-1192, Japan*

e-mail : smiura@mail.kanazawa-u.ac.jp

Structural fluctuation of small protonated water clusters, $H^+(H_2O)_N$, $N = 5 - 8$, is study by the molecular dynamics method. A polarizable and dissociable potential model developed by Ojamae *et al.* [1] is adopted to describe proton transfer processes among water molecules. Quantum nuclear fluctuation is accounted for by the path integral quantization technique. Temperature dependent fluctuation is analysed using the inherent structure method [2, 3] applied to both classical and path integral molecular dynamics trajectories.

References

[1] L. Ojamae, I. Shavitt, and S. J. Singer, J. Chem. Phys. **109**, 5547 (1998).

[2] F. H. Stillinger and T. A. Weber, Phys. Rev. A **25**, 978 (1982).

[3] F. H. Stillinger, J. Chem. Phys. **89**, 4180 (1988).

2PE08 Effect of methanol and trifluoroethanol on thermal denaturation of β-lactoglobulin

Y. Fukushima, K. Yoshida, and T. Yamaguchi

Department of Chemistry, Fukuoka University, Fukuoka 814-0180, Japan

e-mail: sc090431@cis.fukuoka-u.ac.jp

An investigation of folding/unfolding and aggregation of proteins has drawn much attention in food process and cosmetic manufacture. It would be useful to elucidate the mechanism of folding of proteins for understanding the formation of amyloid fibrils due to misfolding of protein. Denaturation and aggregation of proteins are induced by heat, pressure, pH, and co-solvent. Alcohol is widely used as a co-solvent. Since alcohol, which is an amphiphile molecule, is miscible with water, the hydrophobic/hydrophilic nature of the solvent is controllable by changing alcohols and their concentration.

In the present study, the effect of alcohol on the thermal denaturation of β-lactoglobulin (β-LG) in alcohol-water mixtures at various temperatures was studied by small-angle X-ray scattering (SAXS). β-LG (30 mg/mL), 50 mM KCl (pH=7) and 0-70 vol% methanol or trifluoroethanol (TFE) were stirred with a vortex mixer. SAXS was measured on a NANO-Viewer (Rigaku). A mica plate cell was used at room temperature, whereas borosilicate glass capillary at higher temperatures. Measured temperatures were 298-363 K.

Fig.1 shows Guinier plots of β-LG at various methanol concentrations (C_{MeOH}) at 298 K. β-LG monomer exists at $C_{MeOH} \leqq 20$ vol%, and its aggregates at $C_{MeOH} \geqq 30$ vol%. In water, β-LG monomer exists at temperatures $\leqq$ 343 K, and its aggregates at temperatures $\geqq$ 353 K. Thermal denaturation temperature decreased with increasing alcohol concentration. The effect of TFE on thermal denaturation was larger than that of methanol. This is probably because TFE has a larger hydrophobic group than methanol. Fractal dimension after thermal denaturation of β-LG in TFE (2.1-2.8) was larger than that in methanol (1.5-1.6). This indicates that complex aggregates are formed in TFE. In addition, Kratky plots showed that the protein changes from a globular to an unfolded form when it aggregates. It is concluded that thermal denaturation of β -LG is affected by alcohol and its concentration.

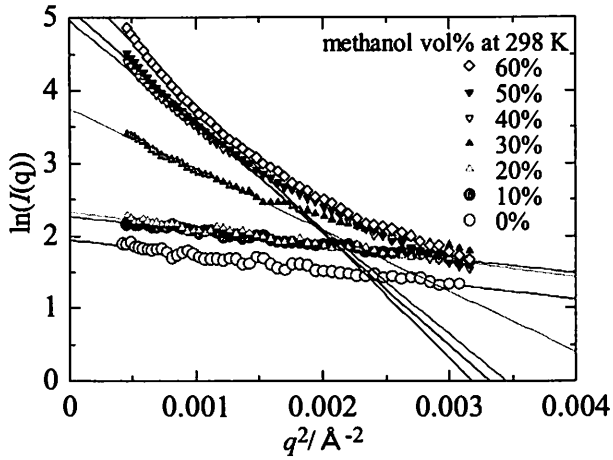

Fig.1. Guinier plots of β-LG in methanol-water mixtures as a function of methanol concentration at 298 K

References

[1] K. Yoshida, et al., Phys. Chem. Chem.Phys. **12**, 3260(2010).

2PE09 Diffusion change reveals conformational dynamics of the N- and C-terminal helical regions of the phototropin1 LOV2 domain

Kimitoshi Takeda[1] , Yusuke Nakasone[1] , Kazunori Zikihara[2] ,
Satoru Tokutomi[2] , Masahide Terazima[1]

[1]*Department of Chemistry, Kyoto University, Kyoto 606-8502, Japan*
[2]*Osaka Prefecture University, Osaka 599-8531, Japan*
e-mail : t_kimitosi@kuchem.kyoto-u.ac.jp

Phototropin is a blue-light sensor protein, which regulates phototropism, chloroplast movement, and stomata opening of higher plants. This protein consists of two LOV (LOV1 and LOV2) domains, the kinase domain, and a linker helix, which connects the LOV2 and the kinase. The LOV2 domain plays a main role for the regulation of the kinase activity. In the signal transduction processes, importance of the conformational change in the N- and C- terminal helical regions (A'α helix and Jα helix) (Fig.1) has been suggested by the molecular dynamics simulation. Indeed, we experimentally found that the Jα helix is detached from the LOV2 domain and finally it unfolds with a time constant of 1 ms upon photoexcitation.[1] However, the reaction of the A'α helix has not been revealed yet.

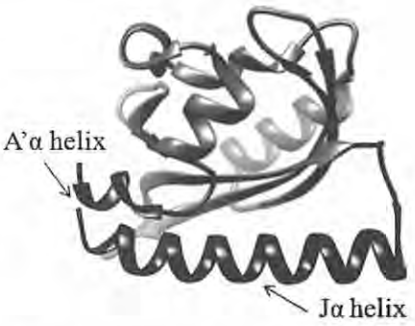

Fig. 1 Structure of phot1-LOV2 linker

In order to clarify the role of the A'α helix on the signal transduction, we studied the dynamics of the conformational change of the A'α helix by using the diffusion coefficient (D) measurements in time-domain. Our group previously showed that D is a good property reflecting the helix conformation in solution. The time dependence of D and secondary structures of several mutants were measured by the transient grating (TG) method and the circular dichroism (CD) spectroscopy, respectively. When we truncated the A'α helix, the Jα helix was unfolded according to the CD spectra. This indicates that the Jα helix was stabilized by the interaction with the A'α helix. The TG signal of the wild type showed a significant D change, which was attributed to the change of the interaction between the solvent and the protein molecule upon the unfolding of the Jα helix.[1] On the other hand, the TG signal of a mutant whose Jα helix was destroyed in advance showed very small change in D, which was assigned to the unfolding process of A'α helix. Monitoring the time development of D change of the mutant, we determined the reaction rate of the unfolding of the A'α helix to be 12 ms. At the symposium, we will discuss the importance of A'α helix at the molecular level based on these results.

References

[1] Nakasone et al.2007.J.Mol.Biol.367:432-42

2PE10 Optical Spectroscopic Studies on Structural Change of Proteins in the Aqueous Ionic Liquid Solutions

T. Takekiyo[1], A. Nihei[1], K. Yamazaki[1], E. Yamaguchi[1], M. Aono[2], H. Abe[2], and Y. Yoshimura[1]

[1] *Department of Applied Chemistry and* [2] *Department of Materials Science and Engineering, National Defense Academy, 1-10-20, Hashirimizu, Yokosuka, Japan 239-8686.*

e-mail:take214@nda.ac.jp

Recently, the use of ionic liquids (ILs) constructing the organic cation and anion in bioscience fields has focused on applications in biotechnology such as biocatalysis and protein storage [1]. Because ILs provide not only a novel and highly efficient reaction medium but also serve as effective participants in various biological processes. Thus, the structural stability and activity of proteins in aqueous IL solutions have been investigated to determine the effect of ILs on protein stability.

Regarding the intriguing features of the aqueous IL solutions, Weing□rter *et al.* reported that the solvent properties such as viscosity and dielectric constant of ILs change drastically at a certain IL concentration from typical electrolyte solution-like behavior to molten salt-like behavior depending on the content of water in the mixtures [2]. Recently, we demonstrated that aqueous 1-butyl-3-methylimidazoliunm nitrate ([bmim][NO_3]) solutions above 20 mol%IL showing the molten salt-like behavior induce the partial refolding of once unfolded lysozyme (38% α-helix and 10% β-sheet) [3]. An understanding of the features contributing to protein stability over a wide IL concentration range in aqueous ILs is necessary to investigate the relationship between the molten salt-like behavior and the protein structure in these media.

In this study, we have investigated structural changes of myoglobin (>80% α-helix) and lysozyme in the aqueous [bmim]-based ILs([bmim][X] X=Cl, NO_3, and SCN) solutions using Nicolet 6700 FT-IR and Jasco J-820 CD spectroscopy. Our results showed that the changes in the concentration of ILs induced disruption of tertiary structure of both proteins. On the other hand, with the addition of ILs, the secondary structure of myoglobin showed the structural transition of the folded state → unfolded state → aggregation, and that of lysozyme showed the folded state → unfolded state → partial refolded state. In view of these results, we suggested that the IL-induced structural change of proteins correlates to the contents of secondary structure and protein size.

References

[1] S. Park, R. J. Kazlauskas, *Curr. Opin. Biotechnol.* **14**, 432 (2003).

[2] H. Weing□rtner, C. Cabrele, and C. Herrman, *Phys. Chem. Chem. Phys.* **14**, 415 (2012).

[3] T. Takekiyo, K. Yamazaki, E. Yamaguchi, H. Abe, and Y. Yoshimura, *J. Phys. Chem. B,* **116**, 11902 (2012).

2PE11 Conformation of ATP and ADP Molecules in Aqueous Solutions Determined by High-energy X-ray Diffraction

T. Miyazaki[1], Y. Kameda[2], Y. Umebayashi[3], H. Doi[3], Y. Amo[2], T. Usuki[2]

[1]*Graduate School of Science and Engineering, Yamagata University, Yamagata 990-8560*

[2]*Department of Material and Biological Chemistry, Faculty of Science, Yamagata University, Yamagata 990-8560*

[3]*Graduate School of Science and Technology, Niigata University, Niigata 950-2181*

e-mail to Y. Kameda: kameda@sci.kj.yamagata-u.ac.jp

Adenosine 5'-triphosphate (ATP) is an important biomolecule which concerning many biological reactions in cells. These reactions use the released energy from hydrolyses of ATP molecule into adenosine 5'-diphosphate (ADP) molecule. In order to understand the biological processes driven by the ATP hydrolysis, it is necessary to obtain information on hydration and conformation of ATP and ADP molecules in aqueous solutions.

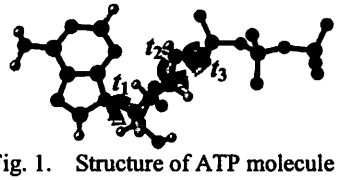

Fig. 1. Structure of ATP molecule and angular parameters, t_1-t_3.

Aqueous 2.05 mol% ATP disodium salt solution and aqueous 2.05 mol% ADP disodium salt solutions were prepared. The samples were contained in a flat plate cell of 2 mm thickness (windows with Kapton 25 μm film). X-ray diffraction measurements were carried out at 25°C using the BL04B2 beam line of the SPring-8 at Japan Synchrotron Radiation Research Institute (JASRI). Scattered X-ray intensities from the sample solutions were counted over the angular range of $0.3 \leq 2\theta \leq 42.0°$ using incident wavelength of 0.2009 Å, corresponding to scattering vector magnitude range of $0.16 \leq Q \leq 22.4$ Å^{-1} ($Q = 4\pi\sin\theta/\lambda$). Measurement time was 6 hours per sample.

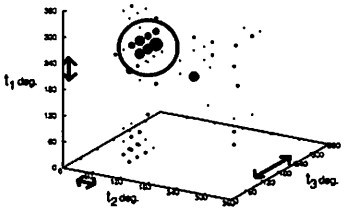

Fig. 2. The distribution of dihedral angles, t_1-t_3, for ATP molecule.

Observed scattering intensities from the sample solutions were corrected for instrumental background, absorption, and polarization to obtain total interference term $i^{total}(Q)$. The least-squares fitting procedure was applied to the $i^{total}(Q)$ in order to obtain the dihedral angles, t_1-t_3 (Fig. 1), that determine special correlation among these components, adenine - ribose - triphosphate groups of ATP and ADP molecules. In the present analysis, internal geometry of adenine and ribose groups were fixed to that reported for crystal of ATP disodium salt determined by neutron diffraction [1], and that for the triphosphate group was fixed as shown in Fig. 1. The sum of squares for the difference between observed and calculated interference terms was calculated at the interval of 30° of dihedral angles, t_1-t_3, and obtained the angular distribution of residual sum of squares (Fig. 2, 3). Distribution of the residual sum of squares are found to different between ATP and ADP molecules in aqueous solutions.

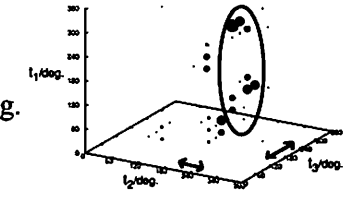

Fig.3. The distribution of dihedral angles, t_1-t_3, for ADP molecule.

Reference [1] O. Kennard, N. W. Isaacs, W. D. S. Motherwell, J. C. Coppola, D. L. Wampler, A. C. Larson, D. G. Watson, *Proc. R. Soc. Lond.* **A325**, 401(1971).

2PE12

Why Are TFE and HFIP Much More Helix-forming than Ethanol and Isopropanol? : IR Studies of O–H Stretching and H–O–H Bending Vibration Bands of the Water in Mixtures with TFE or HFIP

K. Mizuno[1], T. Moroyose[1], Y. Tamai[2], and T. Sumikama[3]

[1] *Depart. of Appl. Chem. and Biotech., Grad.School of Engi., Univ. of Fukui, Fukui, 910-8507 Japan.* [2] *Depart. of Appl. Physics, Grad. School of Engi., Univ. of Fukui, 910-8507 Japan.* [3] *Faculty of Medical Sciences, Univ. of Fukui, 23-3, Matsuoka-shimoaizuki, eiheiji-cho, Yoshida-gun, Fukui, 910-1193 Japan*

e-mail : kmizuno@u-fukui.ac.jp

Purposes: 2,2,2-Trifluoroethanol(TFE) and 1,1,1,3,3,3-hexafluoroisopropanol(HFIP) have been known as a much stronger helix-forming reagent for proteins than ethanol(EtOH) and isopropanol (iPrOH). We have been considering that the differences of the effect as the helix forming reagents may come from the different effects of the alcohols on the property of the water in each aqueous mixture. In the present work, we carried out IR measurements of O-H stretching, ν(O-H), and H-O-H bending, ν(H-O-H), vibration spectra in aqueous solutions of EtOH, TFE, iPrOH or HFIP to study the hydrogen bonding properties of the water molecules in each mixture.

Experiments: IR spectral changes of ν(O-H) was examined by observing O–D stretching vibration band of HDO used as a probe molecule of water[2]. The changes of the ν(H-O-H) were examined by observing the H–O–H bands of the mixture [H_2O + D_2O] of 2:3 volume ratio instead of water.

Results and Discussion: In [water + EtOH], blueshiftings of both ν(O-H) and ν(H-O-H) were observed with increasing EtOH. This meant the formation of less polar, but more bound water than bulk water. We have found that the strange water is also formed on mixing with iPrOH, tetrahydrofuran, or dimethyl sulfoxide. In anyway, hydrogen bond donating property of the water in the mixtures decreased, and the property of water as a solvent became less polar. This can induce formation of intermolecular hydrogen bond N-H•••O=C, and helix formation within protein.

In [water + TFE] and [water + HFIP], on the other hand, blueshiftings of ν(O-H) and redshifting of ν(H-O-H) were observed with increasing the alcohols, showing that intermolecular hydrogen bond network within liquid water were completely broken. Thus, the property of water as a solvent became much less polar than that in the mixtures with EtOH and iPrOH. This also means that TFE and HFIP make the water in their mixtures much effective helix-forming reagent than the water in mixtures of EtOH and iPrOH. The differences in the propertis of the water in mixtures are shown as plots of ν(H-O-H) vs ν(O-D) in Figure 1.

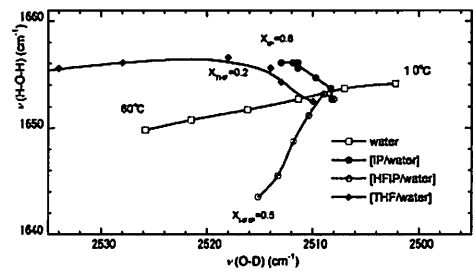

Figure 1. Relationship between ν(O-D) and ν(H-O-H) of the water in [iPrOH/water] and [HFIP/water].

2PF01 Effect of Molecular Orientation on Mscibility and Domain Formation of Fluorocarbon-1-ol and Fluorocarbon-α,ω-diol at Oil/Water Interface

R. Fukuhara, T. Hiroki, H.Matsubara, M.Aratono, and T.Takiue

Department of Chemistry, Faculty of Sciences, Kyushu University, Fukuoka 812-8581, Japan

e-mail : r.fukuhara@chem.kyushu-univ.jp

Gibbs adsorbed films at liquid/liquid interfaces are fundamental structures of soft matters such as biological membranes. Therefore it is required to investigate the character of the adsorbed films in order to clarify the function of the soft matters. Especially, evaluating the miscibility of several kinds of amphiphiles in adsorbed film is of great significance because it involves the formation of important structure of the film such as lateral organization (found in cell membrane as 'raft').

In our previous studies on the adsorbed films at the hexane/water interface by interfacial tensiometry and X-ray reflection, it was found that 1H,1H,2H,2H-perfluorodecanol (FC10OH) form condensed monolayer with molecular orientation normal to the interface. On the other hand, 1H,1H,10H,10H-perfluorodecane-1,10-diol (FC10diol), which have two terminal hydroxyl groups at both ends of hydrophobic chain, adsorb to the interface with parallel orientation.

In this study, we focus on the effect of molecular orientation on the miscibility of film forming substances and the structure of the adsorbed film, and thus employed the FC10diol-FC10OH mixed systems. We measured the interfacial tension γ and X-ray reflectivity of their hexane solutions against water as a function of total molality m ($=m_1+m_2$) of the solution and the composition of FC10OH in the mixture X_2 ($=m_2/m$) under atmospheric pressure at 298.15K.

The γ vs. m curves at constant X_2 have break points corresponding to the phase transition of the adsorbed film. The Interfacial pressure π vs. area per molecule A curves indicated four kinds of film states in the present system; expanded, condensed①, condensed②, and multilayer states. These are shown in the molality at phase transition points m^{eq} vs. X_2 curves in Fig.1. The π vs. A curves and the two-dimensional phase diagram (phase diagram of adsorption; PDA) suggested that the condensed state② is the normal–oriented monolayer in which FC10diol as well as FC10OH molecules orient perpendicularly to the interface, and the condensed state ① is the monolayer in which the normal- and parallel-oriented molecules coexist. Furthermore, the X-ray reflectivity measurement manifests that the condensed state② is heterogeneous structure with micro phase separation into the condensed phase domains with normal and parallel orientations.

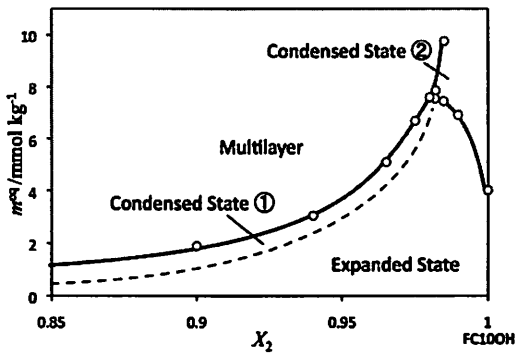

Fig.1 m^{eq} vs. X_2 curve

2PF02 Surface Reorganization of Isotactic Polypropylene Film

K. Yamamoto[1] and K. Tanaka[1,2]

[1]*Department of Applied Chemistry and* [2]*International Institute for Carbon-Neutral Energy Research (WPI-I2CNER), Kyushu University, Fukuoka 819-0395, Japan*

e-mail : k.yamamoto.203@s.kyushu-u.ac.jp

Thin polymer films have been used in a wide variety of technological applications such as selective membranes, medical coatings, etc. In these applications, since the polymer surface is in contact with a water phase, the structure and physical properties of the polymer at the water interface should be directly examined as the first benchmark. We have hitherto worked on this issue using amorphous polymers and accumulated experimental results showing a strong impact of the water phase on the polymer interface. However, we have not embarked on a class of semi-crystalline polymers because the aggregation states of semi-crystalline polymers are more complicated than amorphous ones. In this study, the interfacial characterization of thin films of *isotactic* polypropylene (*i*PP), which is a typical crystalline polymer, was made by sum-frequency generation (SFG) spectroscopy.

As a material, additive free *i*PP was kindly supplied from Japan Polychem. Co. Films of *i*PP were prepared onto quartz prisms by a spin-coating method. They were then melted at 473 K under a vacuum and then quenched to 298 K. SFG spectroscopic measurement was applied to examine the local conformation of *i*PP at the air and D_2O interfaces. The excitation light was guided into the outermost interface from the substrate side through the hemispherical prism. The measurements were carried out at room temperature with the *ssp* (SF output, visible input, and infrared input) polarization combination.

Figure 1 shows the SFG spectra with the *ssp* polarization for an *i*PP film at the air and D_2O interfaces. Three peaks were clearly observed at 2858, 2900 and 2950 cm^{-1}. They can be assigned to the symmetric C-H stretching vibration of methyl groups and the antisymmetric stretching vibration of methylene and methyl groups, respectively. On the other hand, signals from the symmetric stretching of methylene groups were not clearly discerned. These make it clear that the main chain part as well as the side chain portion of iPP oriented in the plane of the air interface. In the case of the D_2O interface, while the peak originated from methylene groups was clearly observed around 2900cm^{-1}, the peak from the symmetric stretching of methyl group disappeared. The peak from the corresponding antisymmetric stretching was observed as a shoulder. This implies that the methyl side chains somehow lost the orientation at the D_2O interface. Thus it can be claimed that the local chain conformation at the outermost region changes even in the semi-crystalline film responding to the environment.

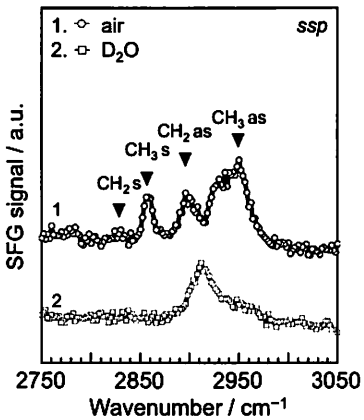

Figure 1 SFG spectra with the *ssp* polarization for an *i*PP film at air and D_2O interfaces.

2PF03 Surface Light Scattering and Surface Viscoelasticity on DTAB Aqueous Solution

S. Ueno[1], Y. Takajo[1], H. Takumi[1], Y. Ohmasa[2], T. Takiue[1], H. Matsubara[1] and M. Aratono[1]

[1]*Department of Chemistry, Faculty of Sciences, Kyushu University, Japan*

[2]*Research Center for Condensed Matter Physics, Hiroshima Institute of Technology, Japan*

e-mail : s.ueno@chem.kyushu-univ.jp

[Introduction] The dilational viscoelasticity represents the rigidity and the fluidity of films at the fluid - fluid interfaces. It is well known that these properties often dominate the stability of foams and emulsions, and play an important role in the biological behaviour of membranes. However, the understanding the dilational viscoelasticity of the adsorbed film has not yet fully progressed. In order to understand these properties, we started the study on the surface viscoelasticity of the adsorbed film of dodecyltrimethylammonium bromide (DTAB) because many data of surface thermodynamic properties have already reported. In this presentation, the details of experimental setup and theoretical background will be introduced and then some results of the data analysis will be demonstrated.

[Experiment] The surface viscoelasticity on aqueous solution of DTAB was measured as a function of the molarity m_1 at a high frequency by the SQELS (Surface Quai-Elastic Light Scattering) method at room temperature under atmospheric pressure. In our SQELS measurement, surface wave that is generated by thermal motion of molecules at the interface, called ripplon, was detected accurately by employing the heterodyne method. The spectrum of scattered light were monitored in frequency domain and analysed on the basis of the dispersion relation.

[Results and Discussion] Figure.1 shows the surface (a)elasticity ε and (b)viscosity κ vs. molality m_1 curves of the adsorbed film of DTAB. The surface elasticity increases drastically around the boundary concentration between the gaseous and expanded states which was exactly determined by surface tension measurement. The surface elasticity of the gaseous film increases slightly as molality increases, but that of the expanded film decreases gradually. Furthermore, we obtained the negative surface viscosity in the region of the expanded film similarly to the report on Langmuir films [1]. We will discuss the gaseous – expanded phase transition and the states of adsorbed film from the view point of molecular interaction derived from our SQELS and thermodynamic studies.

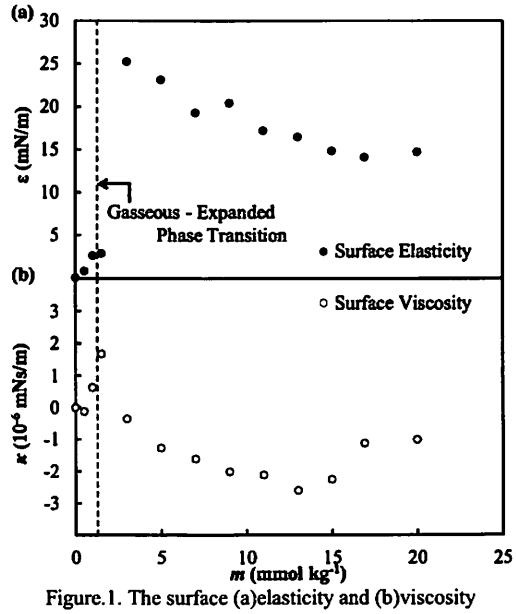

Figure.1. The surface (a)elasticity and (b)viscosity vs. molality curves of DTAB adsorbed film.

[References]

[1] J. Giermanska-Kahn, F. Monroy, D. Langevin, *Phys. Rev. E* **60**, 6, 7163 (1999).

2PF04 Effect of Solvent on Gibbs Adsorbed Films of Decane-1,10-diol at Air/Water and Perfluorohexane/Water Interfaces

N. Obayashi, T. Tottori, T. Hiroki, H. Matsubara, M. Aratono, and T. Takiue

Department of Chemistry, Faculty of Sciences, Kyushu University, Fukuoka 812-8581, Japan

e-mail : n.obayashi@chem.kyushu-univ.jp

The structure and the property of Gibbs adsorbed film are influenced appreciably not only by the structure of adsorbed molecule but also by the molecular interaction including solute-solvent and solute-solute interactions. Our previous study on the adsorbed 1-tetradecanol (C14OH) films at hexane (C6)/water and perfluorohexane (FC6)/water interfaces indicated that C14OH forms condensed film at much lower concentration at the FC6/water interface than at the C6/water interface due to the enhanced interaction between C14OH molecules by the weak interaction between C14OH and FC6 molecules. In this study, we employed decane-1,10-diol(C10diol) as materials, and aimed at elucidating the effect of solute-solvent interaction on the molecular orientation in the adsorbed film.

The interfacial tensions γ of aqueous solution of C10diol against air and FC6 was measured as a function of molality of C10diol m_1 and temperature T under atmospheric pressure by pendant drop method. The X-ray reflectivity (XR) was measured as a function of scattering vector Q_z (= $(4\pi/\lambda)\sin\alpha$) at fixed m_1 and 298.15 K at BL37XU in SPring-8.

The γ value decreases with increasing T and m_1 in both systems. The difference between the two interfaces was clearly seen in the interfacial pressure π vs. mean area per adsorbed molecule A curves at high π shown in Fig. 1. The curve at the FC6/water interface is almost vertical where the A value is around 0.75 nm^2 and close to the cross-sectional area along major axis of C10diol with all-trans conformation, suggesting that C10diol forms condensed monolayer with molecular orientation parallel to the interface. At the air/water interface, on the other hand, the adsorbed film is still compressible even at high π, and the A value is smaller than 0.75 nm^2. According to the electron density profile obtained by XR indicated that C10diol molecules are lying with loop conformation at the surface.

The values of entropy change associated with adsorption Δs are positive at both interfaces. It indicates that the entropy gain due to the dehydration around C10diol molecule accompanied by adsorption is larger than the entropy loss due to the molecular orientation at the interface. Furthermore, the partial molar entropy change of adsorption is smaller at the FC6/water than at the air/water interface mainly due to the difference in the molecular orientation at the FC6/water and air/water interfaces.

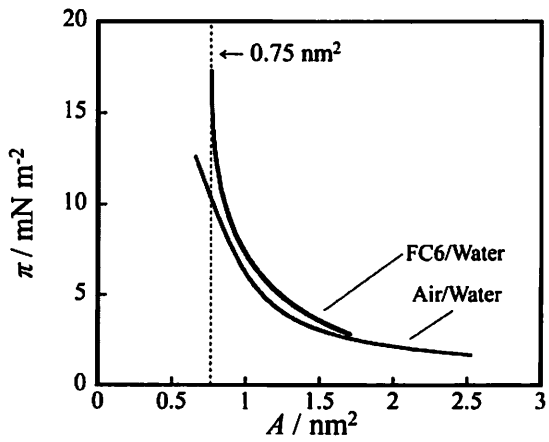

Fig. 1 π vs. A curves at 298.15 K

2PF05 Spherical Harmonics Analysis of the Surface Structure of Spherical Ionic and Nonionic Micelles and Its Relevant Dynamics - A Molecular Dynamics Study

Y. Nimura[1], L. Wang[2], K. Fujimoto[3], N. Yoshii[4], and S. Okazaki[1]

[1]*Department of Applied Chemistry, Nagoya University, Furo-cho, Chikusa-ku, Nagoya 464-8603, Japan*

[2]*School of Chemistry and Chemical Engineering, Shanghai Jiao Tong University, Shanghai 200240, China*

[3]*College of Pharmaceutical Sciences, Ritsumeikan University, 1-1-1 Noji-higashi, Kusatsu, Shiga 525-8577, Japan*

[4]*Center for Computational Science, Graduate School of Engineering, Nagoya University, Furo-cho, Chikusa-ku, Nagoya 464-8603, Japan*

e-mail : yoshii@ccs.engg.nagoya-u.ac.jp

In order to investigate influence of electric charges of hydrophilic group on the micelle structure and its dynamics, molecular dynamics calculations have been performed for ionic sodium dodecyl sulphate (SDS) micelle and non-ionic octaetyleneglycol mono dodecyl ether ($C_{12}E_8$) micelle.

Here, in order to clarify two-dimensional surface structure of the micelles and its dynamical fluctuation as well as fluidity of surfactant molecules, new statistical-mechanical functions has been defined by spherical harmonics, e.g., surface structure factor, intermediate scattering function, pair correlation function, and space-time correlation function. The functions describing two-dimensional spherical surface structure and dynamics are the analogue of the ones usually defined for three-dimensional fluid. [1] From the analysis we observed the relaxation time for the periodic surface structure of the surfactant molecules and the lateral diffusion coefficient for the single surfactant molecule on the micellar surface. Breathing and deforming motions of the micelle are also extracted by the spherical harmonics analysis.

The spherical harmonics analysis presented her is a powerful tool and it is useful for not only the spherical micelle but also other spherical materials such as clusters, nano particles, vesicles, and viruses.

References

[1] J. P. Hansen, I. R. McDonald, Theory of Simple Liquids, Academic Press. London (2006).

2PF06 Effects Phase Transition in the Adsorbed Film on the Foam Film Thickness

H. Tanaka[1], E. Ohtomi[1], N. Ikeda[2], T. Takiue[1], M. Aratono[1], and H. Matsubara[1]

[1]*Department of Chemistry, Faculty of Sciences, Kyushu University, Fukuoka 812-8581, Japan*

[2]*Faculty of Human Environmental Sciences, Fukuoka Women's University, Fukuoka 813-8529, Japan*

e-mail : h.tanaka@chem.kyushu-univ.jp

Foam film is a basic unit of foams in which the thin water phase is stabilized in the air by the repulsive interactions between the two opposing surfactant adsorbed films. The foam film stabilized by the electrostatic repulsion is called the Common Black Film (CBF) and the one stabilized by the steric repulsion is the Newton Black Film (NBF).

We have previously demonstrated that the alkane – surfactant – mixed adsorbed film shows surface phase transition from the liquid like state to the solid like state upon cooling. In this study, we studied the influence of the surface phase transition on the interactions between the adsorbed films and on the foam film thickness. For this purpose, we applied tetradecane (C14) – hexadecyltrimethylammonium chloride (HTAC) mixed adsorbed film to create the foam film (Figure 1) in the presence of sodium chloride (NaCl). We measured the ellipticity and surface tension to determine the state of adsorbed film, and foam film thickness was determined by the micro-interferometry.

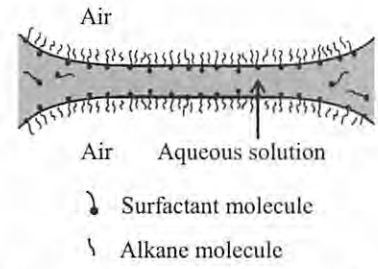

Figure 1 A Schematic picture of the foam film stabilized by the alkane - surfactant mixed adsorbed film

From the experimental results, it was clarified that no remarkable change in foam film thickness was observed in the absence of oil but there was a clear discontinuous change in the presence of oil at the temperature close to the surface phase transition point (Figure 2). One of the most important findings is h remains about 18nm even after the thickness transition. Taking into account of the previous TR–XAFS measurement [1], we suppose that the adsorption of the chloride ions onto the surfactant adsorbed films is induced by the surface phase transition and results in the thin-thick transition between the different thickness CBFs with decreasing of electrostatic repulsion.

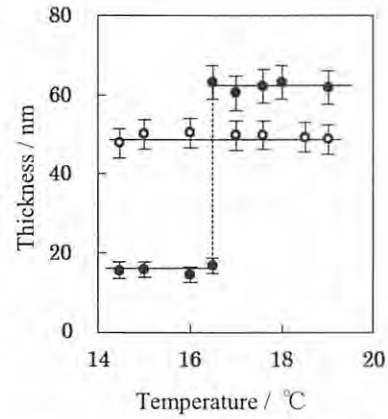

Figure 2 Foam film thickness vs. temperature curves for HTAC foam film in the presence (black) and in the absence (white) of tetradecane at 2.2 mmol kg^{-1} NaCl and 0.3mmol kg^{-1} HTAC

References

[1] E. Ohtomi, N. Ikeda, Y. Tokiwa, I. Watanabe, H. Tanida, T. Takiue, M. Aratono, H. Matsubara, *Chemistry Letters*, **41**, 10, 1300 (2012).

2PF07 Spectroscopy of hydroxyl radical formed in microwave excited bubble plasma

T. Kaga[1], R. Yamase[1], C. Kurosawa[1], Y. Fukumura[1], T. Ishijima[2], K. Takahashi[1,2]
[1]*Institute of Science and Engineering, Kanazawa University, Japan*
[2]*Research Center for Sustainable Energy and Technology, Kanazawa University, Japan*
Email: second@stu.kanazawa-u.ac.jp

Plasma involves activate chemical species that do not exist in the conventional chemical environment. Recently, much attentions have been paid to plasma produced on the interface between liquid and gas[1]. However, our understanding for the reactions at gas-liquid interface is very limited. The aim of this study is to clarify chemical species produced in a microwave bubble plasma and reaction mechanism at the gas-liquid interface.

Figure 1 shows the experimental device for the microwave bubble plasma. The reactor was equipped with a scroll pump by which the pressure inside the vessel can be decreased down to saturated water vapor pressures. Pulsed 2.45 GHz microwave was injected into the solution through a rectangular waveguide and a slot antenna. Microwave plasma was produced in bubbles formed by the front of the slot antenna. Firstly, the emission spectrum was measured in order to examine the chemical specie formed in the bubbles. Then, we used terephthalic acid(TA) aqueous solution as hydroxyl radical scavenger to perform the quantitative analysis of the radical. The TA is known to specifically react with hydroxyl radical and produce 2-hydroxy terephthalic acid(HTA). The HTA absorbs light at wavelength of 310 nm. The absorption spectra of the plasma treated TA aqueous solutions was measured and based on them the concentration of hydroxyl radical was evaluated.

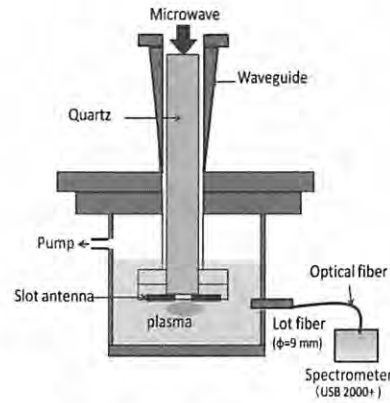

Fig.1.Experimental device.

Figure 2 shows the emission spectrum of microwave bubble plasma formed in ultrapure water. The generation of hydroxyl radical, H_α, H_β and O atoms was confirmed. Figure 3 shows the effect of duty ratio on the amount of HTA produced. The HTA concentration increased with increasing of duty ratio. This is due to the increase of microwave irradiation time. Figure 4 shows the effect of frequency on the HTA formation. The sharp increase of HTA at 50 kHz was observed. We are thinking that this may be related to the life time of electron in plasma and the microwave electric field which accelerate electrons in plasma.

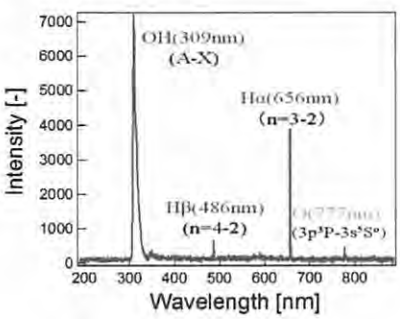

Fig.2.Emission spectrum.

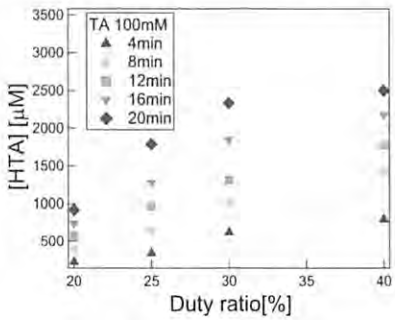

Fig.3.Effect of duty ratio.

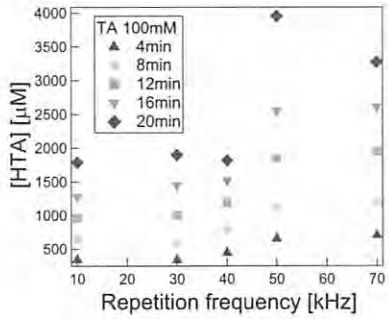

Fig.4.Effect of repetition frequency.

References

[1] T. Ishijima, H. Hotta, M. Sato, and H. Sugai, Appl. Phys. Lett. **91,** 121501(2007).

2PF08 Effect of Condensed Film Formation at Alkane Mixture/Aqueous Solution Interface on Its Composition and Emulsion Stability

Y. Tokiwa, T. Takiue, M. Aratono and H. Matsubara

Department of Chemistry, Kyushu University, Fukuoka 812-8581, Japan

e-mail : y.tokiwa@chem.kyushu-univ.jp

The adsorbed film at oil/water interface is fundamental structure of oil-in-water (O/W) and water-in-oil (W/O) emulsions. So far, it has been considered that the adsorbed film is in the expanded state in which surfactant molecules are loosely packed due to the electrostatic or hydration repulsion between head groups. However, Lei et al recently showed that the condensed film formation can be occurred at hexadecyltrimethylammonium bromide (HTAB) aqueous solution/tetradecane (C_{14}) interface due to the penetration of C_{14} into HTAB adsorbed film upon cooling [1]. In this study, we examined the effect of the difference of alkane chain length on the condensed film formation. In addition, the influence of the adsorbed film structure on the emulsion stability was studied.

For this purpose, we adopted C_{14}–hexadecane (C_{16}) mixture as the oil phase and measured interfacial tension (γ) and ellipticity against HTAB aqueous solution as a function of temperature (T), molality of HTAB (m) and composition of C_{16} in the oil phase (x_2).

Figure 1 shows the phase transition temperature of adsorbed film determined as a function of x_2. It is clearly showed the phase transition temperature increases with increasing x_2 indicating that the adsorption of C_{16} is favorable for condensed film formation. This view was supported by the ellipsometry which revealed that the condensed film is composed mainly by HTAB and C_{16} and C_{14} is expelled from interface. The similar result is obtained from thermodynamic analysis of interfacial tension data.

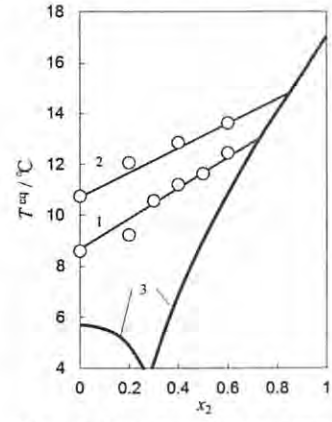

Figure 1 : Phase transition temperature of adsorbed film at m = 0.2 (1) and 0.6 (2) mmol kg^{-1}. The curve No.3 shows oil melting point.

Figure 2 shows the picture of emulsions prepared by stirring HTAB aqueous solution and alkane mixture with VORTEX MIXER. They were kept at fixed T for 24 hours. It was demonstrated that the emulsion stability change abruptly at the temperature very close to phase transition temperature of adsorbed film. In addition, we are now performing the similar experiment at another m. We will also discuss the effect of m on the emulsion stability.

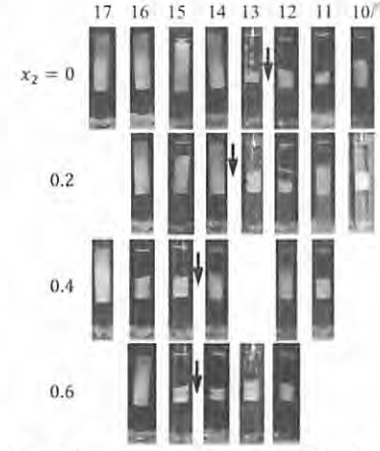

Figure 2 : Emulsion stability examined as a function of T and x_2 at m = 3.0 mmol kg^{-1}. Arrows show the phase transition temperature of adsorbed film.

References

[1] Q. Lei, C. D. Bain, *Phys. Rev. Lett.* **92**, 167103 (2004).

2PF09 Time-dependent Heterogeneity in a Supramolecular Solution System

Y. Matsumoto[1], A. Shundo[1], K. Matsumoto[2,3], M. Ohno[3], K. Miyaji[3], M. Goto[1], and K. Tanaka[1,2]

[1]*Department of Applied Chemistry and* [2]*Department of Automotive Science, Kyushu University, Fukuoka 819-0395, Japan*

[3]*Nissan Chemistry Industries, Ltd., Tokyo 101-0054, Japan*

e-mail : k-tanaka@cstf.kyushu-u.ac.jp

Peptide amphiphiles in water often form hierarchical fibril structures, leading to a supramolecular hydrogel. In contrast to conventional polymeric gels, supramolecular hydrogels exhibit a sol-gel transition by external stimuli. For example, the sol state obtained by mechanically disrupting the gel returns to the gel state spontaneously (re-gelation). However, it is pointed out that repeating re-gelation cycle often causes the change in original physical properties of the gel. In this study, we report how the local physical properties depend on the repeated cycle of disrupting and aging by a particle tracking technique, where the viscoelastic information at the micrometer scale can be accessed by observing the thermal diffusion of embedded probe particles [1].

The probes used in this study were polystyrene particles with a diameter of 1.1 ± 0.03 μm. The diffusion of individual probe particles embedded in the gelator-water mixture was followed by a charge-coupled device camera. From the trajectory of the particles, we calculated the mean-square-displacement ($<\Delta r^2(\tau)>$). Figure 1 shows the double logarithmic plot of $<\Delta r^2(\tau)>$ against the lag time (τ). Each solid line was obtained by monitoring a particle 10 times and averaging them. For the gel, the slope of all plots was less than 1, meaning that the diffusion of the particles was not controlled by the random walk statistics. A reasonable explanation for it is that the particles were trapped within the fibrous networks in the gel. For the sol obtained by shaking the gel, two types of the slope were observed: the slope is equal to and is less than 1. This indicates that the physical properties, thereby network structure, in the sol was heterogeneous. After aging the sol for 72 hours, the slope of plots returned to be smaller than 1. Thus, the re-gelation process was accompanied by a homogenization of the network. Interestingly, when the cycle of the shaking and aging was repeated, two types of the slope were still observed in the gel obtained by aging for 72 hours. Thus, it is most likely that the required aging time to form the homogeneous network became longer depending on the number of cycles of the shaking and aging.

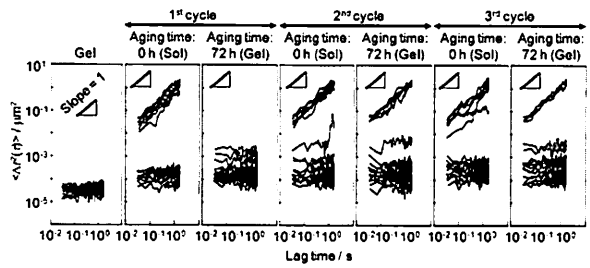

Figure 1 Double logarithmic plot of $<\Delta r^2(\tau)>$ against τ obtained for 20 different particles embedded in the gelator-water mixture.

References

[1] D. P. Penaloza, K. Hori, A. Shundo, K. Tanaka, *Phys. Chem. Chem. Phys.* **14**, 5247 (2012).

2PF10 Cooperative dynamics of water molecules in Water/ Amphiphilic polymer mixed system

T. Akahane[1], L. K. Shrestha[2], and T. Sato[1],

[1]*Dept. of Materials and Chemical Engineering, Shinshu Univ. Ueda 386-8567, Japan*
[2]*National Institute for Materials Science (NIMS), Tukuba 305-0044, Japan*
e-mail : takaakis@shinshu-u.ac.jp (T.S), 13fm502k@shinshu-u.ac.jp (T.A)

We have undertaken to renovate our understanding of a dynamical property of water molecules in soft condensed systems, such as lyotropic liquid crystals. In order to investigate dynamical behavior of water confined to nanostructures in lyotropic liquid crystal, we performed dielectric relaxation spectroscopy (DRS) for water/octaethylene glycol monododecyl ether ($C_{12}E_8$) for the nearly entire concentration range in $0 \leq w \leq 0.9$, where w is the weight fraction of $C_{12}E_8$, covering aqueous micellar (L_1), liquid crystal (hexagonal (H_1) and bicontinuous cubic), and liquid phases at 25 °C

The complex permittivity, $\varepsilon(\nu)^* = \varepsilon'(\nu) - i\varepsilon''(\nu)$, was determined in the frequency range of ca.0.7 $\leq \nu$/GHz $\leq$ ca.25 using a time-domain reflectometry (TDR). The concentration dependence of the relaxation times and amplitudes was determined by fitting the experimental $\varepsilon(\nu)^*$ spectra assuming the superposition of two relaxation functions ($j = 1, 2$), having the relaxation time, τ_j, and amplitude, $\Delta\varepsilon_j$.

An assignment of each process is done on the basis of the concentration dependence of τ_j and $\Delta\varepsilon_j$. The resolved low-frequency process reflects motion of hydrated polyethylene glycol (PEG) chain and hydrated water, whereas the high-frequency process is due to dynamics of cooperative rearrangement of hydrogen bonding network of bulk water.

The relaxation time of bulk-like water, τ_2, increases almost continuously with increasing surfactant concentration, w (Fig.1(a)). This indicates that bulk-like water still presents in liquid crystal phases. In contrast, the relaxation time of hydrated PEG chain, τ_1, increases drastically above the L_1–H_1 transition point, showing the critical-like behaviour.

The relaxation amplitude of the hydrated PEG chain, $\Delta\varepsilon_1$, grows continuously even above the L_1–H_1 phase boundary, showing the maximum at $w \approx 0.5$, and then in turn decreases at higher w (Fig.1(b)). We consider that in $w > 0.5$, the number of the water molecules is no longer sufficient to exhibit such large polarization fluctuation as observed in $w < 0.5$. $\Delta\varepsilon_1$ becomes closer to the amplitude of bare $C_{12}E_8$ with a further increase of the surfactant concentration.

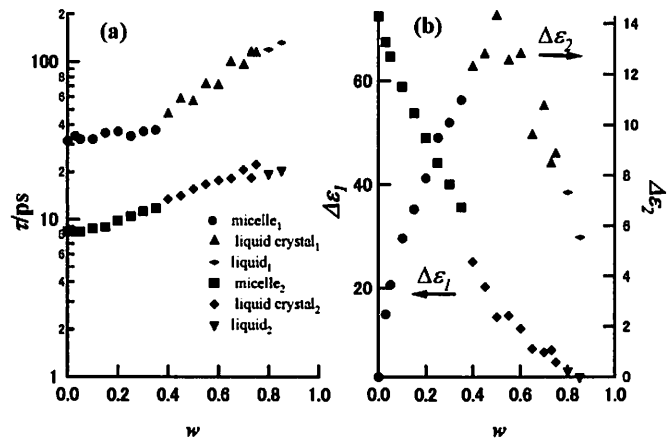

Fig. 1 Relaxation times (a) and amplitudes (b) of the aqueous $C_{12}E_8$ as a function of the surfactant weight fractions, w, at 25°C

References

[1] Schrödle,S., G. Hefter, et.al. *Langmuir*,22,924-932 (**2005**).

[2] Mitchell, D. J., Tiddy, G. J. T. et.al . *M.P.J.Chem.SOC.,Faraday Trans.I*,79,975-1000(**1983**)

2PF11 MESOSCOPIC SIMULATION OF SODIUM DODECYL SULFATE AGGREGATES ON GRAPHENE NANOSHEETS

Wijak Patsinsiri[1], Manaswee Suttipong[2], Alberto Striolo[2], Boonyarach Kitiyanan[1]

[1]*The Petroleum and Petrochemical College, Chulalongkorn University, Bangkok, 10330, Thailand*

[2]*School of Chemical, Biological and Materials Engineering, The University of Oklahoma, Norman, Oklahoma, 73069, USA.*

e-mail : Wijak.Patsinsiri-1@ou.edu

Sodium dodecyl sulfate (SDS) aggregates on graphene sheets (GS) and graphene nanoribbons (GN) were studied using dissipative particle dynamics (DPD) simulations. The effects of GS size and GN width on aggregate morphology were investigated. The SDS aggregates were studied on 3×3 nm^2, 6×6 nm^2, and 12×12 nm^2 GS and on 3 nm, 6 nm, and 12 nm wide GN, at ambient conditions. Our results proved that the SDS aggregate shape depends on the size of the GS and GN. The quantification of the results was in the form of SDS contact angles, order parameter, and density profiles. Both GS and GN were modified with functionalized edges to mimic graphene oxide. To understand the effect of the surfactants on stabilization of GS dispersion, GS of different sizes and surfactant amounts, were allowed to diffuse in an aqueous system. The results were quantified using snapshots, and by quantifying the simulation time required for the GS to agglomerate. The mechanism of agglomeration was discussed qualitatively. Increasing the amount of surfactant decreased the likelihood of GS aggregation and also affected the GS agglomeration mechanism.

2PF12 Using graphene nanosheets/ extended-polymer composites to fabricate transparent and conductive films

Hsi-Wen Tien, Yuan-Li Huang, Sheng-Tsung Hsiao, Wei-Hao Liao, Yu-Sheng Wang, Shin-Ming Li, Chen-Chi M. Ma*

Department of Chemical Engineering, National Tsing-Hua University, Hsin-Chu 30013, Taiwan, ROC

e-mail : ccma@che.nthu.edu.tw

The intercalation reaction of graphite oxide (GO) with poly(acryl amide)/poly(acrylic acid) (PMA) was studied as a method for controlling the spacing between GO through control of the pH value. In order to fabricate transparent conductive films (TCFs), GO must be reduced to graphene nanosheets (GNS) by hydrazine to increase electrical conductivity. Aggregation and restacking of GNS can be efficiently inhibited by extended polymer chains of PMA polymer chains resulted from adjusting the pH value by adding NaOH solution. The existence of ion Na+ also improves the electrical conductivity between GNS layers. The PMA grafted GNS (PMA-g-GNS) composite films showed a lowest sheet resistance of 4.38×10^{3} $\Omega\square^{-1}$ for pH=9.0, which was one order of magnitude lower than that for pH=3.2 system (4.89×10^{4} $\Omega\square^{-1}$), and the value of DC conductivity to optical conductivity ratio (σ_{DC}/σ_{OP}) was 0.09 instead of 0.005. The higher σ_{DC}/σ_{OP} ratio indicates a higher performance of TCFs.

2PF13 Dry Particle Coating Using Ultrasonic Cavitation in High-Pressure CO_2

K. Matsuyama[1], Satoshi Tanaka[1], T. Okuyama[2]

[1]*Department of Biochemistry and Applied Chemistry, Kurume National College of Technology, Kurume 830-8555, Japan*

[2]*Department of Materials Science and Engineering, Kurume National College of Technology, Kurume, 830-8555, Japan*

e-mail : mtym@kurume-nct.ac.jp

Dry particle coating techniques have attracted considerable attention as modification of surface properties and/or functionality of powders in the field of pharmaceutical, cosmetic, food or ceramics industries. These coating materials have obtained much interested remarkable change in properties such as flowability, hydrophobic and hydrophilic property, dispersability, electrostatic, electric, magnetic etc., compared with unmodified powders. For example, to improve the flowability of powders with relatively large particle size (host particles), the fine particles (guest particles) is discretely coated onto the surface of host particles by using the dry coating techniques. However, most fine gust particles have a strong tendency to form agglomerates. The dispersion of guest particles is very important to obtain the discrete coating of host particles with guest particles. Several dry particle coating approaches (dry process) have been developed such as mechanofusion, hybridizer and rotating fluidized bed coater etc. On these dry particle coating methods, the guest particles are attached or embedded onto the surface of host particles by means of high shear and/or impaction forces.

We describe particle coating using ultrasonic irradiation in high-pressure carbon dioxide (CO_2). Host microparticles were coated with guest nanoparticles[1-3]. Shock waves generated by collapsing cavitation bubbles induced with ultrasonic irradiation accelerated the deagglomeration and dispersion of guest nanoparticles and achieved dry particle coating in liquid CO_2. Host microparticles coated with guest nanoparticles were observed using scanning electron microscopy (SEM). This revealed that the guest particles were completely coated with guest nanoparticles, and a smooth coating surface was obtained.

References

[1] K. Matsuyama, K. Mishima, *Ind. Eng. Chem. Res.*, **49**, 1289 (2010).

[2] K. Matsuyama, K. Mishima, T. Kato, K. Ohara, *J. Supercritical Fluids*, **57**, 198(2011).

[3] K. Matsuyama, K. Mishima, *Review of High Pressure Science and Technology/Koatsuryoku No Kagaku To Gijutsu*, **22**, 104 (2012).

2PG01 A New Approach of pH-determination at the Air/water Interface with Confocal Fluorescence Microscope

H. Yang, A. Harata

Department of Molecular and Material Sciences, Interdisciplinary Graduate School of Engineering Sciences, Kyushu University, Fukuoka 816-8580, Japan

e-mail : harata@mm.kyushu-u.ac.jp

Liquid surface and interfaces are fundamentally essential in many physical, chemical and biological processes. The air/water interface is one of the most common interfaces. However, it is still unclear of physical and chemical properties of neutral and charged molecules at the air/water interface. The pH value is a fundamental chemical property. Decades ago, second-harmonic generation [1] and two-photo ionization [2] have been applied to determine the pH at the air/water interface. However, both of these two methods lack high sensitivity to work under a low surface density. Confocal fluorescence microscope (CFM) has been applied to observe fluorescence emission of water-soluble rhodamine dyes adsorbed at the water surface even under the surface density of solute molecules being $1\text{-}10^3$ molecule/μm^2 [3][4][5]. In this work, CFM was applied to study the pH at the air/water interface, by observing fluorescence spectra of two types of pH-indicator dyes adsorbed at the interface between the air and aqueous solutions of various pH.

Rhodamine B was studied as an acid dye in this research, while 5-(and-6)-carboxy SNARF-1 as a basic dye. The experimental setup of CFM was similar to that described elsewhere [3]. The laser was focused at the air/water interface to obtain the fluorescence spectra of dyes surface-selectively.

The pH-dependence of fluorescence peaks of rhodamine B and 5-(and-6)-carboxy SNARF-1 were discussed. Solvent effects on fluorescence spectra of these two dyes were also discussed. Absorption parameters and surface density of dyes were obtained through surface tension experiments. Final results of pH-determination will be evaluated by comparing with previous methods. This work will contribute to understand the physical and chemical properties of the air/water interface.

References

[1] X. Zhao, S. Ong, H. Wang, K. Eisenthal, *Chem. Phys. Lett.* **214**, 2(1993).

[2] M. Sato, A. Harata, Y. Hatano, T. Oagawa, T. Kaieda, K. Ohmukai, H. Kawazumi, *J. Phys. Chem. B*, **108**, 12111(2004).

[3] Y.-Q. Li, M. N. Slyadnev, T. Inoue, A. Harata, and T. Ogawa, *Langmuir*, **15**, 3035(1999).

[4] Y.-Q. Li, T. Inoue, A. Harata, T. Ogawa, *Instrum. Sci. and Tech.* **27**, 159(1999).

[5] X.-Y. Zheng, A. Harata, T. Ogawa, *Spectrochim. Acta Part A.* **57**, 312(2001).

2PG02 A laser trapping-spectroscopy study on mass transfer processes across a single micro-droplet/air interface

Jiang Ma[1], Shoji Ishizaka[1], Terufumi Fujiwara[1]

[1] *Graduate School of Science, Hiroshima University*

e-mail : m111464@hiroshima-u.ac.jp

Clouds regulate the earth's energy balance by reflecting and scattering solar radiation and by absorbing the earth's infrared radiation. The fundamental knowledge about mass transfer processes across a micro-droplet/air interface is very important to give mathematical equations that describe the growth process of clouds for climate models. So far, experimental studies on the condensation growth of water droplets have been conducted by using either an aerosol flow tube or a vibrating orifice aerosol generator. However, the mass accommodation coefficients evaluated by such techniques are very scattered and, therefore, the detailed mechanisms of condensation growth of micrometer-sized water droplets are still controversial. The primary reason for this is difficulties in observing the growth processes of single water droplets in air. In this study, we demonstrate a novel approach for in situ observation of the evaporation and condensation processes of single water droplets levitated in air by means of a laser trapping technique.

As shown in Fig. 1, a micrometer-sized aqueous ammonium sulphate droplet was trapped in air by a focused 532nm laser beam from a CW-Nd: YVO_4 laser introduced to an inverted optical microscope through an objective lens (×60, NA = 0.70). Since vapor pressure of the droplet is governed by both the solute concentration and the temperature, an irradiation of an infrared (IR) laser beam (1064nm, 3.1mW) to the droplet led to an increase in the temperature and thus a decrease in the size of the trapped droplet to attain an equilibrium state at which the droplet vapor pressure is balanced by the surrounding relative humidity. We succeeded in reversible control of the size of the trapped aqueous ammonium sulfate droplets by switching on/off of the IR laser beam irradiation, as shown in Fig. 1. Here, we show that resolving the time evolution of the change in size provides a novel approach for investigating the mass transfer accompanying condensation or evaporation at the single micro-droplet/air interface.

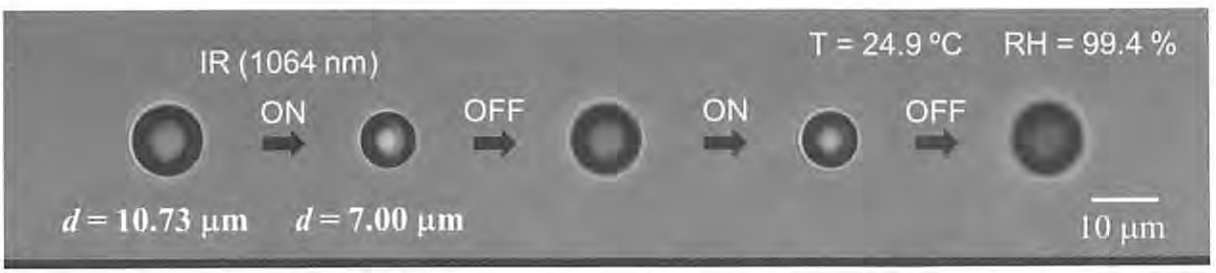

Fig. 1 Reversible size changes of the aqueous ammonium sulfate droplet in air upon switching on-off of IR laser irradiation.

2PG03 Amperometric Detection of Heparin Polyion at a Polarized Water/Ionic Liquid Membrane Interface

J. Langmaier[1], Z. Samec[1], P. Tůma[2], and E. Samcová[2]

[1]*J. Heyrovsky Institute of Physical Chemistry, Prague 8, Czech Republic*

[2]*Third Faculty of Medicine, Charles University in Prague Prague 10, Czech Republic*

e-mail : eva.samcova@lf3.cuni.cz

Amperometric detection of the anticoagulant heparin at the polarized liquid/liquid interfaces and polymeric membranes was shown to be facilitated by the asymmetric tetraalkylammonium cations, e.g., tridodecylmethylammonium cation ($TDMA^+$), via a counter-ion association mechanism [1]. Analogously, the potentiometric response of the PVC plasticized membrane doped with TDMACl to heparin was attributed to the ability of $TDMA^+$ to bind to heparin polyion [2].

In the present study, cyclic voltammetry was used to investigate for the first time the transfer of heparin polyion across the polarized interface between water and the ionic liquid (IL) membrane composed of tridodecylmethyl ammonium cation and tetrakis[3,5-bis(trifluoromethyl)phenyl]borate anion (TDMATFPB). Study reveals a tunable effect of the symmetric tetraalkylammonium cations, e.g., tetrapentylammonium cation ($TPeA^+$), present at trace concentrations in the aqueous solution containing heparin.

The capillary electrophoretic measurements of the heparin migration times in the absence and presence of $TPeA^+$ do not show any change in the heparin charge and, hence, the formation of a new transferable cation in the aqueous phase by the counterion binding of $TPeA^+$ on heparin should be excluded. Theoretical considerations based on the mixed-potential concept and experimental evidence suggests that the tetraalkylammonium cations promote the extraction of heparin into the IL phase, from which heparin can be stripped off by applied potential providing a well-separated current signal. A new method for the amperometric detection of heparin is proposed [3].

This work was supported by grant no. P206/11/0707 from Grant Agency of the Czech Republic.

References

[1] S. Amemiya, Y. Kim, R. Ishimatsu, B. Kabagambe, *Anal. Bioanal. Chem.* **399**, 571(2011).

[2] B. Fu, E. Bakker, V.C. Yang, M.E. Meyerhoff, *Macromolecules* **28**, 5834 (1995).

[3] J. Langmaier, Z. Samec, E. Samcová, P. Tuma, *Electrochem. Commun.* **24**, 25 (2012).

2PG04 Voltammteric Study of Ion Transfer from Water to Highly Hydrophobic Ionic Liquids

J. Langmaier, and Z. Samec

J. Heyrovsky Institute of Physical Chemistry of ASCR, Prague 8, Czech Republic

e-mail : jan.langmaier@jh-inst.cas.cz

Cyclic voltammetry (CV) was used to study the ion transfer from water to various highly hydrophobic ionic liquids (ILs) composed of tridodecylmethylammonium ($TDMA^+$) or redox-active (ferrocenylmethyl)dodecyldimethyl ammonium ($FcMDDA^+$) cations and tetrakis[3,5-bis (trifluoromethyl)phenyl]borate ($TFPB^-$), tetrakis(pentafluorophenyl)borate ($TPFPB^-$) or redox-active Co dicarbollide ($CoDCC^-$) anions [2-4]. CV behavior of several semi-hydrophobic ions ($I^{+/-}$) at a TDMATFPB membrane supported on a thin (ca. 110 μm) micro-porous filter is demonstrated in Figure 1. CV data were used to evaluate the standard Gibbs energy of ion transfer ($\Delta G_{tr,i}^{0,w\rightarrow IL}$), and to establish a Gibbs energy relationship between $\Delta G_{tr,i}^{0,w\rightarrow IL}$ ion transfer the standard Gibbs energy of ion transfer from water to an organic solvent immiscible with water such as 1,2-dichloroethane ($\Delta G_{tr,i}^{0,w\rightarrow DCE}$), cf. Figure 2. Nearly 1:1 correlation indicated that the ion solvation energies in IL and DCE could be similar. In order to clarify this surprising result, we used the dielectric relaxation spectroscopy (DRS) to evaluate and to compare the static dielectric constant ε_S of TDMATPFPB and TDMADCC [5]. On this basis, a conclusion was made that the correlation established between the standard Gibbs energies of ion transfer from water to the studied ILs and to DCE has the origin in similar solvophobic (neutral) contributions rather than in the comparable polarity of TDMADCC (ε_S =11.7) and TDMATPFPB (ε_S =7.1) and DCE (ε_S = 10.5), as characterised by the static dielectric constant.

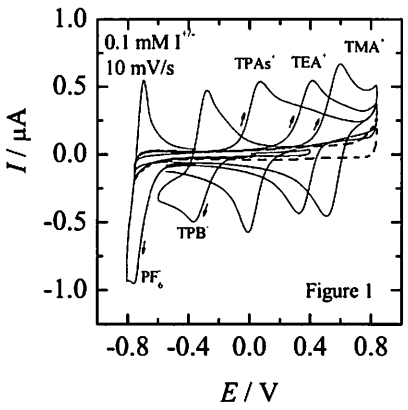

Figure 1

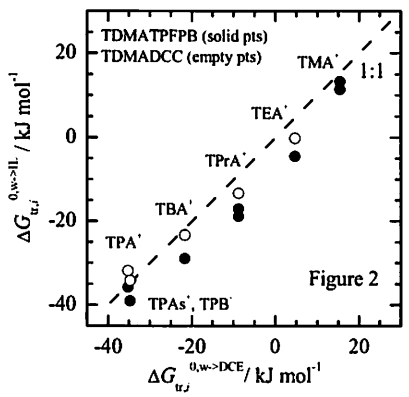

Figure 2

References

[1] Z. Samec J. Langmaier, T. Kakiuchi, *Pure Appl. Chem.* **81**, 1473 (2009).

[2] J. Langmaier, Z. Samec, *Electrochem.Commun.* **9**, 2633 (2007).

[3] J. Langmaier, A. Trojánek, Z. Samec, *Electroanalysis* **21**, 1977 (2009).

[4] J. Langmaier, Z. Samec, *Electrochim.Acta* **58**, 606 (2011).

[5] J. Langmaier, Z. Samec, *Electrochim.Acta* **87**, 591 (2013).

2PG05 Magnetic Orientation of Nematic Liquid Crystal in Contact with Aqueous Solution

A. Arima[1], Y. Nakatsuka[1], M. Suwa[1], and S. Tsukahara[1]

[1]*Department of Chemistry, Graduate School of Science, Osaka University, Toyonaka, Osaka 560-0043, Japan*

e-mail : msuwa@chem.sci.osaka-u.ac.jp

Magnetic orientation of Liquid Crystal (LC) strongly anchored by a functionalized solid has widely been studied to determine the elastic constants of LCs. Recently, Abbott et al. demonstrated that LC molecules were able to be weekly anchored at several aqueous solution/LC interfaces[1, 2]. In this study, we observed the magnetic orientation of LC in contact with aqueous solution and investigated the mechanism.

We examined 4-cyano-4'-pentylbiphenyl (5CB), which exhibits nematic LC phase at 25 °C. According to the procedure reported by Brake and Abbott[1], a stable thin film of 5CB was confined in a copper specimen grid for an electron microscope (100 lines / inch and 20 μm in thickness). One surface of the grid was covered with a glass treated with octadecyltrichlorosilane (OTS). One μL of 5CB was dropped on the grid. The excess of 5CB was removed by contacting a capillary tube, and then a flat film of 5CB was formed in each compartments of the grid. The other surface of 5CB was exposed to air or aqueous solution of sodium dodecyl sulphate (SDS) or was covered with OTS-treated glass. The magnetic orientation of 5CB was measured with polarization microscope with crossed polarizers. The average tilt angle of LC was estimated from the intensity of the transmitted light. A magnetic field, whose angle with respect to the direction of the polarization of incident was 45°, was applied to the sample by using a pair of Nd-Fe-B permanent magnets with a gap of 1 cm. The strength of the magnetic field up to ~500 mT was controlled by positioning the magnets.

In the absence of the magnetic field, the transmittance was almost zero in every case. This means that homeotropic alignment of 5CB was performed. By applying the magnetic field, the transmittance increased as shown in Fig. 1. The LC in contact with SDS solution was easier to align along the magnetic field than that anchored with OTS treated glass.

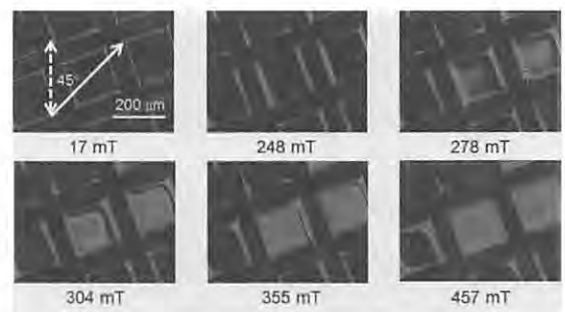

Figure 1 Increase of transmittance accompanied with the magnetic orientation of 5CB in contact with SDS aqueous solution of 2 mM: The solid and dashed arrows indicate the direction of the polarization of incident and the external magnetic field, respectively.

References

[1] J. M. Brake, N. L. Abbott, *Langmuir* **18**, 6101(2002).

[2] R. J. Carlton et al., *Langmuir* **28**, 12796(2012).

2PG06 Synthesis of ZnSe quantum dots using apoferritin as a sensor media for neurotransmitters

Song Li, and Sang Joon Park
Department of Chemical & Biological Engineering, Gachon University, Seongnam, 461-701, Korea
e-mail : psj@gachon.ac.kr

Apoferritin (AFt) is the demineralized form of the cellular iron storage protein ferritin. The 24 polypeptide subunits of AFt assemble automatically to form a hollow protein cage with internal and external diameters of 8 and 12 nm, respectively. Eight hydrophilic channels of *ca.* 4 A° permeate the protein cage, which facilitate the influx and efflux of metal ions and small molecules of appropriate size [1]. In the present work, ZnSe QDs were successfully prepared into the AFt cage with the aid of EDTA. AFt acts as a nanoreactor for ZnSe mineralization firstly and serves as a coating material for the formed QDs subsequently. Accordingly, the prepared ZnSe QDs were water soluble and stable against photo-oxidation after one day aging. In addition, we obtained two-dimensional ZnSe-ferritin nanodots by simple touch method with modification of silicon wafer surface. Then, the PL intensity of the QDs in solution and array were studied accompanying its conjugation reaction with neurotransmitters such as glycine, dopamine and GABA in order to utilize this material as a sensor media. In addition, the possible mechanism for PL enhancement and quenching was investigated and the results were discussed.

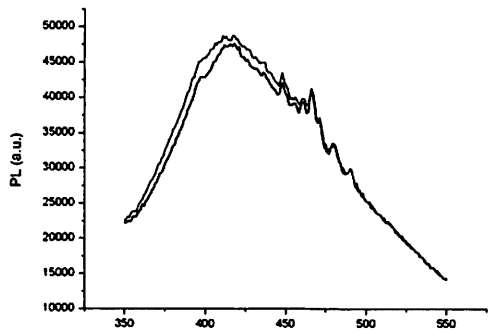

Fig. 1. PL spectrum of ZnSe quantum dots in apoferritin;
back line (as synthesis), red line (after one day aging).

References

[1] T. Ueno, M. Suzuki, T. Goto, T. Matsumoto, K. Nagayama Y.Watanabe, *Angew. Chem., Int. Ed.*, **43**, 2527(2004)

2PG07 Solvent Extraction of Sr and Cs in Solid/liquid Interface

T. Tanaka[1]

[1]*Nuclear Safety Research Center, Japan Atomic Energy Agency, Ibaraki 319-1195, Japan*
e-mail : tanaka.tadao26@jaea.go.jp

Radioactive Sr and Cs dispersed into environment by the Fukushima Daiichi Nuclear Power Plant accident in March, 2011. The decontamination activities of radioactive Cs which widely deposited in living environment are just going to remediate the environment. For the planning the environmental remediation activities, it is effective to understand beforehand the migration behaviour and sorption mechanism of Sr and Cs on ground surface, in order to select the rational decontamination methods. In this research, applicability of a solvent extraction technique was examined to clarify interactions of Sr and Cs on interface of sand with solutions.

By inflowing radioactive Sr (^{85}Sr) and Cs (^{137}Cs) solution into a column packed a sand, the sand sample contaminated with Sr and Cs was prepared. The Sr and the Cs sorbed on sand was sequentially extracted with deionized water, calcium chloride solution, potassium chloride solution, hydrochloride solution of hydroxylamine, potassium oxalate solution, and hydrogen peroxide.

1st step: Exraction with deionized water.
2nd step: Extraction with 0.5M $CaCl_2$ to remove ion-exchangeable sorptive fractions.
3rd step: Extraction with 0.5M KCl to remove specific sorptive fractions into interlayer of clay minarals.
4th step: Extraction with 0.1M NH_2OH-HCl to remove sorptive fractions onto amorphous Fe and/or Mn oxyhydroxide/oxide.
5th step: Extraction with 0.1M K-oxalate to remove sorptive fractions onto crystallized Fe and/or Mn oxyhydroxide/oxide.
6th step: Reaction with 30 w% H_2O_2 to digest fractions interacted with organic substances.

All the Sr sorbed on the sand was extracted by the deionized water and the $CaCl_2$ solution, and this shows that the sorption of the Sr was dominated by reversible ion-exchange. About 40 % of the Cs was extracted by the KCl solution, and considerable amount of the Cs remained on the sand after the 6th step. These results suggested that the Sr and Cs fractions sorbed reversibly on the sand, which will be a target for the decontamination activity, can be estimated by the extraction procedure with the KCl solution.

The extraction procedure is indirect technique to identify sorption mechanisms. In the case of difficulty of direct analysis, example for identification of minor constituent like radioactive elements in environment, the extraction procedure is a simple and an effective technique.

2PG08 Observation of large hydrolytic aluminum polyoxocation (Al_{26} and Al_{30}) using electrospray ionization mass spectrometry

T. Urabe[1] and M. Tanaka[2]

[1] *RIKEN, Hirosawa 2-1, Wako-shi, Saitama 351-0198, Japan*

[2] *Graduate School of Marine Science and Technology, Tokyo Univ. of Marine Sci. and Tech., Konan 4-5-7, Minato-ku, Tokyo 108-8477, Japan*

e-mail: t-urabe@riken.jp

The behaviour of hydrolytic aluminum species in solution has been extensively studied. In particular, special attention has been paid to polynuclear species, such as $[AlO_4Al_{12}(OH)_{24}(H_2O)_{12}]^{7+}$ (Al_{13}). In 2000, two independent groups found aluminum polyoxocation larger than Al_{13} existed in solution, and it was identified as $[Al_{30}O_8(OH)_{56}(H_2O)_{26}]^{18+}$ (Al_{30})[1,2]. Such a large polyoxocation shows specific characteristics (*e.g.* surface activities due to its charge and size). And a number of studies have been reported for the nature of Al_{30}. However, these studies were limited by analytical difficulties. Only one technique, nuclear magnetic resonance (^{27}Al-NMR), can be applied for the direct detection of Al_{30} in solution, but not all species were identified or even detected. In this study, we observed polynuclear species including Al_{30} using electrospray ionization mass spectrometry (ESI-MS) as a powerful tool for enlightening solution chemistry of large metal polyoxocation.

A sample solution containing Al_{30} was prepared by the following procedure. The 1 mol/L (M) of NaOH was added dropwise to 1 M of $AlCl_3$ solution maintained at 80 °C with water bath under fast stirring. The degree of neutralization was $[OH]_{add}/[Al]_T$=2.4. Then, the solution kept heated at 80 °C for 2 h with stirring. And the solution in a sealed vial was settled in an oven at 95 °C for 12 h. The solution was measured by ESI-MS (Shimadzu LCMS-2010A) in the positive ion mode.

From ESI mass spectra, the dominant peaks were identified as Al_{30} with trivalent and tetravalent charges, namely $[Al_{30}H_{35}O_{61}(H_2O)_n]^{3+}$ (n=0-11) and $[Al_{30}H_{48}O_{67}(H_2O)_n]^{4+}$ (n=0-7). These species were charge-reduced from $[Al_{30}O_8(OH)_{56}(H_2O)_{26}]^{18+}$ in the solution during ion transfer to gas phase. Similarly, $[AlO_4Al_{12}(OH)_{24}(H_2O)_{12}]^{7+}$ in the solution was observed with divalent and trivalent charges. Another species, which may correspond to unidentified species reported with ^{27}Al-NMR[3], was observed as $[Al_{26}H_{37}O_{56}(H_2O)_n]^{3+}$ (n=0-8). This suggests direct dimerization of Al_{13} in the formation process of Al_{30} although Al_{14} was postulated as a precursor by ^{27}Al-NMR[3]. This study shows that such a large complex (Al_{30} and Al_{26}) was successfully detected with ESI-MS at the first time, and reveals a suitability of ESI-MS not only for organic macro molecules (*e.g.* protein) but also for giant inorganic polyoxocation. Further investigation will be shown for chemical process of Al_{30} formation.

References

[1] L. Allouche, C. Gerardin, T. Loiseau, G. Ferey, F. Taulelle, *Angew. Chem. Int. Ed.* **39**, 521(2000).

[2] J. Rowsell, L. F. Nazar, *J. Am. Chem. Soc.*, **122**, 3777(2000).

[3] L. Allouche, F. Taulelle, *Inorg. Chem. Commun.* **6**, 1167(2003)

2PG09

Theoretical Investigation of the Electron Transfer Process in Water

○ K. Usui, D. Yokogawa, and S. Irle

WPI-ITbM & Department of Chemistry, Nagoya University, 464-8601, Japan

e-mail : usui.kosuke@f.mbox.nagoya-u.ac.jp

In biochemical and medical fields, bioimaging probes are greatly required, and based on their emission, one can understand what happens *in vivo*. Up to now, some typical but effective molecular frameworks, such as fluorescein, rhodamine, BODIPY, and cyanine, have been suggested in experimental works, and they are also studied in terms of the molecular design.

Quantum chemistry is a powerful tool to theoretically predict molecular properties. However, there are some difficulties for the design of bioimaging molecules using present theoretical approaches. One important point is how to treat both the electronic structure and solvent, especially water. Therefore, we focused on this point and investigated three different electronic states (ground, charge transfer, and excited states) for several Donor-Acceptor pairs in water.

In the present study, the RISM-SCF-SEDD method[1] was employed to include the solvent effect and combined with multi-configuration quasi-degenerate 2nd order perturbation theory (MCQDPT2) to describe the electronic structures. In this approach, due to the non-equilibrium treatment of solvation with hypothetical charge distribution [2], free energy plots were obtained. As an example, simulated free energy curves are shown in **Figure 1**. As the acceptor strength increases (*p*-DCB < NB < *p*-QN), the charge transfer state curve shifts to lower energies. This result implies that our approach can be applied to discuss the energetics of the charge transfer process. Specifically speaking, the activation free energy becomes small corresponding to the acceptor strength. The predicted order agrees with the experimentally observed redox potentials. The charge transfer mostly occurs from a donor molecule at excited state to an acceptor at ground state, so our approach was also applied to the "true" excited state, and our method allows us to discuss the energy relaxation path. Detailed discussion will be performed in the poster session.

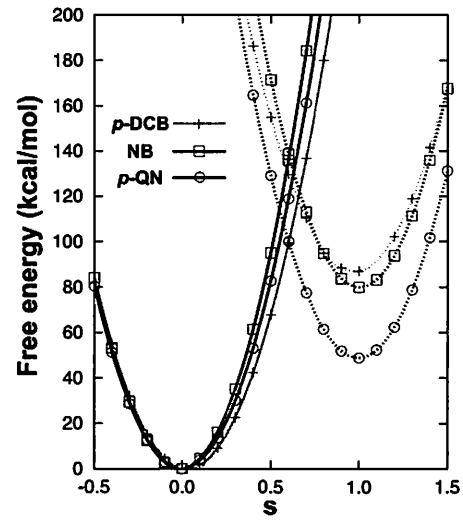

Figure 1. Simulated free energy curves (solid : ground state, broken : charge transfer state) for phenol with *p*-dicyanobenzene (*p*-DCB), nitrobenzene(NB), and *p*-quinone(*p*-QN) systems. *s*, is a mixing coefficient to reproduce the hypothetical charge distribution.

References

[1] D. Yokogawa, H. Sato, and S. Sakaki, *J. Chem. Phys.* **126**, 244504 (2007).

[2] H. Sato, F. Hirata, *J. Phys. Chem. A.* **106**, 2300, (2002)

2PG10 Accelerated Molecular Dynamics Study of Cis-Trans Isomerization of Azobenzene: Kramers Theory Validation

Y. Shigemitsu[1,2], and Y. Ohga[3]

[1]*Industrial Technology Center of Nagasaki, Ikeda Omura Nagasaki 856-0026, Japan*
[2]*Gaduate School of Engineering, Nagasaki University, Nagasaki 852-8521, Japan*
[3]*Department of Applied Chemistry, Oita University, Oita 870-1124, Japan*
e-mail : shige@tc.nagasaki.go.jp

The reaction kinetics of 4-dimethylamino-4'-nitrobenzene (DNAB) in solution was experimentally analysed in wide range of pressure (up to GPa), where the cis-trans isomerisation takes place on milliseconds or longer time scale [1]. Such long time scale is not reachable by normal MD simulations. Instead, Accelerated Molecular Dynamics (aMD) [2] can realize longtime MD simulations (nanoseconds or longer) in explicit solvents in terms of biased energy potential. In general, isomerisation reaction rate is obeyed to transition state theory (TST), where reactant and transition state are kept in thermally equilibrium. It is well known, however, that non-TST behaviours of isomerization kinetics have been studied in the area of laser-pumped excited dynamics. Under high solvent pressure as well, the reaction rate is retarded by solvent friction and deviates from that of TST owing to high solvent viscosity. Kramers theory and its derivatives, alternative formulations of reaction rate to TST, does not suppose chemical equilibrium between reactant and TS, and models chemical reaction as random walk processes through the collision between solute and solvent molecules to surmount potential energy barrier.

In the present study, aMD simulations were carried out by mean of AMBER version12 program. DNAB was constructed by means of Leap module with AMBER99 force field. The cis-trans twist barrier of the central bond (-C-N=N-C-) was replaced by the value refined by DFT(B3LYP)/6-31G(d). The molecule was immersed in 1566 TIP3P water molecules in a cubic box and the whole system was thermally equilibrated. Several aMD production runs were carried out under NPT ensemble (1atm, 300K) and the cis-trans isomerisation frequencies were counted from the extracted trajectories. The reaction rate was retrieved by extrapolating the aMD rate to zero bias limit. The aMD-obtained rates are compared with those of normal MD and of experiments are discussed.

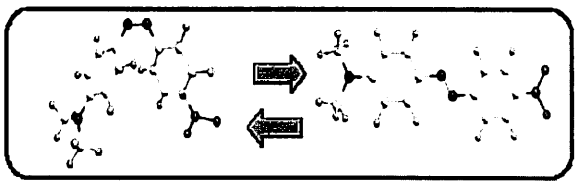

$$\ln(k_{KGH}^{(\alpha,p,q)}) = \ln(\frac{\lambda_{KGH}}{2\pi}) - (F_0 - \frac{q}{\alpha + p}) / k_B T$$

References

[1] T.Asano, T.Yano, T.Okada, J.Am.Chem.Soc., 104, 4900 (1982); T.Asano, T.Okada, J.Org.Chem., 104, 4900 (1982)

[2] U.Doshi and D.Hamelberg, JCTC, 7, 575 (2011).

2PG11

Phosphonate modified silica For adsorption of Cu(II), Co(II), Ni(II), and Zn(II)

Dian M. Widjonarko[1,2], Jumina[3], Indriana Kartini[3], Nuryono[3]

[1] *Doctorate student at Department of Chemistry, Faculty of Mathematics and Natural Science, Gadjah Mada University, Yogyakarta, Indonesia*

[2] *Department of Chemistry, Faculty of Mathematics and Natural Science, Sebelas Maret University, Surakarta, Indonesia*

[3] *Department of Chemistry, Faculty of Mathematics and Natural Science, Gadjah Mada University, Yogyakarta, Indonesia*

e-mail: nuryono_mipa@ugm.ac.id

A new phosphonate modified silica (PMS) has been investigated for adsorption of Cu(II),Co(II), Ni(II), and Zn(II) in aqueous solution. The adsorbent was synthesized by immobilizing aminoethyl-dihydrogen phosphate ($AEPH_2$) on 1,4-dibromobutane grafted silica. The properties of adsorbent were investigated using Fourier Transform Infrared (FTIR) spectroscopy, X-ray Fluoresence (XRF), and N_2 gas adsorption-desorption. The adsorption was carried out in a batch system by mixing solution of metal ions with the adsorbent at various pHs, contact times, and initial metal ion concentrations. The unadsorbed metals were determined by Flame Atomic Absorption Spectrophotometerer (FAAS). Results of characterization showed that PMS has been successfully prepared, and the product contained 1.33 % (w/w) phosphorus with the surface area, pore volume, and pore size of 115.3 m^2g^{-1}; 0.7578 mL g^{-1}; and 131.4 A^o, respectively. Adsorption of metal ions investigated on PMS occurred quite fast, less than 30 minutes. Modification of phosphate on silica increased the adsorption capability, up to 8 times higher than that of unmodified silica with various increase degrees, depending on metal ion types and pH solution. The capacity order adsorption was Cu>Co>Ni>Zn. Based on the adsorption characteristic, the adsorbent has potency to be applied as the material for solid phase extraction of trantion metal ions.

2PI01 Understanding the thermophysical properties of the dissolution of CO_2 in aqueous solutions of demixing amines

K. Ballerat-Busserolles[1,2], Y. Coulier[1,2] , J-Y. Coxam[1,2]

[1] *Clermont Université, Université Blaise Pascal, Institut de Chimie de Clermont - Equipe Thermodynamique et Interactions Moleculaires, BP 10448, F-63000 CLERMONT-FERRAND*

[2] *CNRS, UMR 6296, ICCF/TIM, BP 80026, F-63171 AUBIERE*

e-mail : karine.ballerat@univ-bpclermont.fr

Carbon Capture and Storage (CCS) is one of the main options for CO2 mitigation. Post-combustion capture processes using amines are considered as one of the most adequate methods for CCS [1,2]. However, the energetic cost of avoided CO2 is very high and must be significantly reduced. Thus, several research groups are presently interested in the identification of new solvents with the aim to reduce the cost of the regeneration step. The objective of this research is to study a new class of amines. Demixing amines have the singularity to undergo a liquid-liquid phase separation in aqueous solutions as a function of temperature, composition and CO2 loading charge. These compounds can be considered as new absorbents for CO2 capture. New processes using such demixing amines in removing carbon dioxide from post combustion effluent will require less energy [3]. An overview of the first thermophysical properties of demixing amines based on piperidine skeleton is reported. The specific amines investigated were N-methylpiperidine, 2-methylpiperidine and N-ethylpiperidine. The liquid-liquid equilibria (LLE) were first determined and analyzed [4]. Excess molar volumes and excess molar enthalpies in aqueous solutions of methylpiperidines were then measured over a range of temperatures where the amine is fully miscible in water.

The enthalpies of solution and solubility limits of CO2 in binary solutions were also studied. The experimental data was obtained for {CO2 - 2-methylpiperidine - water} system using a flow calorimetric technique.

Finally a strategic program for the characterization of carbon dioxide absorption in aqueous solutions of demixing amines will be presented. The objective of the project, supported jointly by ANR in France and NSERC in Canada, is to analyze the structure-properties relationships for different substituted piperidines.

References

[1] Rao, A.B. and E.S. Rubin, Environmental Science & Technology, 2002. 36(20), 4467-4475.

[2] L. Raynal, P-A. Bouillon, A. Gomez, P. Broutin, Chemical Engineering Journal, DOI : 10.1016/j.cej.2011.01.008

[3] Zhang, J., et al., Chemical Engineering & Technology, 2011. 34(9): p. 1481-1489

[4] Y. Coulier, K. Ballerat-Busserolles, L. Rodier, J-Y. Coxam, Fluid Phase Equilibria, 296, 206-212 (2010)

2PI02 Interactions of Mo(VI) oxyanions with metal cations: thermodynamic modeling in natural waters

E. Kremer[1], L. Gonzatto[1], F. Tissot[2], G. Peinado[1], J. Torres[1], C. Kremer[1]

[1]*Cátedra de Química Inorgánica, DEC, Facultad de Química, Uruguay*

[2]*Cátedra de Química Analítica, DEC, Facultad de Química, Uruguay*

e-mail: ekremer@fq.edu.uy

Reliable thermodynamic data describing aqueous chemical speciation are essential for developing models to predict the fate of the trace elements in natural systems. A useful chemical model must include experimental values of the appropiate thermodynamic equilibrium constants. In most conditions prevailing in low depth natural waters, Mo(VI) anions are the only soluble thermodynamically stable species of this element. Molybdenum(VI) forms oxo/hydroxospecies including polyanions[1]. The mobility of this element in aquatic media is highly dependent on the presence of free molybdate anion, MoO_4^{2-}, its prevalent species in natural waters. The mobility of this and other Mo(VI) polyanions may, however, be hindered by the interaction with the major cations present in the aquatic environment. The available experimental thermodynamic data concerning the interaction of molybdate anions with metal cations are very scarce. Most of them involve the measurement of +2 cations molybdate salts solubility, but do not include the detection of soluble species[2].

In this work we report the potentiometric study of oxyanions of Mo(VI) and their interaction with some other metal cations: Ca^{2+}, Mg^{2+}, Sr^{2+}, Ba^{2+}, Mn^{2+}, Fe^{2+}, Co^{2+}, Ni^{2+}, Cu^{2+}, Zn^{2+} and Cd^{2+}. Experimental conditions were chosen to simulate natural waters conditions: 20.0 °C and low ionic strength. The influence of the supporting electrolyte was also evaluated for some selected systems.

Results show that the interaction of molybdate anion with M(II) cations is relatively weak (log *K* for the $[M(MoO_4)]$ species formation in the order of 2) and very similar for all studied systems. Polyoxomolybdate anion $Mo_7O_{24}^{6-}$ also interacts with all studied metal cations giving place to $[M(Mo_7O_{24})]^{4-}$. For total molybdenum concentration below 1 mM, the predominant form of molybdenum(VI) is MoO_4^{2-} above pH 4.4, with a variable percentage of $[M(MoO_4)]$, depending on the M(II) concentration. For more acidic conditions, $HMoO_4^-$ is formed, together with $[M(HMoO_4)]^+$ in some systems. For higher total molybdenum concentrations, polyanions and $[M(Mo_7O_{24})]^{4-}$ become predominant. For natural waters simulation, taking for example 10^{-7} M Mo(VI) total concentration, in the presence of mean natural groundwater concentrations of major cations, $[Ca(MoO_4)]$ predominates, accounting for *ca.* 80% of the element. Thus, molybdenum(VI) mobility and availability is infuenced by pH value and the presence of major cations in the natural waters.

This work was partially supported by CSIC (Programa de Apoyo a Grupos).

References

[1] Richens, D.T., 1997. The Chemistry of Aqua Ions, Wiley and Sons, New York

[2] IUPAC, Stability Constants Database, 2007

2PI03 Excess Gibbs energy of activation of binary mixtures of {water + poly(ethylene glycol)} at different temperatures and atmospheric pressure

Heloisa E. Hoga[1], Ricardo B. Tôrres[2], Pedro L.O. Volpe[1]

[1]*Departamento de Físico-Química, Universidade Estadual de Campinas, Cidade Universitária Zeferino Vaz, 13083-970, Campinas, São Paulo, Brazil.*

[2]*Departamento de Engenharia Química, Centro Universitário da FEI, Av. Humberto de Alencar Castelo Branco, 3972, 09850-901, São Bernardo do Campo, São Paulo,Brazil.*

e-mail: helhoga@iqm.unicamp.br

Experimental data of density and viscosity of liquid mixtures and the derived properties are very important in many industrial processes where fluid flow is important. Moreover, knowledge of the dependence of viscometric properties of mixtures liquid is a powerful tool in understanding the physico-chemical behavior of liquid systems. In this work, density and viscosity values of binary mixture of water + monoethylene glycol, or + diethylene glycol, or + triethylene glycol, or + PEG200, or + PEG300, or + PEG400, or + PEG600 have been used to calculate excess Gibbs energy of activation of viscous flow over the entire composition range at (293.15, 298.15, 303.15 and 308.15) K and atmospheric pressure. Density and viscosity of both pure liquids and their mixtures were measured using a commercial densimeter and speed of sound analyzer (Anton Paar DSA 5000) and a Stabinger viscosimeter (Anton Paar SVM 3000M), respectively. For all systems studied, the excess Gibbs energy of activation values was positive and becomes less positive with increasing temperature. Excess Gibbs energy of activation for viscous flow can be used to detect molecular interactions. The positive values of excess Gibbs energy of activation can be an indicative of specific interactions between the unlike molecules present in the mixtures

2PI04 Hydration Thermodynamics by Simple Molecular Models

J. Jirsák[1,2], J. Škvor[2], and I. Nezbeda[1,2]

[1]*Faculty of Science, J. E. Purkinje University in Ústí nad Labem, 400 96 Ústí nad Labem, Czech Republic*

[2]*Institute of Chemical Process Fundamentals, Academy of Sciences of the Czech Republic, 165 02 Praha 6, Czech Republic*

e-mail : jan.jirsak@ujep.cz

Water exhibits anomalous behavior as both a pure liquid and a solvent. Aqueous solutions of solutes ranging from nonpolar over polar and associating to ionic show unusual thermodynamic effects, which are often not properly described by common chemical-engineering models. In order to obtain more sophisticated and thermodynamically consistent expressions with a higher potential for true prediction, one can employ a molecular theory based on a suitable model for molecular interactions. The model has to be simple enough to make a mathematical treatment possible, yet complex enough to preserve the traits necessary for a qualitatively correct description. A number of simple molecular models have been proposed, based on different opinions on what is essential for a water-like behavior, each model qualitatively reproducing some of the desired properties of pure water and simple aqueous solutions. [1]

In the present contribution, an associating fluid theory based on simple, so-called primitive, models is described and its application to aqueous solutions demonstrated. The model has already been used by the group of the present authors to reproduce, qualitatively, the anomalies of pure liquid water and some properties of aqueous mixtures. [1, 2] An attempt is made to move further along this path toward a concise molecular-level understanding of hydration phenomena, especially the hydrophobic hydration.

Equations of state are derived within the thermodynamic perturbation theory using strongly non-additive, pseudo-hard bodies as a reference system. The construction of a pseudo-hard body reflects the finding that not only attractive but also repulsive interactions are needed to appropriately describe the structural effects of hydrogen bonding. [1] Simulation data on mixtures of pseudo-hard water and hard models of selected inorganic solutes – such as rare gases, carbon dioxide, or hydrogen sulphide – are parametrized into a reference pressure function, which is then combined with attractive terms to form a molecular-based equation of state for the solution. The equation of state allows for a consistent calculation of all thermodynamic properties of the mixture.

This research has been supported by the Czech Science Foundation (Grant No. P208/12/P710).

References

[1] I. Nezbeda, J. Jirsák, *Phys. Chem. Chem. Phys.* **13**, 19689(2011).

[2] M. Rouha, I. Nezbeda, *Mol. Phys.* **109**, 613(2011).

2PI05 Quantum Chemical Study of Glucose Hydrolysis in Acid Environment Using RISM-SCS-SEDD

Arifin[1,2], D. Yokogawa[1,2], and S. Irle[1,2]

[1]*Department of Chemistry, Nagoya University, Nagoya 464-8601, Japan*

[2]*Institute of Transformative Bio-Molecules (WPI-ITbM), Nagoya 464-8602, Japan*

e-mail : arifin@b.mbox.nagoya-u.ac.jp

Introduction:

Transformation of glucose into 5-(Hydroxymethyl)furfural (HMF) is believed to be one of many key reactions for producing 'green chemicals'. Previous research suggests that transformation of glucose to HMF can occur after the isomerization to fructose (**B**); fructose can then be directly dehydrated to HMF (**A**), as shown in Scheme 1 [1]. These reactions were experimentally performed in the alkylimidazolium chloride ionic liquid, such as 1-ethyl-3-methylimidazolium. Before we model these reactions with ionic liquids as solvent, we decided to study these mechanisms under acidic aqueous condition.

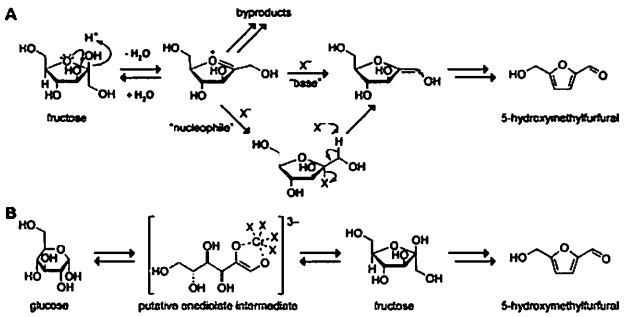

Scheme 1

Computational Detail:

All of the geometries and frequencies were calculated at the DFT B3LYP level of theory, and single-point energies were calculated with the CCSD(T) method. The RISM-SCF-SEDD method [2] was used for solvation, as implemented in the GAMESS program.

Results and discussion:

Fig 1. shows that the free energy of activation for the isomerization into fructose was 25.87 kcal mol^{-1} (from **1** to $\mathbf{TS_{23}}$) with RISM method. In other hand, the popular solvation method, CPCM, seems underestimated the barrier (17.15 kcal mol^{-1}). The activation energy that produced by RISM was about 28.61 kcal mol^{-1}, show good agreement with previous experimental result, 33.20 kcal mol^{-1}. The whole results are presented in the poster.

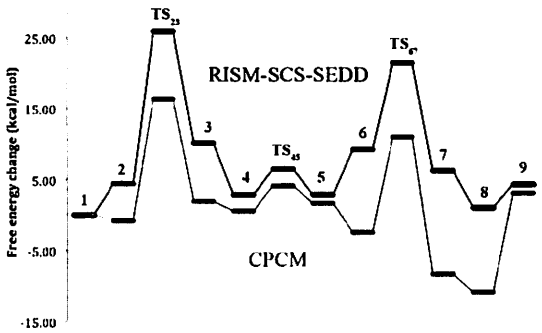

Fig 1. Free energy change of isomerization from glucose to fructose

References

[1] J. B. Binder, R. T. Raines, *J. Am. Chem. Soc.* **131**, 1979(2009)

[2] D. Yokogawa, H. Sato, S. Sakaki, *J. Chem. Phys.* **126**, 244504(2007).

2PI06 An Approach to Partial Molar Volume of Ions Based on Molecular Simulation

Y. Kawabata[1], R. Akiyama[1]

[1]*Department of Chemistry, Kyushu University, Fukuoka 812-8581, Japan*

e-mail : ykawa@chem.kyushu-univ.jp

Partial molar volume change ΔV_p for a reaction is an important quantity to transform ΔS_V to ΔS_P for the reaction, where ΔS_V and ΔS_P are the entropy changes under isochoric condition and under isobaric condition, respectively. Various ions participate in many chemical reactions and partial molar volume of ions cannot be obtained easily by experiments. We, therefore, examined a method to calculate partial molar volume of an ion in water on the basis of molecular simulations and Kirkwood-Buff (KB) theory. In KB theory, partial molar volume of a solute at infinite dilution can be obtained from Kirkwood-Buff integral (KBI) G that is defined by radial distribution function (RDF) $g(r)$ as follows[1]:

$$V_p = \kappa kT - G,$$

$$G = \lim_{R\to\infty} G(R) = \lim_{R\to\infty} \int_0^R 4\pi(g(r)-1)r^2 dr \quad ,$$

where κ is isothermal compressibility of the system. According to literature[2], the value of KBI is independent on the definition of "position of molecule". Actually, the value for a solute does not depend on the definition of molecular position, when the net charge of solute molecule is zero. Two kinds of definitions of the position of water are examined and Fig. 1 shows KBIs as functions of integral cut-off distance R obtained from methane-water RDFs. Those KBIs converge to same value. In case of ions, however, it is not always adequate in simulation condition. Fig. 2 shows KBI for bromide ion in water. Unlike the methane case, two KBIs don't converge to same value within this integral cut-off distance. We will discuss our results and this problem at the poster presentation.

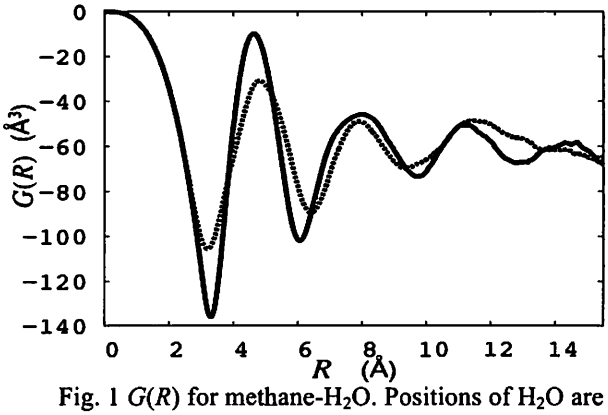

Fig. 1 $G(R)$ for methane-H_2O. Positions of H_2O are defined as O(−) and H(--).

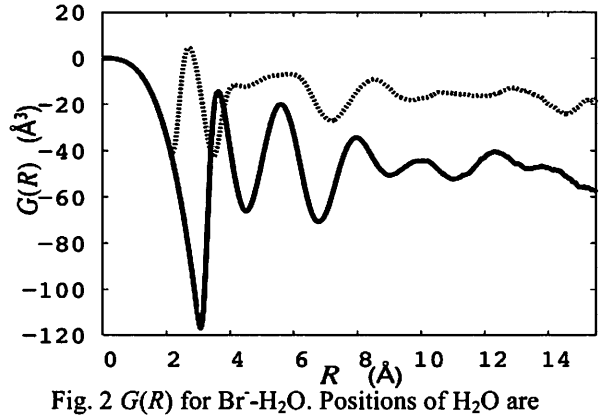

Fig. 2 $G(R)$ for Br^--H_2O. Positions of H_2O are defined as O(−) and H(--).

References

[1] Kirkwood, J. G., Buff, F. P., *J. Chem. Phys.* **19**, 774(1951).

[2] Lockwood, D. M., Rossky, P. J., *J. Phys. Chem. B* **103**, 1982(1999).

2PI07 Theoretical Study of the additive decomposition in Lithium-Ion Batteries

K. Kasahara[1], and H. Sato[1,2]

[1]*Department of Engineering, Graduate School of Engineering, Kyoto University, Nishikyo-ku, Kyoto 615-8510, Japan*

[2]*ESICB, Kyoto University*

e-mail : kasahara.kento.56s@st.kyoto-u.ac.jp

[Introduction] Vinylene carbonate (VC) is one of the most used electrolyte additives of Lithium-Ion batteries. VC plays a very important role in the performance and safety of Lithium-Ion batteries. In the presence of VC, the solid electrolyte interface (SEI) film is formed on the surface of graphite anode and the solvent decomposition is inhibited [1]. It was reported that VC is decomposed into CO and CO_2 [2], and it is expected to get a clue of understanding the mechanism for the formation of SEI by investigating the emission processes. In this study, we focused on the CO emission process shown in **Fig. 1** and evaluated the solvation effects on this process using RISM-SCF-SEDD method.

[Computational Details] Geometry optimizations were carried out by DFT (B3LYP) with aug-cc-pVDZ, followed by CCSD energy evaluation. Computations in pure ethylene carbonate (EC) and 1 M $LiClO_4$/EC at 298.15 K were then carried out with the RISM-SCF-SEDD using GAMESS modified by us. The RISM integral equations were solved with Kovalenko-Hirata closure.

[Results and Discussion] Through the ionization of VC, the structure around C_{v1} is changed from planar to tetrahedral. Then the dissociation of C_{v1}-O_{v3} bond occurs and finally CO is produced by the dissociation of O_{v2}-C_{v1} bond. The free energy changes along the CO emission process are given in **Fig. 2**. In solution phases, all states are stabilized compared with those in the gas phase. In the presence of $LiClO_4$, they are further stabilized. This result indicates that the reaction easily occurs due to the electrostatic interaction between VC^- and Li^+.

[References]

[1] P. B. Balbuena, Y. Wang, *Lithium-Ion Batteries – Solid-Electrolyte Interphase –* , Imperial College Press (2004).

[2] H. Ota et al., *J. Electrochem. Soc.*, **151**, A1659 (2004).

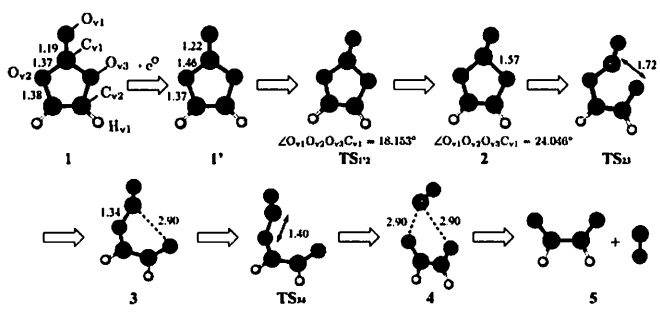

Fig. 1 : Geometry changes in CO emission of VC in gas phase. Bond lengths are in angstrom.

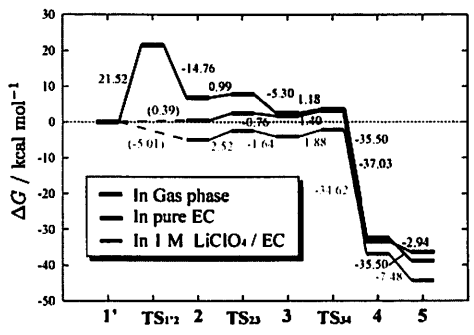

Fig. 2 : Free energy changes.

2PI08 Volumes and Isentropic Compressions of Solvation of Hydrofluoroether in Alcohol, Alkoxyalcohol and Ether

K. Inagaki [1], H. Ogawa [1,2], F. Kimura[2], T. Minamihonoki[2]

[1] *Graduate School of Tokyo Denki University, Hatoyama, Saitama, Japan*

[2] *Tokyo Denki University, Hatoyama, Saitama, Japan*

e-mail: 12rmr01@ms.dendai.ac.jp

In order to make clear the volumetric behavior of hydrofluoroether, HFE solvated in organic solvents, apparent partial molar volumes $V_{m,2}^{\infty}$ and apparent partial molar isentropic compressions $K_{s\,m,2}^{\infty}$ at infinite dilution of HFE in heptane, alcohols(methanol, ethanol, 1-propanol, 1-buthanol), alkoxyalcohols (2-methoxyethanol, 2-ethoxyethanol, 2-propoxyethanol, 2-buthoxyethanol, 2-(2-methoxyethoxyethanol)) and polyethers (1,2-dimethoxyethane, bis(2-methoxyethyl)ether) have been determined from density and sound velocity measurement. Density and sound velocity measurements were carried out using a vibrating-tube densimeter (DMA-602M, Anton Paar) and a sing-around unit (UVM-2, Cho-onpa Kogyo) with 5.000 cm of acoustic cell at 298.15K, respectively.

Results obtained were plotted against the number of carbon atom contained in solvent molecule, n_C in Figs 1. As shown in Fig. 1a, $V_{m,2}^{\infty}$ of HFE is increased especially in alcohols and alcoxyalcohols solvents as increase of n_C, and which will be attributed to weakening of dipole-dipole interaction between HFE and solvent molecular. However, compression does not vary so much in the same chemical species as obsreved from Fig. 1b. The magnitude of volume and compressibility of vicinity of HFE are seen in order heptane > alcohol > alcoxyalcohol > ether, that is considered to be contractin by hydrogen-bonding formed between positively polarized hydrogen atom near fluorine atom in HFE and ether oxygen atom in alcoxyl and ether group. These phenomena could not be expected from the results of previous study measured against the whole composition range [1].

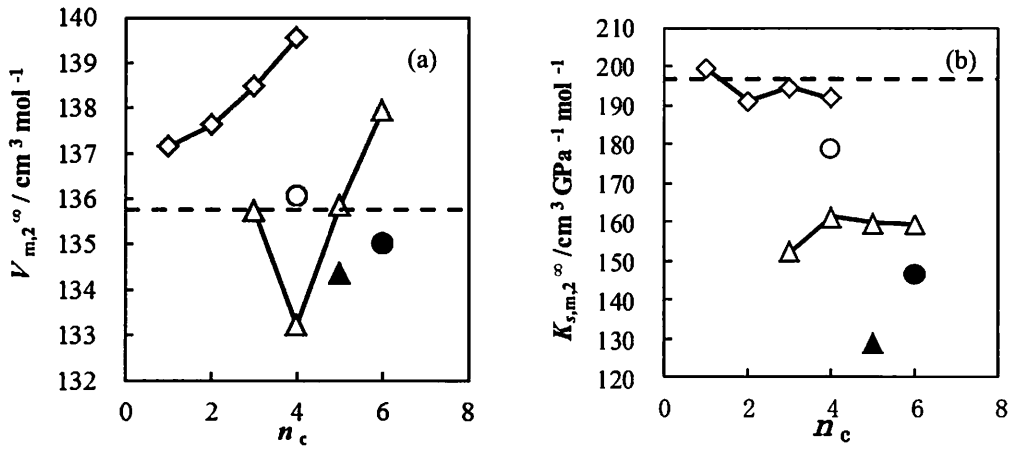

Figs. 1 Partial molar volume, $V_{m,2}^{\infty}$ (a) and partial molar isentropic compression, $K_{s\,m,2}^{\infty}$ (b) of HFE against the number of carbon atom in solvent molecule n_c. Solvents; ◇, alcohol: △, alcoxyalcohol: ▲, 2-(2-methoxy-ethoxyethanol: ○, 1,2-dimethoxyethane: ●, bis(2-methoxyethyl)ether. Line; ···, value of pure HFE

Reference

[1] H. Ogawa, S. Karashima, T. Takigawa, S. Murakami, J. Chem. Thermodynamics, 35 (2003) 763-774.

2PI09 Solvation of cyclic hydrogen-bonding acceptor compounds in alkan-1-ols (n=1-6)

N. Matsui *, F. Kimura **, H. Ogawa **

*Graduate School of Science and Engineering, Tokyo Denki University, Hatoyama, Hikigun, Saitama 350-0394 Japan

** School of Science and Engineering, Tokyo Denki University, Hatoyama, Hikigun, Saitama 350-0394 Japan

E-Mail to Matsui: 12rmr13@ms.dendai.ac.jp

Due to the strong hydrogen-bonding acceptor ability of C=O oxygen and NCH_3 nitrogen, 1-methyl-2-pyrrolidone (NMP) is capable of interacting with hydrogen bond donor alcohols. [1]

Partial molar quantities of NMP as well as cyclopentanone, a 5-membered cyclic ketone and 1-methylpyrrolidine, a 5-membered cyclic tertiary amine, at infinite dilution in a series of n-alcohol solvents were determined and compared each other to investigate the hydrogen bond forming ability of the C=O oxygen and the NCH_3 nitrogen with alcoholic OH.

Partial molar excess enthalpies $H_{m,1}^{E,\infty}$,partial molar excess volumes $V_{m,1}^{E,\infty}$ and partial molar compressibilities $\kappa_{s,1}^{\infty}$ of NMP, cyclopentanone and 1-methylpyrrolidine at infinite dilution in alkan-1-ols (n=1-6) were determined from enthalpies of solution, densities and sound velocities of their dilute solutions measured at 298K under atmospheric pressure.

Results of $H_{m,1}^{E,\infty}$ and $V_{m,1}^{E,\infty}$ are shown in Fig. 1, and $\kappa_{s,1}^{\infty}$ are plotted against $V_{m,1}^{E,\infty}$ in Fig. 2. Values of $H_{m,1}^{E,\infty}$, $V_{m,1}^{E,\infty}$ and $\kappa_{s,1}^{\infty}$ of NMP as well as cyclopetanone in a series of alcohol solutions increase with increasing number of carbon atoms of n-alcohol solvents, while the values of $H_{m,1}^{E,\infty}$, $V_{m,1}^{E,\infty}$ and $\kappa_{s,1}^{\infty}$ of 1-methylpyrrolidine are hardly dependent on the number of carbon atoms of n-alcohol solvents.

Resemblance of the solvation behaviors of NMP solutions and cyclopentanone solutions suggests the C=O oxygen of amide group plays dominant role for the hydrogen bond forming ability of NMP with alcoholic OH in NMP - n-alcohol solutions.

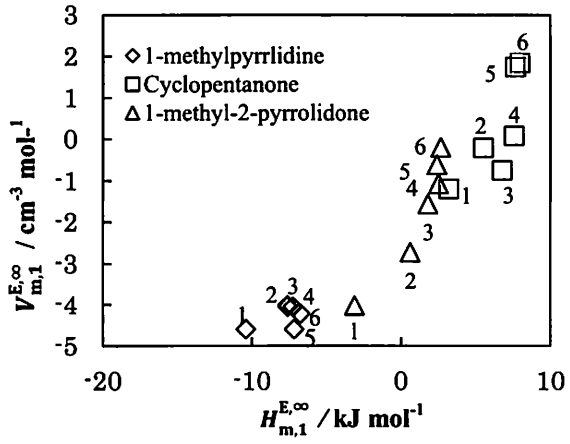

Fig. 1 Correlation of $H_{m,1}^{E,\infty}$ and $V_{m,1}^{E,\infty}$.

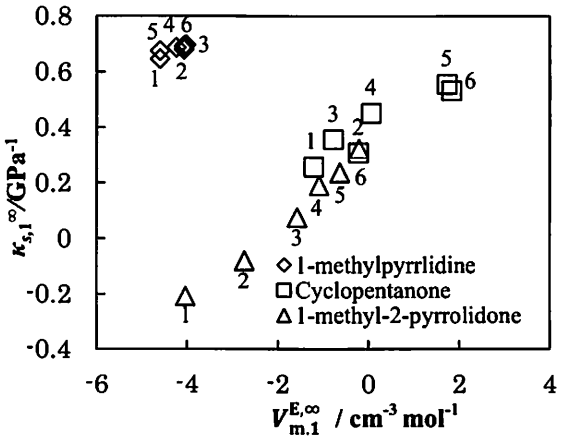

Fig. 2 Correlation of $V_{m,1}^{E,\infty}$ and $\kappa_{s,1}^{\infty}$.

References

[1] Begoña García, Rafael Alcalde,Santigo Aparicio and Jose M. Léal *Phys. Chem. Chem. Phys.* 2002, 4, 1170-1177

2PI10 Chiral interaction between limonenes in BtOH

Y. KOSUGE, T. KAMIYAMA, M. FUJISAWA and T. KIMURA*

Department of Chemistry, Kinki University, 3-4-1 Kowakae, Higashi-Osaka 577-8502, Japan

*E-Mail : kimura@chem.kindai.ac.jp

Enantiomers are chiral molecules that are mirror images of one another. The molecules are non-superimposable on one another. It is negligible small difference and very difficult to determine their difference of physical and chemical properties. However they show very unique properties in biological reactions. In our previous study, mixing enthalpies H^E of hetero *R*- and *S*-enantiomer were showed very small enthalpy changes and almost were positive. To clarify the effect of solvation on chiral discrimination in solution, mixing enthalpies of non-polar chiral limonene (4-Isopropenyl-1-methyl -1-cyclohexene) + non-polar solvents have been reportes for whole concentration of chiral compounds. The experimental results for H^E of chiral compounds of limonenes and solvents of ethanol, hexane, cyclohexane and benzene [1,2] showed endothermic reaction whole range of mole fraction. H^E of chiral limonenes solution of ethanol, hexane, cyclohexane and benzene showed unique concentration dependence of chiral limonenes. H^E showed exothermic behavior in low concentration. However enthalpic stabilization decreased extremely with increasing the concentration of limonene. And finally H^E showed slightly endothermic behavior. In order to know the molecular recognition in solution, H^E of hetero chiral limonene in solvents of structural isomer groups have been measured and showed in Fig. 1 for chiral limonene solutions of BtOH, 2-BtOH, *i*-BtOH and *t*-BtOH at equilimolar concentration of limonene + butanols. H^E of binary mixtures of limonene + BtOH, 2-BtOH, *i*-BtOH and *t*-BtOH were large endothermic and unstabilized on mixing. H^E of hetero chiral limonenes in butanols were increased with decreasing the concentration of Limonene. Chial oriented solvents in butanols solutions might be interaction each other by mixing and change the solvation state to make more stable or less unstable solution. Furthermore H^E of limonenes + butanol isomers were larger than those of limonenes + EtOH and HxOH. To estimate molecular properties chiral compounds and molecular interaction in solvents were carried out by using *ab initio* quantum chemical methods based on the Gaussian programs 09 at the MP2/6-311G(d,p) level of theory.

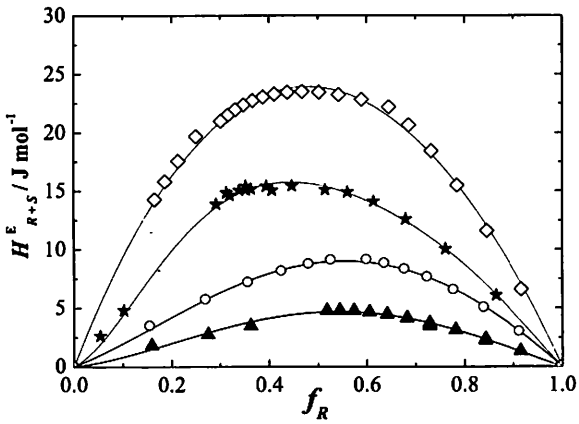

Fig. 1 Excess enthalpies of (1-f_R) *R*-limonene + f_R *S*-limonene at 50 mol% solvents.
▲, BtOH○, 2-BtOH; ★, *i*-BtOH; ◇, *t*-BtOH.

References

[1] Kimura *et. al. J. Chem. Thermodyn.*, **41**, 1170 (2009)

[2] Kimura et. al. *Chirality* **23**:E98-104(2011).

2PI11 Thermodynamic Properties of L-Alanine in NaCl - Water and KCl - Water Mixtures in the Temperature Range 273-323 K

O. Antonova, V. Korolev, M. Fedotova

G.A. Krestov Institute of Solution Chemistry of the Russian Academy of Sciences, Academicheskya str., 1, Ivanovo, 153045, Russia

e-mail : mvf@isuct.ru

Amino acids are used as the model compounds for study of the thermodynamic behaviour of proteins in aqueous solutions. It is known that electrolytes can destroy or strengthen water structure. This property is widely used for investigation of their influence on structure and functions of proteins in aqueous solutions. The purpose of the present report is to investigate the features of interaction of L-alanine (Ala) with NaCl and KCl in aqueous solution at different temperatures.

Enthalpies of solution of L-alanine (Ala) in mixtures of water with NaCl ($m \leq 5$ mol/kg) and KCl ($m \leq 4$ mol/kg) at 288, 298 and 313 K have been measured by calorimetry[1]. The concentration of Ala was 0.02-0.05 mol/kg. The standard enthalpies for the transfer of Ala from water to aqueous NaCl or KCl solutions have been determined from the experimental solution enthalpies. Enthalpic parameters of pair (h_{AE}) and triple (h_{AEE}) interactions of Ala with NaCl and KCl have been calculated within the limits of McMillan-Mayer formalism according to

$$\Delta_{tr}H^0(W \rightarrow W+E) = 2\, h_{AE}\, m + 3\, h_{AEE}\, m^2 \quad (1)$$

Where it is assumed that

$$h(T) = h(\Theta) + c(\Theta)\,(T-\Theta), \quad (2)$$

with h as the enthalpic parameter of pair (h_{AE}, J kg mol^{-2}) or triple (h_{AEE}, J kg^2 mol^{-3}) interaction at temperatures T and a fixed reference temperature, Θ ; c is the heat capacity parameter of interaction.

Eqs. 1, 2 allow to predict the enthalpies of transfer of Ala from water to saturated aqueous NaCl or KCl solutions in the temperature range 273-323 K. Partial molar heat capacities of Ala in aqueous salt solutions have been defined. It has been established, that in the temperature range under study these values do not depend on temperature and increase with electrolyte concentration (m=0-5 mol kg^{-1}). Based on these data the temperature changes in the reduced enthalpy, Gibbs energy and entropy of transfer have been calculated. The value for $\Delta(\Delta_{tr}G^0/T)$ is close to zero for systems under study. Entropic and enthalpic contributions are almost the same and completely compensate each other, i.e the Barclay-Butler rule is followed.

This work was supported by the Russian Foundation for Basic Research (grant No. 12-03-97508–r_centre_a).

References

[1] A. V. Kustov, A. A. Emel'yanov, A. F. Syschenko, M. A. Krest'yaninov, N. I. Zheleznyak, V. P. Korolev, *Russ. J. Phys. Chem.* **80**, 1532(2006).

2PI12 Treating hydrophobic hydration on a simple 3D MB level

T. Urbic[1]

[1]*Faculty of Chemistry and Chemical Technology, University of Ljubljana, Askerceva c. 5, 1000, Ljubljana, Slovenia*

e-mail : tomaz.urbic@fkkt.uni-lj.si

We developed a statistical model which describes the thermal and volumetric properties of water-like molecules. A molecule is presented as a three-dimensional sphere with four hydrogen-bonding arms. Each water molecule interacts with its neighboring waters through a van der Waals interaction and an orientation-dependent hydrogen-bonding interaction. This model, which is largely analytical, is a variant of a model developed before for a two-dimensional Mercedes-Benz model of water [1] and parameterized for 3D Mercedes-Benz model of water [2].

Here a theory of the hydrophobic hydration is extended to 3D, based on a recently proposed 2D statistical mechanical concept [3]. The proposed model of transferring a nonpolar solute into water accounts for the physical balance between water's hydrogen bonding and van der Waals interactions, as well as considers the orientation-dependent hydrogen bonding of water molecules in the hydrophobic effect. The theory is analytical and, in contrast to the integral equation or thermodynamic perturbation based methods, computationally inexpensive. A partition function for a water molecule in the bulk and in the first hydration shell of a hydrophobic solute is built on the expressions for the average energies of different states that the water molecule can be classified to (hydrogen-bonded, van der Waals or non-interacting), and upon considering the geometric restrictions through which a solute dictates the formation or breakage of the hydrogen bonds between water molecules in the first solvation shell. From the expressions for the partition functions, the characteristic thermodynamic functions of transfer follow straightforwardly: changes in the Gibbs free energy, enthalpy, entropy, and heat capacity. Comparison of the results with the machine calculations and with real experiments reveals the theory to qualitatively correctly describe the temperature dependence of the transfer thermodynamics, as well as the trends in the solute size.

References

[1] T. Urbic and K. A. Dill, *J. Chem. Phys.* **132**, 224507(2010).

[2] A. Bizjak, T. Urbic, V. Vlachy, and K. A. Dill, *Acta Chim. Slov.* **54**, 532(2007).

[3] M. Luksic, T. Urbic, B. Hribar-Lee and K. A. Dill, *J. Phys. Chem. B*, **116**, 6177(2012).

2PJ01 Total organic carbon and calcium carbonate distribution in the northern marine of Kuwait

Ahmed Al-Mutairi[1],

[1]*Kuwait Institute for Scientific Research (KISR), Environmental Sciences Department, P.O. Box 24885, Safat 13109, Kuwait.*

e-mail: mrhelala@yahoo.com OR murad.helaleh@mailcity.com

The objective of this research activity is to record total organic carbon and calcium carbonate percentages in a set of samples (43 samples) that cover the northern marine environment of Kuwait. The TOC results show that the present area is impacted by anthropogenic pollutants that are spilled into Kuwait bay from several emergency outlets that are located at the southern part of the Kuwait bay. The carbonate results on the other hand infer the existence of three areas that are recorder as depositional areas. Total organic distribution ranges from 0.2 to 2.5%. Interestingly the inner parts of Kuwait bay and near shore area of bubiyan have lower TOC. The observed distribution of TOC may reflect the effect of the counterclockwise current circulation in Kuwait bay, oil deposition. As carbonate formations related to wormer seawater temperature, it can be inferred that the three areas stated have different oceanographic characteristics.

2PJ02 Effect of Molecular Structure of Nitrogen-Doped Graphene on the Simultaneous Detection of Dopamine, Ascorbic Acid and Uric acid

Shin-Ming Li[1], Shin-Yi Yang[1], Yu-Sheng Wang[1], Chien-Hung Lien[1], Hsi-Wen Tien[1], Sheng-Tsung Hsiao[1], Wei-Hao Liao[1], Hsiu-Ping Tsai[1], Chien-Liang Chang[2], Chen-Chi M. Ma[1] and Chi-Chang Hu[1]

[1]*Department of Chemical Engineering, National Tsing Hua University, Hsin-Chu, TAIWAN, 30013*

[2]*Chung-Shan institute of Science and Technology, Armaments Bureau. M.N.D., Taoyuan, TAIWAN, 32546*

e-mail : ccma@che.nthu.edu.tw

A simple, low-cost method for fabricating nitrogen-doped graphene (NG) is demonstrated by combining the ultrafast thermal exfoliation and covalent transformation from the melamine (MA)-graphene oxide (GO) mixture. NGs prepared at 300, 600, and 900°C, designated as NG300, NG600 and NG900, respectively were systematically characterized by X-ray photoelectron spectroscopy, in which pyridinic-N, pyrrolic-N and graphitic-N are the main nitrogen-doped structures in various ratios. These NGs possess large specific surface area and porous microstructures, confirmed by the N_2 adsorption-desorption isotherms. The NG-modified screen-printed carbon electrodes (SPCEs) were fabricated to detect ascorbic acid (AA), dopamine (DA) and uric acid (UA) simultaneously by cyclic voltammetry and linear sweep voltammetry. Due to the large specific surface area, mesoporous structures and nitrogen-doped sites, these NGs show highly electrochemical sensitivity for AA, DA and UA. Obviously, the pyrrolic-N structure makes the negative shift in the oxidation peak potential of these biomolecules, showing the better catalytic activity than pyridinic-N and graphitic-N structures. The large surface area of NGs provides more nitrogen-doped sites to oxidize bio-compounds and enhances the corresponding currents. The good sensitivity of NG-modified SPCEs makes them become effective sensors for determining AA, DA and UA simultaneously. The discrimination to peak potential and current among these NGs can be observed.

2PJ03 One pot synthesis of indazolo[2,3-a]quinolines derivatives via visible-light photoredox catalysis

W. C. Lin and D. Y. Yang

Department of Chemistry, Tunghai University, Taichung 40704, Taiwan

e-mail : yang@thu.edu.tw

Indazoles have received considerable attention in the past decades due to their diverse biological activities. While existing indazole synthetic strategies mainly involves base-mediated cyclizations, cycloaddition reactions, organometallic catalysis, and azides, utilization of visible-light photoredox catalysis (VLPC)[1] for their preparations has never been reported. In this poster, we will report an efficient, one-pot tandem synthesis of indazolo[2,3-a]quinoline derivatives in moderate yields via VLPC from readily available starting materials (shown below). This synthetic approach involves a novel ruthenium-catalyzed intramolecular formation of the *N-N* bond of the indazole ring, which presumably can provide a greener and more atom-economical access to the highly important heterocyclic indazole derivatives[2]. The scope of this synthetic methodology as well as a possible mechanism for the visible light promoted indazole formation will be presented.

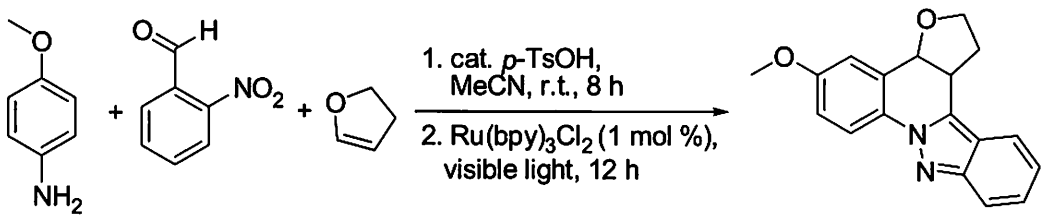

References

[1] J. M. Narayanam, C. R. Stephenson, *Chem. Soc. Rev.* **40**, 102(2011).

[2] W. C. Lin, D. Y. Yang, *J. Org. Chem.* submitted (2013).

2PJ04 Localized vs. Delocalized Ground and Excited States of Mn(III) and Ni(II) Salen Complexes: Theoretical Study of Solvation Effects

S. Aono[1], M. Nakagaki[1], and S. Sakaki[1]

[1]*Fukui Institute for Fundamental Chemistry, Kyoto University, Kyoto 606-8103, Japan*
e-mail : saono@fukui.kyoto-u.ac.jp

Interestingly, one-electron-oxidized Mn(III) and Ni(II) salen complexes contain localized or delocalized salen radical depending on metal and ligand. For instance, the Mn(III) salen complexes show the broad and weak absorption in solution but the Ni(II) salen complexes show the sharp and strong one when the salen ligand is symmetrical. The absorption of the Mn(III) salen complex is experimentally discussed by the inter-valence charge transfer (CT) between two localized states of phenolate moieties and that of the Ni(II) salen complex is the excitation between two delocalized states. To understand the difference in electronic structure and solvation structure between the Mn(III) and the Ni(II) salen complexes, we applied the three dimensional reference interaction site model self-consistent field (3D-RISM-SCF) to these complexes in CH_2Cl_2 solution. The geometry of solute and the solvation structure were optimized by the 3D-RISM-DFT/M06 in self-consistent manner. The vertical excitation energy and the oscillator strength of the first excited state were evaluated by the 3D-RISM general multi-configuration reference quasi-degenerate perturbation theory (GMC-QDPT), including the solvation effects. This calculation provided a good agreement with the tendency of the experimentally observed absorption spectra and reproduced the differences between the Mn(III) and the Ni(II) and those among the salen ligands. Solvation effect is necessary for correctly describing the geometrical distortion, the electronic localization, and the inter-valence CT absorption specrum.

2PJ05 Electrochromic Property of Metalloporphyrins in Solution

K. Ogawa, K. Kamimura, Y. Uchida, and K. Maekawa

Interdisciplinary Graduate School of Medical and Engineering, University of Yamanashi, 4-3-11 Takeda, Kofu, Japan

e-mail : kogawa@yamanashi.ac.jp

The interest in electrochromism and electrochromic materials have increased in recent years, because electrochromism offers a way of modulating light which can be used in various optical devices. An electrochromic device is a non-emissive device similar to a liquid crystal display device. Porphyrins and phthalocyanines are expexted to be the electrochromic materials since they have rich π-electrons that allow not only strong absorption in visible region but also easy oxidation to change their colors. Although redox properties of porphyrins and phthalocyanines have been studies for a long time, no systematic research for electrochromic property has been reported. Here, we will report the electrochromic properties of tetraphenylporphyrin (TPP), its metal complexes, and related compounds in solution.

Oxidation was performed by the addition of Ce(IV) methanol solution into chloroform solution of porphyrin. The central metals investigated were 2H (free base), Zn, Fe, Co, Ag, Ni, Sn, Al, Cu, Pd, TPP complexes of Cd, and Mn. Ni, Sn, Al, Cu, Pd, Cd, and Mn did not show any color change. On the other hand, the solutions of those of free base, Zn, Fe, Co, and Ag showed drastic change in color as summarized in Table 1. The color change by reduction in solution is now under investigation.

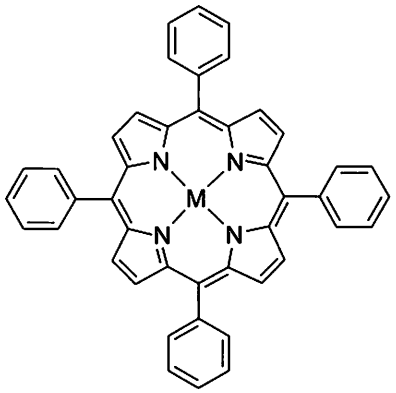

TPP

Table 1. Color change of porphyrin metal complexes by oxidation

	Soret band (nm)		Q band (nm)		color	
	neutral	oxidixed	neutral	oxidixed	neutral	oxidixed
H_2	415	435	515, 550, 592, 648	512, 654	purple	green
Zn	421	407	557, 595	-	purple	brown
Fe	336, 414	314, 395	542	532	brown	green
Co	411	427	528	540	purple	green
Ag	424	broad	540	no change	purple	orange

2PJ06 Synthesis and characterization of high purity gallium oxide nanoparticles by controlled precipitation

K. S. Han[1], J. H. Kim[1], K. T. Hwang[1], W. S. Cho[1], S. H. Hwang[2], Y. J. Choi[2], and D. I. Jeon[2]

[1]*Icheon Branch, Korea Institute of Ceramic Engineering and Technology, Icheon, Gyoenggi, Republic of Korea*

[2]*TSM Co., Ltd., Chilgok, Gyeongbuk, Republic of Korea*

e-mail : kh389@kicet.re.kr

Nano-sized particles are important due to their unique electronic, optical, magnetic and mechanical properties compare to their bulk forms. These properties of nanoparticles are often dependent on their synthesis conditions and corresponding morphologies. The monoclinic gallium oxide (β-Ga_2O_3), which is the most chemically and thermally stable phase among the various phase of gallium oxide, has a wide range of potential applications such as transparent conducting oxide (TCO) of optoelectronic devices, luminescent materials and gas sensors. Here we report the synthesis of high purity gallium oxide nanopowders using gallium nitrate and ammonium hydroxide as starting materials by a scalable precipitation technique. Gallium oxide nanopowders were obtained under various precipitation conditions including Ga concentration, solution pH and aging temperature. The crystal structure of gallium oxide nanopowders was confirmed as β-Ga_2O_3 by X-ray diffraction pattern. The various morphologies of β-Ga_2O_3 nanoparticles from the different precipitation conditions were investigated by using SEM, BET, FT-IR and TG-DTA.

2PJ07 Synthesis and characterization of SnS/Polyvinylbutyral composite fibers by electrospinning route

K. -C. Hsu[1], J. -D. Liao[1], P. -Y. Lin[2], D. -Y. Wu[3], and Y. -S. Fu[3*]

[1]*Department of Materials Science and Engineering, National Cheng Kung University, Tainan, 701, Taiwan*

[2]*Department of Photonics, National Cheng Kung University, Tainan, 701, Taiwan*

[3]*Department of Greenergy, National University of Tainan, 701, Taiwan*

e-mail : ysfu@mail.nutn.edu.tw

Tin sulfide(SnS)/polyvinylbutyral(PVB) composite fibers were synthesized via a relatively simple electrospinning process. From the reactions of stannous chloride dehydrate($SnCl_2 \cdot 2H_2O$), thiourea($SC(NH_2)_2$) and polyvinylbutyral as precursor, SnS/PVB composite fibers with diameter in the range of 100–200 nm were obtained for SnS/Polyvinylbutyral precursor ratios of 20% at an applied voltage of 15 kV after annealing treatment at 400 °C for 3 h. These fibers were composed of very small crystalline grains uniformly linked with an average size. SnS/PVB composite fibers were characterized using X-ray powder diffraction (XRD), scanning electron microscopy (SEM), thermogravimetric analysis (TGA), and transmission electron microscopy (TEM). The optical properties of the SnS composite fibers were also recorded by UV-vis absorption spectroscopy.

References

[1] J. -C. Kuo, S. -C. Lee, K. -C. Hsu, S. -J. Liu, B. -Y. Chou, Y. -S. Fu, *Materials Letters*. **62**, 4594(2008).

[2] K. -C. Hsu, J. -D. Liao, J.-R. Yang, Y.-S. Fu, *CrystEngComm*. Accepted Manuscript. (2013) DOI:10.1039/C3CE00052D.

[3] M. Jayalakshmi, M. Mohan Rao, B. M. Choudary, *Electrochemistry Communications*. **6**, 1119(2004).

2PJ08 Development of chalcopyrite $CuInS_2$ nanorods by electrospinning assisted hydrothermal process

P. Y. Lin[1], K. C. Hsu[2], Y. S. Fu[3], and T. F. Guo[1]

[1]*Department of Photonics, National Cheng Kung University, Tainan, 701, Taiwan*

[2]*Department of Materials Science and Engineering, National Cheng Kung University, Tainan, 701, Taiwan*

[3]*Department of Greenergy, National University of Tainan, 701, Taiwan*

e-mail: ysfu@mail.nutn.edu.tw

The solar cell light absorption materials $CuInS_2$ (CIS) has received attention due to its high absorption coefficient, suitable band gap, and good radiation stability. In this study, we have prepared $CuInS_2$ nanorods through combining electrospinning technique and hydrothermal process. One-dimensional (1-D) CIS/PVB nano-fibers with diameter about 150~300nm have been first prepared by using copper chloride, indium chloride and thiourea dissolve in a mixed solvent of ethanol-ethylene glycol (4:1,v/v) and the polymer used poly(vinyl butyral) via electrospinning approach. Further, those as-prepared 1-D CIS/PVB nano-fibers were employed as precursors to fabricate $CuInS_2$ nanorods through hydrothermal process. The morphology of $CuInS_2$ was similar to that of the precursor CIS/PVB nano-fibers. The CIS/PVB nano-fiber is believed as template lead to the formation of $CuInS_2$ nanorods. The structure, morphology and composition of the samples were characterized using an X-ray diffraction, transmission electron microscopy, an energy dispersive X-ray spectroscope and scanning electron microscopy.

References

[1] J. Xiao, Y. Xie, R. Tang, Y. Qian, *J. Solid State Chem.*, **161**, 179(2001).

[2] G. Shen, D. Chen, K. Tang, Z. Fang, J. Sheng, Y. Qian, *J. Cryst. Growth*, **254**, 75(2003).

[3] Y. Akaki, T. Matsubara, Y. Ohno, T. Momiki, *Curr. Top. Solid State Phys.*, *5*, 1027(2009).

[4] J. Zhou, S. Li, X. Gong, Y. Yang, Y. Guo, *Mater. Lett.*, *65*, 2001(2011).

[5] T. He, H. Ma, Z. Zhou , W. Xu, F. Ren, Z. Shi, J. Wang, *Polym. Degrad. Stab.*, **94**, 2251(2009).

[6] H. Hu, B. Yang, X. Liu, R. Zhang, Y. Qian, *Inorg. Chem. Commun.*, **7** , 563(2004).

[7] S. E. Wark, C.H. Hsia, Z. Luob, D. H. Son, *J. Mater. Chem.*, **21**, 11618(2011).

2PJ09 Linear response approximation to RISM-SCF-SEDD

D. Yokogawa[1,2]

[1]*Department of Chemistry, Graduate School of Science, Nagoya University, Chikusa, Nagoya 464-8602, Japan*

[2]*Institute of Transformative Bio-Molecules (WPI-ITbM), Nagoya University, Chikusa, Nagoya 464-8602, Japan*

e-mail : d.yokogawa@chem.nagoya-u.ac.jp

Introduction

In theoretical study of solution chemistry, hybrid approaches between quantum mechanics (QM) calculation and solvation theory become popular. Reference interaction site model self-consistent field explicitly including spatial electron density distribution (RISM-SCF-SEDD)[1] is one of the hybrid methods. In this work, we applied linear response approximation to RISM-SCF-SEDD and derive new method (LR-RISM-SEDD)[2].

Results and discussion

Radial distribution function (RDF) is one of the most important properties RISM-SCF-SEDD can calculate. In this method, RDF is obtained with the following equation,

$$g_{\alpha s}^{(0+1)}(r) = g_{\alpha s}^{(0)}(r) + \sum_i \left(\frac{\partial h_{\alpha s}}{\partial d_i}\right)^{(0)} (d_i - d_i^0). \quad (1)$$

$g^{(0)}$ is the RDF calculated using the electron density obtained in gas phase calculation and d is the expansion coefficient employed in the fitting of electron density of the solute molecule. In Fig. 1, $g^{(0)}$ and $g^{(0+1)}$ are shown. For comparison, the RDFs computed with RISM-SCF-SEDD were also shown. When RDF is calculated with the electron density obtained in gas phase, the height of each peak is somewhat underestimated. By adding the second tern in Eq. (1), this underestimation is greatly improved.

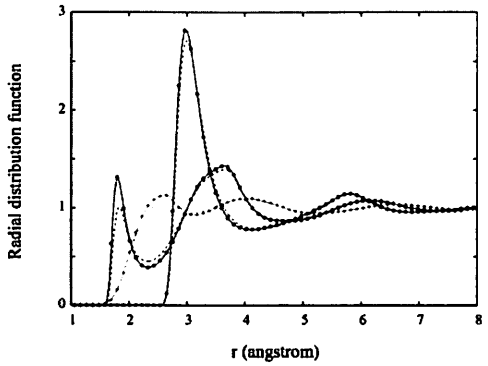

Fig. 1. Radial distribution functions of H_2O between O-O (red), O-H (blue), and H-H (green). Dashed and solid lines are $g^{(0)}$ and $g^{(0+1)}$, respectively. RDFs computed with RISM-SCF-SEDD were shown with filled circles.

To discuss the efficiency of this method, we summarized the computational time required in the present method and RISM-SCF-SEDD. When 12 cores were used, the required computational time for *p*-nitroaniline (PNA) is about one-fifteenth of the time required in RISM-SCF-SEDD.

Table 1. Required computational time[a] (unit: second)

	LR-RISM-SEDD			RISM-SCF-SEDD		
	1 core	6 cores	12 cores	1 core	6 cores	12 cores
H_2O	32	22	22	193	193	194
H_2CO_3	241	189	186	1880	1967	2003
PNA	2538	1895	1904	28194	28480	29049

[a] This benchmark was performed using Xeon X5675 3.07GHz.

References

[1] D. Yokogawa, H. Sato, and S. Sakaki, *J. Chem. Phys.* **126**, 244504 (2007).

[2] D. Yokogawa, *J. Chem. Phys.* accepted.

2PJ10 Ionic Conduction in Electrolyte Solution

S. Matsunaga[1], S. Tamaki[2]

[1]*Nagaoka National College of Technology, Nagaoka 450-8532, Japan*

[1]e-mail : matsu@nagaoka-ct.ac.jp

[2]*Department of Physics, Faculty of Science, Niigata University, Niigata 950-2181, Japan*

The phenomena of transport properties in ionic liquids are of great important in the industrial science and technology, as well as in physics and chemistry. In connection with these, a number of experimental and theoretical studies have been published until the present time[1,2,3]. Ionic liquids are mainly classified into two categories; one is a group of molten salts and the other is a large number of electrolytic solutions, in particular, aqueous solutions of electrolytes.

In the case of molten salts, most of scientific studies have been developed from 1960's by several researchers. In order to study the structural and transport properties in molten salts, experimental investigations and molecular dynamics simulations have also been carried out from mid-seventies of the last century. Following to these, we have been recently engaged in the study of transport properties in molten salts.

It has been required to investigate the static and dynamic properties of dissolved ions in aqueous solutions from the microscopic view point. Along this requirement, the technique of molecular dynamic simulation has been applied, using some qualified inter-particle potentials. Various theoretical attempts have been recently tried to establish the dynamical behaviors of dissolved ions in these solutions, which is able to discuss parallel with results obtained by MD simulations.

However there still remains the task to obtain how to derive the theoretical formula for the dilute limit of the conductivity Λ_0 in terms of inter-particle potentials and corresponding pair distribution functions.

In the present paper, we will try to apply the linear response theory for the electrolytic solution and to obtain Λ_0 and the concentration dependence of the conductivity in terms of pair-wise potentials and pair distribution functions among ions and water molecules, which allow us to compare parallel with the dynamical properties of MD simulation.

In addition we will also try to clarify how the electrophoretic and relaxation effects treated by many researchers are explained in a microscopic view point.

From these, we will see what is similar and what is different for the case of molten salts and that of electrolytic solutions.

References

[1] G. J. Janz, *Molten Salts Handbook*, (Academic Press, New York, 1967)

[2] S. I. Smedley, *The interpretation of ionic conductivity in liquids*, (Plenum Press, New York, 1980)

[3] B. E. Conway, *Physical chemistry (An advanced Treatise)* Vol. IX A; Electrochemistry, ed. H. Eyring, (Academic Press, New York, 1970)

2PJ11 Electro-oxidation of ethanol over Pt(Sn)/TiO_2-C anodic catalysts

Ying-Huei Liou[1,2], Yi-Ping Tsai[1,2], Josh Y.Z. Chiou[1],
Shu-Hua Chien[2,3] and Chen-Bin Wang[1]

[1]*Department of Chemical and Materials Engineering, Chung Cheng Institute of Technology, National Defense University, Tahsi, Taoyuan, 33509, Taiwan, ROC*

[2]*Institute of Chemistry, Academia Sinica, Taipei, 11529 Taiwan, ROC*

[3]*Department of Chemistry, National Taiwan University, Taipei, 10764, Taiwan, ROC*

e-mail : chenbinwang@gmail.com

This research focused on the modified Pt/C anodic catalyst with titania (30 wt% TiO_2) and tin (5 wt% Sn) to improve the utilization and efficiency of direct ethanol fuel cell. The TiO_2-doped on active carbon support was prepared by impregnation method. Then, the Pt(Sn)/TiO_2-C (10 wt% Pt) anodic catalyst was synthesized by formic acid reduction method using platinum chloride ($PtCl_4$) and tin dichloride dihydrate ($SnCl_2 \cdot 2H_2O$) as precursors. The carbon paper coated with Pt(Sn)/TiO_2-C catalyst was used as the working electrode. Evaluation of the catalytic activity for the electro-oxidation of ethanol on working electrodes was performed with cyclic voltammetry (CV) in 0.5 M H_2SO_4 and 1 M ethanol electrolyte at room temperature. The results of XRD and TEM show that all the prepared Pt(Sn)/TiO_2-C anodic catalysts present uniform dispersion of platinum with a diameter around 3 - 6 nm. The activity for electro-oxidation of ethanol was affected remarkably by the content of TiO_2 and Sn in the anodic catalyst. The addition of TiO_2 can promote the CO stripping by the surface oxygen functional groups to reduce CO oxidizing potential. Also, the formation of PtSn alloy can enhance the CO stripping at lower oxidizing potential.

Keywords: Pt(Sn)/TiO_2-C anodic catalyst; Electro-oxidation; Cyclic voltammetry.

References

[1] B.E. Hayden, D.V. Malevich, D. Pletcher, *Electrochem. Commun.* **3**, 395 (2001).

[2] F.C. Simoes, D.M. dos Anjos, F. Vigier, J.M. L'eger, F. Hahna, C. Coutanceau, E.R. Gonzalez, G. Tremiliosi-Filho, A.R. de Andrade, P. Olivi, K.B. Kokoh, *J. Power Sources* **167**, 1 (2007).

2PJ12 A study of phase transition using interaction potential with two minima

A.Suematsu[1], A. Yoshimori[1], M.Saiki[1], J.Matsui[1], T.Odagaki[2]

[1]*Department of Physics, Kyushu University, Fukuoka 812-8581, Japan*

[2]*School of Science and Engineering,Tokyo Denki University, Hatoyama, Saitama 350-0394, Japan*

e-mail : a.suematsu@cmt.phys.kyushu-u.ac.jp

The final goal of the present study is establishment of relationship between interaction of particles and crystallization of the system. The establishment is useful for actual application. For example, it is important in crystallization of protein. The interaction of protein can be controlled by addition of other solutes.

– As an interaction model, we use Lennard-Jones-Gauss (LJG) potential. The LJG potential have two minima: a standard Lennard-Jones minimum and a Gaussian pocket. We can change the depth and position of the Gaussian pocket by parameters of the potential. We calculate melting points in a wide range of the parameters.

– To study the relationship between interaction and crystallization, we use a thermodynamic perturbation theory [1]. We split the LJG potential into hard-sphere reference and perturbation parts using method by WCA. By expansion in terms of the perturbation part, we calculate the Helmholtz free energy of the system in the liquid and solid phases. Then, we obtain a coexisting density and freezing pressure by drawing common tangents. As stable solid phases, we assume fcc and bcc crystals.

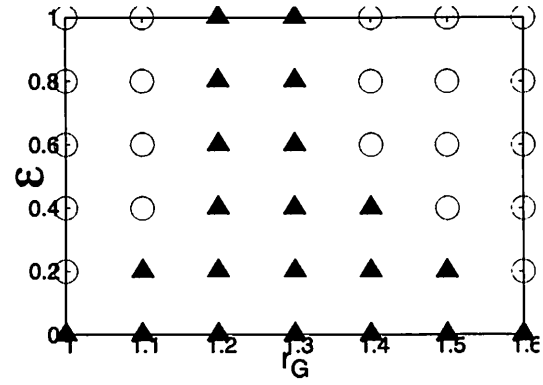

fig. 1: Phase diagram at $P^*=2.0*2^{1/2}$,$T^*=1.0$. P^* and T^* are scaled by the depth and position of the standard Lennard-Jones minimum. ○ and ▲ represent a stable fcc crystal and liquid phase, respectively.

– As a result of calculation, we obtain a phase diagram in the parameter space of the LJG potential (fig.1). Here, ε and r_G represent ratios of the depth and position of the Gaussian pocket to that of the standard Lennard-Jones minimum. By the obtained phase diagram, we find that the system is crystallized at r_G = 1.0, 1.1, and 1.4-1.6.

– We explain the reason for the crystallization at the values of r_G, by relative positions of the Gaussian pocket to the crystal structure. At the values of r_G, the Gaussian pocket is located near the position of the first or third nearest neighbor particles of the fcc crystal. Then, the free energy of the fcc crystal decreases more rapidly than that of the liquid phase. The decrease in the free energy yields the stability of the fcc crystal. By these results, we can conclude that the stable phase can be changed by the position of the Gaussian pocket.

References

[1] A. Suematsu, A. Yoshimori, T. Odagaki: J. Phys. Soc. Jpn. **80** (2011) 025001

2PJ13 Investigation of Silica Nanoparticles as Immunoadjuvants in Animal Vaccine

P.H. Mou[1], G.F. Chen[1], P.F. Hsieh[2], C.C. Yu[3], M.S. Chien[3], M.K. Hsieh[2],

M.Y. Liao[1]

[1]*Department of Chemistry, National Chung Hsing University, Taichung, Taiwan R.O.C.*

[2]*Graduate Institute of Microbiology and Public Health, National Chung Hsing University, Taichung, Taiwan R.O.C.*

[3]*Graduate Institute of Veterinary Pathobiology, National Chung Hsing University, Taichung, Taiwan R.O.C.*

e-mail: mliao@dragon.nchu.edu.tw

Biocomparable and biodegradable soluble silica nanoparticles [1], have a great potential as a delivery system for drug or gene carrier in biological system [2, 3], which can protect effective antigen and prolong its retention in vivo. In this research, positive-charge and water-soluble silica nanoparticles were synthesized by sol-gel method. The surfaces of these particles were directly modified by diaminosilane and hence were mixed with protein to form complexes. The amino-functional silica particles were positive-charge in neutral solution. For particle control, we used different silica source: sodium silicate (MSSNps) and commercial silica gel (60-200 nm, MCSNps) and compared there results in immunity test. For immune experiment, we mixed BSA (Bovine Serum Albumin) with our functional silica nanoparticles and observed its response. Vaccine testing in animal, we compared our materials with commercial Freund's adjuvant in infectious bursal disease (IBD). The positive-charge silica nanoparticles not only ware packing protein into organism as carrier but enhanced immune response. It's suitable in vaccine design and immune modulation for animals.

References

[1] R.K. Iler, *The chemistry of silica :solubility, polymerization, colloid and surface properties, and biochemistry*, (1979).

[2] X. Li, Q.R. Xie, J. Zhang, W. Xia, H. Gu, *Biomaterials* **32**, 9546(2011).

[3] L.V. Carvalho, C. Ruiz Rde, K. Scaramuzzi, E.B. Marengo, J.R. Matos, D.V. Tambourgi, M. C. Fantini, O. Sant'Anna, *Vaccine* **28**, 7829(2010)

2PJ14 Interfacial cyclodextrin-polyfluorinated compound assemblies on functionalized silicon surface

Anna Szwajca

Department of Chemistry, Adam Mickiewicz University, Poznan, Poland
e-mail : Anna.Szwajca@amu.edu.pl

Self-assembled monolayers (SAMs) containing the cyclodextrins as a host molecules are one of the useful interfacial supramolecular assemblies. These structures, for example, tend to form diverse supramolecular used to mimic functional biosurfaces or ion channel [1].

The assembly of organic layers onto surfaces depends on the surface properties such as wettability, polar or ionic interactions, chemical structures and topography [2]. In the self-assembled monolayers containing host molecules, specific bonding interaction exists between the inorganic surface and organic film and they are generally in contact with a solution. These monolayers offer a structural order over supramolecular distances with low defect densities [3]. Fluorinated acids and alcohols were chosen since the fluoroorganic molecules have attracted particular attention in biomaterial science because of a number of unusual properties. Monolayers of polyfluorinated carboxylic acids or alcohols have been self-assembled on silicone surface and physicochemically characterized [4]. The structure and quality of the resulting SAMs were investigated by the contact angle (CA) analysis, atomic force microscopy (AFM), X-ray photoelectron spectroscopy (XPS) and semiempirical (PM5) methods.

This work was supported by the National Center for Science within the project No.: NN 204 444740.

References

[1] A. McNally, R. J. Forster, T.E. Keyes, *Phys. Chem. Chem. Phys.*,**11**, 848(2009).

[2] A. Szwajca; M. Rapp; M. Bilska; M. Krzywiecki; H. Koroniak, *Appl. Surf. Sci.*, DOI information:10.1016/j.apsusc.2013.03.020.

[3] R. J. Forster at all, *Interfacial Supramolecular Assemblies*, Wiley, Dublin (2003).

[4] A. Szwajca unpublished results (2012).

2PJ15 Preparation of Poly(3-hexylthiophene)/multi-walled carbon nanotube hybrid materials by solution process

Yang-Yen Yu*[1], Yu-Hsin Ko[1], Su-Nu Liu[1]

[1] *Department of Materials Engineering, Ming Chi University of Technology, 84 Gunjuan Road, Taishan, New Taipei City 243, Taiwan*

e-mail:yyyu@mail.mcut.edu.tw

Regioregular poly(3-hexylthiophene) (rrP3HT) and multi-walled carbon nanotube (MWNT) hybrid materials with the desired structure and properties were prepared by a solution process method. The prepared hybrid materials were characterized by ultraviolet-visible spectroscopy, photoluminescence spectroscopy, fourier transform infrared spectroscopy, X-ray diffraction, scanning electron microscopy, and transmission electron microscopy. Different concentrations of MWNT were suspended in the polymer solutions and spin-casted onto ITO glass. Then, solar cells with the structure of ITO/PEDOT:PSS(DMSO)/P3HT:MWNT/Al were fabricated by the evaporation of aluminum as the back contact. The results showed that the ratio of rrP3HT to MWNT had a great influence on the performance of solar cell. The efficiency of the solar cell increased with the increase in MWNT content.

2PJ16 Increased Open Circuit Voltage of Solution Process Organic Photovoltaic through Conformational Twist of Indacenodithiophene based Conjugated Polymer

Chih-Ping Chen, Hsiang-Lin Hsu

Department of Materials Engineering, Ming Chi University of Technology, 84 Gunjuan Road, Taishan, New Taipei City, 243, Taiwan

e-mail: cpchen@mail.mcut.edu.tw

Organic photovoltaics (OPV) based on solution process nano–phase segregation blends morphology of electron–donating p–type conjugated polymers and electron–accepting fullerenes have been attracting considerable attention recently due to their unique advantages of low cost, light weight, and capacity for roll–to–roll technology.[1] We have prepared a fused ladder indacenodithiophene (**IDT**) based D-A type alternating conjugated polymer, **PIDTHT–BT**, possessing n–hexyl–thiophene side chain. The prepared polymer is soluble in common solvents. Optical measurement indicates that the bandgap of **PIDTHT–BT** being 1.81 eV. By extended intramolecular repulsion through the side chain conjugated moiety, deeper highest occupied molecular orbital (HOMO) energy level (–5.46 eV) was obtained. When compared to the counterpart (**PIDTDT–BT**), the HOMO level was approximately 0.27 eV lower, and subsequently leads to high open circuit voltages of ca. 0.94 V of fabricated solar cell. The hole mobility (space charge limited current (SCLC) measurement) of blend film containing 25 wt% **PIDTT–BT** and 75 wt% [6,6]–phenyl–C_{71} butyric acid methyl ester (**$PC_{71}BM$**) is 2.0×10^{-9} $m^2V^{-1}s^{-1}$ which is in the reasonable range for organic photovoltaic application. A power conversion efficiency of 4.5% is obtained under simulated solar illumination (AM 1.5G, 100 $mWcm^{-2}$).

References

1. (a) Espinosa, N.; Hosel, M.; Angmo, D.; Krebs, F. C., *Energy & Environmental Science* **2012,** *5* (1), 5117-5132; (b) Espinosa, N.; García-Valverde, R.; Urbina, A.; Krebs, F. C., *Solar Energy Materials and Solar Cells* **2011,** *95* (5), 1293-1302; (c) Chen, J.-T.; Hsu, C.-S., *Polymer Chemistry* **2011,** *2* (12), 2707-2722; (d) Liao, C.-Y.; Chen, C.-P.; Chang, C.-C.; Hwang, G.-W.; Chou, H.-H.; Cheng, C.-H., *Solar Energy Materials and Solar Cells* **2013,** *109* (0), 111-119; (e) Li, X.; Choy, W. C. H.; Huo, L.; Xie, F.; Sha, W. E. I.; Ding, B.; Guo, X.; Li, Y.; Hou, J.; You, J.; Yang, Y., *Advanced Materials* **2012,** *24* (22), 3046-3052.

2PJ17 Morphological Transformation and Photophysical Properties of Rod-Coil Amphiphilic block copolymers in Solution

Yang-Yen Yu*[1], Chia Liang Tsai [1], Su-Nu Liu[1]

[1]: *Department of Materials Engineering, Ming Chi University of Technology, 84 Gunjuan Road, Taishan, New Taipei City 243, Taiwan*

e-mail:yyyu@mail.mcut.edu.tw

Morphologies, synthesis and photophysical characterization of amphiphilic rod-coil poly[2,7-(9,9- dihexylfluorene)]-block- poly[2-(diethylamino)ethyl methacrylate] copolymers PF-*b*-PDEAEMA block copolymer were investigated in the present study. The morphologies of aggregates for block polymers could be manipulated by tuning the selectivity of mixied THF/methanol solvents in which the methanol concentrations ranging from 0 to 90 vol%. The results showed that the morphologies had a great influence on the photophysical properties of PF-*b*-PDEAEMA block copolymers. Moreover, the heating temperature had a great influence on the thermal stability of PF-*b*-PDEAEMA block copolymers. The present study showed that the selectivity of solvent and annealing temperature had an obvious influence on the morphologies of aggregates between copolymers and the photophysical properties of the rod-coil block copolymers.

2PJ18 Simple SPC/E-based models of electrolytes: Simulation study on limits of their applicability

F. Moučka[1], I. Nezbeda[1], and W. R. Smith[2]

[1]*Faculty of Science , J. E. Purkinje University, Usti nad Labem, Czech Republic*
[2]*University of Ontario Institute of Technology, Oshawa, Ontario, Canada*
e-mail : filip.moucka@ujep.cz

Eleven of the most common aqueous NaCl solution force fields have systematically been examined with respect to the accuracy of their prediction of the solution density and chemical potential over the entire concentration range at ambient pressure and temperature. The density was obtained by standard Monte Carlo simulations at constant pressure, temperature, and number of molecules. Dependence of the electrolyte chemical potential on concentration was obtained using a recently developed Osmotic Ensemble Monte Carlo method [1] simulating the system at constant pressure, temperature, number of solvent molecules, and electrolyte chemical potential.

It is found that the results of the force fields considered are scattered over a wide range of values, and none is capable of producing quantitatively accurate results over the entire concentration range for the properties considered [2].

References

[1] F. Moučka, M. Lísal, J. Škvor, J. Jirsák, I. Nezbeda, W. R. Smith *J. Phys. Chem B* **115**, 7849(2011).

[2] F. Moučka, I. Nezbeda, W. R. Smith *J. Chem. Phys.* **138**, 154102(2013).

Poster Session II

3PA13 Liquid and Li^+ Local Structures in Li-glymes Complex Ionic Liquids Revealed by Raman and X-ray Scattering Techniques with the Aid of Theoretical Calculations

Soshi Saito[1], Hiroyuki Doi[1], Seiji Tsuzuki[2], Wataru Shinoda[2], Shiro Seki[3], Kaoru Dokko[4], Masayoshi Watanabe[4], and Yasuhiro Umebayashi[1]

[1]*Graduate School of Science and Technology, Niigata University, Niigata 950-2181, Japan*
[2] *National Institute of Advanced Industrial Science and Technology (AIST), Tsukuba, 305-8565, Japan*
[3]*Materials Science Research Laboratory, Central Research Institute of Electric Power Industry, Komae, 201-8511, Japan*
[4]*Department of Chemistry and Biotechnology, Yokohama National University, Yokohama 240-8501, Japan*
e-mail : s10c312e@mail.cc.niigata-u.ac.jp

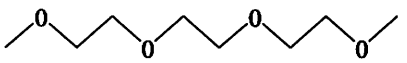

Triglyme (G3)

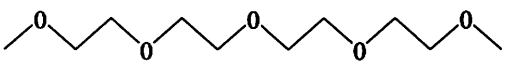

Tetraglyme (G4)

glymes

Room-temperature ionic liquids currently attract much attention as electrolyte materials for lithium batteries. Among them, a new class of ionic liquids containing Li^+ ion have been proposed; Li-glymes complex ionic liquids that consists of equimolar lithium salt and glyme ligand to form the Li-glymes complex. In a working electrolyte of the lithium battery used the Li-glymes complex ionic liquids, specific Li^+ ion conduction mechanism was proposed. In order to realize next generation lithium batteries, it is indispensable to elucidate structure and dynamics of electrolyte at a molecular level. On the other hand, from the viewpoint of solution chemistry, particularly ion solvation, we have already understood structure, reactivity and dynamics of ions in mono-dentate solvents systems to some extent. However, as clearly seen in molecular structure, glymes should act as a multi-dentate ligand forming Li^+ ion complexes. The knowledge of ions in such a multi-dentate solvent systems is scarce so that it is necessary to clarify structure, reactivity and dynamics of ions at a molecular level.

We have so far investigated liquid structure of and Li^+ ion solvation in ordinary ionic liquids.[1-4] We extended our work to this new class of ionic liquids. In this contribution, we report liquid and Li^+ local structures in the Li-glymes complex ionic liquids revealed by Raman spectroscopy and high-energy X-ray diffraction techniques with the aid of theoretical calculations such as ab initio molecular orbital calculations and molecular dynamics simulations. Finally, Li^+ ion conduction mechanism in the Li-glymes complex ionic liquids will be discussed.

References

[1] Y. Umebayashi et al., *J. Phys. Chem. B* **111**, 13028 (2007).
[2] A. Shirai et al., *Anal. Sci.* **24**, 1291 (2008). .
[3] Y. Umebayashi et al., *J. Phys. Chem. B* **114**, 6513 (2010).
[4] Y. Umebayashi et al., *J. Phys. Chem. B* **115**, 12179 (2011).

3PA14 Determination of KAT and EDH Coefficients for the Complexation of Dioxovanadium (V) with D-(-)-Quinic Acid in Different Water + [bmim]BF_4 Solutions

K. Majlesi, S. Rezaienejad

Department of Chemistry, Science and Research Branch, Islamic Azad University, Tehran, Iran

e-mail : kavoshmajlesi@srbiau.ac.ir

This presentation is part of the paper which has been accepted for publication in Journal of Solution Chemistry[1]. Several papers have been published by our group regarding the complexation of dioxovanadium (V) and molybdenum (VI) with D-(-)-quinic acid and aminopolycarboxylic acids in aqueous and non aqueous solutions with the aim of clarifying the role of ionic strength and solvent effects in the solutions[2-5]. Vanadium(V) oxometalates have found application as analytical reagents for the determination of various pharmacologically active substances and biochemical parameters. The biological effects of vanadium (V) vary greatly in different biological systems. Vanadium plays a catalytic role in metalloenzyme systems such as nitrogenase and haloperoxidases. D-(-)-quinic acid is a cyclic polyol and can act as calcium carrier in biological systems. It could therefore also be an effective carrier for other metal ions, due to the formation of coordination compounds. It is also a very useful chiral raw material for total synthesis of complex molecules and chiral reagents for asymmetric synthesis. Although research on room-temperature ionic liquids (RTILs) has gained new attention during the last years, there are only a few papers in the literature about equilibriums analysis in the ionic liquid + water medium. Potentiometric and UV spectrophotometric methods have been utilized in this research for the collection of experimental data in order to determine the stability constants of dioxovanadium (V) complexation with D-(-)-quinic acid at $T = 298$ K, $I = 0.1$ mol.dm^{-3} of sodium chloride for various H_2O + 1-butyl-3-methylimidazolium tetrafluoroborate, [bmim]BF_4, solutions ranging in concentration from 0 to 40 percent of [bmim]BF_4. Kamlet-Abboud-Taft (KAT) model has been used for the calculation of solvatochromic regression coefficients in order to find out the role of various specific and non specific interactions. It was found that hydrogen bonding and polarizability were the most important interactions for the dissociation and stability constants respectively in the aqueous solutions of [bmim]BF_4. The contribution of [bmim]BF_4 as a supporting electrolyte will be also discussed on the basis of the extended Debye-Hückel (EDH) theory.

References

[1] K. Majlesi, S. Rezaienejad, *J. Solution. Chem.* accepted for publication, JOSL2056R1 (2012).

[2] K. Majlesi, S. Rezaienejad, *J. Solution. Chem.* **41**, 937(2012).

[3] K. Majlesi, S. Rezaienejad, *J. Chem. Eng. Data* **56**, 3194(2011).

[4] K. Majlesi, S. Rezaienejad, *J. Chem. Eng. Data* **55**, 4491(2010).

[5] K. Majlesi, N. Momeni, *J. Chem. Eng. Data* **54**, 2479(2009).

3PA15 Physical and CO_2-Absorption Properties of Imidazolium Ionic Liquids with Tetracyanoborate and Bis(trifluoromethanesulfonyl)amide anions

T. Makino[1], Y. Masuda[1], M. Kanakubo[1], and H. Mukaiyama[2]

[1]*National Institute of Advanced Industrial Science and Technology, Sendai 983-8551, Japan*

[2]*Panasonic Co., Gunma 370-0596, Japan*

e-mail : makino.t@asit.go.jp, m-kanakubo@aist.go.jp

Room temperature ionic liquids (ILs) are salts, the melting points of which are at or below ambient temperatures. ILs generally have extremely low vapor pressure, thus they are considered as potentially "green" alternatives to volatile organic solvents. They also have some remarkable properties, including non-flammability, high thermal and chemical stability as liquids over an extended temperature range, wide electrochemical window, high solubility of certain specific gases, and so on. Because of these favorable characteristics, ILs have attracted considerable attention in a wide range of areas. One of the most interested applications is the gas absorbent for the gas separation, gas compression, and gas storage processes. The primarily important property for the performance as gas absorbents is the gas solubility in IL, especially the molarity scaled solubility. Besides the gas absorption property, the volumetric, transport, and thermal properties are required for developing the related technologies using ILs.

We have focused on the imidazolium based ILs with the tetracyanoborate ($[TCB]^-$) and bis(trifluoromethanesulfonyl)amide ($[Tf_2N]^-$) anions, that have been reported as good physical absorbents for CO_2 [1,2]. Herein, the density, viscosity, electrical conductivity, and heat capacity of the imidazolium ILs have been measured at atmospheric pressure. Furthermore, the pressure-volume-temperature-composition (*p-V-T-x*) relations have been investigated for the CO_2 + IL systems under the pressures up to 8 MPa. 1-ethyl-3-methylimidazolium tetracyanoborate ([emim][TCB]) has lower density, lower viscosity, higher electrical conductivity, and lower heat capacity than 1-butyl-3-methylimidazolium bis(trifluoromethanesulfonyl)amide ([bmim][Tf_2N]). The molarity scaled solubility of CO_2 in [emim][TCB] is superior to that in [bmim][Tf_2N] at certain temperatures and pressures, although the CO_2 mole fraction in [emim][TCB] is comparable to that in [bmim][Tf_2N].

References

[1] J. L. Anderson, J. K. Dixon, J. F. Brennecke, *Acc. Chem. Res.* **40**, 1208(2007).

[2] S. M. Mahurin, J. S. Lee, G. A. Baker, H. Luo, S. Dai, *J. Membr. Sci.* **353**, 177(2010).

Acknowledgement

This study was partially supported by the New Energy and Industrial Technology Development Organization (NEDO) of Japan.

3PA16 Vapor-Responsive Ionic Liquids from Cationic Metal-Chelate Complexes

Y. Funasako and T. Mochida

Department of Chemistry, Kobe University, Kobe 657-8501, Japan
e-mail: tmochida@platinum.kobe-u.ac.jp

Recently, metal-containing ionic liquids (ILs) that show interesting physical properties have been reported. We have developed ILs containing metallocenium cations [1–3]. In this presentation, we report the preparation and properties of a new series of metal-containing ILs from cationic chelate complexes (Fig. 1) [4]. These ILs exhibit reversible changes in color, as well as in thermal and magnetic properties in response to organic vapors and gases.

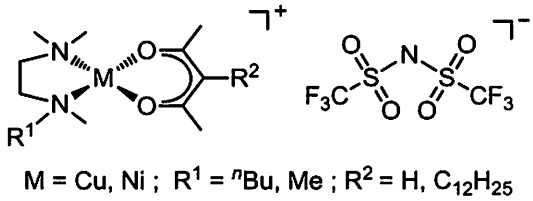

Fig. 1. Structural formulae of the vapor-responsive ionic liquids.

The Cu^{II}-containing ILs are purple, and change color to blue-purple, blue, or green when exposed to different organic vapors (Figure 2). The color change is caused by coordination of vapor molecules to the cation, and the resultant colors depend on the coordination strength (donor number, *DN*) of the vapor molecules. The vapor absorption changes the melting points and viscosities and alters the phase behavior of the ILs. The IL bearing a long alkyl chain changes from purple solid to brown liquid at its melting point. The Ni^{II}-containing IL is dark-red diamagnetic liquid, and changes into a green paramagnetic liquid when it absorbs vapors with high *DN*. The liquid exhibits thermochromism and temperature dependent magnetic susceptibility after absorbing methanol.

We also prepared Cu^{II}-containing ILs from cationic chelate complexes with tripodal ligands.

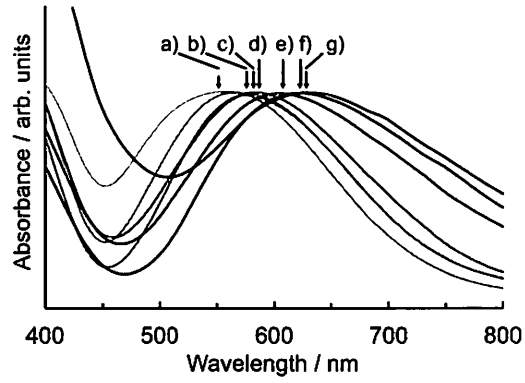

Fig. 2. UV-Vis absorption spectra of Cu^{II}-containing IL a) before and after the absorption of b) acetonitrile, c) acetone, d) methanol, e) DMF, f) DMSO, and g) pyridine.

References

[1] (a) T. Inagaki, T. Mochida, *Chem. Lett.* **2010**, *39*, 572; (b) T. Inagaki, T. Mochida, M. Takahashi, C. Kanadani; T. Saito, D. Kuwahara, *Chem. Eur. J.* **2012**, *18*, 6795; (c) Y. Funasako, K. Abe, T. Mochida, *Thermochim. Acta*, **2012**, *532*, 78; (d) A. Chakraborty, T. Inagaki, M. Banno, T. Mochida, K. Tominaga, *J. Phys. Chem. A* **2011**, *115*, 1313.

[2] Y. Funasako, T. Mochida, T. Inagaki, T. Sakurai, H. Ohta, K. Furukawa, T. Nakamura, *Chem. Commun.* **2011**, *47*, 4475

[3] (a) T. Inagaki, T. Mochida, *Chem. Eur. J.* **2012**, *18*, 8070; (b) S. Mori, T. Mochida, *Organometallics*, **2013**, *32*, 780.

[4] Y. Funasako, T. Mochida, K. Takahashi, T. Sakurai, H. Ohta, *Chem. Eur. J.*, **2012**, *18*, 11929.

3PA17 Metal-Containing Ionic Liquids from 16 Electron Half–Ruthenocenium Cations

S. Yamasaki, and T. Mochida

Department of Chemistry, Kobe University, Kobe 657-8501, Japan

e-mail: tmochida@platinum.kobe-u.ac.jp

Ionic liquids are salts with melting points below 100 °C, and they have interesting properties, such as low vapor pressure, high thermal stabilities, and high ionic conductivities. In our laboratory, a variety of metallocenium ionic liquids, which are functional liquids exhibiting unconventional physical properties and chemical reactivities, have been developed [1].

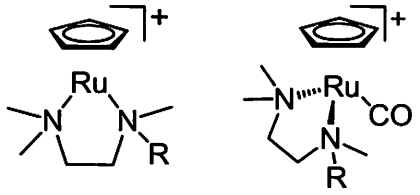

Fig. 1. Structural formulae of (a) 16 electron cations and (b) 18 electron cations with a carbonyl ligand.

In this presentation, we report the preparation and properties of ionic liquids containing 16-electron half-ruthenocenium cations ([CpRu(tmeda)]X). The 16-electron cations have characteristic reactivities toward small molecules due to their unsaturated coordination properties [2]. In the design of ionic liquids, an alkyl chain was introduced to the ligand, and bis(fluorosulfonyl)amide (FSA) anion was employed (Fig. 1a). The product with a butyl substituent was obtained as green liquid with high viscosity.

The 16-electron half-ruthenocenium ionic liquid absorbed acetonitrile vapor (Fig. 2), which resulted in the formation of ionic liquid with 18-electron half-ruthenocenium cation. This reaction, accompanied by a color change from green to red, was reversible. The 16-electron ionic liquid also reacted with carbon monoxide, which resulted in the generation of a carbonyl complex as yellow solid (Fig 1b).

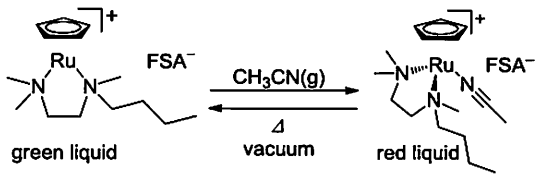

Fig. 2. Adsorption/desorption of acetonitrile by the 16 electron salt.

References

[1] (a) T. Inagaki, T. Mochida, *Chem. Lett.* **2010**, *39*, 572; (b) T. Inagaki, T. Mochida, M. Takahashi, C. Kanadani, T. Saito, D. Kuwahara, *Chem. Eur. J.* **2012**, *18*, 6795; (c) T. Inagaki, T. Mochida, *Chem. Eur. J.*, **2012**, *18*, 8070; (d) Y. Funasako, T. Mochida, T. Inagaki, T. Sakurai, H. Ohta, K. Furukawa, T. Nakamura, *Chem. Commun.* **2011**, *47*, 4475.

[2] (a) C. Gemel, J. C. Huffman, K. G. Caulton, K, Mauthner, K. Mauthner, *J. Organomet. Chem.* **2000**, *593-594,* 342; (b) C. Gemel, K. Mereiter, R. Schmid, K. Kirchner, *Organometallics*, **1997**, *16,* 5601.

3PA18 Liquid-Liquid Equilibria Containing Ionic Liquids for Extraction of Citrus Essential Oil

H. Matsuda, Y. Noriduki, M. Kawai, K. Kurihara, K. Tochigi, and K. Ochi

Department of Materials and Applied Chemistry, Nihon University, Tokyo 101-8308, Japan

e-mail : matsuda.hiroyuki@nihon-u.ac.jp

Ionic liquids (ILs) have attracted a great deal of interest. One of the promising application of ILs is an alternative environmentally friendly solvent in separation processes, such as an extractive solvent for liquid-liquid extraction, and an entrainer for extractive distillation. Recently, ILs have been proposed as a potential extractive solvent for the separation of citrus essential oil using the liquid-liquid extraction. For the design and development of the extraction processes of the essential oil using ILs, the accurate LLE data for binary mixtures IL + essential oil are needed. However, the reported LLE data for these mixtures are scare.

The object of this study is to measure the LLE data in binary mixtures containing ILs and citrus essential oil. We investigated linalool as citrus essential oil. Firstly, the experimental apparatus and procedure for the measurements of LLE containing ILs were verified by measuring the LLE of the binary mixture 1-hexyl-3-methyl-imidazolium bis(trifluoromethanesulfonyl) imide ($[HMIM]^+[TFSI]^-$) + 1-hexanol as a suitable test system recommended by Marsh et al. [2]. Next, the LLE data for IL + linalool were obtained. The LLE data of two binary mixtures 1-butyl-3-methyl-imidazolium bis(trifluoromethanesulfonyl) imide ($[BMIM]^+[TFSI]^-$) or $[HMIM]^+[TFSI]^-$ + linalool were determined. The experimental LLE data were represented using three activity coefficient models, e.g., NRTL, Tsuboka and Katayama's modification of Wilson (T-K-Wilson), and UNIQUAC.

Cloud point method using laser scattering technique developed in our laboratory [3] was used for these measurements. The experimental LLE data for the mixture $[HMIM]^+[TFSI]^-$ + 1-hexanol as a test system agrees reasonably with the recommended value by Marsh et al. and the literature data by Lachwa et al. [4] Therefore, the experimental apparatus and procedure is available for the measurements of LLE containing ILs. The system $[BMIM]^+[TFSI]^-$ + linalool has two solubility curves with UCST and lower critical solution temperature (LCST) from the experimental results of LLE, while the system $[HMIM]^+[TFSI]^-$ + linalool has only one with UCST. Finally, the experimental LLE data for three binary mixtures were correlated using the NRTL, T-K-Wilson, and UNIQUAC models. These models provided a reasonable description of the LLE data for mixtures studied.

References

[1] A. Arce et al., *AIChE J.* **52**, 2089 (2006).

[2] K. N. Marsh, et al., *Pure Appl. Chem.* **81**, 781 (2009).

[3] H. Matsuda et al., *Fluid Phase Equilib.* **297**, 187 (2010).

[4] J. Lachwa et al., *J. Chem. Eng. Data* **51**, 2215 (2006).

3PA19 Green Synthesis of Butyl Salicylate by Dual-site Phase-Transfer Catalyst and Ionic Liquid in Tri-Liquid System

Yu-Hung Hung, Hung-Ming Yang*

Department of Chemical Engineering, National Chung Hsing University, 250 Kuo-Kuang Road, Taichung 402, Taiwan, ROC

e-mail: hmyang@dragon.nchu.edu.tw

Esterification of sodium salicylate (ArCOONa) and 1-bromobutane (RBr) using novel dual-site phase-transfer catalyst 1,4-bis(trihexylammoniomethyl)benzene dibromide (BTHAMBB, QBr_2) to synthesize butyl salicylate via third-liquid phase-transfer catalysis (TLPTC) under ultrasound irradiation was investigated. TLPTC is an environmentally benign technology due to high reaction rate and product selectivity, with green solvent, at mild reaction conditions, and easy reuse of catalysts [1-3]. The catalyst BTHAMBB was synthesized from the reaction of p-xylylene dibromide and excess trihexylamine in acetonitrile at 70 °C. The third-liquid phase containing concentrated catalyst can be prepared simply by using BTHAMBB without extra addition of inorganic salts in the aqueous/organic (toluene or n-heptane) phases. In the tri-liquid system, the intrinsic reaction mainly occurred in this third-liquid phase. Ionic liquid trihexyl(tetradecyl)phosphonium bis(2,4,4-trimethylpentyl)phosphinate (THTDPBTMPP) was employed to enhance the overall reaction rate. The reaction mechanism for ultrasound-assisted third-liquid phase-transfer catalyzed esterification is shown in the following scheme.

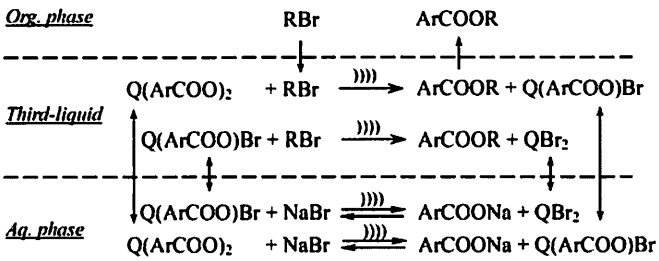

The overall reaction rate can be described by pseudo-first-order kinetic equation. Without using catalyst, no product in the organic phase was observed, but the product yield was 69.7% by BTHAMBB in 4 h of reaction at 70°C, and 250 rpm of stirring speed under ultrasonic irradiation (28 kHz/300 W). By introducing ionic liquid THTDPBTMPP, the product yield can be further increased to 94.1% in the tri-liquid system. It is observed that the product yield can be improved up to 12% increase under ultrasonic irradiation, also showing a higher apparent reaction rate achieved under ultrasound. In this study, the green esterification by dual-site phase-transfer catalyst in TLPTC with ionic liquid was developed.

References

[1] H.M. Yang, G.Y. Peng, *Ultrasonics Sonochem.* **17**, 239-245 (2010).

[2] H.M. Yang, C.C. Chiu, *Ultrasonics Sonochem.* **18**, 363-369 (2011).

[3] H.M. Yang, Y.C. Chen, *J. Taiwan Inst. Chem. Eng.* **43**, 897–903 (2012).

3PA22 *N*-ethyl-*N*-methylpyrrolidinium Fluorohydrogenate Ionic Liquid - Polymer Composite Membranes Prepared by Living Radical Polymerization (LRP) for a Nonhumidified Fuel Cell

P. Kiatkittikul[1], J. Yamaguchi[1], T. Nohira[1], R. Hagiwara[1], Y. Tsujii[2], and T. Sato[3]

[1]*Graduate School of Energy Science, Kyoto University, Kyoto 606-8501, Japan*
[2]*Institute for Chemical Research, Kyoto University, Uji 611-0011, Japan*
[3]*Tsuruoka National College of Technology, Tsuruoka, Japan 997-8511*
e-mail : hagiwara@energy.kyoto-u.ac.jp

Operation at intermediate temperature (> 100 °C) without humidification offers several prominent benefits for PEFCs such as reduction of noble catalyst and simplicity of the unit. In the previous study, we reported a non-humidified fuel cell using a composite membrane of EMPyr$(FH)_{1.7}F$ (EMPyr = *N*-ethyl-*N*-methylpyrrolidinium) ionic liquid and HEMA (2-hydroxyethylmethacrylate) polymer [1]. However, the single cell performance was largely decreased when the operation temperature was elevated from 80 °C to 120 °C [1].

In this study, living radical polymerization (LRP), an efficient method for preparing well-defined and low-polydispersity polymers [2], was employed. EMPyr$(FH)_{1.7}F$ and HEMA monomer were mixed in the molar ratio of 8:2. Small amount of AIBN (2,2'-Azobis(isobutyronitrile)) was added as a radical initiator. CP-I (2-cyanopropyliodide) was also added to produce a dormant species. PTFE filter (thickness: 65 μm, porosity: 80%) used as a porous supporting material was immersed in the mixed solution. Then, polymerization was conducted at 70 °C in Ar-filled oven for 12 h.

Single cell tests were conducted under nonhumidified conditions at 25-120 °C. The GDEs with 1.0 mg Pt cm^{-2} were used for both the anode and cathode. It was revealed that, contrary to the conventional membrane, the cell performance properly improved with temperature due to the increase of electrochemical reaction rate. The maximum power density of 16 mW cm^{-2} was observed at 120 °C. The reason for this difference is possibly explained as follows. At high temperature, the conventional membrane was softened and the composite electrolyte penetrated into GDEs to partially plug the gas channels in the gas diffusion layer. On the other hand, the LRP membrane was supposed to have higher mechanical strength even at high temperatures to properly preserve the MEA structure.

References

[1] P. Kiatkittikul, T. Nohira, R. Hagiwara, *J. Power Sources*, **220**, 10 (2012).

[2] A. Goto, T. Suzuki, H. Ohfuji, M. Tanishima, T. Fukuda, Y. Tsujii, H. Kaji, *Macromolecules*, **44**, 8709 (2011).

3PA19 Green Synthesis of Butyl Salicylate by Dual-site Phase-Transfer Catalyst and Ionic Liquid in Tri-Liquid System

Yu-Hung Hung, Hung-Ming Yang*

Department of Chemical Engineering, National Chung Hsing University, 250 Kuo-Kuang Road, Taichung 402, Taiwan, ROC

e-mail: hmyang@dragon.nchu.edu.tw

Esterification of sodium salicylate (ArCOONa) and 1-bromobutane (RBr) using novel dual-site phase-transfer catalyst 1,4-bis(trihexylammoniomethyl)benzene dibromide (BTHAMBB, QBr_2) to synthesize butyl salicylate via third-liquid phase-transfer catalysis (TLPTC) under ultrasound irradiation was investigated. TLPTC is an environmentally benign technology due to high reaction rate and product selectivity, with green solvent, at mild reaction conditions, and easy reuse of catalysts [1-3]. The catalyst BTHAMBB was synthesized from the reaction of p-xylylene dibromide and excess trihexylamine in acetonitrile at 70 °C. The third-liquid phase containing concentrated catalyst can be prepared simply by using BTHAMBB without extra addition of inorganic salts in the aqueous/organic (toluene or n-heptane) phases. In the tri-liquid system, the intrinsic reaction mainly occurred in this third-liquid phase. Ionic liquid trihexyl(tetradecyl)phosphonium bis(2,4,4-trimethylpentyl)phosphinate (THTDPBTMPP) was employed to enhance the overall reaction rate. The reaction mechanism for ultrasound-assisted third-liquid phase-transfer catalyzed esterification is shown in the following scheme.

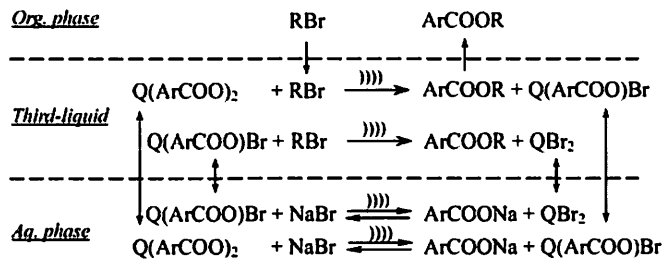

The overall reaction rate can be described by pseudo-first-order kinetic equation. Without using catalyst, no product in the organic phase was observed, but the product yield was 69.7% by BTHAMBB in 4 h of reaction at 70°C, and 250 rpm of stirring speed under ultrasonic irradiation (28 kHz/300 W). By introducing ionic liquid THTDPBTMPP, the product yield can be further increased to 94.1% in the tri-liquid system. It is observed that the product yield can be improved up to 12% increase under ultrasonic irradiation, also showing a higher apparent reaction rate achieved under ultrasound. In this study, the green esterification by dual-site phase-transfer catalyst in TLPTC with ionic liquid was developed.

References

[1] H.M. Yang, G.Y. Peng, *Ultrasonics Sonochem.* **17**, 239-245 (2010).

[2] H.M. Yang, C.C. Chiu, *Ultrasonics Sonochem.* **18**, 363-369 (2011).

[3] H.M. Yang, Y.C. Chen, *J. Taiwan Inst. Chem. Eng.* **43**, 897–903 (2012).

3PA20 Functional Ionic Liquids from Metallocenium Cations

T. Mochida, Y. Funasako, and T. Inagaki

Department of Chemistry, Kobe University, Kobe 657-8501, Japan

e-mail: tmochida@platinum.kobe-u.ac.jp

Metallocenium cations exhibit a variety of physical properties and chemical reactivities. In this presentation, we show that metallocenium salts with various substituents, anions, and metal ions afford a variety of functional ILs [1].

The structural formulae of the ionic liquids with sandwich-type metallocenium cations are shown in Fig. 1. The ferrocenium ILs (Fig. 1a) are blue or green paramagnetic liquids, whereas the cobaltocenium ILs (Fig. 1b) are orange diamagnetic liquids. The arene-ferrocenium ILs (Fig. 1c) are reddish-brown liquids. Correlations between the molecular structure and thermal properties were investigated. The metallocenium ILs exhibited interesting physical properties and chemical reactivities. Paramagnetic ferrocenium ILs exhibited magnetic susceptibility changes coupled with liquid–solid phase transformation near room temperature [2]. Chemical reactivities and catalytic activities of metallocenium ILs including half-metallocenium ILs [3] are also discussed.

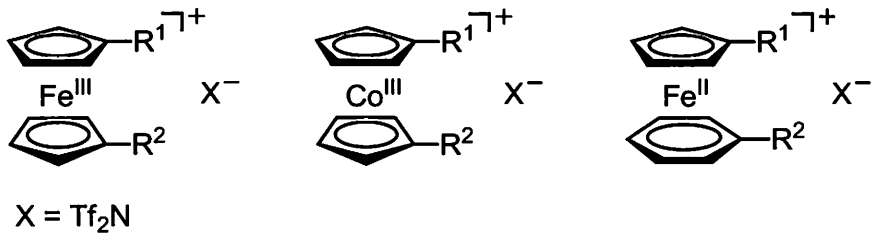

Fig. 1. Structural formulae of the metallocenium ILs.

References

[1] (a) T. Inagaki, T. Mochida, *Chem. Lett.* **2010**, *39*, 572; (b) T. Inagaki, T. Mochida, M. Takahashi, C. Kanadani, T. Saito, D. Kuwahara, *Chem. Eur. J.* **2012**, *18*, 6795; (c) Y. Funasako, K. Abe, T. Mochida, *Thermochim. Acta*, **2012**, 532, 78; (d) A. Chakraborty, T. Inagaki, M. Banno, T. Mochida, K. Tominaga, *J. Phys. Chem. A* **2011**, *115*, 1313.

[2] Y. Funasako, T. Mochida, T. Inagaki, T. Sakurai, H. Ohta, K. Furukawa, T. Nakamura, *Chem. Commun.* **2011**, *47*, 4475.

[3] (a) T. Inagaki, T. Mochida, *Chem. Eur. J.*, **2012**, *18*, 8070; (b) S. Mori, T. Mochida, *Organometallics*, **2013**, *32*, 780.

3PA21 Physicochemical Properties of Ionic Liquids Consisting of 1-Butyl-3-vinylimidazolium Cation and Halide Anions

T. Tsuda[1], R. Taniki[2], M. Baba[1], H. Narikawa[1], Y. Iwasaki[1],

K. Matsumoto[2], R. Hagiwara[2], and S. Kuwabata[1]

[1]*Department of Applied Chemistry, Osaka University, Osaka 565-0871, Japan*
[2]*Department of Fundamental Energy Science, Kyoto University, Kyoto 606-8501, Japan*
e-mail: ttsuda@chem.eng.osaka-u.ac.jp

Ionic liquid (IL) is a curious salt having a liquid phase at room temperature. It is well-known that IL has various physicochemical features, but one of the most important points is that we can add the functionality that we want by a simple chemical synthesis. Recently, we have focused on 1-butyl-3-vinylimidazolium ($[C_4Vyim]$)-based ILs that are easily polymerized by adding a radical initiator, because such ILs are widely employed in materials chemistry due to the interesting functionality [1]. However, there is a limited number of physicochemical data on the $[C_4Vyim]$-based ILs. In this study, we revealed that the physicochemical properties of the functional ILs consisting of $[C_4Vyim]^+$ and various halide anions, $[(FH)_nF]^-$ (n = 2 or 3) , Cl^-, Br^-, I^-, $[BF_4]^-$, and $[(CF_3SO_2)_2N]^-$ [2].

Unfortunately $[C_4Vyim]Cl$ and $[C_4Vyim]Br$ did not show a physically-stable liquid phase at 293 K, and the melting points were 384 K and 340 K, respectively. We could not estimate other physicochemical properties of these two salts except thermophysical ones. Thermal decomposition temperature, T_{dec} (K), of the $[C_4Vyim]$-based ILs and salts strongly depended on the anionic species. The T_{dec}, which was estimated at the temperature of 1 wt% loss, increased with decreasing the nucleophilicity of the anions because the decomposition pathway most likely proceeds via S_N1 or S_N2 reactions [2], but as for the $[C_4Vyim][(FH)_{2.1}F]$, it should be due to the liberation of HF molecules from the $[(FH)_2F]^-$ or $[(FH)_3F]^-$ [3]. The major decomposition initiated at the temperature similar to that for $[C_4Vyim]Cl$, $[C_4Vyim]Br$, and $[C_4Vyim]I$. As we expected, the $[C_4Vyim]^+$-based ILs with thermally-stable and bulky fluoroanions, $[BF_4]^-$ and $[(CF_3SO_2)_2N]^-$, showed better thermal stability than other ILs reported in this investigation. All the T_{dec} of the $[C_4Vyim]^+$-based ILs were lower than those for 1-butyl-3-methylimidazolium ($[C_4mim]^+$)-based ILs that have an analogous cationic structure if the anion is the same, although their glass transition temperatures were almost the same as the $[C_4mim]^+$-based ones. The vinyl group on the cations would relate to the destabilization of the ILs. Other properties will be given in our presentation, too.

References

[1] T. W. Smith, M. Zhao, F. Yang, D. Smith, P. Cebe, *Macromolecules* **46**, 1133 (2013).

[2] T. Tsuda, C. L. Hussey, *in* Modern Aspects of Electrochemistry Vol.45, R. E. White, ed., Springer, pp. 63-174 (2009), and references therein.

[3] K. Matsumoto, T. Tsuda, R. Hagiwara, Y. Ito, O. Tamada, *Solid State Sci.* **4**, 23 (2002).

3PA22 *N*-ethyl-*N*-methylpyrrolidinium Fluorohydrogenate Ionic Liquid - Polymer Composite Membranes Prepared by Living Radical Polymerization (LRP) for a Nonhumidified Fuel Cell

P. Kiatkittikul[1], J. Yamaguchi[1], T. Nohira[1], R. Hagiwara[1], Y. Tsujii[2], and T. Sato[3]

[1]*Graduate School of Energy Science, Kyoto University, Kyoto 606-8501, Japan*
[2]*Institute for Chemical Research, Kyoto University, Uji 611-0011, Japan*
[3]*Tsuruoka National College of Technology, Tsuruoka, Japan 997-8511*
e-mail : hagiwara@energy.kyoto-u.ac.jp

Operation at intermediate temperature (> 100 °C) without humidification offers several prominent benefits for PEFCs such as reduction of noble catalyst and simplicity of the unit. In the previous study, we reported a non-humidified fuel cell using a composite membrane of $EMPyr(FH)_{1.7}F$ (EMPyr = *N*-ethyl-*N*-methylpyrrolidinium) ionic liquid and HEMA (2-hydroxyethylmethacrylate) polymer [1]. However, the single cell performance was largely decreased when the operation temperature was elevated from 80 °C to 120 °C [1].

In this study, living radical polymerization (LRP), an efficient method for preparing well-defined and low-polydispersity polymers [2], was employed. $EMPyr(FH)_{1.7}F$ and HEMA monomer were mixed in the molar ratio of 8:2. Small amount of AIBN (2,2'-Azobis(isobutyronitrile)) was added as a radical initiator. CP-I (2-cyanopropyliodide) was also added to produce a dormant species. PTFE filter (thickness: 65 μm, porosity: 80%) used as a porous supporting material was immersed in the mixed solution. Then, polymerization was conducted at 70 °C in Ar-filled oven for 12 h.

Single cell tests were conducted under nonhumidified conditions at 25-120 °C. The GDEs with 1.0 mg Pt cm^{-2} were used for both the anode and cathode. It was revealed that, contrary to the conventional membrane, the cell performance properly improved with temperature due to the increase of electrochemical reaction rate. The maximum power density of 16 mW cm^{-2} was observed at 120 °C. The reason for this difference is possibly explained as follows. At high temperature, the conventional membrane was softened and the composite electrolyte penetrated into GDEs to partially plug the gas channels in the gas diffusion layer. On the other hand, the LRP membrane was supposed to have higher mechanical strength even at high temperatures to properly preserve the MEA structure.

References

[1] P. Kiatkittikul, T. Nohira, R. Hagiwara, *J. Power Sources*, **220**, 10 (2012).

[2] A. Goto, T. Suzuki, H. Ohfuji, M. Tanishima, T. Fukuda, Y. Tsujii, H. Kaji, *Macromolecules*, **44**, 8709 (2011).

3PA23 $Na_2FeP_2O_7$ Pyrophosphate Positive Electrode for Sodium Secondary Battery Utilizing $NaN(SO_2F)_2$ – $KN(SO_2F)_2$ Ionic Liquid Electrolyte

C.Y. Chen[1], K. Matsumoto[1], T. Nohira[1], R. Hagiwara[1], A. Fukunaga[2], S. Sakai[2], K. Nitta[2], and S. Inazawa[2]

[1]*Graduate School of Energy Science, Kyoto University, Sakyo-ku, Kyoto 606-8501, Japan*

[2]*Sumitomo Electric Industries Ltd., 1-1-3 Shimaya, Konohana-ku, Osaka 554-0024, Japan*

e-mail: nohira@energy.kyoto-u.ac.jp, hagiwara@energy.kyoto-u.ac.jp

In our previous study, a new class of ionic liquids (ILs) consisting of alkali metal cations and bis(fluorosulfonyl)amide ($N(SO_2F)_2$) anions has been explored. Especially, the non-volatile $NaN(SO_2F)_2$–$KN(SO_2F)_2$ binary electrolyte has been proved to enable the fabrication of sodium secondary battery with decent electrochemical properties when $NaCrO_2$ is used as a positive electrode active material [1-2].

In this study, we focused on $Na_2FeP_2O_7$ as a positive electrode active material and investigated its charge-discharge behaviour in $NaN(SO_2F)_2$–$KN(SO_2F)_2$ ionic liquid at 363 K. $Na_2FeP_2O_7$ was prepared by a simple solid-state reaction, modified from ref. 3. The electrode gives a reversible capacity of 91 mA h g^{-1} with excellent rate capability and outstanding capacity retention of 97.8% over 250 cycles, which enables low-cost and high-safety Na secondary battery for large-scale energy storage applications.

References

[1] A. Fukunaga, T. Nohira, Y. Kozawa, R. Hagiwara, S. Sakai, K. Nitta, S. Inazawa, *J. Power Sources* **209,** 52 (2012) .

[2] C.Y. Chen, K. Matsumoto, T. Nohira, R. Hagiwara, A. Fukunaga, S. Sakai, K. Nitta, S. Inazawa, *J. Power Sources*, in press (DOI: 10.1016/j.jpowsour.2013.03.006).

[3] P. Barpanda, T. Ye, S. Nishimura, S.C. Chung, Y. Yamada, M. Okubo, H.S. Zhou, A. Yamada, *Electrochem. Commun.* **24**, 116 (2012).

[4] J. Angenault, J.C. Couturier, M. Quarton, F. Robert, *Eur. J. Solid State Inorg. Chem.* **32**, 335 (1995).

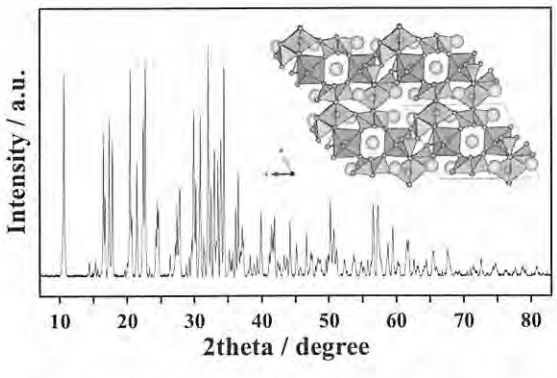

Fig. 1 X-ray diffraction pattern for as-synthesized $Na_2FeP_2O_7$. (Inset) A representative illustration of the crystal structure viewed normal to the *bc* plane which is modified from ref. 4.

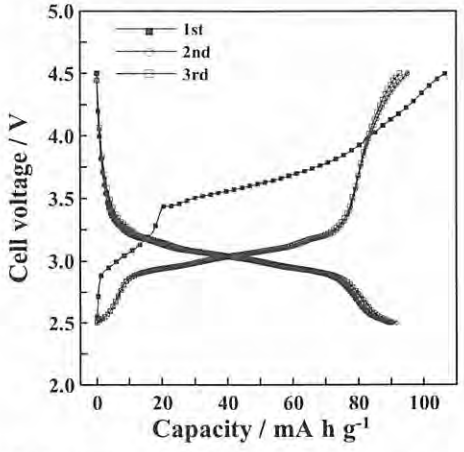

Fig. 2 Galvanostatic charge-discharge curve of the initial three cycles of $Na_2FeP_2O_7$ at a current density of 10 mA g^{-1} in the voltage range of 2.5 – 4.5 V in $NaN(SO_2F)_2$–$KN(SO_2F)_2$ ionic liquid at 363 K.

3PA24 Scanning Electron Microscope observation of nano/ biological materials with Room Temperature Ionic Liquids

S. Abe[1], A. Hyono[2], K. Kawai[2, 3] and T. Yonezawa[2]

[1]*Graduate School of Dental Medicine, Hokkaido University, Sapporo 060-8586, JAPAN*

[2]*Division of Materials Science and Engineering, Faculty of Engineering, Hokkaido University, Sapporo 060-8628, JAPAN*

[3]*Miyoshi Oil and Fat Co., Ltd, Tokyo 124-8510, JAPAN*

e-mail : sabe@den.hokudai.ac.jp

A novel pre-treatment method for scanning electron microscopy (SEM) observation using room temperature ionic liquids (RTILs) was used for several nano/biological materials. By immersion in only an RTIL solution, clear SEM images of several types of nano/biological samples were successfully observed. The quality of images was almost the same as that obtained with conventional platinum/palladium (Pt/Pd) spattering pre-treatment. The highest resolution in this study was less than 30 nm. For the pre-treatment of biological samples, we synthesized novel choline-type RTILs series, which have a molecular structure resembling that of the vitamin-like active substance choline. They have high water solubility, high osmotic pressure, and high cell membrane permeability. Their physical properties make them a very useful pretreatment agent for SEM observation of hydrous samples because they can replace water in the samples, causing them to retain their shapes. These results suggest that the pre-treatment with RTIL can form ultra-thin layer on the sample surface at several molecules level. Thus, the RTILs pre-treatment can be a simple and easy tool for SEM observation of nano/biological materials.

References

[1] K. Kawai, K. Kaneko, H. Kawakami, and T. Yonezawa, *Langmuir* **27**, 9671 (2011).

[2] K. Kawai, K. Kaneko, H. Kawakami, T. Narushima, and T. Yonezawa, *Colloids Surf. B,* **102**, 9 (2013).

[3] S. Abe, A. Hyono, Y. Machida, F. Watari, and T. Yonezawa, *Nano Biomedicine*, **4**, 18 (2012).

[4] S. Abe, A. Hyono, K. Nakayama, T. Takada, and T. Yonezawa, *Jpn J. Appl. Phys.* **52**, p01AH02 (2013).

[5] S. Abe, A. Hyono, and T. Yonezawa, *Thin Solid Films (submitted).*

3PA25 Measurement and Correlation of Viscosity for Binary Mixtures Containing Ionic Liquids at Temperature from (293.15 - 353.15) K Using Falling Ball Viscometer

Y. Itazu, K. Ishii, K. Kurihara, H.Matuda K. Tochigi, and K. Ochi

Department of Materials and Applied Chemistry, Nihon University, Tokyo 101-8308, Japan

e-mail : kurihara.kiyofumi@nihon-u.ac.jp

There has been an increasing in ionic liquids (ILs). ILs have some unique properties, e.g. negligible low pressures, thermal stability etc. and these can lead to their application as an alternative environmentally benign solvent for the reaction and separation processes, and as an electrically conducting fluids.[1-2] The viscosity is a key property for the development of processes and products containing ILs. The measurements of viscosities for ILs have been recently pursued actively. But, the experimental data on the viscosity of ILs are still scarce. The viscosity data of binary or multicomponent mixtures containing ILs are important for the design and development in the liquid-liquid extraction using ILs as an extractive solvent. However, these data have not been reported enough.

The object of this study is to measure the viscosities at atmospheric pressure for binary mixtures containing IL. We investigated water + 1-butyl-pyridinium tetrafluoroborate [BuPy][BF_4] as the binary mixture.

A falling ball viscometer was used for the measurements of the viscosities. Before the measurements of the binary mixture, the viscosities of 1-hexyl-3-methylimidazolium bis(trifluoromethylsulfonyl)imide [HMIM][TFSI] on a reference IL recommended by Marsh et al.[3] was measured, in order to confirm the experimental apparatus and procedure. The comparison of the experimental data with the recommended values by Marsh et al. shows that the experimental apparatus and procedure are available for the measurements of viscosities containing IL.

The viscosities for the binary mixture water + [BuPy][BF_4] were determined at the temperature (293.15 to 353.15)K, and over whole mole fraction range of water. The experimental data of this mixture shows that the viscosity decreases with an increase in temperature and the composition of water. The experimental viscosity data were also correlated by Redlich-Kister(R-K) polynomial function. The R-K equation gave a reasonable correlation accuracy of the experimental data.

References

[1] A. P. Froba, H. Kremer, A. Leipertz, J. Phys. Chem. B 112 (2008) 12420–12430.
[2] M. Ge et al., J. Chem. Eng. Data 54 (2009) 1400–1402.
[3] Marsh N. et al.; *J. Pure Appl Chem.*, **81**, 781-828 (2009)
[4] Mokhtarani B. et al.; *J. Chem. Thermodynamics*, **41**, 323-329 (2009)

3PB11 Monitoring Migration of Heavy Metal into Food Simulants from Food Contact Materials

Dong-Woo Shin, Jae-Myoung Oh, Jae-Chon Choi, Ho-Soo Lim, Se-Jong Park, Hyeah Goh and Meehye Kim

[1]Food Additives and Packages Division, *National Institute of Food and Drug Safety Evaluation, Ministry of Food and Drug Safety, Cheongwon-gun, Chungcheongbuk-do, Korea*

e-mail : dwsh@korea.kr

Ceramics raw materials which are mostly soil could contain harmful heavy metals (especially lead, cadmium, and arsenic). The way of ceramic manufacture has been developed to produce better lustrous ceramics using heavy metal compounds as a glaze. Also, glass which is added at the time of manufacture stabilizer and fresheners could contain toxic heavy metals such as lead, arsenic. So, there are concerns that food packaging and containers manufacturing impurities as residual heavy metals are migrated into food. This study was to investigate the migration of heavy metals (cadmium, lead, arsenic, antimony) from food packaging and containers (glass, ceramics, porcelain enamel) using Inductively Coupled Plasma - Optical Emission Spectrometer (ICP-OES). Method validation was performed by determining linearity, limit of quantification (LOQ) and recovery. The method presented good linearity over the range assayed 0.005-10 mg/L and the LOQ ranged from 0.005-0.1 mg/L. The heavy metals were leached out with 4% acetic acid stored in the samples at room temperature for 24 h. These migration results of heavy metal will provide a scientific basis for the management of the safety food packaging and container materials.

3PB12 Vibrational dynamics of a solute molecule in aqueous solution studied by two-dimensional infrared spectroscopy

Masaki Okuda[1], Kaoru Ohta[2], Keisuke Tominaga[1,2]

[1]*Graduate School of Science and* [2]*Molecular Photoscience Research Center, Kobe University*

Address: 1-1 Rokkodaicho, Kobe, Hyogo 657-8501, Japan

e-mail : 120s205s@stu.kobe-u.ac.jp

In liquid water, three-dimensional hydrogen-bonded network structures are formed by intermolecular hydrogen bonds. Making and breaking of the hydrogen bonds and rearrangement of the hydrogen bond network accompany large fluctuation in the potential energy of the system. These fluctuations play an important role in the chemical reactions and biological functions in aqueous solutions. Two-dimensional infrared (2DIR) spectroscopy is a powerful technique to investigate fluctuations of vibrational transition frequencies of solute molecules in solution. In the present study, we focus on a thiocyanate group (-SCN) of 2-nitro-5-thiocyanatobenzoic acid (NTBA) as a probe to examine vibrational fluctuation in aqueous solutions by 2DIR spectroscopy.

The obtained 2DIR spectrum and its center line slope (CLS) are shown in Figure 1 and Figure 2, respectively. The CLS is plotted against the population time T. It is theoretically shown that the CLS is directly proportional to the frequency-frequency time correlation function (FFTCF) [1]. The CLS of NTBA can be fitted by a single-exponential function ($\Delta_1^2\exp(-t/\tau) + \Delta_0^2$). The value of Δ_0 is approximately 0.15 ps^{-1} and, for SCN^- in D_2O, the value of Δ_0 is 0 ps^{-1} [2]. Comparing the values of Δ_0 of NTBA and SCN^-, the vibrational dynamics of hydrophobic probe is different from that of hydrophilic probe. It can be thought that the value of Δ_0 of NTBA reflects the existence of slow dynamics around NTBA which proceeds over more than 2 ps, or inhomogeneous environment distribution of different molecular conformations of NTBA

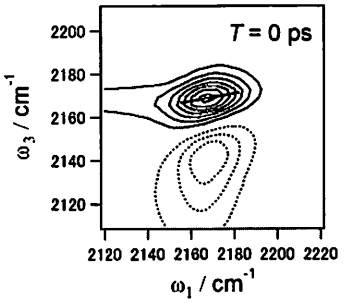

Figure 1. The 2DIR spectrum of NTBA at $T = 0$ ps. Solid and dotted lines indicate positive and negative amplitude, respectively. The straight line in the spectrum is centre line of the spectrum.

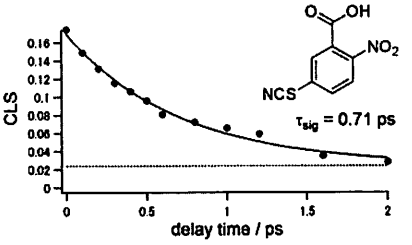

Figure 2. The CLS curve from each 2DIR spectra of NTBA plotted against the population time T. The molecule used in this study is shown in the figure.

References:

[1] K. Kwak, et al., J. Chem. Phys., **127**, 124503 (2007).

[2] K.Ohta *et al.*, Acc. Chem. Res., **45** 1982–1991 (2012).

3PB13 Theoretical study on the absorption and emission spectra of squaraine molecule in solvents

H. Ozawa[1], K. Yashiro[1], T. Yamamoto[1], and S. Yabushita[1]

[1]*Department of Chemistry, Keio University, Yokohama 223-8522, Japan*

e-mail: ozawa@sepia.chem.keio.ac.jp

Bis[4-(dimethylamino)-phenyl]squaraine(squaraine) has the absorption and emission bands in the range of 550-750nm. Law indicated that this molecule has three emission bands and called α, β, and γ bands. He considered the α band is emission from the excited state of free squaraine in solution, the β emission is from the excited state of the solute-solvent complex and the γ emission is from the twisted intramolecular charge transfer (TICT) state[1]. However, Kamat et al. reported later that the α and β emissions were merged in the emission peak[2]. Furthermore, Rettig et al. stated the fluorescence is from one single species and a TICT state acts as a nonemissive funnel to the ground state[3]. In this way, the origin of the emission bands has long been controversial. In this study, we try to resolve these problems theoretically.

Firstly, we calculated free energy changes going from the planar Franck-Condon state to nine twisted structures in the excited states by the PCM-TDBOP method, and found that all of the internal rotation paths require large endothermic energy to arrive at twisted structures. The result suggested that internal rotations are less likely. Secondly, we calculated the theoretical absorption and emission spectra of the planar structure by evaluating the Franck–Condon factor with including Duschinsky effect. The S_0 and S_1 structures were optimized by the CASSCF and MRMP2 methods, and the vibrational frequencies were obtained by the (TD)B3LYP method. The result indicated that the responsible excited state is the lowest B_{1u} state with a planar structure because the theoretically simulated spectral shape and the Stokes shift are in good agreement with the corresponding experimental results.

In conclusion, our study suggests that the fluorescence is from one single species, and the responsible state is the B_{1u} excited state of the planar structure.

References

[1] K. Y. Law, *J. Phys. Chem.*, **91**, 5184, (1987) .

[2] P. V. Kamat et al., *J. Phys. Chem.*, **96**, 195, (1992).

[3] W. Rettig et al., *J. Phys. Chem. A*, **101**, 9673, (1997).

3PB14 Effects of salts on the hydrogen bond network of water studied by near-infrared spectroscopy

N. Uchida[1], K. Fukuhara[1], N. Yoshimura[2] and M. Takayanagi[2]

[1]*Graduate School of Agriculture, and* [2]*United Graduate School of Agricultural Science, Tokyo University of Agriculture and Technology, Fuchu, Tokyo 183-8509, Japan*

e-mail : masaot@cc.tuat.ac.jp

The hydrogen bond network of water is affected by dissolving salt. Although the effect is well known to depend on the kind of salt, it is not easy to elucidate the dependence in detail. We observe the change of the hydrogen bond network of water on dissolving salt by near-infrared (NIR) spectroscopy suitable for the observation of the change; NIR spectra reflect sensitively the hydrogen bond network.

NIR absorption spectra of aqueous solutions of various salts consisting of sodium ion as the cation at various concentrations in a quartz cell with an optical path-length of 1 mm were measured with an FT-NIR spectrophotometer (Bruker, MPA, Resolution: 8 cm^{-1}, Accumulation: 32 scans). The temperature of sample is stabilized at 30°C with the thermostat equipped on the spectrophotometer. The observed spectra were corrected with the densities of water determined by weighing the solutions of a fixed quantity.

In 7400-6200 cm^{-1} region of the NIR absorption spectra of aqueous solutions, a broad band corresponding to the overtone of OH stretching mode is observed. The higher wavenumber side of the band is due to non-hydrogen bonded OH, while the lower wavenumber side is due to hydrogen bonded OH. Therefore, the shape of whole band, which reflects the degree of hydrogen bonding of water, changes upon dissolving salt. By dissolving Na_2CO_3, absorption intensity in the higher wavenumber region due to non-hydrogen bonded OH decreases while that in the lower wavenumber region due to hydrogen bonded OH increases, showing the expansion of hydrogen bond network. On the other hand, in the case of NaI aqueous solution, absorption intensity in the higher wavenumber region increases and that in the lower wavenumber region decreases, suggesting the reduction of hydrogen bond network upon the dissolution of the salt. The completely opposite effects on the hydrogen bond network of water were clearly observed for CO_3^{2-} and I^-.

Although the variation of OH band of water observed in NIR spectrum upon the dissolution of salt depends on the kind of salt, PCA (principal component analysis) of the spectra of aqueous solution of various salts revealed that only two components are mainly related to the variations. The first component reflects the degree of hydrogen bonding of water, while the second component presumably reflects the concentration of OH^-.

We have found that NIR spectroscopy is a powerful tool for the investigation of the effect of salt on the hydrogen bond network of water.

3PB15 Liquid Structure and the Noncoincidence Effect of Liquid Dimethyl Sulfoxide Revisited

Maurizio Musso[1], Maria Grazia Giorgini[2], and Hajime Torii[3]

[1]*Fachbereich Materialforschung und Physik, Abteilung Physik und Biophysik, Universität Salzburg, Hellbrunnerstraße 34, A-5020 Salzburg, Austria*

[2]*Dipartimento di Chimica Industriale 'Toso Montanari', Università di Bologna, Viale del Risorgimento 4, I-40136 Bologna, Italy*

[3]*Department of Chemistry, School of Education, Shizuoka University, 836 Ohya, Shizuoka 422-8529, Japan*

e-mail : torii@ed.shizuoka.ac.jp

Liquid structure and intermolecular interactions of liquid dimethyl sulfoxide (DMSO) have been studied for past decades. While this is sometimes regarded as a strongly associated liquid because of its high boiling point and other unusual thermodynamic properties [1,2], it is suggested in recent studies on the neutron and X-ray diffractions and molecular dynamics (MD) simulations [3,4] that the liquid structure is mainly governed by dipolar interactions. Analysis of the vibrational spectra is expected to clarify the situation, and the large magnitude of the noncoincidence effect (NCE) and/or the peculiar band profile of the S=O stretching band are regarded as indicating the strong molecular association in the liquid [5,6]. However, the true meaning of the band profile is not yet well known.

In the present study, polarized Raman spectra are measured for the liquid of the ^{13}C substituted species [$O=S(^{13}CH_3)_2$]. It is shown that the S=O stretching band profile of this species is much simpler than that of the normal species, indicating that the peculiar band profile observed for the latter arises from the coupling with the combinations of low-frequency modes rather than the molecular association. The magnitude of the NCE is about 7 cm^{-1}, much smaller than previously suggested. To obtain rather precise estimation of the magnitude of vibrational coupling (which is needed to relate this spectral feature to the liquid structure), DFT calculations are carried out for the DMSO dimer with a few different molecular configurations. Spectral simulations on the basis of the vibrational coupling thus obtained and a few different potential functions of MD clearly show that the magnitude of the NCE is related to the relative configurations of the S=O groups of neighboring molecules.

References

[1] D. Martin, A. Weise, H.-J. Niclas, *Angew. Chem. Int. Ed.* **6**, 318 (1967).

[2] A. J. Parker, *Q. Rev. Chem. Soc.* **16**, 163 (1962).

[3] U. Onthong, T. Megyes, T. Radnai, T. Grosz, K. Hermansson, M. Probst, *Phys. Chem. Chem. Phys* **6**, 2136 (2004).

[4] S. E. McLain, A. K. Soper, A. Luzar, *J. Chem. Phys.* **124**, 074502 (2006).

[5] C. Czeslik, Y. J. Kim, J. Jonas, *J. Chem. Phys.* **111**, 9739 (1999).

[6] W. N. Martens, R. L. Frost, J. Kristof, J. T. Kloprogge, *J. Raman Spectrosc.* **33**, 84 (2002).

3PB16 Raman spectroscopic study on the conformational equilibria of 1,4-dioxane in aqueous solution

Ryoichi Wada[1], Hozumi Tsuda[1], and Minoru Kato[1,2]

[1]*Graduate School of Science and Engineering and* [2]*College of Pharmaceutical Sciences, Ritsumeikan University, Kusatsu 525-8577, Japan.*

e-mail to M. Kato: kato-m@ph.ritsumei.ac.jp

Polyethers such as poly(oxyethylene) and crown-ether, which have O-CC-O segment, are infinitely soluble in water. It has been though that the intramolecular distance between two oxygen atoms, 2.9 Å, which is similar to the intermolecular distance of oxygen atoms of neighboring water molecules in bulk water, plays an important role in hydration. 1,4-Dioxiane is a simple cyclic-ether and has three conformers i.e. the chair, boat and twist conformers. The intramolecular distances between two oxygen atoms of the conformers are different from each other. In this study, we investigated the conformational equilibria of 1,4-dioxiane in aqueous solution using Raman spectroscopy.

Raman spectra of 1,4-dioxnae in water at various concentrations are shown in figure 1 .The bands at 490 cm^{-1}, 520 cm^{-1} and 560 cm^{-1} are assigned to the OCC deformation mode of the chair, twist and boat conformers, respectively. The relative intensity of the boat conformer decreases with increasing water concentration, while that of the twist conformer increases. In polar organic solvents such as methanol, the opposite results were obtained.

We discuss the thermodynamics difference between the conformers determined from the temperature dependence of Raman intensity ratio of the conformers. We divided the thermodynamic differences into the electrostatic and local contributions to discuss the solvent effect. The electrostatic contribution was estimated by DFT calculation with polarizable continuum model (PCM).

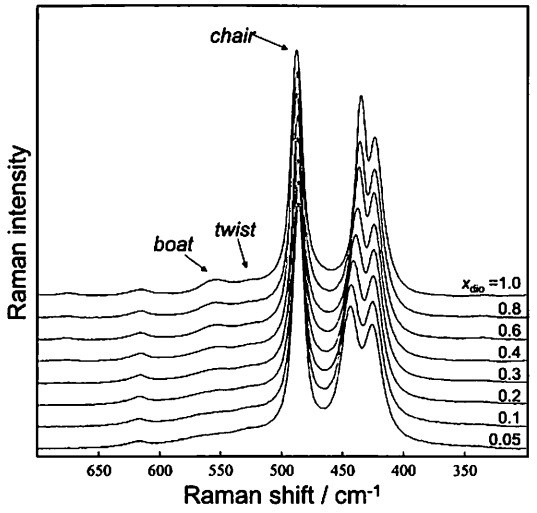

Figure 1. Raman spectra of 1,4-dioxane in water at various concentrations and 298.2 K.

3PB17 Detailed insight to the hydrogen bonding interactions in acetone-methanol mixtures. An Infrared spectroscopy and Voronoi polyhedra analysis study

A.Idrissi[1*], K. Polok[2*], J. G. Da Cunha[3] , I. Dewale[1], M. Bria[4] and W. Gadomski[2]

[1] *University Nord de France, Lille1,LASIR (UMR CNRS A8516) 59655 Villeneuve d'Ascq Cedex, France*

[2] *Laboratory of Physico-chemistry of Dielectrics and Magnetics, Department of Chemistry, University of Warsaw, Zwirki i Wigury 101, 02-089 Warsaw, Poland*

[3] *CAPES Foundation, Ministry of Education of Brazil, 70040-02, Brasilia, Brazil*

e-mail : nacer.idrissi@univ-lille1.fr

The microscopic structure of acetone/methanol mixture in the whole mole fraction range has been investigated using Infrared spectroscopy and molecular dynamic simulation. The excess spectra approach combined with the excess partial molar absorption were used in order to detangle between the dipole-dipole and hydrogen bonding interactions contribution to the O-H, C=O,C-O and C-C vibration spectral profile. The results show that acetone molecules are not homogeneously distributed in the mixture, particularly, in the mole fraction range of acetone between 0.05 and 0.55. This correlates with the appearance of a second peak in the C=O and C-C vibration modes of acetone. This inhomogeneity is driven by the prevalence of the dipole-dipole interactions over those of hydrogen bonding between acetone and methanol molecules. The inhomogeneous distribution of methanol molecules is found to occur in the mole fraction range of acetone between 0.55 and 1. In this case the hydrogen bond interactions between methanol molecules are prevailing over those between methanol and acetone. However, the extent of this inhomogeneity is small as compared with that of acetone in the low mole fraction range.

This IR study was complemented by molecular dynamics simulation. This study is based on the behavior of distributions of metric and topological properties of the Voronoi polyhedra (VP). This inhomogeneous distribution of acetone and methanol molecules is clearly seen in the behavior of the fluctuation of the local density, as measured by the Voronoi polyhedra. More interestingly, the maximum in the heterogeneity coincide with the maximum of the fluctuation in the density of the VP.

3PB18 Multielement solution determination by portable total reflection X-ray fluorescence (TXRF) spectrometer

Y. LIU, S. IMASHUKU, K. YUGE, and J. KAWAI

Department of Materials Science and Engineering, Kyoto University, Kyoto 606-8501, Japan
e-mail : liu.ying.48r@st.kyoto-u.ac.jp

Kunimura *et al.* have developed portable TXRF spectrometer using an X-ray tube of a few watts, and found when a low power X-ray tube is used, polychromatic excitation improves the detection sensitivity compared with monochromatic excitation[1]. Although the portable TXRF spectrometer has proved to be an economical tool for rapid trace elemental determination, its versatility in practical applications of providing rapid multielemental profiles of a wide range of elements have not been demonstrated yet. For that purpose, the present study was carried out to assess the capability of portable TXRF spectrometer on multielement determination. The portable TXRF spectrometer used in this study weighed less than 5 kg, mainly consisted of a 4 W X-ray tube (Rh target,40 kV Magnum, Moxtek, USA), a waveguide slit restricting the incident radiation to be a parallel beam of 10 mm in width and 10 μm in height, and a Si-PIN detector (X-123, Amptek, USA)[2].

Multielement solutions containing 11 elements of S, K, Sc, V, Mn, Co, Cu, Ga, As, Br and Y were analyzed by the portable TXRF spectrometer. Excitation parameters (glancing angle ϕ, tube voltage and current) and sample amount were optimized for the portable TXRF in order to reach the smallest possible detection limits for all elements. Excitation parameter dependences of fluorescence signal and background for detected elements were explained in detail. Background contributed by sample carrier was also discussed. Numerical simulation and convolution approaches were applied to determine the effective X-rays of the polychromatic incident beam to excite the analyte. Consequently, nine elements were detectable at sub-nanogram level in a single measurement under the optimum experimental conditions (Fig. 1).

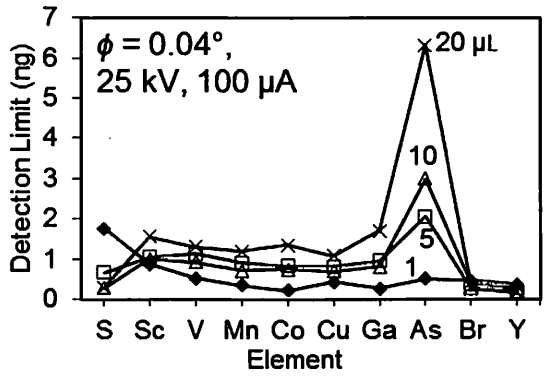

Fig. 1 Detection limits (measurement time of 10 mins) as functions of sample amount of 1 (◆), 5 (□), 10 (△) and 20μL (×).

The portable TXRF spectrometer has shown suitability for simultaneous multielement analysis with low detection limits. The features of high sensitivity, small sample amount required, and fast detection of the wide range of elements make the portable TXRF a valuable tool in versatile applications, such as field studies in environmental and geological investigations.

References

[1] S. Kunimura, J. Kawai, *Analyst* [London], **135**, 1909(2010).

[2] S. Kunimura, J. Kawai, *Anal. Chem.*, *79*, 2593(2007).

3PB19 Soft X-ray recombination emission of liquid water

Y. Harada[1,2], T. Tokushima[2], Y. Horikawa[2], H. Niwa[2,3], M. Oshima[3] and S. Shin[1,2]

[1]*Institute for Solid State Physics, The University of Tokyo, Hyogo 679-5165, Japan*
[2]*Riken SPring-8 center, Hyogo 679-5148, Japan*
[3]*Department of Applied Chemistry, The University of Tokyo, Tokyo 113-8656, Japan*
e-mail : harada@issp.u-tokyo.ac.jp

Recently many have reported O 1s X-ray absorption/emission spectroscopy of water to discuss the local structure of water. Relation between the local structure of water and the profile of the X-ray absorption/emission spectra are, however, much debated. From ice to liquid water there exists a substantial decrease of 540 eV peak in the post edge of XAS, which has been assigned as tetrahedrally coordinated water [1]. This assignment has been challenged by density functional theory since the profile much depends on the model used, namely, half or full core holes [2]. Not only the post edge, assignment of the near-edge peak around 535 eV as the presence of broken hydrogen bond has also been questioned by recent temperature dependent XAS experiment [3]. Meanwhile in X-ray emission spectrum of water, two distinct $1b_1$ peaks were observed and it has been debated whether these peaks represent two distinct local structure of water [4] or they are only the manifestation of core hole induced dynamics which produces dissociated species resulting in the splitting of the $1b_1$ peak [5].

Here we show ultrahigh resolution O 1s X-ray recombination emission spectra of H_2O/D_2O water around pre-edge resonance. The low energy tail of the elastic scattering line at pre-edge resonance has commonly been interpreted as vibronic coupling due to core hole induced dynamics. Using ultrahigh resolution soft X-ray emission spectrometer [6] we have successfully obtained well separated multiple vibrational structures extending several eV below the elastic scattering line. We will present a complete match of the energy separation with the stretching mode of isolated water molecule and discuss the origin of the pre-edge structure in O 1s XAS.

References

[1] Ph. Wernet *et al.*, Science **304**, 995 (2004).
[2] D. Prendergast and G. Galli, Phys. Rev. Lett. **96**, 215502 (2006).
[3] T. Pylkkänen *et al.*, J. Phys. Chem. B **115**, 14544 (2011).
[4] T. Tokushima *et al.*, Chem. Phys. Lett. **460**, 387 (2008).
[5] O. Fuchs *et al.*, Phys. Rev. Lett. **100**, 249802 (2008).
[6] Y. Harada *et al.*, Rev. Sci. Instrum. **83**, 013116 (2012).

3PB20 Electronic Transitions from Liquid Amides Studied by Attenuated Total Reflection Far-Ultraviolet Spectroscopy and Quantum Chemical Calculations

Yusuke Morisawa[1*], Manaka Yasunaga[2], Ryoichi Fukuda[3], Masahiro Ehara[3], and Yukihiro Ozaki[2]

[1]*Department of Chemistry, Kinki University, Higashi-Osaka City 577-8502, Japan*

[2]*Department of Chemistry, Kwansei Gakuin University, Sanda, 669-1337, Japan*

[3]*Institute for Molecular Science, Okazaki 444-8585, Japan*

e-mail : morisawa@chem.kindai.ac.jp

Attenuated total reflection far-ultraviolet (ATR-FUV)[1-2] spectra in the 145-260 nm region were measured for several kinds of liquid amides (Formamide; FA, *N*-methylhormamide; NMF, *N*-methylacetamide; NMA, *N,N*-dimethylharmamide; NdMF, and *N,N*-dimethylacetamide; NdMA) to investigate their electronic transitions in the FUV region. The obtained spectra (figure 1) were compared with the corresponding spectra measured in a gas phase reported by Kaya et al. to investigate the shift of a major absorption band in the 180-200 nm region from the gas phase to the liquid phase. The peak shift depends upon the kinds of amides. FA and NMF, which from intermolecular C=O···H-N hydrogen bonding, show a large lower energy shift by about 0.60 eV but NMA, which also has the hydrogen bonding, show only a small shift. NdMF and NdMA seem to have coupling between the C=O groups and give a small peak shift. Two kinds of quantum chemical calculations, time-dependent density functional theory (TD-DFT) and Symmetry Adapted Cluster-Configuration interaction (SAC-CI), were carried out to explore the cause the shifts and band assignments. In TD-DFT the shift from the monomer gas model to the dimer gas model reproduces well the observed shift from the gas phase to the liquid phase. This suggests that the intermolecular interaction due to the hydrogen bonding affects significantly the shift. In contract, in SAC-CI the shift from the monomer gas model to monomer PCM model reproduces better, indicating that the interaction arising from the polarization of molecule itself appears strongly. As for the band assignments, it was found that the major band in mainly due to the π-π^* transition but several kinds of Rydberg transitions also exist in the vicinity of the π-π^* transition and the π-π^* transition is mixed with the Rydberg transitions. This mixing happens when orbitals have the same symmetry. The number and the kinds of Rydberg transitions appealing the spectra depend upon the kinds of amide molecules.

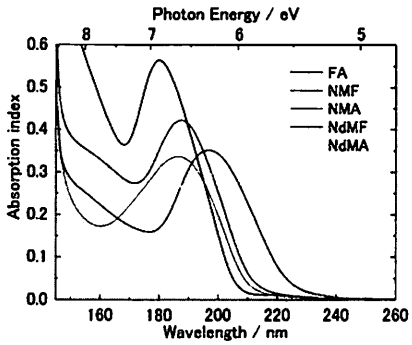

Figure1 FUV absorption index spectra of amides in the region of 145-260 nm

References

1) N. Higashi, *et al. Rev. Sci. Instrum.* **2007**, 78, 103107.

2) Y. Ozaki *et al.*, *Appl. Spectrosc.* **2012,** 66, 1.

3PC01 X-ray diffraction and EPSR modeling of an aqueous NaCl solution from ambient pressure to 2 GPa

N. Fukuyama[1], X. C. Li[1], K. Yoshida[1], Y. Katayama[2], T. Yamaguchi[1]

[1]*Department of Chemistry, Fukuoka University, Jonan, Fukuoka 814-0180, Japan*
[2]*Synchrotron Radiation Research Center (SPring-8), Japan Atomic Energy Agency, Hyogo 679-5148, Japan*
e-mail: yamaguch@fukuoka-u.ac.jp

The structure of electrolyte solutions under high temperature and high pressure condition is very important for understanding chemical processes in earth science and for supercritical water technology. Ion-water and water-water interactions play important roles in various properties and processes in the systems. The size and charge of ions dominate ion-water interaction. Hydrogen bonding in water affects the ion hydration. To understand the properties and chemical reactions in aqueous electrolyte solution at high temperatures and high pressures, we need the microscopic structural information of the solutions. In the present study, X-ray diffraction measurements using synchrotron radiation were made on a 3 *m* (=mol/kg) aqueous NaCl solution at pressures from ambient to 2 GPa. The 3-dimensional structures of water and hydration of ions in the NaCl solution were elucidated through empirical potential structure refinement (EPSR) modeling combined with the X-ray data.

X-ray diffraction experiments were carried out using a cubic-type multi anvil press installed on BL14B1 at the SPring-8 synchrotron radiation facility [1]. A 3 *m* aqueous NaCl solution was inserted in a single-crystal diamond cup and sealed with a thin gold foil in a high pressure container. The thermodynamic states of measurements were 300 K/0.1 MPa, 1.3, 1.7 GPa, 363 K/2.0 GPa. In EPSR modeling, the initial potentials were selected as SPC/E for water and [2] for the ions.

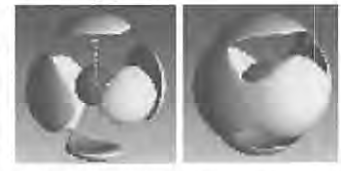

Fig.1. Spatial density functions of water around a central Cl^- at 0.1 MPa (left) and 1.3 GPa (right)

Fig.2. Spatial density functions of water around a central Na^+ at 0.1 MPa (left) and 1.3 GPa (right)

It was found that the tetrahedral-like water structure at 0.1 MPa is completely broken down, giving rise to a simple-liquid-like structure at 1.3~2.0 GPa. The EPSR modeling showed that an average coordination number of Cl^- increases from 6.3 at 0.1 MPa to 16.1 at 1.3 and 1.7 GPa (Fig.1). On the contrary, the hydration structure of Na^+ does not show a significant change with pressure (Fig.2). Pressure of 1–2 GPa applied to the 3 *m* NaCl aqueous solution induces a drastic change in the structure of water and the hydration shell of Cl^-, but not for the hydration shell of Na^+. This is because a large Cl^- has weaker electrostatic interaction with water than a small Na^+.

References

[1] Y. Katayama, et al. *Phys. Rev.* B **81**, 014109 (2010).

[2] J. P. Brodholt, *Chem. Geol.* **151**, 11 (1998).

3PC02 Temperature and Pressure Effects on the Reorientational Correlation Time of Water in DEF- and DMA-Water Mixtures

M. Okada[1,2], T. Suwa[2], Y. Katsuura[2], Y. Yasaka[2], K. Ibuki[2], and M. Ueno[2]

[1]*Depertment of Applied Chemistry, Nagoya University, Aichi 464-8603, Japan*

[2]*Depertment of Molecular Chemistry and Biochmistry, Doshisha University, Kyoto 610-0321, Japan*

e-mail : sk112652@mail.doshisha.ac.jp

Mixtures of water and organic liquids have been an important subject of numerous physico-chemical investigations because of their interesting properties arising from the effect of organic components on the hydrogen-bonded water structure. In order to examine the effects of the length of functional groups and the number of hydrophobic methyl groups on the reorientational dynamics of water molecules in the mixtures, *N*,*N*-diethylformamide (DEF) and *N*,*N*-dimethylacetamide (DMA) were used as organic components. A DEF molecule possesses two ethyl groups which are substituted for methyl groups in a DMF molecule. A DMA molecule has three hydrophobic methyl groups, that is, a hydrogen atom in the aldehyde group of a DMF molecule is substituted by methyl group. Both amides have a relatively large dipole moment, 3.93 D (DEF) and 3.72 D (DMA), respectively, in gas phase.

In this work, we determined the reorientational correlation times (τ_c) of heavy water (D_2O) in DEF- and DMA-D_2O mixtures from the measurements of NMR relaxation times at 10, 25 and 45 °C under atmospheric pressure and at 25 °C under high pressure up to 196.1 MPa, and also performed the molecular dynamics (MD) simulations for the DMA-D_2O mixture to support our interpretations for the experimental results on NMR. Furthermore the densities and viscosities of the mixtures were measured at 25 °C up to 196.1 MPa to examine the relationship between macroscopic and microscopic properties of the mixtures.

The composition dependence of τ_c exhibited a remarkable maximum at about 40 mol% of amides in DEF-, DMA-, and DMF-D_2O[1,2] mixtures at each temperature and pressure; the maximum of τ_c in the DMA-D_2O mixture was highest among three mixtures. The presence of the maximum of τ_c in the composition dependence in these mixtures indicates that the hydrophobic hydration play an important role in the retardation of water molecules in the mixtures. The viscosities showed a similar behavior in the composition dependence though the Stokes-Einstein-Debye law is absent. The highest value of τ_c in the DMA-D_2O mixture indicates that the hydrogen bonds between amides and water would strengthen with increasing the number of hydrophobic groups, which was supported by MD simulations.

[1] M. Okada, K. Ibuki, M. Ueno, *Bull. Chem. Soc. Jpn.* **85**, 189(2012).

[2] M. Okada, K. Ibuki, M. Ueno, *Bull. Chem. Soc. Jpn.* **85**, 1192(2012).

3PC03 Low-frequency Raman scattering of supercritical propanol

Y. Amo[1], T. Sato[1], Y. Kameda[1] and T. Usuki[1]

[1]*Department of Material and biological chemistry, YamagataUnifersity, Yamagata 990-8560 Japan*

e-mail : apj@cm.kj.yamagata-u.ac.jp

Low-frequency Raman spectra of 1- and 2-propanol from -50 cm^{-1} to 400 cm^{-1} have been observed and analysed by using a spectral fitting metnod.

Raman scattering spectra were obtained by a double grating monochrometor (Jobin-Yvon U-1000). The resolution is about 2 cm^{-1}. A specific high-pressure cell was used and right angle scattering geometry is adopted.

The reduced Raman spectra, the imaginary part of the complex susceptibility, were obtained form the Raman intensity spectra detected by the photon counting method. The central component of reduced spectra have been analysed by a revised MRT (Multiple Random Telegraph model) relaxation function [1] instead of the conventional Debye type relaxation function. Below critical temperature, one MRT model and damped harmonic oscillators reproduce spectra. In the supercritical region, one MRT model and one Gaussian function reproduce spectra.

The relaxation time becomes shorter (faster) with increasing temperature, then it turns longer (slower) with increasing temperature toward to the supercritical temperature. This result is qualitatively consistent with the behavior of the dielectric relaxation[2]. The number of free OH increases[3], the lineshape of the second component changes DHO to Gaussian like.

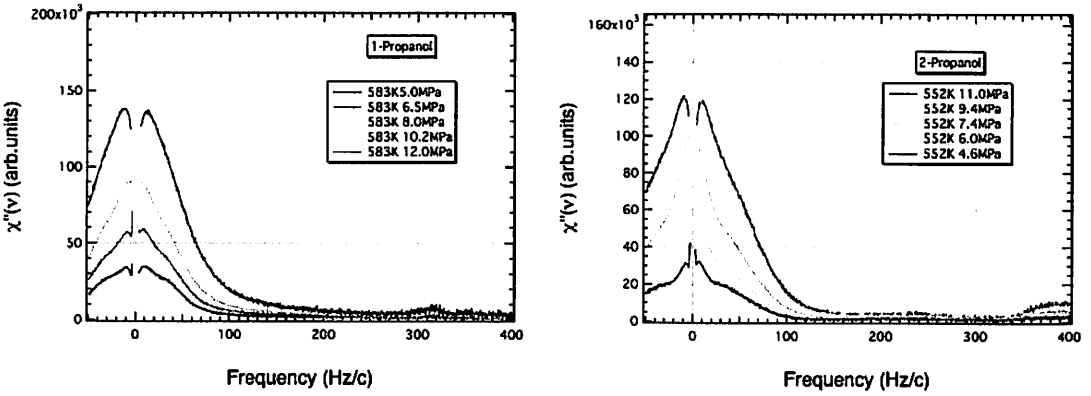

Fig.1 Reduced low-frequency Raman spectra of 1-propanol(left) and 2-propanol(right)

References

[1] F. Shibata,, C. Uchiyama, and K. Maruyama, *Physica A* **161**, 42(1989) .

[2] Y. Hiejima and Makoto Yao, *J. Chem. Phys.* **119**, 7931(2003).

[3] S. J. Barlow, G. B. Bondarenko, Y. E. Gorbaty, T. Yamaguchi and M. Polilakoff, *J. Phys. Chem.* **A106**, 10452(2002).

3PC04 Measurement of Solubility of Anthracene in Supercritical Carbon Dioxide from Nearcritical to High Temperatures by the Determination of the Saturated State Using UV-Visible Spectroscopy

H. Uchida, K. Takahara

Department of Chemistry and Material Engineering, Faculty of Engineering, Shinshu University, Nagano-city, 380-8553, Japan

e-mail : uchida@shinshu-u.ac.jp

Solubilities of anthracene were measured in the pressure range 9–24 MPa and the temperature range 313.2, 333.2, 353.2 and 373.2 K by the saturation pressure determination using the UV-Visible spectroscopy, which was proposed by Ngo et al. [1]. In the method, known amounts of solutes were introduced into a high-pressure optical cell, having a direct path with two sapphire windows. After loading, the cell was heated to a desired temperature by heating tapes. The pressurized carbon dioxide was then introduced into the cell to a desired pressure, and stirred constantly. The supercritical carbon dioxide was in contact with solid solutes at the pressure and temperature. Equilibrium of the mixture was observed in situ by periodically taking UV spectra of the solution. The carbon dioxide pressure was increased up until there was no further increase in the peak absorbance. The absorbance was plotted versus pressure. As the pressure increased, there was a large increase in solubility. Once all the solute in the cell dissolved, there was an abrupt change in the slope and the absorbance became almost constant. The pressure at saturation was then determined from the intersection of the two linear regions on the graph. At this point, solubility can be calculated by knowing the mass of solute in the cell, the fluid density at saturation, and the cell volume. The results obtained were shown in Figure 1 and those were in good agreement with the literature data [2-4] with an average absolute deviation of lower than 10%. The present measurement technique enables us to measure the high accuracy solubility in a short time and it is effective for the solubility measurement of the solutes with very low solubility. The solubilities were correlated by the Chrastil equation [5] and the Predictive Soave-Redlich-Kwong (PSRK) group contribution equation of state [6]. The present models gave good correlation results for the experimental data as shown in Figure 1.

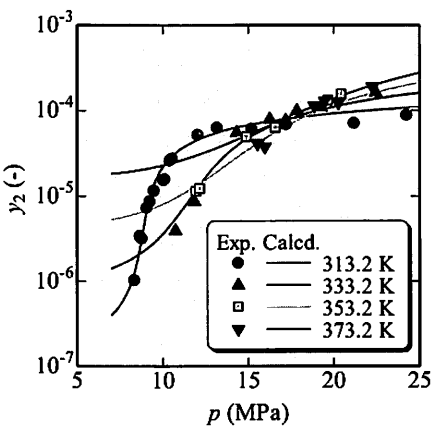

Figure 1. Experimental and Calculated Results of Solubility of Anthracene in Supercritical Carbon Dioxide.

References

[1] T.T. Ngo, D. Bush, C.A. Eckert, C.L. Liotta, *AIChE J.*, **47**, 2566 (2001).

[2] D.J. Miller, S.B. Hawthorne, *Anal. Chem.*, **67**, 273 (1995).

[3] J.W. Hampson, *J. Chem. Eng. Data*, **41**, 97 (1996).

[4] X. Lou, H.-G. Janssen, C.A. Cramers, *J. Chromatorgr. A*, **785**, 57 (1997).

[5] J. Chrastil, *J. Phys. Chem.*, **86**, 3016 (1982).

[6] T. Holderbaum, J. Gmehling, *Fluid Phase Equilib.*, **70**, 251 (1991).

3PC05 Applicability of UV-Visible Spectroscopic Measurement Technique to the Determination of Solubilities of Organic Compounds in Supercritical Carbon Dioxide Using Calibration Curve (Molar Absorptivity) Determined with Organic Solvents

H. Uchida, D. Kondo

Department of Chemistry and Material Engineering, Faculty of Engineering, Shinshu University, Nagano-city, 380-8553, Japan

e-mail : uchida@shinshu-u.ac.jp

This work elucidated the applicability of UV-Visible spectroscopic measurement technique of solubilities of two types of organic compounds, type 1: disperse red 1 and disperse blue 14, which have an absorption in the visible region, and type 2: racemic ibuprofen and theophylline, which have an absorption in the ultraviolet region, in supercritical carbon dioxide using calibration curve (molar absorptivity) determined with organic solvents. The spectroscopic measurement technique using calibration curve prepared with organic solvents was not able to apply to disperse red 1 and disperse blue 14 because the absorption spectra obtained in several organic solvents such as hexane, ethanol, acetone, toluene, chloroform, dichloromethane and N,N-dimethylformamide (DMF) were different from those in supercritical carbon dioxide owing to the solvatochromism. The absorption spectra of racemic ibuprofen and theophylline in organic solvents, on the other hand, were almost the same as those in supercritical carbon dioxide. These results lead to the non-applicability of the spectroscopic measurement technique using calibration curve prepared with organic solvents to organic compounds which have an absorption in the visible region. Moreover, solubilities of racemic ibuprofen and theophylline were measured in the pressure range 14-22 MPa and at temperatures 313.2-343.2 K in order to examine the availability of the spectroscopic measurement technique using calibration curve prepared with organic solvents such as hexane and ethanol. The present measurement technique enables us to measure the high accuracy solubility in a short time and it is effective for the solubility measurement of the drugs with very low solubility. The solubilities were correlated by the Chrastil equation [1] and the Peng-Robinson equation of state [2] and van der Waals type mixing rules with two binary interaction parameters introduced into attraction and size terms, respectively. The present models gave good correlation results for the experimental data.

References

[1] J. Chrastil, *J. Phys. Chem.*, **86**, 3016 (1982).

[2] D.-Y. Peng, D.B. Robinson, *Ind. Eng. Chem. Fundam.*, **15**, 59 (1976).

3PC06 Solubilities of Anthraquinone Dyestuffs in Supercritical Carbon Dioxide

A. Ratna, K. Tamura
Division of Material Engineering, Graduated School of Natural Science & Technology
Kanazawa University, Kanazawa 920-1192, Japan
e-mail : tamura@se.kanazawa-u.ac.jp

The conventional dyeing process needs a large amount of water in a dyeing medium as well as the dispersing agents and surfactants in addition to disperse dye. This process causes the emission of wastewater with various toxic chemical additives to the environment. The Supercritical dyeing technology is capable of substantially reducing wastewater discharge and energy consumption. The saturated solubility of dyestuffs in supercritical fluids is essentially important in the development and design of supercritical dyeing technology. However, only a limited number of the experimental data for solubilities of dyestuffs in supercritical carbon dioxide (SC-CO_2) is available in the literature [1, 2].

The present research focused on the solubility of two anthraquinone dyestuffs in supercritical carbon dioxide. C.I. Disperse Violet 1 is a notation of 1,4-diaminoanthraquinone and C.I. Disperse Red 15 is that of 1-amino-4-hydroxyanthraquinone. We measured the solubility of the disperse dyestuffs at temperatures of 323.15, 353.15 and 383.15K and at pressure ranges from 10.0 to 25.0 MPa by using a flow-type apparatus. We examined how the solubility of C.I. Disperse Violet 1 and C.I. Disperse Red 15 in SC-CO_2 changes with the substituent groups of amino and hydroxyl onto anthraquinone. It was found that the hydroxyl group on the anthraquinone molecule causes higher the solubility of the anthraquinone dye in supercritical CO_2. This suggests that -OH group has an affinity to the carbon dioxide, compared with -NH_2 group. The experimental results were correlated by the Mendez-Santiago equation and the Peng-Robinson equation of state (PR EOS) with the van der Waals mixing rule. Good agreement between the experimental and calculated solubilities of the dispersed dyes was obtained.

References

[1] T. Shinoda, K. Tamura, *Fluid Phase Equilibria* **213**, 115–123 (2003).
[2] H.m. Lin, C.C. Ho, M.J. Lee, *J. Supercritical Fluids* **32**, 105–114(2004).

3PC07 Solubility Phenomena of Methionine in Water under High Pressure

S. Sawamura[1], N. Kunimasa[1]

[1]*Department of Applied Chemistry, Ritsumeikan University, Kusatsu 525-8577, Japan*
e-mail : sawamura@sk.ristumei.ac.jp

Solubilities, m_S, of nonpolar solid solutes such as naphthalene [1] usually decrease as pressure increases following the thermodynamic principle [2];

$$(\partial \ln m_S / \partial p)_T = (V'_{sat} - V_{solid})/(RTf_\gamma), \qquad (1)$$

where $f_\gamma = 1+(\partial \ln \gamma/\partial \ln m)$ and γ is activity coefficient of solute, because the molar volume, V_{solid}, of most solid solutes is generally smaller than the partial molar volume, V'_{sat}, of them in saturated solution and $f_\gamma > 0$. On the other hand, our recent solubility measurements for several amino acids in water showed a variety of pressure dependence, e. g., solubility of glycine decreased as pressure increased, alanine and leucine increased, and valine and isoleucine showed a maximum in solubility-pressure curves though the solubility of these solutes increased as temperature increased without any variety [2]. In the present study, we took methionine as another amino acid for a high-pressure solubility. This solute has a large volume difference, $V'_{sat} - V_{solid}$, compared with the amino acids shown above. So we expected a large increase of the solubility with pressure increasing.

Solubility was measured at 298.2 K and up to 200 MPa using high-pressure piston-cylinder vessels (200 mm length, 70 mm outer diameter, and 15 mm bore size, made of 17-4 PH stainless steel)with an outlet valve designed by one of us. Solute, water and a ball for stirring was put in the vessel and shaken for one week at high pressures using a seesaw in a thermo regulated water bath. Concentration of the saturated solution was estimated by weighing the sample before and after drying. Detail for the measurement was described in Ref. [3].

Solubility was increased as

$$\ln [m_S / (\text{mol kg}^{-1})] = -4.62\text{x}10^{-6}(p/\text{MPa})^2 + 2.65\text{x}10^{-3}(p/\text{MPa}) - 0.970 \qquad (2)$$

Using Eq. (1) and reference data of the thermodynamic parameters, we can estimate the slope of Eq.(2) to be $(2.62\pm0.34)\text{x}10^{-3}$ MPa^{-1} at 0.10 MPa It is near to the second term in Eq.(2) suggesting a reliability of our experiment. This value is larger than $0.80\text{x}10^{-3}$ MPa^{-1} for alanine and $1.76\text{x}10^{-3}$ MPa^{-1} for leucine [2].

References

[1] S. Sawamura, H. Ise, *J. Solution Chem.* **40** 1899 (2011).

[2] H. Matsuo, Y. Suzuki, S. Sawamura, *Fluid Phase Equilibria*, **20**, 227 (2002).

[3] S. Sawamura, *Pure and Applied Chem.*, **79**, 861 (2007).

3PC08 Conformational Preference of Disulfide Model Compound of Proteins under High Pressure

T. Takekiyo[1], Y. Yoshimura[1], R. Wada[2], and M. Kato[3]

[1] *Department of Applied Chemistry, National Defense Academy, 1-10-20, Hashirimizu, Yokosuka, 239-8686, Japan.*[2]*Graduate School of Science and Engineering, and* [3]*Department of Pharmacy, College of Pharmaceutical Sciences, Ristumeikan University, 1-1-1, Noji-Higashi, Kusatsu, 525-8577, Japan*

e-mai:take214@nda.ac.jp

To study on the denaturation of proteins, pressure is a useful parameter thought it has been much less used than temperature. Although the pressure denaturation of proteins have been studied using various experimental techniques [1], the mechanism of pressure denaturation is still unclear. It is necessary to investigate the local structural change such as disulfide bond to understand the mechanism of pressure denaturation. It is well-known that disulfide (SS) bonds between cysteine (Cys) residues are very important determinants for the folding and stability of peptides and proteins and that the disulfide linkage plays an important role in enzyme and in the biological activity of molecular systems [2]. Then, we focused on pressure-induced conformational preference of disulfide linkage to understand the mechanism of pressure denaturation of proteins. The disulfide linkage has a CCSSCC unit, and possibly takes three conformations: the *gauche-gauche-gauche* (*ggg*), *trans-gauche-gauche* (*tgg*), and *trans-gauche-trans* (*tgt*) [3].

We have investigated the pressure effect on conformational equilibria of $_{L}$-cystine (Cys-Cys), which is a model disulfide bond, using Raman spectroscopy. Our result showed that the relative population of *ggg* conformer having the smallest partial molar volume (PMV) increases with increasing pressure throughout the studied pHs. In viewing of this result, it was suggested that disulfide bond in proteins promotes the decrease of the conformational entropy associated with pressure denaturation because the disulfide linkage takes a compact conformation under high pressure.

References

[1] W. Dzwolak, M. Kato, and Y. Taniguchi, *Biochim. Biophys. Acta*, **1595**, 131 (2002).

[2] S. Dai, C. Schwendmayer, P. Schurmann, S. Ramanswamy, and H. Eklund, *Science,* **287**, 655S (2000).

[3] N. Primor and A. T. Tu, *Biochem. Biophys. Acta*, **626**, 299, (1980).

3PC09 The effect of high hydrostatic pressure on sterilization and quality attributes of minced fish

A. Yamasaki and A. Shimizu

Dept. Environmental Engineering for Symbiosis, Soka Univ., Tokyo 192-8577, Japan
e-mail : e13m5720@soka.ac.jp

Surimi (minced fish) is a specialty of the areas that have a greatest damage in the Great East Japan Earthquake. Essentially, the disaster areas boast a fishing industry so reconstruction of fisheries is extremely important. Therefore with the object of fishery processing and distribution, to extend the shelf-life of minced fish and create product with high value added is important. To resolve these issues, high hydrostatic pressure treatment has been recognized as a one of method, but the detail of component change has not been researched during storage periods after pressure treatment. In this study we observed the change of microbiological shelf-life (viable bacteria count) and chemical shelf-life (K values, compounds related to ATP and free amino acid contents). Minced fish with or without table salts was vacuum-packed and subjected to high pressure processing (400 MPa at 4℃ for 30 minutes) or left untreated as controls. The samples were stored at 4℃ for up to 28 days

High pressure significantly delayed microbial growth and increase of K values in minced fish. The microbiological shelf-life was extended from 1-2 weeks in controls to 28 days in pressure-treated at 400 MPa for 30 min with or without table salts. The chemical shelf-life was also extended in the minced fish. In the case of contain of table salts, while K values in control samples reached unacceptable limits between 7 and 14 days, in treated samples remained below the limits of acceptability to 28 days. Without table salts, while K values in control samples reached unacceptable limits within 21 days, in treated samples remained below the limits of acceptability. Pressure treatment also effected a change in the umami taste. The amount of Glutamic acid, in minced fish showed the maximum value after 14 - 21 days storage at 4 ℃and inhibited decomposition of ADP and IMP with or without table salts.

3PC10 Effect of pressure and temperature on the survival rate of adherent A-172 cells

R. Kushida, R. Yasuhara, K. Nei, B. Yamanoha and A. Shimizu

Department of Environmental Engineering for Symbiosis, Soka University, Tokyo 192-8577, Japan

e-mail : ryo.ccolion@gmail.com

Most often, cells are preserved with cryopreservation. However, this method can be toxic to cells because of a cryoprotectant, cells are physically damaged by intracellular and extracellular ice crystals without a cryoprotectant. Hence other alternatives permitting preservation and transportation of cells are desired.

As the alternative cell preservation, we suggest the unfrozen preservation by the exposure of hydrostatic pressure which could cause metabolic suppression. Yasuhara et al. (2013) reported that when A-172 cells were preserved at 25 °C, the highest survival rate was observed with 20.1 MPa regardless of the preservation period (4 - 10 days) [1]. However, the survival rate after the preservation with pressurization at another temperature is not clarified. In this study, we investigated the survival rate after A-172 cells are preserved with pressurization at temperatures other than 25 °C (4 days).

The survival rates of A-172 cells after 4 days preservation in the pressure range (0.1 - 25.1 MPa) at 4, 10, 15 and 20 °C were examined. When preserved at 20 °C with pressurization (4 days), survival rate was remained up to 20.1 MPa, but survival rate with pressurization decreased with increasing pressure when preserved at 4, 10 and 15 °C. We clarified that the effect of temperature change on survival rate of A-172 cells is small, when they are pressured with 20.1 -25.1 MPa at around room temperature.

Reference

[1] Yasuhara R, Kushida R, Ishii S, Banri Y and Shimizu A. High Pressure Research (2013)

3PC11 Effect of pressure and temperature on the survival rate of rat primary astrocytes

K. Nei[1], K. Nakajima[2], S. Yamamoto[2], and A. Shimizu[1]

[1]*Department of Environmental Engineering for Symbiosis, Soka University, Tokyo 192-8577, Japan*

[2]*Department of Bioinformatics, Soka University, Tokyo 192-8577, Japan*

e-mail :e13m5715@soka.ac.jp

The effects of pressure on cell viability and function are complex and have not been fully clarified. We have reported that astrocytes and A172, an adherent cell line, show higher viability when preserved for 4 days at about 1.6-2.0 MPa than at ambient pressure. In this study, we investigated the effects of solution environments, hydrostatic pressure (0.1-30 MPa) and temperatures (4, 10, 15, 20, 25 and 37°C), on the viability and function of rat primary astrocytes after 4 days preservation.

The number of astrocyte cells used in this experiment was controlled to 1 to 2×10^6 in 300 μl DMEM media. The 300-μl cell suspension was placed in a silicon tube (5-mm inner diameter, 7-mm outer diameter) and sealed on both sides by Teflon rods (6-mm diameter, 7-mm length). The inner container was placed in a stainless steel pressure vessel and filled with water. After preservation under each condition, survival rates were determined using Muse Count and Viability Kit (Merck Millipore, Darmstadt, Germany).

The astrocytes preserved for 4 days at 10-25 °C showed the high survival rate at ambient pressure. Also, adhesive and proliferative capacities of cells after 4 days preservation at these temperatures were similar to the cells before preservation. Next we studied the pressure effect on survival rate of astrocytes. At 10, 15, 20°C, the survival rate after 4 days preservation was decreased with increasing pressure up to 30 MPa. The other hand, the survival rate preserved at 25 °C was increased with increasing pressure up to 30 MPa. These results indicated that the astrocytes can be remained in good survival rate and good condition by pressure.

3PC12 Combined effects of pressure and temperature on cyst hatching of *Artemia salina*

Y. Hirao, A. Shimizu

Department of Environmental Engineering for Symbiosis, Faculty of Engineering, Soka University, Tokyo 192-8577, Japan

e-mail : e0957123@soka.ac.jp

Pressure and temperature are known to be important physical factors in the life of water organisms.

The brine shrimp *Artemia*, a micro-crustancean, are found in inland salt lake. Temperature and salinity have been reported to interact with cyst hatching of *Artemia*[1]. *Artemia* dry eggs resist the high hydrostatic pressure of 7.5 GPa[2], but tolerance of underwater eggs has not been clarified.

The hatching rate of *Artemia* has been known to affect by dissolved oxygen [3]. So, we studied the effect of quality of material of culture vessel (silicon, glass, plastic) on hatching rate. As the result, silicon was the optimum culture vessel. At ambient pressure, *Artemia* hatched about 80% at about 24 h. Next, we studied the pressure effects (0 to 30 MPa) on hatching at various temperatures (10 to 34 °C). From these results we discuss the combined effect of pressure and temperature on hatching rate and hatching time of *Artemia salina*.

References

[1] P. Vanhaecke, P. Sorgeloos, *Ann. Roy. Soc. Zool. Belgium.* 118, 7–23(1989).

[2] K. Minami et al., *J. Phys. Conf. Ser.* 215, 012164(2010)

[3] Murakami, *Graduation Thesis. Okayama University of Science* (2009)

3PC13 Amorphous Ices: Glass transitions in LiCl aqueous solutions

G. Ruiz[1,2], H. Corti[1] and T. Loerting[2]

[1]*Faculty of Sciences, University of Buenos Aires, 1426 Buenos Aires, Argentina*

[2]*Institute of Physical Chemistry, University of Innsbruck, A-6020 Innsbruck, Austria.*

guadaruiz@gmail.com

Amorphous polymorphism is one of the key concepts in our current understanding of phase transitions taking place in supercooled water and aqueous solutions. Amorphous water is responsible for several anomalies described in aqueous systems and its study is relevant for astrophysics, cryopreservation and many other disciplines. Three amorphous solids are known for pure water and LiCl solutions, which differ in terms of their densitiy: very high- (VHDA), high- (HDA) and low-density amorphous ice (LDA) [1,2]. Introduction of ionic solutes has been shown to affect the structure of water in a manner similar to the application of pressures, e.g., in salt solutions such as LiCl-H_2O [3,4]. One highly debated question is whether LDA and HDA are states related to crystalline phases or to supercooled liquids having low and high density (LDL and HDL). In this work we address this fundamental question by resorting to the study of glass transition in supercooled aqueous systems.

Previous studies of LiCl aqueous solutions with slow-cooling methods at ambient pressure faced the problem of inaccessibility of the glassy state at low salt concentrations due to crystallization and phase segregation (e.g. [5,6]). Hyperquenching methods used afterwards allow to avoid these problems and showed that glass transition temperature T_g does not vary linearly with concentration, but shows a complex dependence with salt/water ratio, especially at very low salt content [7]. Both methods mentioned above lead to the formation of LDA-type solutions upon cooling. LiCl solutions were also studied by cooling of the pressurized solution, leading to the segregation of HDA-type plus LDA-type regions in the sample [8,9]. We have now studied HDA-type LiCl solutions by the route of pressure-amorphization at 77 K (unrelaxed HDA, according to the method by *Mishima et al.* [10]) and HDA-type LiCl solutions after relaxation at 140 K and 0.1 GPa (according to the method by *Winkel et al.* [11]). In the broad range between 0 and 25mol% LiCl, which includes the elusive dilute concentration range these procedures minimize the issue of phase-segregation and allow to study separately the HDA-type solutions and, after heating at ambient pressure, the LDA-type solutions. We could clearly discriminate between "water-dominated" and "salt-dominated" phase-behaviour of the solutions, with a rather sharp boundary at about 11mol% LiCl. We have observed, for the first time, the glass transition in the HDA-type solutions, and also a glass transition in the LDA-type solutions, both associated with water instead of segregated salt solutions.

References

[1 T. Loerting, N. Giovambattista; *J. Phys.Condens. Matter* **18**, (2006) R919.
[2] L. E. Bove, S. Klotz, J. Philippe, and A. M. Saitta; *Phys. Rev. Lett.* **106**, (2011) 125701.
[3] K.. Winkel, M. Seidl, T. Loerting, L.E. Bove, S. Imberti, V. Molinero, F. Bruni, R. Mancinelli, M. A. Ricci; *J. Chem. Phys.* **134**, (2011) 024515.
[4] Y. Yoshimura and H. Kanno; *J. Phys.: Condens. Matter* **14**, (2002) 10671.
[5] C.A. Angell, E.J. Sare; *J. Chem. Phys.* **52**, (1970) 1058.
[6] C.A. Angell, J.M. Sare and E.J. Sare; *J. Phys. Chem.* **82**, (1978) 2622.
[7] K.Hofer, A. Hallbrucker, E. Mayer and G.P. Johari; *J. Phys. Chem.*. **93**, (1989) 4674.
[8] O. Mishima; *J. Chem. Phys.* **121**, (2004) 3161.
[9] O. Mishima; *J. Chem. Phys.* **126**, (2007) 244507.
[10] O. Mishima, L.D. Calvert and E. Whalley; *Nature* **310**, (1984) 393.
[11] K. Winkel, M.S. Elsaesser, E. Mayer, and T. Loerting; *J.Chem Phys.* **128**, (2008) 044510.

3PE13 Membrane fusion studied by molecular dynamics simulations

S. Kawamoto[1] and W. Shinoda[1]

[1]*National Institute of Advanced Industrial Science and Technology (AIST), Osaka 563-8577, Japan*

e-mail : s.kawamoto@aist.go.jp

Membrane fusion is important for vesicle traffic, such as exocytosis in neuronal synapses and transportation of bioactive molecules between organelle in a cell. There are several intermediate structures in the fusion process, and the stability of each intermediate is related to lipid components and fusion proteins. A stalk intermediate is a negatively curved membrane bridge between two lipid bilayers tentatively observed during the membrane fusion process (Fig. 1). The negative spontaneous curvature is observed in the membrane composed of the inverted cone shaped lipid, which is believed to stabilize the stalk [1].

We investigate the effect of lipid composition on the stability of stalk intermediate by molecular dynamics simulations using realistic coarse grained model [2]. We found that phosphatidylethanol (PE) lipid stabilizes the stalk by assembling around the negative curvature region of the stalk. Thus, the fusion process should be largely modulated by the lipid composition. To investigate the free energy change along the fusion process, we also explored the methodological issues in the free energy computation. Namely, we have tried several possible collective variables [3] to evaluate the free energy barrier for the stalk formation as well as the fusion pore formation processes. The details will be discussed in this presentation.

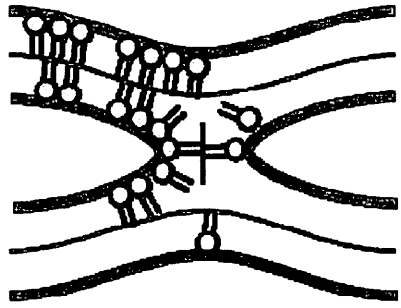

Figure 1. The stalk bridges between two bilayers

References

[1] L. V. Chenomordik, M. M. Kozlov, *Current Topics in Membranes*, **68** (2011)

[2] W. Shinoda, et al., *J. Phys. Chem. B*, **114** 6836 (2010)

[3] M. Müller, Y. G. Smirnova, G. Marelli, M. Fuhrmans, A. C. Shi, *Phys. Rev. Lett.* **108**, 228103 (2012).

3PE14 Photochemical reaction of a blue light sensor protein YtvA in solution

Seokwoo Choi[1], Yusuke Nakasone[1], Klaas J Hellingwerf[2], Masahide Terazima[1]

[1]*Department of Chemistry, Kyoto University, Kyoto 606-8502, Japan*

[2]*Swammerdam Inst Life Sci., Amsterdam University, Amsterdam, Nederland*

e-mail : swchoi@kuchem.kyoto-u.ac.jp

YtvA is a blue light sensor protein consists of the N-terminal LOV (Light-Oxygen-Voltage) domain, linker domain, and the C-terminal STAS (Sulphate Transporter and Anti Sigma factor antagonists) domain. YtvA acts as a positive regulator for environmental stress responses (light and salt stresses) via the activation of the transcriptional factor σ^B. Although the biological function has been studied, the signal transduction process at the molecular level has not been revealed yet. For understanding this mechanism, the photochemical reaction dynamics of the protein in solution has to be elucidated. Until now, we have reported the photochemistry of the shorter fragments such as the LOV domain and the LOV domain with the linker helix of YtvA by using the time-resolved transient grating (TG) method. In this study, we examined the photo-reaction dynamics of the full-length protein of YtvA to discuss how the light signal is transferred from the LOV domain to the STAS domain.

The concentration dependence of the TG signals and cross-linking measurement showed that YtvA is in equilibrium between the hexamer and the dimer in the ground state. Diffusion coefficient (D) change of the dimer was not observed during its photoreaction, which indicates that the structural change of the dimer is minor. In the case of the LOV-linker construct, however, the rotational movement of the linker helix was reported by X-ray crystallographic analysis [1] and the TG measurement of this construct showed significant D-change associated with the rotation. Consequently, we considered that the presence of the STAS domain constrained the movement of linker helix with decreasing its flexibility. On the other hand, the hexamer underwent the global reaction which was manifested as a decrease in D. The D change of the hexamer might be caused by the change in inter-protein interaction between the dimers. YtvA is one of the proteins which composes protein complex called stressosome in *Bacillus subtilis*. In the stressosome, the dimer of YtvA interacts with RsbRA which is a positive regulator of YtvA-dependent light stress response and the interaction should change upon light illumination for its functioning [2]. Therefore, we believed that the observed D change of the hexamer should represent the inter-protein interaction change in the stressosome. Additionally, we have found significant effect of the salt concentration on the equilibrium in the ground state. We will discuss the detail of photoreaction dynamics of the full-length YtvA and the effect of the salt stress on it.

References

[1] Andreas Möglich et al. *J. Mol. Biol.* (2007)

[2] Marcel Jurk et al. *Biochemical and Biophysical Research Communications.* (2013)

3PE15 A 3-D RISM/MD Study of a Small Hydrated Protein Molecule

S. Gyoubu[1], T. Yoshida[2] and S. Miura[2]

[1]*Graduate School of Natural Science and Technology, Kanazawa University, Kakuma, Kanazawa 920-1192, Japan*

[2]*School of Mathematics and Physics, Kanazawa University, Kakuma, Kanazawa 920-1192, Japan*

e-mail : smiura@mail.kanazawa-u.ac.jp

Thermodynamic properties of a small protein molecule, chignolin [1], are studied by the 3-D RISM integral equation theory [2 - 4]. The protein molecule consists of 10 amino acid residues, which is dissolved in the aqueous solution. In order to obtain thermodynamic properties of the flexible molecule, the 3-D RISM integral equation is first numerically solved for a fixed configuration of the molecule. Then, the gradient of the excess free energy is evaluated for the given configuration. Using the gradient, the molecular coordinates are updated by the standard molecular dynamics method. By the repeated application of the above procedure, the 3-D RISM/MD method samples the structural fluctuation on the free energy surface [5, 6]. In the present study, calculations for the hydrated chignolin are performed over a wide temperature range covering from the folded to the denatured states to examine the thermodynamic stability of the protein molecule.

References

[1] S. Honda *et al.*, Structure **12**, 1507 (2004).

[2] D. Beglov and B. Roux, J. Phys. Chem. B **101**, 7821 (1997).

[3] A. Kovalenko and F. Hirata, Chem. Phys. Lett. **290**, 237 (1998).

[4] A. Kovalenko and F. Hirata, J. Chem. Phys. **110**, 10095 (1999).

[5] T. Miyata and F. Hirata, J. Comp. Chem. **29**, 871 (2007).

[6] T. Luchko *et al.*, J. Chem. Theory Comput. **6**, 607 (2010).

3PE16 Molecular Mimicking of Tea Phenolic Compounds as Umami Ligands: A Molecular Docking Study

C.-C. Hung[1], T.-R. Jinn[2], S.-M. Wang[3] and F.-Y. Li[1]

[1]*Department of Chemistry, National Chung Hsing University, Taichung 402, Taiwan*
[2]*School of Chinese Medicine, China Medical University, Taichung 404, Taiwan*
[3]*Institute of Nuclear Energy Research, Lungtan Taoyuan 325, Taiwan*
e-mail : feng64@nchu.edu.tw

The phenolic compounds of tea are known to responsible to both the healthy effects and complex umami-like taste sensation. Compared to the prototypical umami compound, monosodium glutamate (MSG), with notorious Chinese Restaurant Syndrome, these tea phenolics can act as a healthy substitute. With the above consideration, we performed a molecular docking simulation to search the possible umami phenolics in tea beverages. To facilitate the investigation, umami receptor, such as T1R1, was constructed through homology modeling. The docking results suggested that several tea phenolic compounds can act as umami ligands and some other phenolic compounds can synergistically augmented the umami taste as enhancers. This means that the tea phenolic compounds can trigger the umami sensation through the same molecular mechanism by MSG and its enhancers. However the umami sensation can not be equivalently replaced with any of the major tea phenolic compounds, such as Epigallocatechin gallate (EGCG). Regardless the induced fitness, the detailed molecular interactions between the tea umami phenolic compounds and the receptor were drastically different from those of prototypical umami compounds and the receptor. It seems that the tea phenolic compounds may be developed as a natural sweetener.

.

3PE17 Aggregate of Nonionic Surfactant in Dilute Aqueous Solution Studied by MD/3D-RISM Method

T. Miyata[1], Y. Ikuta[2], and F. Hirata[3]

[1]*Department of Physics, Ehime University, Matsuyama, Ehime 790-8577, Japan*
[2]*Collaborative Research Division, Frontier research Center, Toyota Central R&D Labs., Inc., Nagakute, Aichi 480-1192, Japan*
[3]*College of Life Sciences, Ritsumeikan University, Kusatsu, Shiga 525-8577, Japan*
e-mail : miyata.tatsuhiko.mf@ehime-u.ac.jp

The structure and hydration of aggregates or micelles composed of nonionic surfactant octaethylene glycol monododecyl ether ($C_{12}E_8$) are studied by MD/3D-RISM method. The potential of mean force (PMF) along a radius of gyration, R_g, of an aggregate at the aggregation number (N_{agg}) 80 is evaluated by a blue moon method using MD/3D-RISM, which is shown in Fig. 1. With increasing R_g, the PMF exhibits a local minimum, and then increases by ca. 10 kcal/mol to show plateau. The local minimum of PMF indicates an optimal value for the radius of gyration of the aggregate: that is, ca. 23 Å. We examined a structural change of aggregate along R_g, and revealed that its hydrophobic core is maintained when R_g < 23 Å, whereas hydrophilic chains are gradually extended so that they are effectively hydrated with increasing R_g. When R_g becomes larger than 23 Å, a breakup of hydrophobic core is observed. These features in structural change of aggregate along R_g can be attributed to the solvent effect. Analysis concerning energy decomposition indicates that conformational entropy term plays an important role in determining the shape of the PMF curve. We shall point out that the conformational entropy is related to the structural change of aggregate along R_g, which reflects the solvent effect. The analysis upon hydration entropy term will also be presented.

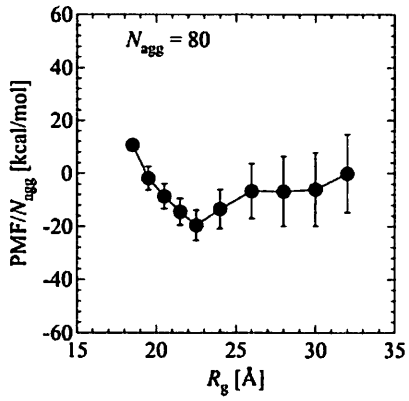

Fig. 1 Potential of mean force along a radius of gyration.

References

[1] T. Miyata, F. Hirata, *J. Comput. Chem.* **29**, 871 (2008).
[2] T. Miyata, Y. Ikuta, F. Hirata, *J. Chem. Phys.* **133**, 044114 (2010).
[3] T. Miyata, Y. Ikuta, F. Hirata, *J. Chem. Phys.* **134**, 044127 (2011).

3PE18 Macromolecular crowding effect on a protein reaction; phototropin 1 LOV2 domain with the linker region

Tomoyuki Yoshitake [1], Yusuke Nakasone [1], Tsuguyoshi Toyooka [1],

Kazunori Zikihara[2], Satoru Tokutomi [2], Masahide Terazima[1]

[1] *Department of Chemistry ,Kyoto University, Kyoto 606-8501, Japan*

[2] *Osaka Prefecture University, Okazaki 599-8231, Japan*

e-mail : t-yoshitake@kuchem.kyoto-u.ac.jp

For studies on molecular mechanisms of protein reactions by physical methods, most of researches have been performed in buffer solutions. However, since cells contain many kinds of macromolecules such as proteins, polysaccharides, RNA, DNA with high concentrations (crowding condition), the environment is very much different from the simple buffer solution. The different environment may induce different reaction from that observed in the buffer. Here, we studied photochemical reaction of a blue light sensor protein phot1LOV2-linker under crowded conditions. So far, the photochemical reaction of phot1LOV2-linker has been studied by the transient grating (TG) method in a buffer solution.[1] Upon photoexcitation of its chromophore FMN, a covalent bond between FMN and a Cys residue in the LOV2 domain is formed with a time constant of 2 μs. This reaction leads to the unfolding of helical structure in the linker region. We studied the photochemistry of phot1LOV2-linker using the transient grating (TG) method in a crowding environment, which was mimicked by adding Ficoll 70 to the sample solution.

Fig.1 shows the molecular diffusion signals of phot1LOV2-linker with and without Ficoll 70. In the absence of Ficoll 70, a strong diffusion peak was observed, which represents the diffusion coefficient change due to the unfolding of the linker helix. On the other hand, adding Ficoll results in the decreases of the intensity of the diffusion peak and a new component was appeared before the diffusion of protein molecule. We assigned the new component to the diffusion signal of FMN, which was dissociated from the LOV2 domain. As a result, the number of molecule which showed normal photoreaction was decreased, and subsequently, the intensity of the diffusion signal was weakened. In addition, we have found that the value of diffusion coefficient was affected by the crowding. We will discuss the crowding effect on the photoreaction of this protein.

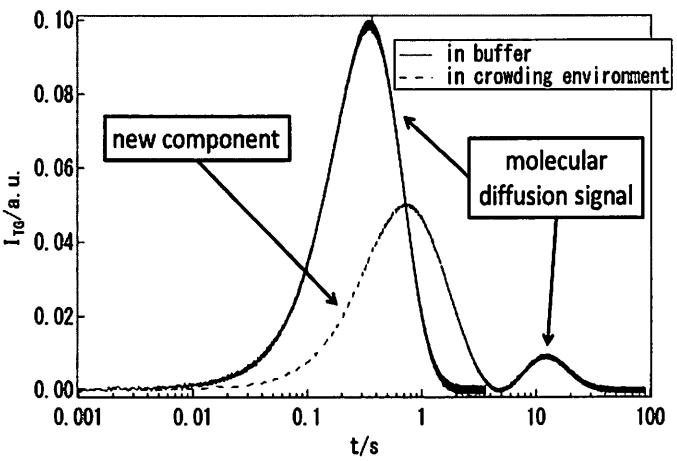

Fig.1 molecular diffusion signals

Reference

[1] Nakasone et al. 2007. *J. Mol. Biol.* 367:432-42.

3PE19 Kinetics of Dissociation Reaction of UVR8 in Solution Measured by the Transient Grating Method

Takaaki Miyamori[1], Yusuke Nakasone[1], Kenichi Hitomi[2],

John M Christie[3], Elizabeth D Getzoff[2], Masahide Terazima[1]

[1]*Department of Chemistry, Kyoto University, Kyoto 606-8502, Japan*

[2]*The Scripps research institute, California, USA*

[3]*University of Glasgow, Glasgow, Scotland*

e-mail : miyamo@kuchem.kyoto-u.ac.jp

In this study, we used the diffusion coefficient (D) change in time-domain to trace the reaction dynamics of a UV-light sensor protein, UVR8. UVR8 from *Arabidopsis* mediates gene expression responses to establish the UV protection. Generally, light sensor proteins possess specific chromophore molecules to absorb light and initiate photochemical reactions for signal transduction. Interestingly, however, UVR8 employs Trp residues to sense the environmental light condition instead of having such specific chromophores. The crystal structure has been reported for the construct which lacks the C-terminal flanking region and it showed doubly hydrogen-bonded salt bridges (R286-D107 and R146-E182) made the dimer stable under dark condition.[1] It was also proposed that the interfaces between dimer employ Trp residues to sense UV-B and induce the dissociation. However, the mechanism of the dissociation process is still not clear, and the photoreaction dynamics in solution has not been examined. Here, we investigated the kinetics of its dissociation reaction and structural change in the C-terminal region by the time-resolved transient grating (TG) method.

The TG signal of UVR8 was measured with a fourth harmonic light of Nd-YAG laser (266nm) as an excitation light and a blue diode laser (449nm) as a probe light. Molecular diffusion signal showed rise and decay features, which indicated that D changed with the dissociation reaction. From the time-profile of the TG signals at various grating wavenumbers, we estimated the time constant of the dissociation reaction to be 100 ms. Under the same condition, the R146A/R286A mutant existing monomer stably in both dark and light state also showed D-change but the profile was different from that of the wild type. We attributed the observed D-change to the conformational change of the UVR8 monomer. We consider the change occurred mainly in C-terminal region. In order to confirm this, we are trying to measure the reaction of the R146A/R286A mutant which lacks the C-terminal region. We will report the photoreaction of UVR8 and its mutants in more detail.

The crystal structure of UVR8 dimer[1]

References

[1] John M. Christie *et al. Science* **335**, 1492 (2012)

3PE20 Stilbene Analogs for Modulating Metal-Mediated Aggregation of Amyloid-*beta* Peptide

L. S. Hsu[1], Y. F. Liao[2], and M. K. Hu[1]

[1]*School of Pharmacy, National Defense Medical Center, Taipei 114, Taiwan*
[2]*Laboratory of Molecular Neurobiology, Institute of Cellular and Organismic Biology, Academia Sinica, Taipei 115, Taiwan*

e-mail : hmk@ndmctsgh.edu.tw

Amyloid-*beta* peptide and its metal-mediated oligomerized states have been proposed to play an important role of the pathogenesis of Alzheimer's disease [1]. Interruption of these metal-mediated amyloid peptides using metal-chelating functionalities implied considerable promise of a strategy for the treatment of the disease [2]. Presented here are stilbene analogs that contain amyloid-binding and metal-chelating molecular motifs, which exhibited effective modulation on amyloid-*beta* aggregation in this study.

The stilbene analogs were prepared straightforward with satisfactory yields by treating quinoline derivative with phenylenediamine and benzyltriphenylphosphonium salt, respectively, as shown in the scheme. Two metal-mediated amyloid-*beta* aggregation studies were carried out in a buffer solution at pH 7.4. We first investigated their abilities for the inhibition of forming metal-induced amyloid aggregation and second, the effects for the disruption of metal-induced aggregated fibrils. The degree of amyloid-*beta* aggregation in the presence of these stilbene analogs was investigated by transmission electron microscopy. The resulting metal-chelating abilities and the images are depicted.

References

[1] A. Rauk, *Chem. Soc. Rev.* **38**, 2698(2009).
[2] K. J. Barnham, A. I. Bush, *Curr. Opin. Chem. Biol.* **12**, 222(2008).

3PE21 Identification of critical structural motifs in steroid compounds for triggering nuclear migration of glucocorticoid receptor: A molecualr docking study

Ya-Lin Liu[1], Tzyy-Rong Jinn[2], Soonmin Jang[3], Shih-Min Wang[4], Feng-Yin Lia*[1]
[1]*Department of Chemistry, National Chung Hsing University, Taichung, Taiwan 402, ROC*
[2]*School of Chinese Medicine, China Medical University, Taichung, Taiwan 404, ROC*
[3]*Department of Chemistry, Sejong University, Seoul 143-747, Korea*
[4]*Institute of Nuclear Energy Research, Lungtan, Taoyuan, Taiwan 325, ROC*
e-mail : irene0211@gmail.com

Antcin, unique steroidal compounds in Niuchangchih (*Antrodia camphorate*), was used to probe the structural basis for triggering nuclear migration of glucocorticoid receptor (GR), along with cortisone and dexamethasone, the regular GR ligands. Even with the highly structural similarity between the five major antcins (A, B, C, H, and K) isolated from fruiting bodies of Niuchangchih (*Antrodia camphorate*), only antcin A was capable of triggering nuclear migration of glucocorticoid receptor as found in our previous study. The structural motifs in the antcins, responsible for triggering this nuclear migration were identified as Docking simulation, along with two common GR ligands (cortisone and dexamethasone) as the positive control. The results indicate that antcin A can effectively dock onto GR in the same active site as cortisone and dexamethasone with similar orientation. The other four antcins show different docking mode lead to poor inhibitory activity. The main reason for this difference in binding affinity is mainly due to the existence of the hydrophilic group at C-7 in the structural skeleton of these antcins, which is exposed to the hydrophobic region in the GR binding cavity. Although antcin A is capable of docking into the GR binding cavity, its linear chain at C-17 reduces the binding affinity to GR compared to cortisone and dexamethasone.

3PE22 Docking simulation of Low-Molecular-Weight Antagonists to Human Thyrotropin Receptor

Kailun Lin, Peilee Chan, Fengyin Li

Department of Chemistry, National Chunghsing University, Taichung 402, Taiwan
e-mail : superdlb@gmail.com

The thyroid-stimulating hormone receptor (TSHR), a G protein-coupled receptor (GPCR), responds to thyroid-stimulating hormones and then stimulates the production of thyroxine (T4) and triiodothyronine (T3). This receptor plays an important role in throid hormone regulation, and is responsible to Graves' disease.

Recently, some low-molecular-weight (LMW) compounds were proposed to be used as agonists for some GPCRs, such as LH/chorionic gonadotropin receptor (LHCGR) and follicle-stimulating hormone (FSH) receptor. In this study, the homology model of TSHR was constructed and docking simulations were also performed in Discovery Studio enviroment (http://accelrys.com). We characterized the design rules of the antagonist according to the activity of the thyroid-stimulating antibody through the LMW compounds docking in Cluster I of the TSHR. We found that the compounds containing 40-70 atoms may have the suitable size to dock into the active site of TSHR. Besides, if the molecules contain functional groups, such as OH and SH groups, that are likely to form hydrogen bonds to those residues on the surface of the active site, the complexes may be stablized.

With those conditions mentioned above, we proposed some molecules to be potential candidates as TSHR antagonists and we also performed molecular docking simulation to verify whether they are capable of binding onto the active site of the receptor or not.

3PE23 Light induced signal transduction reaction of LOV2-kinase fragment of phototropin2 from *Arabidopsis*

A.Takakado[1], Y. Nakasone[1], K. Okajima[2], S. Tokutomi[2] and M. Terazima[1]

[1]*Department of Chemistry, Kyoto University, Kyoto 606-8502, Japan*

[2]*Osaka Prefecture University, Osaka 599-8531, Japan*

e-mail : takakado@kuchem.kyoto-u.ac.jp

For understanding chemical reactions of biomolecules in solution, conformation change dynamics during the reactions should be detected in time domain. In this research, we use the time-resolved diffusion coefficient measurement to study the reaction dynamics of a blue light sensor, phototropin, which is a blue light receptor protein in higher plants. This protein consists of two light sensing domains (LOV1 and LOV2) at N terminal half and a Ser/Thr kinase domain at C terminal half.

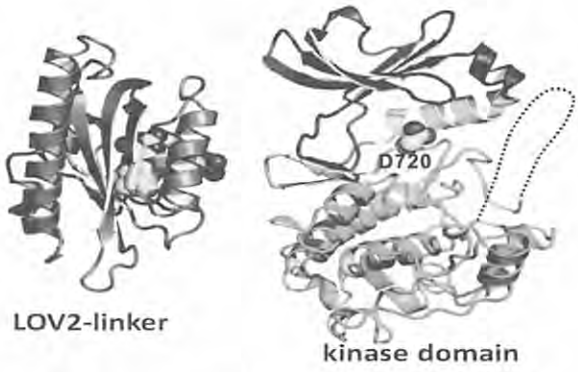

Fig.1 Structures of LOV2-linker and kinase

The LOV2 domain and the kinase domain are connected by a linker domain which forms helical structure at the dark state. The LOV2 domain suppresses the kinase activity by docking on it in the dark and light-induced dissociation of the LOV2 from the kinase leads to the activation of the kinase. So far, our group has been studying the reactions of the LOV2 domain [1], but the reactions of a construct containing both LOV2 and kinase domains (LOV2-kinase) has not been revealed yet. In this study, we report the reaction dynamics of the LOV2-kinase using the time-resolved transient grating (TG) and transient lens (TrL) methods.

The TG signals of the LOV2-kinase showed time dependent diffusion coefficient (D) changes during its photoreaction. The D changes reflect the changes of the interaction with the solvent caused by conformational changes of the LOV2-kinase in solution. Analysing the time development of the diffusion signal, we determined the time constant of the D change to be 2 ms, which was identical to the reaction time constant of the LOV2-linker helix. The TrL measurement also showed a signal which was attributed to a volume change associated with the unfolding process of the linker helix. Therefore, we concluded that the conformation change of the linker helix was conserved in the presence of the kinase domain. Furthermore, we also detected another component in the D change which occurs in the slower time scale (> 10ms). We consider that this reaction takes place in the kinase domain which may reflect the activation process of the kinase.

Reference

[1] T. Eitoku et al. *J.Am.chem.soc.* **127**:13238(2005)

3PE24 3D-RISM Study of Ion-Molecular Complex Formation of Alanine Zwitterion with Inorganic Ions in Biologically Relevant Aqueous Electrolyte Solutions

M. Fedotova[1,2], O. Dmitrieva[2]

[1]*G.A. Krestov Institute of Solution Chemistry of the Russian Academy of Sciences, Academicheskya st., 1, Ivanovo, 153045, Russia*

[2]*Ivanovo State University, Physical Department, Ermak st., 39, Ivanovo, 153025, Russia*

e-mail : mvf@isuct.ru

Biomolecular systems are complex solutions involving not only the considered biomolecule but also the solvent and generally various co-solutes (often ions), with the composition of the matrix significantly modulating the physicochemical properties of these systems[1]. Because salts and other electrolytes are ubiquitous in biological systems, understanding their effects on protein behavior at the molecular level is important to quantify their interactions in biological and biochemical processes. The study of entire biomolecules or biopolymers in an aqueous solution is often inconvenient, because of the difficulties with separating the effects originating from many types of interactions. Therefore, it is often more suitable to study simple model compounds having the typical functional groups encountered in biological systems, like amino acids. However, even for such model systems the complex nature of the involved interactions has hampered thorough understanding so far.

In this contribution we present the results of a 3D-RISM-study into the ion binding of the alanine zwitterion (Ala-ZW) in biologically relevant aqueous electrolyte solutions , XCl(aq), X=Na, K, Ca, Mg. The features of ion-molecular complex formation were analyzed in terms of spatial distribution functions and the spatial potential mean force. As expected, all cations (Cat^+) form complexes with the $-COO^-$ group, whereas Cl^- forms a complex with the $-NH_3^+$ group of Ala-ZW. It was found that the probability of $(-COO^-:Cat^+)_{aq}$ complex formation, and hence the stability of this complex, increases in the sequence $K^+<Na^+<Ca^{2+}<Mg^{2+}$. For all studied salts the probabilities for the formation of $(-NH_3^+:Cl^-)_{aq}$ complexes and the resulting complex stabilities are similar. A structural mechanism for this binding is discussed. Except for K^+, the $(-COO^-:Cat^+)_{aq}$ complex adopts a conformation where one oxygen atom is close to the $-NH_3^+$ group. For KCl(aq) the chloride ion bound to the ammonium group of Ala-ZW is embedded between oxygens of $-COO^-$ up to 2 M KCl(aq). At higher concentrations the conformation taken by the carboxylate residue becomes similar to that of other studied salts. In all investigated systems the $(-NH_3^+:Cl^-)_{aq}$ complex is formed via the hydrogen atom closest to the $-CH_3$ group.

This work was supported by funding from the European Union' Seventh Framework Program (FP7-PEOPLE-2009-IRSES, Marie Curie Project) under grant agreement No. 247500 and by the Russian Foundation for Basic Research (grant No. 12-03-97508–r_centre_a).

References

[1] P. Auffinger, Y. Hashem, *Curr. Opin. Struct. Biol.* **17**, 325(2007).

3PE25 Small angle x-ray scattering and integral equation approach for intermolecular interaction potential of globular proteins

H. Imamura[1], T. Morita[1], T. Sumi[2], Y. Isogai[3], M. Kato[4], and K. Nishikawa[1]

[1]*Graduate School of Advanced Integration Science, Chiba University, Chiba 263-8522, Japan*

[2]*Department of Chemistry, Okayama University, 3-1-1 Tsushima-Naka, Kita-ku, Okayama 700-8530, Japan*

[3]*Department of Biotechnology, Toyama Prefectural University, Toyama 939-0398, Japan*

[4]*Department of Pharmacy, Ritsumeikan University, Shiga 525-8577, Japan*

e-mail : himamura@chiba-u.jp

Self-assemblies of proteins such as precipitation and aggregation are often problematic when handling protein solution for research and commercial use. While naturally occurring proteins are water-soluble, currently designed proteins, the structures of which resemble the target natural proteins, are prone to precipitate (e.g. [1]). We are interested in key factors governing intermolecular interaction, which induces self-association of proteins. A small-angle X-ray scattering (SAXS) provides information from protein's interparticle interference called structure factor and protein's self-scattering. A structure factor is connected to a protein-protein radial distribution function through use of Fourier transform. With theories for analyzing pure liquid structure [2], in addition, intermolecular potential of a protein can be estimated. The present study measured SAXS profiles of myoglobin in aqueous solution. It was reported that the apo-form of myoglobin is prone to aggregate, compared to the holo-form [3]. It is interesting to test how removal of the heme changes the intermolecular interaction. The apo-form of myoglobin shows weaker interparticle interference at low scattering vectors than the holo-form, suggesting that removal of the heme from myoglobin reduces repulsion between the protein molecules. In addition to analysis of the intermolecular potential assuming DLVO potential, we developed a method to determine intermolecular potential of proteins from experimental structure factor by applying an integral equation theory, without assuming any model potential. The analysis of SAXS profile of concentrated lysozyme solution by this method reveals multi peaks in the radial distribution function and the interaction potential between the protein molecules. This information will be useful for understanding protein's arrangement in aqueous solution before the self-assemblies.

References

[1] H. Imamura, Y. Isogai, M. Kato, *Biochemistry* **51**, 3539(2012).

[2] J. P. Hansen, I. R. McDonald, Theory of simple liquids, (1976).

[3] M. Fändrich, V. Forge, K. Buder, M. Kittler, C. M. Dobson, S. Diekmann, *Proc. Natl. Acad. Sci. U.S.A.* **100**, 15463(2003).

3PF14 The high performance graphene-silver nanowire transparent, conductive films

Fong-Chi Lin, Hsi-Wen Tien, Sheng-Tsung Hsiao, Wei-Hao Liao, Yu-Sheng Wang, Shin-Ming Li, Chen-Chi M Ma*

Department of Chemical Engineering, National Tsing-Hua University, Hsin-Chu 30013, Taiwan, ROC

e-mail : ccma@che.nthu.edu.tw

The high surface area graphene nanosheets (GNs) can be incorporated with a high electrical conductive silver nanowires (AgNWs) which were modified by cysteamine to form AgNW-GN hybrid nanomaterials. The high transmittance and low surface electrical resistance transparent conductive films (TCFs) can be prepared a highly controllable dip-coating method. AgNW-GN hybrid nanomaterials were adsorbed by waterborne polyurethane surfaces in an alkaline environment. The AgNWs not only play vital roles to prevent GNs from restacking and aggregation after reduction from graphene oxide but increase the electrical conductivity between the GN interlayers. The AgNW-GN hybrid-based TCFs possess high performance which show a sheet resistance of 86 Ω/sq with 80% light transmittance and high DC conductivity to optical conductivity ratio (19.81).

3PF15 In-situ Polymerization Approach to Amine-Functionalized Graphene Oxide/Polyimide Composite Films with Outstanding Properties

Wei-Hao Liao, Hsi-Wen Tien, Sheng-Tsung Hsiao, Yu-Sheng Wang,

Shin-Ming Li, Chen-Chi Ma, Shin-Yi Yang, and Jen-Yu Wang

Department of Chemical Engineering, National Tsing-Hua University, Hsin-Chu 30013, Taiwan, R.O.C.

e-mail : s9930606@m99.nthu.edu.tw

This study fabricates amine (NH_2)-functionalized graphene oxide (GO)/polyimide(PI) composite films with high performance using in situ polymerization. Linear poly (oxyalkylene) amines with two different molecular weights 400 and 2000 (D400 and D2000) have been grafted onto the GO surfaces, forming two types of NH2-functionalized GO (D400-GO/D2000-GO). NH2-functionalized GO, especially D400-GO, demonstrated better reinforcing efficiency in mechanical and thermal properties. The observed property enhancement are due to large aspect ratio of GO sheets, the uniform dispersion of the GO within the PI matrix, and strong interfacial adhesion due to the chemical bonding between GO and the polymeric matrix. The Young's modulus of the composite films with 0.3 wt % D400-GO loading is 7.4 times greater than that of neat PI, and tensile strength is 240% higher than that of neat PI. Compared to neat PI, 0.3 wt % D400-GO/PI film exhibits approximately 23.96 °C increase in glass transition temperature (T_g). The coefficient of thermal expansion below T_g is significantly decreased from 102.6 μ m/°C (neat PI) to 53.81 μ m/°C (decreasing 48%) for the D400-GO/PI composites with low D400-GO content (0.1 wt %). This work not only provides a method to develop the GO-based polyimide composites with superior performances but also conceptually provides a chance to modulate the interfacial interaction between GO and the polymer through designing the chain length of grafting molecules on NH_2-functionalized GO.

3PF16 Formation Process of Triangular Gold Nanoplates by Tartaric Acid Reduction

M. Takezaki, T. Hirai, and T. Tominaga

Department of Applied Chemistry, Okayama University of Science, Okayama 700-0005, Japan

e-mail: mtake@dac.ous.ac.jp, ttominaga@dac.ous.ac.jp

Metal triangular nanoplates show interesting localized surface plasmon resonances. Around their tips, the electromagnetic field is strongly enhanced. Recently, we have reported simple synthesis methods of gold triangular nanoplates[1, 2]. In order to control the size and shape of gold triangular nanoplates, it is important to elucidate their formation processes. In this work, we have examined the formation processes of gold triangular nanoplates prepared by the tartaric acid reduction method.

Gold nanoplates were synthesized by the method reported elsewhere[2]. The solutions containing 0.5 mM (1 M= 1 mol dm^{-3}) $HAuCl_4$, 2.2 mM hexadecyltrimethylammonium chloride (HTACl) as a protective agent and 60 mM tartaric acid (H_2tart) as a reducing agent were prepared in an oil bath kept at 30 °C. The bath temperature was increased to reach 70 °C in 13 minutes. Then the solutions were taken out of the bath and were characterized by UV-vis spectroscopy and transmission electron microscope (TEM) observation.

The gold nanoparticle solution is clear bluish purple just after being taken out of the bath and changes to be turbid maroon after a day. The extinction spectra are shown in Fig. 1. The nanoparticles show two extinction peaks at 570 and 850 nm 30 s after being taken out. The longer wavelength peak blue-shifted with time and was merged into the shorter wavelength peak. The shorter wavelength peak also blue-shifted and its height increased with time. From these spectral features, large and thin triangular nanoplates are considered to have become smaller and thicker. From TEM observations, triangular nanopaltes having 100 nm side lengths after 30 s changed to smaller and thicker triangular nanoplates after 15 h.

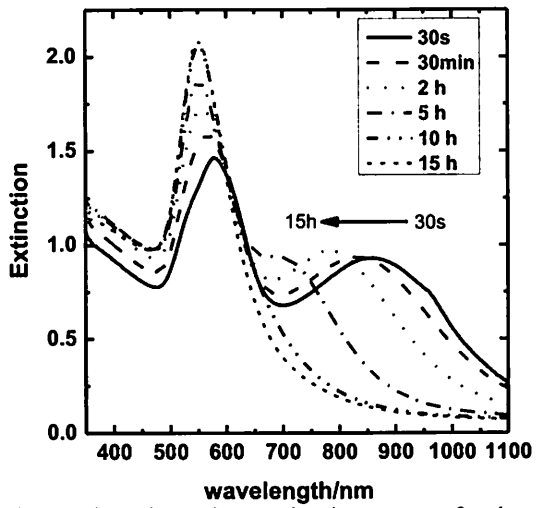

Fig. 1. Time-dependent extinction spectra for the gold nanoparticles.

References

[1] M. Takezaki, R. Kida, Y. Kato, T. Tominaga, *Chem. Lett.* **38**, 1022 (2009).

[2] M. Takezaki, M. Shibata, T. Tominaga, *Chem. Lett.* **41**, 1166 (2012).

3PF17 Electromagnetic interference shielding effectiveness of non-covalent modified graphene nanosheet/ water-born polyurethane composites

Sheng-Tsung Hsiao, Chen-Chi M. Ma*, Hsi-Wen Tien,

Wei-Hao Liao, Yu-Sheng Wang[1], Shin-Ming Li, Yu-Chin Huang

Department of Chemical Engineering,

National Tsing-Hua University, Hsin-Chu 30013, Taiwan

e-mail : s9932538@m99.nthu.edu.tw

This study investigates the preparation and properties of flexible, lightweight and high EMI shielding graphene nanosheet (GNS)/water-born polyurethane (WPU) composites. WPU, with sulfonate functional groups, was used as the polymer matrix. By adsobing the cationic surfactant (trimethylstearylammonium chloride, STAC) on the surface of GNS (S-GNS), restacking and aggregation of GNSs can be suppressed efficiently, which also attracted sulfonate groups of WPU matrix. Due to the favorable interfacial interactions arising from electrostatic attraction, the S-GNS exhibits a good compatibility in the WPU matrix. Such homogeneous dispersion was contributive to construct an electrical conductive network. The S-GNS/WPU composite exhibits a low electrical conductivity percolation threshold (~0.43 vol. %) and an outstanding enhanced electrical conductivity ~5.1 S/m. A high EMI shielding effectiveness (SE) of the WPU composites ~32 dB was obtained by adding 5 vol. % (~7.7 wt. %) S-GNS.

3PF18 Blue colored gold nanoparticles for lateral flow immunochromatographic test

Yuya Kato[1], Hisahiko Iwamoto[1], and Yoshiko K. Takahara[1]

[1]*Medical Department, Technical Division, TANAKA KIKINZOKU KOGYO K. K.,*
2-73, Shinmachi, Hiratsuka, Kanagawa 254-0076, Japan
e-mail : y-kato@ml.tanaka.co.jp

Lateral flow immunochromatographic test (ICT) is used for clinical diagnosis and environment analysis by the reason of simplicity to use, rapid detection and low cost. In addition, ICT does not require for pre-treatment, washing process and sophisticated instruments. However, ITC is inferior to other immunoassays such as ELISA and CLEIA in the detection limit and capability of multiplex simultaneous measurement. Antibody is labelled by reporter carriers such as colored latex beads, quantum dots and metal nanoparticles in ICT. The sensitivity of ICT is influenced by the reporter carrier. As gold nanoparticles have high extinction coefficient caused by the localized surface plasmon resonance, gold nanoparticles are suitable as a reporter carrier. We have succeeded in improving the detection limit of ICT by using monodisperse gold spherical nanoparticles so far[1)].

We have studied blue colored gold nanoparticles for ICT. Various colored gold nanoparticles were synthesized according to wang's method[2)]. And larger particles were grown by own seed-growth method to investigate the size effect of the sensitivity of ICT. Each particle is confirmed by UV-vis spectroscopy, TEM and ICT. We found that the sensitivity of ICT is influenced by the size than the shape in this study. We have developed the new reporter carrier for ICT that can give high sensitivity and multiplex simultaneous measurement.

References

[1] Tanaka precious metals press release, sep. 3 2010.

[2] J. Xie, J. Y. Lee, D. I. C. Wang., *Chem. Mater.*, 2823-2830, **19**, (2007).

3PF19 Interaction potential between the particles adsorbed at an oil-water interface

T. Sakka[1], D. Kozawa[2], K. Tsuchiya[2], N. Sugiman[2], G. Øye[3], K. Fukami[2], and Y. H. Ogata[2]

[1]*Department of Energy and Hydrocarbon Chemistry, Graduate School of Engineering, Kyoto University, Kyoto 615-8510, Japan*

[2]*Instituteof Advanced Energy, Kyoto University, Uji, Kyoto 611-0011, Japan*

[3]*Department of Chemical Engineering, Norwegian University of Science and Technology (NTNU), Trondheim, Norway*

e-mail : sakka.tetsuo.2a@kyoto-u.ac.jp

Self-assembled monolayer of polystyrene particles at oil-water interfaces was studied. Polystyrene (PS) particles with the diameter of 3 μm formed two-dimensional hexagonal array structure, of which the interparticle distance can be as long as ~20 μm. The mechanism justifying such structure is a long-range repulsion among the particles, as well as a limited size of the interfacial area into which the particles are dispersed. In order to precisely control such two-dimensional self-assembled ordering structure, it is crucial to know the interaction potential as a function of interparticle distance. Such interaction potential curve can be measured by using a vertical oil-water interface. In this configuration [1] the gravity partly compensated by buoyancy is used as an externally applied force. Since the magnitude of the gravity is known, and the distance between the particles is readily measured by the optical microscope images, the interaction potential can be obtained as a function of the distance between the particles.

In the present work we obtained the interaction potential curves for the PS particles adsorbed at *n*-decane/water and n-decane/aqueous solution interfaces. As a solute in the aqueous phase, NaCl, sodium dodecyl sulfate (SDS), sorbitan oleate (Span80) were used. SDS is an anionic surfactant, while Span80 is nonionic surfactant. The results show that NaCl does not change the interaction potential curve significantly, while SDS greatly lowers the repulsive nature of the particles. On the other hand the effect of Span80 is very limited. The plot of the interaction potential against $1/r$ or $1/r^3$, where r is the center-to-center interparticle distance, shows a linear dependence in case of $1/r^3$, suggesting a dipole-dipole electrostatic interaction [2] rather than the Coulombic interaction. The lowering of the interaction potential in case of SDS is explained by the effective adsorption of the surfactant to the particles, as well as the effective shielding of the surface charge of the particle due to the ionic nature of the surfactant.

References

[1] A. Law, D. M. A. Buzza, T. S. Horrozov, *Phys. Rev. Lett.* **106**, 128302 (2011).

[2] A. J. Hurd, *J. Phys. A: Math. Gen.* **18**, L1055 (1985).

3PF20 Colloidal Synthesis of Germanium Nanocrystals: Tuning the Color of Luminescence in Wide Range of UV-VIS-NIR

N. Shirahata

[1]*WPI-MANA, National Institute for Materials Science (NIMS), Tsukuba 305-0047, Japan*
[2]*PRESTO, JST, 4-1-8 Honcho Kawaguchi, Saitama 332-0012, Japan*
e-mail : SHIRAHATA.Naoto@nims.go.jp

The luminescent materials in the emission ranging from NUV through VIS to NIR have been attracting research attention owing to a variety of potential optics applications. In particular, the nanoparticles of crystalline Si and Ge offer a number of advantages for the industrial use because of their high compatibilities with microelectronics and inherent non-toxicities against environment surrounding us and human health; however, the element investigated is weighted in Si compared to Ge. The distinctive advantages of Ge over Si for optical applications are the smaller effective mass of its electron-hole pairs and its larger static dielectric constant. Effective mass is inversely related to the bulk exciton Bohr radius, so the quantum confinement (QC) effect appears at a larger dimension for Ge (~24 nm) than Si (~10 nm). A further advantage of Ge is its narrow bulk bandgap (0.67 eV at 300 K), suggesting the possible tuning of light emission over as much as 3.3 eV, corresponding to wavelengths from near-UV through visible to near-IR (~1.5 μm).

In the present study, it is revealed that rigorous control over size and surface of Ge nanoparticles allows the fine color-tuning of efficient fluorescence emission in the very wide wavelength range. The spectral linewidths of each emission were very narrow. Furthermore, the absolute fluorescence quantum yields of each emission were high enough to be used as fluorescence labeling tags. Another scientific impact is the finding of new family of luminescent Ge. Such superior properties of fluorescence were, respectively, observed from the fractions separated from one mother Ge nanoparticle sample by fluorescence color using our developed combinatorial column technique. It is commonly believed that a broad spectral linewidth frequently observed from Ge nanoparticle appears due to an indirect bandgap nature inherited even in nanostructures, but the present study argues that such a broad luminescence spectrum is expressed as ensemble of different spectral lines, and can be separated into the fractions emitting the lights in each wavelength region by the appropriate postsynthetic process.

References

[1] N. Shirahata, *Phys. Chem. Chem. Phys. (Perspective Article)* **13**, 7284 (2011).
[2] N. Shirahata, D. Hirakawa, Y. Masuda, Y. Sakka, *Langmuir* (2013) DOI: 10.1021/la303482s.
[3] J. Zhou, N. Shirahata, et al., *J. Phys. Chem. Lett.* **4**, 402 (2013)
[4] B. Ghosh, Y. Sakka, N. Shirahata, *J. Mater. Chem. A* **1**, 2747 (2013).
[5] B. Ghosh, M. Ogawara, Y. Sakka, N. Shirahata, *J. Nanosci. Nanotechnol.* (2013) in press.
[6] N. Shirahata, *Chem. Commun.* (2013) submitted for publication.

3PF21 Contribution of solvent hydrophobicity on absorption of quercetin by zeolite

Kentaro Tamura and Masanao Imai*

Course in Bioresource Utilization Sciences,
Graduate school of Bioresource Sciences, Nihon University,
1866 Kameino, Fujisawa, Kanagawa-pref. 252-8510 , Japan
*e-mail : XLT05104@nifty.com

Quercetin is known a plant flavonoid, a kind of polyphenol act as an antioxidative supplement. It is a yellow pigment contained in some vegetables such as onion and asparagus. It has hydrophobic characters and is insoluble in water. For recovery of quercetin, suitable choice of solvent is important to realize a maximum yield. This paper demonstrated that the effect of hydrophobicity of solvent on adsorption equilibrium on zeolite. Typical five alcohols (methanol, 1-butanol, 1-hexanol, 1-octanol and 1-decanol) were employed in adsorption study. Zeolite was spherical particles whose effective size range was 1.4~2.4 mm. Adsorption examination was performed for two days shaking in a shade and temperature controlled bath (288K) to avoid degradation of quercetin. Equilibrium concentration of quercetin in alcohol phase was determined by HPLC. Adsorbed amount onto zeolite was calculated from difference of concentration of alcohol phase.

Freundlich isotherm ($Q = K_F C^{1/n}$) presented well the adsorption equilibrium of quercetin. Adsorption parameters K_F and n were obtained for each alcohol. Hydrophobicity of alcohol was evaluated by LogP [1]. The K_F was decayed with increasing LogP and then levelled off over LogP 1.8. The change of (1/n) showed a bell-shaped curve, a maximum value was appeared at LogP 1.8. The criteria of Freundlich isotherm parameters were similar value with LogP value of quercetin reported (1.82) [2]. Similar hydrophobicity between solvent and quercetin was a key factor for high yield adsorption of quercetin.

Table1. Results of K_F and 1/n.

	K_F	1/n
Methanol	0.607	0.373
Butanol	0.147	0.594
Hexanol	0.027	1.070
Octanol	0.045	0.759
Decanol	0.022	0.897

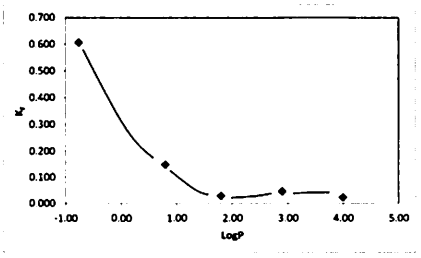

Figure1. K_F vs. LogP

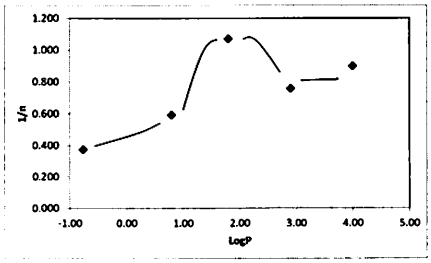

Figure2. 1/n vs. LogP

References

[1] C.Laane, S.Boeren, K.Vos, C.Veeger, *Biotechnol. Bioeng.* 30, 81-87(1987).

[2] J.A.Rothwell, A.J.Day, M.R.A.Morgan, *J.Agric.Food. Chem.*53, 4355-4360(2005)

3PF22 Surface Modification of ZnO-nanoparticle Quantum Dots by Silane Coupling Agents

K. Matsuyama[1], Neil Ihsan[1], T. Okuyama[2], H. Muto[3]

[1]*Department of Biochemistry and Applied Chemistry, Kurume National College of Technology, Kurume 830-8555, Japan*

[2]*Department of Materials Science and Engineering, Kurume National College of Technology, Kurume, 830-8555, Japan*

[3]*Department of Electrical and Electronic Information Engineering, Toyohashi University of Technology, Toyohashi, 441-8580, Japan*

e-mail : mtym@kurume-nct.ac.jp

Recently, ZnO-nanoparticle quantum dots (QDs) have also been shown to be potentially applicable in the manufacture of light-emitting diodes (LEDs) and optical devices. ZnO is relatively nontoxic, whereas other semiconductor materials, including Cd-related compounds, are harmful to cells and human health, and they eventually damage the environment. Although ZnO-nanoparticle QDs can be synthesized by various processes, including chemical vapor deposition (CVD), hydrothermal synthesis, the polyol process, and the sonochemical method, the sol-gel process in an alcoholic medium is the conventional method, with a high production rate and relatively low energy cost. To stabilize ZnO photoluminescence, surface modification can be achieved by using organic ligands, SiO_2, and polymers.

In this work, we investigated a method of surface modification of ZnO QDs using organic ligands to obtain polymeric hybrid films of ZnO-nanoparticle QDs and poly(methyl methacrylate) (PMMA) with high luminescence and tunable emission color. ZnO nanoparticle QDs/PMMA composites are synthesized by conventional radical polymerization in the presence of 3-(trimethoxysilyl)propylmethacrylate (TPM)-modified ZnO nanoparticle QDs[1].

Furthermore, we report the preparation of biotinylated ZnO-nanoparticle QDs and the labeling of avidin-immobilized beads with these QDs by use of the adivin–biotin interaction[2]. Highly luminescent silica-coated ZnO-nanoparticle QDs dispersed in an aqueous medium were synthesized using the sol-gel process. The ZnO-nanoparticle QDs were coated with silica using tetraethyl orthosilicate (TEOS) to improve the water stability of the ZnO nanoparticles. To demonstrate the applicability of this method, we attempted to use the biotinylated ZnO-nanoparticle QDs in cell-labeling applications.

References

[1] K. Matsuyama, K. Mishima, T. Kato, K. Irie, K. Mishima, *J. Colloid & Interface Sci.* **367**, 171(2012).

[2] K. Matsuyama, Neil Ihsan, K. Irie, K. Mishima, T. Okuyama, H. Muto, *J. Colloid & Interface Sci. in press.*

3PF23 Preparation of CdSe/CdS and CdSe/SiO2 Core-Shell Nanoparticles Using Reverse Micelles

K. Liu[1], A. R. Lee[1], H. H. Yoon[1], H. W. Choi[2], K. H. Kim[2], and S. J. Park[1]

[1]*Department of Chemical & Biological Engineering, Gachon University, Seongnam, 461-701, Kore*

[2]*Department of Electrical Engineering, Gachon University, Seongnam, 461-701, Korea*

e-mail : psj@gachon.ac.kr

II-VI semiconductor nanocrystals such as CdSe are attracting much interest as novel bright phosphors, i.e., quantum dots (QDs), with tunable photoluminescence (PL) wavelength for possible uses including as light-emitting devices [1] and in biological labeling. In our previous work, CdSe nanoparticles with relatively high PL quantum yield (30%, Fig. 1) were prepared by a safe, low cost, and simple synthesis method, utilizing a sodium bis (2-ethylhexyl) sulfosuccinate (AOT)/water/ cyclohexane microemulsion. However, the ultrasensitivity of their fluorescence to the surface states hinders its application to a great extent. The formation of a core/shell structure is a typical example of a solution. On the other hand, for applications in biological labeling, the primary problem is how to make QDs biocompatible. Silica is an ideal choice, since it will protect the QDs from oxidation and agglomeration. Furthermore, a silica shell provides biocompatibility and the surface of silica can be easily modified for linking bioconjugators [2]. In the present work, CdSe/CdS and CdSe/SiO_2 core-shell nanoparticles were prepared with TEOS. Then, the optical properties of those nanoparticles were investigated utilizing UV-VIS, and photoluminescence and the structure of core-shell nanoparticles was observed by TEM. Finally, the optimum synthetic conditions were determined to obtain the higer PL yields and photochemical stability of the nanoparticles.

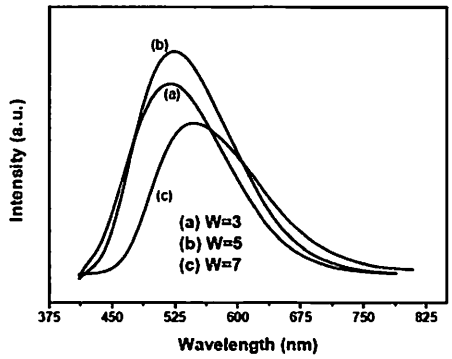

Fig. 1. Fluorescence spectra of CdSe NPs in AOT reverse micellar solutions as a function of W with Cd/Se = 2/1: (a) W=3, (b) W=5, (c) W=7.

References

[1] V. L. Colvin, M. C. Schlamp, A. P. Alivisatos, *Nature* **370**, 354 (1994).

[2] M. Darbandi, R. Thomann, T. Nann, *Chem. Mater.* **17**, 5720 (2005).

3PF24

A simple synthesis of chitosan-silica film using sodium silicate solution

F. Widhi Mahatmanti[1,2], Narsito[3], and Nuryono[3]

[1] *Department of Chemistry, Faculty of Mathematics and Natural Sciences, State University of Semarang, Jl. Raya Sekaran, Gunungpati, Semarang, Indonesia 50229*
[2] *PhD Student at Department of Chemistry, Faculty of Mathematics and Natural Sciences, Universitas Gadjah Mada, Sekip Utara, Yogyakarta, Indonesia 55281*
[3] *Department of Chemistry, Faculty of Mathematics and Natural Sciences, Universitas Gadjah Mada, Sekip Utara, Yogyakarta, Indonesia 55281*
E-mail: nuryono_mipa@ugm.ac.id

Recently, development of film materials is focused on finding the films with high chemical and physical stability. Organic based material such as chitosan produces films with low mechanical stability, and hence addition of inorganic matrices is necessary. In this research, the effect of silica addition on the properties of chitosan based films has been investigated. Precursors used to produce films included chitosan with the deacetilation degree of 83 % and sodium silicate solution as the silica source. A simple synthesis in a one-pot process was carried out by mixing 1 %(wt) of chitosan solution in 2 %(v/v) acetate acid and sodium silicate solution (25 % SiO_2) in various composition ratios and casting the solution on a glass dish. Additionally, the effect of polyethylene glycol (PEG) on the properties of the film was also examined. Based on the measurement of the mechanical parameters showed that chitosan-silica-PEG film with the weight ratio of chitosan:silica:PEG 4:2:1 gives the highest values of tensile strength and elongation at break. Hydrophilicity of the film increased with the addition of PEG and decreased with increasing the pH. X-ray diffraction pattern, infrared spectra and thermal gravimetric analysis data revealed that the addition of silica and PEG in the chitosan film do not significantly change the crystalline degree, absorbance bands and the thermal stability, respectively, indicating the domination of physical interaction among active sites in the film components.

3PF25 Controlling morphologies of hexagonal prisms and hexagonal pyramids ZnO microstructures by microwave radiation method

A. Phuruangrat

Department of Materials Science and Technology, Faculty of Science,

Prince of Songkla University, Hat Yai, Songkhla 90112, Thailand

E-mail : phuruangrat@hotmail.com

Flower-like ZnO nanostructures with composed of hexagonal prisms and hexagonal pyramids were successfully synthesized by a microwave radiation method. The precursor solutions were prepared using zinc nitrate hexahydrate and hexamethylenetetramine at pH 7 and 13 by 3 M NaOH solution. XRD, SEM and TEM analysis reveal that the as-synthesized samples are pure wurtzite hexagonal ZnO structure which show a hexagonal prisms flower-like shape for pH9 and hexagonal pyramids flower-like shape for pH 13. Raman spectra detect a sharp and strong optical phonon Raman-active E_2 and E_1L modes at 438 and 585 cm^{-1} which are characteristic wurtzite hexagonal ZnO phase. UV-Visible spectra show excitonic character with the absorption peak at 397 nm and 384 nm for flower-like ZnO nanostructures with composed of hexagonal prisms and hexagonal pyramids. Photocatalytic efficiency of RhB with hexagonal prisms flower-like and hexagonal pyramids flower-like ZnO samples are 77 % and 87% after Hg lamp irradiation for 120 min.

References

[1] R. Yi, N. Zhang, H. Zhou, R. Shi, G. Qiu, X. Liu, *Mater. Sci. Eng. B* **153**, 25 (21008).

[2] S.J. Kim, H.H. Kim, J.B. Kwon, J.G. Lee, B.H. O, S.G. Lee, E.H. Lee, S.G. Park, *Microelectron. Eng.* **87**, 1534 (2010).

3PF16 Hydrothermal synthesis of Bi_2MoO_6 nanoplates with their optical and photocatalytic properties

A. Phuruangrat

Department of Materials Science and Technology, Faculty of Science,

Prince of Songkla University, Hat Yai, Songkhla 90112, Thailand

E-mail : phuruangrat@hotmail.com

This research was studied the effect of pH on phase, morphologies and photocatalytic properties. Bi_2MoO_6 nanoplates were synthesized by a hydrothermal method at 180 °C for 24 h at pH 2-12. XRD pattern found that products are pure phase orthorhombic Bi_2MoO_6 structure at pH 4 and pH 6. Increasing pH higher than 6, the cubic Bi_4MoO_6 phase was obtained. SEM and TEM reveal the morphologies of Bi_2MoO_6 are a nanoplates. The molecular vibration of Bi_2MoO_6 was investigated by Fourier transform infrared spectroscopy and Raman spectroscopy which detected the symmetric stretching, asymmetric stretching, stretching vibration and bending mode of BiO_6 and MoO_6 octahedra. Photocatalytic activity of Bi_2MoO_6 nanoplates was determined from the degradation of rhodamine-B by Xe light at 98 % for 180 min irradiation.

References

[1] Z. Zhang, W. Wang, M. Shang, W. Yin, *J. Hazard. Mater.* **177**, 1013 (2010).

[2] C. Belver, C. Adán, M.F. Garća, *Catal. Today* **143**, 274 (2009).

3PF27 EFFECT OF DIFFERENT PARAMETERS ON THE DISPERSION STABILITY OF SILICA

Q.A. Bhatti[1], M.K. Baloch[1], S. Schwarz[2], G. Petzold[2]

[1]*Department of chemistry Gomal University Dera Ismail Khan, Pakistan,*
[2]*Leibniz-Institut für Polymerforschung Dresden e.V., Germany*

Abstract

Silica dispersion has a number of applications in our daily life and needs detail investigation to establish the effect of various parameters over the size, size distribution and its stability. Therefore, the silica was dispersed and the size and size distribution and surface charge have been investigated as a function of ultrasonication time, added polymer (Polyvinylpyrrolidone) concentration and molecular mass. It has been concluded that though the size distribution remains almost unaffected by the ultrasonication time but the surface charge was increased with the increase in ultrasonication time up to 20 minutes and then it leveled off. Further the polymers added were adsorbed over the surface of the particles and increased the surface charge (Zeta potential) and the increase proportional to the molecular mass of the polymer. Due to the reason the added polymers introduced the steric as well as electrostatic stabilization and the dispersions became stable. However, if the particles were not properly dispersed before the addition of polymer then the available agglomerates did not break by ultrasonication and hence the distribution of the particles size was widened.

Keywords: Silica dispersion; Zeta potential; Poly (vinylpyrrolidone); pH; ultrasonication; stability of dispersion.

References

[1] G.Petzold, S.Schwarz Interactions between Polyelectrolytes and Inorganic particles. In: Encyclopedia of Surface and Colloid Science, 2nd edn. Taylor & Francis, New York (2006)

[2] Bhatti QA, Schwarz S, Petzold G European Coatings journal. 08:33-37 (2010)

[3] I.F.Kuz'kina, I.I .Ivankova, V.P .Zubov, T .Schauer, M .Entenmann, C.D .Elsenbach European coatings journal .12:18-23. (2000) .

[4] V.P .Zubov, N.A .Serebryakova, I.A .Arutyunov, Bulychev , I.F.Kuz'kina, Y.A .Khrustalev Kolloidin Zh. 3 .66:346 (2004).

[5] D .Lerche J. Disp. Sci. and Technol. 23:699 (2002).

3PH01 Electrowetting of aqueous electrolytes: Simulation study in an open statistical ensemble, confined geometry, and electric field

F. Moučka[1]

[1]*Faculty of Science , J. E. Purkinje University, Usti nad Labem, Czech Republic*
e-mail : filip.moucka@ujep.cz

Phenomena observed at liquid-solid interfaces in the presence of an external electric field have been studied at molecular level. Of particular interest were density and concentration profiles, pressure tensor components, and wetting free energy. For this purpose, a novel efficient method for computer simulations in an open statistical ensemble, that allows studying aqueous solutions of electrolytes at these conditions, have been developed. The method simulates confined solutions at prescribed chemical potential values of its individual species. The particles are inserted/deleted to/from the nanopore through a sequence of intermediate states containing fractional particles that are partially coupled to the solution.

The method have been applied to aqueous solutions of NaCl confined in nanopores of various widths and considered to be in equilibrium with infinite bulk reservoirs of various concentrations and ambient pressure and temperature. Dependence of several properties on the external electric field was examined [1]. Both simplified model, considering plain pore walls, and complex model of structured walls have been considered. Values of the electrolyte chemical potential and of water chemical potential corresponding to various bulk reservoir concentrations at ambient conditions were calculated [2] by a recently developed Osmotic Ensemble Monte Carlo method [3].

References

[1] F. Moučka, D. Bratko, A. Luzar *To be published* (2013).

[2] F. Moučka, I. Nezbeda, W. R. Smith *Submitted to Mol. Simul.* (2013).

[3] F. Moučka, M. Lísal, J. Škvor, J. Jirsák, I. Nezbeda, W. R. Smith *J. Phys. Chem B* **115**, 7849(2011).

3PI13 Solvation structures of FAMSO + water, + methanol

M. Takahashi[1], T. Sato[1], T. Kamiyama[1], M. Fujisawa[1], A. Wakisaka[2], and T. Kimura[1]*

[1] *Department of Chemistry, Kinki University, 3-4-1 Kowakae, Higashi-Osaka 577-8502, Japan*

[2] *National Institute of Advanced Industrial Science and Technology, Onogawa 16-1, Tsukuba, 305-8569 Japan*

*e-mail : kimura @chem.kindai.ac.jp

FAMSO (**F**ormaldehyde dimethyl**m**ercaptal-**S**-**o**xide) has not only polar sulfoxide and thioether groups but also non-polar methyl and methylene groups. It may be used as a universal solvent from the viewpoint of its molecular structure. In this work, vapor pressures of FAMSO + water, +MeOH at 298.15 K were measured. The excess Gibbs energies and excess entropies of these systems were determined with previously reported values of excess enthalpies of mixing [1, 2]. In order to clarify the solution structures in these systems, the mass spectrometic analyses of clusters isolated from liquid droplets [3] were carried out for the solutions.

The vapor pressures of FAMSO + water, + MeOH were determined by using isoteniscope method at (298.15 ± 0.001) K over the whole range of mole fractions with an accuracy of ±1 Pa and shown in Fig. 1. The concentrations of the solutions were determined by a refractometer and vibrating-density meter. A straight line in Fig. 1 shows vapor pressures of the ideal solution of Raoult's law. The mixtures of FAMSO + water were unstable than the ideal solution and those of FAMSO + MeOH were unstable than the ideal solution at low concentration of FAMSO. The excess thermodynamic properties of excess Gibbs energies and excess entropies were determined with excess enthalpies of mixing [1, 2]. Excess entropies of FAMSO + water were unstabilized but those of FAMSO + MeOH were stabilized. Excess partial molar thermodynamic quantities were determined. Excess partial molar enthalpies of water and MeOH showed inflection points. In order to clarify the unique behavior, mass spectrometric analyses were carried out. In the system of FAMSO + water, clusters of water, FAMSO and FAMSO + water were observed before inflection. But after inflection, only FAMSO clusters were observed. The cluster structures were changed considerably before and after inflection. The system of FAMSO + MeOH also showed similar to that of FAMSO + water. These results will be discussed with results of MO calculations by Gaussian 09. And the role of interaction energies of electrostatic exchange, charge transfer and dispersion force will be discussed.

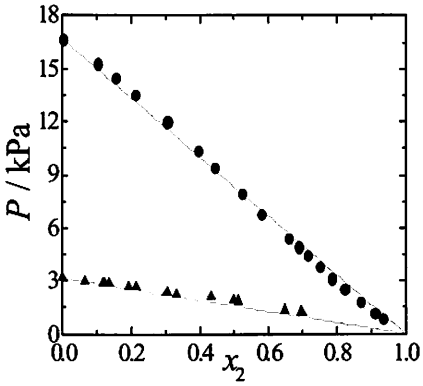

Fig. 1 Vapor pressures of solvent (1) + FAMSO (2) at 298.15 K : ▲, water; ●, MeOH

References

[1] T. Kimura and S. Takagi, *Netsu Sokutei*, **13**, 2 (1986).

[2] T. Kimura, T. Morikuni, T. Chanoki, and S. Takagi, *Netsu Sokutei*, **17**, 67 (1990).

[3] A. Wakisaka and T. Ohki, *Faraday Discuss.* **129**, 231 (2005).

3PI14 Interpretation of Singular Behaviour of Excess Enthalpies near Critical Points for Mixture of Carbon Dioxide and Ethane

K. Tsukamoto, G. Fang, M. Maebayashi and M. Ohba

Faculty of Agriculture, Meijo University, Nagoya 468-8502, Japan

e-mail : n0961501@ccalumni.meijo-u.ac.jp

Excess enthalpy of binary fluid mixtures behaves singularly with the changes in temperature, pressure and composition near critical points. In order to interpret the singular behaviour, we have calculated the excess enthalpies for two models in which molecules interact through the 12-6 LJ potential by using the PY equation. For one model, the critical pressures of the pure component fluids were the same. For the other model, the critical temperatures of the pure component fluids were the same. The excess enthalpies near the critical points for the former model agreed qualitatively with those for (C_2H_6 + C_2H_4) [1] which has almost the same critical pressures, however, the excess enthalpies for the latter model disagreed apparently with those for (CO_2 + C_2H_6) [2] which has almost the same critical temperatures. The critical locus on the *p-T* plane for the latter model differed in shape from that for (CO_2 + C_2H_6), whereas the critical locus for the former model and that for (C_2H_6 + C_2H_4) were almost the same shapes. When the shape of the critical locus for the latter model was fitted to that for (CO_2 + C_2H_6) by adjusting the calculation temperatures, the excess enthalpies near the critical points for the latter model agreed qualitatively with those for (CO_2 + C_2H_6).

From the result of analysis by focusing on the position on the *p-T* plane, it was clear that the singular behaviour relates to the positional relation between the critical locus and the thermodynamic states where the excess enthalpies is obtained. The singular behaviour was interpreted as the mixing of between a gas-like fluid and a liquid-like fluid. We named this behaviour observed remarkably between two extended vapour-liquid coexistence curves of the pure component fluids as "Phase Transition-like Phenomenon: PTLP". Figure 1 shows the states on the *p-T* plane where the PTLP was observed remarkably for (CO_2 + C_2H_6) [2,3]. The critical locus is leftward-convexed, thus the states in which the phase separation and the PTLP was observed concurrently exists.

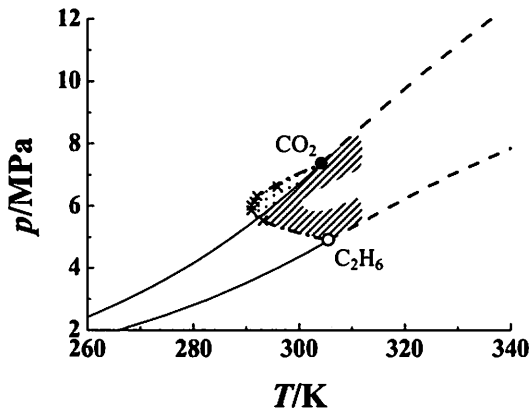

Figure 1. The thermodynamic states on the *p-T* plane where the PTLP is observed remarkably for (CO_2 + C_2H_6) [2,3]. The shaded and dotted regions indicate the states where the PTLP is observed and the phase separation and the PTLP are concurrently observed, respectively.

References

[1] M. S. Gruszkiewicz, J. T. Sipowska, J. B. Ott, P. R. Brown, J. D. Moore, *J. Chem. Thermodyn.*, **27**, 507(1995).

[2] C. J. Wormald, J. M. Eyears, *J. Chem. Thermodyn.*, **20**, 323(1988).

[3] C. J. Wormald, R. W. Hodgetts, *J. Chem. Thermodyn.*, **29**, 75(1997).

3PI15 Isopiestic Determination of Osmotic Coefficient of Some Heavy Metal Sulfates at 323.15 K

H. Yang, and D. Zeng

[1]*College of Chemistry and Chemical Engineering, Central South University, Changsha 410083, China*

e-mail : hai.tang.ouyang@hotmial.com

In hydrometallurgical processes, the solubility phase diagram of heavy metals aqueous solution systems like $CaSO_4$+H_2SO_4+MSO_4+H_2O (M=Zn, Cu, Mn, Ni, Co) are extremely complex while very important for improving production quality and production process. In order to use thermodynamic models to describe and predict the muti-temperature diagram of these systems, the accurate thermodynamic experimental data especially osmotic coefficient for systems MSO_4 (M = Zn, Cu, Mn, Ni, Co)+H_2O at higher temperature than 25 ℃ is quite necessary[1].

At room temperature, the isopiestic experimental set-up and procedure is quite simple and most of the osmotic coefficient data for MSO_4 (M=Zn, Cu, Mn, Ni, Co)+H_2O systems therefore have been determined by this method at 25 ℃[2-5]. However, only a few apparatus have been attempted to apply at 50 ℃. In this paper, based on the isopiestic container of Voigt [6], a complete set of apparatus (Fig. 1) for isopiestic measurements at enhanced temperature is described. Measurements were made in some heavy metal sulfates systems MSO_4 (M=Zn, Cu, Mn, Ni, Co)+H_2O at T=323.15 ±0.01 K, at molarities in the range from 0.1 mol.kg^{-1} to saturation. Both of H_2SO_4+H_2O and $CaCl_2$ +H_2O systems have been chosen as reference system. The reproducibility of the results is better than 0.08 %. The results show the osmotic coefficient of all MSO_4 (M = Zn, Cu, Mn, Ni, Co)+H_2O heavy metal sulfates systems increase with the molarity increase, and furthermore, the increased trend are exactly similar.

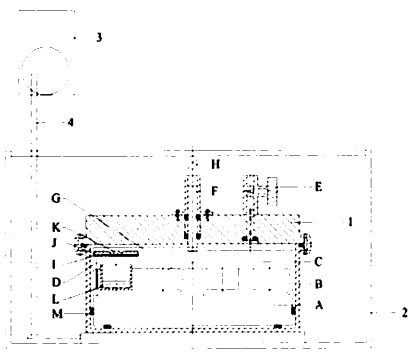

Fig.1 Profile map of the apparatus for isopiestic measurements. 1: Isopiestic container, 2: Bath wall, 3: Electrical machinery, 4: Rocking axis; A: Aluminum block, B: Aluminum container, C: Holes for sample cups, D: Piece of wire, E: Needle valve, F: Steel bolt, G: Stainless steel plate, H: Screw, I: Silicone gasket, J: Lid, K: Spring, L: Sample cup, M: PTFE shim.

References

[1] D. Zeng, W. Wang, *Pure Appl. Chem.*, **83(5)**, 1045(2011).

[2] R. Robinson, R. Jones, S. Ronald, *J. Am. Chem. Soc.*, **58**, 959(1936).

[3] L. Wlodzimierz, S. Teresa, L. Zofia, *J. Sol. Chem.*, **9(5)**, 341(1980).

[4] M. Jelena, T. Milica, N. Rozalija, *J. Chem. Therm.*, **34(11)**, 1769(2002).

[5] R. Joseph A, *J. Chem. & Eng. Data.*, **29(4)**, 443(1984).

[6] K. Grjotheim, W. Voigt, B. Haugsdal, D. Dittrich, *Acta Chem. Scandi.*, **A 42**, 470(1988).

3PI16

Formation of supramolecular structures in aqueous solution of Tetrahydrofuran

S.Z.Mirzaev, K.B.Egamberdiev, M.R.Zaitdinov
Institute of Ion-plasma and laser technologies, Uzbek Academy of Sciences, Do'rmon yo'li str. 33, 100125 Tashkent, Uzbekistan
e-mail : kegamberdiev@yandex.ru

Study unusual properties of aqueous solutions are the most important for the liquid condensed matter. There are can be expected many structures like clathrate-like structures, self-associated water molecules forming cages with small voids and supramolecular structures. These molecular structures have significant interests for the nanotechnology and renewable energy.

Tetrathydrofuran (THF) is one of the structure-making solute and has dipole-dipole interactions. In the aqueous solution have appeared guest-host interactions. Therefore we are decided to investigate aqueous solution of THF. By using pulse method [1] we have measured ultrasonic attenuation and ultrasonic velocity in the aqueous solution of THF at all range of concentrations and various temperatures.

For each concentration measurements were made between 10 and 150 MHz. Ultrasonic velocity sharply increases up to 0,18 mol fraction (m.f.) of THF. After that it decreased with increase the THF concentration. But maximum values of velocity shift to the low concentration with increase the temperature. The ultrasonic attenuation reached maximum value between 0,16 and 0,18 m.f. of THF. At the higher concentration of THF in solution supramolecular structures break down and passed to another state.

Past studies of this solution have implicated the importance of pseudoclathrate structures [2] and fluctuations [3] in determining the properties of this solution. In the work [4] aqueous solution of THF studied by dynamic light scattering. C.M. Sorensen caught liquid-liquid phase separation at 0,22 m.f. of THF and 71,85°C. Location of phase separation point is near to maximum point of both velocity and attenuation versus concentration and it is affected to supramolecular structure.

To consider previously results we are suggested formation of supramolecular structures in aqueous solution of THF by form of $THF+nH_2O \rightarrow THF{\cdot}nH_2O$, $n=4\div6$, where n is number of water molecules.

References

[1] U. Kaatze, V. Kuhnel, K. Menzel, S. Scherdtfeger, *Meas. Sce. Technol.* 1257(1993).
[2] S.R. Gough, *J. Solution Chem.* **8**, 371(1979).
[3] G. Atkinson, S. Rajagopalan, B.L. Atkinson, *J .Phys. Chem.*, **85**, 733(1981).
[4] C.M. Sorensen, *J. Phys. Chem.* **92**, 2367(1988).

3PI17 Application of Prigogine-Flory-Patterson theory to excess molar volumes of mixtures of {methyl tert butyl ether (MTBE) + alcohols} mixtures at different temperatures and atmospheric pressure

Heloisa E. Hoga[1], Ricardo B. Tôrres[2], Pedro L.O. Volpe[1]

[1]*Departamento de Físico-Química, Universidade Estadual de Campinas, Cidade Universitária Zeferino Vaz, 13083-970, Campinas, São Paulo, Brazil.*

[2]*Departamento de Engenharia Química, Centro Universitário da FEI, Av. Humberto de Alencar Castelo Branco, 3972, 09850-901, São Bernardo do Campo, São Paulo,Brazil.*

e-mail: helhoga@iqm.unicamp.br

In the present study, data of excess molar volumes of binary mixtures of methyl tert butyl ether (MTBE) + methanol, or + ethanol, or + 1-propanol, or + 2-propanol, or + 1-butanol, or + 1-pentanol, or + 1-hexanol have been used to test the applicability of the Prigogine-Flory-Patterson theory (PFP) as a function of composition at different temperatures and atmospheric pressure. This theory has been used to analyze excess thermodynamics properties of different kinds of mixtures, including polar components. According to the PFP theory, excess molar volumes calculations include three contributions: (i) interactional contribution which is proportional to the Flory parameter; (ii) the free volume contribution which arises from the dependence of the reduced volume upon the reduced temperature as a result of the difference between the degree of expansion of the two components, and (iii) the P* contribution which depends both on the differences of internal pressure and differences of reduced volumes of the components. It may be observed that the PFP theory reproduces the main features of the experimental data by using only one fitted parameter adjusted. The results of each contribution are discussed.

3PI18 Formation of Weak Hydrogen Bonds C–H•••O_{water} is Responsible for Hydrophobic Hydration: IR and Simulation Studies on [Water+Dimethyl Sulfoxide]

K. Mizuno[1], T. Moroyose[1], Y. Tamai[2], and T. Sumikama[3]

[1] *Depart. of Appl. Chem. and Biotech., Grad.School of Engi., Univ. of Fukui, Fukui, 910-8507 Japan.* [2] *Depart. of Appl. Physics, Grad. School of Engi., Univ. of Fukui, 910-8507 Japan.* [3] *Faculty of Medical Sciences, Univ. of Fukui, 23-3, Matsuoka-shimoaizuki, eiheiji-cho, Yoshida-gun, Fukui, 910-1193 Japan*

e-mail : kmizuno@u-fukui.ac.jp

Abstract: We carried out FT-IR measurements of O–H stretching and H–O–H bending vibration bands of the water in [water + dimethyl sulfoxide(DMSO)] followed by MD and QM simulations, to identify roles of the O–H groups and the oxygen(O_w) in water in the hydration. We observed blueshiftings of both ν(O–H) over the whole concentration range and of ν(H–O–H) up to $X_{dmso}\approx$ 0.35. We also observed blueshiftings of the ν(C–H) bands of methyl groups with increasing water content, which showed the formation of C–H•••OH_2. From all these experimental results, we can attribute the hindered rotational and translational motions of the strange water to formation of weak H-bonds C–H•••O_w between the methyl groups and water. MD and QM calculations carried for a mixture at X_{dmso}=0.33 has provided us with the blueshifts of ν(O–H) and ν(H–O–H), and the formation of the C–H•••OH_2, in agreement with the experimental results.

Introduction: Thermodynamic anomalies such as negative excess enthalpy and excess entropy have been observed on dissolving an organic solute into water, but underlying reasons remain unexplained. Since the anomalies were related with a structure resembling solid clathrate hydrates around hydrophobes, O–H groups in water have been used as probes and an increase of their hydrogen bonding strength has been noted to investigate hydrophobic hydration even up to recent years. We, however, observed a decrease of the H-bonding strength of the O–H groups in [water + DMSO] by measuring NMR spectra[1]. We also observed continuous decrease of the H-bond donating strength of the O–H groups with increasing tetrahydrofuran in aqueous binary mixtures[2]. All these results were against the above picture of the structure formation, and suggested participation of weak hydrogen bonds[3], C–H•••OH_2, in hydration. In the present work we revisited [water + DMSO] to identify roles of O–H groups and O_w in water and weak H-bonds, C–H•••O_w, in hydrophobic hydration of DMSO.

Experiments: IR spectral changes of O–H stretching vibration band was examined by observing O–D stretching vibration band of HDO used as a probe molecule of water[2]. The changes of the H–O–H bending vibration bands were examined by observing the H–O–H bands of the mixture [H_2O + D_2O] of 2:3 volume ratio instead of water. Changes of the C–H stretching vibration bands of DMSO with concentration were observed for [D_2O + DMSO]. Classical MD simulations were carried out to simulate bulk water and the mixture at X_{dmso}=0.33. Then from the MD data sets, we obtained [W_{36}] and [W_{24}+$DMSO_{12}$] assemblies, as input files of the molecular configurations for subsequent QM structure optimizations, where W indicates a water molecule. Four data sets of the assemblies were used, respectively, for the optimization with DFT method at a level of B3LYP/6-31G(d,p). After the vibration analyses, we selected all the W's in the second and more inner molecular layers from the surface of each assembly. Totally, 32 and 31 W's were selected as the water molecules in pure water and in the mixture, respectively.

References

[1] K. Mizuno *et al.*, *J. Phys. Chem. B* **104,** 11001 (2000).

[2] K. Mizuno *et al.*, *J. Phys. Chem. B* **113,** 906 (2009).

[3] E. Arunan *et al.*, *Pure Appl. Chem.* **83,** 1619(2011).

3PI19 Enthalpic descrimination of chiral fenchones in cyclic compounds

H. Togashi, T. Kamiyama, M. Fujisawa, T. Kimura*

Department of Chemistry, Kinki University, 3-4-1 Kowakae, Higashi-Osaka, 577-8502 Japan

*e-mail : kimura@chem.kindai.ac.jp

Enantiomers are very unique molecules. While difference of hetero-chiral compounds was discussed qualitatively, were not defined quantitatively. In order to clarify the molecular interactions between enantiomers of dicarboxylic acids, camphor and its derivatives in ethanol solution were determined in dilute concentration[1-3]. In order to clarify the effect of solvation, excess enthalpies H^E of non-polar chiral limonenes and nonpolar solvents of hexane, cyclohexane, benzene, carbon tetrachloride and ethanol were determined over the whole range of concentrations at 298.15 K. The experimental results for H^E of *R*- and *S*-enantiomer in solutions showed very unique behavior.[3] In order to clarify the unique behavior, a polar chiral compound of fenchones and with polar solvents of ethanol was determined over the whole range of concentrations at 298.15 K.

H^E of fenchones solutions showed exothermic behavior over the whole range of mole fractions in benzene and cyclohexane solutions. And enthalpic stabilization was increased with decreasing the concentration of fenchones. The concentration dependences of fenchone systems were similar as that of limonene. H^E of binary mixtures of benzene, cyclohexane were not small endothermic and unstabilized on mixing. Chiral oriented solvents in the solutions might be different interaction and change the solvation state to make less stable solution. To estimate molecular properties chiral compounds, molecular interactions in solvents were carried out by using *ab initio* quantum chemical methods based on the Gaussian programs 09 at the mp2/6-311++G** level of theory.

The experimental results of excess enthalpies and interaction energies by supermoleclar method will be compared and discussed.

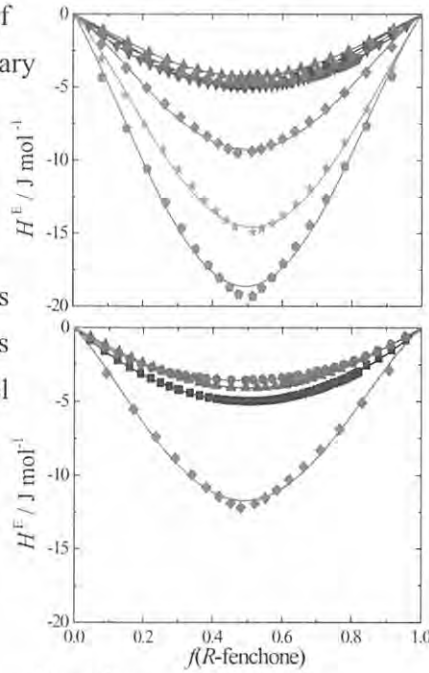

Fig. 1 Excess enthalpies for {(1-*f*)*S*+*fR*}- fenchone in benzene and cyclohexane solution at different molar fractions: ■, pure; ●, 0.7; ▲, 0.5; ▼, 0.3; ◆, 0.1;★, 0.05; ⬟, 0.03

References

[1] T. Kimura, T.Ozaki, S.Takagi, *Chirality* **10,**722(1998).

[2] T.Kimura, M. A. Khan, T. Kamiyama, *J .Thermal. Anal. & Calori.* **85,** 559 (2006). *idem ibit,* **85,** 575 (2006).

[3] T. Kimura, S. Kido, T. Kamiyama, M. Fujisawa, *Chirality*, **23,** 98 (2011).

[4] H. Liu, S. Kido, T. Kamiyama, M. Fujisawa, T. Kimura, *J Chem Thermodyn* **40,**627 (2011).

3PI20 Enthalpy of Mixing of Binary Mixtures of Water + *n*-Alkanol at High Temperature and High Pressure

Y. Sugawara[1], H. Ogawa[1], Y. Kataoka[1] and F. Kimura[1]

[1]School of Science and Engineering, Tokyo Denki University, JAPAN

E-mail: 13hz003@ms.dendai.ac.jp

To discuss behaviour of component molecule and intermolecular in the mixtures of water + *n*-alkanol (number of carbon atom n = 1 to 4) at high temperature and high pressure, enthalpy of mixing $\Delta_{mix}H_m$ has been measured at temperature of 348, 373, 398 and 423K and at pressure of 5, 10, 15 and 20 MPa, using home-made twin conduction type of flow calorimeter. Results of water + ethanol agreed with reliable reference values [1],[2].

The results of $\Delta_{mix}H_m$ obtained for equimolar mixture increased as increase of chain length of the *n*-alkanol at 373 K, as shown in Fig. 1, which will be attributed to weakening of hydrogen bond between water by introducing alkyl group. However, negative values were observed for water rich region of + methanol, + ethanol and + 1-propanol mixtures at lower temperature, which suggest strengthening of hydrogen bonding at the vicinity of small alcohol molecule. Parabolic curve were obtained for the results of water + 1-butanol as plotted in Fig. 2, which means mixture is miscible at measurement high temperature. Negative pressure dependence was observed at higher temperature and value of $\Delta_{mix}H_m$ increased as increase of temperature. Such phenomena will be explained by rather active thermal motion and longer distance between molecules at higher temperature and lower pressure.

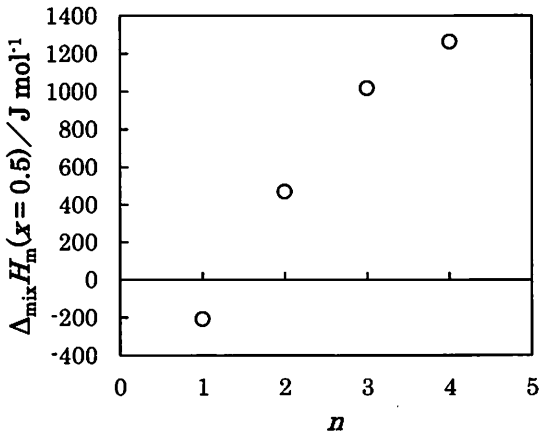

Fig. 1 Plots of enthalpy of mixing (x= 0.5) of binary mixtures of water + *n*-alkanols against number of carbon atom n contained in alkanol. T= 373 K, P= 5 MPa.

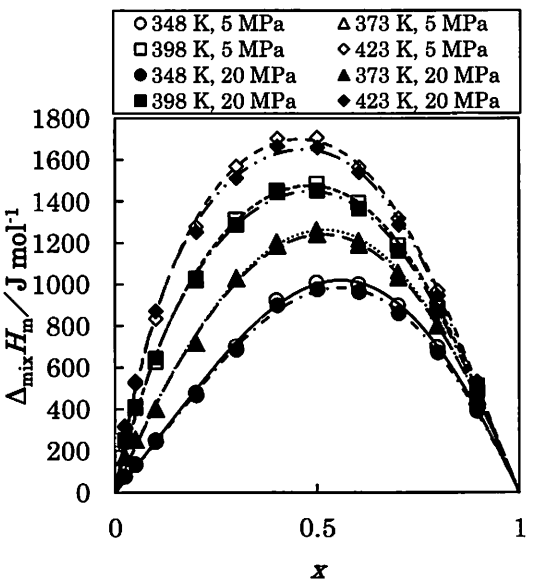

Fig. 2 Enthalpy of mixing of binary mixtures of water + 1-butanol at 348, 373, 398 and 423 K and 5, 20 MPa.

References

[1] J. B. OTT, C. E. STOUFFER, *et al*, *J. Chem. Thermodynamics*, **19** (1987) 337-348

[2] C. Mathonat, V. Hynek, V. Majer, and J-P.E Grolier, *J. Sol. Chem*, **23** (1994) 1161-1182

3PI21 Energy Aspects for Beta-Lactum Antibiotic + Cyclodextrin Inclusion Complexes in Aqueous Solutions

M. Fujisawa[1], S. Tsujikawa[2] T. Yasukuni[1], H. Ikeda[3], and T. Kimura[2]
e-mail : 1233310102d@kindai.ac.jp

[1] *Department of Biotechnological Science, Kinki University, Wakayama 649-6493, Japan*
[2] *Department of Chemistry, Kinki University, Osaka 577-8501, Japan*
[3] *Department of Pharmaceutical Science, Fukuoka University, Fukuoka 814-0180, Japan*

In our previous work, for the cyclodextrin(CD) system of a pharmaceutical drug, theoretical calculations of molecular interactions of the complex (β-CD + chlorambucil) were carried out using the molecular orbital method[1]. The correlation between energy changes and molecular structures were examined. The large interaction energies calculated by the molecular orbital method showed the inclusion phenomenon. However, the major contributions to the interaction energy were not discussed in detail. In addition, the direction from which ampicillin enters the CD cavity could not be clearly concluded using the semiempirical molecular orbital method and the NMR spectrum [2].

In this study, we were interested in clearly detailing the major contribution to the interaction energy of CDs and guest molecules. The interaction energies for the inclusion complex of the β-lactam antibiotic ampicillin and the nonsteroidal anti-inflammatory drug ibuprofen with β-CD in aqueous solutions were analyzed by molecular mechanics/Poisson–Boltzmann surface area (MM/PBSA) analysis and pair interaction energy decomposition analysis (PIEDA). Predictions regarding the direction of inclusion of drugs into the cavity of β-CD were made on the basis of the computational results.

We predict that a phenyl ring of ampicillin exists outside of the secondary hydroxyl side of β-CD and that the lactam ring exists inside the β-CD cavity. It seems that the inclusion occurs to give the form in which the hydrophobic group of the drug is not exposed to water. These observations were borne out by the dispersion forces determined using PIEDA. Thus, the lactam ring of ampicillin was inside the β-CD cavity, which protected it from aggregation. This indicates that the inclusion complexes of ampicillin and β-CD would be useful as drug delivery systems. The structures of the complexes could be predicted using two different methods that contain no empirical parameters.

References

[1] M. Fujisawa, T. Kimura, *J. Therm. Anal. Calorim.* **85**, 589(2006).
[2] H. Aki, T. Niiya, Y. Iwase, Y. Kawasaki, K. Kumai, T.Kimura, *Thermochim Acta*, **416**, 87(2004).

3PI22 Thermodynamic properties of binary mixtures of limonene+ nine alcohols at 298.15 K

T. Kimura and Y. Kosuge

Department of Chemistry, Kinki University, Higashi-Osaka 577-8502, Japan
e-mail : kimura@chem.kindai.ac.jp

Limonene{1-methyl-4-(1-methylethenyl)-cyclohexene}, a monoterpene, made up of two isoprene units. Limonene has two optically active forms even the simplest cyclic olefin, and it has been shown to prevent cancer[1]. There have been studies on the thermodynamic properties of limonene as a liquid and in the gas phase. Excess enthalpies of mixing were determined by Atick *et al.* [2] and Kimura *et al.* [3] Excess enthalpies(HE) were negligible small but positive over the whole range of mole fractions. Intermolecular interaction between heterochiral limonenes were unfavorable than homochiral interactions. To clarify heterochiral interaction in solutions, HE of heterochiral solutions of benzene, cyclohexane, hexane, carbon tetrachloride and ethanol were reported[4]. HE of these systems were large and unique behaviors. In order to understand solvents-limonene interaction, HE of eleven aliphatic alcohols from methanol to pentanols were determined by Thermal Activity Monitor (Thermometric) at (298.15±0.001) K and showed in Fig. 1. All excess enthalpies measured were endothermic. HE of MeOH+ Limonene and BtOH+Limonene were showed the least and most unstable enthalpies, respectively. The size of aliphatic group did not show simple effect on excess enthalpies on mixing. Excess enthalpies of solvents + limonene were also estimated by regular solution theory, the group contribution theory of UNIFAC and dielectric continuum solvation models (COSMO-RS), and compared with experimental results.

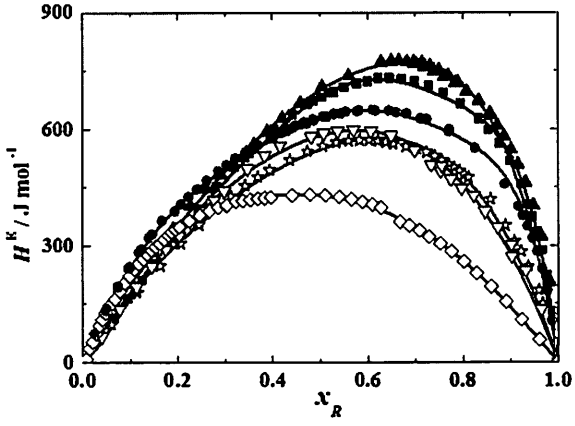

Fig. 1 Excess enthalpies of mixing of (1- x_R) alcohols + x_R *R*-limonene at 298.15 K: ◇, MeOH; ●, EtOH; ▽, PrOH; ▲, BtOH; ☆, PeOH; ■, HxOH.

All interaction energy between limonene and solvents were performed with Gaussian 09. The interactions of limonene + solvents were optimized with MP2/6-311G(d,p) in solvent by self-consistent reaction field (SCRF) calculation. And the role of interaction energies of electrostatic exchange, charge transfer and dispersion force will be discussed for limonene +alcohols.

References

[1] P.L. Crowell and M. N. Gould, *Critical Rev. Oncogen.***5**,1(1994).

[2] Z. Atik, M. B Ewing, M. L.McGlashan, *J. Chem. Thermodyn.*, **15**,159(1983).

[3] T. Kimura, T. Ozaki, S. Takagi, *Enantiomers*, **6**, 5(2001).

[4] T. Kimura, S. Kido, *J. Thermal. Anal. & Calori.*, **99**, 87(2010).

3PI23

Thermodynamics of solvation of nonpolar solutes

T. Urbic[1], T. Mohoric[1], and B. Hribar-Lee[1]

[1]*Faculty of Chemistry and Chemical Technology, University of Ljubljana, Askerceva c. 5, 1000, Ljubljana, Slovenia*

e-mail : tomaz.urbic@fkkt.uni-lj.si

Understanding the solute-solvent interactions in aqueous solutions is important for biology and chemistry. Theoretical models of various degree of sophistication have been developed to capture the anomalous properties of water and aqueous solutions. One simple model, the so called Mercedes-Benz (MB) has recently been reinvented in his 3D form [1]. MB molecules are three-dimensional Lennard-Jones spheres, with four hydrogen-bond arms (HB). Monte Carlo simulations have shown that MB model predicts qualitatively the density anomaly, the minimum in the isothermal compressibility as a function of temperature, as also the experimental trends for the thermodynamic properties of solvation of nonpolar solutes [1].

Here we apply the IET and TPT to the hydrophobic effect, the transfer of a nonpolar solute into 3D MB water. The Gibss free energy, enthalpy and entropy of transfer of nonpolar solute to a model water are calculated as a function of the size of the solute and temperature. As before, we find that the theories reproduce the Monte Carlo results quite accurately for liquid water at higher temperatures, they predict the qualitative trends in cold water, and they are computationally much more efficient for exploring the properties of water models such as this. An important conclusion of this work is that the Gibbs free energy of transfer is not very sensitive to the details of solvent modelling.

References

[1] A. Bizjak, T. Urbic, V. Vlachy, and K. A. Dill, *Acta Chim. Slov.* **54**, 532(2007).

3PI24 Liquid-solid equilibrium of butanol isomers + *i*-butylamine

Y. Kasai[1] and T. Kimura[2]

[1]*Hitachi High-Tech Science Corporation, Toyonaka, Osaka 560-0083, Japan*

[2]*Department of Chemistry, Kinki University, Higashi-Osaka, Osaka 577-8502, Japan*

e-mail: kasai-yuichi@hhs.hitachi-hitec.com

Mixtures of alcohol + amine showed a characteristic concentration-dependence of glass transition temperatures, viscosity and were extremely large exothermic reaction on mixing[1,2]. Hydrogen-bonding between amines and alcohols might be large effect on stability of solution. Also the steric effect and the influences of hydrophobic groups on hydrogen bonding are interesting in understanding of interaction of alcohols and amines. In order to clarify the steric effect on alcohols and amine, excess enthalpies of alcohols + amines were determined and discussed by thermodynamic properties of formation of alcohols-amine complexes, raman spectrometry, quantum chemical calculation and association model of solution theory.

However most of those have been reported in liquid state and there are a few results of the liquid-solid equilibrium. To clarify the steric effect on amine and alcohols, phase diagrams of butanols and butylamine have been determined. Butanols and butylamines have four isomers and excess enthalpies of butanols and butylamines showed unique results by means of those steric effects. In this study, mixtures of 1-butanol, 2-butanol + *i*-butylamine were determined to clarify the positional effect of the hydroxyl group of butanol.

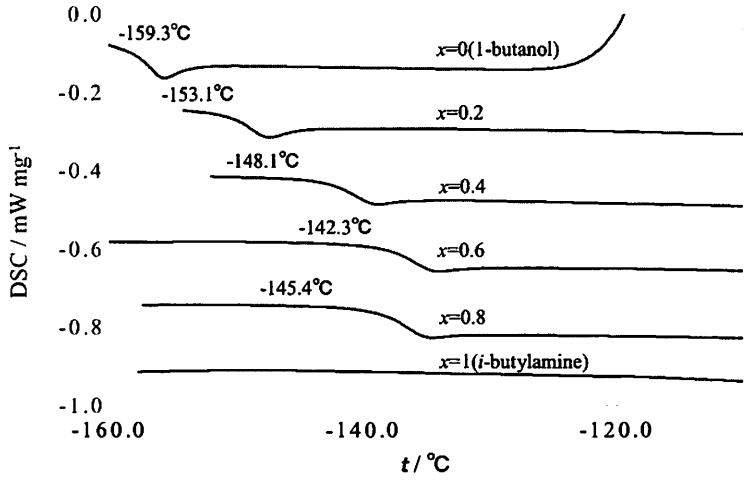

Fig.1 An example of thermoprofiles of *x i*-butylamine + (1-*x*)1-butanol

Thermoprofiles of the mixed of *xi*-butylamine + (1-*x*)1-butanol and *x i*-butylamine + (1-*x*) 2-butanol were determined by a differential scanning calorimeter (Hitachi High-Tech Science X-DSC7000), and made the phase diagrams from an analysis of phase transition temperature(glass transition, melting temperature and etc.).

The glass transition temperatures of mixtures were increased with increasing the concentration of *i*-butylamine. Phase behaviours and excess thermodynamic properties will be discussed.

References

[1] T. Kimura, T. Ozaki, S. Takeda, Y. Nakai, S. Takagi, *J. Thermal Anal.*, **54**, 285 (1998).

[2] T. Kimura, T. Kitai, T. Kamiyama, M. Fujisawa, *Thermochimica Acta.*, **450**, 91 (2006).

3PI25 Experimental Determination and Modelling of Solubility Phase Diagram of the Quaternary System $MgCl_2$+LiCl+NH_4Cl+H_2O and its Application

H. Yang, and D. Zeng

[1]*College of Chemistry and Chemical Engineering, Central South University, Changsha 410083, China*

e-mail : hai.tang.ouyang@hotmial.com

In this work, we determined the solubility data as well as the corresponding solid phases of the system $MgCl_2$+LiCl+NH_4Cl+H_2O at 298.15 K by equilibrium isothermal method (Fig.1a). The thermodynamic model of Pitzer–Simoson–Clegg (PSC) [1] was used to predict the complete phase diagram at 298.15 K, whose parameters were obtained by simulating the experimental solubility and water activity of binary systems LiCl+H_2O, NH_4Cl+H_2O, $MgCl_2$+H_2O and ternary systems NH_4Cl+LiCl+H_2O, $MgCl_2$+LiCl+H_2O, $MgCl_2$+NH_4Cl+H_2O. Four crystallization fields including two double salt phases, one crystalline hydrate phase and one solid–solution phase were found in this system. The calculated results (Fig.1b) are in good agree with the experimental results, while the solid solution crystallization fields was calculated with assuming solid phase as ideal solution. The experimental and predicted phase diagram proved to be trustworthy and reliable for the industrial process design of separating $MgCl_2$ from Li(Mg)+containing natural brine as adding NH_3 to precipitate $MgCl_2$.

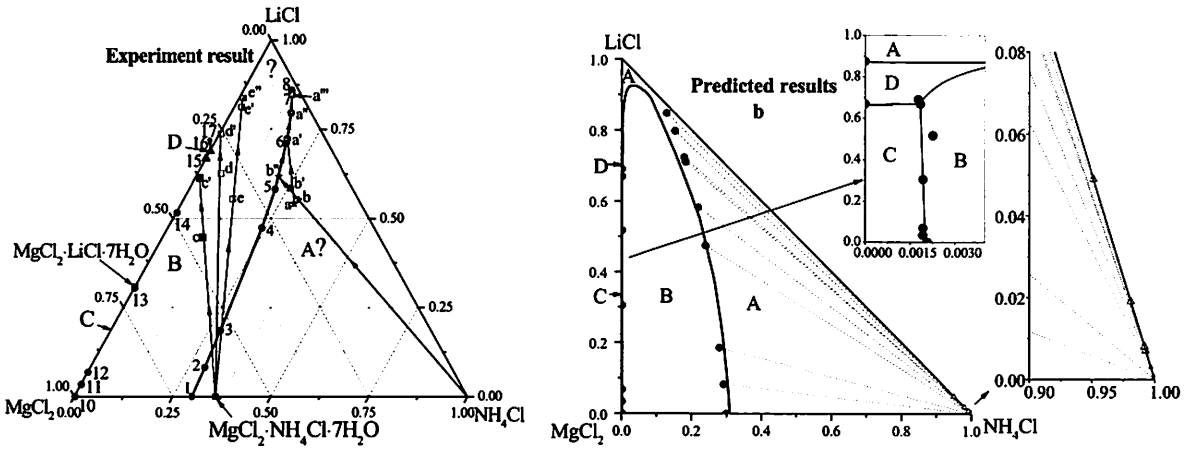

Fig. 1a and 1b. Isothermal solubility phase diagram as a function of dry–solid of the quaternary system $MgCl_2$+LiCl+NH_4Cl+H_2O at 298.15 K; ●, experimental data located on two phases isotherm curve; ☆, ★, □, ■: experimental data located on one phase isotherm surface; ?: the isotherm curve not completely defined; Crystallization fields: A=solid–solution (LiCl·H_2O and NH_4Cl), B=NH_4Cl·$MgCl_2$·$6H_2O$, C=$MgCl_2$·$6H_2O$, D=LiCl·$MgCl_2$·$7H_2O$; —(1b): predicted results using PSC model; △: the mass fraction of NH_4Cl and LiCl·H_2O in solid-solution solid phase; Point o is the dissolved point of salt LiCl·$MgCl_2$·$7H_2O$.

References

[1] Clegg S. L., Ptizer K. S., Brimblecombe P. *J. Phys. Chem.*, **96**, 3513(1992).

3PJ19 A Novel Computational Scheme for Standard Hydrogen Electrode and Redox Potentials

T. Matsui[1,2], Y. Kitagawa[2], Y. Shigeta[3], and M. Okumura[2]

[1]*Advanced Institute for Computational Science, RIKEN, Kobe 650-0047, Japan*

[2]*Department of Chemistry, Graduate School of Science, Osaka University, Toyonaka 560-0043, Japan*

[3]*Department of Material Science, Graduate School of Engineering Science, Osaka University, Toyonaka 560-8531, Japan*

e-mail : toru.matsui@riken.jp

Redox potential is one of the most important properties of the molecules in the field of electrochemistry. Many studies in both experiment and computation focusing on the redox potential employ the standard hydrogen electrode (SHE) potential as a reference in the half-cell reaction. Though many experiments reported SHE potential different from the IUPAC recommending value (4.44 V), most of the computational studies employ the same value (4.44 V) like as a physical constant for its practical use. The use of this value is appropriate only when very accurate and high-cost calculation method, i.e. CCSD(T), is employed. This is because the treatment of the Gibbs energy of the proton in aqueous solution, which relates to the pK_a value of H_2O, is difficult in nature and the electron correlation effects are essential for describing this physical property. This consideration requests us to use high-cost computation method to evaluate the redox potential with the IUPAC value of 4.44 V. However, this is difficult for given reaction which we want to investigate. Our work provides a new scheme to compute the SHE potential and emphasizes that the same method must be employed to evaluate the SHE and the redox potentials for a given reaction. [1] The important insights within this manuscript are as follows:

(1) We estimated the pK_a value of H_2O by using the linear fitting. The computed pK_a value is very accurate, which corresponds to the ion product of water: $[H^+]\,[OH^-]=5.0 \times 10^{-15} - 1.5 \times 10^{-14}$ $(mol/l)^2$.

(2) SHE potential can be evaluated well by our computational schemes. It should be noted that the CCSD(T)/aug-cc-pVTZ reproduces very well the SHE potential which is almost the same as the IUPAC value. The DFT-calculated SHE potentials are somewhat different from the IUPAC value, indicating that the redox potential should be presented with respective to the SHE potential calculated at the same computational method. Our scheme also reproduces well the redox potentials of several typical reactions within almost 0.1 V by typical density functional theory. We will show further applications of SHE tuned redox potential to larger molecules such as nucleic acid and vitamin. [2]

References

[1] T. Matsui *et al.*, *J. Comp. Chem.* **34**, 21(2013).

[2] T. Matsui, Y. Kitagawa, Y. Shigeta and M. Okumura, *in preparation.*

3PJ20 Shear Relaxation Spectra of Liquid Mixtures

T. Yamaguchi, T. Akatsuka, S. Koda

Graduate School of Engineering, Nagoya University, Nagoya 464-8603, Japan

e-mail : tyama@nuce.nagoya-u.ac.jp

Shear viscosity of liquids, liquid mixtures and solutions has been studied for more than a century due to the relative ease and accuracy of its measurement. In particular, various structural models on liquid mixtures have been proposed based on the composition dependence of the shear viscosity. However, the validity of these models is not confirmed because the mechanism of the shear viscosity of liquid mixture is yet to be resolved at present.

In spite that shear viscosity is a dynamic variable, conventional studies have determined merely the steady-state values of the shear viscosity. We have applied shear impedance spectroscopy to various liquids including lubrication oils, ionic liquids and lithium electrolytes, and determined the complex shear relaxation spectra of these liquids in the MHz region. The origin of the variation of the steady-state shear viscosity was discussed based on these relaxation spectra. The shear relaxation spectrometry is extended to liquid mixtures in this work.

The experiments are performed on three binary mixtures as squalane + 2,4-dicyclohexyl 2-methylpentane (DCMP), bis(2-ethylhexyl)sebacate + benzylbutylphtarate, and the mixtures of two silicone oils of different molecular weights. These three pairs of liquids are chosen because their high-frequency shear moduli are different from each other. The temperature is fixed at 298 K, and the mass fraction is varied from 0 to 1 with the interval of 0.25.

Figure 1 shows the shear relaxation spectra of squalane + DCMP mixtures of various compositions. The relaxation frequency of neat squalane (circles) is lower than that of neat DCMP (squares), though the viscosity of the former is smaller than that of the latter. Two relaxation processes are observed in the spectra of mixtures, and their relaxation frequencies look close to those of neat liquids. Therefore, the shear viscosity of the mixture is not explained by the variation of the frequency or the amplitude of the single relaxation process.

We tried to reproduce the relaxation spectra of mixtures as the linear combination of those of neat liquid, which is found to work fairly well. The results of the analysis and the composition dependence of the coefficients of the linear combination will be presented at the conference.

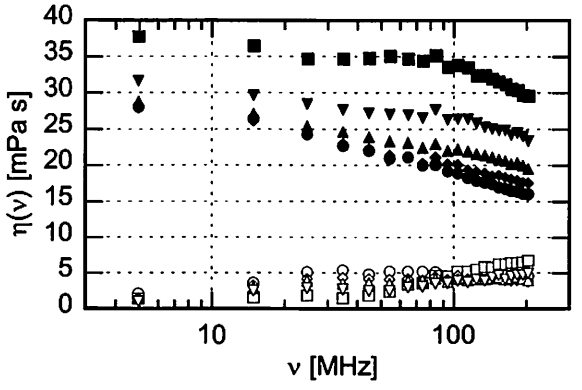

Fig.1 The shear relaxation spectra of squalane + DCMP mixtures. The mass fraction of squalane is 1.00 (circles), 0.75 (diamonds), 0.50 (upward triangles), 0.25 (downward triangles) and 0.00 (squares). The filled and open symbols denote the real and imaginary parts, respectively.

3PJ21 Preparation of Photocatalyst and its Application in Degradation of Congo Red

Wen-Chen Chien*[1,2], Chien-Fu Lin, Wan-Chien Liao

[1]*Department of Chemical Engineering, Ming Chi University of Technology*

[2]*Battery Research Center of Green Energy, Ming Chi University of Technology*

e-mail : wcchien@mail.mcut.edu.tw

Titania photocatalysts were prepared by direct precipitation of titanium tetrachloride and ammonium hydroxide at various annealing temperature between 200 and 800°C at different solution pH. Effects of solution pH and annealing temperature on the properties of titania were studied. The results showed that the prepared titania had a particle-shape and the aggregation between primary titania crystallines occurred after high temperature annealing. The prepared titania had the pure anatase phase as the precipitation process was conducted under acidic or natural reactive environments and the annealing temperature was less than 600°C. At pH=9 and pH=11, parts of anatase titania could be transferred into rutile phase as the annealing temperature reached 600°C. Pure rutile titania would be prepared as the annealing temperature reached 800°C. However, the prepared titania showed the mixture phase of anatase and rutile as the annealing temperature reached 800°C at pH=7. In addition, the bar-shape titania could be obtained at pH=11 and annealing temperature at 800°C. Finally, the titania was applied to decompose the Congo red dyes. The results showed that the prepared titania with a size 10-20nm and mixed crystal phase had the best performance for the decomposition of Congo red dyes

TEM image of bar-shape titania prepared at annealing temperature 800°C.

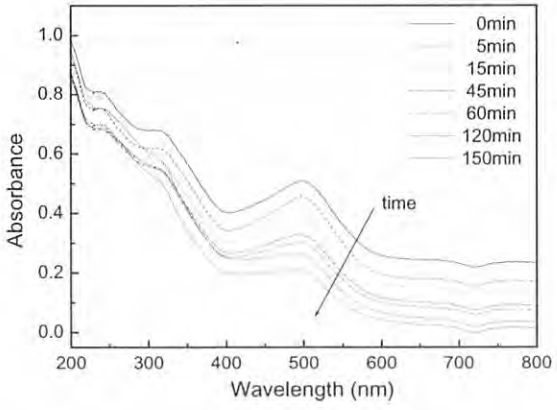

UV-vis spectra of Congo red solution under degradation by titania at different time.

3PJ22 Photodegradation of methylene blue catalyzed by graphene-silica/TiO2 nanosheets composite

Yan Huang[1], and Sam Fong Yau Li[1]

[1]*Department of Chemistry, National University of Singapore, Singapore, 117543*

e-mail : g0900988@nus.edu.sg

Graphene oxide or graphene-silica as a support for immobilizing TiO2 nanosheets was prepared by hydrothermal reaction. The morphology, porosity, adsorption property, and composition of as-prepared composites were characterized in detail. The textural properties of the as-prepared composites were controlled by changing graphene loading and titania ratio. Subsequently, these composites were applied to the photodegradation of methylene blue under UV irradiation. Enhanced photocatalytic activity of these as-prepared composites compared with pure TiO2 nanosheets was obtained. Their degradation kinetics was investigated, and the reason for the enhanced performance was revealed.

3PJ23 PEGylated Poly(ethylene imine) Copolymers as Adjuvant for the Application of Veterinary Vaccine

M.L. Chen[1], G.F. Chen[1], P.F. Hsieh[2], C.C. Yu[3], M.S. Chien[3], M.K. Hsieh[2], M.Y. Liao[1]

[1]*Department of Chemistry, National Chung Hsing University, Taichung, Taiwan R.O.C.*
[2]*Graduate Institute of Microbiology and Public Health, National Chung Hsing University, Taichung, Taiwan R.O.C.*
[3]*Graduate Institute of Veterinary Pathobiology, National Chung Hsing University, Taichung, Taiwan R.O.C.*
e-mail: dolphineddie@yahoo.com.tw

In this study, hydrophilic copolymers (PEI-PEG) are synthesized by branched poly(ethylene imine) (cationic polyelectrolytes) and poly(ethylene glycol) (nonionic hydrophilic polymers) as a functional biodegradable adjuvant for animal subunit and DNA vaccine. Appropriate PEGlation of PEI can reduce its cytotoxicity and extend its clinical application, but also maintain the high efficiency for transfection [1] and stimulate immune response. In addition to properties of polyelectrolyte, forming the complex proportion of polycation and DNA or protein plays an important role to influence the efficiency and cytotoxicity [2]. Therefore, the physicochemical characteristics of PEI-PEG, including protein binding ability, zeta potential and the particle size in different ratio of polycomplexes, were explored. The experiments revealed that PEI-PEG blending with DNA showed high transfection efficiency in 293T cells with DNA, and good binding ability with protein in the proper ratio. PEI-PEG copolymers exhibit good potential as efficacy immunoadjuvant.

References

[1] B.Y. Chua, M.A. Kobaisi, W. Zeng, D. Mainwaring, D.C. Jackson, *Mol. Pharm.* **9**, 8190(2011).
[2] T. Behera, P. Swain, S.K. Sahoo, *Int. Immunopharmacol.* **11**, 907(2011).

3PJ24 Neutron Diffraction Study on the Structure of Aqueous $LiNO_3$ Solutions

Y. Kameda[1], T. Miyazaki[1], Y. Amo[1], T. Usuki[1]

[1]*Department of Material and Biological Chemistry, Yamagata University, Yamagata 990-8560, Japan*

e-mail : kameda@sci.kj.yamagata-u.ac.jp

Hydration structure of Li^+ has extensively been investigated by means of experimental and theoretical methods. However, reported hydration number of Li^+ is still uncertain, widely spreading out from 4 to 6[1,2]. According to neutron diffraction studies with $^6Li/^7Li$ isotopic substitution method, indication of the concentration dependence of the hydration number of Li^+ has been suggested[3-5]. Environmental structure around Li^+ obtained from neutron diffraction can be affected by large absorption of ^6Li. In order to avoid this experimental difficulty, the use of incident neutrons with shorter wavelength and excellent counting statistics must be necessary. In the present study we describe results of neutron diffraction measurements on aqueous $LiNO_3$ heavy water solutions using newly constructed time-of-flight total scattering spectrometer NOVA installed at BL21 of the MLF facility in J-PARC.

$^6Li/^7Li$ isotopically substituted 1, 5 and 10 mol% $LiNO_3$ heavy water solutions were sealed in cylindrical vanadium foil cell with diameter of 6mm. Neutron diffraction measurements ware carried out at 25 °C. The first-order difference, $\Delta_{Li}(Q)$, between observed scattering cross sections from isotopically distinct samples involves partial structure factors relating the substituted atom[3]. The distribution function around Li^+ was derived from the Fourier transform of the observed $\Delta_{Li}(Q)$. Structural parameters concerning the first hydration shell of Li^+ were obtained from the least squares fitting analysis of the observed $\Delta_{Li}(Q)$ as indicated in Fig. 1. The nearest neighbour $Li^+\cdots O(D_2O)$ and $Li^+\cdots D(D_2O)$ distances were determined to 1.972(8) and 2.58(1) Å, and 1.958(8) and 2.56(1) Å, for 10 and 5 mol% $LiNO_3$ solutions, respectively. Hydration number of Li^+ for 10, 5 and 1 mol% $LiNO_3$ solutions was determined to 3.95(6), 5.18(5) and 6.0(3), respectively, clearly indicating existence of concentration dependence of hydration number of Li^+.

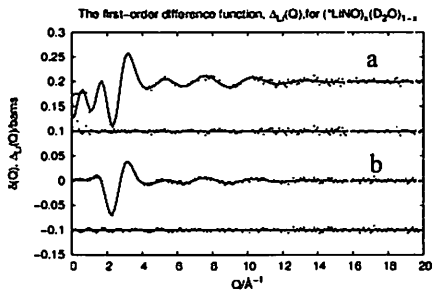

Fig. 1 Difference function, $\Delta_{Li}(Q)$, around Li^+, observed for a) 10 and b) 5 mol% $LiNO_3$ solutions in D_2O.

References

[1] H. Ohtaki, T. Radnai, *Chem. Rev.* **93**, 1157(1993).

[2] P. R. Smirnov, V. N. trosin, *Russ. J. Gen. Chem.* **76**, 175(2006).

[3] J. R. Newsome, G. W. Neilson, J. E. Enderby, *J. Phys. C: Solid State Phys.* **13**, L923(1980).

[4] I. Howell, G. W. Neilson, *J. Phys.: Condens. Matter* **8**, 4455(1996).

[5] Y. Kameda, S. Suzuki, H. Ebata, T. Usuki, O. Uemura, *Bull. Chem. Soc. Jpn,* **70**, 47(1997).

3PJ25 Integral equation theory for solvation effects on molecular structural fluctuation

Y. Matsumura[1], and H. Sato[1,2]

[1]*Department of Molecular Engineering, Kyoto University, Kyoto 615-8510, Japan*
[2]*ESICB, Kyoto University, Kyoto 615-8510, Japan*
e-mail : matsumura.yoshihiro.36s@st.kyoto-u.ac.jp

【Introduction】 Structural fluctuation of a protein may be essentially influenced by the medium environment. The solvation effects on structural fluctuation of chain molecules are important to understand chemical and biological phenomena in solution. N-butane, which has only one conformational degree of freedom, is the fundamental model to investigate the solvation effects [1].

In the present study, we developed a new integral equation theory (IET) combined with Monte Carlo (MC) simulation to investigate molecular structural fluctuation in various solution systems. Thanks to the analytical nature of IET, we can compute a statistical ensemble of the conformation with reasonable computational cost, including solvation effects [2, 3]. We examined hydration effects on structural fluctuation of n-butane (all-atom model [1]).

【Theory】 Solute structural fluctuation is expressed by the intra-molecular correlation function, $\omega = \omega^{ref}+\Delta\omega$. ω^{ref} is calculated using MC simulation of an isolated molecule. The deviation $\Delta\omega$ due to solvation is calculated based on new integral equations as follows;

$$\omega_{ab}^{ref}(r)\Delta\tilde{\omega}_{ab}(r)=\sum_{c<d}\int dr' c_{cd}^{UU}(r')\chi_{cd,ab}(r',r), \quad \text{and} \quad c_{ab}^{UU}(r)=\begin{cases}\Delta\tilde{\omega}_{ab}(r)-\ln(\Delta\tilde{\omega}_{ab}(r)+1)-\beta u_{ab}^{S}(r) & for \quad \Delta\tilde{\omega}_{ab}(r)\le 0,\\ -\beta u_{ab}^{S}(r) & for \quad \Delta\tilde{\omega}_{ab}(r)>0.\end{cases}$$

Here, $\Delta\tilde{\omega}_{ab}=\Delta\omega_{ab}/\omega_{ab}^{ref}$. Subscript denotes a solute site. c^{UU} is the intra-molecular direct correlation function, χ is the intra-molecular density-density correlation function, u^S is the intra-molecular solvation potential, and $\beta=1/k_BT$, k_B is Boltzmann constant. Solvation free energy ΔF including solute structural fluctuation effects can be derived analytically based on the present theory.

【Results and Discussion】 ΔF was calculated at the four thermodynamic state points, for which experimental data are available (Table 1, [1]). The result ΔF (calc.) becomes larger when temperature increases, which is in qualitative agreement with experimental data ΔF (exp.). This is consistent with the typical thermodynamics of hydrophobic hydration. The origin of this dependency on thermodynamic condition is the negative hydration entropy. This may be related to the orientational restrictions for water molecules around the n-butane [4].

Table1: Solvation free energy, ΔF (kcalmol^{-1})

Temperature(K)	density(gcm^{-1})	ΔF (calc.)	ΔF (Cui)	ΔF (exp.)
283.15	0.9997	1.622	1.345	1.658
298.15	0.9970	2.297	2.034	2.082
313.15	0.9922	2.888	2.638	2.439
328.15	0.9875	3.459	3.166	2.731

【References】[1] Q. Cui, and V. H. Smith, Jr. *J. Phys. Chem.* **B106**, 6554(2002). [2] T. Munakata, S. Yoshida, and F. Hirata, *Phys. Rev.* **E123**, 3687(1996). [3] D. Yokogawa, H. Sato, and S. Sakaki, *Chem. Phys. Lett.* **487**, 241(2010). [4] R. L. Mancera, and A. D. Buckingham, *J. Phys. Chem.* **99**, 14632(1995).

3PJ26 Perturbation Theory of Large Particle Diffusion in a Binary Solvent

Y. Nakamura[1], A. Yoshimori[1], R. Akiyama[2] and T. Yamaguchi[3]

[1]*Department of Physics, Kyushu University, Fukuoka 812-858, Japan*

[2] *Department of Chemistry, Kyushu University, Fukuoka 812-8581, Japan*

[3] *Department of Molecular Design and Engineering, Graduate School of Engineering, Nagoya University, Nagoya464-8603, Japan*

e-mail : y.nakamura@cmt.phys.kyushu-u.ac.jp

I. Purpose

The purpose of the present study is to develop a theory for studying of diffusion in a binary solvent for studying effects of solvation structure around a large diffusing particle. When a solvent consists of two components, the solvation structure greatly depends on a particle number ratio of each solvent. Thus, some experiments of biomolecules in a binary solvent have showed the effect of solvation on diffusion when changing the number ratio.

II. Theory

Assuming that a solvent particle was much smaller than a diffusing (solute) particle, we expanded microscopic equations for binary-solvent particles [1]. By the expansion, we derived hydrodynamic equations with new boundary conditions of the surface on a solute particle. The boundary conditions are calculated by the radial distribution functions of a binary solvent. We can consider the solvation effect through the functions, because they represent the density distribution of solvent particles around the solute. Solving the hydrodynamic equations with the boundary conditions, we can obtain an analytical expression of diffusion coefficient.

III. Application

The developed theory is applied to a large hard sphere solute immersed in a binary hard-sphere mixture (solvent and co-solvent). Due to the solvation structure, the diffusion coefficient deviates from the value predicted by the Stokes-Einstein (SE) relation (Fig.1). The deviation increases with the mole fraction of the co-solvent. Furthermore, these tendencies are stronger at a large size of a co-solvent than at a small size. For instance, the diffusion coefficient is 1.39 times as large as that of the SE relation when the mole fraction of a co-solvent was 0.002 (The ratio of sizes was 50 : 1 : 5).

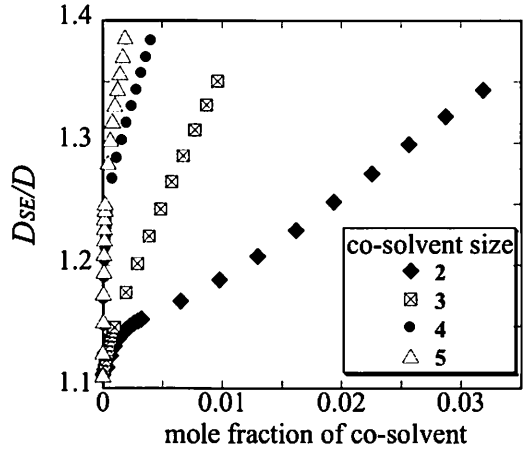

Fig.1 The diffusion coefficient D calculated by our theory. Here, D_{SE} is the value predicted by the Stokes-Einstein relation (slip condition). The size ratio of solute, solvent and co-solvent particles is 50 : 1 : X, where X = 2, 3, 4 and 5.

References

[1] Y. Nakamura, A. Yoshimori, R.Akiyama, J. Phys. Soc. Jpn. Suppl., **81** (2012) SA026 (2012).

3PJ27 A graphene-CNT based support for enhancing the electrochemical properties and tolerance of Pt-Ru catalysts

Yu-Sheng Wang, Shin-Yi Yang, Shin-Ming Li, Hsi-Wen Tien, Sheng-Tsung Hsiao,

Wei-Hao Liao, ,Chen-Chi M. Ma and Chi-Chang Hu

Department of Chemical Engineering, National Tsing Hua University,
101 Section 2, Kwang Fu Rd., Hsin-Chu 30013, TAIWAN
e-mail: ccma@che.nthu.edu.tw

This study demonstrates that platinum-ruthenium (PtRu) nanoclusters decorated on a composite consisting of graphene sheets (GS) and carbon nanotubes (CNTs), named as PtRu/GS-CNT, exhibit great electrocatalytic activity for methanol oxidation with excellent CO tolerance. From the SEM image, CNTs act as useful nanospacers for diminishing the face-to-face aggregation of GS due to the strong graphitic interaction. This 3-D porous structure exposes highly surface area for evenly depositing PtRu nanoclusters and facilitates the electrolyte/reactant diffusion, leading to the highly catalytic performances. The voltammetric forward peak current density to the reverse peak current density for PtRu/GS-CNT (If/Ib=6.33) is much higher than that of commercial catalyst, PtRu/Vulcan XC-72 (If/Ib=1.33), revealing the synergistic effects between GS and CNT on enhancing electrochemical activities of PtRu nanoclusters for the methanol oxidation and the carbon monoxide (CO) tolerance.

3PJ28 Synthesis of Carbon Dots by Means of Double Electrospray Microreactor

Y. Hiejima[1], K. Nitta[1], M. Kanakubo[2], and A. Wakisaka[3]

[1]*Kanazawa University, Kakuma, Kanazawa 920-1192, Japan*

[2]*National Institute of Advanced Industrial Science and Technology (AIST), 4-2-1 Nigatake, Sendai 983-8551, Japan*

[3]*National Institute of Advanced Industrial Science and Technology (AIST), 16-1 Onogawa, Tsukuba 305-8569, Japan*

e-mail : hiejima@se.kanazawa-u.ac.jp

Carbon dot (C-dot), which is a photoluminescent carbon-based nanomaterial, has attracted much attention [1]. Although several methods of synthesis in solution have been reported, most of those are based on batch pyrolysis reactions, which require purification procedures to remove byproducts. In this study, micrometer-sized droplets, which are generated by an electrospray method, are utilized as the microreactors, and the synthesis of the C-dots is conducted successfully.

A schematic picture of the experimental set up is shown in Fig. 1. The charged droplets of the solutions of citric acid (CA) and ethylenediamine (EDA) in 1-propanol (1 M) were formed with a pair of electrosprays in the opposite polarities. Due to the coulombic attraction between the positively and negatively charged droplets, CA and EDA were mixed in the merged droplet, and the salt (CA-EDA) was formed. The salt in the droplets was sucked into the furnace, and carbonized after evaporation of the solvent. The carbogenic particles were collected with a cold trap. The product was dispersed in water as obtained, and the emission spectra of the aqueous solution were measured with a fluorospectrometer (Jasco, FP-6200).

Typical emission spectra at various excitation wavelengths are shown in Fig. 2. The emission spectra show red shifts at longer excitation wavelengths, which are commonly observed for the C-dots [1]. The relevant parameters for determining the properties of the C-dots and the reaction mechanism will be discussed in the presentation.

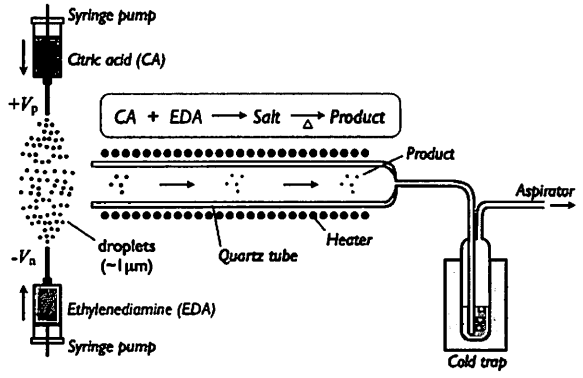

Fig. 1 Schematic picture of the experimental set up.

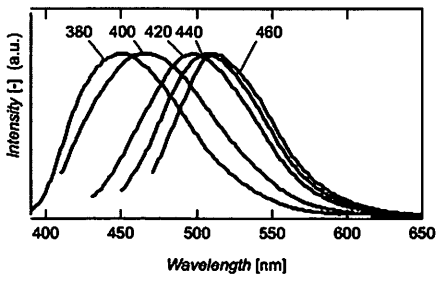

Fig. 2 Normalized photoluminescence spectra of the product synthesized at 400 °C. The excitation wavelengths are shown by the numbers.

References

[1] S. N. Barker and G. A. Barker, *Angew. Chem. Int. Ed.* **49**, 6726 (2010).

3PJ29 Effect of Alkyl Chain Length on the Structure of the Liquid Phase of Primary Alcohols – A Molecular Dynamics Study

G. Matisz[1,2], A-M. Kelterer[3], W.M.F. Fabian[4] and S. Kunsági-Máté[1,2]

[1]*Department of General and Physical Chemistry, University of Pécs, Ifjúság 6, H-7624 Pécs, Hungary*

[2]*János Szentágothai Research Center, Ifjúság 20, H-7624 Pécs, Hungary*

[3]*Institute of Physical and Theoretical Chemistry, Graz University of Technology, Stremayrgasse 9/I, A-8010 Graz, Austria*

[4]*Institute of Chemistry, Karl-Franzens University of Graz, Heinrichstr. 28, A-8010 Graz, Austria*

e-mail : gmatisz@gamma.ttk.pte.hu

The structure determining factors on constant pressure and temperature in liquids which consist of molecules capable to form hydrogen bonds (e.g. water, primary alcohols) are the strength of the hydrogen bonds and the length of the alkyl chains.

The strength of the hydrogen bonds not only depends on the type of the interacting molecules, but increasing with the number of molecules which are taking part in the OH...O network, in a non pair-wise additive way. This latter property is known as cooperativity effect [1] and mainly associated to the formation of cyclic structures [1-3].

In this contribution, based on molecular dynamics simulations using the DFTB+ program[4,5] which is capable to describe partly (approx. 60%) the cooperativity effect, the effect of the length of the alkyl chains on the liquid structure will be discussed in case of the liquid phase of various primary alcohols (e.g. methanol, ethanol, propan-1-ol and butan-1-ol).

Acknowledgement: The calculations are performed using the DFTB+ program on the Hungarian HPC infrastructure (NIIF Institute, Hungary).
Financial support of the SROP-4.2.2.A-11/1/KONV-2012-0065 project is gratefully acknowledged.

References

[1] S.L. Boyd and R.J. Boyd, *J. Chem. Theory Comput.* **3,** 54 (2007).

[2] R. Ludwig, Angew. Chem. Int. Ed. **40**, 1808 (2001).

[3] G. Matisz, W.M.F. Fabian, A-M. Kelterer, S. Kunsági-Máté, *Theochem* **956**, 103 (2010).

[4] B. Aradi, B. Hourahine and T. Frauenheim, *J. Phys. Chem.* **A111**, 5678 (2007).

[5] M. Elstner, P. Hobza, T. Frauenheim, S. Suhai and E. Kaxiras, *J. Chem. Phys.* **114**, 5149 (2001).

3PJ30 Competitive Adsorption of Cd(II) from the Solution Containing Mg(II) and Cu(II) Ions Using Dithizone-Immobilized Natural Zeolite

Mudasir, A. N. Rosmadewi, and Roto

Chemistry Department, Faculty of Mathematics and Natural Sciences, Universitas Gadjah Mada, Sekip Utara, Yogyakarta 55281, Indonesia

e-mail : mudasir@ugm.ac.id

Competitive adsorption of Cd(II) ion from the solution in the presence of Mg(II) and Cu(II) ions using dithizone-immobililized natural zeolite (DIZ) has been systematically studied. Results of the study were compared to those adsorbed competitively using non-modified active natural zeolite (NZ).

The study included preparation and characterization of modified adsorbent, optimization of solution pH as well as determination of kinetic and adsorption isotherm parameters. The modification of adsorbent was done by refluxing activated natural zeolite with dithizone in toluene for several hours[1, 2] and the obtained modified adsorbent (DIZ) was characterized using X-ray diffraction analysis and FT-IR spectrophotometry.

Results of study show that dithizone has been successfully immobilized onto the surface of natural zeolite and the immobilization process does not significantly affect zeolite crystalinity. The adsorption of Cd(II) from the solution in the presence of Mg(II) and Cu(II) ions using DIZ adsorbent reaches optimum value at pH = 5. Kinetics parameters of the adsorption has been studied using 1st order Langmuir-Hinshelwood model and the result suggests that adsorption rate constant (k) of NZ and DIZ is 1.00 x 10^{-4} and 3.00 x 10^{-3} mins^{-1}, respectively. Equilibrium constant (K) of NZ and DIZ is found to be 2.95 x 10^{4} L mol^{-1} and 3.96 x 10^{4} L mol^{-1}, respectively. The adsorption of Cd(II) in the presence of Mg(II) and Cu(II) on NZ and NIZ is categorized as chemisorption with the adsorption energy (E) of 30.17 and 32.11 kJ mol^{-1} respectively[3]. In general, it has been clearly shown that the ability of natural zeolite for the adsorption of Cd(II) ions from the solution containing Mg(II) and Cu(II) ions is significantly improved by the immobilization of dithizone on the surface of zeolite.

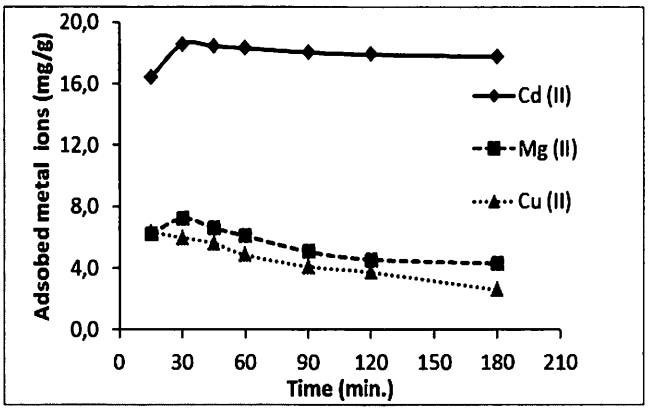

Fig. Effect of contact time on the adsorbed metal ions

References

[1] Mudasir, D. Siswanta, P. D. Ola, *J. Ion Exchange.* **18**, 418 (2007).

[2] Mudasir, G. Raharjo, I. Tahir, E.T. Wahyuni, *J. Phys. Sci.* **19**, 63 (2008)

[3] A.W. Adamson, *Physical Chemistry of Surface,* 5th ed., John Wiley and Sons, Inc., New York, 1990.

3PJ31

Adsorption Studies on Chromium Based Dyes in Aqueous Solution Using Silica Based Schiff base Adsorbent

S.Theodore David, R.Antony,S.Asha Jebamary,M.Seethalakshmi,R.Biju Bennie, S.Daniel Abraham and C.Joel.

Post Graduate Department of Chemistry, St.John's College, Tirunelveli-627002, India
e-mail : s.theodore.david@gmail.com

Water polluted by Chromium based dyes cause many harmful diseases. Hence, the removal of chromium dyes from the water has been the fascinated field of research in solution chemistry. Many types of adsorpents have been reported till date for the removal of chromium dye from the water solution. But, the silica based materials are more effective due to their high surface area and porous structure. In this work, we have derived the organo functionalized silica based Schiff base from SiO_2, APTES and isatin for the separation of chromium dye and water by adsorption phenomenon. This Schiff base has been structuraly characterized by FT-IR, UV-Vis., 1H NMR, and XRD spectroscopic techniques. The morphology of the Schiff base hase been studied by SEM technique. TG-DTG analysis has been used to investigate the thermal properties of the Schiff base. The adsorption studies of chromiun dye on silica based Schiff base have been discussed using UV-Vis. spectroscopy.

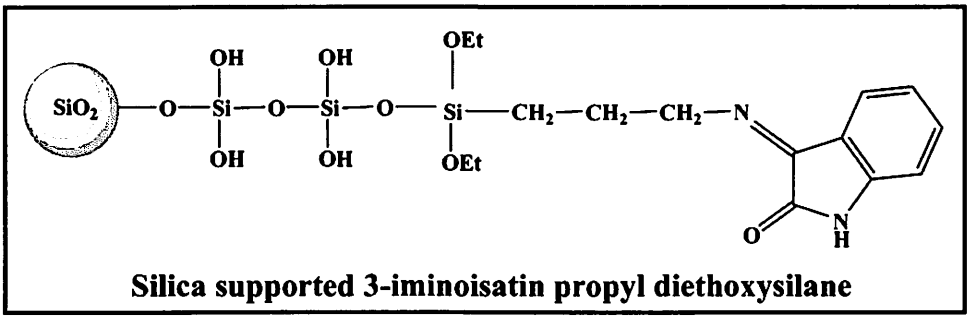

Silica supported 3-iminoisatin propyl diethoxysilane

Key Words: Schiff base, Adsorbent, Water pollution, Chromium dyes, Silica support.

3PJ32 Ethanol induced formation of graphene fractions suspended in acetonitrile

Heng Li,[1,2] Jia Cai Nie,[3] Jin Chai Li,[1] Sándor Kunsági-Máté[2,4]

[1] *Department of Physics, Xiamen University, Xiamen, 361005, P. R. China*

[2] *Department of General and Physical Chemistry, University of Pécs, H-7624 Pécs, Ifjúság 6, Hungary*

[3] *Department of Physics, Beijing Normal University, 100875, Beijing, People's Republic of China*

[4] *János Szentágothai Research Center, Pécs, H-7624 Pécs, Ifjúság 20, Hungary*

e-mail : kunsagi@gamma.ttk.pte.hu

A recent trend in research shows a growing interest in lengthwise (i.e., along the CNT axis) cutting, e.g. by solution-based oxidative process [1,2] to produce graphene fractions and/or graphene nanoribbons which have plenty of applications when fabricating nanodevices. Recently, a series of work [3] showed that ethanol has etching effect on the side wall of multiwalled carbon nanotubes (MWCNTs).

In this work, a new treatment process was developed, that under proper temperature and employing ultrasonic treatment, graphene fractions could be obtained and suspend in acetonitrile due to the ethanol induced breaking down of the ektexine of the MWCNTs. High resolution images by transmission electron microscopy validated these processes [4]. Using this procedure, high coverage of surfaces can be fabricated due to the reduced entropy in solution phase [5,6]. Therefore this procedure can be applicable for preparing heterostructures in the design optoelectronic devices [7].

Acknowledgement: Financial supports of the TÉT-10-1-2011-0126 and the SROP-4.2.2.A-11/1/KONV-2012-0065 projects are acknowledged.

References

[1] D.V. Kosynkin, A.L. Higginbotham, A. Sinitskii, J.R. Lomeda, A. Dimiev, B.K. Price, et al., *Nature* **458**, 872 (2009).

[2] Z. Zhang, Z. Sun, J. Yao, D.V. Kosynkin, J.M. Tour, *J. Am. Chem. Soc.* **131**, 13460 (2009).

[3] G. Yu, J. Gong, S. Wang, D. Zhu, S. He, Z. Zhu, *Carbon* **44**, 1218 (2006).

[4] H. Li, J.C. Nie, J.C. Li, S. Kunsági-Máté, Carbon **54**, 495 (2013).

[5] H. Li, J.C. Nie, S. Kunsági-Máté, *Chem. Phys. Lett.* **531**, 183 (2012).

[6] H. Li, J.C. Nie, S. Kunsági-Máté, *Chem. Phys. Lett.* **492**, 258 (2010).

[7] H. Li, A. Petz, H. Yan, J. C. Nie, S. Kunsági-Máté, *J. Phys. Chem. C* **115**, 1480 (2011).

3PJ33 Preparation of rod-coil diblock copolymers as sensory materials by atom transfer radical polymerization

Yang-Yen Yu*, Chia-Liang Tsai [1], Su-Nu Liu[1]

[1:] *Department of Materials Engineering, Ming Chi University of Technology,*

84 Gunjuan Road, Taishan, New Taipei City 243, Taiwan

e-mail:yyyu@mail.mcut.edu.tw

The rod-coil diblock copolymers, poly[2,7-(9,9- dihexylfluorene)]-block-poly[2-(dimethylamino)ethyl methacrylate] copolymers with different repeating units of coil, 90 and 197, were synthesized by atom transfer radical polymerization in this study. The surface structures and photophysical properties of the synthesized polymers were studied through the variation of solvent composition, temperature, and pH. The micellar aggregates of copolymers in water were observed at temperature and pH ranging from 25-75 ℃ and 2-9, respectively. The intermolecular PF aggregations led to fluorescence quenching and a blue-shift in the absorption spectra of the block copolymer as the water content increased. The aggregates of PF_{10}-b-$PDMAEMA_{90}$ and PF_{10}-b-$PDMAEMA_{197}$ micelles in water induced by pH variation showed a spherical and cylindrical structure at pH=2 and pH=7, respectively. The PL characteristics suggested the copolymers could be used as an on/off fluorescence indicator. The present study suggests that PF-b-PDMAEMA copolymers have potential applications as multifunctional sensory materials toward solvent, temperature, and pH.

3PJ34 An analytical expression of the Ornstein-Zernike integral equation of hard-sphere liquid derived from the extended scaled particle theory

Takuya Fukudome[1] and Masayuki Irisa[1]

[1] *Faculty of Computer Science and Systems, Engineering, Kyushu Institute of Technology, Iizuka 820-8502, Japan*

e-mail : fukudome@irisa-lab.bio.kyutech.ac.jp

The integral equation methods based on the Ornstein-Zernike equation have been widely used to obtain radial distribution functions, g(r), of molecular liquids. The closer which connects a direct correlation function, c(r), with a total correlation function, h(r), is necessary for solving the integral equation. However, in most cases physical meaning of the closer is ambiguous, even if the distribution functions are reproduced quantitatively. Until now, we succeeded in reproduce a radial distribution function of hard-sphere liquid in the range up to first solvation shell. In this work, we have obtained an analytical expression of the radial distribution function of hard-sphere liquid at all radial distances through a cavity function derived from the extended version of scaled particle theory (XSPT) which we have developed for non-spherical particles. The closer in this work is derived in the same manner as the Kovalenko-Hirata closer [1] but cavity functions in the closer have the analytical expression given in XSPT. In the case of hard-sphere liquid, our new integral equation gives quantitative values of the radial distribution function. Especially, the contact value, which is a value of the first peak of the function, agrees with the Monte Carlo simulation results better than that of the PY equation. Our integral equation method in this work is expected to extend to the particles with non-spherical shapes in the next step in order to apply the method to hydration of a protein.

References

[1] A. Kovalenko and F. Hirata, *Chem. Phys. Lett.* **349**, 496 (2001).

3PJ35 The Inverse Problem for Molecular Liquids: from Site-Site Bridge Function toward Effective Pair Potentials

I. Vyalov[1], G. Chuev[1,2], and N. Georgi[1]

[1]*Max-Planck Institute for Mathematics in Natural Sciences, Leipzig, 04103, German*
[2]*Inistute for Theoretical and Experimental Biophysics, Puschino, 140290, Russia*
e-mail : vyalov@mis.mpg.de

The determination of interaction potential from microscopic structure of molecular liquids is one of the crucial challenges of the theory of liquids that could play the key role in understanding of structure and thermodynamics of solutions. We present a recently developed methodology to extract effective site-site potentials from the data accumulated in site-site radial distribution functions [1]. The method is based on the inverse solution of integral equations for molecular liquids in particular interaction site model equations. Interaction site approach seems to be the most suitable to treat structural input data obtained from either scattering experiments or molecular simulations. Our approach requires only negligible computational efforts unlike other methods based on reverse Monte Carlo technique serving the same purposes.

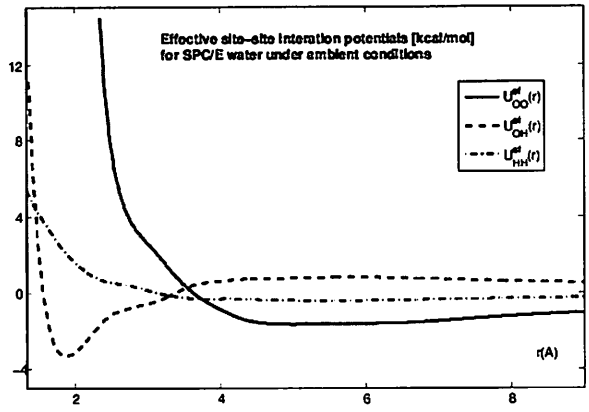

In general case, an inverse solution of site-site integral equation results in an ill-posed problem which cannot be solved without additional regularization. We impose additional constraints using the known asymptotic behaviour of site-site direct correlation functions. Such a procedure allows us to invert matrix of partial structure factors and avoid problems associated with singularities of the matrices. Finally, we are able to reconstruct the site-site bridge functions and then evaluate effective pair potential between interacting sites.

The method was applied to water, methanol, and ethanol under ambient conditions. The effective pair potential obtained for SPC/E model of water is depicted on the Figure. Our results indicate that the obtained bridge functions induced by many-body correlations strongly modify the interactions between sites. Accurate evaluation of the effective potential opens the way to reliable calculations of thermodynamic quantities such as: Compressibility, internal energy, chemical potential.

References

[1] Chuev G. et al., Chem. Phys. Lett., **561–562**, 175–178 (2013)

3PJ36 The Photoresponsive Behavior and Aggregation State of Azobenzene-Containing Block Copolymer in a Solvent

Chieh-Tsung Lo and Shu-Chi Tsao

Department of Chemical Engineering, National Cheng Kung University, Tainan 701, Taiwan
e-mail: tsunglo@mail.ncku.edu.tw

Stimuli-response polymers are the subject of intense research because they offer the possibility to tune their properties via environmental changes. As block copolymers exhibit distinct sequences, the stimuli responsiveness can be localized in either part of the block and the obtained systems can distinctly respond to different stimuli. In this work, the rod-coil diblock copolymer of poly(tert-butyl acrylate)-*block*-poly(6-[4-(4-methoxyphenylazo)phenoxy]hexyl methacrylate) (P*t*BA-b-azobenzene) was synthesized using atom transfer radical polymerization (ATRP) [1]. Our results reveal that the rod-like block containing the azobenzene group exhibited the characteristics of photoisomerization. After UV irradiation, the structure of P*t*BA-b-azobenzene changed from the trans to the cis isomer. The cis isomer was able to recover to the stable trans state under the visible light. The aggregation state of azobenzenes showed a strong function of the solvent selectivity and solution concentration. In a neutral solvent, no specific association between azobenzenes was observed. On the contrary, azobenzenes tended to pack in the H-aggregation form in a P*t*BA-selective solvent due to the poor interaction between azobenzene and solvent molecules. When the solvent concentration increased, the population of H-aggregation increased.

Acknowledgement: This work is supported by the Technology Development Program for Academia No. 101-EC-17-A-08-S1-204 by Ministry of Economic Affairs in Taiwan.

References

[1] G. Wang, X. Tong, Y. Zhao, *Macromolecules* **37**, 8911-8917(2004).

3PJ37 Structure of Liquid Water at Temperatures down to −35°C in the Supercooled State

H. Yokoyama[1], M. Kajiwara[2], and H. Kanno[3]

[1] *Yokohama City University, Yokohama 236-0027, Japan*

[2] *Yokohama Environmental Planning Bureau, Yokohama, Japan*

[3] *National Defense Academy, Yokosuka, 239-8686, Japan*

e-mail : yokoyama@yokohama-cu.ac.jp

X-ray diffraction measurements have been carried out for pure liquid water at various temperatures down to −15 °C in the supercooled state from 95 °C. In the radial distribution functions (RDF) a specific peak was found at ~10.8 Å and strengthened in the supercooled state. The RDF at −15 °C could be well explained by theoretical RDFs based on structure models assuming hydrogen-bonded networks in gas-hydrate crystals with some free water molecules in polyhedron cages, such as Pauling's model [1].

The gas-hydrate-like structures have pentagon structures composed of five water molecules as the structural unit, constructing the dodecahedrons and their aggregates. The formations of these structures seem to start at rather high temperatures above ~25 °C. The existence of the ice I-like structure could not be confirmed at temperatures down to −15 °C, but the clusters having this structure were found to be formed in the emulsion particles by supercooling from −15 °C to −35 °C together with the formation of gas-hydrate-like structures [2]. The structure of heavy water (D_2O) was also investigated and elucidated to be essentially similar to that of ordinary water (H_2O) although the hydrogen bonds in D_2O were developed slightly more than in H_2O at the same temperature [2].

References

[1] H. Yokoyama, M. Kannami, H. Kanno, *Chem. Phys. Lett.* **463**, 99 (2008).

[2] H. Yokoyama, M. Kjiwara, H. Kanno, 低温科学(*Low Temperature Science*), **71**, 39 (2013).

Author Index